INTERNATIONAL HYDROLOGICAL PROGRAMME

Interdisciplinary approaches in small catchment hydrology: Monitoring and research

9th Conference of the European Network of Experimental and Representative Basins (ERB)
Demänovská dolina (Slovakia), 25 – 28 September 2002

Convened by: ERB and UNESCO/IHP (NE FRIEND Project 5)

PROCEEDINGS

Edited by L. Holko and P. Miklánek

IHP-VI | Technical Documents in Hydrology | No. 67
UNESCO, Paris, 2003

(SC-2003/WS/30)

Published in 2003 by the International Hydrological Programme (IHP) of the United Nations Educational, Scientific and Cultural Organization (UNESCO)
1 rue Miollis, 75732 Paris Cedex 15, France

IHP-VI Technical Document in Hydrology N°67
UNESCO Working Series SC-2003/WS/30

ISBN 92-9220-001-1

The designations employed and the presentation of material throughout the publication do not imply the expression of any opinion whatsoever on the part of UNESCO concerning the legal status of any country, territory, city or of its authorities, or concerning the delimitation of its frontiers or boundaries.

Publications in the series of *IHP Technical Documents in Hydrology* are available from:

IHP Secretariat | UNESCO | Division of Water Sciences
1 rue Miollis, 75732 Paris Cedes 15, France
Tel: +33 (0)1 45 68 40 01 | Fax: +33 (0)1 45 68 58 11
E-mail: ihp@unesco.org
http://www.unesco.org/water/ihp

Printed in UNESCO's workshops
Paris, France

INTERDISCIPLINARY APPROACHES IN SMALL CATCHMENT HYDROLOGY: MONITORING AND RESEARCH

International Conference held in Demänovská dolina, Slovakia,
September 25-28, 2002

Convened by:
European Network of Experimental and Representative Basins (ERB)
IHP UNESCO Northern European FRIEND Project 5 Catchment Hydrological and Biogeochemical Processes in a Changing Environment

Organised by:
Slovak Committee for Hydrology-NC IHP UNESCO,
Institute of Hydrology, Slovak Academy of Sciences

Scientific Advisory Committee:
Mike Bonell, UNESCO, Paris, France
Václav Eliáš†, Institute of Hydrodynamics ASCR, Prague, Czech Republic
Andreas Herrmann, Braunschweig University, Braunschweig, Germany
Ladislav Holko, Institute of Hydrology SAS, Liptovský Mikuláš, Slovakia
Hubert Holzmann, University of Agricultural Sciences (BOKU), Vienna, Austria
Franca Maraga, Italian Researches Council, IRPI, Torino, Italy
Pavol Miklánek, Institute of Hydrology SAS, Bratislava, Slovakia
François de Troch, Ghent University, Ghent, Belgium
Daniel Viville, CEREG & CGS, Strasbourg, France
Piet Warmerdam, Wageningen University, Wageningen, The Netherlands

Local Organising Committee:
Pavol Miklánek, Ladislav Holko, Zdeněk Kostka, Juraj Parajka, Eva Záhorová, Martin Rusina, Zuzana Pecušová (Institute of Hydrology SAS), and Miroslav Trizna (Water Supply and Treatment)

Proceedings papers reviewed by:
R. Dijksma (Wageningen), F. Doležal (Prague), F. Gallart (Barcelona), H. Holzmann (Vienna), W. Chełmicki (Cracow), L. Pfister (Luxembourg), P. Seuna (Helsinki), D. Viville (Strasbourg), P. Warmerdam (Wageningen)

Linguistic review and correction:
Darcy K. Molnar, PhD

Previous ERB conferences and proceedings:

Oct 1986	Aix en Provence (France)
Oct 1988	Perugia (Italy) *Erosion and sediment transport* Quad. Idronomia Montana [Special Issue], A.I.D.I., Fac. Di Agraria, Univ. Padova
Sep 1990	Wageningen (The Netherlands) *Hydrological research basins and the environment* TNO Comm. On Hydrol. Res., Proc. and Informat. No. 44, The Hague, 347 pp.
Sep 1992	Oxford (United Kingdom) *Methods of hydrological basin comparison* Institute of Hydrology Rep. No. 120, Wallingford, 198 pp.
Sep 1994	Barcelona (Spain) *Assessment of hydrological temporal variability and changes* Acta Geol. Hisp., [Special Issue], vol. 28, no. 2-3, Barcelona, 1993, 138 pp.
Sep 1996	Strasbourg (France) *Ecohydrological processes in small basins* Technical Documents in Hydrology 14, IHP UNESCO, Paris, 1997, 199 pp.
Sep 1998	Liblice (Czech Republic) *Catchment hydrological and biochemical processes in a changing environment* Technical Documents in Hydrology 37, IHP UNESCO, Paris, 2000, 296 pp.
Sep 2000	Ghent (Belgium) *Monitoring and modelling catchment water quantity and quality* Technical Documents in Hydrology 66, IHP UNESCO, Paris, 2003, 112 pp.
Sep 2002	Demänovská dolina (Slovakia) *Interdisciplinary approaches in small catchment hydrology: Monitoring and research* Technical Documents in Hydrology 67, IHP UNESCO, Paris, 2003, 256 pp.

ERB Member Countries and National Correspondents (in 2002):

Austria	Hubert Holzmann	The Netherlands	Piet Warmerdam co-ordinator since 2002
Belgium	François de Troch	Poland	Wojciech Chełmicki
Bulgaria	George Gergov	Romania	Pompiliu Miţă
Czech Republic	Václav Eliáš✝	Russia	Sergey Zhuravin
Finland	Pertti Seuna	Slovakia	Pavol Miklánek
France	Daniel Viville	Spain	Francesc Gallart
Germany	Siegfried Demuth	Switzerland	Manfred Spreafico
Italy	Franca Maraga	United Kingdom	Jim Hudson
Luxembourg	Laurent Pfister		

NE FRIEND Project 5 participating countries (in 2002):

Czech Republic, Finland, Germany, The Netherlands, Poland, Russia, Slovakia, Sweden, co-ordinator L. Holko (Slovakia)

Preface

The Proceedings contain contributions selected for oral presentation at the 9th International conference of the European Network of Experimental and Research Basins (ERB). The conference was organised jointly with the IHP UNESCO Northern European FRIEND Project 5 "Catchment hydrological and biogeochemical processes in a changing environment".

The ***European Network of Experimental and Research Basins (ERB)*** was recommended by the European Council and launched in 1986. The main objectives of the network are:

- to establish and maintain relationships between member countries and research teams by means of information exchange, mobility and regular conferences
- to initiate and enable co-operation between members and other organisations
- to maintain a database of small research and experimental basins

The ERB network currently has 17 member countries. Member countries are represented by their national correspondents in the ERB Steering Committee, which assembles once per year. National correspondents are appointed by national IHP committees. The ERB General Assembly meets once every two years during the ERB international conference. Regular ERB conferences represent the main forum for meeting and exchanging knowledge among the ERB participants.

The ERB reports on its activities in the ERB Newsletter, which is published approximately twice a year. It provides information about national and international activities, catchments, projects, research findings and progress with the ERB database.

The ERB database ICARE (Inventory of the Catchments for Research in Europe) contains metadata from about 142 basins and several sets of validation data measured during short time intervals. The database is maintained by CEMAGREF in Lyon, France.

The Northern European FRIEND Project 5 "Catchment hydrological and biogeochemical processes in a changing environment" is focused on a better understanding and synthesis of the processes and mechanisms responsible for streamflow generation, variation in flow components and cycling of the main nutrients under different physiographic and climatic conditions. FRIEND is a bottom-up programme with free participation. About 10-15 participants representing universities and research institutes typically contribute to Project 5.

Similar interests of ERB and NE FRIEND Project 5 communities have lead to close co-operation in the exchange of knowledge and organisation of the latest ERB conferences.

Additional information about the ERB and NE FRIEND Project 5 can be found on:
http://erb.lyon.cemagref.fr/en/index.html
http://www.ih.savba.sk/ihp/friend5/index.html

Note from the editors

The conference was attended by 96 scientists from 16 countries. Participants presented 40 oral presentations in 3 sessions and 26 posters. This volume contains 37 of the oral presentations submitted by authors from 14 countries and a list of presented posters in the annex.

The contributions are devoted to research of various aspects of the water cycle in catchments. Most of them are focused on monitoring and modelling of streamflow generation, water quality, and the impact of climate and land use changes on the hydrological regime.

Manuscripts were refereed for their technical and scientific suitability for publication by international experts, mainly members of the Scientific Advisory Committee and chairmen of the conference sessions. The editors are greatly indebted to the reviewers (listed on page i) for undertaking the review procedure.

Readers of the proceedings are requested to bear in mind that the papers are all but one by authors whose first language is not English. Editing for the readability of the written English was undertaken by Darcy Molnar. The editors are indebted to Darcy for careful review and her husband Peter for technical help with the reviewing process.

In addition to the papers published in this volume, three other oral contributions were presented during the conference:

Schumann, S., Herrmann, A. – Flood formation and modelling on a small basin scale from Integrative Catchment Approach (ICA);

Šútor, J., Štekauerová, V. – Water balance in vertical of atmosphere – plant canopy – soil aeration zone – groundwater system in lowland forest ecosystems;

Weiler, M., McDonnell, J. – Soft experiments: A new approach to study water flow and solute transport at the hillslope scale.

Ladislav Holko and Pavol Miklanek, Institute of Hydrology SAS, Bratislava, Slovakia

ERB and Northern European FRIEND Project 5 Conference
Interdisciplinary Approaches in Small Catchment Hydrology: Monitoring and Research
Demänovská dolina, Slovakia
26-28 September 2002

Table of Contents

<u>Session 2: Data processing and hydrological modelling</u>

Session 3: Hydrological processes at larger spatial and temporal scales

SEASONAL ASPECTS OF HYDROLOGICAL PROCESSES IN THE VALLCEBRE CATCHMENTS (SOUTH-EASTERN PYRENEES)

Francesc Gallart, Pilar Llorens, Jérôme Latron, David Regüés

Institute of Earth Sciences 'Jaume Almera' (CSIC), Lluis Solé Sabarís s/n, E-08028 Barcelona, Spain

ABSTRACT

Rainfall interception, soil moisture regime, runoff generation and sediment transport have been investigated in the Mediterranean middle-mountain catchments at Vallcebre, using data collected for a period of over 5 years. The climate of this area is characterised by water surplus in autumn and spring, and water deficit in summer and winter. The seasonally varying role of rainfall intensity and atmospheric demand for evaporation counteracted and resulted in a rather uniform relative interception rate throughout the year. The spatial pattern of soil moisture showed the occurrence of semi-permanent saturated areas in downslope locations that dried out during summertime. Three different kinds of runoff events were characterised: flash summer floods caused by overland flow over impervious areas, moderate and relatively short floods at the end of the dry seasons caused by saturation 'from above' of soils, and large and sustained floods caused by precipitation over previously saturated areas and baseflow contribution during wet seasons. Sediment transport in the catchments is strongly dominated by the role of severely eroded 'badland' areas on clayey bedrock. The sediment yield increased from winter, when physical weathering dominated, to autumn, when erosion and transport was very effective because of active runoff generation on badland surfaces and on larger parts of the catchment.

Keywords mediterranean region, rainfall interception, soil moisture, runoff generation, erosion

INTRODUCTION

Subhumid Mediterranean mountains have two different kinds of interests for hydrological investigations: first, they share the hydrological processes from both wet and dry environments; and second, they are the source for water resources necessary for human life and activity in the drier downstream areas. Furthermore, most of these areas were deforested in the past, but in the European Mediterranean area most of the human activity decreased since the middle 20^{th} century, which led to the recovery of bush and forest vegetation. The knowledge of the hydrological functioning of these areas may help to anticipate the hydrological consequences of both climate and land cover change, as well as to design land use strategies that might counteract these consequences.

The purpose of this paper is to summarise the hydrological functioning of the Vallcebre catchments, paying attention to the rainfall interception process, the moisture regime of the soils, the runoff generation mechanisms, and the sediment transport processes.

Site characteristics

The Vallcebre catchments (Fig 1) are located in a middle mountain area of the Pyrenean ranges, built up by sedimentary rocks and loamy soils. The vegetation cover is dominated by pastures and forests of *Pinus sylvestris*, mostly occupying former agricultural terraces. Seasonal or temporary saturated areas occur in downslope locations, as well as in the inner part of terraces, being easily identified by the growth of hydrophile grasses such as *Molinia coerulea*. Some small heavily eroded areas (badlands) exist in the catchments, with important hydrological and geomorphic roles.

Mean annual temperature at 1440 m a.s.l. is 7.3 ºC and mean annual precipitation is 924 mm with 91 rainy days per year on average. Autumn is the main rainy season with the heaviest precipitation events, followed by spring with less rainfall amounts but more rainy days (Fig 2). Some intense rainstorms occur in summer, whereas winter is the season with less precipitation. Mean annual potential evapotranspiration is about 700 mm; June, July, August, February and March are months with water deficit.

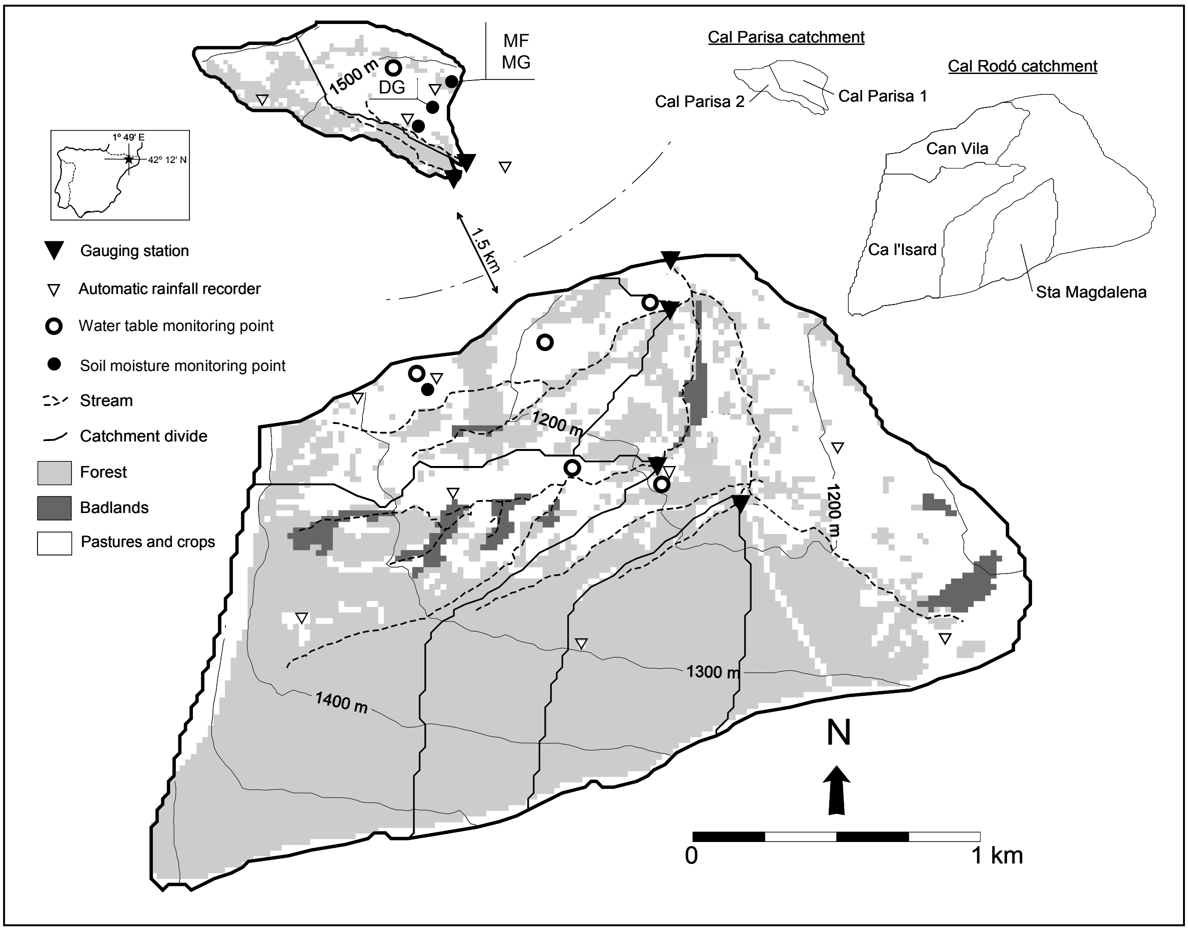

Fig 1: Map of the Vallcebre catchments, showing the instrumentation and the sites cited in the text. The Cal Parisa cluster consists of two catchments of similar size (Cal Parisa 1: 17 ha, Cal Parisa 2: 13 ha). The Cal Rodó cluster (417 ha) contains three sub-catchments (Can Vila: 56 ha, Ca l'Isard: 132 ha, Sta. Magdalena: 53 ha).

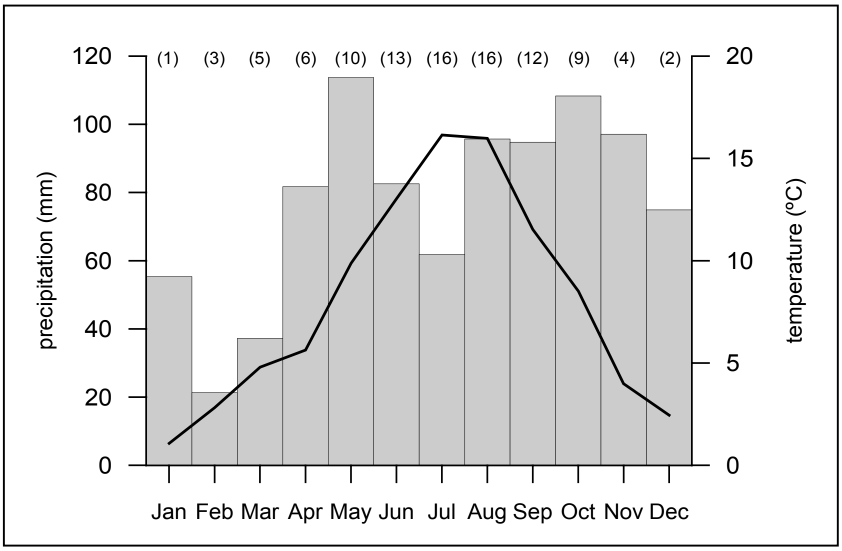

Fig 2: Monthly precipitation depths (bars), number of rainy days per month (figures between brackets), and mean monthly air temperature at 1450 m a.s.l.

Instrument set-up

Two clusters of small catchments (a paired set and an arrangement of 4 nested basins, see Fig 1) were instrumented since 1989 for the study of hydrological processes, including sediment yield, in relationship to land-use changes. The pluviometric network consisted of 12 tipping-bucket rain gauges, situated in pasture areas or clearings, and connected to data-loggers that recorded 0.2 mm precipitation increments at a temporal resolution of 1s. Two standard automatic weather stations (measuring global and net radiation, air temperature and humidity, wind speed and direction and soil temperature) were installed in Cal Parisa 1 and Can Vila sub-catchments.

All six streamflow gauging stations have control structures where water level and temperature measurements were recorded at intervals between 2 and 60 minutes. Three of the gauging stations (Cal Rodó, Ca l'Isard and Can Vila) were equipped with infrared backscattering turbidity sensors as well as automatic water sampling devices controlled by data-loggers. Two of these stations (Cal Rodó, Ca l'Isard) were also provided with suspended sediment sensors based on ultrasonic beam attenuation, which are appropriate for the high range of sediment concentrations observed during storms (sometimes higher than 100 g l^{-1}).

Soil water content has been measured in the Vallcebre catchments since 1993 using the Time-Domain Reflectometry (TDR) method at 9 profiles distributed in the main geo-ecological units (only the more relevant profiles are shown in Fig 1). These profiles consisted of sets of four vertical 20 cm-long probes permanently installed in the ground at 0, 20, 40 and 60 cm depths, read every week with a Tektronix 1502-C cable tester. A network of soil tensiometers was installed in late 1996 close to the soil moisture profiles. Depths to the water table were measured weekly at two old wells and four continuously recording piezometers were instrumented in the catchments in late 1995 to study the dynamics of the water table during rainfall events.

An experimental forest plot (site MF on Fig 1) has been monitored since 1993 to evaluate the water balance of a representative afforestation patch of *Pinus sylvestris*. The plot was instrumented for the continuous monitoring of rainfall interception (throughfall and stemflow collectors), tree transpiration (sap flow gauges) and soil water potential, as well as for periodical measurements of soil moisture (see Llorens et al., 1997ab for more details).

RESULTS AND DISCUSSION

Rainfall interception

Rainfall interception in the *Pinus sylvestris* forest plot was about 24% of bulk rainfall. Interception rates were the highest (49%) during moderate rainfall events of low intensity under atmospheric dry conditions, intermediate (15%) during long rainfall events of low intensity under atmospheric wet conditions, and the lowest (13%) during short intense summer events under dry atmospheric conditions (Llorens et al., 1997b). Nevertheless, the counteracting role of rainfall intensity and atmospheric conditions meant that the process of rainfall interception was relatively similar throughout the year, with relative interception rates of 28, 25, 21 and 27% in spring, summer, autumn and winter respectively (Gallart et al., 2002).

Soil moisture

As a result of the seasonal distribution of precipitation and the annual pattern of evapotranspirative demand, soil moisture showed a temporal pattern (Fig 3), characterised by the occurrence of a marked deficit period in summer.

During most of the year, subsurface flow on hillslopes drove the spatial organisation of soil moisture and the occurrence of saturated areas. Nevertheless, this spatial organisation was also controlled by the micro-topography created by the old agricultural terraces and the patterns of vegetation cover. Wetter soils were prevalent under grass cover and in inner parts of terraces, and drier ones under forest and in external rims of terraces. During dry periods, subsurface flow was discontinued, causing the disappearance of the saturated areas and the change of the spatial patterns of soil moisture (Gallart et al., in revision).

The temporal pattern of soil water content reflects the chief role of the dry period during summer that started in late June, after the large rainfall input in spring, and ended between September and October, when large rainfall events were able to restore soil water content and the subsurface water transfer along hillslopes (Gallart et al., 2002).

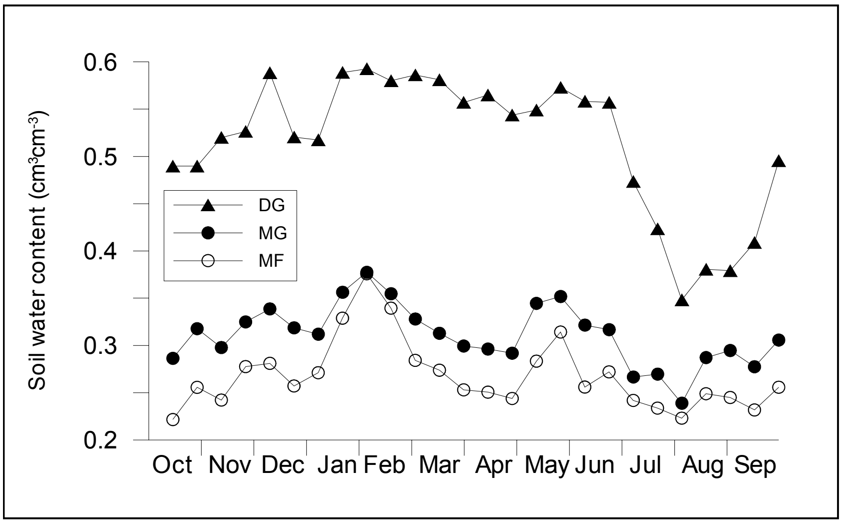

Fig 3: Fortnightly averages of volumetric soil water content measured in three 80-cm deep profiles. MF and MG are adjacent profiles located in a mid-slope position, covered by pine trees and mesophile grass respectively. The DG profile is located in a downslope frequently saturated area, covered by hydrophile grass.

Runoff generation

Streamflow from the studied catchments was dominated by storm flow (Fig 4). The runoff generating mechanisms showed a clear seasonal pattern, controlled by the soil moisture and the extent of saturated areas (Latron et al., 2000; Latron and Gallart, 2002; Gallart et al., in revision).

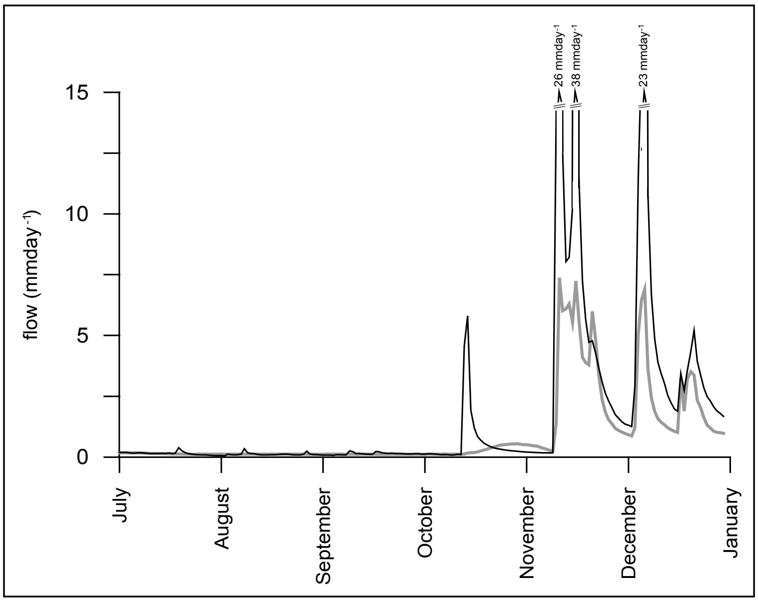

Fig 4: Daily runoff depths (black line) measured at the Can Vila sub catchment and base flow contribution (grey line) estimated for this catchment from water table records using an exponential relationship (Gallart et al., 2002). Data from year 1996.

During summer, intense rainstorms produced flash floods (small peaks on Fig 4) with very low runoff coefficients but high sediment concentrations. The dry condition of soils meant that during these events runoff was only produced on the relatively small impervious and badland areas. At the end of the dry period, the occurrence of large rainfall events could generate significant runoff in spite of the low water table (intermediate event with low base flow estimated from the water table shown in Fig 4) because of the perched saturation of the shallow soil horizons. Finally, during the wet season, runoff generation was dominated by the role of precipitation over saturated areas and baseflow.

The hydrological response of the catchment during the year showed therefore a 'switching' behaviour between a dry and a wet season, driven by the temporal pattern of soil moisture. A range of hydrological models tested in the catchments showed particular difficulties in the simulation of the events at the end of the dry period, as the models predicted either earlier or later saturation of soils than actually occurred. These models had also some difficulties in reproducing the overall water balance, presumably because of the large changes in water storage in the soils (for more details see Gallart et al., 2000; Anderton et al., 2002; Latron et al., in press).

Sediment transport

Very low concentrations of suspended sediments in waters draining areas devoid of badlands were observed, which confirms the protective role of the vegetation cover and the old soil conservation structures. In contrast, stream waters in catchments with badlands showed very high suspended sediment concentrations.

The seasonal pattern of erosion processes in badlands was characterised by regolith formation due to the weathering action of freeze-thawing cycles, regolith compaction and moderate erosion during spring, mild erosion in summer, and active erosion and transport in autumn (Regüés et al., 2000).

The results of 5 years of sediment yield monitoring in the sub-catchment with a larger relative area covered by badlands (4.5%) showed that the seasonal transport of suspended sediment increased progressively from winter to summer, and rose suddenly in autumn (Fig 5). The seasonal distributions of precipitation and runoff did not follow the same pattern, showing the non-linearity of the relationships between rainfall, runoff and sediment transport.

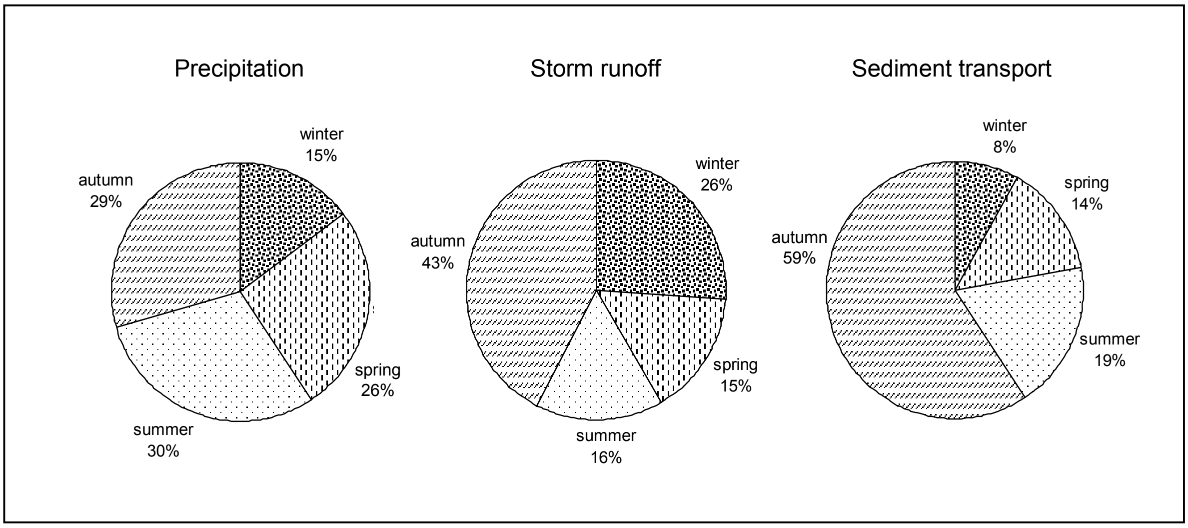

Fig 5: Seasonal distribution of precipitation, storm runoff and suspended sediment transport obtained for the Ca l'Isard sub-catchment with 4.5% of badland surface.

ACKNOWLEDGEMENTS

The authors are indebted to O. Avila for his assistance with instruments and fieldwork, to D. Rabadà and M.C. Salvany for soil moisture measurements and to M. Soler for her assistance with laboratory and desk work.

The Vallcebre catchments were operated with support from the RESEL network, through an agreement between CSIC and DGCONA. This research was supported by the projects VAHMPIRE (ENV4-CT95-0134) funded by the European Commission and PROHISEM (REN2001-2268-C02-01/HID) funded by the Programa Nacional de Recursos Naturales / Recursos Hídricos, Spanish Government.

REFERENCES

Anderton, S., Latron, J., Gallart, F. (2002) Sensitivity analysis and multi-response, multi-criteria validation of a physically-based distributed model, *Hydrol. Process.*, 16, 333-353.

Gallart, F., Latron, J., Llorens, P., Salvany, C., Anderton, S., Quinn, P., O'Connell, P.E., White, S., Ciarapica, L., Todini, E., Buchtele, J., Herrmann, A. (2000) Intercomparison of hydrological models in a small research catchment in the Pyrenees, In: *Proceedings of the ERB 2000 Conference*, R. Hoeben, Y. Van Herpe, F.P. De Troch (Eds.), Ghent University, Belgium (CD).

Gallart, F., Latron, J., Llorens, P., Salvany. M.C., Josa, R., Anderton, S., White, S. (in revision). Analysis of the hydrological functioning of a Mediterranean mountain catchment through monitoring of internal dynamics. *J. Hydrol.*

Gallart, F., Llorens, P., Latron, J., Regüés, D. (2002) Hydrological processes and their seasonal controls in a small Mediterranean mountain catchment in the Pyrenees. *Hydrol. and Earth System Sci.,* 6, 527-537.

Latron, J., Gallart, F., Salvany C. (2000) Analysing the role of phreatic level dynamics on the stream flow response in a Mediterranean mountainous experimental catchment (Vallcebre, Catalonia). In: *Catchment Hydrological and Biochemical Processes in Changing Environment*, V. Elias and I.G. Littlewood (Eds.), IHP-V, Technical Documents in Hydrology 37, UNESCO, Paris, 107-111.

Latron, J., Gallart, F. (2002) Seasonal dynamics of runoff variable contributing areas in a Mediterranean mountain catchment (Vallcebre, Catalan Pyrenees). In: L. Holko, P Miklánek, J. Parajka and Z. Kostka (Eds), *Interdisciplinary approaches in small catchment hydrology: monitoring and research*, proceedings of the ERB 2002 International Conference, Demänovská dolina, Slovakia, 25-28/09/2002, 173-179.

Latron, J., Anderton, S., White, S., Llorens, P., Gallart, F. (in press) Seasonal characteristics of the hydrological response in a Mediterranean mountain research catchment (Vallcebre, Catalan Pyrenees): Field investigations and modelling. IAHS publication.

Llorens, P., Abril, M., Salvany, M.C., Poch, R., Gallart, F. (1997a) Monitoring evapotranspiration and interception from grassland and forst patches ovegrown in abandoned terraces at the Cal Parisa basin. In: *Ecohydrological Processes in Small Basins*, D. Viville and I.G. Littlewood (Eds.), IHP-V, Technical Documents in Hydrology 14, UNESCO, Paris, 1-6.

Llorens, P., Poch, R., Latron, J., Gallart, F. (1997b). Rainfall interception by a Pinus sylvestris forest patch overgrown in a Mediterranean mountainous abandoned area. I- Monitoring design and results down to the event scale. *J. Hydrol*., 199, 331-345.

Regüés, D., Balasch, J.C., Castelltort, X., Soler, M., Gallart, F. (2000). Relación entre las tendencias temporales de producción y transporte de sedimentos y las condiciones climáticas en una pequeña cuenca de montaña Mediterránea (Vallcebre, Pirineos orientales). *Cuadernos de Investigación Geográfica*, 26, 41-65.

RUNOFF FORMATION IN A SMALL CATCHMENT

Miroslav Tesař[1], Miloslav Šír[1], Ľubomír Lichner[2]

[1]*Institute of Hydrodynamics, Academy of Sciences of CR, Praha, Czech Republic*
[2]*Institute of Hydrology, Slovak Academy of Sciences, Bratislava, Slovakia*

ABSTRACT

This article shows how soil water transport determines runoff formation from a small forested catchment during the vegetation season. Areal homogeneity of the soil water regime is also studied. Analysis of the relation between the soil water regime and runoff from a catchment shows that: (i) the small catchment covered by vegetation behaves hydrologically as a homogenous unit, (ii) runoff in a small catchment can be investigated as two transformations: rainfall to the outflow from the soil, and outflow from the soil to runoff. The proportion of both transformations in runoff generation changes following the running phase of the soil water regime.

Keywords runoff formation, soil water regime, small catchment

INTRODUCTION

The so-called rainfall-runoff relationship has been studied in depth in the past. Its formulation was based on the finding that in large catchments (with areas exceeding 100 km^2), a well definable relationship between the actual discharge in the closing profile and the precipitation total for a given antecedent period can be found. Gradually it became evident that models conceived in this way are unable to describe the reality of runoff formation from small catchments (with areas up to 10 km^2). The detailed description of soil water transport offers a promising direction for further research activities (Kostka and Holko, 1997; Tesař et al., 2001).

EXPERIMENTAL CATCHMENT

The experimental catchment Liz is located at altitudes ranging from 828 to 1074 m a.s.l. in the Šumava Mts. in the Czech Republic. The fully forested watershed (spruce) has a drainage area of 0.99 km^2. The soil cover (acid brown soil) is composed of several horizons with different hydraulic properties. Infiltrated water largely flows downward through the soil profile, so that surface and subsurface runoff is a rare phenomenon. The highly permeable subsoil forms a shallow drainage layer transporting water from the soil to a small brook. This layer is not fully filled with water, so that no significant areas with a ground water table can be found in the catchment. Geological bedrock (paragneiss) forms an impermeable layer. The experimental area is described in detail in a publication by Pražák et al. (1994). Air temperature, precipitation, global radiation, tensiometric pressure at different depths in the soil, and discharge in the closing profile are measured in the catchment.

The outflow from the soil is evaluated using a soil water balance equation on a daily time step: outflow from the soil into the drainage layer = daily precipitation – daily evapotranspiration – daily change of the soil water content. Time series of tensiometric pressures, daily precipitation and evapotranspiration totals are measured. Retention curves are used in the recalculation of tensiometric pressures in the soil water (Pražák et. al, 1994). The soil water content is the total amount of water contained in the particular soil layers. The daily change of the soil water content is determined as the difference between the soil water content at the end and at the beginning of each day. Actual evapotranspiration is evaluated as the water requirement for plant cooling (Pražák et al., 1994; Tesař et al., 2001). The outflow from the soil into the drainage layer is the only unknown variable in the balance equation. It is a computed value.

Water transport in the Liz catchment – from the onset of rainfall up to the discharge in a stream – can be divided into two parts: (1) the water movement in the soil, and (2) the flow of water through the subsoil (drainage layer) into the stream. Following the proposed schematisation, water transport in the soil can be excluded from the hydrological cycle in the catchment and investigated separately. The outflow from the soil is the only inflow into the drainage layer. Water contained in the drainage layer does not flow back into the soil cover. In principle, the soil water movement is one-dimensional and vertical. Water in the sloping drainage layer moves downhill to the stream. In an article by Tesař et al. (2001), two types of soil water transport are discussed: the diffusion type flow (DTF) in drier soils, and the instability driven flow (IDF) in soils with a higher soil water content. This corresponds to two phases of soil water flow – the percolation phase (when IDF is taking place) and the accumulation phase (when DTF is taking place). In the course of the percolation phase, the infiltrating rainwater flows through the soil without causing any considerable increment of soil water content. During the accumulation phase, rainwater accumulates in the soil without flowing through the soil profile.

AREAL HOMOGENEITY OF THE OUTFLOW FROM THE SOIL COVER

The influence of areal heterogeneity of the soil and vegetative cover on the outflow from the soil in the Liz catchment was studied on data from 1999. Ten randomly distributed monitoring stands were located in the catchment. Tensiometric pressures at depths of 0 – 17 cm, 17 – 40 cm, 40 – 50 cm, and 60 – 100 cm were measured. Fig 1 shows the typical pressure variation in the soil horizon at a depth of 17 – 40 cm at three different stands. The general impression is chaotic and it would seem that the soil water regime of the upper horizon is very heterogeneous. Pressure variations show the same pattern in all soil horizons. On the other hand, as is shown in Fig 2, the relation between the soil water content and precipitation is quite evident. Precipitation in Fig 2 is presented as a total depth between two consecutive measurements of the soil water content.

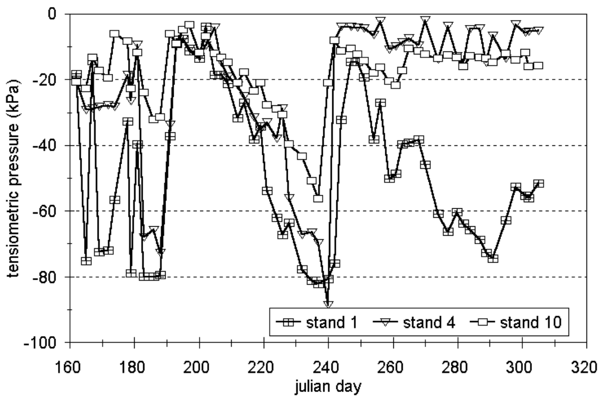

Fig 1: Tensiometric pressures at a 17 – 40 cm depth in the soil horizon (stands 1, 4, 10).

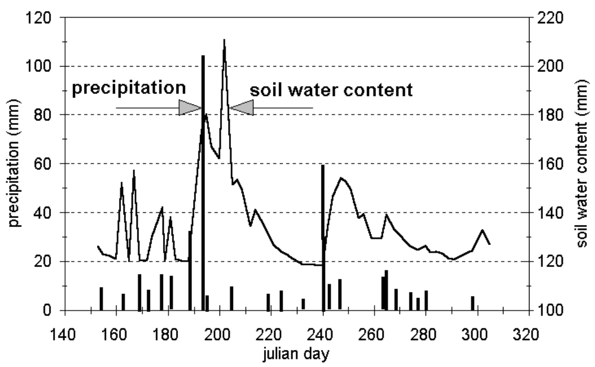

Fig 2: Soil water content (stand 1) and precipitation.

The mutual relationship between precipitation, evapotranspiration and outflow from the soil into the drainage layer can be seen in the mass curves presented in Fig 3. It can be said that the infiltrated precipitation outflows into the drainage layer only during percolation phases. The soil draining happens practically at the same time in all stands (Fig 4). The seasonal outflow varies in the range of 187 to 259 mm. If we eliminate the distant stands (No. 2 and 4), the range narrows to 209 to 234 mm. This means that for a seasonal precipitation total of 367 mm, approximately 55 to 64 % of the precipitation flows from the soil into the drainage layer. The variability in outflow is 9 % of the precipitation total.

If we consider that precipitation is measured with an error margin of 10 %, this means that the water outflow from the soil is measured with the same inaccuracy as precipitation (due to the soil cover heterogeneity). In the Liz catchment, it was thus demonstrated that the soil water regime is homogeneous from the hydrological point of view. This conclusion is supported not only by the measurements in the wet year 1999, when a precipitation deficiency did not appear (potential transpiration in 143 days was about 160 mm, precipitation 367 mm), but also in the dry year 2000, when potential transpiration (282 mm in 149 days) reached the precipitation total (280 mm).

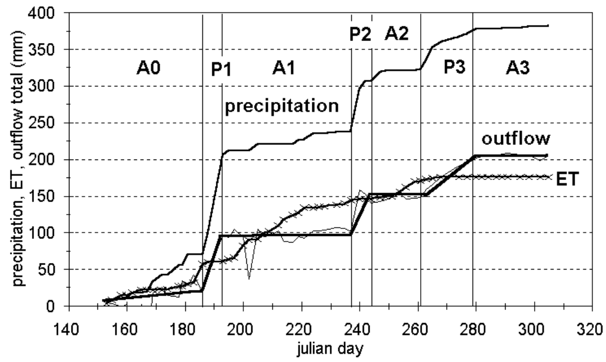

Fig 3: Mass curves of precipitation, outflow from the soil (stand 1) and evapotranspiration. P – percolation phase, A – accumulation phase.

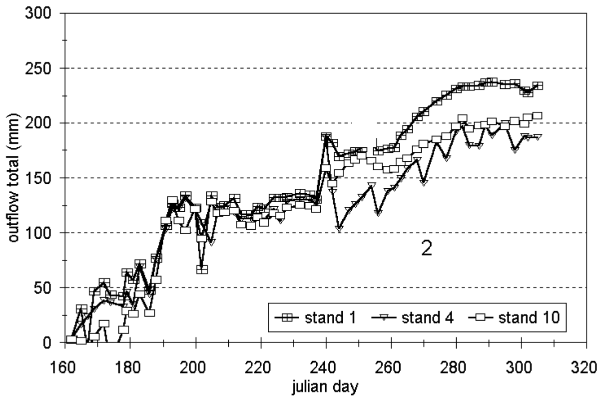

Fig 4: Mass curves of the outflow from the soil (stands 1, 4, 10).

RUNOFF FORMATION

The rainfall-runoff relationship in the Liz catchment during the vegetation season of 1999 is shown in Fig 5. Three significant precipitation events (S1, S2, S3) and the consequent generated discharge waves (O1, O2, O3) are marked out. In the figure, P1, P2, P3 represent percolation phases caused by precipitation, and A1, A2, A3 represent consecutive accumulation phases. It is obvious how significantly the soil water outflow depends on the soil water content (Table 1). In the situation S3 (where there is the highest soil water content of all situations), 100 % of the precipitation on the soil surface outflows, even when the precipitation total is the lowest of all the situations. In the situation S1 (when the soil water content is lower than in the situation S3), an almost seven times higher precipitation amount generates an outflow equal to only 44 % of the precipitation. Such discrepancies (as seen in data in Table 1) are caused by the oscillation phenomena in gravity driven drainage (Pražák et al., 1992).

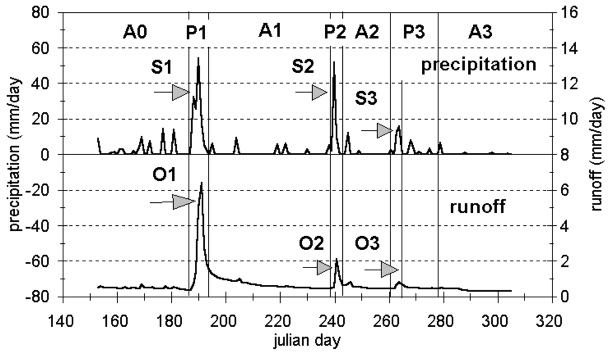

Fig 5: Precipitation and runoff from the catchment.

Table 1: Precipitation events in the vegetation season 1999.

Precipitation event	Duration (days)	Pressure (kPa)	Precipitation (mm)	Runoff (mm)	Outflow (mm)	Runoff (%)	Outflow (%)
S1	6	-55	137	17	60	13	44
S2	4	-73	70	3	60	4	86
S3	3	-36	20	0,7	20	4	100

Pressure (kPa) in Table 1 represents the tensiometric pressure at a depth of 100 cm. Precipitation (mm) is the total precipitation during the event. Runoff (mm) is the volume of the discharge wave in the stream decreased by baseflow. Outflow (mm) is the volume of the outflow from the soil. Runoff (%) and outflow (%) are related to the precipitation total.

Discharge waves in the stream have the same duration as the precipitation in all three cases. The percolation phases in situations S1 and S2 have the same duration as well. The percolation phase ends with the end of precipitation (successive precipitation does not outflow from the soil into the drainage layer) and the accumulation phase begins (runoff in the stream continuously decreases as the drainage layer empties and does not react to precipitation).

However, in the situation S3, the percolation phase persists for about 15 days after the discharge wave in the stream. Successive precipitation flows through the soil into the drainage layer. Fig 3 indicates an explanation of the phenomenon. In the period following the situation S3 there was very low water uptake for plant transpiration, the soil cover was not sufficiently depleted to be able to accumulate precipitation. The soil water content decline (Fig 2) is due to the water outflow into the drainage layer and not due to its uptake by transpiration. Moreover, the deepest soil horizon was amply saturated by the water at the beginning of the precipitation, because the tensiometric pressure at a depth of 100 cm was the highest (Table 1).

Mass curves in Fig 6 and Fig 7 show differences between the precipitation-runoff transformation, and the precipitation-soil water outflow transformation. In Fig 6 symbols S1, S2, S3 denote precipitation (Fig 5). In Fig 7 symbols V1, V2, V3 denote outflow from the soil due to precipitation S1, S2 and S3 (Fig 5), and K1, K2, K3 denote the tangents of the steady outflow. While the outflow from the soil is markedly an episodic event (the mass curve has a step-like form), water outflows from the catchment steadily (the mass curve is more continuous).

It is possible to deduce by the analysis of both mass curves (Figs 6, 7) that the soil water outflow-runoff transformation behaves exactly as the precipitation-runoff transformation. During the percolation phase the water fills up the drainage layer. Water flows into the stream and generates a perceptible discharge wave of short duration (several hours to days) when the drainage layer is sufficiently replenished by the outflow from the soil. During the accumulation phase the drainage layer slowly empties by outflow into the stream.

Water forms the so-called baseflow in the stream. The baseflow decreases in time but usually not to zero. The lowest value of the baseflow, the steady runoff, is the characteristic constant value for the studied catchment. Fig 7 shows that the steady runoff is practically identical at the end of every accumulation phase (tangents of runoff mass curve K1, K2 and K3 are parallel).

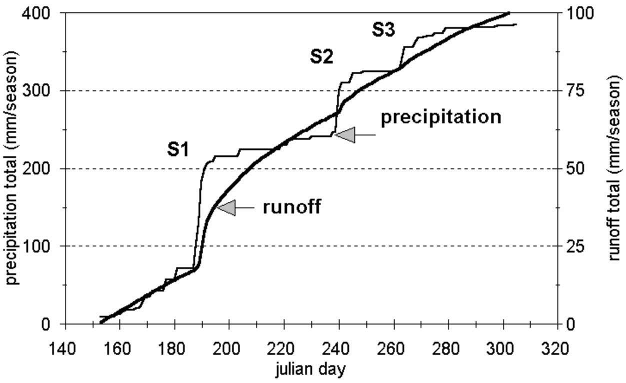

Fig 6: Mass curves of precipitation and runoff.

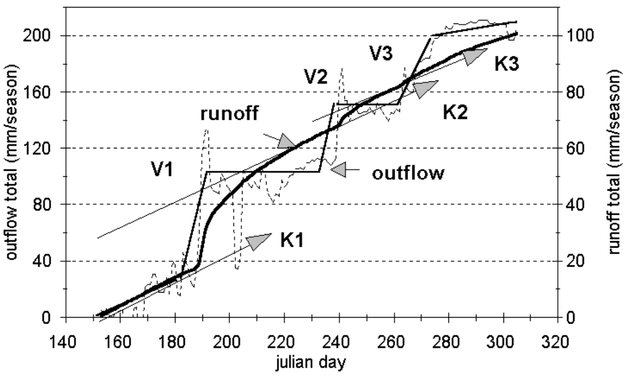

Fig 7: Mass curves of the outflow from the soil (stand 1) and runoff.

DISCUSSION

It appears that the rainfall-runoff transformation takes place in two steps in the Liz catchment. In the first step the soil behaves as a reservoir, filled with rainwater and emptied by the water uptake for plant transpiration. In the course of the vegetation season, the soil water content oscillates between two typical values – maximum and minimum. The maximum value corresponds to a soil water content where the infiltration of further rain results in instability driven flow and a percolation of water to the drainage layer. The minimum value corresponds to a soil water content where insufficient soil moisture renders a further withdrawal of water for plant transpiration impossible.

Table 2: Water balance in the vegetation season 1999.

Season	day 162 – 305	duration 143 days	
Precipitation	367 mm/143 days		2.6 mm/day
Evapotranspiration	158 mm/143 days	43 % of precipitation	1.1 mm/day
Outflow	203 – 234 mm/143 days	55 – 64 % of precip.	1.4 – 1.6 mm/day
Runoff	103 mm/143 days	28 % of precipitation	0.7 mm/day
Drainage layer recharge	106 mm/143 days	28 % of precipitation	0.7 mm/day

The second step of the rainfall-runoff transformation, water movement in the drainage layer, is not complicated from the hydraulic point of view. The drainage layer forms a reservoir in which water is stored for a long time. An interesting point concerning the catchment water regime is noticeable in the summarised data of the 1999 vegetation season presented in Table 2. Only half of the water from the soil flowed out of the catchment; the remaining half was retained in the drainage layer. In such a manner, water storage in the catchment is generated, which feeds the baseflow during the frost period when water does not flow into the drainage layer.

The mechanism of increasing oscillation outflow explains why there is no clear connection between the so-called causal precipitation and the runoff in a small catchment, typically up to 10 km^2. In such a small catchment, a correlated effect of the oscillation outflow in a large area appears from time to time resulting from the soil water regime homogeneity. Due to the above, a considerably higher amount of water outflows from the catchment than would correspond to the causal rainfall. The soil profile is drained and the next precipitation is held back in the soil, therefore it does not affect the runoff from the catchment. Thus another factor enters into the rainfall-runoff relationship: the soil water content. On the other hand, in a large catchment with a drainage area of more than 100 km^2 the areal correlation of the oscillation outflow is highly improbable. The oscillation outflow from partial areas is not large enough to substantially affect the runoff from the entire catchment. At the same time however, it holds that increased rainfall activity brings about greater runoff from the catchment, and vice versa. This is why, in a large catchment, the rainfall-runoff relationship is well described by the concept of antecedent rainfall.

CONCLUSIONS

Analysis of the relationship between the soil water regime and runoff from a catchment shows that: (i) a small catchment covered by vegetation behaves hydrologically as a homogenous unit, (ii) runoff in a small catchment can be investigated as two transformations: (1) rainfall to the outflow from the soil and (2) outflow from the soil to runoff. The proportion of both transformations in the generation of runoff changes following the running phase of the soil water regime.

Two phases interchange in the soil water regime: the percolation phase (rainwater percolates through the soil into the drainage layer, through which it flows into the stream) and the accumulation phase (rainwater accumulates in the soil and does not outflow into the drainage layer). Different mechanisms of runoff formation act in both phases. In the percolation phase, water storage recharges into the drainage layer and outflows into the stream in discharge waves immediately reacting to precipitation. In the accumulation phase, water slowly outflows from the drainage layer and forms baseflow. Alterations of the accumulation and the percolation phases can be described with the help of two rules. (1) The percolation of soil water to the drainage layer sets in if the critical soil moisture is exceeded. In this situation, the water supplied by rainfall causes a pronounced water outflow and a decrease in the soil water content. (2) In a situation when the soil moisture is less than critical, percolation is negligible.

Acknowledgements: Support from the Grant Agency of ASCR (Grants No. A30060001 and S2060104), the Grant Agency of the Czech Republic (Grant No. 205-99-1426), and the Ministry of Environment of the Czech Republic (Project No. VaV 610/3/00) is greatly acknowledged.

REFERENCES

Kostka, Z., Holko, L. (1997) Soil moisture and runoff generation in small mountain basin. Publication of the Slovak Committee for Hydrology 2. SVH-NC IHP UNESCO, Bratislava, pp. 90.

Pražák, J., Šír, M., Kubík, F., Tywoniak, J., Zarcone, C. (1992) Oscillation phenomena in gravity driven drainage. *Water Resources Research*, 28, 1849–1855.

Pražák, J., Šír, M., Tesař, M. (1994) Estimation of plant transpiration from meteorological data under conditions of sufficient soil moisture. *J. Hydrol*., 162, 409–427.

Tesař, M., Šír, M., Syrovátka, O., Pražák, J., Lichner, Ľ., Kubík, F. (2001) Soil water regime in head water regions – observation, assessment and modelling. *J. Hydrol. Hydromech*., 49, 6, 355–375.

STORMFLOW COMPONENT DETERMINATION USING HYDROLOGICAL, ISOTOPIC AND CHEMICAL APPROACHES IN THE SMALL FORESTED STRENGBACH CATCHMENT (GRANITIC VOSGES MASSIF, FRANCE)

D. Viville [1, 2*], A. Probst [2, 4*], B. Ladouche [3,5*], S. Idir [2], J.-L. Probst [2, 4*], T. Bariac [3]

[1] *Centre d'Etudes et de Recherches Eco-Géographiques, CEREG/ULP/CNRS, 3 rue de l'Argonne, 67083 Strasbourg Cedex*
[2] *Centre de Géochimie de la Surface, CGS/CNRS, 1, Rue Blessig, 67084 Strasbourg Cedex,*
[3] *Laboratoire de Biogéochimie Isotopique, BGCI/UPMC/CNRS/INRA, Case 120, 4 place Jussieu, 75252 Paris,*
[4] *Laboratoire des Mécanismes de Transferts en Géologie UPS/LMTG, 38 rue des 36 Ponts, 31400 Toulouse*
[5] *BRGM, Direction de la Recherche, 1039 rue de Pinville, 34000 Montpellier, France*
**present address*

ABSTRACT

The hydrological behaviour of the small (0.8 km²) granitic Strengbach catchment (Vosges mountains, Eastern France) was investigated during an intensive summer rainfall event (30 mm) by hydrological, isotopic and chemical measurements of streamflow components. ^{18}O, Si, DOC were selected to assess the different contributing sources using mass balance equations and end-member mixing diagrams. Gauging indicates that most of the water (62%) comes from the lower part of the catchment. Isotopic hydrograph separation indicates that the pre-event water dominates (78% of the total runoff), even at peak flow (55% of the discharge). The chemical separation distinguishes the contribution of water coming from the deep layers of the hillslopes (55-64 %) from that coming from the upper layers of the downslope saturated area (45-36%). Peak flow is mainly produced by the superficial layers of the saturated areas; processes involved could be the superficial runoff due to groundwater exfiltration after rapid infiltration.

Keywords hydrograph separation, ^{18}O, dissolved organic carbon, silica, event water, contributing areas

INTRODUCTION

The understanding of streamflow generation processes in different environmental conditions has been considerably improved by using tracers in hydrograph separation. After the pioneering work of Voronkov (1963) on separating hydrographs on a hydrochemical basis, chemical tracers have been widely used for identifying the origin of contributing reservoirs (as example Pinder and Jones, 1969; Hooper et al, 1990). Later on, stable isotopes (^2H, ^{18}O) have been successfully used (Sklash and Farvolden, 1979; Mc Donnell et al., 1990) to separate hydrographs into the water stored in the catchment prior to an event (pre-event or old water) and into that of the event (event or new water). Subsequently, studies associating both chemical and isotopes tracers (Fritz et al., 1976; Hooper and Shoemaker, 1986; Wels et al., 1991) have been carried out to compare the two methods. Although the hydrological role of the downslope saturation area has long been known (Cappus, 1960), its quantification by a combination of hydrological, isotopic and chemical measurements is not done frequently (Ladouche et al., 2001). In this paper we attempt to estimate the contribution of rainfall, as well as the role of contributing areas and of storages, to streamflow by such a combined approach in the Strengbach catchment (Vosges mountains, Eastern France) for a short summer event (22-23 July 1995).

SITE DESCRIPTION, INSTRUMENTATION AND METHODS OF ANALYSIS

The Strengbach forested catchment is located on the eastern side of the Vosges massif (north-eastern France). This small catchment (0.8 km²) ranges from 883 m to 1146 m (a.s.l.) and lies mainly on base-poor granitic bedrock. Soils are acidic and coarse-textured. The catchment is forested predominantly with Norway spruce (65% of the area), and mixed beech and silver fir (the remainder of the area). The climate is temperate oceanic-mountainous. Mean annual precipitation is 1400 mm regularly spread throughout the year and mean annual runoff is 850 mm with high flow rates in the cold season and low flow rates at the end of summer. A variable saturated area (up to 3% of the catchment area for a 128 $l.s^{-1}$ discharge), close to the outlet, is connected to the stream (Fig 1).

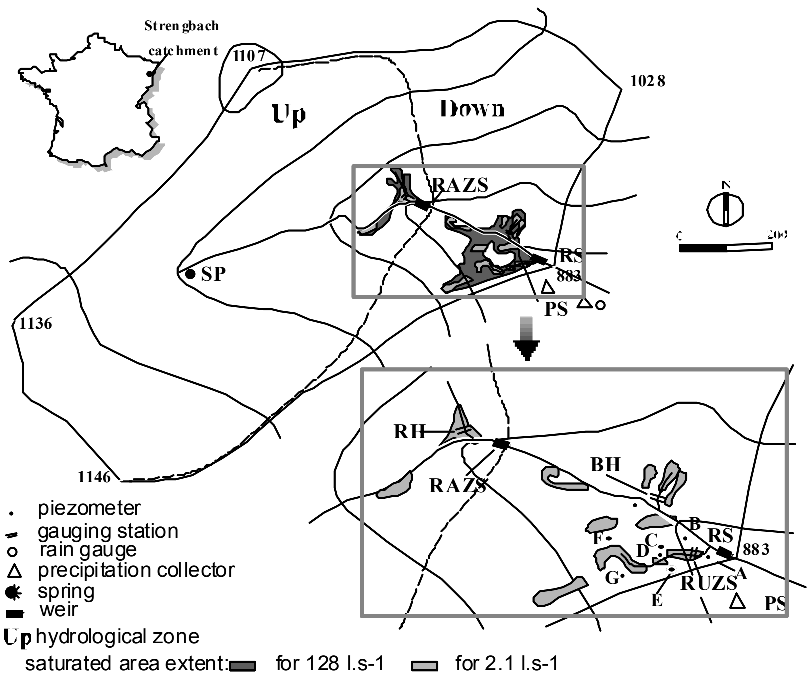

Fig 1: Location and measurement network of the Strengbach catchment.

During the event of 22-23 July 1995, rainfall was sampled at a variable time step (2, 4, 8, or 16 minutes) at the site (PS) close to the outlet. Soil water solutions were collected with porous cups under pressure (500 mbar) at 6 depths (0.15, 0.3, 0.45, 0.6, 0.75, 0.9 m) at 3 sites located at the lower part of the north-facing slope. Water sampling of the groundwater was done using the piezometer network (A, C, D, E, F, G) and 2 micropiezometers at 3 levels (0 to 0.6 m depth). Discharges from the main stream (sites RS, RAZS) and tributaries (sites BH and RUZS) were measured with flumes and sampled simultaneously (Fig 1). The water sampling frequency was adjusted to the temporal evolution of discharge (5, 10 or 15 minutes). The major chemical parameters (Na^+, K^+, Ca^{2+}, Mg^{2+}, SO_4^{2-}, NO_3^-, Cl^-, NH_4^+), silica, alkalinity, dissolved organic carbon (DOC) and stable isotopes (^2H, ^{18}O) were analysed for both groundwater and surface water with methods described in Ladouche et al. (2001). Isotopic ratios are reported in the δ notation (as ‰) relative to the Vienna-Standard Mean Ocean Water (Gonfiantini, 1978).

For both chemical and isotopic tracers, the well-established two to n-component mixing model (Pinder and Jones, 1969) was used to separate the streamflow components. This approach based on two mass conservation laws (water and tracer), allows separating the contribution of the different components (event or pre-event water, superficial or deep layer water) which correspond to different reservoirs or contributing areas.

RESULTS AND DISCUSSION

Hydrological features

The event on 22 July 1995 occurred during low water flow conditions, discharge at the outlet (RS) was only 3.5 $l.s^{-1}$. Rainfall started at 14:30 hours and lasted until 21:00 hours. This event was a typical intensive (up to 60 mm.h^{-1}) summer rainstorm with three short interruptions. The total amount of the four showers was 30 mm (Fig 2). The corresponding hydrograph is characterized by three discharge peaks (40, 34 and 17 l.s^{-1} at the outlet) in response to the successive rainfall events (18, 7.4, 3.3 and 1.5 mm) (Fig 2). The rapid response (5 minutes) of the stream and the tributaries to the rainfall suggests that the contributing areas are close to the brook and especially to the outlet.

Water table measurements show a general water level increase between 15 and 20:00 hours, with a 0.4 to 0.5 m value (Fig 3). The piezometers located in the upper part of the slope (E, for example) indicate a maximum water level at 15:30 hours, and then a plateau or a decrease is observed. Whereas the water level of the downslope piezometer A only begins to increase at 19:00 hours and reaches a maximum at 22:00 hours, which could indicate a downward wave propagation on the slope.

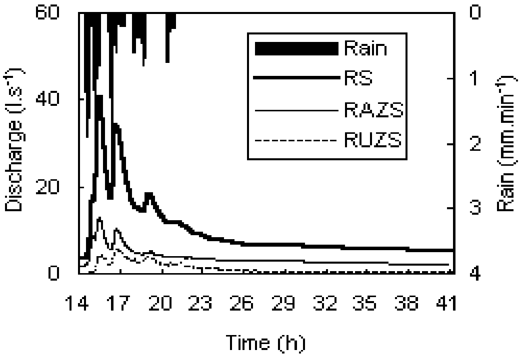

Fig 2: Hyetograph and hydrograph of the stream at the outlet (RS) and at the upper subcatchment (RAZS), and of the tributary draining the saturated area (RUZS).

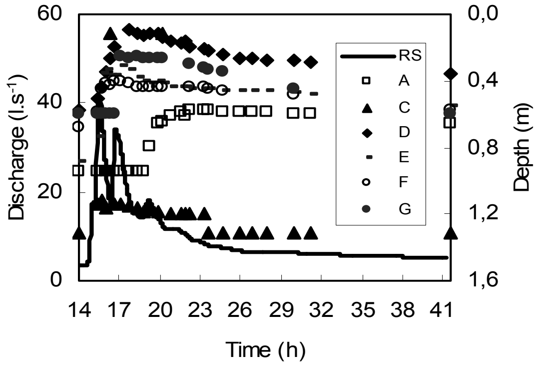

Fig 3: Hydrograph and variations of water table depths in the different piezometers in the saturated area.

The total stormflow volume is estimated to be 927 m^3. A graphical hydrograph separation based on the straight line method determines a direct runoff or 'quickflow' volume of 330 m^3 whereas the remaining 597 m^3 is attributed to 'delayed flow'; quickflow then represents only 1.4 % of the 24000 m^3, assuming rain on the entire basin. That means that most of the rain is stored in the catchment during this event. The specific discharge of the upper subcatchment (RAZS) is only of 25 l.s^{-1}.km^{-2} at the first peak whereas for the downstream zone (between RAZS and RS), it can reach 100 l.s^{-1}.km^{-2}. Hence, considering the specific discharge, the most efficient contributing source area is located in the lower part of the catchment. For the whole event, the contribution of this area is 62 % of the total volume of the flow, while it represents only 32 % of the catchment area.

Isotopic features

The ^{18}O content of streamwater during baseflow conditions (-9.3 ‰) is very similar to the spring value (-9.35 ‰) suggesting that stream baseflow is composed exclusively of groundwater (Ladouche, 1997). Consequently, groundwater flow controls baseflow and its isotopic composition can be used to characterise the pre-event component. The isotopic rainwater composition varies between -3 ‰ and -6 ‰ but most of the data are close to a -4 ‰ value. This temporal variation is not very important compared to another event where a range of 9 ‰ has been recorded (Ladouche et al., 2001). The isotopic composition of streamwater at the outlet varies greatly from -9.3 ‰ before the event to -7.1 ‰ at the peak flow and returns to the initial value during the recession stage (Fig 4). The same behaviour is observed for all the tributaries. This variation of $\delta^{18}O$ value in streamwater suggests that the event water contribution is rather important.

The isotope hydrograph separation has been performed using the event weighted isotopic signature of each shower (McDonnell et al., 1990) and with a constant pre-event signature (-9.3 ‰, stream baseflow value). The hydrograph separation (Fig 5) at the outlet indicates that, the event contribution can reach a maximum value of 40 to 45 % at the two main discharge peaks (40 and 34 l.s^{-1}). The same magnitude is observed at sites BH and RUZS. At the site RAZS, the rain contribution is only 33 % of the discharge. For the whole rainfall event, the new water contribution is 22 % at the outlet and is relatively important in comparison with a 10 % value obtained for a 40 mm rainfall event (Ladouche et al., 2001).

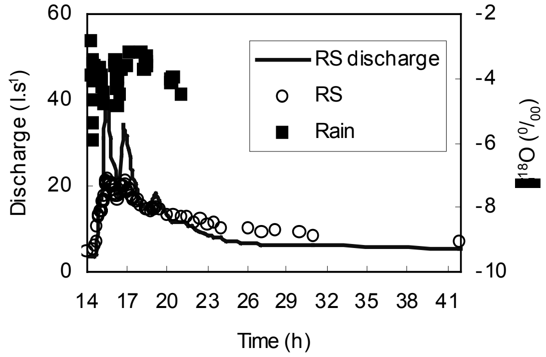

Fig 4: Variations of $\delta^{18}O$ in rainfall and at the stream outlet (RS) and discharge hydrograph.

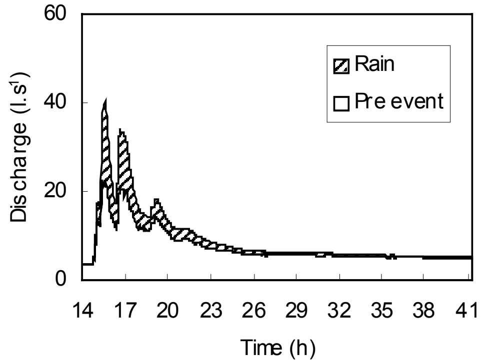

Fig 5: Two-component (event/pre-event) hydrograph separation using ^{18}O and variation of their contribution to streamflow at the outlet.

The analyses of samples of porous cups (site SC) show that there is a layering of the isotopic composition of the water (Fig 6). In the upper layers (0 to 40 cm), the signal is enriched (-4.5 to -7 ‰ value) indicating a mixing of waters (pre-event and rain water) and reflecting an important contribution of the event rain water, whereas in the deeper layers (65-90 cm) the signal is impoverished (-9 ‰) indicating a minor influence of the rain. A comparison with streamflow indicates that, during peak flow the variation of the signal at station RS is strongly influenced by that of station RUZS or the upper layer signal of the saturated area. However, during the recession period the deeper layers of this saturated area dominate.

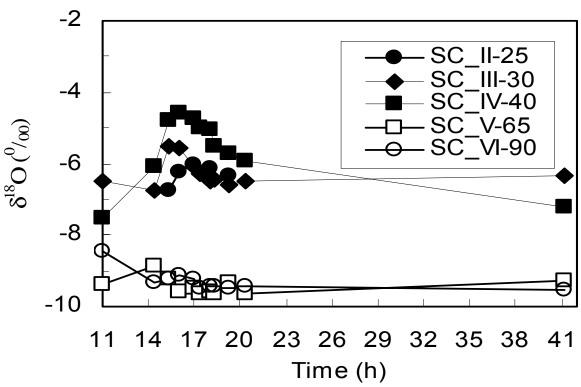

Fig 6: Variations of $\delta^{18}O$ in the porous cups (Site SC) at various depths (25-90 cm).

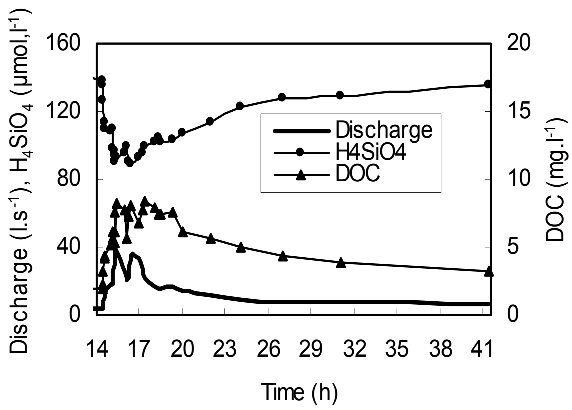

Fig 7: Variations of DOC, silica and discharge at the outlet.

<u>Geochemical features</u>

During the storm event, the rainwater is acidic (mean pH of 4.5), with low concentrations of major elements (Total Dissolved Salts = 5.6 mg.l^{-1}) (Idir, 1998). Ammonium, calcium, nitrate and sulphate are dominant, whereas dissolved silica and DOC are negligible, as already observed (Probst et al., 1990; Ladouche et al., 2001). The concentrations of almost all the elements decrease during the first two showers on 22 July and increase temporarily during the third shower. Streamwater pH is circumneutral (pH 6.0-6.5), indicating an important buffering capacity of the catchment, and calcium and sulphate are the dominant ions.

According to their chemical behaviour in relation to the discharge variations at the outlet (RS), two groups of chemical parameters can be identified at the upper subcatchment site (RAZS) and at the BH tributary: the elements which are diluted with increasing discharge (SO_4^{2-}, Na^+ and H_4SiO_4) and the elements which are concentrated with increasing discharge (DOC, NO_3^-, Cl^-, K^+, Ca^{2+}, Mg^{2+} and alkalinity) (Fig 7). In streamwater, the rapid increase of Ca, K and DOC concentrations could be due to canopy and soil surface leaching by the first rain drops, whereas the high concentrations of sulphate or silica in streamwater are diluted by the low rain content.

In order to identify the contributing sources to the chemical composition of streamwater, end-member mixing diagrams (Christophersen et al., 1990) have been performed for major elements (Idir, 1998). Among analysed parameters, the linear mixing diagram between DOC and silica (Fig 8) shows that streamwater at the outlet (RS) can be explained mainly by two obvious end-members: the component with high DOC and low silica concentrations characterizes the upper horizons of the saturated area (1: *Q sat*), whereas the component with high silica and low DOC content represents the deeper layers of the hillslopes (2: *Q hill*) as already observed for another event (Ladouche et al., 2001).

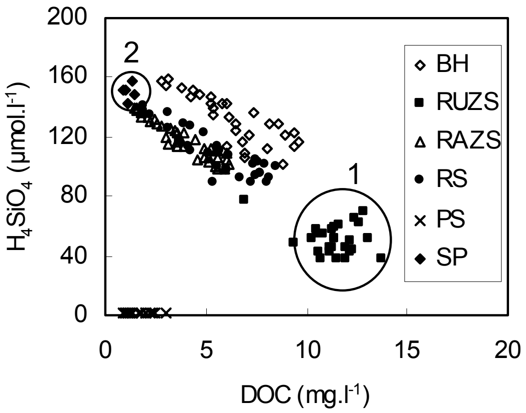

Fig 8: Mixing diagram between DOC and silica for the sampling sites; 1: upper layers of the saturated area; 2: deep layers of the hillslopes.

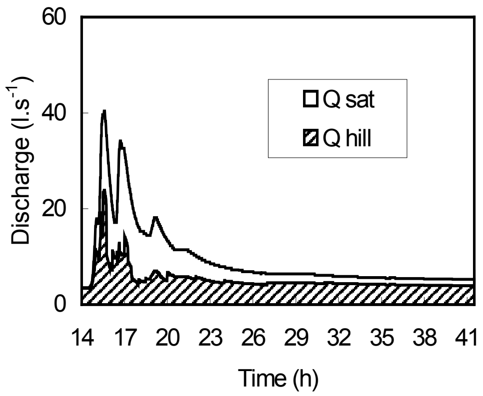

Fig 9: Two-component (deep layers of hill slopes: *Qhill*; surface layers of the saturated area: *Q sat*) hydrograph separation using DOC.

A chemical hydrograph separation has been performed at the outlet using silica and DOC. The results of the separation performed using DOC with constant end-member values (11 and 1.5 $mg.l^{-1}$ values respectively) are presented in Fig 9. For the whole event, the surface waters draining *Q hill* represent 55 % of the total volume while the remaining 45 % is attributed to *Q sat*. Nevertheless, the contribution of *Q sat* can represent 62 % and 68 % respectively of the discharge during the two main peak flows. The results of the separation using silica are similar, even if the *Qhill* contribution (64 %) is slightly higher than that obtained with DOC.

DISCUSSION AND CONCLUSIONS

This study combines three approaches to trace the origin of the water contributing to streamflow generation. The hydrological measurements indicate that the downstream zone of the catchment is the most efficient contributing area to streamflow and that the water table reacts very quickly to rainfall. The stable isotopes show that the peak flows, which are composed of a non-negligible proportion of rain, are generated by pre-event water coming from the superficial layers of the saturated area, whereas during the recession phase, the influence of the deeper layers increases. The chemical tracers clearly exhibit that during peak flows the water comes mainly from the upper layers of the saturated area. Considering these different approaches, the scheme proposed for this event could be as follows. Before the event, streamflow is composed of pre-event water draining the deep layers of the superficial formations. During peak flow, a rapid infiltration of an important part of rain via preferential pathways (macropores) could explain the sharp rising of the water table, the variation of the isotopic signature and the decrease of silica content in the superficial layers. This groundwater ridging causes the extent of the saturated area to increase, which could induce superficial runoff due to groundwater exfiltration. Then, in the final stage, most of the water comes from the downstream hydrological zone and the event water proportion reduces, whereas the deep layer contribution becomes highly dominant.

ACKNOWLEDGMENTS

This work has been carried out within the DBT II "Fleuves et Erosion" research programme supported by the INSU/CNRS. The authors are grateful to all participants in the field and in the laboratory for their contribution which allows this study to progress in good conditions. This is EOST contribution N° 2002.407-UMR7517.

REFERENCES

Cappus, P. (1960) Bassin experimental d'Alrance – Etude des lois de l'écoulement- Application au calcul et à la prévision des débits. *La houille blanche*, A, 493-520.

Christophersen, N., Neal, C., Richard, H., Vogt, R.D., Andersen, S. (1990) Modelling streamwater chemistry as a mixture of the soilwater end-members - a step towards second generation acidification models. *J. Hydrol.*, 116, 307-320.

Fritz, M., Cherry, J.A., Weyer, K.V., Sklash, M.G. (1976) Runoff analyses using environmental isotope and major ions. In *Interpretation of Environmental Isotope and Hydrochemical Data in Groundwater Hydrology*, I.A.E.A., Vienna, 111-130.

Gonfiantini, R. (1978) Standards for stable isotope measurements in natural compounds. *Nature*, 271, 534-536.

Hooper, R.P., Shoemaker, C.A. (1986) A comparison of chemical. and isotopic hydrograph separation. *Water Res. Res.*, 22, 10, 1444-1454.

Hooper, R.P., Christophersen, N., Peters, J. (1990) Modelling streamwater chemistry as a mixture of soilwater end-members- application to the Panola mountain catchment, Georgia, USA. *J. Hydrol.* , 116, 321-343.

Idir, S. (1998) Etude géochimique des crues du bassin versant du Strengbach (Vosges): Origine des écoulements et contribution aux flux d'éléments majeurs dissous exportés. *Thèse Doct.* Univ. Louis Pasteur, pp. 266.

Ladouche, B., (1997) Etude des flux hydriques par le traçage isotopique naturel à l'échelle d'un bassin forestier (Strengbach, Vosges). *Thèse Doct.* Univ. P. et M. Curie, pp. 194.

Ladouche, B., Probst, A., Viville, D., Idir, S., Loubet, M., Probst, J.L., Bariac T. (2001) Hydrograph separation of stormflow components using isotopic, chemical and hydrological approaches: application to the Strengbach catchment (Vosges mountains -France). *J. Hydrol.,* 242, 255-274.

McDonnell, J.J., Bonell, M., Stewart, M.K., Pearce, A.J. (1990) Deuterium variations in storm rainfall: implication for stream hydrograph separation. *Water Res. Res*., 26, 3, 455-458.

Pinder, G.F., Jones, J.F. (1969) Determination of the groundwater component of peak discharge from the chemistry of total runoff. *Water Res. Res.*, 5, 2, 438-445.

Probst, A., Dambrine, E., Viville D., Fritz B. (1990) Influence of acid atmospheric inputs on surface water chemistry and mineral fluxes in a declining spruce stand within a small granitic catchment (Vosges massif, France). *J. Hydrol.*, 116, 101-124.

Sklash, M. G., Farvolden, R. N. (1979) The role of groundwater in storm runoff. *J. Hydrol.*, 43, 45-65.

Voronkov, P.P. (1963) Hydrochemical bases for segregating local runoff and a method of separating its discharge hydrograph, *Soviet Hydrology*, 4, 409-414. Translated by L.G. Robbins from *Meteorology and Hydrology*, 8, 21-28.

Wels, C., Cornett, R.J., Lazarete, B.D. (1991) Hydrograph separation: a comparison of geochemical and isotopic tracers. *J. Hydrol.*, 122, 53-274.

ANALYSIS OF RAINFALL-RUNOFF EVENTS IN A MOUNTAIN CATCHMENT

Zdeno Kostka, Ladislav Holko

Institute of Hydrology, Slovak Academy of Sciences
Ondrašovecká 16, 031 05 Liptovský Mikuláš, Slovakia

ABSTRACT

The study presents results of the analysis of rainfall-runoff events in the mountain catchment of Jalovecký creek, Slovakia, in snow-free seasons. Daily to 10-minute data from the summer seasons 1989-2001 were analysed. Catchment response to rainfall was very fast. The spatial distribution of precipitation did not seem to influence the response. The rainfall amount was the most important parameter determining catchment runoff. There is no evidence of a strong relation between runoff and pre-event saturation. The data indicate the existence of a threshold of about 40 mm of rainfall, which is important for the runoff response of the catchment.

Keywords mountain catchment, rainfall-runoff events, catchment saturation state

INTRODUCTION

Fast response of runoff to precipitation events is a typical feature of mountain catchments. This phenomenon is explained by the low retention capacity of high mountain areas (Hladný and Pacl, 1974). The precipitation amount and its spatial distribution primarily influence runoff volume during a flood event. It is expected that characteristics of the flood wave depend also on the state of catchment saturation before the event. This can be characterised by an antecedent precipitation index (e.g., Hladný and Pacl, 1974), by pre-event soil moisture (Silveira et al., 2000) or by the dynamic source area concept (Myrabø, 1986).

This study was devoted to the analysis of rainfall-runoff events in the mountain catchment of Jalovecký creek, Slovakia. The objectives were to

- describe the frequency and magnitude of flood events in snow-free seasons,
- characterise catchment response to rainfall,
- check the role of the spatial distribution of rainfall and the influence of the catchment saturation state on catchment response to rainfall.

CATCHMENT DESCRIPTION

The Jalovecký creek catchment is situated in the Western Tatra Mountains, north Slovakia, near the town of Liptovský Mikuláš. The catchment area is 22.2 km^2, elevations range between 816 and 2178 m a.s.l. The catchment is formed mainly by gneiss and schist (48% of catchment area), and granodiorites (21%). Mesozoic rocks dominated by limestone and dolomite build up 7% of the catchment. Quaternary loose sediments cover 24% of the catchment. The average slope is 30° and most slopes have south-eastern to south-western orientation. The soil types are Cambisols, Podsol, Ranker and Lithosols. Soil depths vary between 55-125 cm on the average (Kostka and Holko, 1997). Forests dominated by spruce cover 44% of catchment area, dwarf pine covers 31% and alpine meadows and bare rocks cover the remaining 25%. The location of the catchment and the observation network are shown in Fig 1. Catchment mean annual precipitation (1989-2001) is 1575 mm, mean annual runoff is 1030 mm and the average annual air temperature at catchment mean elevation (1500 m) is 3.4 °C.

METHODS AND DATA

Simple statistics and regression analysis are the basic methods used in this study. They are used to describe the frequency, duration and magnitude of flood events and to compare precipitation and runoff characteristics. The catchment saturation state was characterised by the antecedent precipitation index, catchment retention capacity index, and soil water content in the root zone and in the upper 1 m layer of soil.

The antecedent precipitation index IPZ was calculated according to Hladný and Pacl (1974):

$$IPZ_{N,k} = \sum_{i}^{N} P_i \cdot k^i$$

where i – day before the event, N – number of days involved, P_i – precipitation on the i-th day before the event, k – evapotranspiration constant ($0<k<1$). The calculation was performed for various values of N, the value of k was set to 0.98 .

The catchment retention capacity index (Mendel, 1971) was calculated as:

$$IL_{30} = \frac{\sum_{i}^{N} \sqrt{P_i} \cdot (N + 1 - i)}{465}$$

where i – day before the event, N – number of days involved, P_i – precipitation on the i-th day before the event. The value of N was set to 30.

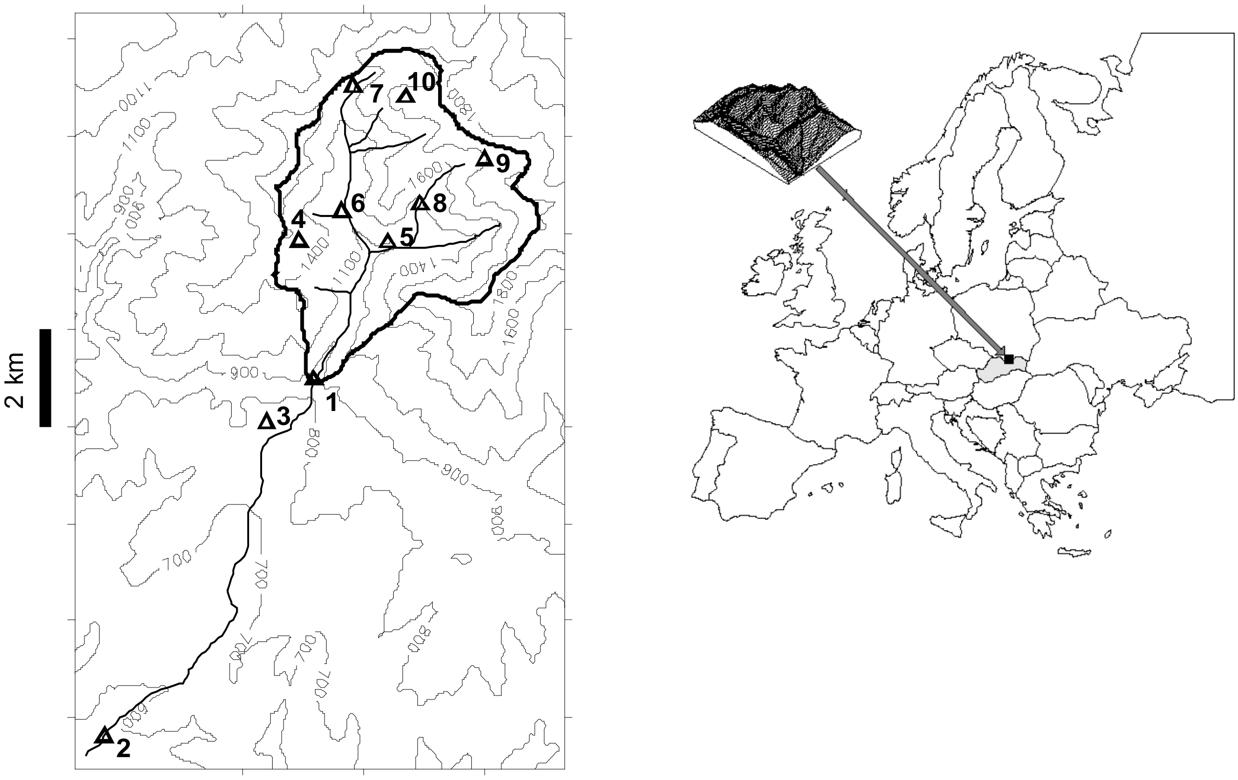

Fig 1: Location of the Jalovecký creek experimental catchment and the measuring sites; site 1 - catchment outlet with discharge measurements and 10-minute rainfall measurements in 2001 and 2002; sites 4, 5, 7 and 10 - hourly (or 10-minute in summer 2001 and 2002) precipitation measurements; site 2 - daily precipitation measurements; sites 3 and 4 - weekly precipitation measurements; sites 3, 4, 6, 7, 8 and 9 - monthly precipitation measurements.

The soil moisture content in the root zone, in the upper 1 m of the soil layer, and evapotranspiration were modelled with the distributed hydrological model WaSiM-ETH (Schulla and Jasper, 1999). The model was calibrated against measured catchment runoff, and point measurements of snow water equivalent and soil moisture.

The analysis of rainfall-runoff data was based on data from 1989-2001. Monthly precipitation was measured by storage gauges at 6 sites. The height of the storage gauge is 3 meters and it is equipped with the Nipher wind shield. Weekly precipitation is measured by standard gauges of the Slovak hydrometeorological service (height 1 m, unshielded) at 2 sites. Hourly or 10-minute precipitation was measured at 1-4 sites by the tipping bucket gauges Sierra Misco (height 30 cm). Hourly or 10-minute runoff was measured at the catchment outlet (Fig 1). The analysis was based on data from summer seasons (June-September) only, in order to exclude the snowmelt events. Basic analyses were done with daily and hourly data. Limited series of 10-minute data were also used. Daily data were measured in the hydrological years 1989-2001 (35 rainfall-runoff events), hourly data were available from hydrological years 1993-2001 (88 events). 10-minute rainfall and runoff data were measured in the summer seasons 2001 and 2002. Catchment rainfall used in the analyses was calculated from uncorrected point measurements by a combination of elevation gradient and inverse distance methods.

Single and complex rainfall-runoff events were distinguished in the analysis. We determined single events as those events which had just one peak followed by longer recession. Complex events had several peaks (Fig 3).

RESULTS AND DISCUSSION

Frequency, magnitude and duration of flood events

Frequent rainfall-runoff events typically occur during the warm period of the year in the Jalovecký creek catchment. Fig 2 gives an idea of the magnitude of precipitation and runoff in the summer seasons 1989-2001. Years 1992, 1994 and 1999 were relatively dry while years 1991, 1996, 1997 and 2001 were relatively wet (Fig 2). Wet years have more runoff events. Seasonal catchment precipitation (total for June-September) varied between 452 mm in 1992 and 1099 mm in 2001. Runoff in the same period varied between 249 mm (1992) and 727 mm (2001). Runoff during the driest and wettest seasons is shown in Fig 3.

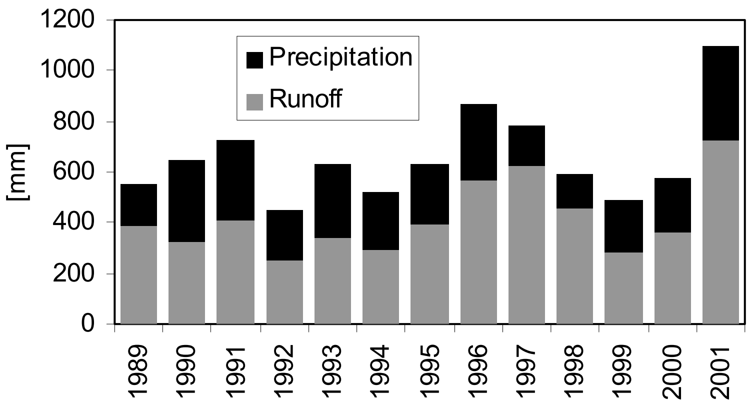

Fig 2: Seasonal catchment precipitation and runoff in years 1989-2001 - totals for June-September.

The number of events in different years varies according to the precipitation amount and the time resolution with which the data are analysed (daily or hourly). Generally, the variability of runoff on the same calendar day in different years was large. Only the period between August 17 and 27 consistently shows rather low runoff. The variability of catchment runoff in that period is the lowest in the season.

Considering a daily time resolution, only up to 3 single events occurred during the season. Often there was no single event in a season. Complex events were more frequent. Typically, two complex events occurred in a season (Table 1). About 2.6-26.5 mm (6.4 mm on the average) of runoff was observed during the day of peak flow. This represents discharges Q_{MAX} of 0.655-3.796 m^3s^{-1} (1.655 m^3s^{-1} on the average). Total precipitation before and during the single flood events varied between 26 mm and 183 mm (average 73 mm) and resulted in runoff of 9 -126 mm (average 48 mm). Total precipitation during complex flood events varied between 100 - 704 mm (average 265 mm). The resulting runoff varied between 53 - 507 mm (173 mm on the average). The mean runoff coefficient of both single and complex events was about 0.66.

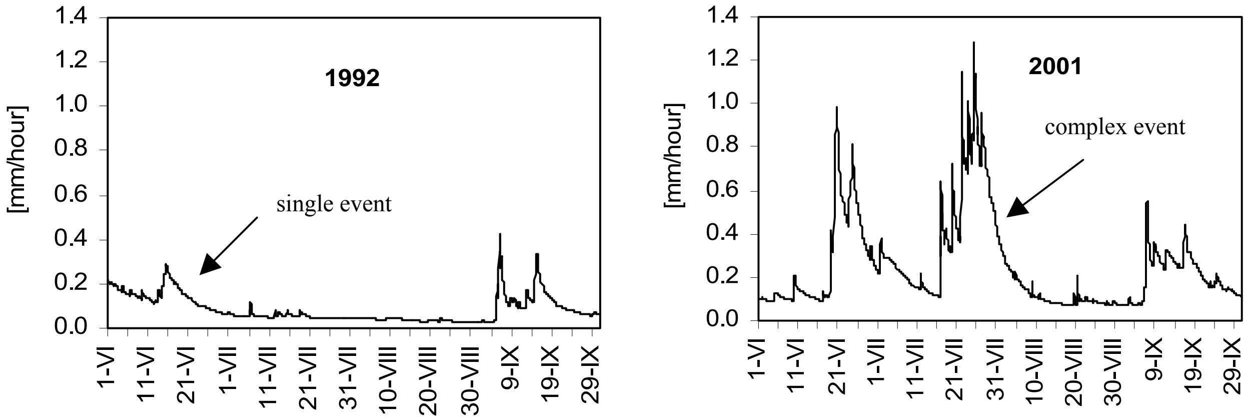

Fig 3: Runoff during the driest and the wettest seasons, examples of single and complex events.

Daily data provided initial information on the frequency and magnitude of runoff events. At the same time, the calculation of catchment rainfall was relatively easy for daily data. Daily data were therefore used in the analysis of relationships between rainfall and runoff volumes. On the other hand, daily data are too coarse to analyse maximum catchment discharge, concentration time or duration of an event. They can even provide contradictory conclusions regarding the discrimination between single or complex flood events (Table 1). Time to peak based on daily data can also be estimated incorrectly in a small mountain catchment. Hourly data are more suitable for such an analysis. Hourly data in the Jalovecký creek catchment revealed substantially more single flood events than the daily data indicated. The typical duration of single flood events was about 2.5 days. Complex events lasted almost 10 days on the average. Corresponding catchment mean hourly runoff was 14.5 and 66.7 mm respectively. Peak hourly runoff varied between 0.04 and 1.38 mm.hour^{-1} (0.244-8.433 m^3 s^{-1}, mean 2.043 m^3 s^{-1}).

Table 1: Basic characteristics of rainfall-runoff events in the Jalovecký creek catchment.

	Daily data (1989-2001)		Hourly data (1994-2001)	
Events	Single	Complex	Single	Complex
Number of events	15	20	61	27
Number of events per year*	0 – 3	0 - 3	8 - 13	2 – 6
Mean duration	12 days	33 days	63 hours	220 hours
P-R delay	0 days	0 days	1 hour	1 hour
Q_o-Q_{max} (time to peak)	3 days	9 days	3 hours	3 hours

*June to September

Response of catchment runoff to rainfall

All data (daily, hourly, 10-minute) showed a fast response of catchment runoff to rainfall. According to hourly data, runoff usually increased within 1 hour after the beginning of precipitation and maximum runoff occurred within 3 hours after the onset of rainfall (Table 1).

Although catchment response to rainfall is very fast, flash floods are not frequent. A flash flood is understood here as a sudden flood of great volume or a flood that crests in a short length of time and is often characterised by high velocity flows (Nevada Division of Water Planning, 2000). Such events occurred in the Jalovecký creek catchment in the summers 1987, 1988, 1994, 1997 and 1998. Catchment discharge rates increased typically 4-10 times within 1-3 hours during flash floods. Extraordinary among the flash floods was the event observed on 7 August 1994. About 36 mm of rainfall occurred in 2 hours. The catchment hourly discharge rose from 0.254 m^3.s^{-1} to 4.05 m^3.s^{-1} within 1 hour, i.e. about 16 times.

Summer months in the Jalovecký creek catchment are usually relatively wet. However, dry periods lasting for several weeks occurred quite often (1990-1992, 1995, 1998-2001). It appears that on a daily time scale there is a threshold of about 40 mm of rain which has to fall after such relatively dry periods before the flood events occur (Fig 4). Approximately the same limit seems also to be important in the case of more complex flood events. This could correspond to the runoff generation mechanism proposed by Tesař et al. (2001), the so called retention-evapotranspiration units RETU. Tesař et al. (2001) demonstrated that the soil profile acts as a reservoir, which is filled up or emptied depending on soil moisture. Water accumulates in the reservoir until a certain threshold is reached. Then, the reservoir is quickly emptied and the process starts again. The existence of a threshold of about 40 mm indicates that a similar mechanism may also influence the response of the Jalovecký creek catchment. However, further research in the catchment will be needed before a generalised conclusion about the threshold can be drawn.

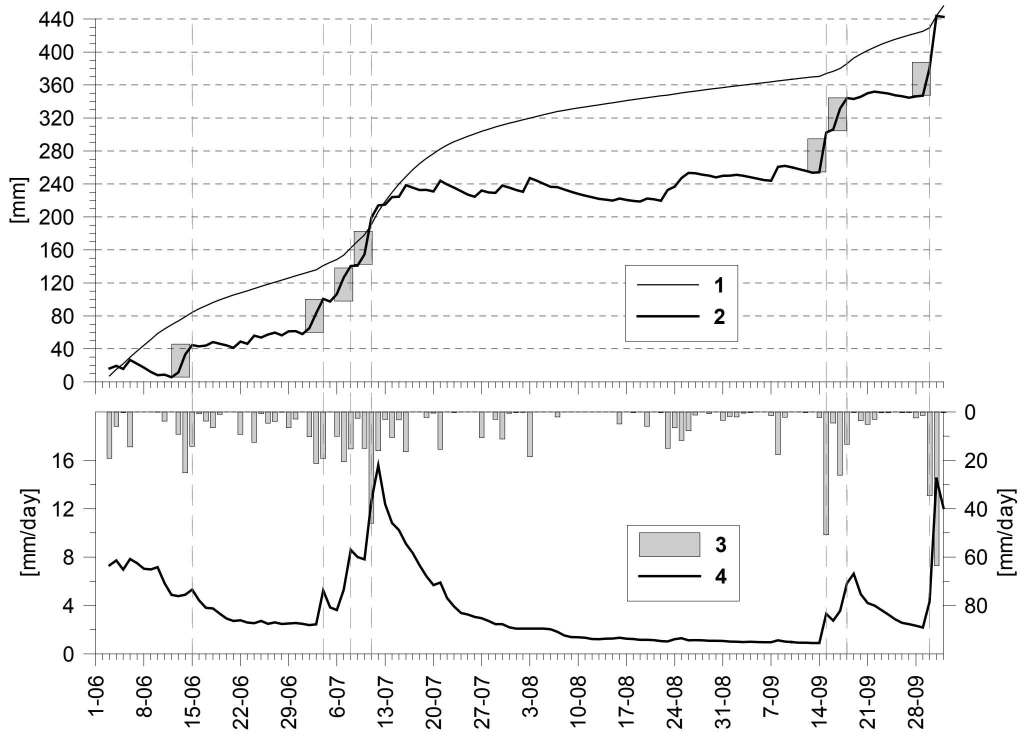

Fig 4: Daily catchment precipitation (3) and runoff (4) in the summer season of 1998 - lower part of the figure; cumulative runoff (1) and "effective" rainfall (2) - upper part of the figure; grey rectangles in the upper part of the figure represent the 40 mm limit of "effective" rainfall; "effective" rainfall is the difference between precipitation and modelled actual evapotranspiration.

Catchment runoff during flood events was best correlated with precipitation amount (Fig 5). Maximum runoff volume during the events was best correlated with maximum precipitation, although this relationship was worse than in the case of total runoff and total rainfall. The correlation of catchment runoff with parameters related to the saturation state of the catchment before the event (IPZ, IL, soil moisture in the root zone, soil moisture at 1 m) was generally very poor. Better correlation was obtained with the catchment retention capacity index (IL_{30}). However, the value of the correlation coefficient R was only 0.31. The correlation between IL_{30} and maximum runoff was only slightly better. Previous results of hydrograph separation and rainfall-runoff modelling (Holko and Lepistő, 1997; Kostka and Holko, 2001) proved that catchment runoff is dominated by subsurface flow. The fact that we did not find a good correlation between runoff during flood events and common indices of catchment saturation state before the event can be interpreted as follows:

1. The major parameter determining the response of a mountain catchment is the amount of precipitation. Saturation of the catchment before the event is not as important.
2. The characteristics of the catchment saturation state used in this study were not suitable.
3. Catchment response is governed by mechanisms other than simple overland flow or continuous subsurface flow.

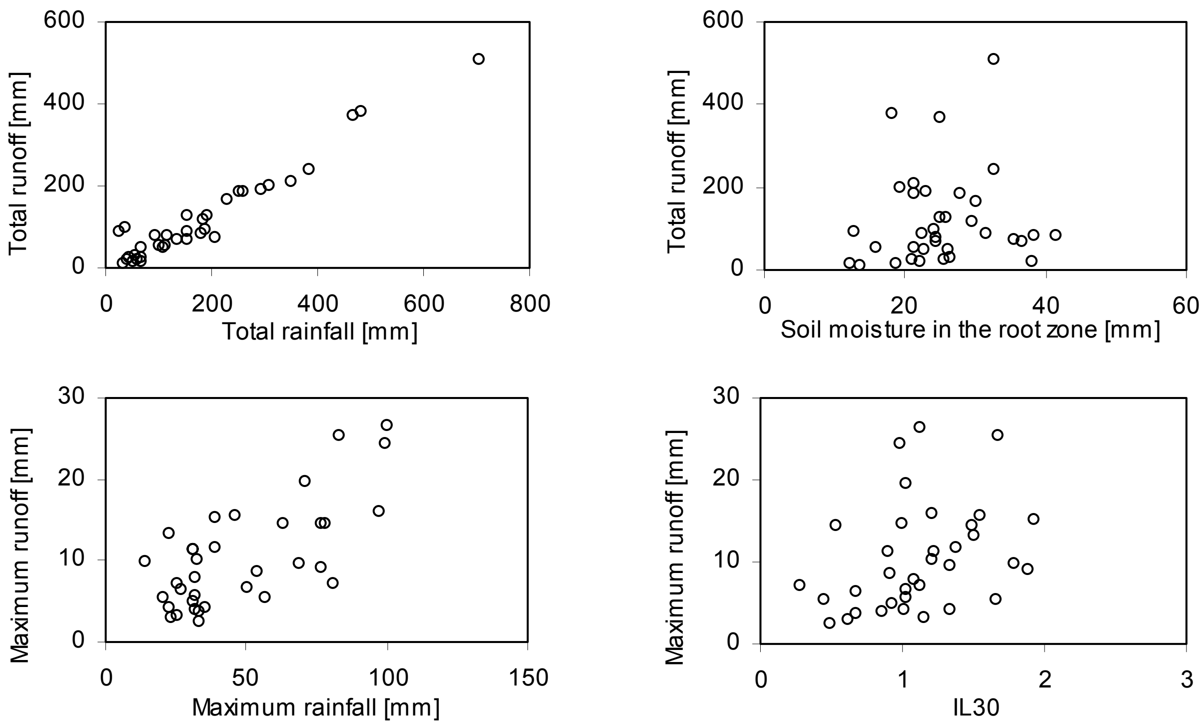

Fig 5: Relation between runoff during flood events and other characteristics; IL_{30} is the catchment retention capacity index.

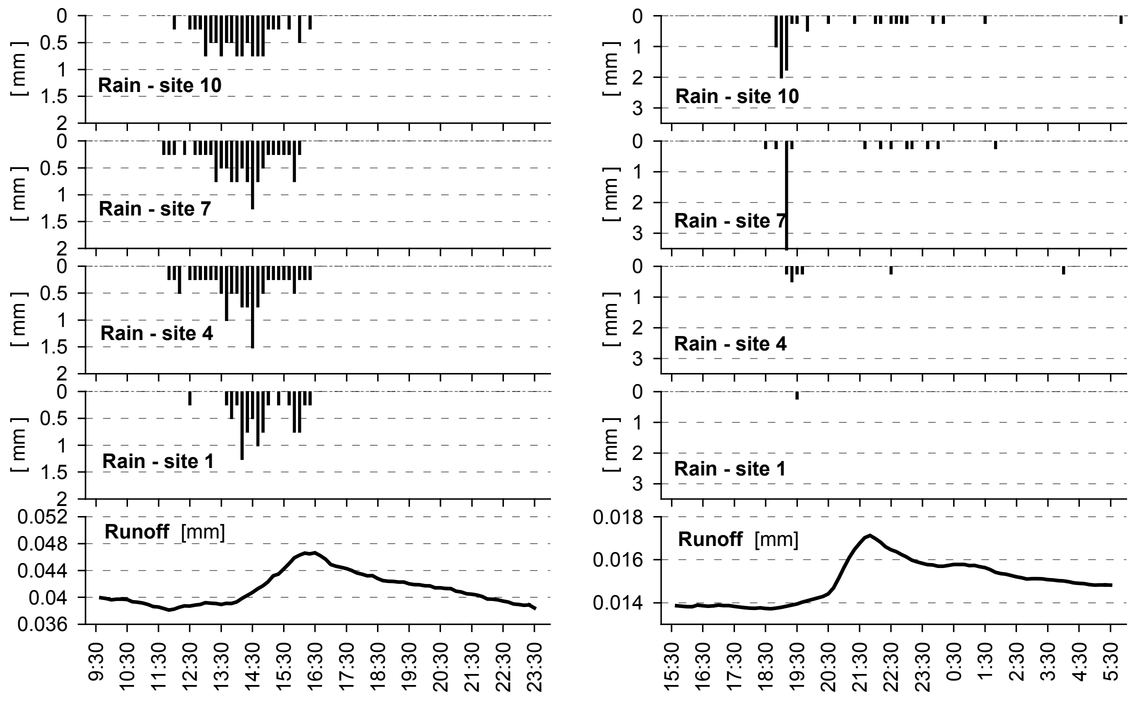

Fig 6: Rainfall-runoff events in summer 2002 - regional rainfall on 18 July (left) and local rainfall on 1 September (right); the data are measured in 10-minute time step, site numbers refer to Fig 1.

Role of spatial distribution of rainfall

The 10-minute rainfall data measured in summers 2001 and 2002 indicate that precipitation patterns at different elevations in the catchment were usually similar. It was interesting to find out that catchment response to regional and local precipitation did not differ (Fig 6). Catchment discharge rose 1 - 2 hours after nearly uniformly distributed rainfall but also after rainfall which occurred only in the most upstream part of the catchment.

Fig 6 also demonstrates the value of rainfall-runoff data in runoff generation research. It can be interpreted as an indication of the role of stream alluvium (riparian zone) in runoff formation. Major alluvium in the catchment occurs in its upper part on relatively small areas. The rest of the catchment has rather steep slopes and practically no alluvium along the channels. Local rainfall presented in Fig 6 fell in the part of the catchment where largest alluvium is found. The time shift between the rainfall and the rising limb of the hydrograph at the catchment outlet roughly corresponds to the travel time of water from the upper part of the catchment to the catchment outlet. It could be hypothesised that the event caused by local rainfall was dominated by the contribution of the riparian zone in the upper part of the catchment.

CONCLUSIONS

The study provided information about the frequency and magnitude of rainfall-runoff events in the mountain catchment of Jalovecký creek during the warm part of the year. The analysis helped to better understand the value of different data and the rainfall-runoff process in the catchment.
The time resolution of the rainfall and runoff data (daily, hourly, 10-minute) determines the information which can be extracted from the data. Daily data allow for a comparison of rainfall and runoff characteristics, because it is relatively easy to calculate catchment precipitation with daily data. The uncertainty of extrapolation of hourly or 10-minute rainfall data is much higher. On the other hand, hourly or 10-minute data are more suitable for a precise analysis of frequency, duration and magnitude of runoff events and the estimation of time shifts between rainfall and runoff events. It should be kept in mind that flood characteristics such as duration and maximum derived from daily and hourly data differ.
The spatial distribution of rainfall does not seem to have a dominant influence on the response of runoff to rainfall at the scale of the catchment (22.2 km^2). Longer data series of higher time resolution may be useful in testing the hypothesis of the dominant contributing role of riparian areas during short floods. The study showed that rainfall amount is the main parameter influencing catchment runoff. The saturation state of the catchment, characterised by antecedent precipitation indices or soil moisture content, was not well correlated with characteristics of flood events (total runoff, flood volume and duration). The existence of a rainfall "threshold" of about 40 mm indicates that concepts such as the retention-evapotranspiration unit (Tesař et al, 2001) may be useful in further runoff generation studies in the catchment.

REFERENCES

Hladný, J., Pacl, J. (1974) Analysis of the precipitation-runoff relationships in mountain watersheds. In Slovak with an English abstract. *J. Hydrol. Hydromech*, 22, 4, 346-356.

Holko, L., Lepistő, A. (1997) Modelling the hydrological behaviour of a mountain catchment using TOPMODEL. *J. Hydrology*, 196, 361-377.

Kostka, Z., Holko, L. (2001) Runoff modelling in a mountain catchment with conspicuous relief using TOPMODEL. *J. Hydrol. Hydromech*, 49, 3-4, 149-171.

Mendel, O. (1971) Influence of surface runoff separation on the accuracy of determination of rainfall-runoff relationships. In Slovak, PhD thesis, Institute of Hydrology and Hydraulics SAS, Bratislava, 155 pp.

Myarbø, S. (1986) Runoff studies in a small catchment. *Nordic Hydrology*, 17, 335-346.

Nevada Division of Water Planning (2000) Water Words Dictionary. A Compilation of Technical Water, Water Quality, Environmental, and Water-Related Terms. (researched and complied by G.A. Horton) http://www.state.nv.us/cnr/ndwp/dict-1/ww-index.htm

Schulla, J., Jasper, K. (1999) Model Description wasim-ETH (Water Balance Simulation Model ETH). Institute of Geography ETH, Zürich, 166 pp.

Silveira, L., Charbonnier, F., Genta, J.L. (2000) The antecedent soil moisture condition of the curve number procedure. *Hydrological Sciences J.*, 45, 1, 3-12.

Tesař, M., Šír, M., Syrovátka, O., Pražák, J., Lichner, L., Kubík, F. (2001) Soil water regime in head water regions-observation, assessment and modelling. *J. Hydrol. Hydromech*, 49, 6, 355-375.

WATER BALANCE COMPONENTS FOR FOREST AND MEADOW LAND USE SYSTEMS IN A CRYSTALLINE CATCHMENT

Christophe André Ruch, Till Harum

Institute of Hydrogeology and Geothermics, Joanneum Research, Elisabethstraße 16/II
A-8010 Graz, Austria, e-mail:christophe.ruch@joanneum.ac.at; till.harum@joanneum.ac.at
Tel.: +43 316 876-148,Fax: +43 316 876 91489

ABSTRACT

Station scale data are compared to determine the local influence of land use and topography on water balance components. Forest influence on the water balance is the most pronounced through interception that is considered totally lost. Including additional spring and catchment data in the analysis demonstrates that data from the forest station are representative for the general hydrological functioning of the headwater catchment Höhenhansl.

Keywords water balance, forest-open area, hydrological functioning

INTRODUCTION

Data collected at the station scale are related to specific local conditions that severely limit upscaling procedures. Water balance components in mountainous areas are strongly influenced by land use, climatic, and topographic conditions that control rainfall distribution in a decisive way. As a result, soil moisture and water balance patterns are very patchy, leading to large spatial variations in evapotranspiration and stream discharge. Nevertheless, station scale measurements provide essential data to evaluate the influence of local factors on water balance components. Moreover, comparison between data measured at different stations and at different spatial scales delivers a good overview of the main processes active in a given hydrological system. In this respect, the goal of this paper is to present the water balance components measured and calculated at the station scale for forest and grassland cover. Data from the Höhenhansl headwater catchment and from its main spring are further used to evaluate the influence of station characteristics on the measured data. The period under investigation (10/95–09/99) is characterised by very variable hydrometeorological conditions that are well documented through the intensive data collection at the Höhenhansl headwater catchment. After a very humid period in 1996 and winter 1997 follows a dry phase in 1998 and 1999. Consequently, differences in soil water tension patterns observed at both stations reflect the impact of local conditions on the water balance components.

DESCRIPTION OF THE TEST SITES AND DATA ACQUISITION

The area under investigation, located in the Pöllau Basin (Eastern Styria, Austria; see Fig 1A), is a well-defined small south-exposed headwater catchment covered with around 70 % forest and 30 % meadow. The catchment area has been a hydrological pilot area since 1991 (Bergmann et al., 1996; Zojer et al., 1996) and was a test site within the EU-project AGREAUALP (Bourjot et al., 1999). The subsurface characteristics consist primarily of crystalline schists with a thick weathered surface layer and five different soil types with sand, sandy loam or loamy sand horizons. The Höhenhansl sub-catchment area (0.392 km², mean altitude 963 m) shows an orographically well-definable enclosed catchment open only to the south, with two main springs and a central drainage to the Hanslbach (see Fig 1B). The total runoff from the catchment area is measured continuously at the gauging station together with water temperature and electrical conductivity. The same variables are measured once a day at the main spring (0.09875 km²). The different types of impacts of land cover on groundwater recharge are being detected at "lysimeter" stations under forest (coniferous trees) and meadow since August 1995. The name of the station corresponds to the local land cover, i.e. station forest and station meadow. The local slope is around 30° and 12° at the station forest and meadow respectively. Each station consists of (1) a profile with TDR-probes for measuring the time dependent water content of the soil at different depths, (2) a profile with tensiometers to get information about the water tension of the soil at the same depths as water content, and (3) a profile for measuring soil temperature. Other variables measured at the stations are rainfall (throughfall for forest), air temperature, air relative humidity (15 minute recordings for all three variables) and overland flow in 1 m² micro catchments. It should be noted that at a 1.30 m depth at the forest station and at a 1.5 m depth at the meadow station suction plates are installed. A sub pressure of 200–250 cm is set up once a week and the collected amount of water is measured every day. As the water is removed from the soil to the collector (bottle), the sub pressure slowly decreases so that the collected water cannot be related to a pressure value or a soil pore diameter. Furthermore, because of the local slope, the water volume collected at the suction plates should correspond to vertical and lateral water flow processes. Therefore, water collected from the suction plates cannot be considered as the "real" groundwater recharge.

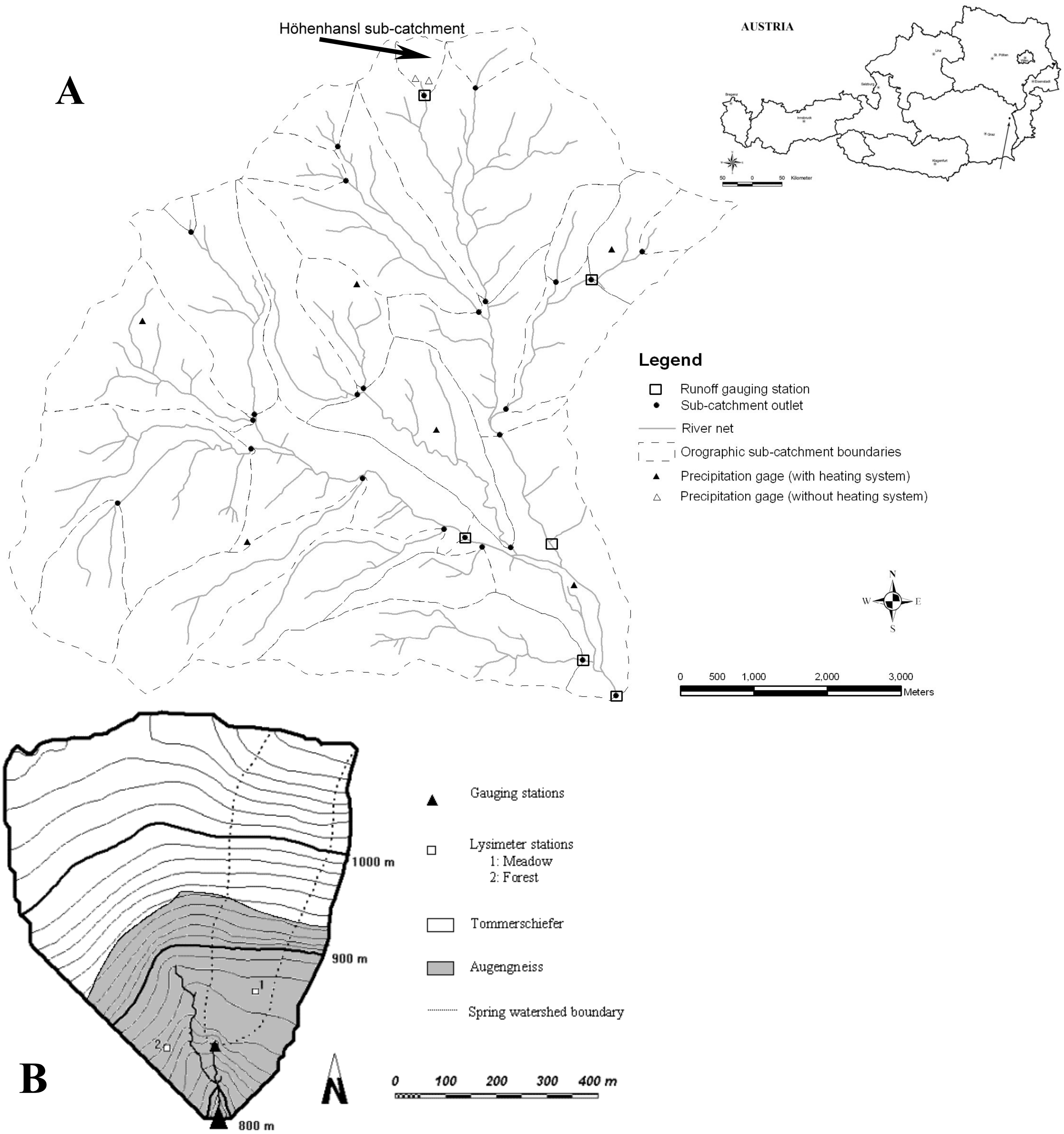

Fig 1: (A) The Pöllau nested research catchments and its hydro-climatic network.
(B) Topo-geological map and measurement network of the headwater catchment Höhenhansl.

THE CATCHMENT WATER BALANCE

The different precipitation amounts measured every year since the gauge was installed are presented in Fig 2. The annual precipitation amount always exceeds 790 mm. The year 1996 was the most humid year since measurements began, and it is also characterised by extreme snow cover. Due to the conjunction of snowmelt and heavy rainfall, April 1996, with a total precipitation of 217 mm, is the most humid month over the whole study period. The mean annual precipitation amount over the nine years is about 930 mm. The average monthly variation of precipitation within the year is presented in Fig 3. A kind of symmetry around the period May to September can be recognised. During these five months, 70 % of the annual precipitation occurs, illustrating on the one hand that convective rainfall is predominant during this time (Bergmann et al., 2000), and on the other hand that less water is available for deep percolation during periods of low evapotranspiration.

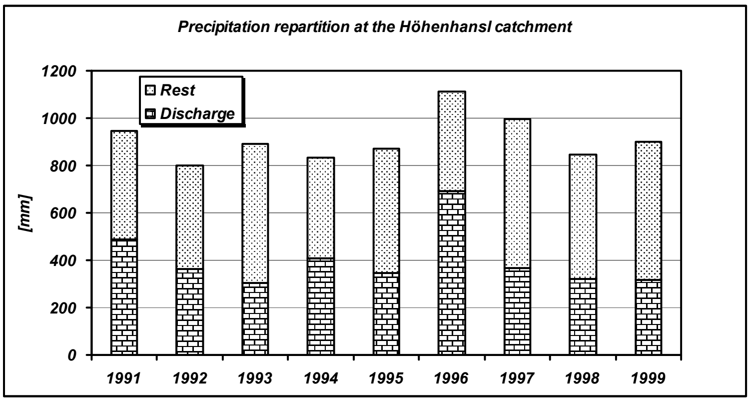

Fig 2: Precipitation and discharge amounts recorded at the Höhenhansl headwater catchment.

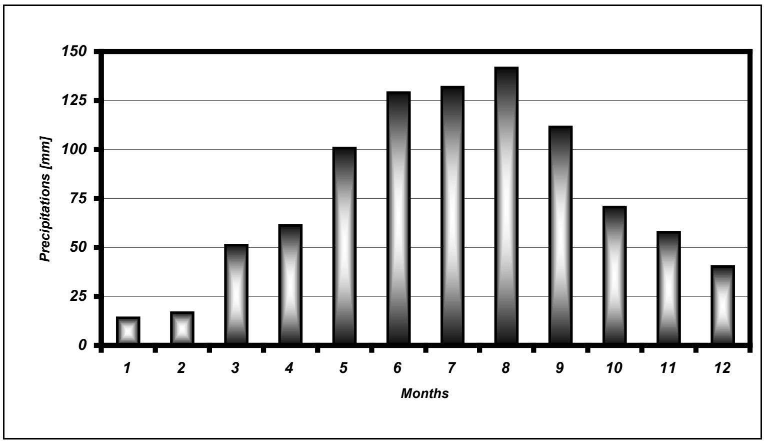

Fig 3: Average monthly precipitation amounts recorded at the Höhenhansl catchment (1991–1999).

The part of precipitation that is discharged is also presented in Fig 2. The mean discharge value over the nine years represents 400 mm or 43 %, which leaves 57 %. The runoff fraction exceeds this average value only for 1991 (52 %), 1994 (49 %) and 1996 (62 %). In contrast to 1996, the years 1997, 1998 and 1999 have a runoff percentage between 35 and 38 %. The year with the lowest precipitation amount (1993) has the smallest runoff fraction of 34 %. The highest mean daily discharge value was calculated to be 60.3 l/s on 25 October 1993 (maximum 63.8 l/s: average calculated over 5 minutes). The next highest value was due to snowmelt in 1996 and was calculated to be 44.8 l/s on 10 April (maximum 48.4 l/s: average calculated over 5 minutes). During this year values over 44 l/s are also found in September and October. In addition, the total discharge of 1996 is the highest, reaching almost 700 mm. The lowest mean daily discharge value calculated since 1991 was 0.92 l/s on 5 March 1998. The winter period in 1998 was in this respect particularly dry: the 22 lowest mean daily discharge values since 1991 (0.92 l/s to 1.03 l/s) are calculated in the period between 11 February and 12 March. This is due on the one hand to the rainless period in January and February (1 mm in February), and on the other hand to the high temperatures during this winter. January and February 1998 recorded the highest average temperatures measured at the station meadow since 1995. In this regard, February 1998 was abnormally warm with a mean temperature of 4.7° C. Only during five days did the daily mean temperature drop below 0° C.

Thus, it can be recognised that the water cycle at the headwater catchment Höhenhansl is dominated by water losses. Even if the average amount of rainfall is rather large (930 mm for the period 1991–1999), only 43 % (400 mm) is released as runoff. This is due (a) to the large forest cover (2/3 of the catchment) that favours interception losses, and (b) to the rainfall repartition centred on the warmest months in the year. The evapotranspiration processes are also reinforced by the catchment southern exposition. However, the ratio discharge/rainfall is quite variable in relation to the winter precipitation and especially to snowfall. In 1996 the ratio is over 60 % and it is lower than 40 % from 1997 to 1999, illustrating that hydro-climatic conditions are very variable for the period under investigation.

WATER BALANCE COMPONENTS AT THE STATION SCALE

Precipitation variability throughout the four hydrological years under investigation (10/95–09/99) and between both stations is rather important. In Fig 4, the cumulated precipitation amount measured at the stations is presented. Clearly, interception processes dramatically influence the rainfall amount measured at the forest station, which is around 75 % of the rainfall at the meadow station: 2980 mm and 3950 mm respectively (it is assumed that stemflow for spruce can be neglected). More then 1030 mm precipitation is recorded at the meadow station for years 95/96 and 96/97, while less than 950 mm is recorded during the last two years. Under forest conditions the precipitation amount per year never exceeds 850 mm. It is remarkable that the interception fraction increases to 30 % in 95/96 (the most humid year) and in 97/98 (the driest year). Forest interception recorded each month is also illustrated in Fig 4. Evidently, this process is the most pronounced during the rainiest period, i.e., the summer months.

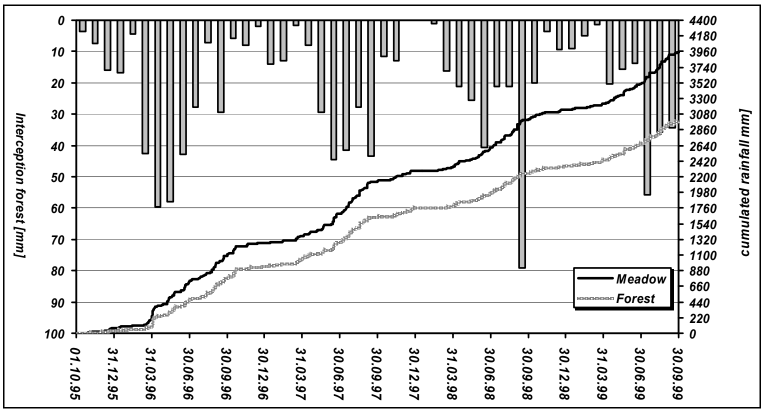

Fig 4: Cumulated precipitation recorded at the forest and meadow stations together with the monthly interception estimated as the difference between both stations (stemflow is neglected).

Surface runoff is measured on 1 m² plots at the Höhenhansl catchment. Surface runoff measured at the meadow station is the highest only in January and April 1996. For the latter, a measurement error due to snowmelt cannot be excluded. At the forest station, surface runoff processes increase considerably during the summer 1997 and 1998 (see Fig 5). The conjunction of high rainfall intensity with extended dryness in the first centimetres of the soil can explain this phenomenon. The forest humus has a high permeability, which varies significantly with the initial moisture content. After long periods of drought, the raw humus of conifer stands is very hydrophobic and constitutes an impermeable layer for the first precipitation events. However, no trace of intense concentrated erosion is visible at the Höhenhansl soil surface.

The effects of high interception losses in the forest and increased overland flow considerably reduce the amount of water that can infiltrate in the forest area. In this study it is assumed that the difference between the rainfall recorded at both stations is lost (interception loss). At this stage, infiltration under forest represents only 65 % of the meadow infiltration over the four years. To estimate local evapotranspiration processes on a daily time step, a simple daily water balance method is used, where (1) potential evapotranspiration (Etp) is calculated using the Haude method (1955), (2) average root depth is defined using field observations for grass and literature data for trees, and (3) the maximum available water-holding capacity of the soil zone reservoir is calculated as the difference between field capacity and wilting point integrated over the root depth. For a complete description see Ruch C. A. (2002). Under trees, the soil-water budget method allows more water to be available for "soil" evapotranspiration calculations. However, results show that evapotranspiration processes are more pronounced for grass. The reasons are twofold: Etp calculated with the Haude method is lower for conifer trees than for grass, and less water is available for "soil" evapotranspiration at the forest station because a reduced amount of water infiltrates to fill up the soil-moisture reservoir. The highest difference in evapotranspiration between both stations is calculated for the year 97/98 where "soil" evapotranspiration at the forest station represents only 54 % of the amount calculated at the meadow station. In 98/99 this percentage is about 75 % and over the entire period, "soil" evapotranspiration under forest represents 65 % of that calculated at the meadow station. All in all, after "soil" evapotranspiration amounts are subtracted from the infiltration amounts, deep percolation represents about 1500 mm and 1000 mm for the whole period at the meadow and forest stations respectively.

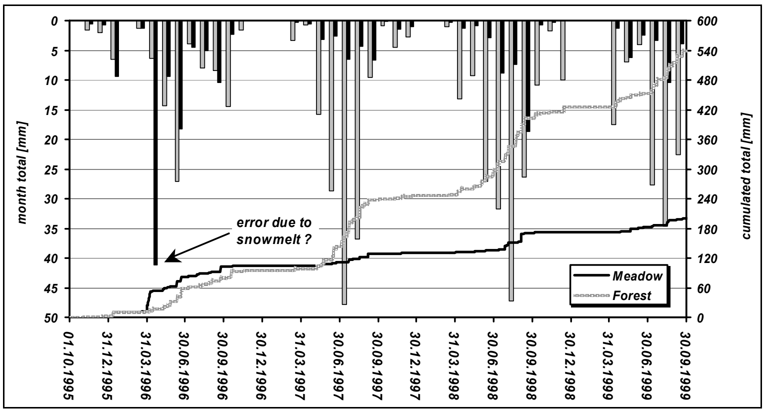

Fig 5: Cumulative surface runoff and monthly totals recorded at the forest and meadow stations.

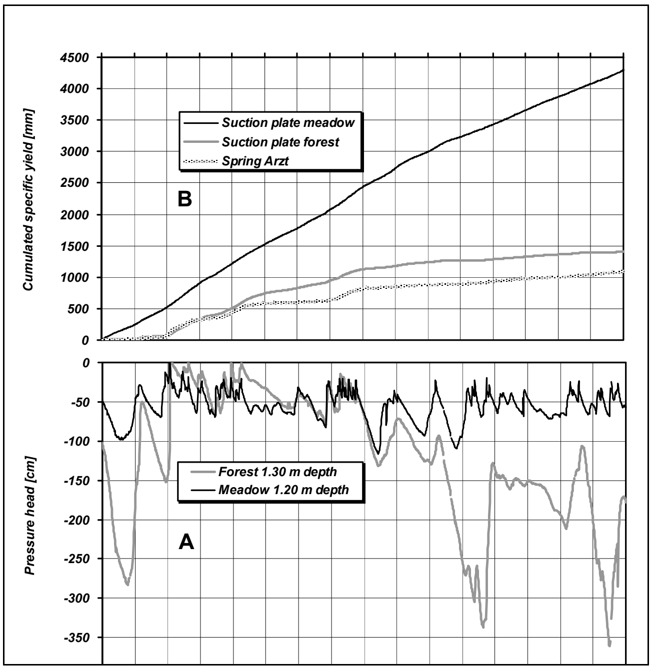

Fig 6: (A) Cumulated percolation water collected at the forest and meadow stations and cumulated spring discharge; (B) Water tension measured at the deepest probe at the forest and meadow stations.

These results can be connected to the pressure head values measured at similar depths at both stations (see Fig 6B). In this figure it is very clear that pressure head values are similar until the winter of 1997. Due to the snowmelt in April 1996 the whole underground can be considered saturated. As already mentioned above, hydrometeorological conditions, high temperatures, and low precipitation in January and February 1998 favour water release processes so that the saturation deficit increases. This phenomenon could be well observed at the forest station: as is shown for example in Fig 6B for summer 1998 and 1999. It is also striking to observe that the cumulated percolation amount collected at this station over the period of four years (about 1400 mm, see Fig 6A) is similar to the cumulated discharge from the spring. It can be recognised that a difference of approximately 400 mm is built up only during the humid phase between October 1996 and June 1997 and remains constant until September 1999. It is assumed that water is removed laterally during the humid period so that also upslope water is collected at the suction plate. This is a good indication that the deep infiltration amount at this station is in good accordance with the spatial deep percolation under forest cover, so that the water balance components measured and calculated at this station can be assumed to be representative for the total forested area from the Höhenhansl watershed. At the meadow station the pressure heads measured at the deepest probe were never lower than -120 cm between 1995 and 1999. The water collected at the suction plate was even higher than the rainfall amount (see Figs 6A and 4). This water tension constancy near saturation is an indication of local conditions that are not in good accordance with the general conditions in this catchment: grassland (only about 30 % of the land cover) and, in particular, a low slope inclination. On the one hand grass water uptake is not as deep as for trees, on the other hand this station is located in a "flat" area compared to the whole catchment. Accordingly, it is assumed that the upslope amount of water inflow is larger than the amount removed downslope. If this hypothesis is correct, the pressure head patterns measured at this station are not representative for the general situation but for small areas like that on the left side of the riverbed.

CONCLUSION

Comparison of the water balance components for forest and meadow evidently demonstrate that the canopy interception (estimated to be totally lost in this work) is the key process in explaining the differences in deep percolation amounts. Although about 25 % of the precipitation is intercepted, overland flow is more pronounced under forest cover. This is due to the local larger slope and to the increasing hydrophobic characteristics of the raw humus layer related to growing dry conditions of 97/98. A huge difference is found for deep percolation volumes: for forest they represent only 2/3 of the meadow volumes (over the four years 1000 mm and 1500 mm respectively). Analyses of spring discharge demonstrate that data from the forest station can be assumed to be representative for the headwater catchment Höhenhansl, whereas the constant humid conditions under grassland are influenced by local factors that are not in good accordance with the general situation for this catchment.

REFERENCES

Bergmann, H., Fank, J., Harum, T., Papesch, W., Rank, D., Richtig, G., Zojer H. (1996) Abflusskomponenten und Speichereigenschaften, Konzeption und Auswertemethoden. *Österr. Wasser- u. Abfallwirtschaft*, 48, Heft 1/2, 27-45.

Bergmann, H., Schatzl, R., Ruch, C. A., Pozarnik, H., Harum T. (2000) Calibration of Weather Radar Data in Different Space and Time Scales. Proc. of *Remote Sens. & Hydro*. 2000, IAHS Publ. no. 267.

Bourjot, L., Boissier, J.M., Dobremez, J.F., Fank, J., Fourneaux, C., Gallet, C., Habsburg-Lothringen, C., Harum T., Marmonier P., Parriaux A., Pelissier F., Schaffter N. & W. Stichler (1999) AGREAUALP - Agri-environmental measures and water quality in mountain catchments. Final report 1995-1998. Unpublished EU-report, 74 p, Chambéry – Graz – Grenoble – Lausanne.

Haude, W. (1955) Zur Bestimmung der Verdunstung auf möglichst einfache Weise. In: *Mitt. d. Deutschen Wetterdienstes*, vol. 11, Bad Kissingen.

Ruch, C. A. (2002) Study of the groundwater flow dynamics in a crystalline headwater catchment and the factors that govern its variability at the sub-catchment scale. Dissertation, K. Franzens Uni., Graz, Austria, pp. 198.

Zojer, H., Fank, J., Harum, T., Papesch, W., Rank D. (1996) Erfahrung mit dem Einsatz von Umwelttracern in der Abflußanalyse. *Österr. Wasser- u. Abfallwirtschaft*, 48, Heft 5/6, 145-156.

THE WATER CIRCULATION IN A PEATLAND ON THE EXAMPLE OF WIELKIE TORFOWISKO BATOROWSKIE IN STOLOWE MOUNTAINS

Dariusz Woronko

University of Warsaw

ABSTRACT

Water circulation is central to the study of wetland hydrology, as the relative significance of the various inputs, outputs and storages underlies the hydrological functions, water quality functions and the management of wetlands for conservation. The key to understanding the functioning of wetlands lies in the water budget, which expresses the movement of water into, out of, and through the wetland, and the storage of water within it. The wetland water balance attempts to take account of all inputs, outputs and storages in the hydrological system, i.e. the terrestrial phase of the water cycle. Unlike a drainage basin, however, the wetland is not delineated by convenient no-flow boundaries, and its water budget must include terms to represent groundwater and surface water inflows as well as outflows. Wielkie Torfowisko Batorowskie is a highmoor peatland situated in the southwestern part of Poland in the Stolowe Mountains, which are mainly built of limestones and sandstones. Basic data to calculate water balance components come from field measurements based on the hydrometeorological monitoring network established in the peatland catchment. The area of Wielkie Torfowisko Batorowskie is under artificial influence that determines the water circulation in this area. The artificial drainage system consists of many ditches crossing the bog and its catchment, and it seems to disturb the natural water circulation, resulting in quite high surface inflow and outflow from the bog, which is more common for fens than for raised bogs. Natural conditions of the water cycle in Wielkie Torfowisko Batorowskie may be achieved after complete land reclamation.

Keywords peat, peatland, water balance

INTRODUCTION

Wetlands and peatbogs connect many elements of the hydrological cycle, especially surface and ground water flow and precipitation. Relationships between water circulation elements mostly depend on physiographic and climatic characteristics of the region. In most cases wetlands increase the storage ability of a catchment.

Solving the water balance, which is one of the most important investigations in a peatbog study, may involve calculations of particular elements of water circulation. When calculating the water balance, all parts of the land water cycle phase must be taken into account including ground and surface encharge and discharge (Dooge, 1975; Gilman, 1994). The estimation of water circulation characteristics is a key to correctly describe qualitative and quantitative processes which occur in a peatland. Many factors, from geology to climate, have their influence on the formation and development of peatlands (Winter, 1988). The relief and lithology force the setting for peatland formation. Then climatic and hydrological conditions influence its development. Characteristics of water encharge and the amount of incoming water cause the peatland to develop into a particular type. The vegetation development is mostly a result of hydrological characteristics of a peatland. Taking water input into account, wetlands may be divided into four groups (Okruszko, 1983):

- ombrogenous (their catchments are rather small and the water input comes from precipitation and sometimes from subsurface flow (e.g. a raised bog);
- topogenous (their catchments cover a large area and are mostly supplied with water from groundwater aquifers);
- soligenous (they are supplied with water coming from springs);
- fluviogenous (the main sources of water input are river floods).

THE SITE OF INVESTIGATION

Wielkie Torfowisko Batorowskie is a peatbog situated in the Stolowe (Table) Mountains (the south-east part of Poland, Fig 1). The mountains are built of horizontally layered sandstones with characteristic floors (Niemczyk, 1999) that form rocky "tables" - hence the name of the mountains. In Poland, these mountains are the only example of mountains made up of sandstone and marl layers of a very differentiated resistance to erosion by wind and water. The peatbog is situated at the border of sandstones and marls at an altitude of about 700 m a.s.l. During field work marl rocks were found underneath the peat cover.

Fig 1: Location of the Stolowe Mountains, Poland.

The type of vegetation shows that Wielkie Torfowisko Batorowskie is a highmoor bog (at least its central part) with characteristic plant species including *Sphagnum* (Potocka, 1999). The beginning of peat formation is dated at about 10 ka BP (Marek, 1998). The peat accumulation probably took place in the sedimentological basin where rushes communities were developed. The deposits contain no remnants of gyttja and such common plants as white waterlily (*Nymphaea alba*) and yellow waterlily (*Nuphar luteum*). The main phenomenon was the boggy process, not shallowing of the water reservoir. Eutrophic communities gradually passed into mesotrophic and oligotrophic communities (Marek, 1998) as evidenced in the peat profile which has a thickness in the central part of about 5 m:

0.0 – 3.2 m – highmoor peat (mostly consisting of *Sphagnum medium*),
3.2 – 3.5 m – topogenous peat,
3.5 – 5.0 m – fen peat.

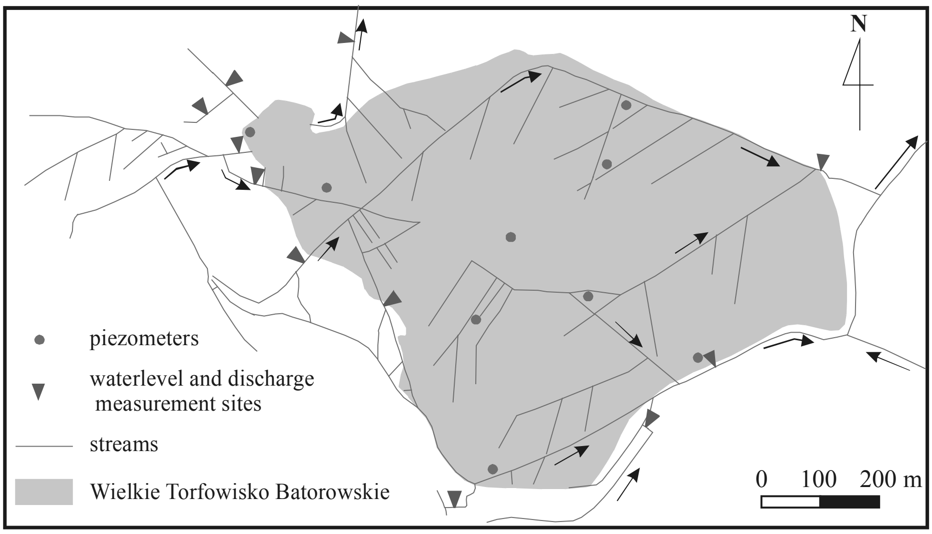

Fig 2: Hydrological monitoring network on Wielkie Torfowisko Batorowskie.

The current functionality of the peatland is dependent on an artificial drainage system (Fig 2) with a total length of about 5000 m. Human activity is also seen in the vegetation cover (Potocka, 1999). A hundred years ago the area of Stolowe Mountains was intensively afforested (Stark, 1936) mostly by Norway spruce (*Picea abies*). This tree species is now dominant in the peatbog flora (Potocka, 1999). The plant coverage in the area of the peatland varies from 0.5 to 0.9 which influences the interception process.

Wielkie Torfowisko Batorowskie is situated on a slight slope which is inclined to the North. Its highest point lies at 715 m a.s.l and the lowest point at 707 m a.s.l. (Fig 3), somewhat similar to blanket bogs for instance in Ireland. The peatbog is not encharged by any groundwater aquifer described in the Stolowe Mountains area (Pacia, 1999). The first groundwater aquifer was located at 690 m a.s.l., which is a few meters below the peatbog bottom.

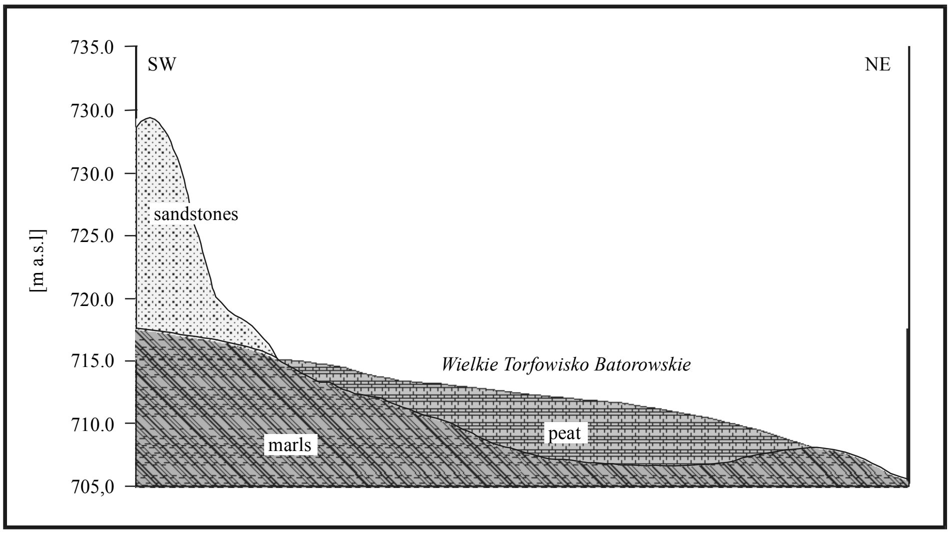

Fig 3: Geomorphological and geological schematic of Wielkie Torfowisko Batorowskie.

WATER BALANCE MEASUREMENTS OF WIELKIE TORFOWISKO BATOROWSKIE

The investigation of the hydrological cycle was conducted for the period from 1 November 1998 to 31 October 1999 using daily observations. This period was chosen because the end of October is in most catchments the time of the biggest groundwater deficit and all water balance calculations and observations in Poland are mostly made from November to October. The measured parameters were: precipitation, discharge, encharge, groundwater level, and meteorological parameters needed to calculate evapotranspiration. The calculation of the water balance was based on these observations using the following formula modified from Bavina (1975), Dooge (1975) and Lensen (1991):

$$P + Q_{in} + G_{in} = I + E + Q_{out}\, G_{out} + \Delta s,$$

where: P – precipitation, Q_{in} – surface inflow to the bog, G_{in} – groundwater inflow to the bog, I – interception, E – evapotranspiration, Q_{out} – surface outflow from the bog, G_{out} – groundwater outflow from the bog and Δs – changes of water storage in the bog.

Precipitation and other meteorological parameters were measured at a meteorological station situated 3000 m to the North-West of the peatland at the same altitude and in similar relief conditions. The current meter discharge measurements, along with daily surface water level observations, allowed the establishment of a rating curve, which was the basis for inflow and outflow calculations. Detailed investigations of vegetation cover (Potocka, 1999) allowed for the calculation of interception and evapotranspiration. Additionally all the meteorological parameters needed for these calculations were measured at the meteorological station. Interception of precipitation was established using the general formula for canopy interception (Von Hoyningen-Hüne, 1983; Braden, 1985):

$$P_i = aLAI\left(1 - \frac{1}{1 + \frac{bP_{gross}}{aLAI}}\right),$$

where: P_i – intercepted precipitation, a – empirical coefficient, b – soil cover fraction, P_{gross} – gross precipitation and LAI – leaf area index. Evapotranspiration calculations were based on the Penman-Monteith formula with respect to the soil and vegetation cover characteristics and measured meteorological parameters. Groundwater level measurements allowed for the calculation of changes in the water storage. During the whole hydrological year the groundwater table was no deeper than 30 cm below the surface Groundwater (subsurface) inflow and outflow was assumed as the difference in the equation.

RESULTS

The hydrological year 1999 (1.11.1998-31.11.1999) in the region of the Stolowe Mountains may be described in terms of precipitation as an average year in the decade of 1990-1999. Measured precipitation during the investigated period (757 mm) is almost the same as the average annual precipitation for 1990-1999 (745 mm). Precipitation was measured using Hellmann's raingauge, and correction of the precipitation was performed. This caused an increase in precipitation by 12 % (Table 1).

Every parameter (except groundwater inflow) of the water balance was calculated separately. The difference in the equation is very small (about 1 %) and proves that the groundwater inflow to the peatland has a small influence on the water circulation.

Table 1: Water balance parameters of Wielkie Torfowisko Batorowskie.

Parameter of the water balance	Q_{in}	P	Δs	I	E	Q_{out}	G_{in}
[mm]	378.1	857.5	-6.7	85.1	433.0	735.3	11.1
[1000 m^3]	110.4	254.3	2.0	25.5	129.9	220.6	9.3

The main parameter in the water balance inputs (Fig 4a) is precipitation (69 %). The large contribution of surface inflow (30 %) is caused by artificial influence where hand-made ditches accumulate water in the channels and transport it to the bog from the upper parts of the catchment, thereby decreasing the subsurface flow to the bog. The water storage changes should be included into the water balance, however the changes are so small that they seem not to be important in the water cycle.

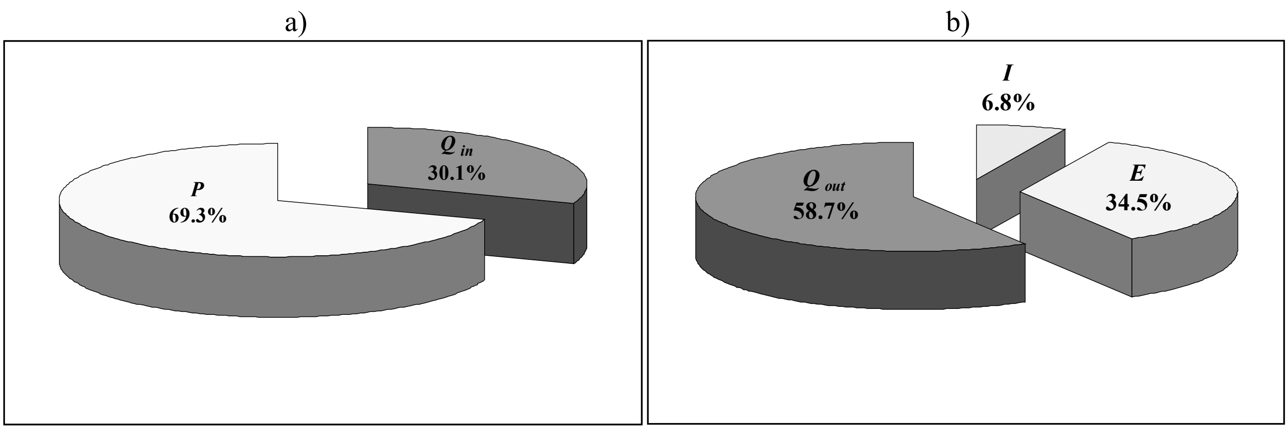

Fig 4: Main parameters of the Wielkie Torfowisko Batorowskie water balance; a – input, b – output.

The output part of the water balance (Fig 4b) is characterised by a large contribution of the surface outflow (59 %). This is a result of the artificial drainage system in the peatbog (Fig 2). The second important contributor is evapotranspiration (34 %). Interestingly, the evapotranspiration contribution is much smaller than the amount estimated on the Irish raised bogs which can be up to 80 % of the water balance output (Lensen, 1991). The interception of precipitation by plant cover (7 % of the output) amounts to about 10 % of the total annual precipitation, which is much smaller than the maximum interception capacity of Sudety spruce forests (Wozniak, 1977). This is the result of the bad condition of the spruce forest on the peatland (Potocka, 1999).

CONCLUSIONS

Wielkie Torfowisko Batorowskie is not a typical highmoor bog. Despite having dominating plant species characteristic for raised bogs, this bog does not lay on the catchment border. The vegetation community is the result of water supply by very poor water coming from precipitation and shallow groundwater flow accumulating in the ditches. This water is characterised by low values of pH and mineralisation. The hydrogeological situation causes an isolated groundwater level to occur in the peatland, without any hydraulic connections with deeper aquifers of the Stolowe Mountains. Apart from precipitation, surface inflow plays an important role in the bog water supply, which is a result of a very dense artificial drainage system. This is why the outflow from the bog is the most important parameter of the water balance output. Relatively small evapotranspiration may be connected with the influence of altitude. In the Stolowe Mountains, with increasing altitude the moisture deficit decreases and relative humidity increases (Kicinska et al., 1999) reducing the ability of the atmosphere to receive water from the soil and plant cover. The results of the water balance differ from those obtained on the raised bogs of the Atlantic type in Ireland (Table 2). Nevertheless, the results are similar to the results of investigations on forested peatlands in the highlands of European parts of Russia (Bavina, 1975). These results indicate a similar scheme of hydrological processes as seen on Wielkie Torfowisko Batorowskie. The significant difference is only in the outflow, which may be explained by the artificial drainage system on Wielkie Torfowisko Batorowskie.

Table 2: Comparison of water balance components in different peatlands.

Parameters of the water balance [mm]	Forested moss peatland (Russia) Annual average from 1955-1966	Wielkie Torfowisko Batorowskie Hydrological year 1999	Raised bog (Ireland) Hydrological year 1990
Precipitation	828	857.5	850
Evapotranspiration	456	433	550
Storage changes	-4	-6.7	0
Surface outflow	376	735.3	270

One of the first Polish scientists who began hydrological investigations on wetlands was Ostromecki, who studied peatlands on Polesie (1938). The water balance was calculated for the Czemerne wetland in the years 1933-1937, resulting in the following average annual values: precipitation 551.2 mm, surface outflow 133.0 mm, evapotranspiration 421.9 mm, and storage changes –2.9 mm. The main phase of the water cycle is the vertical part of the water balance and the value of evapotranspiration may be compared to that of Wielkie Torfowisko Batorowskie. After World War II, the Institute of Meteorology and Water Management established a wetland station in Grodek (the North-East part of Poland) where investigations were conducted on the upper boggy Suprasl catchment (Bortkiewicz, 1959). The measurements were made in the period 1958-1963. The results of hydrological observations described by Mikulski and Lesniak (1975) indicate the big influence of the artificial drainage system, which caused the lowering of the groundwater level in the peatland. The same situation occurs in Wielkie Torfowisko Batorowskie, where a dense ditch network influences the functionality of the peatland resulting in decreasing active peat formation area. The role of Wielkie Torfowisko Batorowskie should rather be considered on a local scale, mostly because of its small dimensions. Nevertheless it is a very important element in the mentioned local scale. The conditions for peat accumulation and wetland formation in the Stolowe

Mountains are rather poor (Woronko, 1988). An object of surface water storage may equalise the hydrological processes, but only after land reclamation focussed on the problem of the ditch network.

REFERENCES

Bavina, L. G. (1975) Water balance of swamps in the forest zone of the European part of the USSR. *Hydrology of marsh-ridden areas*. Proceedings of Minsk Symposium, June 1972. UNESCO Press. Paris.

Bortkiewicz, A. (1959) Stacja bagienna PIHM w Grodku. *Biuletyn Panstwowego Instytutu Hydrologiczno-Meteorologicznego, dodatek do Gospodarki Wodnej*. Rok II, nr 4, 16, Warszawa.

Braden, H. (1985) Ein Energiehaushalts- und Verdunstungsmodell for Wasser und Stoffhaushaltsuntersuchungen landwirtschaftlich genutzer Einzugsgebiete. *Mittelungen Deutsche Bodenkundliche Geselschaft*, 42.

Dooge, J. (1975) The water balance of bogs and fens. *Hydrology of marsh-ridden areas*. Proceedings of Minsk Symposium, June 1972. UNESCO Press. Paris.

Gilman, K. (1993) Hydrology and wetland conservation. John Wiley. Chichester.

Kicinska, B., Zmudzka, E., Olszewski, K. (1999) Ogolne cechy klimatu PNGS. Gory Stolowe (ed. M. Zgorzelski). Wydawnictwo Akademickie Dialog. Warszawa.

Lensen, H. A. (1991) Hydrology of Clara and Raheenmore bogs. Irish-Dutch peatland study, geohydrology and ecology. Wageningen.

Marek, S. (1998) Rozwoj Wielkiego Torfowiska Batorowskiego w swietle badan biostratygraficznych. Szczeliniec, Wydawnictwo Parku Narodowego Gor Stolowych, nr 2. Kudowa Zdroj.

Mikulski, Z., Lesniak, E. (1975) Hydrological research on a peat-bog in the upper Suprasl basin. *Hydrology of marsh-ridden areas*. Proceedings of Minsk Symposium, June 1972. UNESCO Press. Paris.

Niemczyk, V. (1999) Współczesny stan wiedzy geologicznej na temat Gor Stolowych (Sudety Srodkowe). Szczeliniec, Wydawnictwo Parku Narodowego Gor Stolowych, nr 3. Kudowa Zdroj.

Okruszko, H. (1983) Zroznicowanie warunkow hydrologicznych mokradel w aspekcie ich melioracji. *Wiad. IMUZ*, 15, 1.

Ostromecki, J. (1938) Bilans wodny i stosunki odplywu zlewni bagna Czemerne. *Gospodarka Wodna*, IV, 6, Warszawa.

Pacia, G. (1999) Wody podziemne PNGS. Gory Stolowe (ed. M. Zgorzelski). Wydawnictwo Akademickie Dialog. Warszawa.

Potocka, J. (1999) Wspolczesna szata roslinna Wielkiego Torfowiska Batorowskiego. Szczeliniec, Wydawnictwo Parku Narodowego Gor Stolowych, nr 3. Kudowa Zdroj.

Stark, L. (1936) Zur Geschichte der Moore und Wälder Schlesiens in postglazialer Zeit. *Botanische Jahrbücher* LXVII Bd.

Von Hoyningen-Hüne, J. (1983) Die Interception des Niederschlags in landwirtschaftlichen Beständen. *Schriftenreihe des DVWK*, 57.

Winter, T. C. (1988) A conceptual framework for assessing cumulative impacts on the hydrology of nontidal wetlands. *Environ. Man*. 12, 5.

Woronko, D. (1998) Warunki wystepowania i funkcjonowania obszarow podmoklych w Parku Narodowym Gor Stolowych. Szczeliniec, Wydawnictwo Parku Narodowego Gor Stolowych, nr 2. Kudowa Zdroj.

Wozniak, Z. (1977) Wstepne wyniki pomiarów intercepcji w sudeckich drzewostanach swierkowych. *Przegl. Geofiz*., XXII (XXX), 3-4.

DEFINING FLOW CONTRIBUTION SUBAREAS USING WATER CHEMISTRY DATA (ALTUBE RIVER CATCHMENT, BASQUE COUNTRY)

Ane Zabaleta, Virginia Martínez, Iñaki Antigüedad

Group of Hydrogeology, University of the Basque Country, 48940 Leioa, Bizkaia, Basque Country, Spain

ABSTRACT

For the first time in the Basque Country a hydrological study based on river water chemistry has been initiated. The catchment selected for that purpose is the Altube River catchment (116 km^2), due to the spatial variability of various factors (lithology, slopes, vegetation, soils, etc.). That variability causes waters coming from each part of the catchment to be chemically very different, so it is possible to identify where waters are coming from in time by using mass balance. During low flow periods, 24% of the catchment accounts for 60% of the total discharge, whereas during high flow periods, 41% of the basin accounts for 65% of the total discharge. Temporal variability of water chemistry and differences between subareas have also been analysed. Preliminary results are presented here.

Keywords river water chemistry, flow contribution, Altube river catchment, Basque Country

INTRODUCTION

Many connections exist among the physical, chemical and biological processes that shape the chemical composition of water flowing from forested catchments (Christophersen and Neal, 1990; Church, 1997). Studying the chemical composition of running water helps to unravel the pathways that water follows through the catchment, in order to understand how a catchment functions and to predict its hydrochemical response to large-scale stresses. From this point of view the analysis of some specific events, such as the transition from low to high water periods, is particularly useful in studying the hydrological behaviour of catchments. To study the evolution of water chemistry, a field investigation recently started (April 2000) in the Altube headwater catchment. It is the first study of catchment hydrology based on physical controls of stream water chemistry in the Basque Country. The goal is to explain stream water chemistry evolution according to its spatial origin. The preliminary results of systematic monitoring carried out in different subareas of the catchment are presented here.

THE ALTUBE CATCHMENT

The research area is a 116 km^2 forested catchment (Fig 1) situated between the territories of Bizkaia and Araba, in the western part of the Basque Country. Elevation ranges from 200 to 1200 m a.s.l., with a mountainous topography in the Northeast and a smoother one in the Southwest. The average annual precipitation values range from 900 mm in the South to 1400 mm in the North. Precipitation can even reach 1700 mm in the Northeast region. Streamflow is continuous throughout the year. This area has not been substantially impacted by anthropogenic activities, although pine tree forests have been planted, mostly in the North of the catchment. Nevertheless, at the borders of the basin and in the South early vegetation, such as oaks, beech trees, heath and fern can be found.

The bedrock material consists mostly of Supraurgonian (Cenomanian) terrigenous and Upper Cretaceous carbonate rocks disposed in a monoclinal structure that dips to the Southwest. In the Northeast area Supraurgonian sandstones, microconglomerates and lutites appear. Towards the Southwest Upper Cretaceous carbonate platform materials are found, with alternations of limestones, marls, marly-limestones and shales; above these, limestones are predominant only in the Southwest corner of the catchment. The contact between terrigenous materials and carbonated rocks is of transitional character. In the Southeast, breaking the monoclinal structure, appears the Murgia diapir built of Triassic clays and gypsum. To the Northeast some Quaternary coluvial deposits are found. None of these series form aquifers of regional interest.

Discharge data from the catchment are only known for one site (point 17 in Fig 1), where water level data are registered every ten minutes (web.bizkaia.net/Ingurugiro/ Hidrologia/ingles/index.htm). It is very difficult to measure discharge directly in any other place of the basin owing to the irregular sections of the channels, the large width of the streams and the turbulent regimes present during high water periods all over the catchment. Point 17 has been chosen as the outlet of the catchment. The annual discharge at this point ranges from 43 to 120 (10^6) m^3 (1996-2001), which means that the specific discharge ranges between 11.7 and 32.8 l/(s·km^2). Subcatchments considered in this paper are shown in Fig 1.

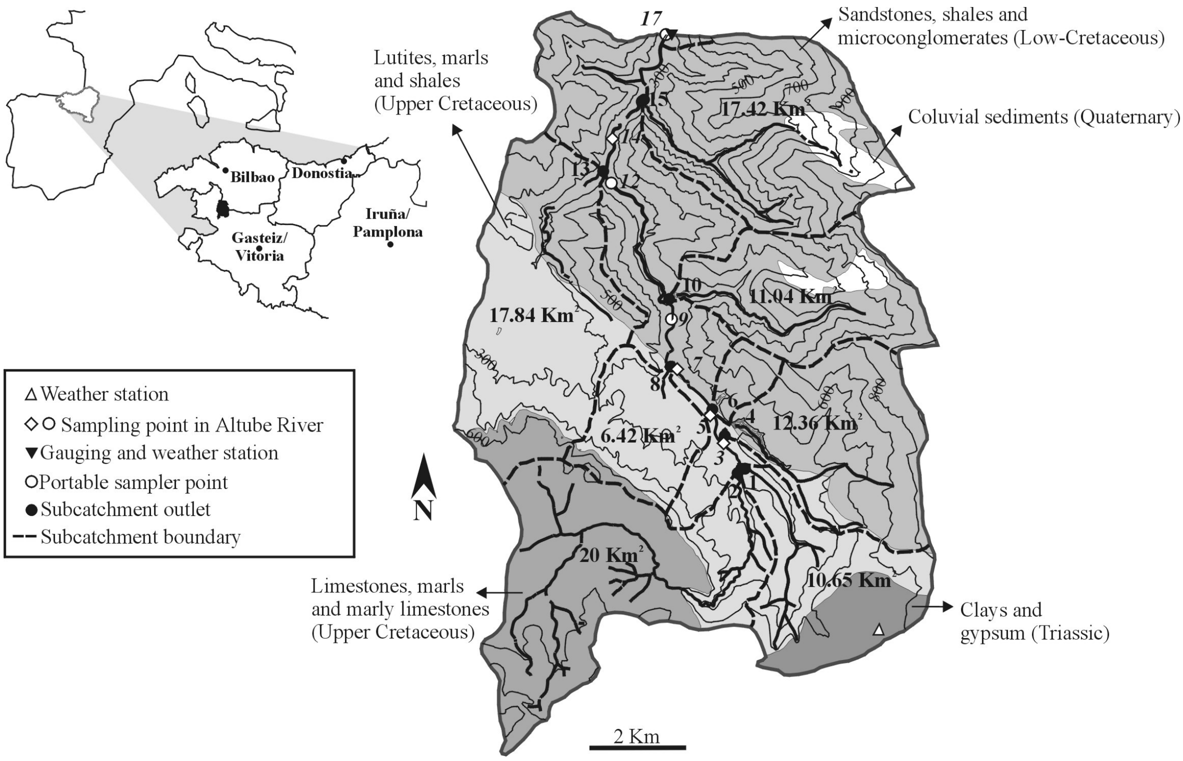

Fig 1: Altube River catchment (Basque Country) and measurement network points.

THE FIELD WORK

A systematic monitoring of the catchment water chemistry at several sites in the drainage network and in different hydrological situationshas been carried out. In all the cases electrical conductivity and temperature were measured in the field, and in some cases (Figs 6 and 7) the major anionic and cationic components were determined in the laboratory. During the transition from the low to the high water period (Fig 2, A-A´) corresponding to the end of the hydrological year 2000-2001 and the beginning of the year 2001-2002, portable water samplers were installed at three sections along the Altube River (points 9, 12 and 17; Fig 1), with a 4-8 hour sampling interval.

Fig 3 shows the electrical conductivity and sulfate concentration evolution during the A-A´ period at points 9, 12 and 17 and the hydrograph at the gauging station (point 17). Sulfate is one of the most important components in the Altube River waters (Table 1) and it is very strongly related to the electrical conductivity owing to the presence of the Murgia diapir in the Southeast of the catchment (Fig 1).

Manual samples were taken simultaneously at all subcatchment outlets (Figs 1 and 2) several times from April 2001 onwards, with discharge at the gauging station (Q_{gs}) at the time of sampling ranging from 25 l/s to 18000 l/s. Water chemistry at any point of the Altube River is then analysed as a chemical mixture of the water upstream and the water of the tributaries flowing into the river just above the sampling point. Electrical conductivity and sulfate have been used as key tracers for the balance. Such an approach allows us to quantify, in percent terms, waters coming to the gauging station (point 17) from each subcatchment in different hydrological situations (Fig 4). As other authors have already observed

(Caissie et. al, 1996), fairly accurate hydrograph separation can be achieved by measuring conductivity alone. So if the results from the two key tracers are similar, we consider here the conductivity-based balance.

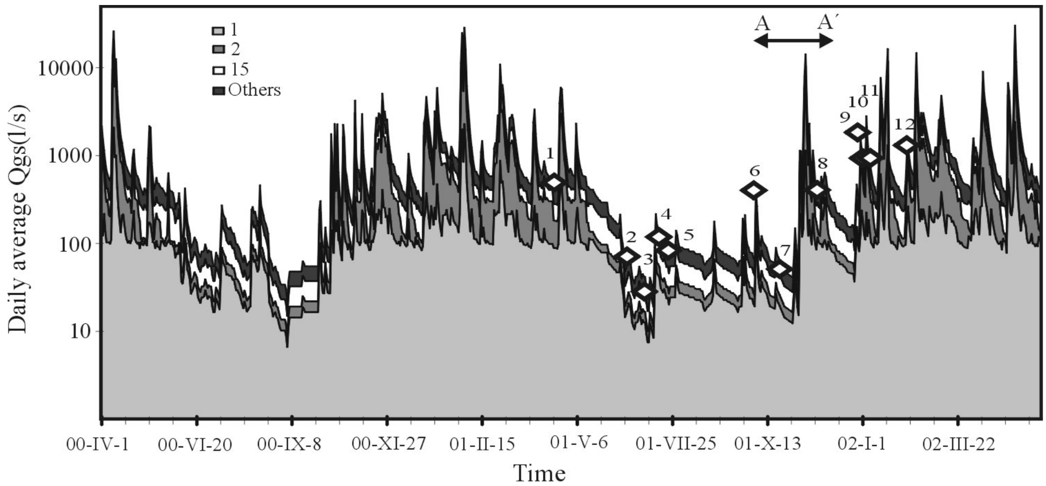

Fig 2: Average daily discharge of the Altube River at point 17 (2000/IV/1-2002/V/31). The hydrograph has been broadly decomposed using water chemistry data from the different subcatchments (1, 2, 15 and others). Diamonds refer to manual sampling times. Continuous sampling was carried out in the A-A´ period.

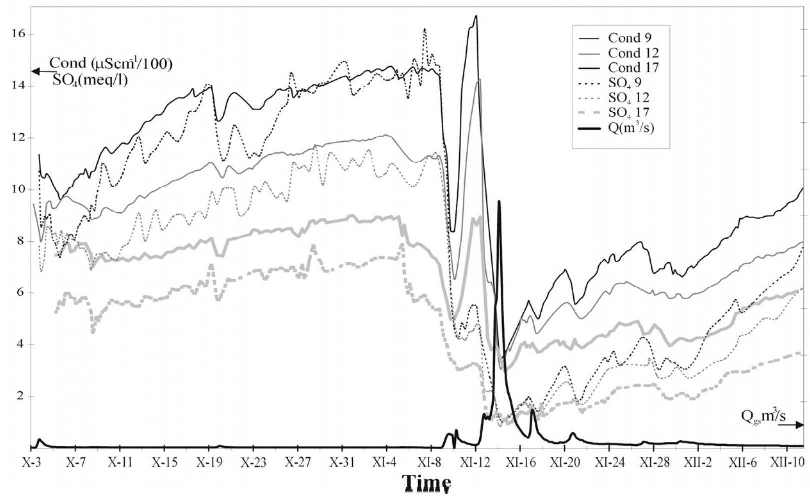

Fig 3: Electrical conductivity ($\mu Scm^{-1}/100$) and sulfate (meq/l) evolution in points 9, 12 and 17, and hydrograph at point 17 over the period A-A´ (Fig 2).

DATA DISCUSSION

Fig 4 shows the contribution to discharge of each subcatchment as a function of the total discharge at the catchment outlet (gauging station) based on the conductivity balance approach. This distribution is shown for every sampling moment (except for the moment when Q_{gs} = 18000 l/s where it remains in general similar to the high flow period). Extraneous discharge contributions were observed for samples taken at the rising limb of the hydrograph (i.e. number 6 and 8). This phenomenon was also observed by Caissie et al. (1996) and Walling et al. (1975), who explained it, for the catchments they studied, as the result of a flushing out of older groundwater into the stream. The figure reflects that during low waters (Q_{gs} less than 400 l/s), subcatchments 1 and 15 (28 km^2) account for about 60% of the total discharge. During high waters (Q_{gs} >700 l/s), these subcatchments account for only 30% of the total discharge, while subcatchment 2 is the one with the highest contribution of about 35%. Therefore, during high waters, a 65% contribution is coming from a 48 km^2 surface out of a total catchment area of 116 km^2.

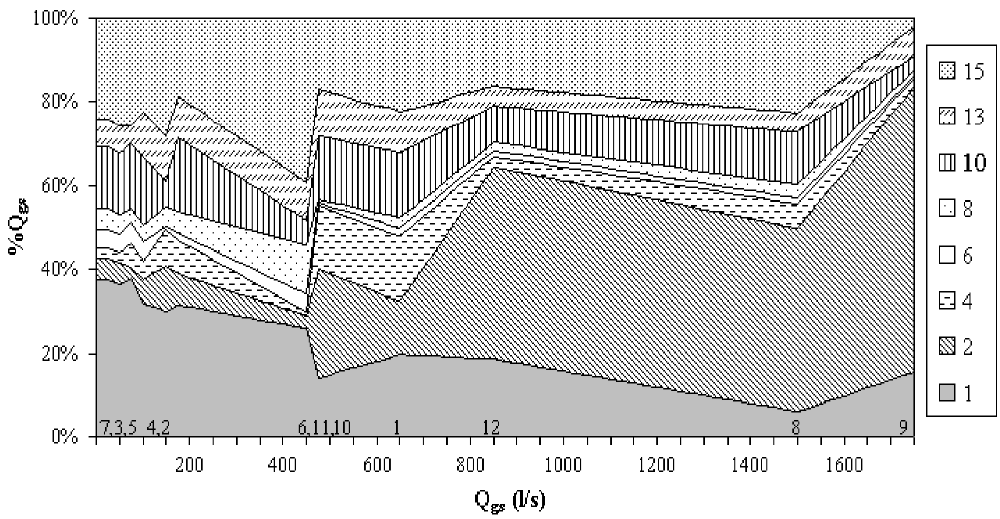

Fig 4: Percentage discharge contribution of each subcatchment (numbers in the legend) to the total discharge at the gauging station. Numbers at the bottom axis refer to the sampling time shown in Fig 2.

Water chemical composition is highly variable within the catchment, in time (Fig 3) and in space. Fig 5 shows a good example of spatial variability of electrical conductivity. Waters in subcatchment 1 show the highest mineralisation (600-1800 $\mu S.cm^{-1}$) with calcium sulfate facies due to the presence of diapir. Waters in subcatchments 15 and 10 (mainly sandstones) show the lowest mineralisation (60-140 $\mu S \cdot cm^{-1}$) with calcium bicarbonate facies. The figure also shows the mineralisation variability (shaded zones) at the sampling points as a function of discharge derived from the chemical balance. Zones can be fitted to ellipses in which the slope of the line corresponding to the main axis is a function of the dilution degree in the waters. Lines are defined by the equation $y = -a.\ln(x) + b$. Slope values (a) are shown in the figure. Except for subcatchment 1, with an important dilution during high water periods, all the others show low dilution. So, in a subcatchment with very high discharge variability (e.g. no. 2), water mineralisation remains within a narrow range, whereas in another catchment with smaller discharge variability (no. 1), mineralisation varies considerably. The subcatchment 15, however, shows low variability in both discharge and mineralisation. Comparing these results with the geological map (Fig 1), the subcatchments with more influence of soilwater-groundwater in the discharge response (smaller value of a; less dilution by piston flow) are related to the sandstones (6, 10, 15) and limestones (2). A smaller influence is seen in subcatchments in lutites (8, 13).

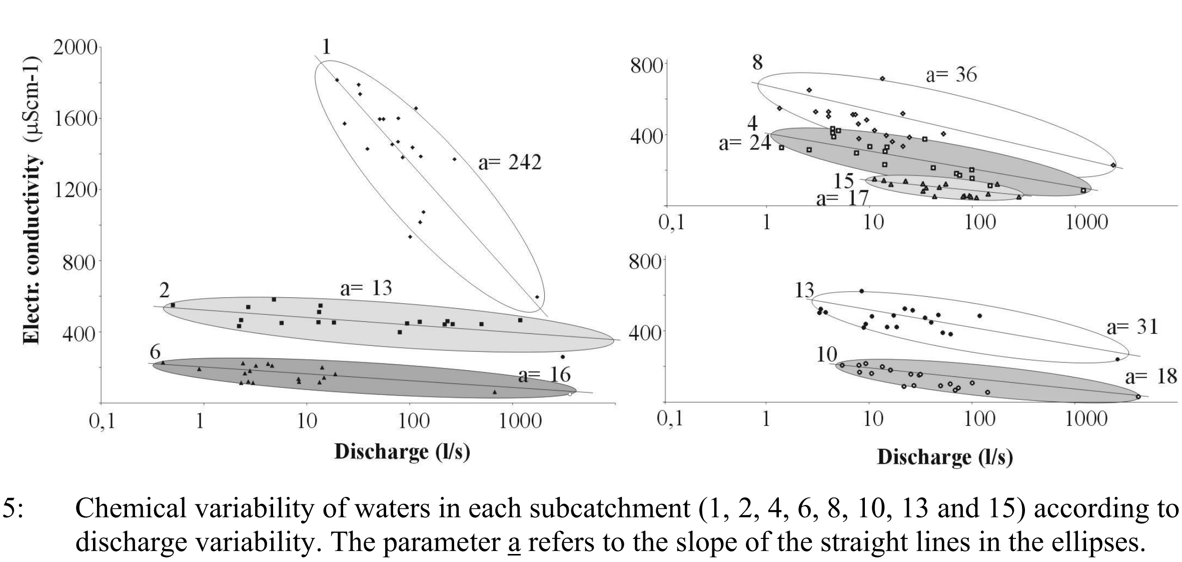

Fig 5: Chemical variability of waters in each subcatchment (1, 2, 4, 6, 8, 10, 13 and 15) according to their discharge variability. The parameter a refers to the slope of the straight lines in the ellipses.

A principal component analysis was conducted on chemical data of the whole catchment (Fig 6). For a better comprehension of chemical variability, Table 1 shows the average values of major elements at the different sampling points. The factorial plane reflects the most information in the analysis, with factor I (61 % of the variance) characterised by $SO_4^{=}$, Cl^-, Ca^{2+}, Mg^{2+}, and Na^+, showing the high mineralisation of waters from subcatchment 1, and factor II (15 %) characterised by HCO_3^-. The subcatchments with higher values in factor II are the ones in the Western part of the Altube River (2, 8, 13), while those of the Eastern part (4, 6, 10, 15) show lower values. This differentiation can be related to lithology, as the bedrock material in the West is carbonated and in the East it is well-washed sandy rock.

Referring to samples taken from the channel of the Altube River, the relation of water in the main channel to the water flowing from each subcatchment can be analysed. Two groups of samples can be distinguished: one group with high values of factor I, related to situations when subcatchment 1 has a larger influence (low waters); the other group with lower values of factor I and higher values of factor II, related to the increasing water contribution of subcatchment 2 during high water periods (Fig 4). Samples taken at the gauging station (point 17) are situated in the bottom-middle part of Fig 6, between subcatchment 1 and waters coming from subcatchments of the Eastern part of the Altube River. This demonstrates once again the importance of the hydrochemical contribution of that part of the catchment.

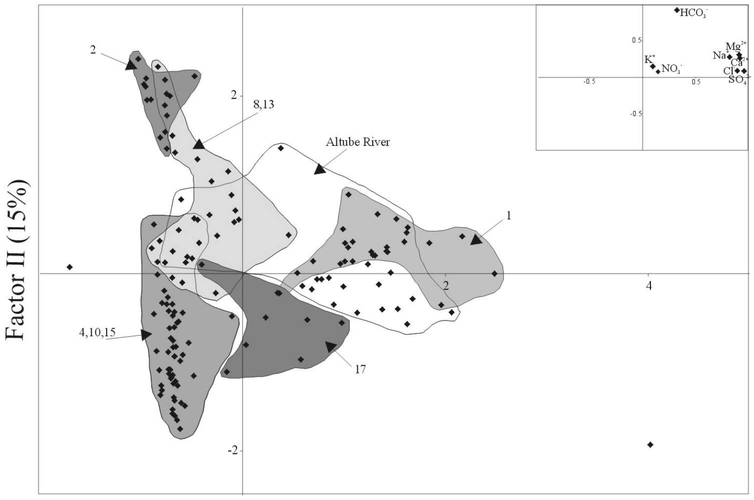

Fig 6: Factorial plane showing the hydrochemical pattern of the Altube River catchment and subcatchments.

So as to have a clearer view of the evolution of water chemistry in the Altube River, another component analysis was made (Fig 7) using data only from control points along the river (Fig 1). The significance of the factors I (56 %) and II (18 %) is identical to that in Fig 6. Waters from subcatchment 1 show the most variable mineralisation, while at point 17 the chemical variability is much lower due to the influence of the tributaries (4, 10, 15) which have lower and less variable mineralisation (Fig 5).

The chemical behaviour of waters does not depend only on the discharge value, but also on the time when samples were taken. Thus, samples taken when the discharge at the gauging station was 80 l/s and 87 l/s show different evolutions, because the first samples were taken on the rising limb of the hydrograph, while the second samples were taken at the peak. The influence of the hydrological context can also be observed by comparing evolutions at discharge values of 445 l/s and 571 l/s; for the first value, the hydrograph was at its maximum point and for the second the water discharge was decreasing but within a period of very high waters. Thus, different chemical evolutions of water flowing along the river at different moments of the hydrograph have been distinguished. The evolutions at the top of the figure (Q_{gs} = 571 and 640 l/s), almost parallel to the factor II axis, occurred during high water when subcatchment 2 had the largest contribution. The chemical evolutions in the middle part of the figure (Q_{gs} = 170, 445, 87, 205 and 1174 l/s), almost 45º from both axes, occurred at a maximum point of discharge. The evolution with Q_{gs} = 80 l/s occurred shortly after the maximum, and the evolution with a discharge value of 25 l/s was during a very calm moment of the hydrograph after a long period without precipitation.

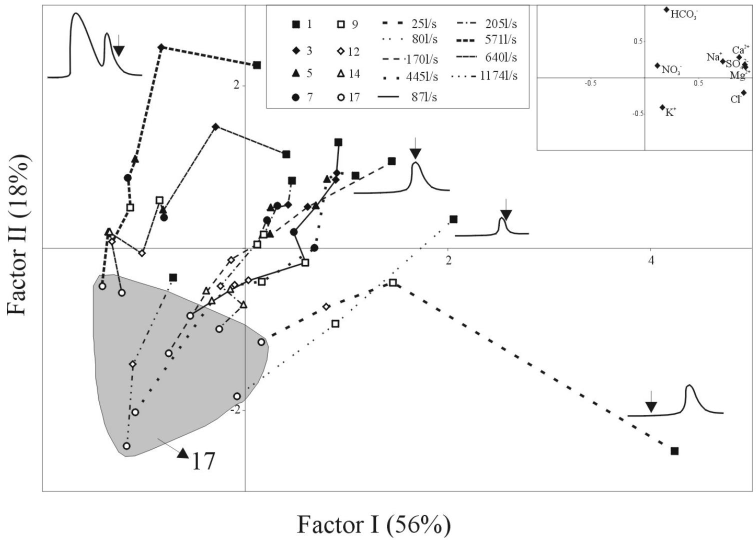

Fig 7: Chemical evolution along sampling points in the Altube River (Fig 1) for different discharge values (referred by lines) and different hydrological situations (described by schematic hydrographs). Factorial plane. Discharges refer to data at the gauging station at the time of sampling. Symbols refer to different sampling points along the Altube River.

Table 1: Average concentration and standard deviation of sulfate (mg/l) (83 values) and electrical conductivity (μScm^{-1}) (170 values) in the subcatchment control points.

Subcatchment		**1**	**2**	**4**	**6**	**8**	**10**	**13**	**15**	**17(the outlet)**
SO_4^{2-}	Average	702	63	51	24	51	18	55	16	293
	St. deviation	167	22	21	12	23	4	8	8	124
Cond.	Average	1416	464	162	465	278	93	463	134	608
	St. deviation	314	68	49	112	107	38	75	55	201

Finally, we tried to broadly separate the annual hydrograph at the gauging station (point 17) according to the sources of waters within the catchment (Fig 2), using the discharge percent contribution shown in Fig 4. Four subareas are considered as sources: the most important subcatchments (1, 2 and 15) and the remaining catchments together. The influence of the three important subcatchments is clearly observed.

CONCLUSIONS

The chemical composition of running water has been used to study the different streamflow sources in the Altube catchment. The most influential subcatchments for different hydrological situations were detected. During low waters, 24% of the catchment accounts for 60% of the total discharge, whereas during high water periods, 41% of the basin accounts for the 65% of the total discharge. Discharge at each point deduced from the chemical mass balance allows us to establish a general relation between discharge and electrical conductivity. Conductivity is therefore used as an easy field tool to estimate water discharge. A principal component analysis shows that lithological signals in waters can help us to differentiate waters coming from subcatchment 1 (diapir), from the West (limestones) and from the East (sandstones) of the Altube catchment. Moreover, the dilution degree (variability of the mineralisation of water with discharge) observed in each subcatchment stream is related to the influence of soilwater-groundwater on discharge response and therefore to its regulation capacity. The principal component analysis also allows us to differentiate the hydrochemical evolution along the Altube river depending on the hydrological situation (Fig 7). It is possible to use these preliminary results as a validation tool for rainfall-runoff models. The next step is to apply water chemistry studies within each subcatchment in order to understand the chemical signature of landuse influence and water pathways.

ACKNOWLEDGMENTS

The authors thank the Basque Meteorological Service of the Basque Government for supporting this investigation. Dr. W. Chełmicki and Dr. L. Holko are thanked for the helpful comments on the manuscript.

REFERENCES

Caissie, D., Pollock, T., Cunjak, R. (1996) Variation in stream water chemistry and hydrograph separation in a small drainage basin. *J. Hydrol*., 178, 137-157.

Christophersen, N., Neal, C. (1990) Linking Hydrological geochemical, and soil chemical processes on the catchment scale: an interplay between modelling and field work. *Water Res. Res.*, 26, 12, 3077-3086.

Church, M.R. (1997) Hydrochemistry of forested catchments. *Annu. Rev. Earth Planet.Sci*., 25, 23-59.

Walling, D.E., Foster, I.D.I (1975) Variation in the natural chemical concentration of river water during flood flows, and the lag effect: some further comments. *J. Hydrol*., 26, 237-244.

HYDROCHEMICAL RESPONSE IN GROUNDWATER TO ABSTRACTION OF BEDROCK GROUNDWATER (CASE STUDY OF SMALL CATCHMENTS IN S SWEDEN)

Siri Knape Hansén, Otto Graffner

Department of Geology, Chalmers University of Technology, Göteborg, Sweden

ABSTRACT

This study shows that natural and artificial fluctuations of the groundwater table influence water quality. This is exemplified by the appearance of pulses of sulphate, cations and chloride in the groundwater and runoff water in periods of low groundwater levels. These effects occur, or are amplified, by the groundwater drawdown associated with groundwater withdrawal. Two catchments are studied. Here, the elements' mass flux is controlled by water flux. If element concentration increases with decreasing runoff, this results in a decrease of the elements' mass flux.

Keywords hydrochemistry, groundwater quality, groundwater recharge, groundwater abstraction, groundwater table fluctuation, hydrogeochemical conceptual model

INTRODUCTION

The alteration of water quality in a catchment is driven by changes in the hydrogeological conditions. De Caritat and Saether (1997) and Stuyfzand (1999), among others, have presented overviews of hydrogeochemical processes along the flow path in catchments. In general, there are large hydrochemistry fluctuations (in both time and space) in the upper part of an aquifer, while the lower part of it has more or less constant hydrochemistry. Natural hydrogeological conditions are often disturbed in a catchment by artificial activities (such as digging, tunnel constructions, domestic wells, etc.) and groundwater abstractions. The impact of these activities on water quality is difficult to estimate. First, the natural fluctuation of the water quality in the catchment has to be considered. Second, the magnitude to which the groundwater abstraction affects the groundwater chemistry in the sediments has to be estimated, depending on the geological and hydrological circumstances.

The aim of this paper is to present the hydrochemical response in groundwater and runoff water to the lowering of the groundwater table in areas with thin sediments and underlying crystalline bedrock. During the period of study, the lowering of the groundwater table has been both natural (according to seasonal fluctuations) and artificial (by groundwater withdrawal from the bedrock).

SITE DESCRIPTION AND METHODOLOGY

About 75% of the Swedish bedrock is of acidic, silica-rich type and most of the Quaternary deposits originate from this material. The deposits are mainly formed during and after glaciation (the latest was 10,000 years ago). At that time, the crust had been pressed down by the ice cap. With the ice regression, land was usually covered by sea from which today's coastland is elevated. The highest traces of the ancient shoreline (*the highest shoreline*) are at different altitudes throughout Sweden, depending on how much the crust had been pressed down, how much the local sea surface rose, and the time when the area became ice free (Fredén, 1994).

Below the highest shoreline, bare-washed bedrock, wave-washed till, gravel, sand, silt and clay are typical results from water processes and sea sedimentation associated with the uplift. These types of deposits are sparse above the highest shoreline, and two different hydrogeological settings emerge. Clay is the key deposit with a high hydrogeological significance, but which exists only below the highest shoreline. Clay tends to divide sediment groundwater into double aquifer systems as it often more or less isolates the lower part from direct groundwater recharge.

The hydrology and hydrochemistry of four small catchments (< 0.05 km^2) with wetlands, thin sediments and crystalline bedrock, were investigated from 1997 to 2001 on the northern Äspö Island (the southeast coast of Sweden), and in the Lake Gårdsjön area (the west coast of Sweden), see Fig 1. Äspö Island (0.8 km^2) is situated below the highest shoreline in the development of the Baltic Sea, and the till is covered by glacial clay. The Lake Gårdsjön area (Andersson and Olsson, 1985; Hultberg and Skeffington, 1998) is situated above the highest shoreline - clay is absent and the till has not been wave-washed.

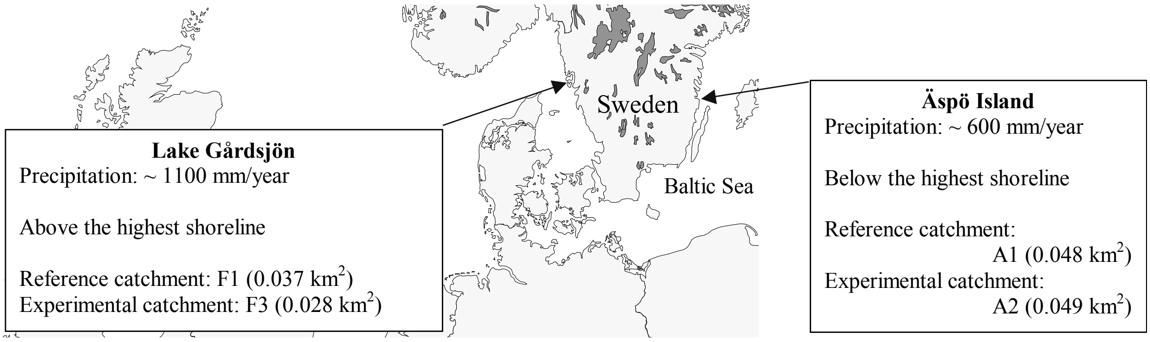

Fig 1: Studied areas: Äspö Island and Lake Gårdsjön.

The two sites show similar hydrological conditions where wetland hydrology dominates the water flux in the catchment. Surrounding areas are thinly covered by glacial till (less than one meter) and most of the water flows to the topographical low points where wetlands are usually found. In addition, the main water storage is found within the wetland where the deposits reach a depth of up to six meters. During most of the year, the groundwater table in the wetland is located less than one meter below surface. Hence, the groundwater fluctuation is controlled by individual rainfall events and runoff responds immediately. Runoff is closely related to the sediment groundwater level and is generated from groundwater drained centrally in the wetland. Therefore, it is difficult to differentiate between groundwater and channel water components in the runoff water. Runoff is measured with V-notched Thomson weirs driven through the deposits down to the bedrock.

The field survey was divided into two phases: seasonal studies under natural conditions and experimental studies where groundwater was withdrawn from the bedrock at a 45 meter depth. Monthly samples of open field precipitation, throughfall, sediment and bedrock groundwater, and runoff water were analysed (Knape, 2001). Bedrock groundwater was generally collected at 10, 30 and 60 meters below ground surface. Analyses of inorganic compounds of bedrock and sediment groundwater and runoff water were conducted to survey the temporal and spatial chemical effects caused both by natural fluctuations of the groundwater table and by an artificial lowering of the groundwater table.

The method used to generalise the complexity of the studied catchments and to enable a comparison between them was the set up of *hydrogeochemical conceptual models*. These models were constructed from the study of natural conditions (Knape, 2001). Such a model of the catchment required a wide range of hydrogeological and hydrochemical information and data, e.g. geologic history, meteorology, land use, the aquifer type, groundwater flow patterns, atmospheric deposition and geochemical processes.

RESULTS AND DISCUSSION

Hydrochemical effects caused by seasonal groundwater fluctuations

An overview is given below of the most significant hydrochemical effects and the processes that occurred during seasonal high and low recharge in the studied catchments. A hydrochemical conceptual model is displayed in Fig 2. It consists of the mass fluxes and the hydrochemical processes in different zones of a wetland profile and in the runoff.

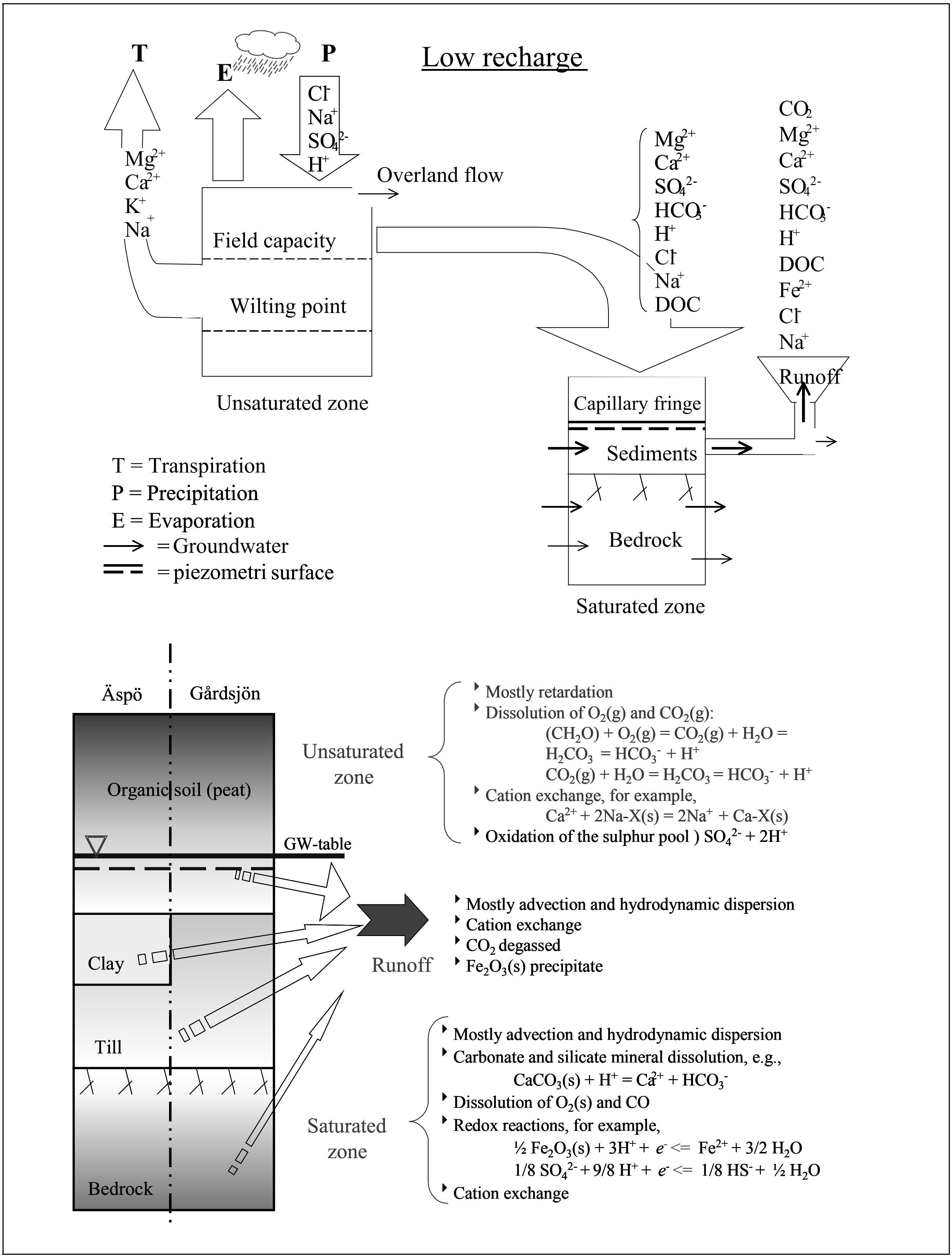

Fig 2: Hydrochemical conceptual model of the mass fluxes and the hydrochemical processes taking place in a wetland profile during natural low recharge in the studied catchments. Resulting effects are the appearance of pulses of sulphate, cation and chloride, as well as the low redox potential in the groundwater. The magnitudes of the water fluxes are represented by the size of the arrows.

The seasonal hydrochemical variations of the groundwater and runoff caused by a natural lowering of the groundwater table were more marked at Äspö Island than at Lake Gårdsjön. The precipitation over Lake Gårdsjön was more evenly distributed over the year, resulting in runoff all year round. In Lake Gårdsjön, the chloride in the precipitation (up to 44 mg/l, due to sea spray) was mostly transported inactively through the catchment and the catchments leached no marine chloride and sulphur from the sediments.

At Äspö Island, a clear effect of naturally increasing recharge was the rainwater flushing of acidic groundwater with high concentrations of sulphate, cation and chloride into the runoff. During dry summer periods, sulphur pulses of maximum 100 mg/l (followed by high concentrations of cations) were recorded in the sediment groundwater (Fig 3). In both groundwater and runoff, the concentrations of dissolved organic carbon (DOC) and iron increased in correlation with drought periods (i.e. periods with low groundwater recharge). In the runoff at Äspö Island the concentration rose to 190 mg DOC/l.

The bedrock groundwater, studied at both sites, did not show seasonal variations in chemical composition. Hydrogeological and hydrochemical studies at Äspö Island indicated that there is low hydraulic connectivity between bedrock fractures (Knape, 1999) and that the hydraulic conductivity is much lower in the bedrock than in the sediments. At Lake Gårdsjön, the hydraulic contact within the bedrock and between the sediment and the bedrock is better.

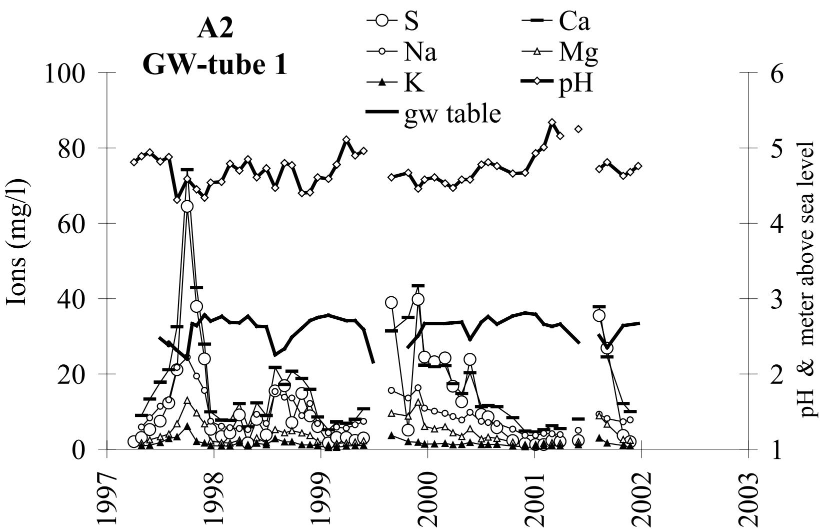

Fig 3: At Äspö Island there were natural pulses of sulphur and cations in the groundwater during periods of low groundwater table (i.e. in autumn).

Hydrochemical effects caused by artificial withdrawal of groundwater

The difference between mass fluxes (i.e. mg/m^2) entering the catchment (by precipitation) and leaving the catchment (runoff and abstraction) reveal whether a catchment stores or releases e.g. sulphate for a given time period. Natural runoff mass fluxes were in general greater at Lake Gårdsjön than at Äspö Island (Knape, 2001). This is due to the higher amount of precipitation and runoff (see Fig 4). It is clear that the mass fluxes are controlled by the water fluxes.

During the study period of natural conditions, the reference catchments F1 in Lake Gårdsjön released chloride and sulphur (see the runoff flux compared to the throughfall flux), while the same compounds were stored in the experimental catchment F3. The Äspö Island catchments indicated a natural leakage of sulphate and chloride, which is expected from an area situated below the highest shoreline with an excess of old marine sulphate and chloride in the sediments.

During the groundwater withdrawal phase in F3, the mass fluxes were affected as water corresponding to 40% of the total natural runoff was abstracted. At F3, there was a clear storage of sulphur and chloride during the withdrawal, compared to the reference catchment F1. At Äspö Island, only water corresponding to 4–8% of the total natural runoff was abstracted from A2, mainly due to low conductivity in the bedrock. The catchment A2 showed no hydrochemical effect on the runoff mass fluxes during the withdrawal phase, as the clay nearly isolates the bedrock groundwater from the sediment.

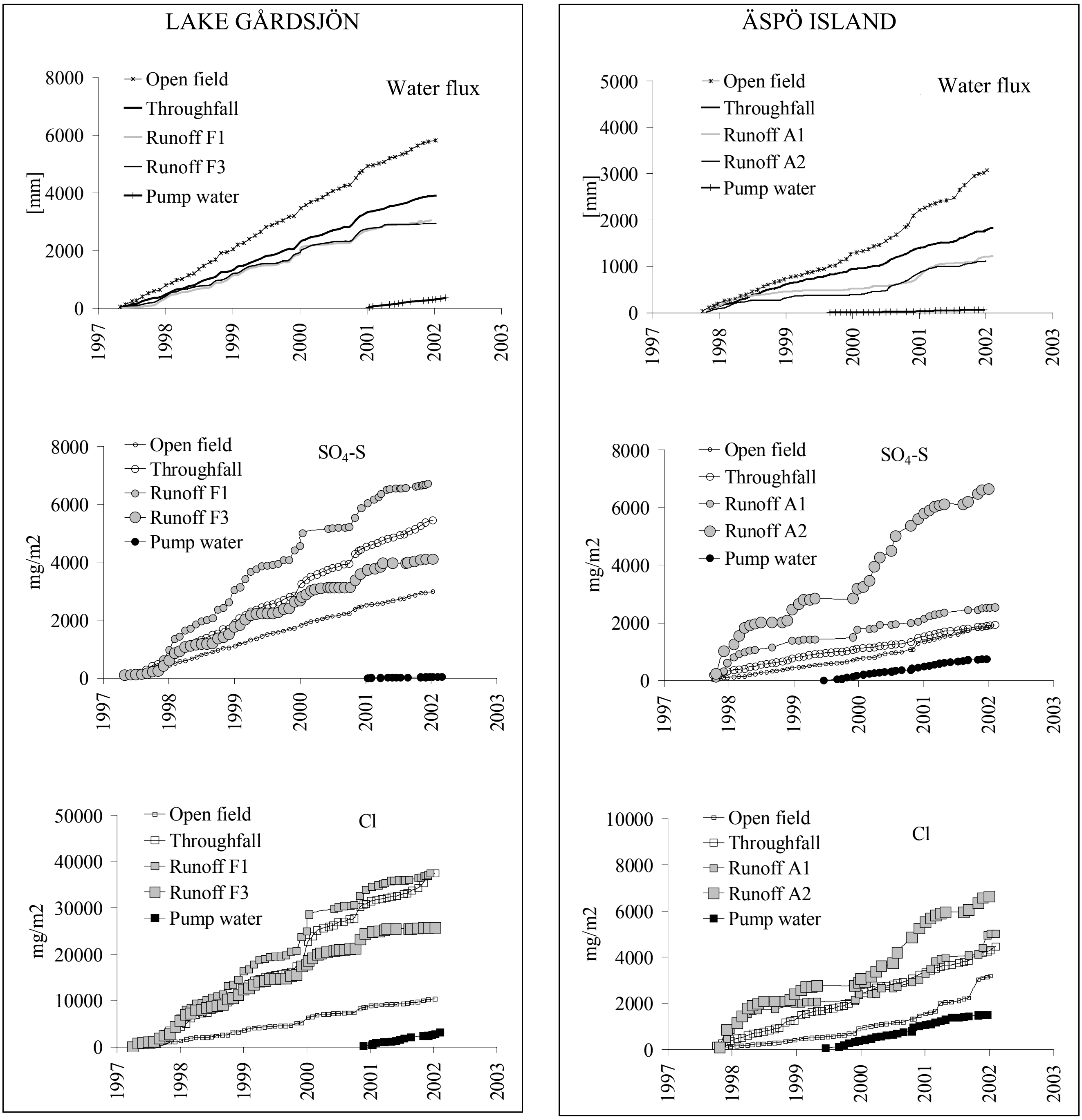

Fig 4: Accumulated water fluxes and accumulated mass fluxes of sulphur and chloride for the reference (F1 and A1) and the experimental (F3 and A2) catchments in Lake Gårdsjön and Äspö Island. At F3, above the highest shoreline, there was a clear storage of sulphur and chloride during the withdrawal, compared to the reference catchment F1. At A2 the bedrock groundwater withdrawal caused no depletion effect on the runoff mass fluxes as the water flux in the sediment was slightly affected.

At the same time as the concentration of an element in runoff increases, the *mass flux* of this element can decrease because of a decline in runoff (Fig 5). At Lake Gårdsjön, there was an evident drop in runoff caused by the lowering of the sediment groundwater level (associated with the withdrawal of bedrock groundwater). When the runoff declined, a pulse in sulphur and cation concentrations appeared. Nevertheless, as mass flux is controlled by water flux, there was a resulting decline of the elements' mass flux. At Äspö Island, an abstraction higher than 4–8% of the total runoff may be required, as the withdrawal did not significantly affect sediment groundwater levels. However, seasonal decreases of the groundwater recharge at Äspö Island gave sulphur pulses. In the end of the year 2000, the groundwater recharge was higher than normal and the sulphur pulse was absent while the mass flux rose.

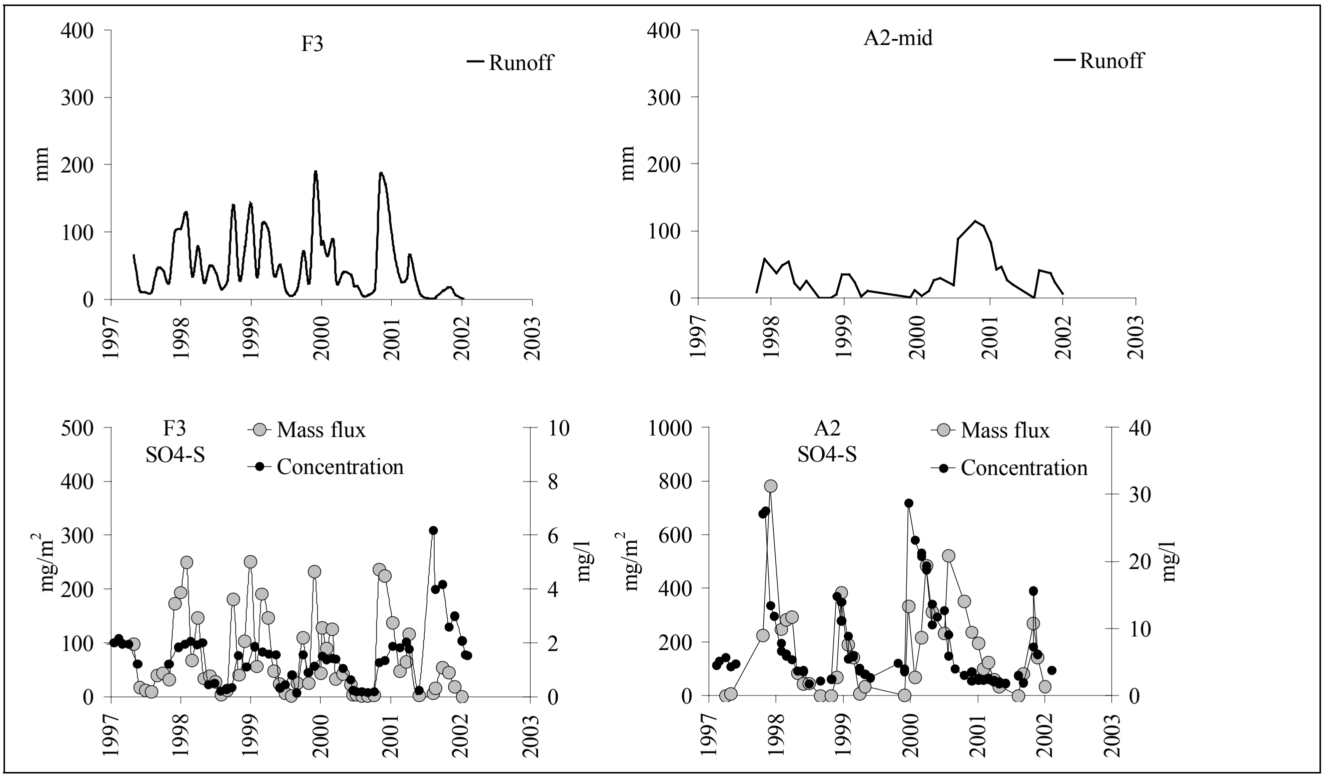

Fig 5: In Lake Gårdsjön, the experimental catchment showed high concentration of sulphur while the runoff declined in year 2001, resulting in a decreasing mass flux of sulphur. In year 2000 at Äspö Island, the concentration of sulphur declined and the runoff rose, which resulted in an increased mass flux of sulphur.

CONCLUSION

The study of four small catchments at Lake Gårdsjön and Äspö Island showed that natural and artificial fluctuations of the groundwater table influence water quality. The groundwater level lowering resulted in the appearance of pulses of sulphate, cation and chloride concentrations, together with low redox potential in the groundwater and runoff. A withdrawal of bedrock groundwater at Lake Gårdsjön caused a considerable decline in runoff, which in turn resulted in concentration pulses of sulphur and cations, but at the same time, a decline of the elements' mass fluxes from the catchment. In addition to precipitation and the amount of groundwater withdrawn, the presence of clay had an impact on the hydrochemistry of the sediment water, dependent on the site location relative to the level of the highest shoreline. Hydrogeochemical conceptual models (Knape, 2001) were applied to support the prediction of groundwater abstraction scenarios of the studied catchments. Further research will formulate *quantitative* conceptual models of the mass fluxes and the hydrochemical processes of the studied catchments.

ACKNOWLEDGEMENTS

The authors wish to thank Äspö Environmental Research Foundation; IVL, Swedish Environmental Research Institute and the Swedish National Railroad Administration for the resources needed to perform the study and for a good collaboration.

REFERENCES

Andersson, F., Olsson, B., (eds.), (1985) Lake Gårdsjön – An acid forest lake and its catchment. *Ecol. Bull (Stockholm) 37*. Sweden.

Caritat de, P., Saether, O. M. (1997) Chemical changes attending water cycling through a catchment – An overview. In: Saether, O. M. and de Caritat, P. (eds.), *Geochemical Processes, Weathering and Groundwater Recharge in Catchments,* A. A. Balkema, Rotterdam, Netherlands, 305 – 328.

Fredén, C., Wastenson, L., (eds.) (1994) Geology. National Atlas of Sweden. Almqvist & Wiksell International, Stockholm, Sweden, 102 – 124.

Hultberg, H., Skeffington, R., (eds.), (1998) Experimental Reversal of Acid Rain Effects. The Gårdsjön Roof Project. John Wiley & Sons Ltd., West Sussex, England.

Knape, S. (1999) Shallow groundwater quality variations within a hardrock aquifer. In: Knutsson, G. (ed.); Proceedings of the Workshop on Hardrock Hydrogeology, Äspö, Sweden. *NHP Report,* No. 45.

Knape, S. (2001) Natural Hydrochemical Variations in Small Catchments with Thin Soil Layers and Crystalline Bedrock. A Two-year Study of Catchments on the East and West Coasts of Sweden. Chalmers University of Technology, Department of Geology, Licentiate thesis, Göteborg, Sweden.

Stuyfzand, P. J. (1999) Patterns in groundwater chemistry resulting from groundwater flow. *Hydrogeology Journal*, Vol. 7, pp. 15 – 27.

DIRECT PROPORTIONALITY BETWEEN TRANSPIRATION AND NUTRIENT UPTAKE FROM SOIL TO PLANT CANOPIES

Viliam Novák [1], Jozef Vidovič [2]

[1] *Institute of Hydrology, Slovak Academy of Sciences, Račianska 75, 831 02 Bratislava 3, Slovak Republic. Phone: +421-2-44259383; fax: +421-02-44259404, novak@uh.savba.sk*
[2] *Research Institute of Plant Production, Piešťany, Slovak Republic*

ABSTRACT

The study presents results of field measurements of nutrient uptake from soil by maize canopy. It confirms that the rate of nutrient uptake by plants during the vegetation period can be expressed by a curve with a maximum approximately at the stage of the maximum growth intensity. It was demonstrated that the nutrient uptake kinetics during a dry season (1981) were different from that during a normal season (1982). The cumulative curve of ion uptake during the dry season (1981) exhibits a maximum for all three ion species studied, after which a decrease of the cumulative nutrient uptake occurs, due to low transpiration intensity and nutrient loss. For a maize canopy and dry year (1981), 174 kg of N (nitrogen) per hectare and season was taken up, while for the normal season of 1982 it was 230 kg N per hectare. More important differences between the two seasons were found in terms of the other two elements, P (phosphorus) and K (potassium). Their seasonal uptake was 7.6 / 38 kg P per hectare and 70 / 127 kg K per hectare for the dry and the normal season, respectively. A linear relationship (direct proportionality) between the uptake rate of nutrients by maize roots and a maize canopy transpiration rate is applicable to the whole vegetation period of 1982 and to the first part of the vegetation period of 1981, until the loss of nutrients from the plants due to drought set on. The direct proportionality is expressed by values of proportionality coefficients. These coefficients are different for each nutrient, but they are similar for both growing seasons and a particular nutrient. The results are based on field studies with a maize canopy grown on a silty Haplic Chernozem soil at the Trnava site (South of Slovak Republic), but general features of the nutrient uptake should be similar in different canopies, which makes it possible to adopt the direct proportionality between the nutrient uptake rate and the water uptake rate in simulation models.

Keywords nutrient uptake, soil, plant, transpiration

INTRODUCTION

The transport of dissolved chemicals in surface water is understood relatively well. The concentration of chemicals and its change in time and space are relatively easy to measure. This has led to numerous mathematical models of such processes and their application.

Quite a different situation can be found in the subsurface, particularly in a soil. The most important obstacles to a quicker advance in understanding the soil solute transport are difficulties in determining soil chemical concentrations. The main problem is the soil solution sampling for analysis - there are difficulties in acquiring basic information about the concentration of dissolved chemicals and its change in time and space.

Soil solute behaviour can be briefly described as follows: chemicals are introduced into a soil usually by fertilising (industrial fertilisers are usually used), by emissions or by the disposal of different kinds of waste. Infiltration of water into the soil is usually the main process which transports chemicals. When over-fertilisation leads to a high concentration of chemicals in soils and is followed by an intensive rain or irrigation, the groundwater can be polluted. Groundwater with a high concentration of chemicals can be a source of secondary "salinisation" of soil. But the most important process of chemical transport is an uptake of ions by plants during their ontogenesis. Its importance is due mostly to its necessity for plant growth. Particular chemicals are uptaken by plants as nutrients and accumulate in plant bodies. The quantification of nutrient uptake by plants is a key problem in modelling the chemical movement in the soil root zone. The current approach to solving this problem starts with a sampling of the soil, followed by a determination of the nutrient concentration in the laboratory. Thus, the concentration of a particular ion is estimated. This laborious and time-consuming method is not acceptable as a standard method for use.

Another method would be to sample the soil solution only, e.g., using suction cups. This method would be more acceptable, in principle, but its practical application meets difficulties. The sampling process is slow, and it can only be used in soil at a soil water content close to saturation. Therefore, our effort is directed to the mathematical modelling of nutrient transport. Such a model has to contain a "nutrient uptake" term.

Leaching is another process of chemical transport influencing the chemical balance in the soil. This process is especially important during the autumn–winter period, when nutrient uptake is negligible and high precipitation amounts infiltrate into the soil and percolate to the shallow groundwater, carrying dissolved nutrients and thus creating a risk of groundwater salinisation, especially in agriculturally utilised catchments. Another negative feature of leaching is the transport of nutrients originally located in the soil root zone downwards, out of the roots' reach, where they cannot be utilised by plants.

Modelling of the ion "uptake" process is based on ideas which are not always sufficiently confirmed by reliable data. In particular, it is generally accepted that the so called "passive" transport of nutrients in plants, carried by the transpiration flux through the soil-plant-atmosphere system is the most important mechanism over a great range of nutrient uptake rates (Dvořák, 1976, Mengel and Kirkby, 1982). It is mainly this approach that has been used for the modelling of this process. Some models assume that the passive transport of nutrients in plants and, consequently, also the uptake of nutrients by plant roots from the soil, are directly proportional to the transpiration rate (Franko et al., 1995). Many "production" models estimate N uptake by a much more simple scheme, e.g. as a function of time during a growing period. It should be mentioned, however, that the so-called "active" transport and uptake of nutrients may also be of significance under specific conditions (Dvořák, 1976).

To our knowledge, a proper experimental substantiation of either a linear or another simple relationship between the uptake of macronutrients and the transpiration flux has not yet been published. The aim of this work is to investigate the relationships between nitrogen (N), phosphorus (P) and potassium (K) uptake and the transpiration rate of the maize canopy, based on measurements at the Trnava site in the South of the Slovak Republic made during two growth periods (Vidovič et al., 1984). It is believed that a generalisation of this approach for a variety of plant canopies (even for forest) is possible, but further research is needed.

UPTAKE OF NUTRIENTS BY ROOTS

The movement of ions in a homogeneous soil under isothermal conditions, can be characterised quantitatively by a convection–dispersion equation describing the solute transport in a variably saturated zone of the soil (Kutilek and Nielsen, 1994), with an additional sink term $M_i(z,t)$ describing the i-th chemical element (nutrient) uptake by plant roots.

$$\frac{\partial c_i}{\partial t} = \frac{\partial}{\partial z}\left[D_a\left(\frac{\partial c_i}{\partial z}\right)\right] - \frac{\partial(v.c_i)}{\partial z} - M_i(z,t) \qquad (1)$$

where c_i is an average concentration of the i-th nutrient (chemical element) in the soil solution [M L^{-3}], v is the solution flux density [L T^{-1}], z is the vertical coordinate [L], t is time [T], D_a is a hydrodynamic dispersion coefficient [L^2 T^{-1}], $M_i(z,t)$ is the pattern of the i-th nutrient uptake rate by roots [M L^{-3} T^{-1}] as a function of z and time t. $D_a = \theta(D_c + D_m)$ is the effective hydrodynamic dispersion coefficient, where D_m is the molecular diffusion coefficient of the i-th nutrient in the soil solution [L^2 T^{-1}], and D_c is the mechanical dispersion coefficient of the i-th nutrient in the soil solution [L^2 T^{-1}].

As is implied in equation (1), the sorption/desorption processes and biochemical reactions are not accounted for; nutrient uptake is the only process involved. The simplest hypothesis used is to express the nutrient uptake rate as proportional to the water uptake rate. Thus, water is supposed to be a passive transporter of chemicals from the soil to a plant. This hypothesis has been used previously (Franko et al., 1995) for the modelling of nitrogen uptake by plants (CANDY model) but without field verification. The nutrient uptake rate can be expressed as a function of the transpiration rate E_t:

$$M_i(t) = n_i \,.\, E_t(t) \qquad (2)$$

where $M_i(t)$ is an average integral uptake rate of the i-th nutrient from the root zone under a unit soil surface area per unit time, evaluated at time t [M L^{-2} T^{-1}], $E_t(t)$ is an average transpiration rate, expressed in mass of water uptaken by plant canopy grown on a unit soil surface area per unit time, evaluated at time

t [M L^{-2} T^{-1}], n_i is the slope of this linear relationship, a dimensionless coefficient which characterises the interaction among specific ions and the properties of the soil-plant-atmosphere system.

Further, by knowing an average concentration of the specific nutrient in a canopy $C_i(t)$, [M L^{-2}], (i.e. the mass of a particular nutrient in a canopy grown on a unit area of soil surface) the rate of the i-th nutrient uptake from the entire soil profile by a particular canopy can easily be estimated. Using an independently estimated transpiration rate $E_t(t)$, which is the rate of water uptake by the canopy from the entire soil profile, we can estimate the average coefficient of proportionality between the two uptake rates as:

$$n_i = M_i(t) / E_t(t) \qquad (3)$$

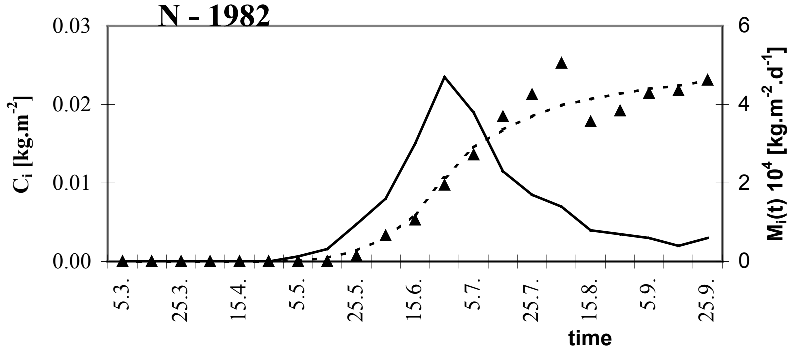

Fig 1: Nutrient content C_i (nitrogen-N) in the above-ground parts of the maize canopy per square meter of soil surface during the vegetation period of the year 1982. Measured values are shown by triangles. The integral uptake rate of nutrients by the maize canopy from the soil $M_i(t)$ during 1982 is shown by the solid line. The maximum uptake rates correspond approximately to the silking phase of ontogenesis in loamy soil at the Trnava site in the South of the Slovak Republic.

SITE DESCRIPTION

The measurements were carried out at the Experimental Station of the Maize Research Institute at Trnava, in the Slovak Republic (48°23′ N, 17°36′ E, 146 m a.s.l.); the region can be characterised as subhumid (Thornwaite, 1948).

The soil is a loamy Haplic Chernozem (FAO classification). The maize plants (Zea Mays L.) were grown with a stand density of 72 000 plants per hectare in rows 0.70 m apart. Industrial fertilisers were applied during the pre-season time. Nitrogen was applied in two doses (in autumn and in spring before sowing) at a total rate 178 = 63 + 115 (N) kg ha^{-1}, while 52.4 kg ha^{-1} (P) and 116.2 kg ha^{-1} (K) were applied in autumn. As will be shown later, the N nutrient amount supplied by mineral fertilisers was completely uptaken by the plants, and even older nitrogen reserves or products of mineralisation were also used.

METHODS

Standard methods of estimating the concentration of chemical elements (nutrients) in plants and soil were used (Vidovič et al., 1984). During the whole vegetation period 10 plants in four replications were sampled every week for chemical analyses; in addition, the dry matter content of all plant organs was estimated. Nutrient accumulation was evaluated per soil surface unit in the plant part above ground, in the root parts and in the whole plants. Additionally, the following nutrient concentrations in the soil were estimated regularly: NO^-_3, NH^+_4, $H_2PO^-_4$, and K^+. Meteorological characteristics were measured at the meteorological station situated in the same field. All necessary soil and plant data were measured during the two seasons of 1981 and 1982 (Vidovič et al., 1984; Novák and Majerčák, 1992).

A potential evapotranspiration rate was calculated by a modified Penman–Monteith method. Its modification is based on the advanced method of the aerodynamic resistance estimation, proposed by Monin and Obukhov

(1954) and briefly described in the literature given below. Evapotranspiration and its components, i.e. transpiration and evaporation, were estimated according to Budagovskij (1981) and Novák (1995) methods. Finally, the seasonal courses of the maize daily average transpiration rates were estimated.

RESULTS AND DISCUSSION

The seasonal courses of three nutrient contents C_i (nitrogen (N), phosphorus (P) and potassium (K)) were measured in the above ground parts of the maize canopy during the vegetation periods of 1981 and 1982. A typical example of results for nitrogen is shown in Fig 1 for 1982. The integral rate of nutrient uptake was obtained from these data by numerical differentiation. Measured data were smoothed by eye (the dashed line in Fig 1), to allow the differentiation of the curve. As can be seen in Fig 1., measured data corresponding to relatively high values of transpiration rates are too dispersed (see the beginning of August). The dispersion of measured data is due to several different factors: spatial variability of the plant's nutrient content and the dry matter weight, the leaching of nutrients from the above ground parts of plants during heavy rainfall, and dry matter loss due to premature senescence (the falling of dry leaves after periods of drought). Plants were sampled randomly from all parts of the field. The variation of the content of N, P, K ions during the 1981 vegetation period was different from that in 1982 and is characterised by a local maximum in the middle of the season followed by a nutrient content decrease during the rest of the season. Conversely, during the 1982 vegetation period (shown in Fig 1), the content of nutrients in the canopy increases during the entire season.

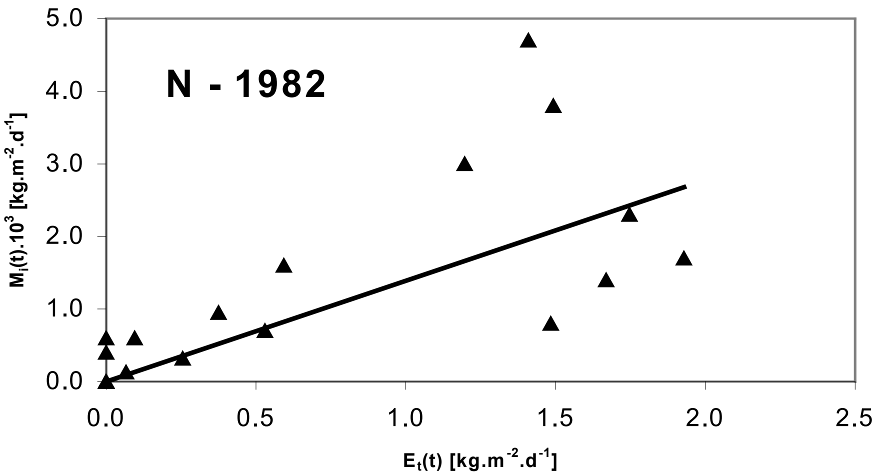

Fig 2: The daily average uptake rate of nitrogen by maize canopy $M_i(t)$ from the soil as a function of the daily average transpiration rate $E_t(t)$ for the vegetation period of 1982 (loamy soil, Trnava site, the South of the Slovak Republic).

Maximum uptake rates of ions by plants were observed approximately at the same ontogenesis stage of the vegetation periods of the years 1981 and 1982, namely at the silking stage. Nutrient loss during the 1981 vegetation period was observed when the decline of the transpiration rate, compared to 1982, became significant. The transpiration rates were higher for the second part of the 1982 season, compared to the same part of the vegetation period of the year 1981. Baier (1987) stated that drought can decrease the P ion uptake of a variety of plant species. The structure of nutrient loss (active efflux and washing out) can hardly be estimated, but a measurable washing out of nutrients – especially N from plants by rain or irrigation – was observed (Kovács, 1982). This effect could have contributed to the decrease of nutrient concentration in plants during September 1981 when a monthly precipitation total of 108.5 mm was observed, as opposed to 10.4 mm of rain during September 1982. But a considerable amount of rain (187 mm) during the time interval 4 July - 9 August 1982 did not lead to a measurable decrease of nutrient content in the maize plants. This implies that the washing out of nutrients was not important at this time interval. Different uptakes of nutrients during the later parts of the vegetation periods of the years 1981 and 1982 can be influenced by the different biomass dry weight due to leaf loss and decay. Maize grain yield was estimated as 6.4 t ha^{-1} for the 1981 season (below average) and 9.7 t ha^{-1} (above average) for the 1982 season (Vidovič et al., 1984).

Table 1: Proportionality coefficients in equation (2) for three nutrients (N, P and K) and vegetation periods of 1981 and 1982 (loamy soil with maize canopy, at the Trnava site in southern Slovakia).

Year	$M_i(t)$		
	N	P	K
1981	$20\ 10^{-5}$	$2.5\ 10^{-5}$	$20\ 10^{-5}$
1982	$15\ 10^{-5}$	$2.7\ 10^{-5}$	$8\ 10^{-5}$

For a maize canopy and the dry year 1981, 174 kg of N (nitrogen) per hectare were uptaken over the season, while for the normal season of 1982, 230 kg of nitrogen per hectare were uptaken. But the more important differences were found for the other two elemental nutrients - P (phosphorus) and K (potassium). The corresponding seasonal uptake totals were 7.6 kg P ha^{-1} / 38 kg P ha^{-1} and 70 kg K ha^{-1} / 127 kg K ha^{-1} for the dry (1981) and the normal (1982) seasons, respectively. In the same two seasons, the transpiration totals were 105 and 128.5 mm per season, respectively (the season duration was 133 days in both years). The difference between transpiration totals in 1981 and 1982 is only 22.5 mm, but the difference in grain yields is more crucial - 3.3 t ha^{-1}. As can be seen from data in previous sections, the seasonal uptake of the main nutrients approximately equals the amount of nutrients applied as industrial fertilisers. The organic matter mineralisation is difficult to estimate, but according to data available (Agricultural soils, 2000), the N mineralisation rate in the Trnava region is about 60 kg per hectare and season, and it can be significant. As was stated by Kafkafi (1971), the average annual daily N uptake by maize in Israel was 1.4 kg N ha^{-1} d^{-1} , which is comparable with our data, while the average seasonal mineralisation rate was estimated by Kafkafi (1971) as 2.5 kg N ha^{-1} d^{-1}, which is significantly more than the average uptake. This means that no additional N fertilisation was in fact needed. It must be noted that this is valid for dry and warm conditions of Israel. The nitrification bacteria activity reaches its maximum at around 31 ºC (in terms of the soil temperature) which is rarely reached in Slovakia. Therefore, the nitrogen mineralisation rates in the soils of southern Slovakia must be lower than those in Israeli soils.

The relationships between the uptake rate of nutrients by maize roots $M_i(t)$ and the canopy transpiration rate $E_t\,(t)$ were estimated from the measured data (Novák and Vidovič, 2002), as demonstrated in Fig 2. It was shown that the relation between the uptake of nutrients by maize roots $M_i(t)$ and the maize canopy transpiration rate $E_t(t)$ can be treated as a direct proportionality and, therefore, can be approximated by a linear equation. The correlation coefficients between $M_i\,(t)$ and $E_t(t)$ were relatively high: r = 0.772 (N), r = 0.926 (P), and r = 0.804 (K) for the vegetation period of 1981, and r = 0.754 (N), r = 0.950 (P) and r = 0.849 (K) for the vegetation period of 1982. It is worth noting that the values of the correlation coefficients, as well as the slopes of the linear relationships (i.e. the regression coefficients) for particular ions are similar for both seasons. In Table 1., proportionality coefficients (slopes) of the relationship expressed by equation (3) are shown. There are differences between particular nutrients (chemical elements), depending on the concentration of particular nutrients in the soil solution and depending on plant needs. Equation (2) is likely valid under the condition of not limiting nutrient concentration in the soil.

It is difficult to draw final conclusions based on the results of only two seasons of measurements. No similar comparisons of nutrient uptake with water uptake were found in the literature. Most authors only present the seasonal course of different nutrient concentrations in canopies, but other data (relating to weather, soil, plant transpiration, etc.) are missing (cf. Lasztity and Biczok, 1988; Biczok et al., 1988). A sort of linear relationship (proportionality) between the transpiration and the nutrient uptake can be expected to be valid for other crops, as well as for forests and meadows, but this should be confirmed by further research. We also recommend that other available data from field experiments in which the soil water uptake totals (transpiration totals) and the ion uptake totals were measured for different plants, soils and climates, are evaluated in a similar way, in order to provide a broader data base for modelling.

CONCLUSIONS

It was shown and confirmed that the seasonal course of nutrient uptake rates by plant canopies during the vegetation period can be expressed by a curve with a maximum (approximately at the milky ripeness phase of maize ontogenesis), as is shown in Fig 1.

The basic difference between the nutrient uptake course for a dry vegetation period (1981) and a normal period (1982) for maize was shown. The course of cumulative ion uptake during the dry season exhibits a maximum followed by a period of decrease in the nutrient content of the plant (i.e. of nutrient loss from the canopy) during the later part of the season, which led to a substantial depression of yields. This pertains to all three ions studied (N, P and K). On the contrary, a continuous increase in nutrient content in the canopy was observed during the normal season of 1982.

An approximate direct proportionality, which was found between the uptake rate of nutrients by maize roots and the maize canopy transpiration rate is applicable over the whole vegetation period of 1982 and for the first part of ontogenesis in the vegetation period of 1981. The interannual variability of proportionality coefficients is not significant except for potassium (Tab.1). From this it follows that equation (1) can be applied as a first approximation to estimate nutrient uptake by maize as a function of the transpiration rate.

The results presented here are valid for maize canopy. Additional research is needed to collect more information in order to generalise the relationship between water and ion uptake for other canopies. The character of this relationship may depend on plant, soil and meteorological characteristics during the vegetation period.

ACKNOWLEDGEMENT

This work was supported by the Slovak Grant Agency (VEGA), Project 2 – 1084 - 21.

REFERENCES

Agricultural soils of Slovak Republic (2000) Facts and figures. Soil Fertility Res. Inst., Bratislava, Slovakia.

Baier, J. (1987) The weather influence on phosphorus, potassium and microelements uptake. (in Czech), In: Petr, J. et al.: *Počasí a úroda*, Praha, SZN, 106-112.

Biczok, G.Y., Lasztity, B., Ruda, M. (1988) Dynamics of nutrient uptake and aboveground phytomass in some winter wheat varieties at major growing sites in Hungary. *Acta Agronomica Hungarica*, 37, 3-19.

Budagovskij, A.I. (1981) Soil water evaporation. (In Russian, with English abstract), In: *Physics of soil water*. Moscow, Nauka, 13-95.

Dvořák, M. (1976) Special plant physiology. Mineral nutrient of plants. (in Czech), Charles University, Prague, 173 pp.

Franko, U., Olschlägel, B., Shenk, S. (1995) Simulation of temperature-water–and nitrogen dynamics using the model CANDY. *Ecological Modeling*, 81, 213-222.

Houba, V.W., Van Vark, I., Walinga, J.J., Van Der Lee (1989) Plant Analysis procedures. Department of Soil and Plant Analysis, Wageningen, The Netherlands.

Kafkafi, U. (1973) Nutrient supply to irrigated crops. In: *Ecological Studies*, 5, Arid zone irrigation (B. Yaron, E. Danfors, and Y. Vaadia, Eds.), Springer Verlag, Berlin–Heidelberg–New York, 177-188.

Kovács, G.J. (1982) Nutrients and water dynamics of maize as a critical ecophysiological relationship. (in Hungarian with English abstract), *Nővenytermelés*, 31, 355-365.

Kutilek, M., Nielsen, D.R. (1994) Soil hydrology. Cremlingen – Destedt, Catena Verl., 370 pp.

Lasztity, B., Biczok, G. (1988) Effect of intensive fertilisation on the phosphorus uptake by winter wheat during a vegetation period. *Zemljište i Biljka*, 37, 201-206.

Mengel, K., Kirkby, E.A. (1982) Principles of plant nutrition. International Potash Institute, Bern, 655 pp.

Novák, V. Majerčák, J. (1992) Simulation of the soil – water dynamics in the root zone during the vegetation period: II. The course of state variables of soil water below the maize canopy. *J. Hydrol. Hydromech*., 40, 380-397.

Novák, V. (1995) Evapotranspiration and methods if its estimation. (in Slovak), VEDA, Bratislava, 260 pp.

Novák, V., Vidovič, J. (2002) Transpiration and nutrient uptake dynamics in maize (Zea Mays L.), *Ecological Modelling*, (submitted for publication).

Thornwaite, C.W. (1948) An approach to a rational classification of climate. *Geo. Rev*., 38, 55 – 94.

Vidovič, J., Novák, V., Hurtalová, T., Matejka, F. (1984) Production function and maize canopy evapotranspiration during ontogenesis. (in Slovak) Research Report, Maize Research Institute, Trnava, pp.206.

FLOODS OF COMBINED ORIGIN - RAINFALL AND SNOWMELT - IN ROMANIAN SMALL CATCHMENTS

Pompiliu Miță, Marinela Simota, Valentina Ungureanu, Simona Matreata

National Institute of Meteorology and Hydrology,Bucharest, Romania

ABSTRACT

In this paper, the differences between the main characteristics (runoff depth, peak discharge) of rainfall-snowmelt originated floods and those corresponding to flood waves generated only by rainfall or only by snowmelt are analysed. The comparison has been made considering that the flood wave parameters have been determined under comparable conditions of water inflow and of previous precipitation amounts.

Keywords flood of mixed origin, synthetic flood wave, runoff depth

INTRODUCTION

In Romania, rainfall and snowmelt originated floods (floods of mixed origin) frequently occur on rivers in mountainous regions. There are years in which the water content of the snow cover in these river basins exceeds 500-600 mm. During the snowmelt period, usually in the spring when high amounts of rainfall superpose the snowmelt process, severe floods occur. In this paper, several results concerning two main characteristics of these floods – runoff depth and peak discharge – brought about by rainfall, snowmelt and combination of these two processes are presented. The issue has proven to be difficult for conditions when the rainfall intensifies the snowmelt process by its heat flux and by changing the snow peak metamorphism. At the same time, rainfall suffers a delay and attenuation through the snow cover. Both sources – rain and snowmelt – exert a certain influence upon the volumes and discharges, both from the quantitative point of view and from the point of view of the evolution in time.

DATA

The paper is based on data recorded at the Iedut and Fantana Galbena representative basins, situated in the western part of Romania. These basins have provided data on the variation of the snow cover (depth, density, water equivalent) in the basins, and also on the recorded flood waves generated by rainfall, snowmelt or their combined action. For all three types of floods, the main characteristics of the flood waves (runoff depth and peak discharge) have been separately analysed. In the case of the two studied basins, the relationships between the flood characteristics and the factors determining them have also been established.

METHODOLOGY

To point out the particularities of rainfall and snowmelt originated floods (mixed origin), a comparative method has been chosen. The main characteristics of flood waves (runoff depth and peak discharge) were determined in the case of floods of mixed origin precisely recorded at the gauging stations, and compared with values of these elements determined in the case of "synthetic" flood waves generated only by rainfall or only by snowmelt. They have been called "synthetic" because these floods have not been recorded at the gauging station. The synthetic flood waves have been created on the basis of flood wave characteristics: peak discharge, increasing duration, decreasing duration, volume. These characteristics were determined from synthesis relations (Mita and Stancalie, 1996; Mita et al., 1999). Such relations are presented in Figs 2 and 3.

To achieve this comparison, the following steps were taken:

1. The values of the flood wave characteristics (runoff depth and peak discharge) have been determined for each flood of mixed origin analysed at the gauging station. These floods have been generated by water inflow ($P+h_z$), where P is a rainfall amount and h_z the water amount coming from snowmelt.
2. For each of the floods of mixed origin a corresponding pair of "synthetic" floods has been created, generated only by rainfall or only by snowmelt (Fig 1).

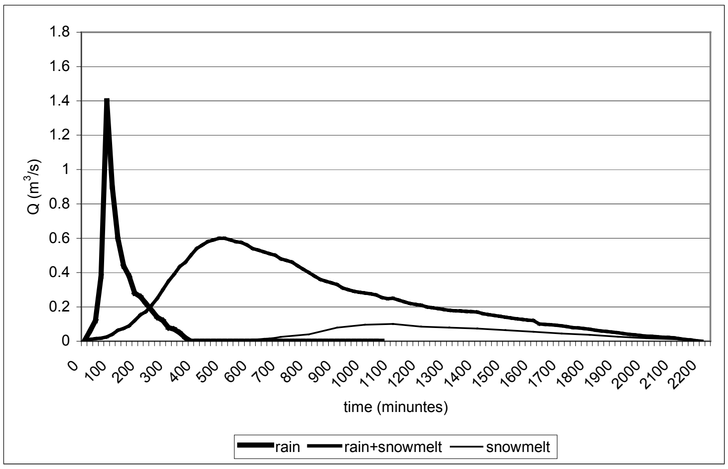

Fig 1: The flood wave of mixed origin (rainfall + snowmelt) recorded at the gauging station Stana de Vale during 19 – 21 April 1980 and the synthetic flood waves only from rainfall and only from snowmelt.

The synthetic flood waves have been created using the same values of the water inflow ($P+h_z$) which generated the flood wave of mixed origin, i.e. the same precipitation, P(mm), in the case of the synthetic flood wave produced by rainfall, and the same water amount from snowmelt, h_z, in the case of the synthetic flood wave produced by snowmelt. A comparison has been made between the values of the runoff depth and the peak discharge corresponding to the flood wave of mixed origin (h_{sM}, $Q_{max\ M}$) and the sum of the values of these characteristics corresponding to the two synthetic flood waves: h_{sp} and $Q_{max\ p}$ in case of the flood waves produced by rainfall, and h_{sz} and $Q_{max,z}$ in the case of the flood waves produced by snowmelt.

The following relationships were used for the floods of rainfall origin:

$$Q_{max\ p} = f(i_p,\ T_p) \qquad t_{cr} = f(T_p)$$

$$t_d = f(T_{tot},\ i_{Xtot}) \qquad h_{sp} = f(p,\ API_{10})$$

where:

$Q_{max,p}$ – peak discharge of the rainfall originated flood (m^3/s); T_p – time interval between the beginning of the rainfall and the end of the rainfall core (min); i_p – intensity of the rainfall for the time interval T_p (mm/min); t_{cr} – flood wave increase duration (min); t_d – flood wave decrease duration (min); T_{tot} – total duration of rainfall (min); i_{Xtot} – intensity of rainfall for T_{tot} (mm/min); h_{sp} – runoff depth of the rainfall originated flood wave (mm); P – amount of rainfall that generates the flood (mm); API_{10} – the soil moisture index calculated from rainfall during 10 days prior to the flood occurrence (mm).

These relationships are presented in Fig 2.

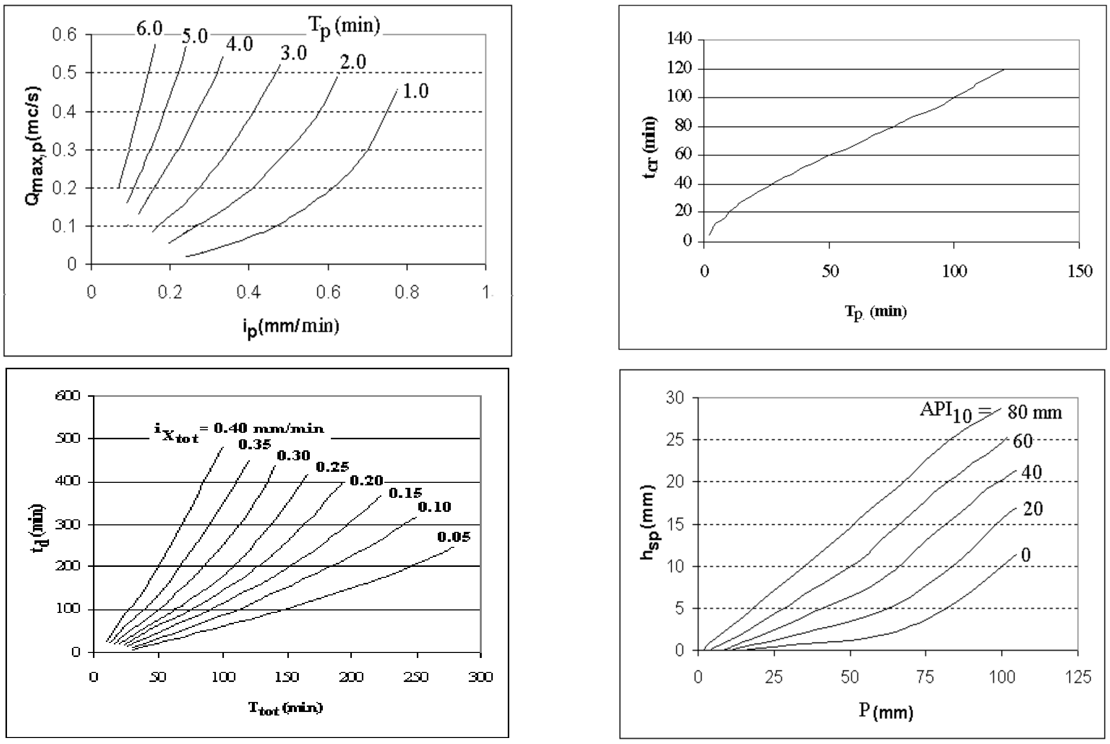

Fig 2: Relationships derived for floods of rainfall origin (explanation of the symbols is given in the text above).

The form coefficient has been adopted for each flood as a function of the precipitation distribution between 0.2-0.3.

For the floods of snowmelt origin, the following relationships were applied:

$$h_{sz} = f(h_z, API_{10}) \qquad\qquad Q_{max,z} = f(i_{hz}, API_{10})$$

where:

h_{sz} – runoff depth of the snowmelt originated flood wave (mm); hz – water yield of snowmelt during a certain time interval (mm); $Q_{max,z}$ – peak discharge of the snowmelt originated flood (m^3/s); i_{hz} – intensity of the water produced by snowmelt (mm/hour); API_{10} – the soil moisture index calculated from the rainfall and water yield of snowmelt during 10 days prior to the flood occurrence (mm).

These relationships are presented in Fig 3.

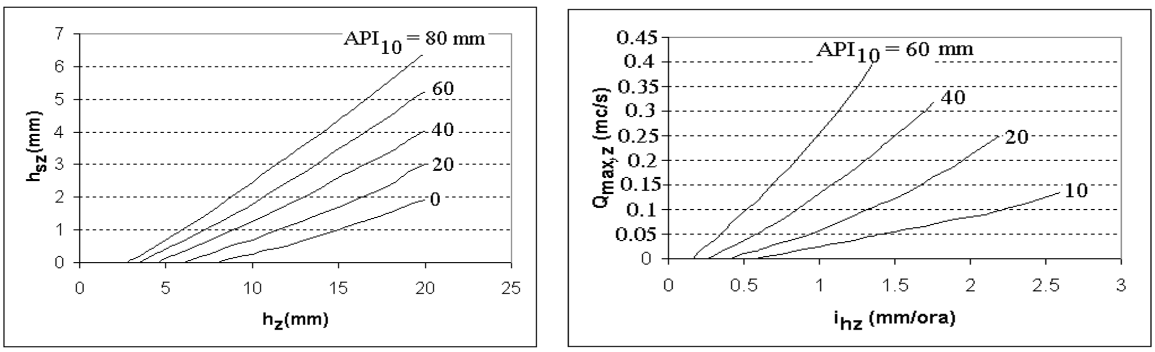

Fig 3: Relationships derived for floods of snowmelt origin (explanation of the symbols is given in the text above).

In the case of the increase and decrease duration of the flood wave, there also exist syntheses showing their dependency on the diurnal duration of the snowmelt process and on its intensity, in accordance with the air temperature variation. Such syntheses have been used to create the "synthetic" floods generated only by snowmelt.

RESULTS

By establishing the values of the flood characteristics (runoff depth and peak discharge) in the case of the floods of mixed origin and of the "synthetic" floods, a comparison of the respective parameters for the three types of floods could be made.

Runoff depth

The values of the runoff depth determined in the case of the flood waves of mixed origin, h_{sM} (mm), generated by certain precipitation amounts, P (mm), and certain water amounts produced by snowmelt, h_z (mm), were compared with the sum of the values of the runoff depth obtained separately from synthetic flood waves: h_{sp} given by rain and h_{sz} (mm) given by snowmelt ($h_{sp} + h_{sz}$).

In all the cases it was found that $h_{sM} > h_{sp}+h_{sz}$. The higher values of the runoff depth in the case of mixed floods, h_{sM}, in comparison with the sum ($h_{sp}+h_{sz}$) are justified through the acceleration of the snowmelt process, which is a function of the precipitation fallen on the snow surface.

The difference h_{sM}- ($h_{sp}+h_{sz.}$) has been calculated for all mixed floods. The analysis has shown that this difference, Δh_{sM}, favouring the mixed floods, depends on the share of the rainfall amount (P) within the total water inflow generating the mixed wave ($P+h_z$); $\beta = P/(P+h_z)$.

In order to prove this fact, both the Δh_{sM} difference and the β ratio have been determined (in percentage).

Thus:

$$\Delta h_{sM}(\%) = [h_{sM} - (h_{sp}+h_{sz})]/ (h_{sp}+h_{sz})*100$$

$$\beta (\%)= P/(P+h_z)*100$$

In the relationship $\Delta h_{SM}(\%)=f(\beta, P+h_z)$ presented in Fig 4, it can be noticed that the highest values of $\Delta h_{SM}(\%)$ are encountered in the area of the values β = 55 - 75%, irrespective of the total water inflow amount ($P+h_z$).

Consequently, the difference between the values of the runoff depth in the case of mixed floods (h_{sM}) and the sum of the runoff depths in the case of the "synthetic" floods ($h_{sp}+h_{sz.}$) is the largest when the share of rainfall (P) in total water inflow ($P+h_z$) varies between 55% and 75%. This means that in the case of such values of the rainfall share its influence upon snowmelt is the largest.

In Fig 4, a decrease of $\Delta h_{sM}(\%)$ values as β approaches 100% can also be observed. This means that when there is a significant increase in the rainfall share β, the water inflow coming from snowmelt (h_z) decreases considerably.

Finally, values of the rainfall share of β = 100% are reached when h_z=0 and the value $\Delta h_{SM}(\%)$=0. Because snow does not exist any more, there are no supplementary yields coming from its melting.

$\Delta h_{sM}(\%)$ also decreases in the region with low values of the β parameter. This means that due to the rainfall share decrease, the accelerating effect of the snowmelt process also decreases. Thus, for values of β=0% values of Δh_{sM}=0% will result because factors affecting the snow depth do not exist.

The same relationship points out the fact that in absolute value Δh_{sM} does not record significant variations in the conditions of the total water inflow variation ($P+h_z$). This means that rainfall has a certain potential with respect to snowmelt process acceleration to induce a higher variation of the water equivalent in the snow depth.

Peak discharge

The comparative analysis of mixed floods ($Q_{max\ M}$) with the peak discharges of the "synthetic" floods generated only by rainfall ($Q_{max\ P}$) and only by snowmelt ($Q_{max\ Z}$), has proved to be more complex than in the case
of the runoff depth analysis. This is due to many factors, affecting not only the peak discharge value but also the time of its occurrence for the mixed floods. It is worth mentioning some of these factors: quantity and intensity of the rainfall over the snow, snow cover characteristics (depth, density, water equivalent), and others.

In addition to this, the rainfall nucleus and the maximum intensity of the snowmelt are recorded at different moments. Rainfall can be observed at any time during the day, while the maximum intensity of snowmelt is recorded only after the maximum air temperature has been reached. Within this context, the peak discharge recorded for mixed floods, ($Q_{max\ M}$), has not been compared to the sum of the peak discharges corresponding to both "synthetic" floods, ($Q_{max\ P}+Q_{max\ Z}$).

Within this analysis, the values $Q_{max\ P}$ were first determined from the synthesis relationships, for the same characteristics of the rainfall P existing in the case of the flood wave of mixed origin (amount, intensity, the moment of recording of the nucleus). In the case of the synthetic flood wave from snowmelt a certain discharge, Q_Z, which corresponded to the time of occurrence of the maximum discharge $Q_{max\ P}$ was considered. Thus, $Q_{max\ M}$ has been compared to the sum ($Q_{max\ P}+Q_Z$). Under these conditions, ($Q_{max\ M}$) was smaller than the sum ($Q_{max\ P}+Q_Z$).

For the comparative analysis, the reducing coefficient of ($Q_{max\ M}$) with respect to the sum ($Q_{max\ P}+Q_Z$) was defined: $\Delta Q_{max\ M}(\%)$.

$$\Delta Q_{\max M}(\%) = [(Q_{\max P} + Q_Z) - Q_{\max M}]/(Q_{\max P} + Q_Z) \cdot 100$$

This coefficient has been correlated, as in the case of the runoff depth, with the β parameter.

In Fig 5 the relationship $\Delta Q_{max\ M}(\%) = f(\beta\ P+h_z)$ is shown.

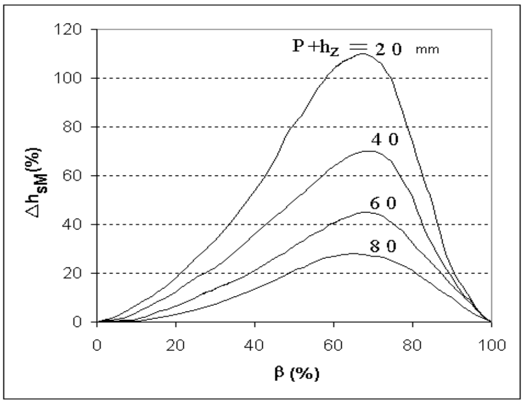

Fig 4: The realationship $\Delta h_{SM} = f(\beta, P+hz)$.

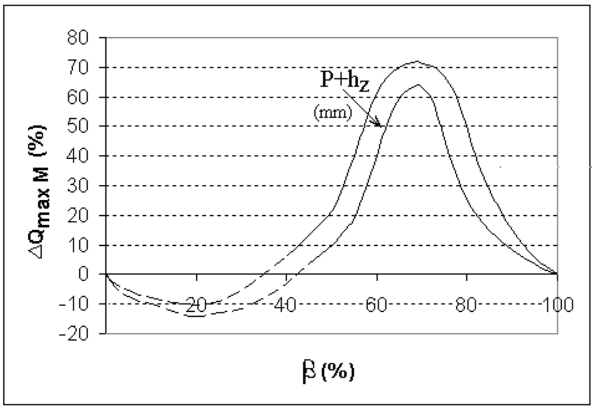

Fig 5: The realationship $\Delta Q_{max,M} = f(\beta, P+hz)$.

It is worth to emphasise the fact that the relationship refers to a more restricted domain of the total water inflow variation ($P+h_z$): between 40 and 60mm. The analysed rainfall intensity has varied between 0.15 and 0.25 mm/min. As the relationship has shown, the biggest attenuation of $Q_{max\ M}$ is recorded in the range β = 60%-80%. This can be explained by the fact that at such rainfall values (amounts, intensity), the synthetic flood wave has a much higher discharge than the mixed floods. (It is taken into account that water inflow $P + h_z = 40 - 60$ mm and the rainfall share β > 60%, P > 25 mm). For β > 80%, the values of $Q_{max\ P}$ increase as the rain increases. To a certain degree the values of $Q_{max\ M}$ will also increase, being determined more by precipitation than by snowmelt. The result will be a decrease of $\Delta Q_{max\ M}$. For β = 100%, $Q_{max\ M} = 0$, because the discharge will be generated only by rainfall. In the case in which the rainfall share decreases towards zero, a significant decrease of the $\Delta Q_{max\ M}$ parameter can be noticed. This parameter may have negative values at rainfall shares less than 30-40%. The explanation is that at such rainfall shares, the rainfall amount is quite small, with a little more than 10 mm (in the relationship in Fig 5, the values $P+h_z$ = 40 - 60 mm).

At such precipitation amounts and intensities (0.15 - 0.20 mm/min) the discharges are very small. In spite of this, the snowmelt originated discharges, at rainfall shares of 60-70%, and h_z>25 mm, are relatively high. They will condition values of the mixed flood peak discharge to be higher than the sum resulting from discharges of both synthetic hydrographs. Because the rainfall originated discharge will not be taken into account, but the rainfall amount, even small, will accelerate the snowmelt process, causing a higher discharge value.

CONCLUSIONS

The comparative analysis of the main characteristics of rainfall–snowmelt originated floods (depth of runoff and peak discharge) with those of flood waves originated from rainfall or snowmelt only, considering the same generating parameters (water inflow and soil moisture index), shows an increase of the runoff depth and a decrease of the peak discharges of the mixed flood waves.

The results of this analysis are very important for flood forecasting, giving the possibility to quantitatively estimate the characteristics of mixed floods, especially the depth of runoff, in small mountain river basins which can be considered "warning basins" for larger basins in a flood forecasting model (Diaconu and Stanescu, 1976).

REFERENCES

Diaconu, C., Stanescu, V. Al. (1976) A mathematical model for flood wave forecasting by means of warning basins. *Hydrological Sciences Bulletin*, XXI, No. 3, Bucharest, Romania.

Miță, P., Stancalie, G. (1996) Methods of computing of the variation of the characteristics of the snow cover and runoff generated by snowmelting.. Ed. Centre d'Etudes et de Recherces Eco-Geographiques. CEREG, Strasburg - France.

Miță, P., Simota, M., Stancalie, G., Popovici, F., Catana, S. (1999) Some results regarding the diminishing role of the forest in sediment runoff for snowmelt – generate floods, Proceedings of the Symposium: *Vegetation, Land Use and Erosion Processes*, Bucharest, Romania.

USING GROUNDWATER LEVEL MONITORING AS A TOOL FOR ESTIMATING RUNOFF COEFFICIENTS IN THE ALZETTE RIVER BASIN (GRAND-DUCHY OF LUXEMBOURG)

L. Pfister[1], G. Drogue[1], A. El Idrissi[1], J. Humbert[2], J.-F. Iffly[1], P. Matgen[1], L. Hoffmann[1]

[1]*CREBS – Cellule de Recherche en Environnement et Biotechnologies, Centre de Recherche Public – Gabriel Lippmann 162a, avenue de la Faïencerie, L-1511 Luxembourg, Grand-Duchy of Luxembourg*
[2]*Université Louis Pasteur – UFR de Géographie 3, rue de l'Argonne, F-67083 Strasbourg cedex, France*

ABSTRACT

The role of groundwater resurgence on runoff coefficients was investigated in the Alzette river floodplain, upstream of Luxembourg-city (Grand-Duchy of Luxembourg). A threshold in the saturation level was identified through the calculation of a water balance at a daily time step. This threshold appeared to coincide with groundwater resurgence in the Alzette river floodplain. Once groundwater resurgence appears, runoff coefficients reach their maximum level of approximately 70%, regardless of individual rainfall event totals. Groundwater level monitoring can thus serve as a tool for evaluating the overall saturation level, as well as the runoff coefficients that are to be expected in case of rainfall.

Keywords Alzette basin, groundwater resurgence, runoff coefficients

INTRODUCTION

In north-western Europe, floods are preferentially caused either by excessively heavy and/or excessively prolonged rainfall. The activation and the interaction of hydrological processes in a river basin are dependent on a combination of various factors; defined as meteorological parameters, land use, soil moisture and physical properties (Ambroise, 1998). Flood generating processes can be classified into four major categories: direct precipitation, overland flow, throughflow and groundwater flow (Musy and Higy, 1998).

Saturation overland flow, combined with return flow, occur on variable source areas, also described as 'saturated contributive areas' by Cosandey and Robinson (2000), as a result of prolonged rainfall, preferentially in riparian zones (Joerin, 2000). These flood-producing processes cause large volumes of quickflow that reach the stream channels very rapidly during and immediately after a rainfall event (Smith and Ward, 1998).

Merz and Plate (1997) have outlined that the influence of the spatial variability of soils and soil moisture on runoff is reduced for very small and for large events, while it plays a major role for medium-sized rainfall events. Hangen et al. (2001) have identified in a micro-scale basin in south-western Germany three stages with different contributions of the single runoff components and source areas: 1) a rapid release of water by soil water displacement/fast infiltration in the near-channel area, supplemented by saturation overland flow, 2) a fast depletion of the near-channel reservoir comprising soil water and groundwater and 3) a delayed reaction of the hillslope aquifer.

The concept of variable source areas has been transposed to the macro-scale Alzette river basin (Grand-Duchy of Luxembourg), where the role of groundwater resurgence on flood genesis has been investigated. Since the early 1990's, high-magnitude floods have caused important damages in the Alzette river basin on several occasions. A significant increase in winter maximum daily streamflow of the Alzette over the last decades has been clearly linked to a positive trend in winter rainfall totals due to westerly atmospheric fluxes (Pfister et al., 2000). With increasing winter rainfall totals, extended periods with groundwater resurgence are expected to increase the probability of conditions that are propitious to flood genesis.

THE ALZETTE RIVER BASIN

The Alzette experimental basin (1172 km^2) is located in the Grand-Duchy of Luxembourg at an altitude ranging from 200 to 539 m.a.s.l. The average annual temperature is 8.3°C and the average annual rainfall is 876 mm. The underlying bedrock mainly consists of superimposed strata of sandstone and marls. On its northern border, the Alzette basin is limited by schists that are part of the Ardennes massif. Since 1995, public authorities and the Public Research Centre – Gabriel Lippmann have built-up a complementary stream and raingauge network in the Alzette basin. The network has been designed to monitor subbasins that are representative of the large physiographic diversity of the Alzette basin. Since 1996, 12 raingauges and 23 streamgauges (recording at a 15-minute time step), in addition to an already existing network of more than 50 pluviometers (measurements at daily time step), are monitoring rainfall and streamflow in the Alzette basin. The sizes of the 23 monitored subbasins vary between 0.8 and 1172 km^2. Upstream of Luxembourg-city, the observation network has been completed with 3 piezographs, monitoring groundwater levels at an hourly time step since 1996.

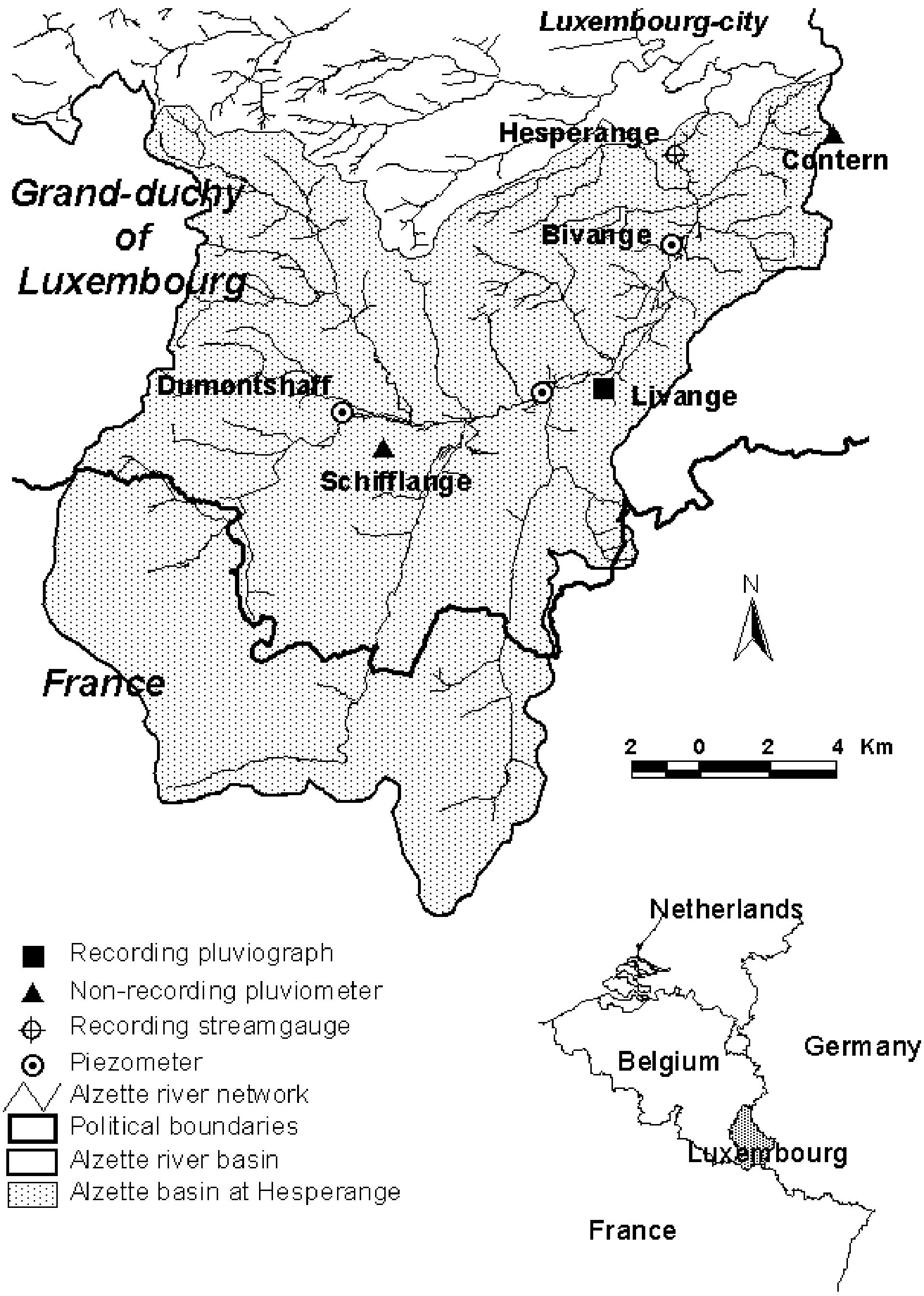

Fig 1: Location of the Alzette river basin and hydroclimatological measuring network upstream of Luxembourg-city.

THE STUDY AREA

The Alzette river originates in France, approximately 4 km south of the French-Luxembourg border (Fig 1). The Alzette river basin covers an area of 1172 km^2 and the valley accommodates almost 2/3 of the population of Luxembourg, as well as an important part of the industrial infrastructure. The study area is restricted to the Alzette floodplain, located upstream of Luxembourg-city and covers 291.3 km^2 (upstream of the Hesperange streamgauge).

The topography of the floodplain is characterised by a natural sandstone bottleneck, located near Luxembourg-city. Upstream of the bottleneck, the valley is up to 2.5 km wide, while in the Luxembourg sandstone the valley is only 75 meters wide. Moreover, the sandstone extends approximately 80 meters below the surface. Over the study area, elevations range from 260 to 441 m.a.s.l. The geological substratum of left-bank tributaries of the Alzette river is dominated by marls, while the right-bank tributaries have limestone and sandstone deposits due to a natural bottleneck of sandstone. The depth of alluvial deposits varies between 4 m (near Dumontshaff) and 8 m (near Hesperange). Sand, gravel, as well as marls and clay alternate in the alluvial deposits (Marx, 1987).

GROUNDWATER RESURGENCE AS A RUNOFF GENERATING PROCESS IN THE ALZETTE RIVER FLOODPLAIN

Observations of rainfall, streamflow and groundwater have confirmed the pluvio-evaporal type of the hydrological regime of the Alzette (Pfister, 2000), with highest runoff values being recorded during winter and lowest runoff values occurring during summer. During winter months, high rainfall totals and lower evapotranspiration cause a progressive rise of both groundwater levels and streamflow. Storm runoff is mainly generated in the western part of the Alzette basin, where highest rainfall totals and impermeable geological substratum are overlapping (Pfister et al., 2002). During winter months, groundwater resurgence starts close to the natural bottleneck near Luxembourg-city and then progressively extends further upstream. Recorded piezometric levels tend to stabilise at a maximum level, once groundwater resurgence is reached (see example of the piezometric well in Bivange, Fig 2).

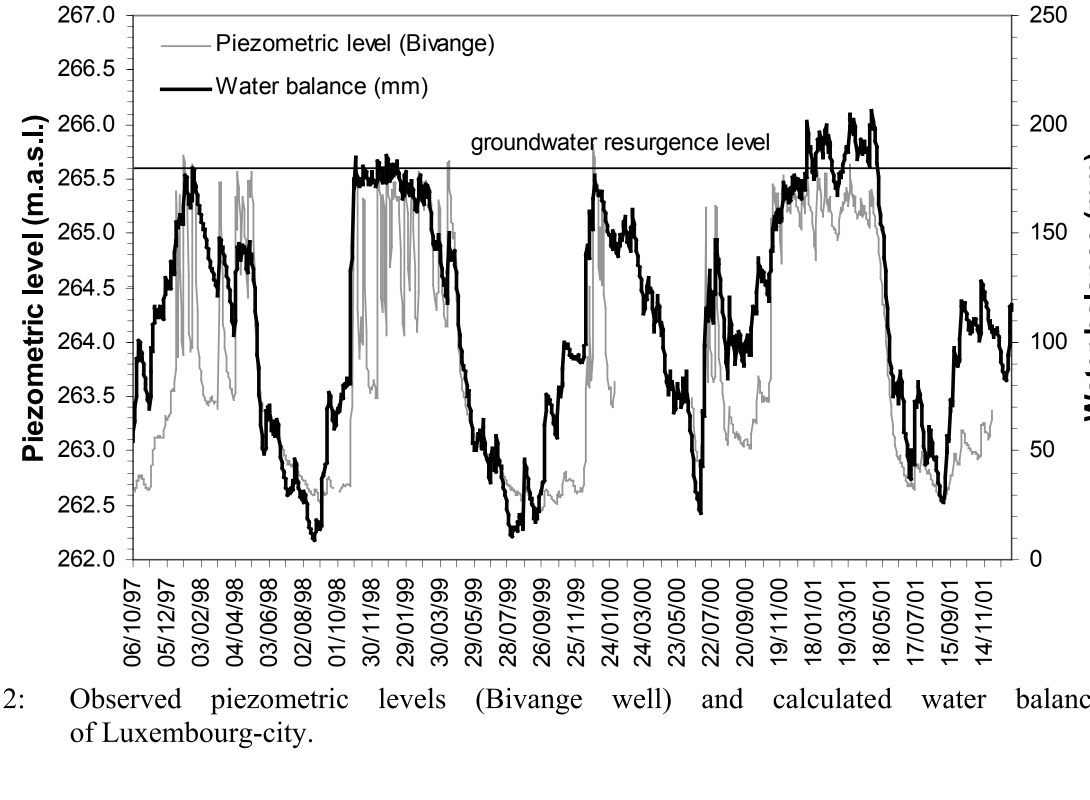

Fig 2: Observed piezometric levels (Bivange well) and calculated water balance upstream of Luxembourg-city.

The assumption was made that the natural bottleneck of the Alzette hampers the downstream progression of groundwater and thus causes a rapid rise of piezometric levels upstream of the bottleneck. As a consequence, once groundwater resurgence covers large areas of the floodplain, runoff coefficients increase and cause an important rise of streamflow and ultimately of flooding.

A water balance was calculated in order to analyse the evolution of the water stock within the Alzette basin throughout the hydrological year, as well as its impact on runoff coefficients and on runoff. The water balance was calculated on a daily time-step as follows:

$$WB_{(t)} = R_{(t)} - Q_{(t)} - AET_{(t)} + WB_{(t-\Delta t)}$$

With, $R_{(t)}$ = mean daily rainfall
$Q_{(t)}$ = mean daily streamflow at Hesperange streamgauge station
$AET_{(t)}$ = mean daily actual evapotranspiration (based on Penman-Monteith PET calculations)
$WB_{(t)}$ = water balance, i.e. amount of water stored at time t in the catchment upstream of Luxembourg-city.

The water balance shows a maximum threshold, around 180 mm, close to the groundwater resurgence level (Fig 2). In each hydrological year, the water balance reaches a maximum level almost at the same time that groundwater resurgence occurs. Groundwater resurgence at the piezometric well at Bivange corresponds to a water balance level of approximately 180 mm.

The impact of the overall basin saturation is illustrated by the almost linear relationship between water balance and runoff coefficients determined for winter rainfall events that occurred between October 1997 and March 2001 (Fig 3). The closer the water balance is to the saturation limit, the higher the runoff coefficients are. In case of snowfall, runoff coefficients are slightly inferior for a given water balance value, due to the progressive snowmelt process.

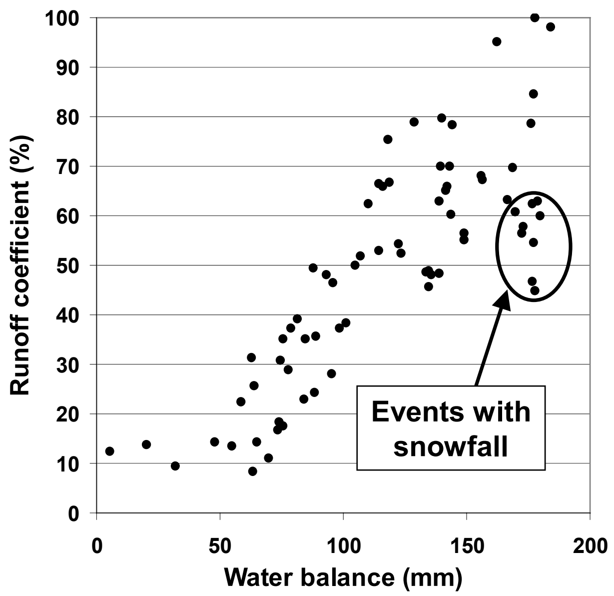

Fig 3: Relationship between water balance and runoff coefficients on rainfall event scale.

For rainfall events that occurred while the water balance was equal to or exceeding 180 mm, a linear relationship was observed between total event rainfall and total event runoff of the Alzette (Fig 4). During overall saturation conditions, runoff thus amounts to more or less 70% on average of total rainfall. This further illustrates the key role played by the complete saturation of the river system.

A very close relationship exists between water balance and piezometric levels in the Alzette river floodplain, upstream of Luxembourg-city (Fig 5). The highest water balance levels are reached at groundwater resurgence, equally corresponding to the highest runoff coefficient, reaching an average of 70% at the rainfall event scale.

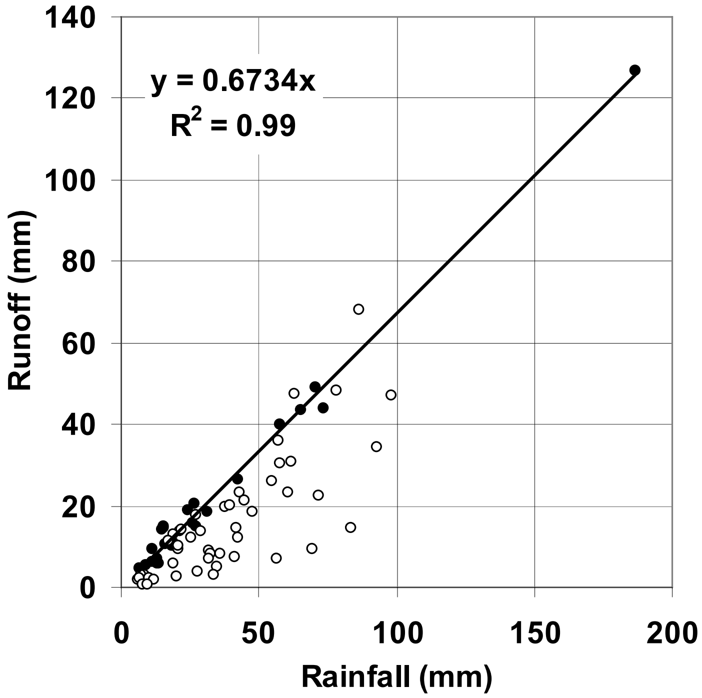

Fig 4: Relationship between rainfall and runoff upstream of Luxembourg-city (black dots = rainfall events occurring at total saturation conditions; formula applies to black dots).

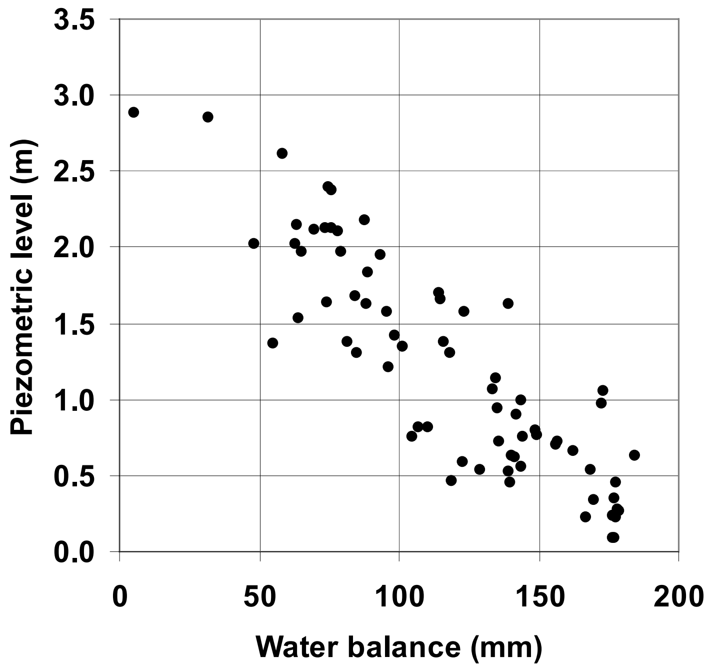

Fig 5: Relationship between water balance and piezometric levels (piezometric level = average distance between soil surface and groundwater at 3 piezometric stations).

CONCLUSION

A clear relationship between the saturation level (documented by water balance values), piezometric levels and runoff coefficients has been determined for the Alzette river basin upstream of Luxembourg-city. During winter months, incident rainfall causes the groundwater table to rise, ultimately saturating large parts of the Alzette floodplain. The storage capacity of the basin is moreover strongly limited by a natural sandstone bottleneck. Runoff coefficients can thus reach very high levels once groundwater resurgence has spread over large parts of the floodplain.

The strong relationship between piezometric levels, water balance values and runoff coefficients suggests the use of groundwater monitoring as a complementary tool in flood alert systems, groundwater levels close to resurgence indicating high runoff coefficients and thus propitious conditions for flood genesis.

REFERENCES

Ambroise, B. (1998) Genèse des débits dans les petits bassins versants ruraux en milieu tempéré: 1- Processus et facteurs. *Revue des Sciences de l'Eau*, 11, 471-495.

Cosandey, C., Robinson, M. (2000) Hydrologie continentale. Armand Colin, Paris, 360 pp.

Hangen, E., Lindenlaub, M., Leibundgut, C., von Wilpert, K. (2001) Investigating mechanisms of stormflow generation by natural tracers and hydrometric data: a small catchment study in the Black Forest, Germany. *Hydrological Processes*, 15, 183-199.

Joerin, C. (2000) Etude des processus hydrologiques par l'application du traçage environnemental. Association à des mesures effectuées à l'échelle locale et analyse d'incertitude. PhD thesis, Ecole Polytechnique Fédérale de Lausanne, Switzerland, 234 pp.

Marx, M. (1987) Verhalten des Grundwasserspiegels im Alluvium des Alzettetals für den Raum Livingen-Berchem. Travail de fin d'études, Institut Supérieur de Technologie, Luxembourg, 43 pp.

Merz, B., Plate, E.J. (1997) An analysis of the effects of spatial variability of soil and soil moisture on runoff. *Water ResourcesRresearch*, 33, 2909-2922.

Musy, A., Higy, C. (1998) Hydrologie appliquée. Ecole Polytechnique de Lausanne. 366 pp.

Pfister, L. (2000) Analyse spatio-temporelle du fonctionnement hydro-climatologique du bassin versant de l'Alzette (Grand-duché de Luxembourg). Détection des facteurs climatiques, anthropiques et physiogéographiques générateurs de crues et d'inondations'. PhD thesis, Université Louis Pasteur, Strasbourg, France, 240 pp.

Pfister, L., Humbert, J., Hoffmann L. (2000) Recent trends in rainfall-runoff characteristics in the Alzette river basin, Luxembourg. *Climatic Change*, 45, 323-337.

Pfister, L., Humbert, J., Iffly, J.-F., Hoffmann L. (2002) Use of regionalized stormflow coefficients in view of hydro-climatological hazard mapping. *Hydrological Sciences Journal*, 47, 479 – 491.

Smith, K., Ward, R. (1998) Floods – Physical processes and human impacts. John Wiley & Sons: New York, 382 pp.

MONITORING HYDROLOGICAL PROCESSES IN MONTANE AND SUBALPINE KARST REGIONS: COMPARISON BETWEEN DIFFERENT TYPES OF VEGETATION. EXPERIMENTAL DESIGN, TECHNIQUES AND FIRST RESULTS.

R. Köck[1], E. Härtel[2], C. Holtermann[2], E. Hochbichler[1], H. Hager[3], K. Schönthaler[2]

[1] *Institute of Silviculture, University of Agricultural Sciences, Peter Jordanstr. 70, 1190 Vienna, Austria.*
[2] *Institute of Landscape Architecture and Landscape Management, Univ. of Agricult. Sciences, Austria.*
[3] *Institute of Forest Ecology, University of Agricultural Sciences, Austria.*

ABSTRACT

On the Rax Alpe, a mountain site in the Northeastern Calcareous Alps of Austria, five experimental plots have been selected with representative types of vegetation cover (forest, krummholz and subalpine grassland) in order to describe hydrological parameters for these vegetation classes. The research area is located in the water resources protection zone for the drinking water supply of the City of Vienna. Three vegetation types were analysed in the montane zone (1000 m a.s.l.): a mixed spruce-fir-beech stand (B1), a homogeneous spruce plantation (F1) and a regeneration area (B2). Two vegetation types were analysed in the subalpine zone (1800 m a.s.l.): a subalpine grassland (A1) and a krummholz area (L1 - *Pinus mugo*). A comparable set of measuring instruments was installed on each experimental plot. Differences between the specific vegetation types, which seem to be significant for the hydrology of these karstic headwaters, could be outlined by the comparison of various parameters.

Keywords karst, forest, krummholz, subalpine grassland, interception, soil moisture

INTRODUCTION

The City of Vienna receives about 95 % of its drinking water from the Northeastern Calcareous Alps of Austria. The watershed areas there are covered with forests, alpine grasslands or are simply barren rock areas. In order to estimate hydrological differences between representative types of vegetation, five experimental plots have been installed on the Rax Alpe, which is a mountain within the water resources protection zone of the City of Vienna. Within the montane and subalpine zones, the investigated vegetation classes are compared with regard to specific hydrological parameters. Through comparison, hydrological differences between the vegetation classes can be emphasized. The study also contributes to the formulation of management guidelines that define the most adequate forest composition, forest structure and land use practices in order to optimise water quality and water yield for the drinking water supply of the City of Vienna.

METHODS

A comparison between the specific vegetation classes, which are represented by the experimental plots, has been conducted on three plots within the montane zone and on two plots within the subalpine zone. In order to represent widespread forest types of the montane zone, a natural old grown mixed stand of spruce, fir and beech (B1, natural vegetation about 150 years old), a homogeneous 60 year old spruce plantation (F1) and a regeneration area (B2, young trees and clearcut vegetation) have been selected as appropriate for the installation of three experimental plots. They are situated at the same altitude (1040 m a.s.l.), they have the same inclination (30°), similar aspects (from SW to W) and relatively similar soil types (with regard to the highly variable karst soils). The soils are calcareous leptosols and the bedrock is dolomite mixed with limestone particles. On the forested plots the humus layers are thick and variable, on the regeneration plot the humus layers are shallow and relatively homogenous. The thickest humus layers can be found on the B1 plot (the natural mixed stand of spruce, fir and beech). On all three plots the potential natural forest community is *Helleboro-Abieti-Fagetum typicum* (Zukrigl, 1973; Köck et al., 2002). On the Rax plateau, two experimental plots have been installed at 1840 m a.s.l. The first one is situated within a krummholz area (L1 - *Pinus mugo*) and the second one within an open subalpine grassland (A1). Krummholz vegetation and subalpine and alpine grasslands cover large areas of these altitudinal regions. The area on the Rax plateau is level and slightly undulating, the soils on both plots are chromic cambisols and the bedrock is limestone. The humus layer on the krummholz area (L1) is shallow and homogeneous (around 5 cm), while there is only mull-humus on the grassland plot (A1).

On all five plots a comparable set of measuring instruments has been installed. In order to guarantee measurement cycles throughout the year, data loggers have been installed in plastic boxes within the soils. The data loggers are MiniCube loggers from EMS (Environmental Measuring Systems, Brno). Air temperature and relative humidity were measured at a height of 2 m on all five plots. Soil temperature was measured at 5 cm, 15 cm, 30 cm and 45 cm depths on all five plots. Wind speed was measured 2 m above the ground on all experimental plots except L1 (krummholz-plot) and 2 m above the crowns of two dominant trees in B1 (spruce-fir-beech plot) and in F1 (spruce plantation plot). Solar radiation was measured 3 m above the ground at two places: in B2 (regeneration plot), which is the open reference base within the montane zone and in A1 (subalpine grassland), which is the open reference base within the subalpine zone. Soil moisture was measured at depths of 20 cm and 50 cm in the montane zone, using "Frequency Domain" (FD) probes (Delta-T Devices Ltd. 1999). These probes have been installed at 5 locations in B1 and three locations in F1 and B2. Within the subalpine zone, soil moisture probes have been installed at depths of 20 cm and 35 cm below the soil surface. Both on the A1 plot and on the L1 plot, the measuring design has been installed in two locations. Because of the high gravel contents of the karstic soils, the theta probes have been installed horizontally in such a way that the rods are surrounded by homogenised autochthonous soil material, settled to its natural bulk density, instead of inserting them into the natural layered soil. This approach was selected because of the significant underestimation of soil moisture content caused by gaps of soil around the rods, which frequently occurs if the sensors are placed into undisturbed rocky soils (v. Wilpert et al., 1998). The soil where the sensor is inserted should also not be compacted (Robinson et al., 1999). The theta probes were installed only into the undisturbed soil within the naturally dense and homogeneous humus layers. Börner et al. (1996) found a strong linear relationship between the volumetric water content of litter measured by TDR probes and the litter water content calculated from gravimetric values.

In order to describe the precipitation events, bulk raingauges have been installed for measuring precipitation in the open area (gross rainfall) in B2, close to B1 and in A1. Within the montane zone, canopy throughfall collectors have been installed at all three plots: five in B1, three in F1 and two in B2. In the subalpine zone, six canopy throughfall collectors have been installed in L1 within the krummholz bushes. At the B1 plot where beech is growing, stemflow gauges have been installed on three beech trees in order to characterise interception losses for this mixed stand (spruce, fir, beech, maple). Stemflow on spruce occurs with quantities around 1 % or less and was therefore considered negligible (Hager and Holzmann, 1997). During the winter season, snow cover (snow depth) and the water equivalent of the snow cover have been investigated at all plots, following a snow course scheme.

At all five plots, lysimeters have been installed in order to obtain seepage water for water quality analysis. The suction lysimeters (ceramic cups with 8 cm diameter) were installed 15 cm and 60 cm below the soil surface at the three plots in the montane zone. In B1 this device has been set up in six locations, in F1 and B2 in three locations. Due to the soil properties in the subalpine zone (high rates of rock material in the deeper soil horizons), the ceramic cups have been installed there at depths of 15 cm and 30 cm. At the A1 and L1 plot the lysimeter device has been set up in two locations. The seepage water samples were analysed for nitrate, ammonium, calcium, potassium, magnesium, sodium, pH value and electric conductivity.

FIRST RESULTS AND DISCUSSION

Monitoring of precipitation, canopy throughfall and stemflow during three summer seasons showed high variation of these parameters as a function of the characteristics of precipitation events. Rainfall in general is a phenomenon which shows high spatial variability (Lopes, 1996; Hanson et al., 1989). Between the two experimental plots B1 (spruce-fir-beech plot) and F1 (spruce plantation) in the montane zone, gross annual rainfall shows some variability (see Table 1, GR). Interception within the stands (B1 and F1) is highly variable (Durocher, 1990), and each precipitation event shows different interception rates depending on the intensity of rainfall (Price et al., 1997) and other meteorological variables (such as temperature, wind, etc.). Due to the high variability of the canopy structure within the mixed stand B1 (spruce-fir-beech plot) in relation to the homogeneous stand in F1 (spruce plantation), the variability of canopy throughfall is also higher in B1 than in F1; the standard deviation of canopy throughfall is therefore higher in B1 than in F1 (Table 1). Stemflow on the beech trees within B1 is responsible for the difference in net precipitation between the mixed stand (B1) and the spruce plantation (F1). It also seems to be obvious that higher values of gross precipitation in wet years (e.g. 1999) lead to higher net precipitation than years with lower values of gross precipitation (e.g. 2001, Table 1). The variation of interception loss for each precipitation event is dependent on the intensity of rainfall. Intensive rainfall leads to lower interception rates than less intense rainfall. In F1 (spruce plantation) interception loss (on an event basis) during the measurement period in 2000 ranged between 8.9 % and 81.3 %. During the measurement period in 2001 the interception loss in F1 ranged between 22.2 and 67.6 %. The years with higher rainfall amounts also show higher net precipitation.

Table 1: Overview for summer canopy throughfall and net precipitation for a mixed spruce-fir-beech stand (*B1*) and a homogeneous spruce plantation (*F1*).

		B1		F1
1999	Ctf	65.8 %	Ctf	69.7 %
	StD	± 5.3 %	StD	± 3.9 %
	Ste	7.3 %	Ste	--
	NeP	73.1 % (GR: 1178 mm)	NeP	69.7 (GR: 1226 mm)
2000	Ctf	60.5 %	Ctf	61.6 %
	StD	± 6.0 %	StD	± 0.8 %
	Ste	6.5 %	Ste	--
	NeP	67,0 % (GR: 882 mm)	NeP	61.6 % (GR: 901 mm)
2001	Ctf	53.6 %	Ctf	53.0 %
	StD	± 4.4 %	StD	± 3.1 %
	Ste	6.6 %	Ste	--
	NeP	60.2 % (GR: 813 mm)	NeP	53.0 % (GR: 891 mm)

Ctf is the canopy throughfall (calculated as the mean of all troughs on each plot), *StD* is the standard deviation of canopy throughfall for each plot, *Ste* is the stemflow on beech (calculated as the value for the whole plot area of B1), *NeP* is the net precipitation (which is identical with canopy throughfall in F1 and which is the sum of canopy throughfall and stemflow in B1), and *GR* is gross rainfall (mm). Values are expressed as a percentage of *GR*.

In the subalpine zone, interception loss within the krummholz plot (L1 - *Pinus mugo*) is highly variable. Interception rates constituted between 19 % and 65 % of gross rainfall, while at the same time one trough received 118 % of gross rainfall. The variations of canopy throughfall within the krummholz plot could be related to stemflow dynamics of the *Pinus mugo* plants, which have not been measured because of technical obstacles due to the shape of this plant. *Pinus mugo* grows with a high variation in the angle of its branches, so that locating the place for mounting stemflow gauges is not simple. In the desert of Arizona it was possible to mount stemflow gauges at the base of creosote bushes (*Larrea tridentata*) (Whitford et al., 1997), by a technique that is not applicable for *Pinus mugo.* Another reason for the canopy throughfall variations could be the capability of *Pinus mugo* to intercept moisture from fog and clouds (occult precipitation). At the edges of the krummholz groups, a higher rate of moisture is likely to be intercepted. In other montane forests of the earth, occult precipitation is an important quantity (Hunzinger, 1997; Flemming, 1993). Wind-driven rainfall can also have the effect of inhomogeneous distribution of canopy throughfall (Herwitz and Slye, 1995). The canopy throughfall troughs quantify occult precipitation only as a unit together with gross rainfall, therefore it is not possible to measure the percentage of total precipitation which is occult precipitation with this technique.

Soil temperature is influenced by vegetation cover. In the subalpine zone, soil temperature (at a 5 cm depth) on the open subalpine grassland (A1) reaches maxima which are more than 7°C warmer than on the krummholz area (*Pinus mugo* plot L1- on 10 June 2000 – Fig 1). The monthly means during the summer season 2000 were also higher in A1 than in L1; the difference, viewed over all measured soil horizons, varied between 0.5°C and 4°C. The trend of higher soil temperatures in A1 during the summer season was inverted during the winter season, where L1 exhibited warmer soil than A1. Within the krummholz, the soil did not freeze during the winter season (e.g. 1999/2000) or froze only slightly in the upper horizon (e.g. 2000/2001), while the soil in A1 froze significantly (less than minus 1°C) and over all measured soil horizons. During the snowmelt period, higher soil temperatures under krummholz vegetation (L1) allowed melting water to percolate into the soil, while on the frozen soil in A1 (open grassland) percolation could not occur on the whole area during the same time.

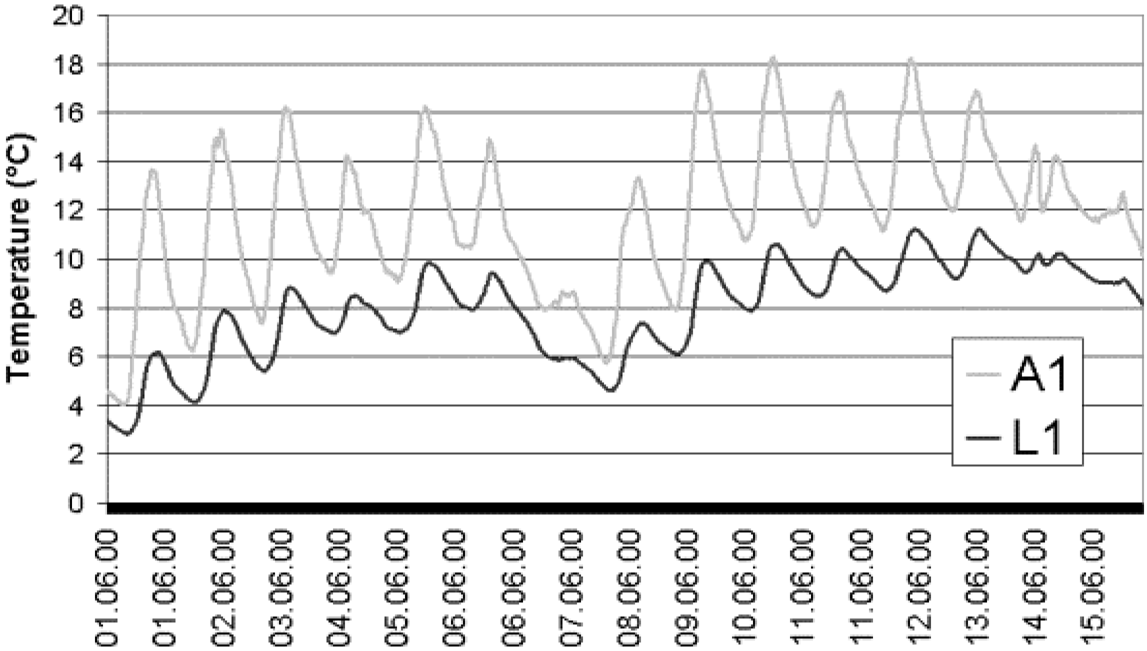

Fig 1: Soil temperature 5 cm below the soil surface: A1 (subalpine grassland) and L1 (krummholz area, *Pinus mugo*).

The effect of soil temperature during the winter season has been estimated by a comparative analysis of soil moisture and soil temperature dynamics during the snowmelt period in the spring season 2000 in the subalpine zone. Melting water or precipitation water percolates more easily into soils without ground frost than into frozen soils (Shanley and Chalmers, 1999). In the montane zone, soil temperature also shows the influence of vegetation cover. Peaks in soil temperature in the upper soil horizons differ on radiation days by 2°C to 7°C during the day time between the mixed forest stand B1 and the open regeneration plot B2, with higher soil temperatures occurring in B2. The homogeneous spruce plantation (F1) exhibits slightly higher soil temperatures than the mixed stand in B1. Soil temperature is a key parameter for many geo-chemical processes, which start to be evident after using the clearcutting technique of harvesting (Likens and Bormann, 1995; Reynolds et al., 1992; v. Wilpert et al., 2000; Martin et al., 2000).

Soil moisture dynamics showed different behaviour for each vegetation type. In the subalpine zone for example, soil moisture remained higher under krummholz vegetation (L1 - *Pinus mugo*) than under subalpine grassland vegetation (A1) after a winter season with a high level of snow accumulation (e.g. 1999/2000). During long lasting dry spells, which occurred in the year 2000 during the month of August, soil moisture dropped more quickly at L1 than at A1. In June 2000, soil moisture at every measurement plot in L1 was higher than in A1. In August the soil moisture levels in L1 were lower than in A1 at two plots. Soil moisture is, especially during dry periods, controlled by the soil type and vegetation (Gautam et al., 2000). During the dry spell in August 2000, soil moisture dropped more quickly under the krummholz vegetation than under subalpine grassland vegetation, which can be explained by a higher transpiration demand of *Pinus mugo* compared to grassland vegetation (Dirnböck and Grabherr, 2000). The high soil moisture content within the krummholz area in the summer months of 2000 can be related to high snow accumulation during the winter season of 1999/2000. The snowmelt water percolated with higher ease into the soils which were covered by krummholz vegetation. Variations of soil moisture conditions are higher within the krummholz area (L1) than within the subalpine grassland area (A1). This can be related to higher variability of precipitation distribution due to the growing shape of the *Pinus mugo* plants. Variations of soil moisture conditions due to the variation of soils within the subalpine zone of the Rax are not substantial, because the soils on A1 and L1 are identical (chromic cambisols). Variations due to differing depths of groundwater table can also be excluded since groundwater is not relevant for karstic sites at this altitude, but variations due to groundwater do occur in watersheds with crystalline bedrocks (Beldring et al., 1999).

The analysis of the seepage water, which has been extracted by the lysimeters, showed the highest nitrate concentrations on the spruce plot F1 (8,7 mg NO^{3-}/l as the highest value). The regeneration area B2 had the lowest nitrate concentrations due to mobilisation and erosion and/or leaching of the nutrients which had been stored in humus and root biomass after the clearcut period. The clearcut was made after wind blowdown, which took place 25 years ago. On the plot in B1 the seepage water shows varying nitrate concentrations, which are generally lower than in F1. After clearcutting, the nitrate concentration in seepage water can reach high values (v. Wilpert et al., 2000; Likens and Bormann, 1995; Reynolds et al., 1992; Martin et al., 2000). In general, nitrate concentrations in seepage water in the Rax area are low, also in comparison with the karstic research area in the Northern Calcareous Alps of Tyrol at the Mühleggerköpfl (Smidt, 2001; Feichtinger et al., 2002). This may be due to lower atmospheric N inputs in the Rax area. The pH value and the electric conductivity of the seepage water generally increase with soil depth. The highest concentrations of nitrate and ammonium in precipitation water (crown throughfall) have been found beneath the crowns of spruce (in F1 and B1). The tendency of spruce to filter higher amounts of pollutants is also highlighted in other studies (Rothe et al., 1998; v. Wilpert et al., 2000; Adamson et al., 1993; Robertson et al.; 2000).

CONCLUSIONS

The installation of a comparable set of measuring instruments on five experimental plots in the water protection zone of the City of Vienna made it possible to monitor some hydrological processes within these karstic headwaters. The five experimental plots represent characteristic vegetation types within the water protection area. The setting of the instrumentation is suited for the operation of the sensors during the summer season as well as during the winter season. The first results of this project show hydrological differences between the monitored vegetation types. These differences can be used in order to elaborate more specific forest and land use management concepts for water protection purposes.

ACKNOWLEDGEMENTS

The project has been funded by the Viennese Water Works (Municipal Department 31), by the Forestry Office and Urban Agriculture (Municipal Department 49) and by the University of Agricultural Sciences, Vienna, Austria (Internal Research Stimulation Program). The continuation of the monitoring processes has been funded by the Austrian Federal Ministry for Education, Science and Culture and by the Municipal Departments 31 and 49 of the City of Vienna. The authors want to express their acknowledgements to the representatives of these institutions.

REFERENCES

Adamson, J.K, Hornung, M., Kennedy, V.H., Norris, D.A., Paterson, I.S., Stevens, P.A. (1993) Soil solution Chemistry and Throughfall Under Adjacent Stands of Japanese Larch and Sitka Spruce at Three Contrasting Locations. *Britain Forestry*, vol 66, no 1.

Beldring, S., Gottschalk, L., Seibert, J., Tallaksen, L.M. (1999) Distribution of soil moisture and groundwater levels at patch and catchment scales. *Agricultural and Forest Meteorology*, 98-99, 305-324.

Börner, T., Johnson, M.G., Rygiewicz, P.T., Tingey, D.T., Jarrell, G.D. (1996) A two-probe method for measuring water content of forest floor litter layers using time domain reflectometry. *Soil Technology*, 9, 199-207.

Delta-T-Devices Ltd (1999) Theta Probe Soil Moisture Sensor, User Manual. Burwell, Cambridge, England.

Dirnböck, T., Grabherr, G. (2000) GIS Assessment of Vegetation and Hydrological Change in a High Mountain Catchment of the Northern Limestone Alps. *Mount. Research and Development,* vol 20, no 2, 172-179.

Durocher, M.G. (1990) Monitoring spatial variability of forest interception. *Hydrological Processes*, vol 4, 215-229.
Feichtinger, F., Smidt, S., Klaghofer, E. (2002) Water and Nitrate Fluxes at a Forest Site in the North Tyrolean Limestone Alps. *Environmental Science and Pollution Research*, Special Issue 2, 31-36.
Flemming, G. (1993) Grundsätzliche Probleme bei der Berücksichtigung des Klimas in der forstlichen Standortslehre und Forstökologie. *Forstw.* Cbl., 112, 370-375, Verlag Paul Parey, Hamburg und Berlin.
Gautam, M.R., Watanabe, K., Saegsa, H. (2000) Runoff analysis in humid forest catchment with artificial neural network. *Journal of Hydrology*, 235, 117-136.
Hager, H., Holzmann, H. (1997) Hydrologische Funktionen ausgewählter naturnaher Waldökosysteme in einem alpinen Flusseinzugsgebiet. Projektendbericht. *Hydrologie Österreichs*, Österr. Akad. der Wissenschaften.
Hanson, C.L., Osborn, H.B., Woolhiser, D.A. (1989) Daily precipitation Simulation Model for Mountainous Areas. *Transactions of the ASAE*, St. Joseph, USA.
Herwitz, S.R., Slye, R.E. (1995) Three-dimensional modelling of canopy tree interception of wind-driven rainfall. *Journal of Hydrology*, 168, 205-226.
Hunzinger, H. (1997) Hydrology of montane forests in the Sierra de San Javier, Tucuman, Argentina. *Mountain Research and Development*, 17, 299-308.
Köck, R., Weidinger, H., Mrkvicka, A (2002) Berichte zur Standorstkartierung der Quellenschutzwälder der Stadt Wien, Teilgebiet I. Wiener Hochquellenwasserleitung. Forstamt und Landwirtschaftsbetriebe der Stadt Wien, Wien.
Likens, G.E., Bormann, F.H. (1995) Biogeochemistry of a forested ecosystem, 2nd edition, Springer Verlag.
Lopes, V.L. (1996) On the effect of uncertainty in spatial distribution of rainfall on catchment modelling. *Catena*, 28, 107-119.
Martin, C.W., Hornbeck, J.W., Likens, G.E., Buso, D.C. (2000) Impacts of intensive harvesting on hydrology and nutrient dynamics of northern hardwood forests. *Can. J. Fish. Aquat. Sci.*, 57 (Suppl. 2), 19-29.
Price, A.G., Dunham, K., Carleton, T., Band, L. (1997) Variability of water fluxes through the black spruce (*Picea mariana*) canopy and feather moss (*Pleurozium schreberi*) carpet in the boreal forest of Northern Manitoba. *Journal of Hydrology*, 196, 310-323.
Reynolds, B., Stevens, P.A., Adamson, J.K., Hughes, S., Roberts, J.D. (1992) Effects of clearfelling on stream and soil water aluminium chemistry in three UK forests. *Environmental Pollution*, 77, 157-165.
Robertson, S.M.C., Hornung, M., Kennedy, V.H. (2000) Water chemistry of throughfall and soil water under four tree species at Gaisburn, northwest England, before and after felling. *Forest Ecology and Management*, 129, 101-117.
Robinson, D.A., Gardner, C.M.K., Cooper, J. D. (1999) Measurement of relative permittivity in sandy soils using TDR, capacitance and theta probes: comparison, including the effects of bulk soil electrical conductivity. *Journal of Hydrology*, 223, 198-211.
Rothe, A., Kölling, C., Moritz, K. (1998) Der aktuelle Kenntnissstand: Waldbewirtschaftung und Grundwasserschutz. *AFZ/Der Wald*, 6, 291-295.
Shanley, J.B., Chalmers, A. (1999) The effect of frozen soil on snowmelt runoff at Sleepers River, Vermont. *Hydrological Processes*, 13, 1843-1857.
Smidt, S. (2001) Luft- Depositions- und Bodenwasseranalysen am Mühleggerköpfl / Nordtiroler Kalkalpen. *FBVA-Berichte*, 119, 61-72.
v. Wilpert, K., Nell, U., Lukes, M., Schack-Kirchner, H. (1998) Genauigkeit von Bodenfeuchtemessungen mit ‚Time Domain-Reflektometrie' in heterogenen Waldböden. Z. Pflanzenernähr. *Bodenk.*, 161, Wiley Vch Verlag, Weinheim, 179-185.
v. Wilpert, K., Zirlewagen, D., Kohler, M. (2000) To what extend can silviculture enhance sustainability of forest sites under the immission regime in Central Europe. *Water, Air and Soil Pollution*, 122, 105-120.
Whitford, W. G., Anderson, J., Rice, P. M. (1997) Stemflow contribution to the "fertile island" effect in creosotebush, *Larrea tridentate. Journal of Arid Environments*, 35, 451-457.
Zukrigl, K. (1973) Montane und subalpine Waldgesellschaften am Alpenostrand. Mitteilungen der Forstlichen Bundesversuchsanstalt No 101, Wien.

THE IMPACT OF INTERCEPTION LOSSES ON THE WATER BALANCE IN FORESTED MOUNTAIN RANGES

C. Cosandey[1], C. Martin[2], L. Savina[1], J.F. Didon-Lescot[2]

[1]*LGP, Cnrs, 1 place A Briand F92 190 Meudon,* cosandey@cnrs-bellevue.fr,
[2] *UMR 6012 "ESPACE", Equipe GVE, Département de Géographie, 98 Boulevard Edouard Herriot, BP 3209, F-06 204 NICE cedex 3, France*

ABSTRACT

Although it is commonly understood that forest reduces annual runoff, the amount of the reduction may vary considerably as a function of the soil and climatic conditions. Forest enhances evaporation through two main processes: 1) Deeper root systems use the water stored in the soil more efficiently during the summer period. As a result, more water is retained in the soil during the following autumn before the resumption of winter discharge, and annual runoff is reduced. 2) Loss by interception is greater in forested areas than for other types of vegetation cover during the winter months, mainly because of more efficient use of advective energy. Studies in small catchments on Mount Lozère (South of France) have shown that during the winter period, "actual" evapotranspiration (calculated by the water balance method) is higher than "potential" evapotranspiration (estimated using a standard equation). These differences are due to interception losses. During the study period, one small spruce-forested catchment was cut and replanted, while another grassland/heath catchment was left undisturbed. Interception losses for the two basins were compared. The study period (1982-1995) covered the pre-cut (1982-1987), cutting (1987-1989) and postcut/regrowth (1990-1995) periods. Results show that cutting the forest did reduce interception losses. However, the hydrological behaviour of the cut catchment changed back to its pre-cut behaviour relatively quickly and clearly before the new plants had developed enough to be considered as forest cover.

Keywords forest hydrology, interception, forest evaporation

INTRODUCTION

The hydrological impact of forest is one of the most controversial issues when it comes to studying the consequences of human activities on water resources (Calder, 1979, 1985; Morton, 1984, 1985). As early as 1982 – and the study is still a reference – Bosch and Hewlett concluded their study "A review of catchment experiments to determine the effect of vegetation changes on water yield and evaporation" by emphasizing the complex nature of the results. Only one thing was certain: "No experiment in deliberately reducing cover caused reductions in yield, nor have any deliberate increases in cover caused increases in yield." Obviously, then, if the forest has an impact on annual runoff, it is to reduce it. The reduction is all the greater when conditions include a large water deficit, abundant water reserves, and also frequent but light rainfall (Cosandey and Robinson, 2000).

Two mechanisms account for the reduction:

- First, the forest provides a larger surface for interception during rainfall and enough roughness to favour high air turbulence and, therefore, more efficient use of advective energy and a higher rate of evaporation. On the other hand, evaporation can limit plant transpiration, and it is difficult to evaluate the increase in overall evapotranspiration that results from the direct evaporation of intercepted water. It is not possible to know the value for the increase from direct measurements of the intercepted water that does not reach the soil, since a partial compensation can occur with a decrease in plant transpiration (the available energy is used more quickly in order to evaporate the water that is more easily available on the surfaces of leaves or branches).
- Second, because the forest is more deeply rooted, it has a greater potential soil moisture reserve (which secures its water supply when evaporation exceeds rainfall). A greater reserve allows more evaporation during the summer months, and therefore lower flows in autumn that start later in the season due to the larger amount of water taken up by the soil.

If a classic sequence of rain events for a hydrologic year in temperate climate is considered (Cosandey and Robinson, 2000), the forest delays the resumption of flows at the start of the rainy season, because the soil moisture reserves have been depleted by the trees during the dry season. Of course the delay is accompanied by a decrease in runoff. The forest also reduces winter flows directly, due to the direct evaporation of part of the precipitation that is intercepted by the canopy and does not reach the soil. Such higher winter evaporation naturally depends on the type of vegetation - a heath with broom growing on it is likely much more efficient than a broad-leaved forest.

Evaporation during the summer period (when evaporation demand exceeds rainfall) is dependent on the available water (precipitation plus the soil water storage). Interception has no impact on precipitation, or on soil water storage, and so it does not change the values for evapotranspiration during the summer. The resulting interception losses, therefore, have an effect on flows only during the winter period and can be estimated only within that framework.

When a forest is cut, the estimation of evaporation before and after the cut should make it possible to estimate the differences between a forested catchment and an unforested one, and therefore the impact of interception losses on runoff.

EXPERIMENTAL SET-UP

Three small catchments on granite in the Mount Lozère Experimental Research Basin (ERB) have been monitored since 1981. These are the spruce-forested Latte (0.195 km^2), the beech-forested Sapine (0.54 km^2), and the grazed-grassland Cloutasses (0.81 km^2). The slopes there are moderately steep - approximately 12° (Latte), 18° (Sapine), and 10° (Cloutasses). The Latte catchment (Fig 1) was the most closely observed catchment, as 80% of its surface was clear-cut of its spruce forest from 1987 to 1989.

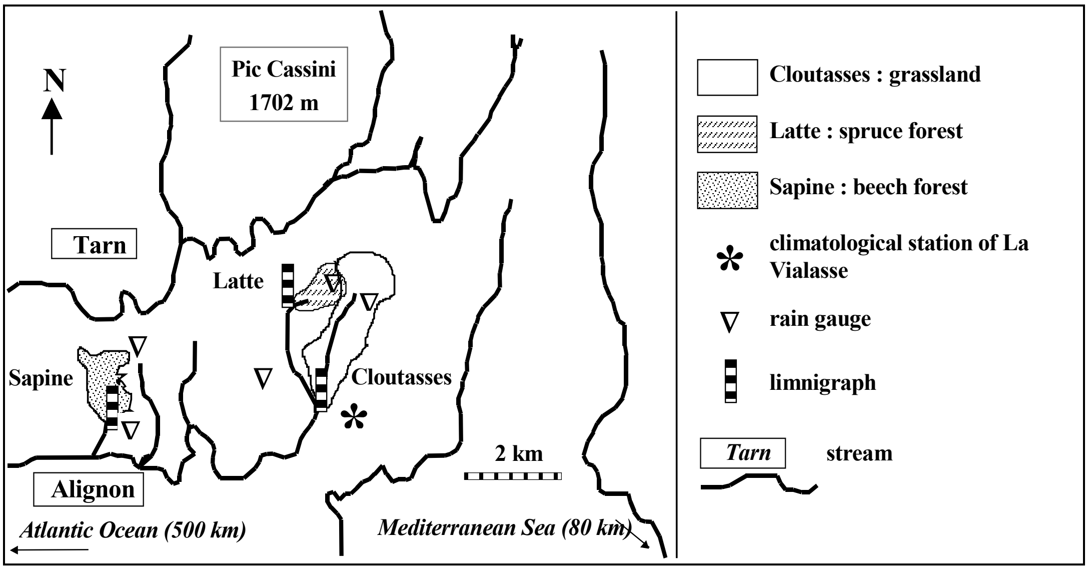

Fig 1: Schematic of Mount Lozère Experimental Research Basin.

At between 1100 and 1500 metres in elevation, the Mount Lozère ERB has a mediterranean climate with mountain characteristics. The mean temperature at 1300 m is 6.9 °C. Mean annual precipitation is about 2000 mm, and ranges between 1100 and 3500 mm. Rainfall can be very intense, especially in autumn during “cévenols” events; for example on the Latte catchment, maximum 30-minute rainfall intensities reached 179 mm h^{-1} on 28 August 1999 and 131 mm h^{-1} on 22 September 1993. On the average, the soils and superficial deposits are from 60 cm (Sapine) to 70 cm (Latte and Cloutasses) thick. Filtration rates for the soils as determined in simulated rain conditions range from 78 to more than 123 mm h^{-1} under undisturbed vegetation and for well-protected soils (Cosandey et al., 1990).

METHODOLOGY

The method is based on the water balance equation calculated during the "excess water period", when rainfall exceeds atmospheric water demand (what is called "hydrologic winter", usually -but not always- from October to April). It is known that during the hydrologic winter (defined by R>Pe), the equation may be expressed as:

$$R = D + Ae + \Delta S$$

Where:
R = measured rainfall
D = measured runoff
Ae = actual evaporation
Pe = potential evaporation (calculated with Turc formula; Turc, 1961):
$\Delta S = \Delta Ru + \Delta Rh$
with ΔRu soil moisture storage (function of soil characteristics and depth of root development)
and ΔRh groundwater storage (deduced from beginning and end-of-period baseflow and the recession curve).
In the following study, the thin soils prevent the vegetation from developing a very deep root system, so there is very little difference in the soil moisture storage. This difference has been estimated at 20 mm (100 mm for the forest and 80 mm for heath/grassland). These reserves probably were somewhat depleted when the forest was cut, at least during the two years following the cut. Because these values are somewhat arbitrary, they do constitute a source of uncertainty in the following developments. If the estimated interception losses are taken into consideration, however, the magnitude of the uncertainty is negligible.

From the basic equation, the following calculation of Ae is obtained for the duration of the hydrologic winter:

$$Ae = R - D - \Delta S$$

This calculation of Ae is done for the two basins. The problem, well known, is that the value of Ae is the residual term of the calculation, which includes errors in rainfall and runoff storage measurements. For this reason, not the values themselves, but only *the ratio between the values* is taken into account, according to the "comparative basins method". This method reduces the error concerning rainfall (which is quite the same for the two basins, and has no consequence on the difference of Ae estimation) and the error concerning runoff, due to calibration curves, which remain the same for each basin respectively.

Of course, the forest cut didn't change only evaporation (with respect to evaporation of intercepted water). It also affected plant transpiration, although we are operating here on the hypothesis that plant transpiration can be ignored during the months of winter dormancy, especially given the low temperatures involved.

RESULTS

Differences in Ae, attributed to differences in interception losses, were estimated over a period of twelve years for two catchments (the heath/grassland Cloutasses, and the initially forested Latte, five years before the cut; then seven years after the cut during the summer of 1987). The results are shown in Tables 1 and 2.

There are two preliminary remarks:

1) Values of Actual evaporation are higher than values of Potential evaporation computed using the Turc formula (from local data). The Turc formula is not the best for Pe estimation. But there is insufficient data for Penman's equation and the Pe values are taken into account only for the winter season. Even if the Turc formula tends towards low values, it seems that interception losses are effective even on the grazed heath/grassland catchment and can probably be explained by the presence of broom plants and clumps of trees.

2) The wide range of values is difficult to explain, even if they are clearly in relation to Pe values. It is clear that measurement errors both on rainfall and runoff play a role; but as seen above, the consequences are negligible.

Table 1: Actual evaporation (mm) in the two basins for the whole period (see Table 2 for details).

hydrologic winter	Ae Cloutasses	Ae Latte	Ae Lat - Ae Clout	Ae Lat / Ae Clout
82/83	555	671	-116	1,21
83/84	349	456	-107	1,31
84/85	463	572	-109	1,24
85/86	121	198	-77	1,64
86/87	348	499	-151	1,43
87/88	504	394	110	0,78
88/89	300	283	17	0,94
89/90	538	498	40	0,93
90/91	226	198	28	0,88
91/92	447	444	-3	0,99
92/93	457	475	18	1.04
93/94	328	347	-19	1,06
94/95	488	470	18	0,96
95/96	347	276	71	0,80

Table 2: Data for Ae calculation.

Latte Basin					Cloutasses Basin				
hydrol. winter	D (mm)	R (mm)	ΔS (mm)	Ae Latte (mm)	hydrol. winter	D (mm)	R (mm)	ΔS (mm)	Ae Cloutasses (mm)
82/83	1500	2269	98	671	82/83	1513	2184	116	555
83/84	874	1490	160	456	83/84	1018	1490	123	349
84/85	1455	2150	123	572	84/85	1452	2052	137	463
85/86	840	1310	272	198	85/86	1049	1310	140	121
86/87	1273	1890	118	499	86/87	1221	1738	169	348
87/88	1959	2608	255	394	87/88	1925	2608	179	504
88/89	624	1065	158	283	88/89	620	1065	145	300
89/90	752	1384	134	498	89/90	720	1384	126	538
90/91	950	1280	132	198	90/91	934	1276	116	226
91/92	805	1380	131	444	91/92	826	1392	119	447
92/93	1185	1798	138	475	92/93	1194	1769	118	457
93/94	1690	2216	179	347	93/94	1754	2216	134	328
94/95	1369	2012	173	470	94/95	1386	2012	138	488
95/96	2797	3227	157	273	95/96	2760	3227	120	347

In order to determine the impact of the forest cut on interception losses, we can take a look at the evolution in the ratio between Ae in the two basins before and after the cut. Fig 2 shows that after the cut, the ratio between evaporation in the two basins, which was larger than 1 before the cut became less than 1 after.

DISCUSSION

Before the cut, interception losses were higher in the spruce-forested Latte catchment than in the Cloutasses catchment. There was a large decrease in interception losses during the winter that followed the cut, explained by the reduction in evaporating surface area: more than a third of the trees were cut and, although debris from the cut was strewn over the ground, there was no plant colonisation to cover the deforested areas. Under these conditions, it is not surprising that interception losses were lower than in the heath/grassland catchment.

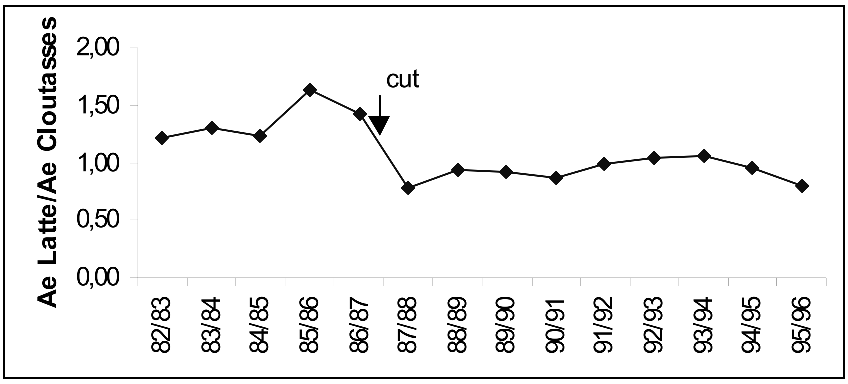

Fig 2: Ratio between actual evapotranspiration values for the Latte and the Cloutasses Basins.

The situation rapidly changed, however. By the following summer, abundant herbaceous (great willow herb) and shrub (raspberry bush) vegetation had developed; nowhere was bare ground to be found. By the second post-cut winter, the deforested catchment's behaviour was similar to that of the heath/grassland catchment, even though cutting operations had resumed in an area where tree growth was less successful. The behaviour remained similar even though some very small trees were planted (very slow growth in the difficult climatic conditions, so their impact was still very limited).

CONCLUSION

This study was based on a certain number of hypotheses and rough calculations. In particular, it is clear that using water balances involves the risk of accumulating errors in data measurements (principally rainfall and discharge). Comparing neighbouring catchments is a way to reduce this type of risk, however, especially since it makes it easier to take any possible impact of climate variability into account.

Beyond such uncertainty, we felt that it was of interest to give further thought to the hydrologic processes that bring about lower flows under forest cover. Once a higher level of evaporation during the winter period was identified on the forested catchment, and it was ascertained that it could be due only to losses by interception, it became easier to understand why the overall increase in runoff that was observed after the cut only affected minor floods. During the "cévenols" rainfall events, the amount of rain and the depth of runoff can be enormous – and the effects of interception losses become negligible. The same cannot be said of a relatively light rainfall event. In that case, the depth of runoff measures only a few millimetres, and can therefore be heavily influenced in terms of relative value by a reduction in the effective rainfall due to the interception of part of the rain by the plant cover.

REFERENCES

Bosch, J.M., Hewlett, J.D. (1982) A review of catchments experiments to determine the effect of vegetation on water yield and evapotranspiration. *J. Hydrol*., 55, 3-23.

Calder, I.R. (1979) Do trees use more water than grass? *Water Services*, 83, 11-14.

Calder, I.R. (1985) What are the limits on Forest Evaporation? – Comment. *J. Hydrol*., 82, 179-192.

Cosandey, C., Boudjemline, D., Roose, E., Lelong, F. (1990) Etude expérimentale du ruissellement sur des sols à végétation contrastée du Mont Lozère. *Z. für Geomorphologie*, N.F. 34-1, Berlin-Stuttgart, März 1990, 61-77.

Cosandey, C., Robinson, M. (2000) Hydrologie continentale. coll. U, Armand Colin, Paris, 360 pp.

Morton, F. I. (1984) What are the limits of forest evaporation? *J. Hydrol.,* 74, 373-398.

Morton, F. I. (1985) What are the limits of forest evaporation? – Reply. *J. Hydrol*., 82, 184-192.

Turc, L. (1961) Evaluation des besoins en eau d'irrigation. Formule climatique simplifiée et mise à jour. *An. Agro*., INRA, Paris, 12, 1, 13-49.

DIFFERENCES BETWEEN THE SNOW WATER EQUIVALENT IN THE FOREST AND OPEN AREAS IN THE JIZERA MOUNTAINS, CZECH REPUBLIC

J. Stehlík, L. Bubeníčková

Czech Hydrometeorological Institute, Department of Hydrological Research,
Na Šabatce 17, 143 06 Prague 4, Czech Republic

ABSTRACT

The study deals with analyses of long-term snow measurements performed in the upper parts of the Jizera Mts. in Northern Bohemia, Czech Republic. The main task is to determine the amount of snow storage in forest based on measurements in open areas. Data from selected pairs of snow profiles in the open area and in the forest, simultaneously measured in the same locality, were tested to prove the homogeneity of measured data and to establish the relationship between snow storage in an open area and in a forest. It was found that: i) the relationship can be defined by means of linear regression (correlations for all profiles are significant); ii) the parameters vary with the site of measurement (profile) and accumulation or melting period, respectively.

Keywords snow measurement, snow water equivalent, forest and open area, Jizera Mts.

INTRODUCTION

Data of snow depth and its water equivalent in winter seasons are very important sources for the estimation of water storages in basins. This information is gained from the network of precipitation and climatological observation stations that, for historical and pragmatic reasons, are all situated in open-area localities. None of them measure the depth of snow cover and its water equivalent in forested areas, though most of the areas where floods are generated lie predominantly in forested regions. The observation-based experience proves that the regime of accumulation and snow cover melting in forested regions differs significantly from the regime in non-forested regions, both in time and space. Especially during snow melting periods there are often considerable differences. To take the different type of land use into account it is necessary to quantify these differences.

In the territory of the Czech Republic and Slovakia several empirical research studies were conducted, mainly in the Moravian and Slovakian mountains, to estimate snow cover variations in forests, differences between the snow regime in deciduous and coniferous canopy, and the areal distribution of snow in watersheds (Babiaková and Kozlík, 1969; Zelený, 1965, 1975; Kantor, 1975). In Bohemia, water snow storage was examined in small basins for water management prediction for reservoirs (Turčan, 1977; Barták, 1978, 1995; Chamas, 1981). The different results of these snow measurements pointed to the necessity of paying more attention to the execution of paired snow measurements – in forest and open area in the same locality – considering the regional topography, altitude and vegetation cover. This would enable the systematic and consistent quantification of differences in measured data. The final goal of this effort is to use this acquired knowledge for the innovation and improvement of hydrological forecasting procedures. Therefore in the last two decades, detailed snow studies were performed at the Experimental Base of the Czech Hydrometeorological Institute in the Jizera Mts. (Hladný et al., 1999). The data were evaluated, analysed and mutually compared (Stehlík et al., 2000). The main goal of this paper is to derive the relationships between the snow water equivalent in forest and open areas.

STUDY AREA AND METHODS

The Jizera Mts. (altitude 750-1085 m) are situated in Northern Bohemia, and are one of the European regions highly affected by atmospheric deposition. As a result the monoculture spruce forest was damaged and started to die. The 7 watersheds (areas of basins vary from 1.87 to 10.6 km^2) included in the Czech

Hydrometeorological Institute Experimental Base lie in the upper part of the mountains close to the watershed divide; 5 on the southern slope and 2 on the northern slope (Fig 1).

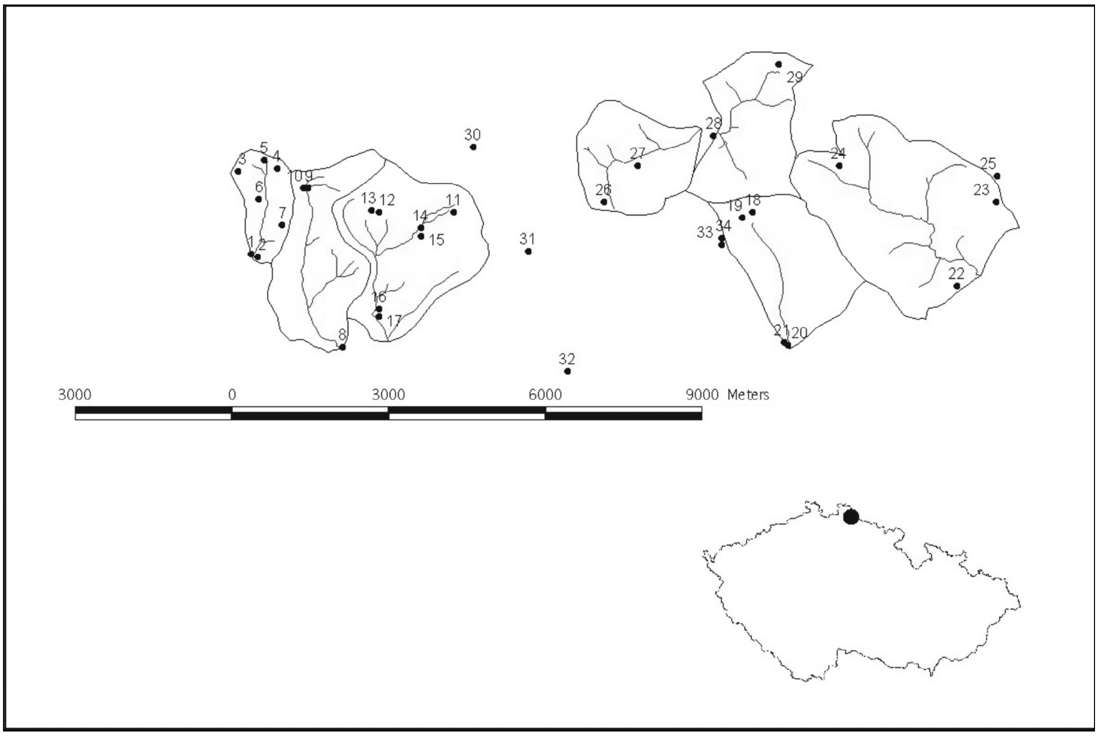

Fig 1: Location of the studied basins and snow profiles in the Jizera Mts.

Time series of snow measurements performed both under trees and on clearings are available. The position of the profiles is given in Fig 1. The aim of measurements concentrates on two topics: to establish the relationship of areal distribution of snow to altitude and to determine the differences in snow accumulation and snow melting in forests compared to open areas. The number of selected measured localities is influenced by the character of the winter season, i.e. it varies due to the duration of the snow cover and its depth, as well as the accessibility to profiles. Usually 15 to 26 profiles are regularly measured in weekly time intervals, which also includes the paired profiles measured in 8 localities (Hladný et al., 1999). The beginning and the end of the winter monitoring season depends on snow cover formation and melting. The beginning usually starts in November or in December and continues to the end of March or to mid April.

The measurements of snow depth and its water equivalent are performed in snow profiles by a weighing snow sampler. The profiles were chosen to be easily accessible from the road but far enough not to be influenced by wind effects. The profiles are 15 to 20 meters long, at the beginning and at the end marked by poles in order to be easily located in the open terrain, in the forest marked by coloured triangles. The snow depth is surveyed at 10 points, at 3 of them the density of snow is also measured. The depths of snow are read on the centimetre scale on the outer side of the sample tube; the density is derived from the weight of the samples evaluated with a digital weighing instrument.

The period 1991-1999, when the snow measuring network became already stabilised, was chosen for the analyses. The data analyses include homogeneity testing, assessment of altitude influence on snow water equivalent (SWE), and the quantification of differences between snow cover accumulation and melting in open space and in forested environments where sufficient data are available. In the profiles listed in Table 1, paired profiles are selected which have enough measurements to be statistically evaluated concerning the relationship between forest and open area SWE.

Table 1: The description of the selected paired snow profiles.

Locality	Profile No.	Clearing or forest	Altitude (m)	Exposition	Slope %	Species of vegetation	Age (years)	Crown Density %
Uhlířská	1	clearing	775	South	0	calamagrostis villosa		
Uhlířská	2	forest	780	South	0	Spruce	70	70
Kristiánov	16	clearing	805	West	3	calamagrostis villosa		
Kristiánov	17	forest	795	South West	10	Spruce	50	65
Jezdecká	20	clearing	775	South West	3	calamagrostis villosa		
Jezdecká	21	forest	780	South East	5	Spruce	70	60
Hřebínek	9	clearing	825	West	1	calamagrostis villosa		
Hřebínek	10	forest	830	East	2	Spruce	70	55
Kasárenská	33	clearing	920	South	5	calamagrostis villosa		
Kasárenská	34	forest	930	South	3	Spruce	30	80
Černá Nisa	4	clearing	820	South East	7	calamagrostis villosa		
Černá Nisa	5	forest	830	South	1	Spruce	40	55
Bílé Buky	12	clearing	900	South West	6	calamagrostis villosa		
Bílé Buky	13	forest	905	South West	6	spruce, beech	80	70
U Podkovy	14	clearing	875	South West	5	calamagrostis villosa		
U Podkovy	15	forest	875	South West	5	Spruce	70	70

RESULTS AND DISCUSSION

As mentioned above, snow profiles in the Jizera Mts. are partly measured in so-called ”pairs”, i.e. in the forest and on clearings (open space) in close proximity to each other. The homogeneity testing proves that the double mass curves are more or less without large deviations, both for the period of snow accumulation and snow melting. An example for the profile Jezdecká is given in Fig 2.

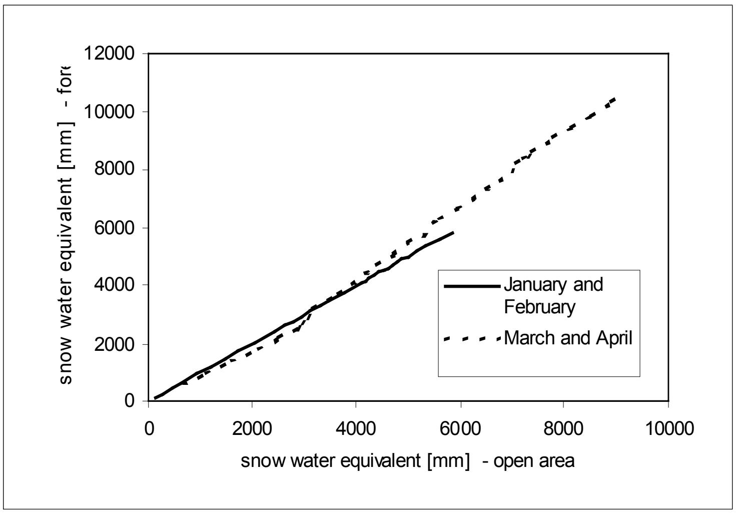

Fig 2: Double mass curve of the SWE for the profile Jezdecká (No. 20 and 21).

In Table 2, the selected profiles are statistically evaluated concerning the relationship between the forest and open area SWE. In three cases the number of measurements is sufficient to divide the winter seasons into two parts: January-February (accumulation) and March-April (melting). This rough division was introduced due to the fact that air temperature (which could be a better criterion) was not measured in the observation period.

For each paired site the parameters of the linear regression between the SWE in forest and SWE in open area were computed:

$$SWE_{forest} = a + b * SWE_{open\_area} \quad (1)$$

The results are listed in Table 2. All correlation coefficients between the SWE in forest and in open areas are significant at the 0.05 % level. The division into winter subseasons makes it easier to interpret the results of the analyses (see below for the profile Jezdecká). However, the results for the whole winter season are also included because they make it possible to derive the snow storage in the forest based on measurements in the open area in the given locality. From Table 2 it also follows that the parameters differ from site to site, and that it would be difficult to derive one equation (relationship) even for such a relatively small region. In most cases there is also considerable uncertainty in the coefficients of regression (especially the intercept value) – see the upper and lower 95 % intervals for both regression coefficients.

The correlation coefficients between the SWE in open areas and in forests are not significantly related to the geographical conditions or vegetation characteristics of the profile (altitude, slope, age and crown density). The influence of the geographical and vegetation parameters on the regression coefficients is difficult to interpret because one has to differentiate between the period of accumulation and snowmelt, and only three profiles provide enough measurements for such analyses. Data from more profiles will be analysed in the future to clarify this question.

Table 2: Parameters of the dependence between the snow water equivalent (SWE) in open area and forest in the paired profiles in the Jizera Mountains ($SWE_{forest} = a + b * SWE_{open\_area}$).

Pair profile	Time period in winter	No. of mea-sure-ments	r correl.	A			b		
				expec-tance	Lower 95 %	upper 95 %	expect-ance	lower 95 %	upper 95 %
Uhlířská	whole season	74	0.900	38.427	22.34	54.510	0.703	0.623	0.783
	Jan. and Feb.	35	0.902	34.689	16.720	52.658	0.645	0.535	0.754
	Mar. and Apr.	13	0.896	80.983	26.600	135.367	0.706	0.474	0.938
Kristiánov	whole season	59	0.899	-3.460	-28.270	21.350	0.847	0.738	0.956
	Jan. and Feb.	30	0.938	-9.570	-31.180	12.038	0.756	0.648	0.864
	Mar. and Apr.	16	0.881	58.526	-3.723	120.775	0.757	0.524	0.990
Jezdecká	whole season	68	0.852	41.74	7,934	75,546	0.880	0,745	1,014
	Jan. and Feb.	33	0.907	-16.987	-53,446	19,471	1.054	0,871	1,235
	Mar. and Apr.	24	0.822	184.17	136.865	231.476	0.523	0.363	0.683
Hřebínek	whole season	32	0.942	-5.448	-30.729	19.833	1.001	0.874	1.141
Kasárenská	whole season	26	0.892	18.895	-47.125	84.915	1.261	0.992	1.531
Černá Nisa	whole season	20	0.864	-3.629	-53.992	46.734	0.739	0.526	0.953
Bílé buky	whole season	21	0.916	-16.603	-74.208	41.001	1.005	0.794	1.216
U podkovy	whole season	21	0.891	15.035	-57.432	87.502	0.848	0.589	1.106

The profile Jezdecká (points 20 and 21 on Fig 1) was chosen for a detailed presentation. The course of the SWE in the winter season 1996 is presented in Fig 3, where the accumulation role of forest in the spring period is demonstrated. In Fig 4 the relationship between the SWE in the forest and in clearings for two winter subseasons is demonstrated. The results can be interpreted as follows: the lines in the figure have different slopes and different intercept values for each sub-season. From the intercept value for the period of snowmelt (Table 2) it follows that in spring more snow is preserved in the forest than in clearings. When the clearings are already free of snow, snow storage in the forest still remains with an expected value of 184.17 mm. The results for the accumulation period substantiate that the snow accumulates earlier in the open areas than in forests (negative intercept). The interpretations for the profiles Uhlířská and Kristiánov can also be done from the values in Table 2. Detailed results for both profiles were reported in Stehlík and Bubeníčková (2002).

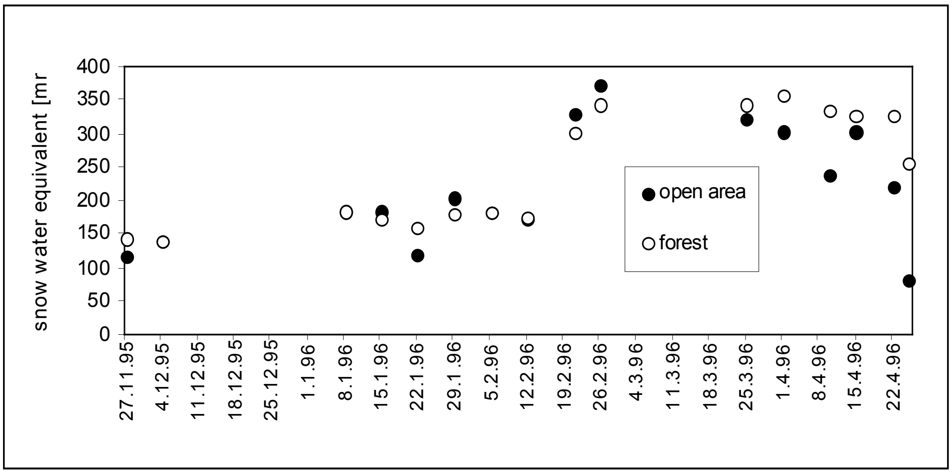

Fig 3: Course of the SWE in forest and in open area in winter 1996 in the profile Jezdecká.

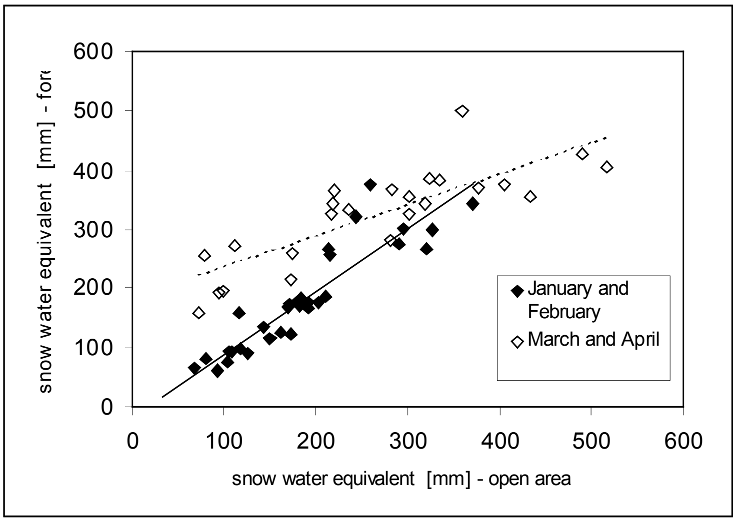

Fig 4: Relationship between the SWE in forest and in open area in the profile Jezdecká (divided into two sub-seasons).

Usually altitude is considered to be one of the most significant parameters influencing snow depth and SWE - when the set of stations covers a sufficient range of altitudes. However this is not the case for stations in the Jizera Mts. The minimum snow profile altitude is 775 m, the maximum one is 985 m. The statistical significance of the relationship between altitude and SWE was tested on the level $\alpha = 0.05$. The average correlation coefficient from a total number of 47 cases is 0.448, and only 8 from 47 relationships are statistically significant.

Results presented in this paper have shown that the relationship between the SWE measured in open areas and in adjacent forests is significant in all analysed profiles. These equations could serve to estimate the snow storage accumulated in the forest based on the measurements in clearings in a given locality. However, the form of the relationship (regression equation) reveals high variability even in such a relatively small research area, and therefore it is not possible to derive one general equation for a given region. Data from more profiles will be evaluated to try to relate the regression parameters to the geographical and vegetation conditions.

REFERENCES

Babiaková, G., Kozlík, V. (1969) Contribution to the determination of the snow storage in forested and non forested areas. *J. Hydrol. Hydromech.*, 17, 3, 243-254.

Barták, Z. (1978) Hydrological forecasting system for the protection of environment. Evaluations of snow cover water storage in the Nýrsko reservoir basin in years 1974-1978. Design of representative snow measuring net. (in Czech), Project Research of stochastic and systematic proceedings in hydrology for the need of water management and creation of environment, Part 3, Czech Hydrometeorological Institute, pp. 42.

Barták, Z. (1995) Hydrological forecasting in the Nýrsko basin. (in Czech), *Works and studies of the Czech Hydrometeorological Institute*, 26, Prague.

Hladný, J., Bubeníčková, L., Hancvencl, R., Kulasová, A. et al. (1999) Sensitiveness of inputs for hydrological models in winter seasons. The Jizera Mts. Experimental watershed. Register 1980/1981-1998/1999 of snow measurements. (in Czech), Project VaV/510/2/99 *Research of methods and development of forecasting models for the need of protection against floods*, Part 6, Czech Hydrometeorological Institute, Prague, 178 and 60 pp.

Chamas, V. (1981) Measurement of snow covers depth and their water equivalent in the Josefův Důl basin. (in Czech), Czech Hydrometeorological Institute, Ústí n. L..

Kantor, P. (1975) Influence of species composition of forest canopy to forming and melting of snow. (in Czech), *Forestry*, 23.

Stehlík, J. Bubeníčková, L. (2002) Relationships between the snow water equivalent in the forest and open areas in the experimental basins in the Jizera Mountains, *J. Hydrol. Hydromech*., 50, 3, 233-246.

Stehlík, J., Bubeníčková, L., Hancvencl, R., Krejčí, J., Kulasová, A., et al. (2001) Sensitiveness of inputs for hydrological models in winter seasons. (in Czech) Project VaV/510/2/99 *Research of methods and development of forecasting models for the need of protection against floods*, Part 6, Czech Hydrometeorological Institute, Prague, 68 pp.

Stehlík, J., Bubeníčková, L., Hancvencl, R., Kulasová, A.(2000) Sensitiveness of inputs for hydrological models in winter seasons. (in Czech), Project VaV/510/2/99 *Research of methods and development of forecasting models for the need of protection against floods*, Part 6, Czech Hydrometeorological Institute, Prague, 29 pp.

Turčan, J. (1977): Evaluation of snow storage in the Kamenice basin for the years 1975-1977. The design of rational snow measuring net. (in Slovak), Report of the Institute of Hydrology, Academy of Sciences, Bratislava.

Zelený, V. (1965) Runoff conditions during snowmelt in the Moravskoslezské Beskydy Mountains. (in Czech), *Journal of Forestry*, 4, 339-358.

Zelený, V. (1975) Contribution to the knowledge of the influence of the forest on the distribution of rainfall. *J. Hydrol. Hydromech*., 23, 4-5, 332-353.

EROSIVE RAINS RELATED TO IN-CHANNEL SEDIMENT DELIVERY IN A SMALL ALPINE BASIN (NORTH-WESTERN ITALY)

I. Maggi[1], F. Maraga[2], C. Ottone[1]

[1]*Earth Sciences Department, University of Pavia (Italy), cottone@manhattan.unipv.it*
[2]*Italian National Research Council (CNR), Research Institute for Geo-Hydrological Protection, Section in Turin (Italy), f.maraga@irpi.to.cnr.it*

ABSTRACT

A hydrological approach to the evaluation of erosion and water transport processes contributing to sediment supply in a river system was developed on the basis of rainfall data (analysed as an erosive factor) and sediment transport data in the channel. The small basin Valle della Gallina (Chicken Valley, $1km^2$) is located in the Alpine region of Piedmont characterised by a Mediterranean climate. Since 1982 it has been equipped with a sedimentary station at its outlet where in-channel transported sediment is trapped in a concrete pool, sediment volume and grain size are measured (mean sediment yield 39 m^3/year; D50 ranging from 16 to 1mm) and related to water discharges. The sediment collected in the concrete pool is delivered by flowing water as bed load transport of materials detached by breaking up and weathering of bedrock (volcanic rhyolite) and azonal soils; suspended load is irrelevant due to soil texture (coarse sand is dominant). In a 10-year period 1991-2000, the erosive rainfall events which exceeded a threshold selected by a standard rainfall depth of 12.6 mm throughout the event were singled out from the total amount of precipitation (mean 1390 mm/year). A correlation analysis was performed by comparing the annual sedimentation amounts measured in the concrete pool at the outlet of the basin with corresponding pluviometric values of annual rainfall and erosive rainfall, number of erosive events, number of rainfall hours, mean erosive rainfall intensity and precipitation erosive factor. Statistical results indicate that in-channel sediment delivery is equally affected by annual rainfall and total erosive rainfall/year calculated following the standard erosive threshold of 12.6 mm/event and by erosive rainfall duration. In fact, longer rainfall duration is considered to be able to lead to sediment discharge of event transportable materials even without surface drainage continuity to the main channel.

Keywords bed load transport, headwater erosion, rainfall erosive factor, sediment grain-size, Italian Alps

INTRODUCTION

This study is part of a wider research activity on sediment mobilisation and transport conducted by the Research Institute for Geo-Hydrological Protection in areas equipped and managed since the late 1970s on small basins in the Alpine and Apennine regions of the upper Po hydrographic network (Caroni and Tropeano, 1981; Tropeano, 1983; Anselmo et al., 1987; Caroni et al., 2000).

It is known that a pluviometric threshold must be reached, above which soil particles are mobilised, detached and carried away by water erosion. The data from 30 years of measurements in many regions of the USA show that cumulative effects of moderate storms and occasional severe storms should be considered in order to estimate average annual soil loss. The erosive capacity seems to be determined by a rainfall height of at least 12.6 mm throughout a given rainfall event (Wischmeier and Smith, 1978). After studies on 18 representative catchment basin in the Apennine region of Central Italy, accelerated soil erosion was noted as the main source of sediment transport in the rivers (Farroni et al., 2002).

Experimental studies following lithological, geomorphological and pedological surveys of the *Valle della Gallina* basin were carried out by field measurements on 7 slope plots and 2 small watersheds (1976-1979). Since 1982, the studies have focused on sediment yield measured by a sedimentary station located at the basin outlet.

Lithological uniformity of the rocks making up the basin and climatic uniformity of the area constitute homogeneous factors that are important for the analysis of erosion and transport processes associated with water as concerns the typology of the rock present (rhyolites), geomorphological evolution (dominant erosion), and azonal soil development.

The data from soil erosion measurements in the sample areas (Caroni and Tropeano, 1981) have shown that slope erosion processes differ, especially depending on the vegetation cover: the rate of erosion on bare soil at the head watershed was 6 mm/year, on grass it was 0.2 mm/year, and no erosion was observed in wooded areas. Depending on the soil texture, the rainfall erosive threshold values were found to range between 4 and 10 mm/hour, regardless of the duration of the event. Sediment transport measurements in the channel have shown that bed load sediment is mobilised at peak flow thresholds of 0.11 m^3/s and 0.33 m^3/s respectively for sand and gravel sized sediment (Anselmo et al., 1987).

In addition to the investigation of relationships between sediment delivery and water discharge at the outlet of the basin, which has been carried out since 1982, the investigation of the relationships between rainfall and sediment supply has started. This work presents the first results of correlation analyses (conducted at the scale of a surface drainage system) between sediment delivery data and rainfall data considered erosive (equal to or greater than 12.6 mm/event).

STUDY BASIN

The *Valle della Gallina* basin is located at the Alpine border of north-western Italy, in a mountainous transition zone between the Alps and the upper Po plain. The basin is defined by a dense dendritic drainage network (52 km/km^2) cutting down to bedrock made up of igneous, volcanic and rhyolite rocks. The main channel is 4 m deep and 5 m wide at the basin outlet.

Since 1982, a rainfall gauging station has been operating in the watershed at 380 m altitude; the basin outlet (330 m a.s.l.) is equipped with a hydrometric station and a sedimentary station to measure sediment delivery volumes and grain sizes related to the water discharge. No man-made works are present.

Table 1: Characteristics of the Valle della Gallina experimental basin.

Area	1.09 km^2
Lithology	volcanic rhyolites
Altitude (max - min)	522 - 330 m a.s.l.
Inclination (mean)	49 %
Soil cover (azonal soils)	99%
Soil dominant grain sizes	2 - 0.25 mm
Vegetation cover	77%
Temperature (mean 1982-1989)	11 °C
Precipitation (mean 1982-2000)	1300 mm/year
Runoff (mean 1982-2000)	750 mm/year
Discharge (mean 1982-2000)	0.02 m^3/s
Peak flow max (19 Sept. 1995)	6.44 m^3/s
Sediment trapped (mean 1982-2000)	39.0 m^3/year
Sediment trapped grain size range	128-0.06 mm

The characteristics of basin morphology and hydrology are shown in Table 1 and Fig 1.

The basin is located in a rainy part of the Italian Alpine region, with heavy rains and extensive soil erosion. The region has high daily rainfall values (some of the highest recorded maxima in Italy). For example, a rainfall intensity of 300 mm/day was exceeded twice in the period 1913-1978 (Anselmo, 1984). Rainstorms are frequent during the summer. The pluviometric monthly regime of the basin was classified within the Mediterranean climate system of the continental type and is characterised by two maximums, the first in spring and the second in autumn, with the principal minimum in winter (Caroni, 1979). According to the map of the Fournier index distribution band (Fournier, 1960) adapted for northern Italy (Maggi et al., 1998; Briggs and Giordano, 1990), the pluviometric variability in the basin, based on annual rainfall data, is in the transition zone between moderate and high classes (Fig 1).

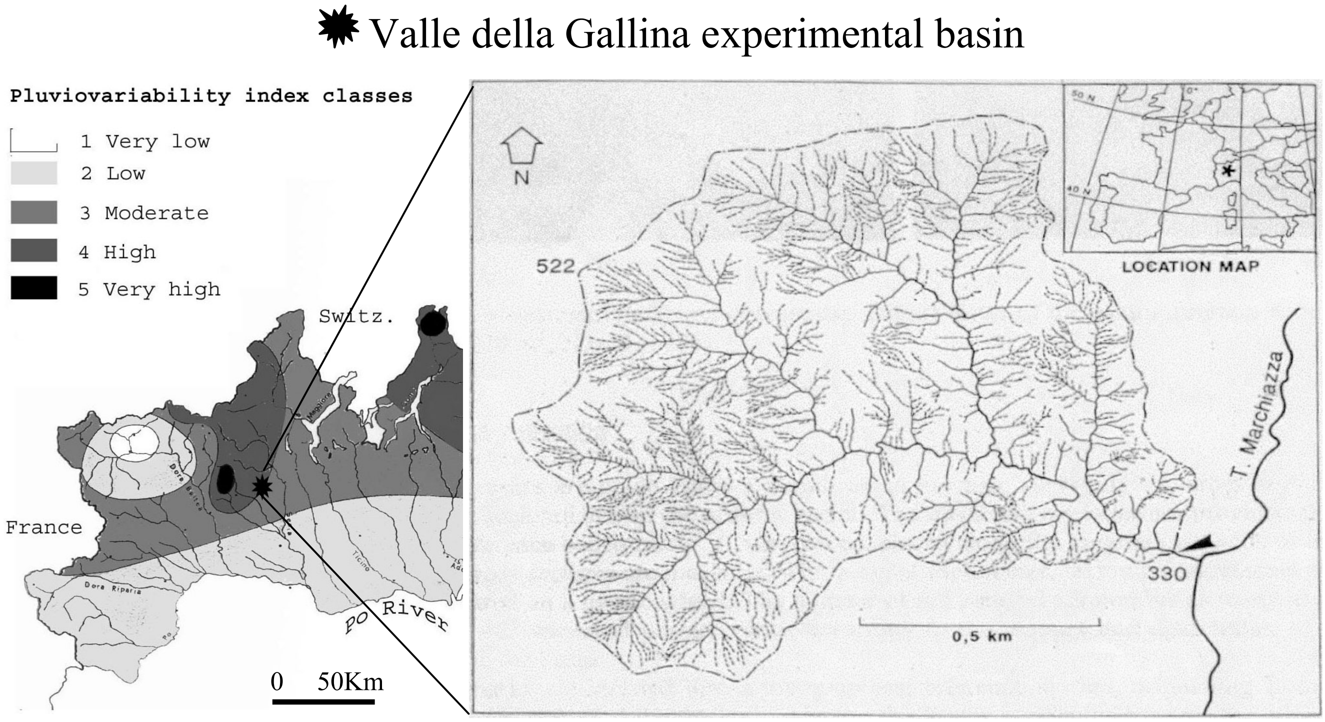

Fig 1: Valle della Gallina experimental basin shown on the pluviovariability index map of the Alpine hydrographic system in north-western Italy (after Maggi et al., 1998, modified). On the right: drainage network of the basin from aerial photographs; the arrow indicates the hydrometric and sedimentary station in the main channel at the outlet of the basin.

Closely related to the pluviometric regime, the discharge regime follows rain showers with a delay of about 1 hour. Compared with mean annual discharge (0.02 m^3/s), some peak discharges of over 1 m^3/s have been recorded every year, with a maximum peak value of 6.44 m^3/s in 1995.

Soil and vegetation cover

Soil cover is present on 99% of the basin area; it consists of lithosol and regosol with a rare clayey matrix. A study of the soil composition and erosion processes conducted by Biancotti (1981) described widespread phenomena of physical disaggregation of the outcrop, which were associated with landforms of accelerated erosion, and which limited pedogenetic development.

In 1992, the soil texture was characterised from 57 manual borings on the entire basin area with a collection of samples down to the bedrock surface at depths from 0.2 to 2.2 m. The grain size distribution showed that in 77% of cases the dominant grain sizes are sand (between 2 and 0.25 mm of the modal class), in 14% dominant muddy-clayey sizes were found, and in 9% gravely sizes (Bellino and Maraga, 1995).

Erosive processes in the watershed, which supply sediment to the drainage system, occur as sheet and rill erosion, beginning at the head of the basin (from gullies several centimetres to several meters deep, from a dense dendritic network incised to the bedrock) down to the main channel.

Vegetation consists of mature broadleaf woods with occasional evergreens. It starts from the middle slope and continues down to the valley bottom and the banks of the water courses, covering 77% of the area.

The watershed features and the main channel at the hydrometric and sedimentary station at the basin outlet are shown in Fig 2.

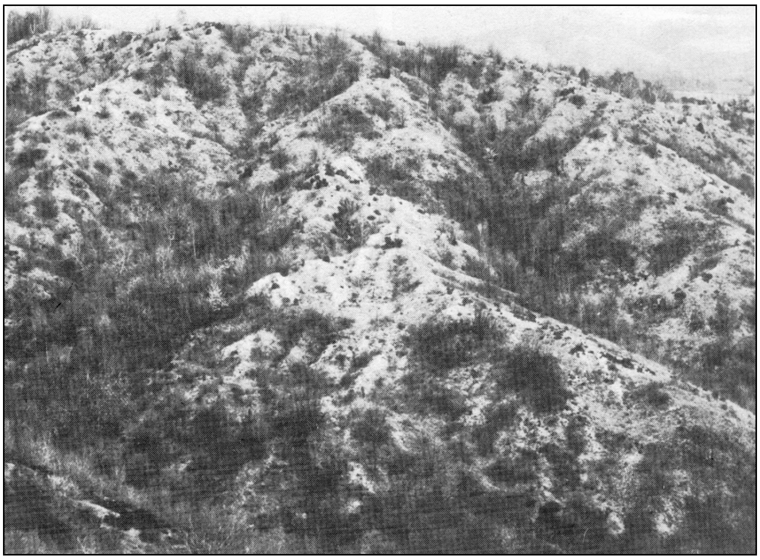

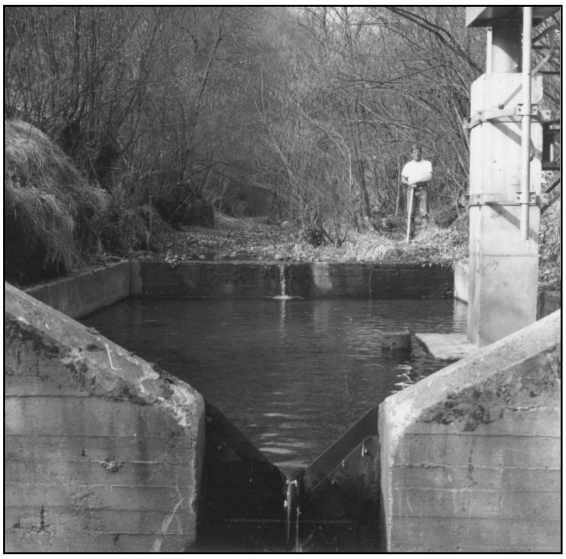

Fig 2. Valle della Gallina experimental basin. On the left: head watershed in winter showing the erosion effects on the watershed divide. On the right: view of the hydrometric and sedimentary station in the main channel at the basin outlet in winter.

Sediment transport

The hydrometric station at the basin outlet was set up to trap sediments transported by water. The trap consists of a pool set into the channel (5 m wide) lined with concrete on the bottom and the banks, extending 8 m upstream from the hydrometric section, with a capacity of nearly 40 m^3. On the pool border longitudinal walls, 32 metallic markers were installed to periodically measure the transverse sections of accumulated sediment which are used in calculating the sediment volume. The pool is usually cleaned manually or with a mechanical hoe, depending on the amount of sediment to be removed, with occasional grain size sampling. So far, the pool has been able to contain the transported material between cleanings.

The sediment delivered to the outlet of the basin is produced by bed load transport processes. It is represented by component fractions having the same grain sizes as the detached parent rock fragments which generate the soil. The sediment ranges in size from rare and occasional boulders (about 300 mm), frequent gravel (with modal class at 16-8 mm), to sand and silt, depending on the peak discharges and sediment transport pulses during the event (Govi et al., 1993).

Since 1982, correlation analyses between discharge and sediment supply have shown that transport occurs with discharges above the threshold of 0.11 m^3/s, moving coarse sands. The trapped volumes are also related to water volumes over 500,000 m^3 (Maraga et al., 2000). The grain sizes increase with peak discharges, whereas the sediment volumes trapped in the sedimentary pool increase with the water flow volumes produced by the rainfall event. However, sediment delivery is related to the sediment recharge in the channel reach upstream from the sedimentary pool (Godone and Maraga, 1992).

Sediment suspension sampled during a flood with a peak discharge of 1.1 m^3/s showed a mean concentration of 0.17 g/l (Anselmo et al., 1982), which was considered moderate, allowing for a reasonable estimate of sediment transport from only the sediment collected in the trap. The sedimentary pool with trapped material and the grain size zone from 27 grain size analyses, based on samples of different amounts (4 to 1540 kg), is shown in Fig 3.

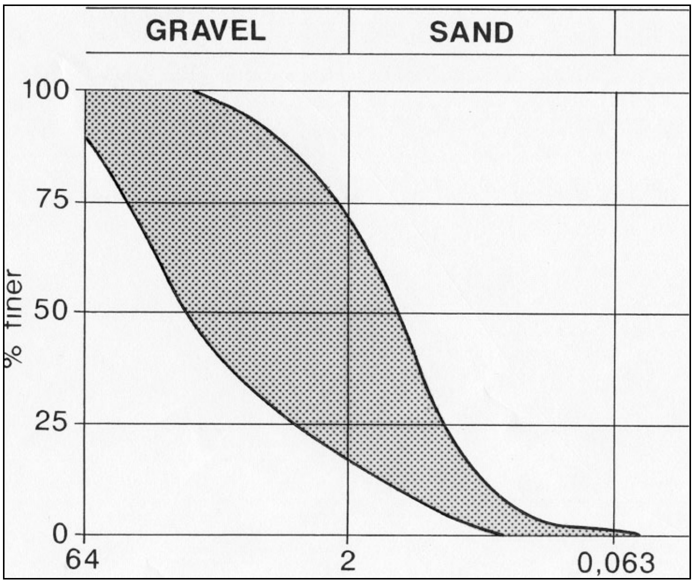

Fig 3. Valle della Gallina experimental basin. On the left: sedimentary pool showing filling condition in November 1992, during the manual cleaning. On the right: grain size zone determined by 27 grain size sample cumulative curves.

EROSIVE RAINFALL FACTOR

To correlate sediment delivery with erosive rain, the study started from the annual sediment volume yield and hourly rainfall data collected during the 10-year period 1991-2000.

In the present study, we adopted the criterion of calculating the annual erosive rain total from single erosive rainfall events (the event amounts were summed to form the annual total). The erosive rainfall events with amounts equal to or greater than 12.6 mm (standard erosive rainfall threshold) were selected for each year. For each erosive rainfall event, the Factor of Precipitation Erosivity (R) was calculated in accordance with the Universal Soil Loss Equation (USLE) for soil erosion estimation, as described in Wischmeier and Smith (1978). The Precipitation Erosivity Factor (R) is determined as follows:

$$R = E\ I_{30}\ \text{(MJ mm)/(ha hour year)}$$

where:
- E is the energy of the event, a function of the quantity and intensity of rain distribution. It is obtained by adding the energy values relative to each constant precipitation intensity interval;
- I_{30} is the maximum intensity of rain in an event for a duration of 30 minutes. It is obtained by dividing the hourly rainfall values.

A statistical analysis of the correlation between transported sediment and related rainfall was applied to the variables reported in Table 2, using an Excel programme which calculates the correlation index (ρ) on the basis of covariance.

RESULTS

For the 10-year period (1991-2000), the rainfall amounts were compared with the sediment volumes recorded at the *Valle della Gallina* basin outlet as an indirect assessment of erosion and sediment source in the basin.

The correlation index is $\rho > 0.69$ for relations between sediment volumes and total annual precipitation, total erosive rainfall (standard erosive rainfall threshold at 12.6 mm), number of erosive events and Erosive Factor (R). Best correlation was found between sediment delivery and total annual precipitation (ρ=0.86), total erosive rainfall (ρ =0.84) and number of erosive rainfall hours (ρ = 0.79).

The time series of the studied variables show a clear peak in the years 1994, 1995 and 1996, particularly for sediment volume delivery. The abnormality in the temporal trend for all variables during those years was found to correspond with a series of rainy years in the western Alpine region (for example the year 2000), which could signal a similar series input (Figs 4, 5).

In the study basin, the peak flows with sediment transport were generated by rainstorms. Appreciable changes in the bed form of the channel were observed during events with sediment trapped in the sedimentary pool. Channel depth variations on the order of 0.5 m generated by sediment supply or bed erosion were observed. Because these highs and lows have been interpreted as a wave translation pattern in the sediment bed load transfer, it appeared logical to conclude that sediment supply by headwaters from small watersheds, whose development times are unknown, could play a role in this process.

To better appreciate the interdependence between sediment delivery in the hydrographic system and rainfall events, the statistical analysis will be widened according to two statistical approaches. One approach will develop on a time scale of 20 years (1982-2002) the same correlation of annual variability to show any recurrent anomalies. The other approach will search for new variables that may influence on an hourly and daily scale the single rainfall events associated with corresponding sediment transport events in the main channel at the outlet of the basin.

Table 2: Data set for the correlation analysis between sediment delivery and rainfall with relative correlation index value (ρ).

Year	Sediment delivery	Rainfall								
		Annual			Erosive					
		Total	Hours	Intensity (mean)	Total	Events	Hours	Intensity (mean)	Intensity (mean)	Erosive factor
	m3	mm	no.	mm/h	mm	no.	no.	mm/h	mm/event	R
1991	34.0	1334.2	740	1.8	1072.6	28	425	2.5	38.3	427.5
1992	23.1	1297.6	881	1.5	1004.2	30	442	2.3	33.5	434.7
1993	18.9	1217.6	959	1.3	957.6	20	475	2.0	47.9	496.0
1994	70.0	1717.2	995	1.7	1434.8	37	601	2.4	38.8	623.7
1995	55.3	1379.2	993	1.4	1129.6	37	550	2.1	30.5	542.3
1996	57.1	1461.6	1131	1.3	1065.6	33	538	2.0	32.3	408.2
1997	12.5	1065.4	711	1.5	757.4	22	293	2.6	34.4	325.6
1998	39.5	1336.8	714	1.9	1017.2	31	367	2.8	32.8	424.0
1999	11.4	1394.0	855	1.6	1040.2	31	432	2.4	33.6	451.0
2000	65.0	1701.6	1047	1.6	1342.4	31	543	2.5	43.3	567.8
ρ		**0.8**	**0.6**	**0.1**	**0.8**	**0.7**	**0.8**	**-0.1**	**0.0**	**0.7**

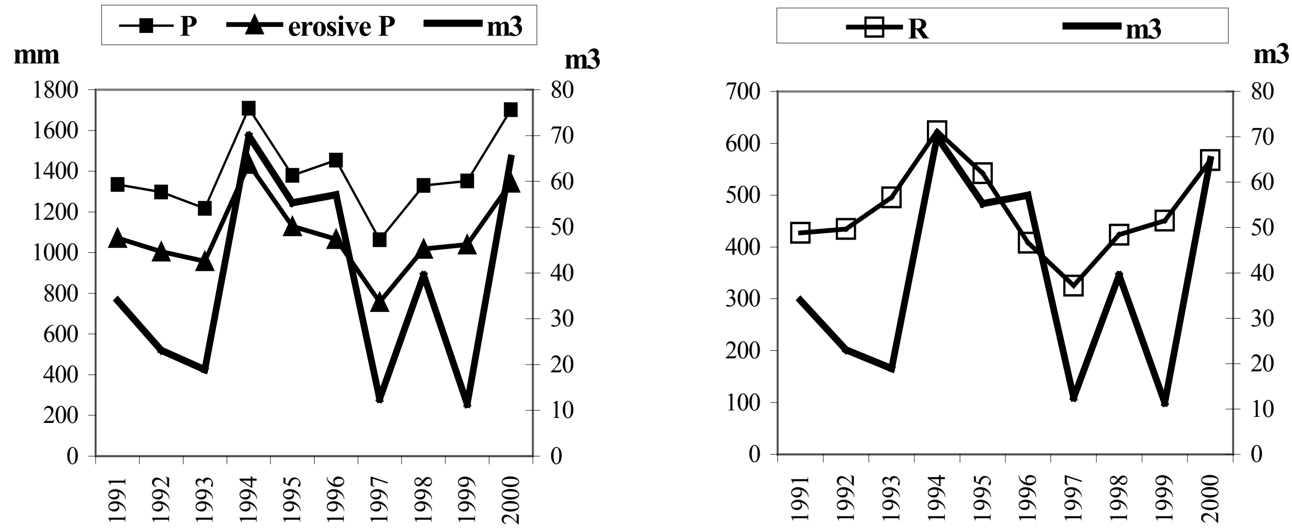

Fig 4. Time variations in annual volumes of sediment delivered (m^3) corresponding in the left panel to total rainfall amount (P) and erosive rainfall amount (erosive P), and in the right panel to the precipitation erosive factor (R).

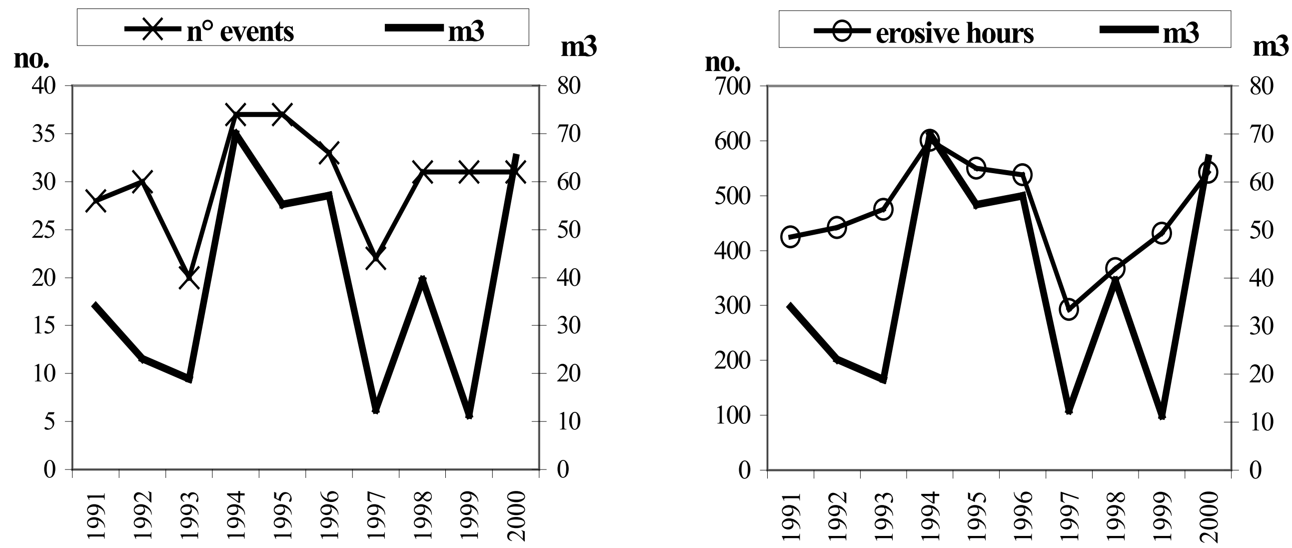

Fig 5. Time variations in annual volumes of sediment delivered (m^3) corresponding in the left panel to the number of events, and in the right panel to the number of erosive hours.

ACKNOWLEDGEMENTS

The authors wish to thank the referee for useful comments that helped to better focus the content and purposes of this preliminary study on sediment supply in the hydrographic network. Field data collection and processing were conducted by F. Di Nunzio (meteorological and hydrometric stations) and by F. Godone, R. Massobrio, M. Trevisiol and E. Viola (sedimentary station). Grain size analysis was conducted by R. Massobrio; figures were drawn by E. Viola). The project was supported by University and CNR funds in the framework of CNR (Italy) and AVCR (Czech Republic) Cooperative Programme 2001/2003, Earth and Environment Sciences, Joint Project n°2.

REFERENCES

Anselmo, V. (1984) Rainfall intensity and spatial distribution of major storms on north-western Italy. Proceedings of *Int. Conf. For Alpine Metereology*, Opatija (Yugoslaia), 25-29 Sept. 1984, 265-268.

Anselmo, V., Godone, F., Tropeano, D. (1982) Eventi idrologici in piccoli bacini montani: osservazioni sulla relazione afflussi-deflussi. Proceedings of Italian National meeting of Italian Association of Genio Rurale, Padova 19 Nov., Italy, 309-324.

Anselmo, V., Maraga, F., Buffa, F., Villi V. (1987) Sediment yield and bedload movement in mountain torrents in the Italian Alps. IUGG XIX General Assembly, IAHS Workshop on *Debris Torrent*, Vancouver, Canada, August 2-22, Poster Session, Abstracts V. 3, IAHS HW6, 979.

Bellino, L., Maraga, F. (1995) Temps de saturation en bassin versants. Proceedings of *2nd Int. Meeting of Young Researchers on Applied Geology*, Peveragno (Italy), Section C, 254-259.

Biancotti, A. (1981) Morfologia, suoli ed erosione in valle Marchiazza (Biellese). *Geografia Fisica e Dinamica Quaternaria*, no. 4, 30-38.

Briggs. D., Giordano, A. (1990) CORINE, Soil erosion risk and important land resource in the southern regions of the European Community. Report EUR 13233 EN, 97 pp.

Caroni, E. (1979) Pluviometria del Biellese Orientale. *Boll. Ass. Mineraria Subalpina*, no 4, 889-909.

Caroni, E., Arattano, M., Maraga, F. (2000) Results from bed load measurements in a small catchment. Idronomia Montana, 20, Special Issue on *Dynamics of water and sediments in mountain basins*, 99-110.

Caroni, E., Tropeano D. (1981) Rate of erosion processes on experimental areas in the Marchiazza basin (North- Western Italy), IAHS Publ., n. 133, 457-466.

Farroni, A., Magaldi, D., Tallini, M. (2002) Total sediment transport by rivers of Abruzzi (Central Italy) : prediction with the RAIZAL model. *Bull. Eng. Geol. Env*., 61, 121-127.

Fournier, F. (1960) Climat et erosion. Presses Universitaires de France, 201 pp.

Godone, F., Maraga, F. (1992) Topographic changes at gravel stream bed induced by sediment tranfer in the Valle della Gallina experimental basin, Alps, Italy. Conference on *Methods of hydrological basin comparison*, Oxford, UK, 28 Sept.-2Oct., Poster Session, Abstracts, 73-74.

Govi, M., Maraga, F., Moia, F. (1993) Seismic detectors for continuous bed load monitoring in a gravel stream. *Hydrological Sciences Journal*, 38, 2, 123-132.

Maggi, I., Ottone, C., Rossetti R. (1998) Distribution et fiabilité de l'indice d'erosion potentielle du climat au Nord du Po (Italie du nord). *Publ. De l'A.I.C.*, vol. 11, 267 pp.

Maraga, F., Di Nunzio, F., Godone, F., Massobrio, R., Viola, E. (2000) Sixteen years field monitoring of debris supply from an incised stream channel network. Proceedings of ERB 1998, UNESCO Technical Documents in Hydrology, n. 37, 131-138.

Tropeano, D. (1983) Soil erosion on vineyards in the Tertiary Piedmontese Basin (Northwestern Italy). Studies on experimental areas. In Jan de Poe (ed.): *Rainfall simulation runoff and soil erosion*, Catena Supplement,n. 4, 115-127.

Wischmeier, W. H., Smith, D. D. (1978) Predicting rainfall erosion losses. A guide for conservation planning; *USDA Agricultural Handbook*, no. 537, 58 pp.

INVESTIGATION OF SOIL MOISTURE REGIME AND PRESSURE CONDITIONS IN A DRAINED SOIL PROFILE

M. Soukup, E. Pilná, H. Baběradová

Research Institute for Soil and Water Conservation, Prague, Žabovřeská 250, 156 27 Prague 5–Zbraslav, Czech Republic. Phone: +420-2-5792 1640, e-mail: soukup@vumop.cz, pilna@vumop.cz

ABSTRACT

Drainage runoff, precipitation, soil moisture regime, underground water level and piezometric pressure were studied on drained soils located in the upper part of the Cerhovický stream catchment (Central Bohemia) for the period 1979-2001. The aim of the study was to evaluate the influence of the soil layers on drainage runoff. Drainage runoff is a component of the hydrologic balance of a drained agriculturally used watershed. The drainage system, first of all, creates drainage runoff and thus affects the soil moisture regime at both the soil profile and at a particular locality. The regulating systems to control drainage runoff were worked out (see Soukup and Kulhavý, 2000; Soukup et. al., 2001). The system of piezometers consists of 20 piezometers placed in two rows parallel to the drain tube. The piezometric heads and the soil moisture regime were analysed in the relatively wet years 1987, 2001 and dry years 1988, 1999. Any layer of the soil can be considered as an underground reservoir partly connected with the neighbouring layers to which it can pass water. Some layers take part in the water circulation process in an active way while others probably act as insulators. Monitoring proves that the circulation unsteadiness is higher in the deeper layers of the drainage system constructed in a sloping terrain. The measurement results show that changes in piezometric heads vary in the different layers of the drained profile and in its substrate layers. The results of the soil moisture regime measurements in the pairs of selected years prove the effect of the inserted retardation elements, particularly during the periods when the soil moisture is changing significantly.

Keywords drainage runoff, soil moisture regime, agricultural catchment, hydrologic balance

INTRODUCTION

This study is directed at an evaluation of the influence of agricultural drainage on the water regime of soils. The aim of the study was to assess the dynamics of the moisture regime of soils drained by the classic way, i.e. without regulation, and with regulation of drainage runoff.

Water streaming in the drained soil profile is usually simplified in theoretical works, and authors generally introduce so-called simplifying preconditions (e.g. the Dupuit-Forcheimer precondition). Computer processing enables now to "reject" some established preconditions, and so it is possible, while calculating water streaming to the drains, to define for instance the layers that participate in water streaming. It will always be necessary, however, to compare the results of theoretical approaches with the values measured in the field. The theoretically experimental approach was used for instance by Švihla (1984) to resolve the hydrological balance of a small drained catchment. We proceeded similarly while evaluating the piezometric pressures measured on the drainage system in the Cerhovický stream catchment where we attempted to clarify the origin of drainage runoff by means of a piezometric system installed on the drainage network.

Precipitation, surface and drainage runoff and further economic and physical aspects were monitored in the long term in the experimental catchment of the Cerhovický stream (district Beroun) that has a character of an agricultural and forested catchment from the point of view of land use. The catchment belongs to the Central Bohemian Hills with elevations 350–500 m above sea level. The geological environment is formed by slaty strata of the early Paleozoic. The agricultural land is farmed partly by the Agricultural Cooperative in Záluží and partly by a private farmer. The land is partly drained by underground pipe drainage. In the year 1998 a part of the drainage system "V lukách" was equipped with flow retardation and damming elements of the underground runoff retardation system (the PRO). The PRO system was designed by VÚMOP Prague (Soukup et al., 2000).

The purpose of the long-term monitoring of partial elements of the hydrological balance in this catchment was to evaluate the influence of drainage as a melioration measure, both on the water regime of soil and on the environment, namely on the quality and quantity of waters (e.g. Švihla, 1991; Soukup et al., 2000).

METHODOLOGY

Pairs of approximately equal years for a wet and a dry period were chosen from a sequence of 21-year long observations of precipitation and runoff from the Cerhovický stream catchment (1980–2001). In this way pairs of the years 1988/1999 were formed - representing a relatively dry period with precipitation lower than 15% in comparison with the precipitation standard from the years 1901–1950, and pairs of the years 1987/2001 - representing a relatively wet period with a positive deviation of more than 12% of the precipitation standard. It was not the value of the deviation from the standard that was decisive for the selection, but the greatest conformity possible of annual precipitation totals. The courses of soil moisture, precipitation, piezometric pressure and runoff data were processed for the above-mentioned years and periods. While precipitation, piezometric pressure and runoff were measured continuously, soil moisture measurements were conducted in an interval of a fortnight.

Soil moisture was measured in three locations (HV2, HV4 and on the retardation drainage), always at the drain and in the middle between parallel pipe drains. Measurements were carried out by a neutron probe (type Troxler) at depths of 0.2 to 1.0 m, spaced by 0.1 m.

Precipitation was measured ombrographically by a precipitation gauge located in the catchment (the catchment area before the year 1994 was 8.76 km^2, now 7.31 km^2). In the catchment, the stream through-flow was measured (at the final measuring profile) and drainage runoff was measured limnigraphically in the manholes (shafts) of three drainage groups. Piezometric heights (pressures) were measured in two places (in a slightly sloping position marked HV2 and on the stream level marked HV4) by a system of 20 piezometers located in parallel with the pipe drains in two rows at the drains and between the drains at a depth of 0.8 m to 2.40 m. Six piezometers were mounted with limnigraphs in the piezometric system HV2 and four limnigraphs in HV4 so that a continuous record was obtained.

In the first phase, a two-month period was chosen from 28 July to 31 September 1986 for the drained area in the sloping gradient of HV2. This was a period with increased precipitation activity and the expected reaction of the piezometric system was confirmed. The time step chosen for computer processing of pressure changes was 1 hour. In the second phase, dry and wet periods were chosen in each year (1987 and 1988) with regard to the drainage runoff response in which piezometric pressures were being stored in the database in an interval of 6 hours.

The piezometers were constructed as vertical cased bores. The casings are of PVC tubes with diameter 0.04 m, they are sealed at the bottom, and at a length of 0.1 m from the bottom they are perforated over a total area of 10cm^2/dm.

Characteristics of soil and drainage system

From the point of view of soil type, the soils are brown gleied and illimerised. As far as the sort of soil is concerned, the soils are clayey-loamy up to loamy-clayey soils the porosity of which is on average 43%, volume weight 1.4 gcm^{-3}, drainage porosity 5–7 %, and hydraulic conductivity in the range of 0.1 to 0.3 $m^{-1}day^{-1}$. The classical underground drainage spacing is 9 m in the surroundings of HV4, 18 m at HV2, and 11 m with the underground retardation of drainage runoff. The depth of the collection drains is 0.8 up to 0.9 m and the leaky drains are placed at a depth of approximately 1.0 m. The drainage piping is of baked clay. Drainage runoff was measured limnigraphically on Thompson´s measuring devices situated in the manholes (shafts) of the drainage groups marked Š5, Š6 and Š7. From the point of view of water streaming to the drains, the important depth is the depth of the so-called impermeable subsoil that is about 0.5 m under the drainage level in the area of HV2 and of the underground retardation of drainage runoff, while in HV4 on the stream level there is an impermeable layer at a depth of about 2 m.

MEASUREMENT RESULTS

The course of the drained soil profile moistures was expressed graphically for the wet years 1987/2001 and for the dry years 1988/1999. Piezometric pressures courses were evaluated in the wet year 1987 and in the dry year 1988. The piezograph of the dry period of the wet year 1987 (Fig 1) and the piezograph of the wet period of the dry year 1988 (Fig 2) is represented in the enclosed pictures. Both graphs (Figs 1and 2) are depicting the situation for the sloping position HV2.

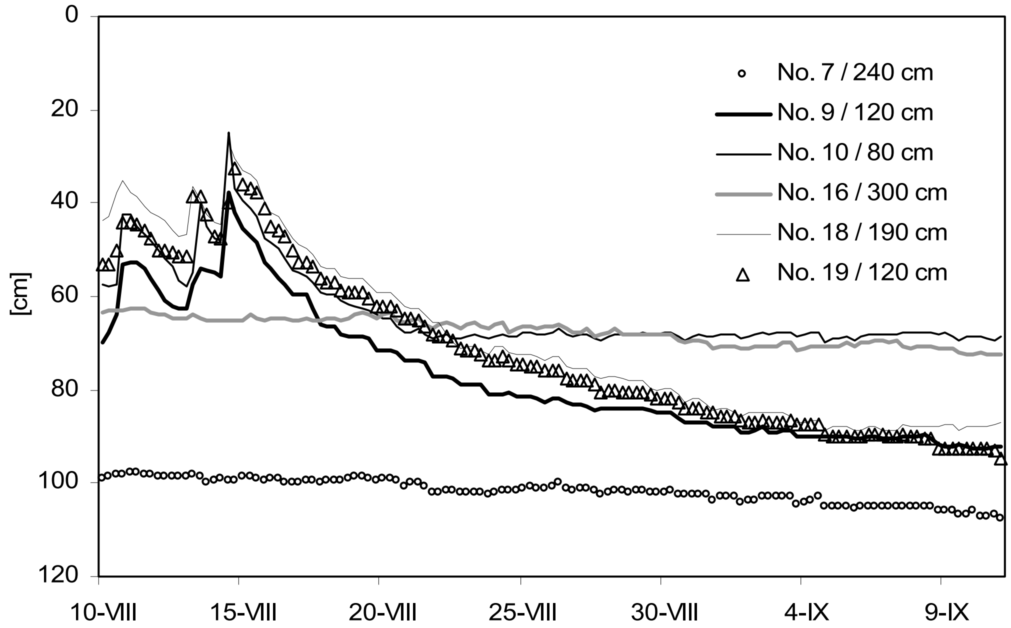

Fig 1: Piezometric pressure [cm] during the dry period of the wet year 1987; Cerhovice HV2.

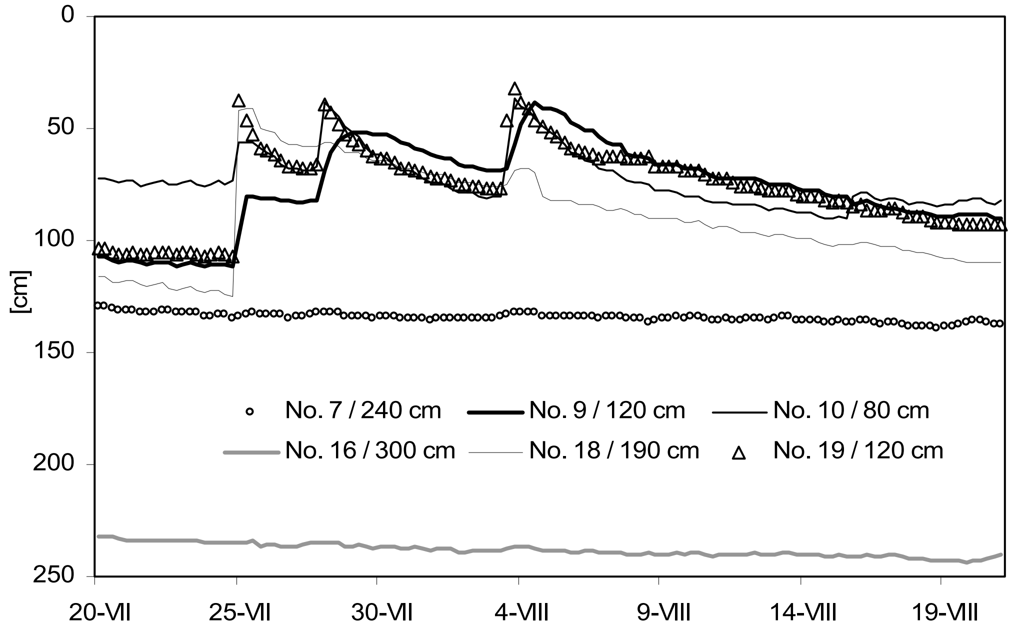

Fig 2: Piezometric pressure [cm] during the wet period of the dry year 1988; Cerhovice HV2.

The soil moisture of the drained profile was expressed in percentage of volume for the depths of 0.2, 0.5 and 0.7 m. In the wet year 1987 the soil moisture on the drained land moved in the range of 28 to 50% of volume, and was slightly decreasing during the vegetation period (with the exception of increases in soil moisture after intense precipitation towards the end of the month of June). The moisture at the depth of 0.3 m was markedly higher in the level position than in the sloping position. In the level position wetting of the soil profile occurs by water from the stream or by underground water inflow. Drainage continues permanently but underground water contributions evidently exceed the precipitation volume. In the depth of 0.5–0.7 m the soil humidity is, on the contrary, higher in the sloping position. In the slightly sloping position in HV2 it is only the excess infiltrated water from precipitation that is carried away. In the dry year 1988 the moisture near the surface of the soil was markedly lower in the level position HV4 than in the sloping position HV2. The opposite is true with increasing depth. With increasing depth the moisture range is also reduced, while the difference of the maximum and the minimum moisture content reached 30% at a depth of 0.2 m, this difference was no more than 12% at a depth of 0.7 m. The course of the soil moisture content at depths 0.5 m, 0.7 m and 1.0 m for site HV2 for 1988 is depicted in Fig 3.

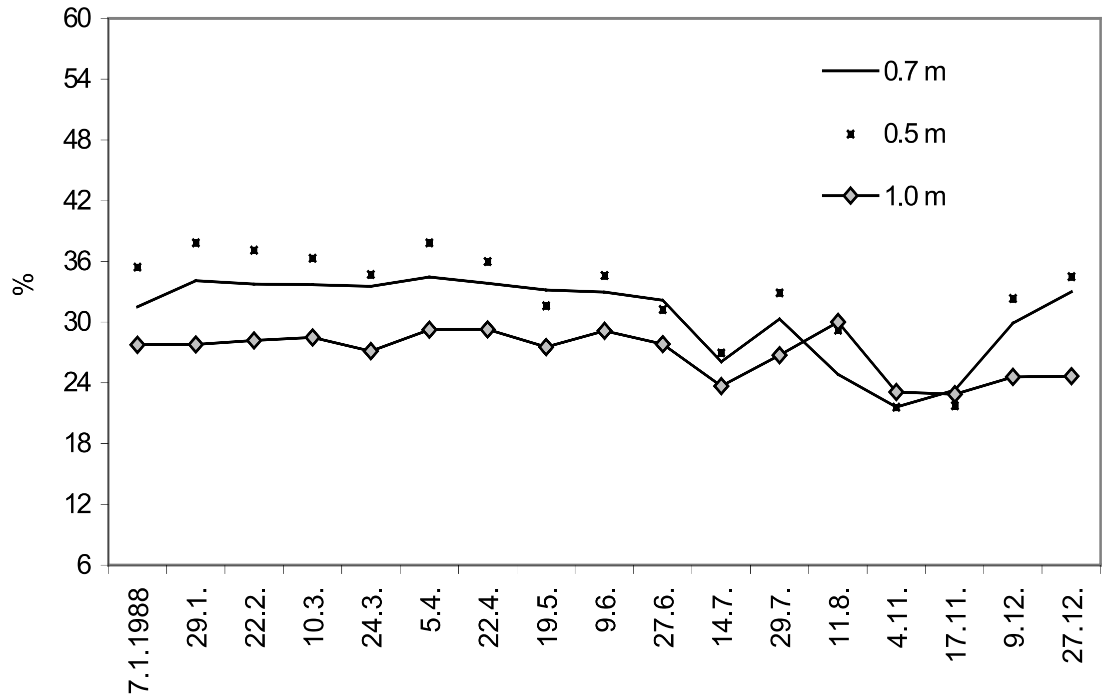

Fig 3: Soil moisture [%] at different depths in the dry year 1988 (January-December); Cerhovice HV2.

In the years 1999 to 2001 soil moisture was also monitored on the retardation drainage in which the damming element – regulator was permanently closed. During closure, the water in the regulation element is dammed by 0.3 m and water flows over the regulator. Drainage occurs also during water retardation, however, the runoff intensity is reduced as a consequence of water retardation. During the summer season, water from the soil profile is extracted by transpiration and partly also by evaporation. Due to the influence of an extreme drought in the year 2000 caused by a period of almost two months without precipitation, the lowest soil moisture values were measured as early as by the end of June. While in the year 1999, maximum soil moisture reduction occurred by the end of September, that is as late as by the end of the vegetation period. Water retardation in the drainage system causes a time shift in the onset of the critical drought period.

Pressure changes in the piezometric system (HV2 as well as HV4) were evident to the depth of 1.80 m. The deepest piezometers (2.4 and 3.0 m) hardly react in a dry year, which means that the water of the deeper layers does not contribute to the creation of drainage runoff. While all the layers are totally saturated, water streaming occurs in the direction to the drains from as far as the depth of 1.8 m. The outlet branches of the piezographs (hydrograms) that usually follow after larger precipitation were analysed from the viewpoint of pressure change in time. However, for the time being it is not possible to evaluate the part of pressure reduction as a consequence of the creation of drainage runoff and of the influence of filtration. While some layers participate actively in “water circulation”, other ones act evidently as insulators. Less permeable layers form impermeable layers from the point of view of streaming.

The monitored situation shows the differences of climatically characteristic years (the wet year 1987 as well as the dry year 1999) and the influence of the position of the drainage system.

Piezometric pressures were put in context with the moisture dynamics of the drained soil profile to the depth of 1.0 m, and with precipitation and drainage runoff. In view of the depth of the soil moisture measurements that was carried out to 1.0 m it was possible to review the given relations to the relevant depth only. The analysis of the results of piezometric pressure measurement in the individual depths of the drained profile can be compared with the results of theoretical models.

DISCUSSION

The neutron probe type Troxler used for the soil moisture measuring records "moisture" in the spherical space of soil around the probe sensor roughly to the distance equal to the radius 0.2 m from the sensor. The method is not dependent on the size and quality of the contact area of the sensor with the porous environment (soil) as it is the case with a whole number of other moisture apparatuses. A measuring accuracy for the sensor is currently stated with an error of ± 1.5%, but in our case the potential error also grows because of further inaccuracies, e.g. due to the spatial variability in the physical properties of the soil. For all the monitoring locations the correction ($-0.849 + 0.628n$) was used, where n is the deduced value of measurement.

From the point of view of water streaming in the drained soil profile the macro-voids (pedohydatodes), soil permeability and drainage parameters (above all the location depth and the parallel drains range) are fundamentally important. The saturated zone thickness fluctuates due to the occurrence of precipitation and of soil profile drainage. In spite of its upper level being approximately identical with the underground water level, it is necessary to mention that the measured underground water level may be distorted as the probe records the pressure from any depth and place on the periphery of the bore (perforated pipe).

The saturated zone is usually not hundred percent saturated, there always remains a certain aeration share that can be ascribed to the debit of the soil particles forces and also to hysteresis. However, oxygen may be gradually extracted by soil organisms. For these reasons the piezometers suitable for the study of water streaming conditions in a porous environment are those that are sensible tools for recording pressures above all in a non-homogenous layered environment.

The choice of the relatively equal pairs of dry and wet years is based on the identity of the annual precipitation totals. It is a criterion that is acceptable from the hydrological point of view. However, if a markedly different precipitation development occurs in the chosen years (in temporal distribution as well as in intensity), then the chosen pairs may be less homogenous.

CONCLUSIONS

The monitored situation showed evident differences and mutual connections of the course of soil moisture and piezometric pressure in climatically and hydrologically characteristic years (the wet year 1987 and the dry year 1999) for two different positions of the drainage system.

Based on the evaluation of the piezometric system in the dry and the wet period of a wet and a dry year, the soil and underlying layers participating in the creation of drainage runoff were defined. The lowest values of soil moisture content were measured during the extreme drought in the spring of the year 2000. The rate of decrease of soil moisture drops with increasing depth. Water retardation used in the drainage system retains soil moisture in the drained soil profile, which means that the critical drought period is shortened.

The obtained results enable us to describe more precisely the conditions of the drainage runoff origin in a slightly sloping and a level position of the drainage system in the experimental catchment of the Cerhovický stream on the loam-clay soils in the area of the Central Bohemian Hills.

ACKNOWLEDGEMENTS

This work was carried out in the framework of the project "Influence of Melioration Interventions Control on Hydrological Soils Regimes and Hydrological Processes in Landscape" which is a part of the research objectives of Research Institute for Soil and Water Conservation Prague. The authors would like to express their thanks to Mr. P. Hospodka for his carefully and systematically performed measurements in the experimental catchment, and to Mr. J. Hanzlík, a student of the Faculty of Natural Sciences of the Charles University, for his assistance in computer processing of the piezometric measurements.

REFERENCES

Soukup, M., Kulhavý, Z., Pilná, E., Mimrová, K., Eichler, J. (2001) Measures for runoff regulation in an agriculturally exploited catchment. Output of the project NAZV EP 0960006150. *VÚMOP Prague methodology*, no.26, pp. 51.

Soukup, M., Kulhavý, Z., Hrádek, F., Eichler, J., Pilná, E., Doležal, F., Hospodka, P., Čmelík, M., Mimrová, K., Čížek, V., Kyzlíková, J. (2000) Regulation of surface and ground water runoff in a catchment with regard to water protection. Final report of the project NAZV EP 0960006150. Prague: VÚMOP Prague, pp. 36. + annexes.

Soukup, M., Kulhavý, Z.(2000) Regulation methods of runoff from drainage systems. *Methodology*, 24, 86 pp.

Švihla, V. (1984) Drainage influence on water management balance in a catchment. The final report of the task C 11-329-208-01-02 VÚZZP Prague, 58 pp. + annexes.

Švihla V. (1991) Drainage systems with hydrological function optimation. *Scientific works of VÚMOP Prague*, no. 7, 64-72.

RUNOFF AND SOIL EROSION FROM TILLED AND CONTROLLED GRASS-COVERED VINEYARDS IN A HILLSIDE CATCHMENT

A. Ferrero, L. Lisa, S. Parena, L. Sudiro

Institute for Agricultural and Earth Moving Machines, CNR, Turin, Italy
Fax: +3911-3489218, E-mail: a.ferrero@ima.to.cnr.it

ABSTRACT

Runoff, soil and nutrient losses from a vineyard with rows across the hillslope (15-35%) were monitored in a hillside catchment of NW Italy over a period of seven years. Conventional tillage (T) and controlled grass cover (GC) of the inter-rows were compared in two hydraulically isolated plots (0.6 ha). Moreover, in the top 30 cm of the soil, water-stable aggregates, bulk density, water content at saturation, saturated hydraulic conductivity (SHC) and soil temperature at two depths were monitored. On average, observed topsoil loss was 2410 kg ha^{-1} per year from the T plot and 480 kg ha^{-1} from the GC plot. Nitrogen loss was 1.27 and 0.75 kg ha^{-1} respectively. Normal rainfall events were analysed separately from rainstorms. Soil loss was considerably greater during rainstorms. Nutrient losses followed the same pattern with rather low absolute amounts. The GC management considerably increased the aggregate stability, while SHC was significantly decreased compared to the T plot management. In the GC soil, bulk density and field water capacity were always higher.

Keywords soil erosion, hillside vineyard, tillage, grass cover

INTRODUCTION

In Piedmont (NW Italy), high quality viticulture is located on sloping or steep hill lands (gradient 20-45 %). Traditional hillside viticulture uses deep and surface tillage. This technique, also due to increased mechanisation, can lead to a deterioration of soil physical properties, causing excessive runoff, surface erosion and sometimes landsliding. Tillage affects soil erosion in that it reduces organic carbon in all size fractions, it decreases the aggregate stability, and it creates surface sealing (Burk et al., 1999) which appreciably reduces the soil hydraulic conductivity of the uppermost horizons.

In different hilly areas of Central Italy (Bazzoffi et al., 1999), the controlled grass cover management in orchards and vineyards has proved to mitigate soil erosion by reducing runoff and to be effective in containing water pollution. Vegetation cover affects runoff and reduces surface erosion in several ways: it shields the soil surface from raindrop impacts and prevents crust formation; roots generate macropores thereby enhancing infiltration (Burk et al., 1999).

After some years of grass cover on vineyard inter-row in our experimental site, we have observed an increase in bulk density in the upper soil, a decrease in hydraulic conductivity, and a halving of soil erosion. In dry years we have observed a decrease in grape production (though improvement in quality), however the effects of management led to recovery in the years with more rainfall (Ferrero et al., 2001; Lisa et al., 1999). To ascertain the efficiency of the grass cover management practice for increasing hydrological protection, a vineyard with conventional tillage and grass cover management in a small hillside catchment was monitored from 1992 to 1998 for rainfall, runoff, soil and nutrient losses.

METHODS

The research was carried out in a hill farm of Northern Monferrato (Piedmont). The climate in this area has cold winters with snow and dry summers with rainstorms. Rainfall averages 836 mm per year. The catchment (425-530 m a.s.l) covers about 11 ha with a SW aspect, it includes arable land and vineyards on less sloping plots (15-30% gradient), and coppices on the steeper plots (up to 50% gradient). The soil is silt-loam (58% loam), overlaying marls of the Baldissero Formation (Middle Miocene).

In a vineyard, with vine rows at 2.75 m across the slope, arranged with slight longitudinal slope (2-10%) and terracing at the head of every four rows which decreases the hill slope to 10-20%, two plots (about 0.56 ha each) were hydraulically isolated by an inter-row with uphill counterslope. One of the plots was treated with conventional tillage (T) with autumn ploughing and two tillings; the other plot was treated with controlled grass cover (GC) with mowing and chopping of the cover three times per year. The plots were supplied with a water capture outlet, measurement devices and a slowing decantation tank.

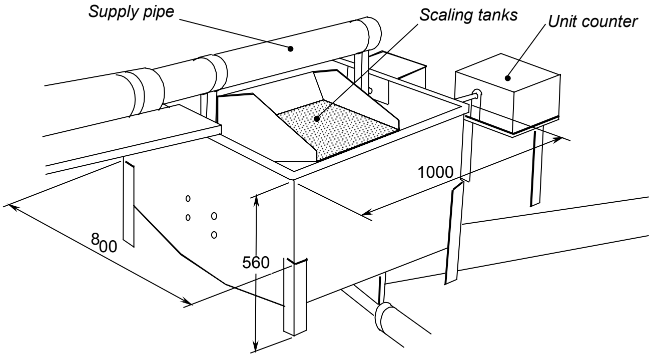

Fig 1: Schematic of the measurement device for the water runoff from the vineyard plots, fitted with scaling tanks and a counter.

The runoff gauge consists of two balancing buckets (12 l capacity) equipped with a click counter and a chart recording system, and of an overflow meter for the water volume if overflowing from the buckets occurs. Part of the water is automatically collected in a container (80 l) for taking samples for soil and nutrient content analyses. Soil deposits in the sedimentation tank were also analysed. The weather station at the farm, equipped with a tipping bucket raingauge (0.2 mm resolution) with chart recorder, was used to obtain the meteorological inputs (a collection of standard meteorological data since 1962 is available).

Moreover some soil characteristics in three layers down to 29 cm depth were monitored in four sub-plots of the compared treatments. At the beginning and end of the experiment, soil samples were collected for chemical analyses, for soil texture, and for water aggregate stability index (WAS), according to Pagliai et al. (1997). Three times per year, bulk density, total porosity, water content at saturation (SP) and at field capacity (FWC) were determined by the method of Luppi (1973) on undisturbed cores (100 cm^3) from three depths. The saturated hydraulic conductivity (SHC) was measured by a Guelph permeameter according to Reynolds and Elrick (1985). Soil temperatures were measured with termocouple sensors, at 6 and 11 cm depths, and registered by datalogger every 10 minutes throughout the year.

The vegetative and productive characteristics of two grape varieties, Barbera and Freisa, commonly grown in the research area, were also monitored.

RESULTS

All the rainfall episodes recorded from 1992 to 1998 were taken into account when their runoff exceeded 0.03 mm (300 l ha^{-1}): this amounted to 101 events. Normal rainfall events (maximum intensity lower than 10 mm h^{-1}) were examined separately from rainstorms and autumnal rains (long lasting rainfalls).

In Table 1, the average features of single events identified as: normal, rainstorm and autumnal rainfall are reported. The events are also grouped by amounts of runoff and soil loss from the two plots.

The mean duration of the 101 events was 47 h, while the rainfall lasted 23.8 h, with a 42.7 mm rainfall depth. The average intensity of rainfall was 5.1 mm h^{-1}, and the maximum intensity was 6.05 and 32.49 mm h^{-1} respectively for normal rainfall and rainstorms.

Very high variability of the rainfall intensity and of the runoff coefficient occurred both for rainstorms and autumnal rains. The runoff coefficient was much higher in the T plot than in the GC one during rainstorms, conversely it was higher in the GC plot for autumnal rainfall events. Also the mean soil losses for each event showed high variability, especially during rainstorms when they rose to 500 kg ha^{-1} in the T plot, while they remained very low (3.1 kg ha^{-1}) during normal events.

Table 1: Mean features of the recorded rainfall events, runoff coefficients and soil losses from tilled (T) and grass covered (GC) vineyard plots for the period 1992 - 1998.

Features		Events		
		Normal	Rainstorm	Autumnal
Duration	(h)	62.2(90.2)*	25.0(144.4)	63.2(60.4)
Rainfall	(mm)	44.4(48.5)	36.0(65.1)	60.7(63.5)
Max.intensity	(mm h^{-1})	6.2(46.8)	31.6(80.1)	4.1(16.6)
°Runoff coeff.	%			
Tilled		0.72(116.9)	2.66(165.9)	1.44(121.4)
Grass covered		0.47(87.2)	1.27(122.2)	2.82(99.5)
°Soil loss	(kg ha^{-1})			
Tilled		3.1(199.5)	500.6(433.3)	1.9(121.9)
Grass covered		2.4(194.2)	99.2(380.6)	1.3(72.2)

* coefficient of variation of single events is shown in parenthesis
° statistically analysed adopting the decimal log

In Fig 2, the hydrograph of a typical short-lived summer rainstorm is shown. It occurred on wet soil, 6.4 mm rainfall the previous day, with 1 h duration, 67 mm rainfall depth, and maximum intensity corresponding to 100 mm h^{-1} for 15 minutes. Runoff started 20 minutes after the beginning of rainfall, at a fairly intense rate of 2.97 mm in the T plot and 2.14 mm in the GC plot. The time lag (peak rainfall to peak discharge) was 52 minutes in the GC plot and 43 minutes in the T one. The runoff coefficients were 4.43% for the T plot and 3.19% for the GC one, the soil losses 953.1 and 617.8 kg ha^{-1} respectively.

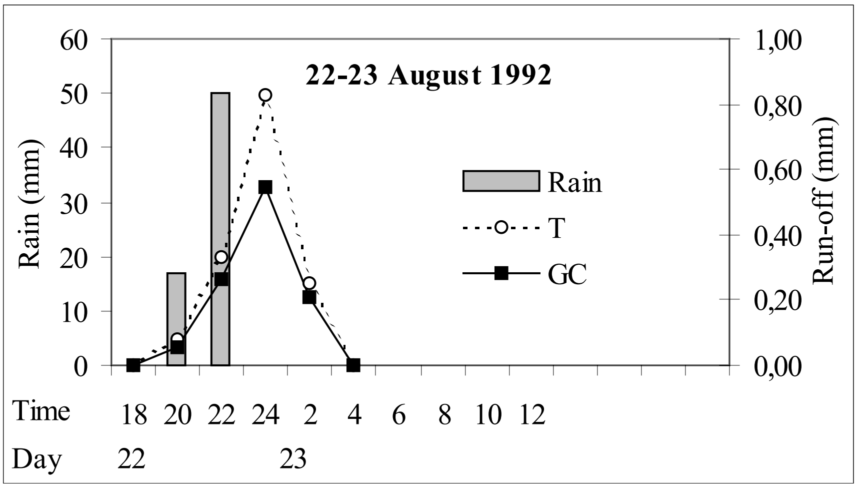

Fig 2: Course of rainfall and runoff during a typical summer rainstorm, from tilled (T) and grass covered (GC) vineyard plots.

Fig 3 shows the time series of annual rainfall and the annual amount of runoff from the T and GC plots. In the years 1992-1993 the runoff amounts were very high, especially for the T plot, as a result of two high intensity short-lived storms. In 1994, total runoff was higher in the GC plot. This behaviour was caused by a heavy autumnal rainfall event, which produced more runoff from the GC plot.

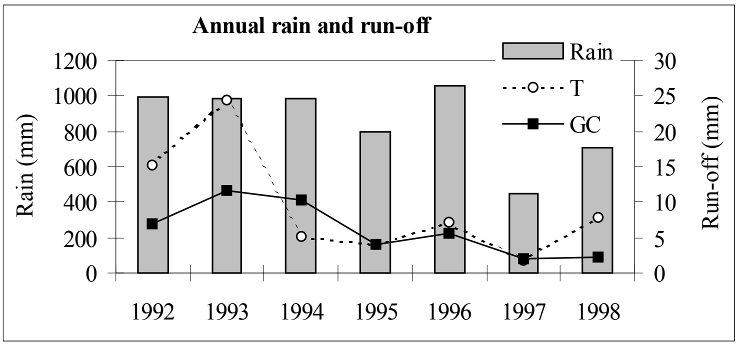

Fig 3: Trend over the years of total annual rainfall and runoff from tilled (T) and grass covered (GC) vineyard plots.

The mean runoff depth of the single events for normal rainfall (57 events) was 0.35 mm from the T plot and 0.22 mm from the GC one. In the case of the 39 rainstorms identified, a larger difference occurred, as the mean amounts were 1.04 and 0.5 mm respectively (Fig 4). It is therefore clear that rainstorms result in heavier runoff which is mitigated by continuous grass cover.

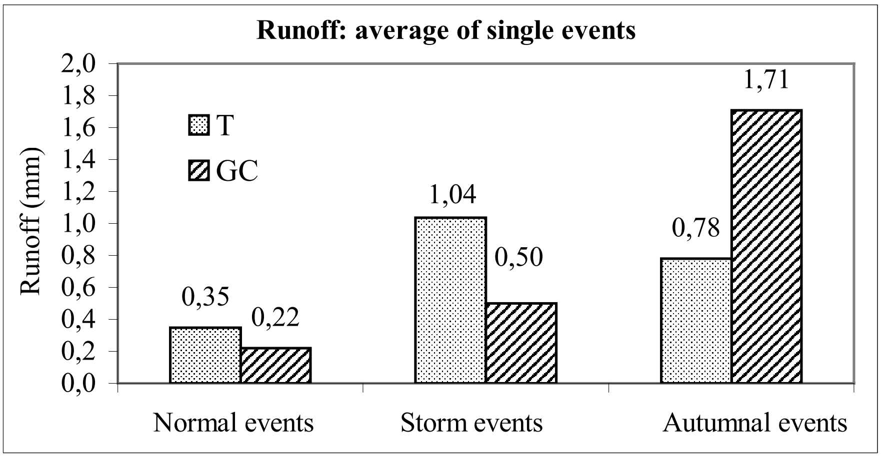

Fig 4: Average runoff, for the period 1992-1998, during normal rainfall and rainstorms, from tilled (T) and grass covered (GC) vineyard plots.

In the case of normal rainfall, moderate annual soil losses were detected: 21 and 18 kg ha^{-1} (mean of seven years) in the T and in the GC vineyard plots; also the nitrogen losses were very low: 0.44 kg ha^{-1} and 0,30 kg ha^{-1} respectively. During rainstorms, soil losses rose to 2390 Kg ha^{-1} from the T plot and only to 459 kg ha^{-1} from the GC one (Fig 5). Nitrogen loss from the T plot almost doubled (0.82 kg ha^{-1}), whereas from the GC one there was only a moderate increase (0.35 kg ha^{-1}).

The permanent grass cover considerably increased (about double near the surface) the organic matter content in the soil compared with the T plot (Table 2). The aggregate stability to water (WAS) was much higher in the first two layers of the GC soil: this can be correlated with the increase of organic carbon in the surface soil.

The bulk density was, on average, higher in the upper two layers the GC soil. In autumn, a considerable increase in bulk density, near 18 cm depth, was noted also in the trafficked areas of T plot inter-rows.

The water content at saturation (SP) and at field capacity (FC) proved to be higher in the first two soil layers of the GC plots. A considerable increase of organic carbon and of aggregate stability in the surface layer was also noted by Carter (1992) when comparing the soil properties of tilled and grassland sites.

The saturated hydraulic conductivity (SHC) was significantly lower in the upper soil of the GC inter-rows, but less variable in time and space: higher differences occurred in spring. Other studies have related the lower water conductivity of no-till practices with higher bulk density (Heard et al., 1988).

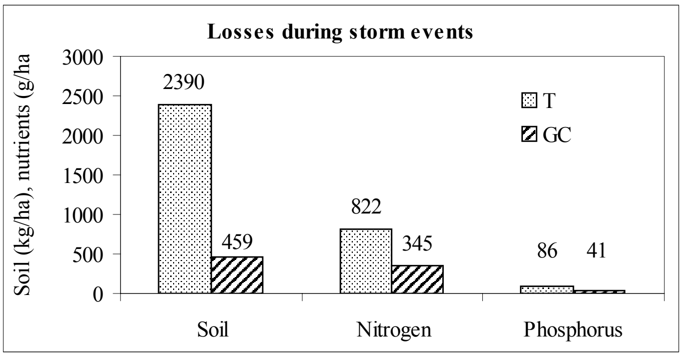

Fig 5: Average annual soil and nutrient losses from the vineyard plots for the period 1992-1998 during the monitored storm events.

Table 2: Selected soil characteristics in a hillside vineyard measured after seven years of applying conventional tillage or grass cover technique.

Parameters measured		Tilled soil, Depth, (cm) 0-9	10-19	20-29	Grass cover, Depth, (cm) 0-9	10-19	20-29
Organic matter	(g kg^{-1})	2.9**	2.6*	1.5	5.5**	3.8*	2.1
Bulk density	(Mg m^3)	1.18*	1.22*	1.20	1.20*	1.24*	1.23
Saturation capacity	(%v/v)	53.8	48.5*	49.5	54.2	52.0*	50.1
Field capacity	(%v/v)	35.0*	33.3**	36.2*	38.1*	36.5**	37.1*
Satur.conductivity, SHC	(m d^{-1})		1.46*			0.88*	
Water-stable aggregate Index, W.A.S.		6.1**	5.5**	ND	20.9**	26.2**	ND

SHC: means the depth of measurement 10-20 cm
Means with * and ** at the same depth are significantly different at the 0.05 level and 0.01 by the LSD test.

The temperature in the upper soil of GC plots showed higher values in winter, lower in summer, and less fluctuation, compared with the T soil. In January, the mean and standard deviation of the minimum daily temperature at 6 cm depth were 3.38$\pm$0.64 °C in the GC plot, and 2.68$\pm$0.78 °C in the T plot. The mean and standard deviation of the maximum were 5.78$\pm$0.80 °C and 4.89$\pm$0.97 °C respectively. A reverse relation occurred in August when minimum and maximum daily temperatures were lower in the GC plot: 20.35$\pm$0.30 °C and 23.04$\pm$1.46 °C, while in the T plot the averages were 22.21$\pm$1.54 °C and 27.24$\pm$2.66 °C.

This trend may be correlated with the grass canopy and the mulching action of the plant residue which decreased the energy available at the soil surface and the evaporative losses. Similar behaviour was noted by Herrero et al. (2001).

The mean qualitative and productive results highlight lower plant vigour and grape yield in the GC vineyard, though significant differences occurred only for the Barbera vine. Over seven years, the mean production (Barbera) and the standard deviations were 2.48$\pm$0.39 kg/plant in the GC plot, and 3.18$\pm$0.55 kg/plant in the T one; the sugar content was 196.91 $\pm$17.09 g/l and 189.86$\pm$21.02 g/l respectively in the GC and T treatments.

CONCLUSIONS

The controlled grass cover of hillside vineyards in the experimental site has proved to be effective in reducing runoff, soil erosion, and environmental impacts. The mean values for the seven years of observations indicate an annual topsoil loss of 2410 kg ha^{-1} from the T plot and 480 kg ha^{-1} from the GC one, and a nitrogen loss of 1.27 kg ha^{-1} and 0.75 kg ha^{-1}, respectively. During autumnal rains, runoff is greater from the GC plot. This behaviour might be induced by higher bulk density and lower hydraulic conductivity of the soil which increase surface runoff, whereas in the tilled soil, the roughness effect prevails producing greater hydraulic gradients (Burk 1999).

The positive effect of the practice is enhanced during rainstorm events. The soil losses are less than in similar experiments in central Italy (Bazzoffi and Chisci, 1999); this may be due to the arrangement of the vineyard, developed to reduce water runoff.

The different topsoil erosion in the two practices would be clarified by the analyses of the soil physical properties, which indicate a considerable increase of water stability of the aggregates in the topsoil under the GC practice. It is well known that soil erodibility is related to detachability and transportability, both of which depend on the physical and chemical properties of the soil (Lal et al., 1994).

To conclude, the results of the above research confirm, in our experimental condition, the positive effect of the controlled grass cover of the vineyard, but also highlight some constraints. Therefore, there is need for further research to deepen some aspects, especially the duration over time of the permanent grass cover.

ACKNOWLEDGEMENTS

The authors thanks G. Benvegnù, M. Parena of the CNR staff of the Vezzolano farm for their technical assistance, and Dr. A. Nosalewicz, Polish Academy of Sciences, for the evaluation of temperature data.

REFERENCES

Bazzoffi, P., Chisci, G. (1999) Soil conservation techniques in vineyards and peach orchards of the Cesena hilly area. *Riv. Agric*., 33, 177-184.

Burk, A. R., Chanasyk, D.S., Mapfumo E. (1999) Influences of land disturbance and management regime on infiltration and runoff . *Canadian Agric. Eng.,* 41, 127-132.

Carter, M.R. (1992) Influence of reduced tillage systems on organic matter, microbial biomass, macro-aggregate distribution and structural stability of the surface soil in a humid climate. *Soil. Till. Res.,* 23, 361-372.

Heard, J.R., Kladivko, E.J., Mamering, J.V. (1988) Soil macroporosity, hydraulic conductivity and air permeability of silty soils under long-term conservation tillage in Indiana. *Soil. Till. Res*., 11, 1-18.

Herrero, E.V., Mitchell, J.P., Lanini, W.T., Temple, S.R., Campiglia, E. (2001) Soil properties in no-till tomato production. *Calif. Agric.*, 55, 30-34.

Ferrero, A., Lipiec, J., Nosalewicz, A., Parena, S. (2001) Conventional tillage or permanent grass cover in hillside vineyards: effects on soil physical characteristics. In: *Proc. Int. Conf. of Physical Methods in Agriculture*, Prague, 27-30 August, 88-92.

Lal, R., Mauhboubi, A., Fausly, N.R. (1994) Long-term tillage and rotation effects on properties of a central Ohio soil. *Soil Sc. Am. J*., 58, 517-522.

Lisa, L., Parena, S., Lisa, L. (1999) Comparison between grass cover and soil working techniques in Piedmont region: vine growing aspects. *11èmes Journées d'Etudes GESCO*. Palermo (Italy)*, 6-12 June*, vol.2, 891-895.

Luppi, G. (1973) Research on the determination of hydrological characteristics of soils. (in Italian): *La Ricerca scientifica*. CNR, Roma, Quad. 79, 72-83.

Pagliai, M., Torri, D., Patruno, A. (1997) Aggregate stability and size distribution. (in Italian). Methods of soil physical analysis. *FrancoAngeli*, Milano, Italia, Part V, 1*,* 7-13.

Reynolds, W.D., Elrick, D.E. (1985) In situ measurement of field saturated hydraulic conductivity, sorptivity, and the alpha-parameter using the Guelph permeameter. *Soil Sci.*, 140, 292-302.

VARIABLE GROUNDWATER CATCHMENT SIZE IN AN AREA WITH DEEP WATER TABLES

R. Dijksma, H.A.J. van Lanen, P. Aalders

Sub-department of Water Resources, Wageningen University, Nieuwe Kanaal 11, 6709 PA Wageningen, The Netherlands

ABSTRACT

In catchments with deep groundwater tables the topographical catchment boundary is often used as a hydrological boundary. The better method, determining the catchment boundary by deep piezometers, is hampered by the scarsity of deep expensive drillings. A simple steady state groundwater model was constructed in order to derive the hydrological boundaries of the Noor catchment. This model indicates a much smaller hydrological catchment than the topographical catchment (716 and 1056 ha, respectively). The simplified model indicated variable catchment boundaries, given the meteorological conditions. Therefore calculations have also been performed to estimate the minimum and maximum size of the catchment. Attempts to relate the NO_3 load of major springs and the Noor brook to the N-input on a field scale are largely influenced by this variable catchment size.

Keywords topographical versus hydrological boundary, deep groundwater tables, NO_3 load, groundwater modeling

INTRODUCTION

In the Noor catchment (The Netherlands), a small catchment with deep water tables, nitrate concentrations are increasing. Many springs have already exceeded the critical concentration of 50 $mg \cdot l^{-1}$ NO_3. The biggest and therefore most important spring (Sint Brigida spring) in the catchment shows an increase from 40 $mg \cdot l^{-1}$ in the early eighties up to 85 $mg \cdot l^{-1}$ NO_3 at present. The discharges of the major springs and the brook are measured continuously. In order to relate the NO_3 loads to the N-input, it is important to know the size of the catchment.

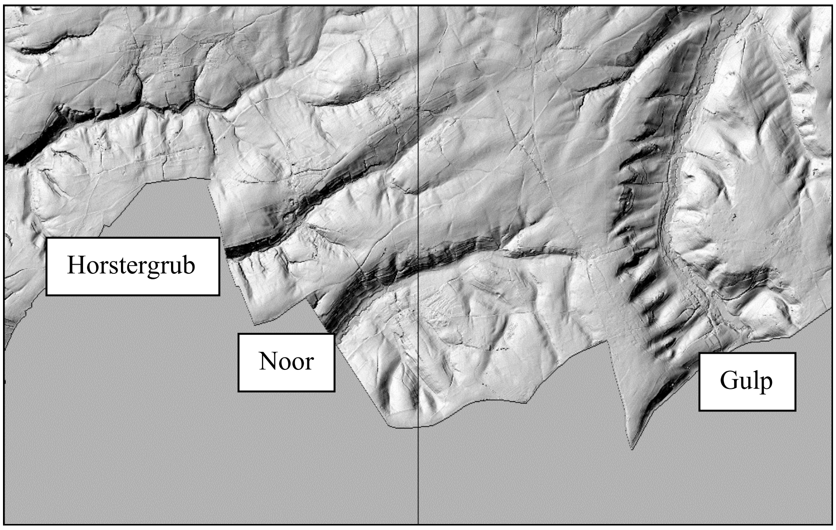

Fig 1: Topography of the Dutch part of the area: South Limburg.

Common practice in determining the catchment boundary in areas with deep groundwater tables is the assumption that the hydrological boundary and the topographical boundary coincide (Querner et al., 1997). In the Noor catchment, with little information on groundwater heads near the assumed catchment boundaries, this assumption led to a catchment of approximately 1056 ha (Dijksma and Van Lanen, 2001). By constructing a simple steady state groundwater model of the area, with as few assumptions as possible, the catchment boundary and catchment size were calculated.

METHODS

The Noor is a small tributary of the river Meuse, located in the south-east of the Netherlands and north-east of Belgium (Fig 1). The surface elevation in this catchment varies between 240 m a.m.s.l. in the south-east and 91 m a.m.s.l. at the outlet. The Noor brook starts as the Sint Brigida spring at 138 m a.m.s.l., has a length of 3 km and discharges into the Voer in Belgium.

Consolidated Upper-Carboniferous shales and sandstone, folded at the Variscan orogeny, form the impermeable base at a depth of 50-150 m below the surface (Heijde et al., 1980). In the downstream part in Belgium these Upper-Carboniferous formations have been eroded and permeable Lower-Carboniferous limestones occur, which implies that the impermeable base is at a depth of more than 800 m. These consolidated rocks are discordantly overlain by subhorizontal Upper-Cretaceous deposits, consisting of a sedimentary series of clayey silts, interbedded with thin layers of consolidated and fractured sandstone (Vaals Formation), and soft and poorly bedded chalk (Gulpen Formation). A poorly sorted regolith is found on top of the chalk (Eindhoven Formation). These formations lead to a hydrological system with deep groundwater tables in the largest part of the area, and shallow water tables near the Noor brook and its springs.

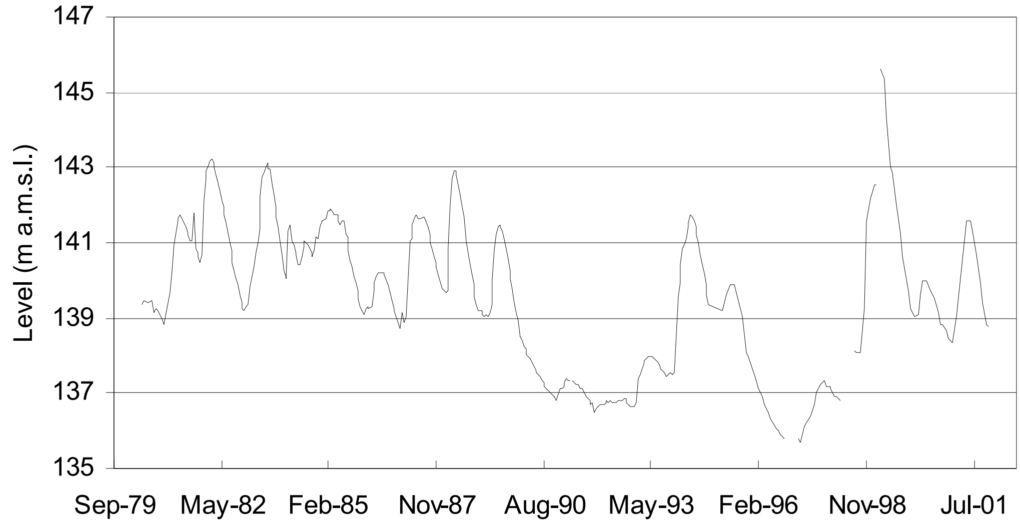

Fig 2: Groundwater table in the Noor catchment (WP98).

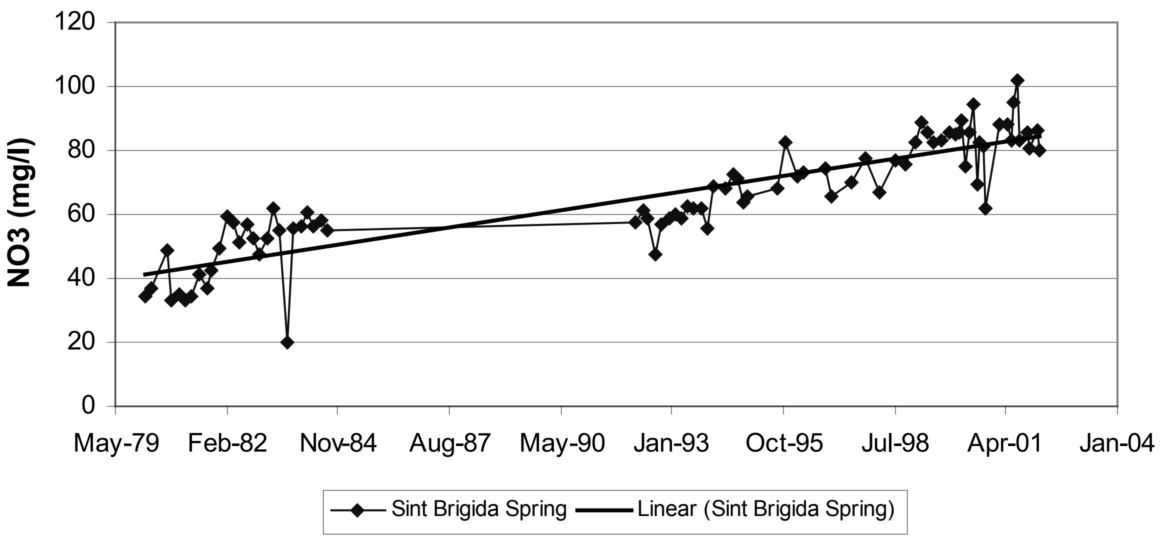

Fig 3: Nitrate concentration of the Sint Brigida Spring.

The deep groundwater tables show large fluctuations over time, due to variations in the annual rainfall surplus (Fig 2). Nitrate concentrations do not show the same fluctuation, but a gradual increase. Fig 3 shows the nitrate concentration of the Sint Brigida Spring over the last 20 years (Van Lanen and Dijksma, 1999).

MODELLING

A simple steady state groundwater model was constructed using Micro-Fem (Hemker and Nijsten, 1996). Its boundaries were chosen at a relatively large distance from the assumed Noor catchment boundaries. The transmissivity of the Cretaceous formations was assumed to be 100 m^2 d^{-1} (Dijksma and Van Lanen, 2000; Peters et al, 2001). Neighbouring brooks were included in the model.

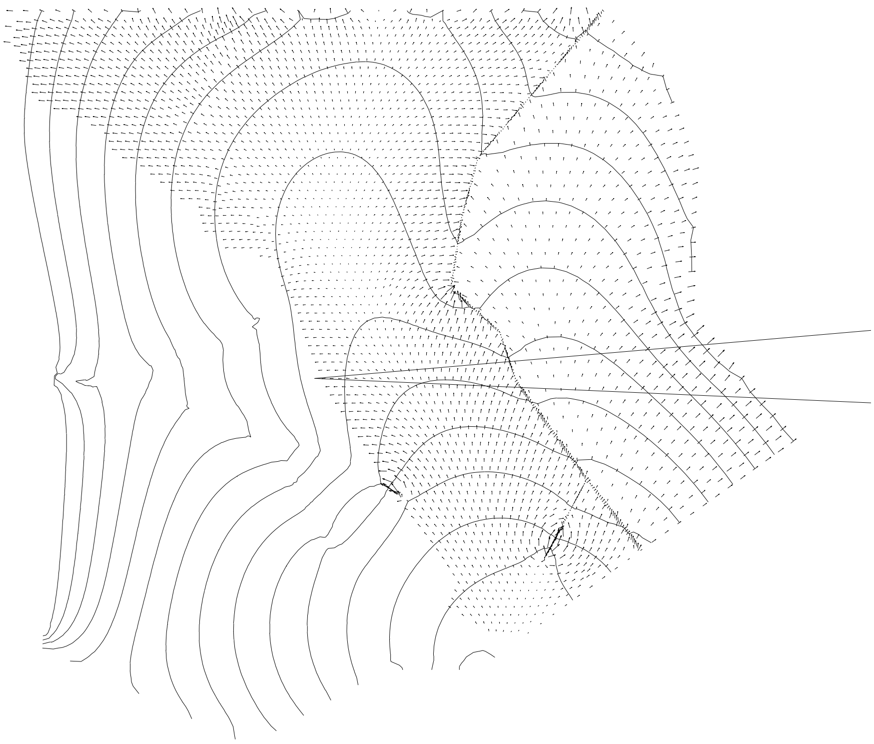

Fig 4: Reference groundwater model of the Noor and neighbouring brooks, depicting flow direction and velocity.

Fig 4 shows the result using the long-term average of 269 mm·year^{-1} as rainfall surplus. The small arrows indicate the flow direction and velocity. The darker area is the resulting Noor catchment. The long tail of the catchment is the result of inaccuracy at the south-east model boundary. In the calculations, this tail is ignored.

This reference model indicates that the catchment extends over only 716 ha, and is thus much smaller than the topography based catchment of 1056 ha. On all sides, the catchment boundary is shifted towards the brook.

Since the catchment is certainly not at steady state with fluctuations in rainfall surplus and accompanied fluctuations of the deep groundwater tables, calculations were also made under wet and dry conditions. The wet condition was represented by a doubled rainfall surplus, the dry condition by half the rainfall surplus (Table 1).

Table 1: Calculated Noor catchment size; maximum variation.

	Rainfall surplus ($mm \cdot year^{-1}$)	Catchment size (ha)
Reference	269	716
Double (x 2)	538	1016
Half (x 0.5)	135	437

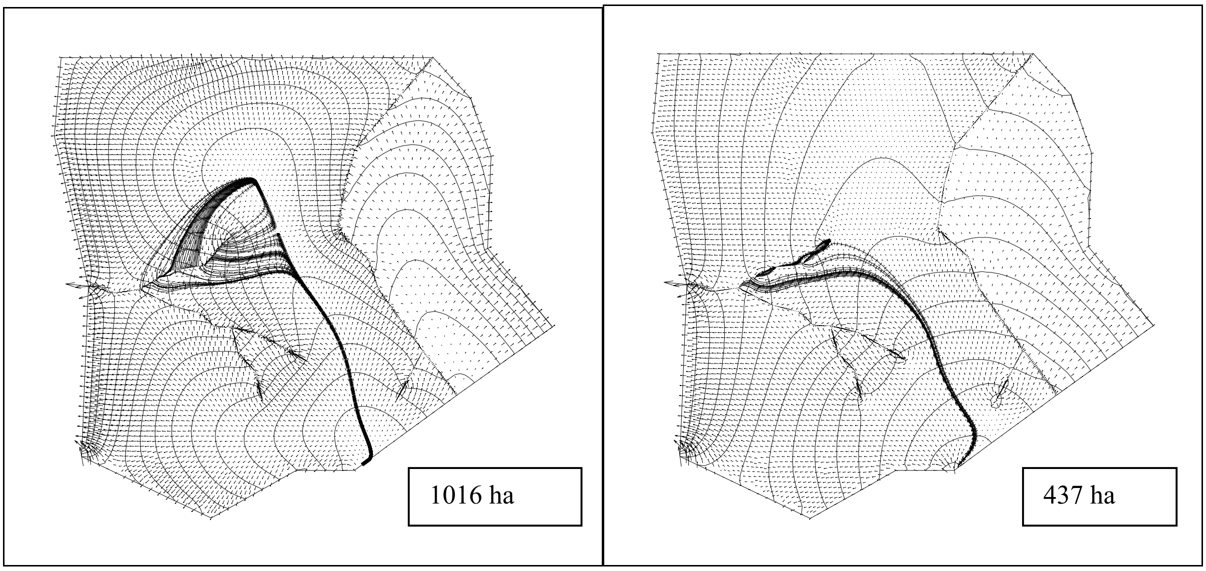

Fig 5: The Noor catchment, with rainfall surplus x 2 and x 0,5 respectively.

These results indicate that the catchment size is strongly dependent on the climatic conditions. As shown in Fig 2, the wet and dry periods only last a few years. Then the conditions change again. Equilibrium in groundwater levels, discharges and therefore catchment boundaries is never reached. Thus, the catchment boundaries in this system are fluctuating over time, but not as much as indicated in Table 1.

It was estimated that, given the duration of the wet and dry periods, it would be more realistic to use less extreme values for rainfall surplus. Another indication that the catchment size fluctuation should be less than that reported in Table 1 was that the calculated groundwater heads (max. and min.) were never reached. A correction factor was derived, using the calculated and real groundwater levels. Table 2 shows the results of these calculations.

Table 2: Calculated Noor catchment size; realistic variation.

	Catchment size (ha)
Reference	716
Wet conditions	781
Dry conditions	644

Another possible check on the most likely catchment size is to calculate the water balance. However, in areas with deep groundwater tables a large quantity of water can be stored in the unsaturated zone. It would be necessary to calculate a water balance over tens of years to eliminate the storage uncertainty.

CONCLUSIONS

In areas with deep groundwater tables the topographical boundary is often used as the hydrological catchment boundary. Piezometers to validate this assumption are often scarce. Water balance calculations to derive the catchment size are hampered by the large storage capacity of the unsaturated zone.

In the Noor catchment, the most likely hydrological catchment area is only 68% of the topographical catchment area. The catchment size is not constant over time, but is related to variations in rainfall surplus (± 10 %). The correlation of Nitrate loads in springs and brooks, and N-input on the field scale can contain large errors (> 25%) because of this phenomenon.

ACKNOWLEDGEMENT

The research was carried out as part of the programme of the Wageningen Institute for Environment and Climate Research (WIMEK/SENSE).

REFERENCES

Dijksma, R., van Lanen, H.A.J. (2000) Monitoring and modelling of springflow in the Noor catchment (the Netherlands) In: *Catchment hydrological and biochemical processes in the changing environment*; IHP 2000, 31-36.

Dijksma, R., Lanen, H.A.J. van (2001) De afvoer van de Noor (Zuid-Limburg); Periode 1992 – 2000 (in Dutch). Subdepartment Water Resources, Wageningen University.

Heijde, P.K.M. van der, Kuyl, O.S., van Rooijen, P. (1980) Grondwaterkaart van Nederland; Kaartblad Maastricht 61 en Heerlen 62 West (in Dutch), Dienst grondwaterverkenning TNO, Delft, the Netherlands.

Hemker, C.J., Nijsten, G.J. (1996) Groundwater Flow Modelling using Micro-Fem; Version 3, Free University Amsterdam, the Netherlands.

Lanen, H.A.J van, Dijksma, R. (1999) Water flow and nitrate transport to a groundwater-fed stream in the Belgian-Dutch chalk region. *Hydrological Processes*, 13, 295-307.

Peters, E., van Lanen, H.A.J., Alvarez, J., Bradford, R.B.B. (2001) Groundwater droughts; Evaluation of temporal variability of recharge in three groundwater catchments. *ARIDE Technical report no. 11*, Wageningen.

Querner, E.P., Tallaksen, L.M., Kašpárek, L. van Lanen, H.A.J. (1997) Impact of land-use, climate change and groundwater abstraction on stream flow droughts, using physically based models. *FRIEND '97 – Regional Hydrology: Concepts and Models for Sustainable Water Resource Management*. IAHS Publ. No. 246.

INTERCOMPARISON OF FIELD OBSERVATIONS AND HYDROLOGICAL MODELLING OF HILLSLOPE RUNOFF COMPONENTS

H. Holzmann

Institute for Water Management, Hydrology and Hydraulic Engineering.
BOKU – University of Natural Resources and Applied Life Sciences, Vienna, Austria

ABSTRACT

A conceptual rainfall-runoff model originally developed for the basin scale was applied in this paper at the hillslope scale. Observation data gained by field experiments were compared with the simulation results of the model. The total amount of simulated runoff showed reasonable agreement with observations. But regarding the specific runoff components, the model overestimated interflow and underestimated (near)surface flow. This was caused by the model design based on the saturation excess concept. Some model parameters and state variables such as soil depth, wilting point, field capacity and soil water storage pertain to physical properties. Therefore the model can be applied on sparsely monitored plots. As hillslope runoff components will hardly be available, soil moisture observations can be used for model calibration and validation.

Keywords hillslope runoff processes, runoff formation experiments, subsurface flow, conceptual hydrological modelling

INTRODUCTION AND OBJECTIVES

One main objective of hydrological field experiments is to gain knowledge regarding runoff formation processes. Based on these experiences simulation models can be developed and evaluated, considering impacts of vegetation cover, soil properties and morphological parameters.

Hydrological runoff models have been applied to numerous problems in hydraulic engineering and water management. In general, water management decision making deals with larger spatial scales than field experiments and, therefore, applies models which have been validated for those particular larger scales. This paper aims to test and verify whether a conceptual hydrological model is applicable also for local plot scale approaches and whether it can reflect the natural behaviour of a hydrological system.

FIELD DATA AND OBSERVATION DESIGN

In the framework of a research project dealing with hydrological functions of alpine forest ecosystems (Hager and Holzmann, 1997), hillslope runoff processes were analysed (see also Holzmann and Sereinig, 1997). The experimental site was located in the western part of the Austrian province of Styria in the upper catchment of the river Enns. The elevation of the subcatchment ranges from 700 to 2200 m a.s.l., the experimental plot was located at 1100 m a.s.l. The slope inclination was about 35 degrees. The plot was situated in a forested stand, stocked by a mixed forest (European beech, Norway spruce, silver firs) with domination of deciduous species. The soil depth was about 160 cm, the permeable bedrock consists of fractured phyllite slate. The field observation design included the measurement of subsurface runoff, soil moisture and soil suction on the plot scale. A scheme is shown in Fig 1. Observations of the meteorological data and rainfall measurements in the forest stands and in the open space enabled the estimation of water balance components like interception, infiltration and runoff. Similar investigations are referred to in Atkinson (1978) or in Peters et al. (1995).

Field measurements were carried out during the summer period in 1995. All data were stored in data loggers and have temporal resolutions of 5 to 15 minutes and have been aggregated to hourly and daily time series. The database of the field observations and derivatives to be used in the hillslope runoff modelling include the following:

- subsurface runoff at 20, 100 and 160 cm depths,
- net precipitation (excluding interception),
- soil moisture at 40, 60 and 90 cm depths and 20, 150 and 300 cm upslope of the drainage pit,
- potential evapotranspiration (estimated by the Penman-Monteith formula),
- soil suction head at 40 and 80 cm depths.

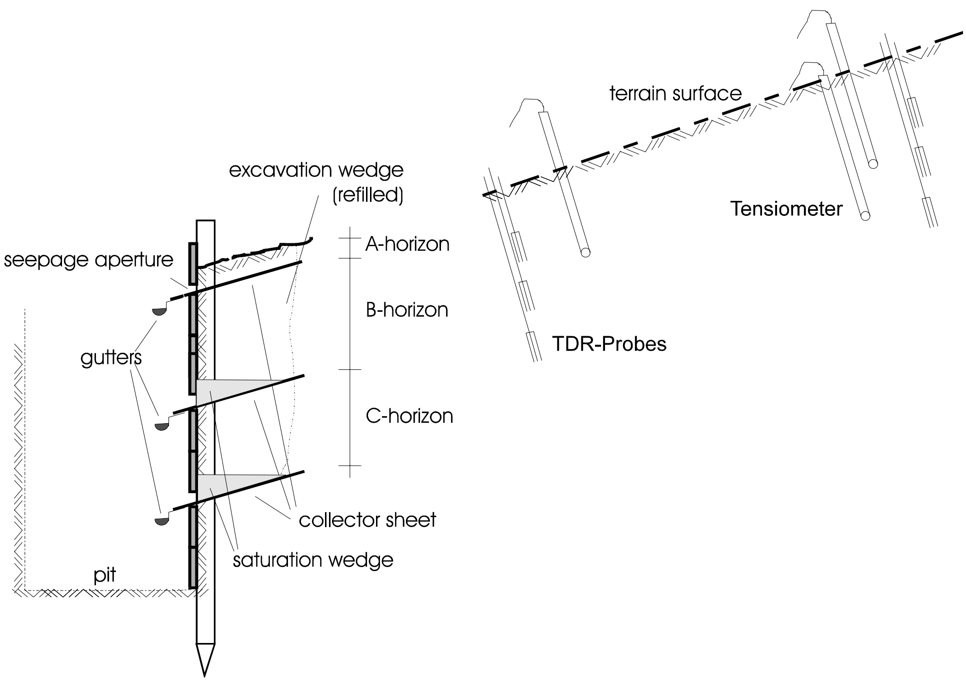

Fig 1: Scheme of the measurement plot and instrumentation (modified from Holzmann and Sereinig, 1997).

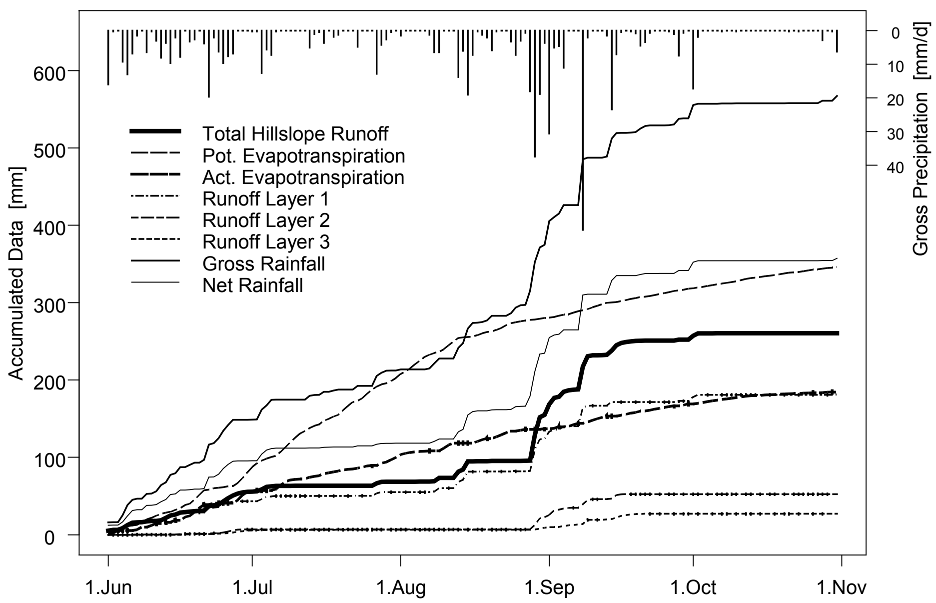

Fig 2: Accumulated water balance components for the summer period 1995.

The cumulative water balance components for the 1995 observations are plotted in Fig 2. For the period from June to November the gross precipitation was 568 mm, the net precipitation (excluding the interception loss) was 357 mm. Interception was directly measured by means of rain gauges in the stand and stem runoff equipment. The total hillslope runoff was 261 mm, which represents 46% of the total rainfall or 73% of the net precipitation. Table 1 shows the monthly water balances for the observation period.

Actual evapotranspiration was estimated by the calibrated conceptual rainfall-runoff model described below, considering the instantaneous available soil moisture content (for plants) and the evaporation demand of the atmosphere. Table 1 shows that this actual evapotranspiration is very near to the observed interception losses (the difference between gross precipitation and net precipitation).

Table 1: Water balance components of the observation period 1995.

	Net Precip. [mm]	Gross Prec. [mm]	Mean Air Temp. [°C]	Pot. ET [mm]	Act. ET [mm]	Runoff total	Runoff 1 [mm]	Runoff 2 [mm]	Runoff 3 [mm]
June	95	149	10.7	80	55	55.3	43.3	6.9	5.1
July	23	64	17.1	122	48	13.3	11.9	0.1	1.3
August	116	163	13.3	77	34	86.7	68.5	15.6	2.6
Sept.	107	163	8.8	38	33	97.3	49.4	29.8	18.1
October	16	29	8.5	27	14	8.4	8.1	0.2	0.1
Total	**357**	**568**	**11.7**	**345**	**184**	**261.0**	**181.2**	**52.6**	**27.2**

Besides the above observations, additional forest ecological investigations were carried out to estimate root depths and densities, stem runoff and interception of vegetation and litter layer.

APPLIED HYDROLOGICAL MODEL

Conceptual models are generally applied at the basin scale. This was also the case for the described model, which was originally developed for runoff forecast purposes for catchments larger than one thousand square kilometres. The scheme of this model is presented in Fig 3. The development process is described in Nachtnebel and Holzmann (1999) and in Holzmann and Nachtnebel (2002). The design of the available model includes three runoff components of quick (near surface) flow, interflow and slow (base) flow, which are to some extent analogous to the runoff components observed in the plot scale investigations (compare with Fig 1). Therefore it was deemed useful to test if the model assumptions of multiple storage release agree with the observations made on the plot scale.

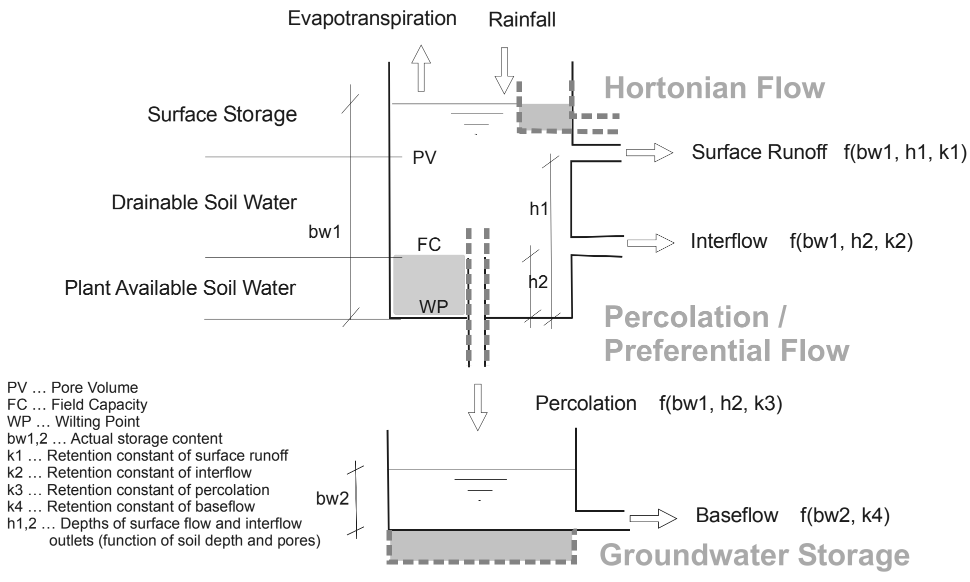

Fig 3: Conceptual rainfall runoff model (after Nachtnebel and Holzmann, 1999) with recommended modifications (dashed modules).

The conceptual rainfall-runoff model consists of two storages. The upper storage represents the soil column. Two outlets correspond to surface runoff (saturation overland flow) and interflow (macropore flow).

The second storage is the groundwater storage, interconnected with the soil column only by the vertical downward flux component (percolation), i.e. not allowing for the upward capillary rise of water. Groundwater release can be interpreted as the slow baseflow component. The basic model, primarily developed for daily time steps, was discretised to hourly intervals. All input data such as rainfall and potential evapotranspiration were transformed to that time scale. The interception process of the vegetation cover is not directly integrated into the model, but its effect can implicitly be considered as being included in the actual evapotranspiration. The dashed and dotted model components of Fig 3, e.g. the Hortonian flow component, did not exist in the original model version but refer to recommendations for improvement mentioned in the conclusions of the present paper.

The model application on the plot scale was made possible due to the availability of specific discharge observations for the quick, medium and slow flow components. This enabled a parameter calibration, which had not only to consider total runoff as the overall response of the system – which is usually available for the model calibration at the catchment scale – but linked the model parameters more closely to the addressed processes. Using the minimum least square criterion as the objective function, the improved calibration follows equation (2) instead of using equation (1). Some subjective weighting coefficients λ can account for different data reliability or for different priorities in the particular runoff components.

$$d = \sqrt{\left(q_{total}^{obs} - q_{total}^{sim}\right)^2} \Rightarrow Min \tag{1}$$

$$d = \lambda_1 \cdot \sqrt{\left(q_1^{obs} - q_1^{sim}\right)^2} + \lambda_2 \cdot \sqrt{\left(q_2^{obs} - q_2^{sim}\right)^2} + \lambda_3 \cdot \sqrt{\left(q_3^{obs} - q_3^{sim}\right)^2} \Rightarrow Min \tag{2}$$

where:

d … value of the objective function

q_i … fluxes (total or for near surface flow (1), interflow (2) and base flow (3)), observed or simulated

λ_i … weighting coefficient for near surface flow (1), interflow (2) and base flow (3)

SIMULATION RESULTS AND INTERPRETATION

Runoff comparison

Due to the short duration of the observations, the model was calibrated for the entire period. Only the first 10 days were excluded in the objective function, allowing a compensation of errors of the initial condition estimation. Both for daily and hourly temporal resolutions, the total hillslope runoff could be modelled well. The correlation coefficient of 0.95 and a Nash-Suttcliffe (NS) value of 0.89 confirm the good performance. Fig 4 shows that the total discharge peaks agree between observed and simulated data; only small runoff peaks in July were underestimated by the model.

For the specific runoff components, bigger discrepancies between observed and simulated data exist and are indicated in Fig 5 by grey ellipses. The upper layer flow – interpreted as near surface flow – was reliably simulated for the bigger peaks, while smaller runoff events were underestimated by the model. The correlation coefficient for the near surface runoff was 0.90 and the NS-coefficient was 0.76. The model parameters (depths of outlets and recession constants) were optimised using equally weighted square errors of the three specific runoff components corresponding to equation (2). As the highest discharges occurred for layer 1, the deviations in the objective function gave higher weight to the parameters of layer 1. The interflow layer was not described so well, correlation coefficient of 0.65 and NS-coefficient of 0.1 show rather weak agreement. The observed intermittent base flow component was not described by the model at all. To prevent the model from percolating too much water – which could not be observed in nature – the calibration resulted in very high retention constants *k3* and *k4* (see Fig 3), reflecting percolation and groundwater flow, which made the simulated base flow delayed and smoothly varying and not corresponding to the observed runoff pattern.

Some difficulties are also caused by the variable contributing area of the plot, which is not a priori known. At the beginning of some rainfall events, the hydraulic head gradient is directed rather perpendicular to the soil surface. With increasing soil moisture content the flux will be more directed parallel to the surface.

Therefore, the runoff measuring troughs receive water from an area which is small at the beginning but gets progressively larger during the course of the event. A closed water balance then cannot be easily made.

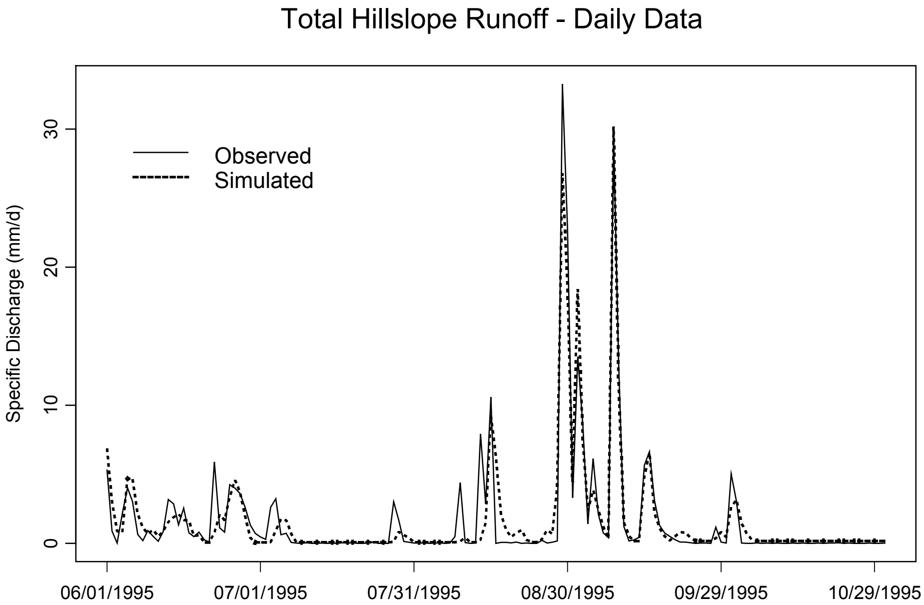

Fig 4: Simulation of Total Hillslope Runoff.

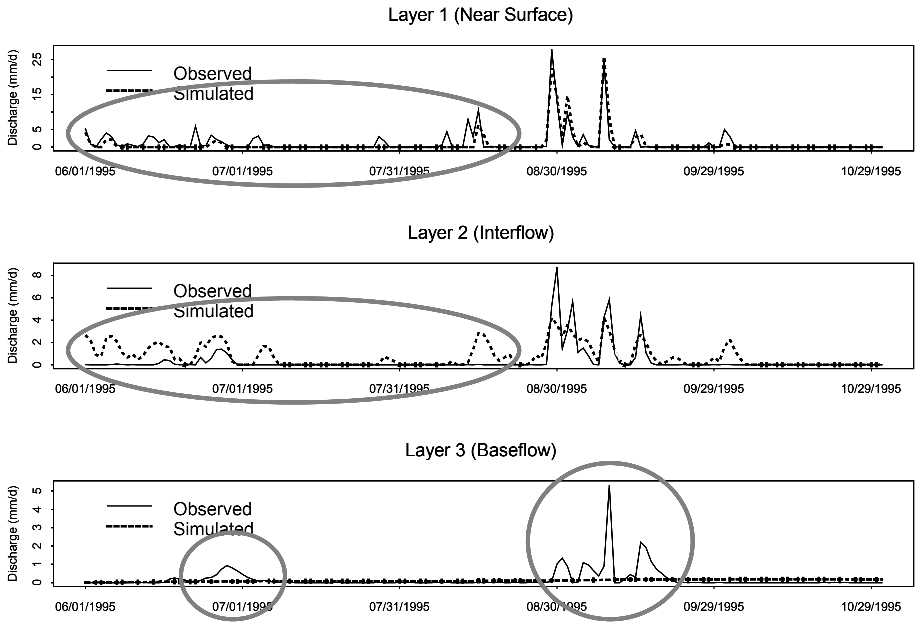

Fig 5: Simulation of specific runoff components.

Soil moisture comparison

The upper storage of the conceptual model represents the soil column (see Fig 3). The water content scale starts with the wilting point (WP), percolation and interflow is initiated at field capacity (FC) and surface runoff at saturation (saturation excess flow).

According to the model concept (see Fig 3), the state variable *bw1* of the model upper storage (soil storage) can be interpreted as

$$bw1(t) = (\theta(t) - \theta_{WP}) \cdot \Delta h \tag{3}$$

where $\theta(t)$ … average instantaneous soil moisture content
θ_{WP} … average soil moisture content at wilting point
Δh … depth of soil column

By solving equation (3) with the observed soil moisture data $\theta(t)$, the corresponding estimate of the state variable *bw1* can be compared with the model results. Fig 6 shows the simulated state variable and the soil water storage according to the TDR measurement at a 40 cm depth estimated by means of equation (3). The absolute variability of the soil moisture storage is reliably modelled, but the observed data show a more pronounced increasing trend than the modelled data and the drainage phases of observed soil moisture variations tend to be delayed. Some deviation may be due to the fact that the soil profile depth considered in (3) was about 90 cm, while the TDR data correspond to a depth of 30 to 50 cm only.

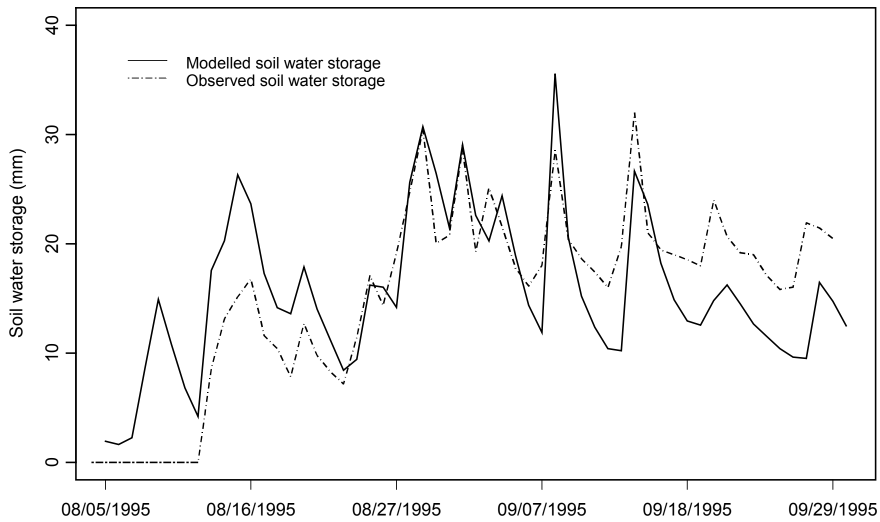

Fig 6: Modelled (conceptual model) and observed (equation (3)) soil water storage.

CONCLUSIONS

Conceptual rainfall-runoff models find a broad range of application at the basin scale. This contribution shows that this type of model is also applicable for the plot scale. But the analysis of actual processes based on field observations indicated that some shortcomings should be recognized. (1) The model's quick flow response is based on a saturation excess flow generation mechanism and can only occur if the soil storage is full. The model output will also generate interflow. The observations showed that quick flow occurred only during certain events. Therefore a submodel representing the Hortonian overland flow may better describe the natural processes and should be added to the model. (2) The observed runoff for the third (lowest) layer should not be interpreted as groundwater flow, as the soil layer in which it is generated is not permanently saturated. It could rather be described as an intermittent perched groundwater flow term, initiated at a predefined average soil water content, higher than the field capacity. A model adaptation consisting of raising the elevation of the percolation outlet can allow for this effect. (3) The spatial boundary of the plot-scale water balance unit can vary in time. This makes the definition of the contributing area difficult and event-dependent. This is not considered in the model. (4) Some model parameters refer to soil physical properties such as soil depth, wilting point and field capacity, and have therefore a better physical meaning on the plot scale and on the scale of Hydrological Response Units (HRU) than on the basin scale, where the retention parameters cannot be directly estimated from physical parameters, but are rather a function of the catchment size and morphological conditions. Future research will focus on these relations to also investigate the applicability of the conceptual model for ungauged catchments or to find upscaling procedures for parameter estimation. (5) The combined approach of in-situ experiments and the application of computer models provides useful insight into the system behaviour, the conceptualisation of the processes and their limitations.

REFERENCES

Atkinson, T.C. (1978) Techniques for measuring subsurface flow on hillslopes. In : *Hillslope Hydrology*. Editor: M. J. Kirkby. Chichester, New York, Brisbane, Toronto: John Wiley & Sons. S. 1-42.

Hager, H., Holzmann, H. (1997) Hydrologic functions of natural forest ecosystems in an alpine catchment. (in German), Final report of research project HÖ/94 by order of the Austrian Academy of Sciences, Vienna..

Holzmann, H., Sereinig, N. (1997) In situ measurements of hillslope runoff components with different types of forest vegetation. In: *FRIEND'97 - Regional Hydrology: Concepts and Models for Sustainable Water Resource Management* (Proc. of the Postojna Conf., Slovenia). IAHS Publ. No. 246.

Holzmann, H., Nachtnebel, H.P., Sereinig, N. (1998) Small scale modelling of runoff components in an alpine environment. In Kovar, K. et.al. (edts.) *Hydrology, Water Resources and Ecology in Headwaters* (Proceedings of the HeadWater'98 Conf.. Meran, April 1998). IAHS Publ. No.248, 231-238.

Holzmann, H., Nachtnebel, H.P. (2002) Sequential development of a conceptual hydrological model considering alpine basin processes. In Rizzoli, A. & Jakeman (Edts.), Integrated assessment and decision support. Proc. of IEMSS conference, Lugano, Vol.1, 416-421.

Nachtnebel, H.P., Holzmann, H. (1999) Development of an operational runoff forecasting system for the Austrian Danube basin. (in German), Report to the customer. Vienna.

Peters, D. L., Buttle, J. M., Taylor, C. H., LaZerte, B. D. (1995) Runoff production in a forested, shallow soil, Canadian Shield basin. *Water Resources Research*. Vol. 31, No. 5, 1291-1304.

USE OF ENVIRONMENTAL TRACING TO CONSTRAIN A RAINFALL-RUNOFF MODEL. APPLICATION TO THE HAUTE-MENTUE CATCHMENT.

D. Balin Talamba[1], C. Joerin[2], C. Higy[1], A. Musy[1]

[1]*Institute of Soil and Water Management (ISTE/HYDRAM), ENAC, EPFL, 1015 Lausanne, Switzerland, email: daniela.talamba@epfl.ch, christophe.higy@epfl.ch, andre.musy@ epfl.ch*
[2]*Office Fédéral des Eaux et de la Géologie (OFEG); Service Hydrologique National, 3003 Berne, Switzerland, email: Christophe.Joerin@bwg.admin.ch*

ABSTRACT

The present study tries to use additional information to improve process representativity in hydrological modelling. The study region is the Haute-Mentue catchment located in the western part of Switzerland, 20 km north of Lausanne. Previous research that has been carried out on this catchment improved the understanding of the runoff generation process by combining point soil moisture measurements (TDR) and integrating measurements both at the hillslope scale (dye tracing) and at the catchment scale (environmental tracing). In this work, environmental tracing information is integrated into a semi-distributed hydrological model, which is a modified version of TOPMODEL, taking into account rapid shallow subsurface stormflow generation above a less permeable soil horizon. Additional information has been incorporated by using a version of simulated annealing adapted for multicriteria optimisation.

Keywords runoff generation, tracing, hydrological modelling, multicriteria optimisation

INTRODUCTION

This work is in line with research at the ISTE / HYDRAM institute which aims at identifying and modelling the hydrological behaviour at the catchment scale. The study region is the Haute-Mentue experimental catchment, located in the western part of Switzerland (Fig 1). Research carried out previously showed that environmental tracing, as an integrating technique, contributed to a better understanding of the hydrological processes at the catchment scale. In order to benefit from this knowledge, we try to use environmental tracing as additional information in the calibration of a modified version of TOPMODEL.

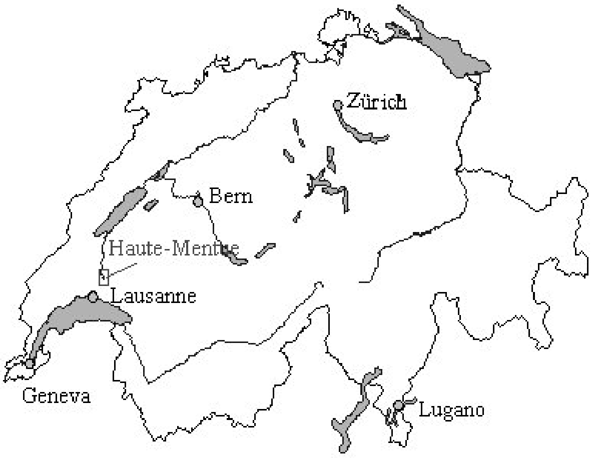

Fig 1: Geographical location of the Haute-Mentue catchment.

ENVIRONMENTAL TRACING ON THE HAUTE- MENTUE CATCHMENT

Chemical mixing models have been intensively used on the Haute-Mentue catchment in order to study the runoff generation process. Environmental tracing considers runoff at the outlet as a result of a mixture of several components the definition of which depends on the number and type of tracers. Calcium, silica and oxygen-18 have essentially been used to monitor the chemistry of the flow. In this study, calcium and silica have been chosen in order to identify three components: precipitation, soil water and groundwater. The chemical signatures were defined by considering temporal variability of the three components and spatial variability of the groundwater. Hydro-meteorological data are treated by the AIDH program developed at the ISTE/HYDRAM (Joerin, 2002). Hydrograph separation performed for October 1998 on the Bois-Vuacoz subbasin of the Haute-Mentue catchment showed that soil water is the most important component contributing to the flow, independent of the antecedent conditions (Fig 2). Several hypotheses have been proposed to explain this rapid subsurface response, one of them highlighting the role of preferential flow and particularly macropores (Joerin, 2000). Because environmental tracing is an integrating measurement at the catchment scale it could be very useful in constraining the performance of hydrological models that make predictions at the same scale.

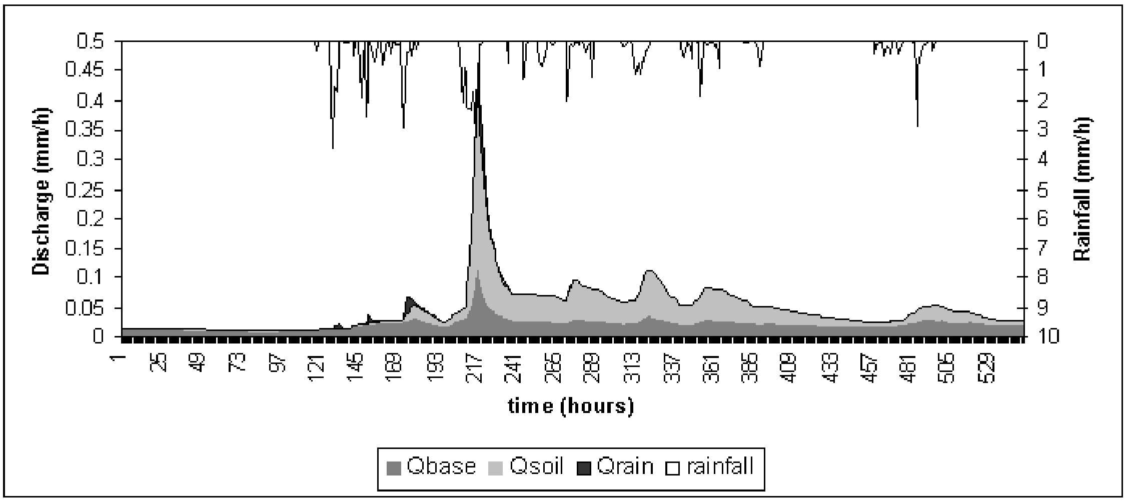

Fig 2: Hydrograph decomposition by the AIDH program; Bois-Vuacoz catchment, October 1998.

HYDROLOGICAL MODELLING

Because we observed a large contribution of soil water to the total flood discharge, we use for modelling purposes, a "3 component" version of TOPMODEL. The main difference with the original version of TOPMODEL consists in introducing a subsurface reservoir from which shallow saturation above a less permeable layer can contribute to the episodic surface saturation near the stream. When perched water develops, the contributing area expands only from the initial saturated area from the groundwater (for more details see Scanlon T.J., 2000). The model works with a set of eight parameters characterising both saturated and unsaturated zones. This version of TOPMODEL is applied on the Haute-Mentue catchment during a humid period of the year 1998. Model parameters are optimised by a version of simulated annealing which belongs to the class of Monte Carlo directed methods. The algorithm includes a parameter called temperature which determines the acceptance or rejection of newly generated parameter sets. Better models are always accepted with probability 1 while worse models are accepted with a probability given by the Metropolis rule:

$$P = \exp(-\Delta E / T)$$

where:

- ΔE is the difference in the objective function between two consecutive iterations;
- T is the temperature parameter.

First, the model is calibrated against total discharge only. The objective function is represented by the sum of the squared errors and the optimisation procedure minimises the objective function using the ordinary least squares method. In order to improve robustness of the calibrated parameters, corrective actions were taken in order to assess the constancy of the residuals' variance (use of logarithm-transformed data) and the time independence of the residuals (introduction of an autoregressive model AR(1,0)). The total discharge is well simulated (Nash-Sutcliffe criterion equal 0.84) but the simulated components are different from the ones obtained by the application of environmental tracing (Fig 3). Thus, in order to improve the model process representativity, the environmental components as given by the AIDH program were used to constrain the model performance. We have formulated for this reason a new objective function that takes into account two responses: total streamflow and baseflow at the outlet. The choice of baseflow to constrain the model was motivated by the parameters' distribution after calibration of the model against single components of the total discharge. The distributions of the parameters obtained by calibration on baseflow are different from the distributions of the parameters obtained by calibration on total streamflow, soil and rainfall contributions. Fig 4 shows the shape of different distributions of the most sensitive model parameters. These are the groundwater zone scale depth parameter (m) and the stormflow zone recession parameter (Qosf). The new objective function was built in accordance with the recommendations of Mroczkovski (1997), each response being weighted by its residual variance. Joint calibration of the model on total streamflow and on baseflow indicates that the general performance of the model is slightly lower (Nash-Sutcliffe criterion equal 0.8), but runoff components, and especially baseflow, are better simulated. In fact, the results show a compromise between a slightly lower simulation of the soil runoff contribution and an improved groundwater contribution (Fig 5). The example we presented highlights the benefits of additional information in order to improve the representativity of conceptual process-based rainfall-runoff models. It might be interesting to further develop this kind of approach in the aim of choosing the most "physical" sets of parameters. As already shown by Beven (2001), calibrating conceptual rainfall-runoff models seems to be very difficult because of the equifinality of the parameters. In this example too, one can identify several parameter sets which give quite similar results in terms of streamflow simulation. This preliminary study shows that the introduction of additional information could contribute to a better definition of the surface response of the parameters.

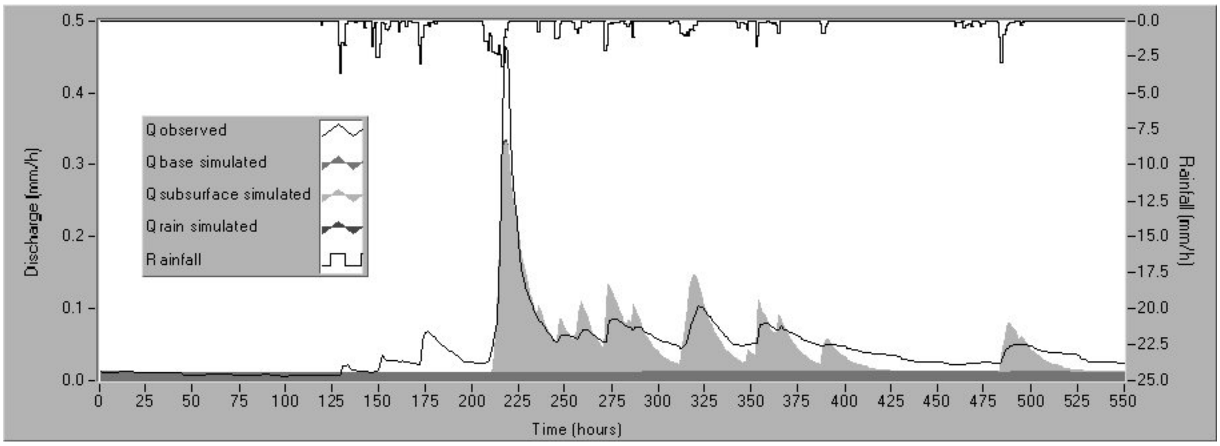

Fig 3: Modified version of TOPMODEL runoff simulation for Bois-Vuacoz catchment, October 1998.

PERSPECTIVES

The next step for working with multiple responses could be the incorporation of a multicriteria approach. More attention should be given to the choice of the most informative responses to work with, in order to better identify subspaces of response surfaces where robust parameters lie. The identification of such robust sets of parameters would allow them to be used on periods without tracer information. In this context, a new version of the simulated annealing algorithm developed by Suppapitnarm (2000) for multiobjective optimisation will be implemented to work with the modified version of TOPMODEL. The method creates an archive of non-dominated solutions, which is generally known as the pareto-optimal set. The final non-dominated population represents a number of different optimal solutions from which a user can choose a compromise solution with full knowledge of what is actually achievable.

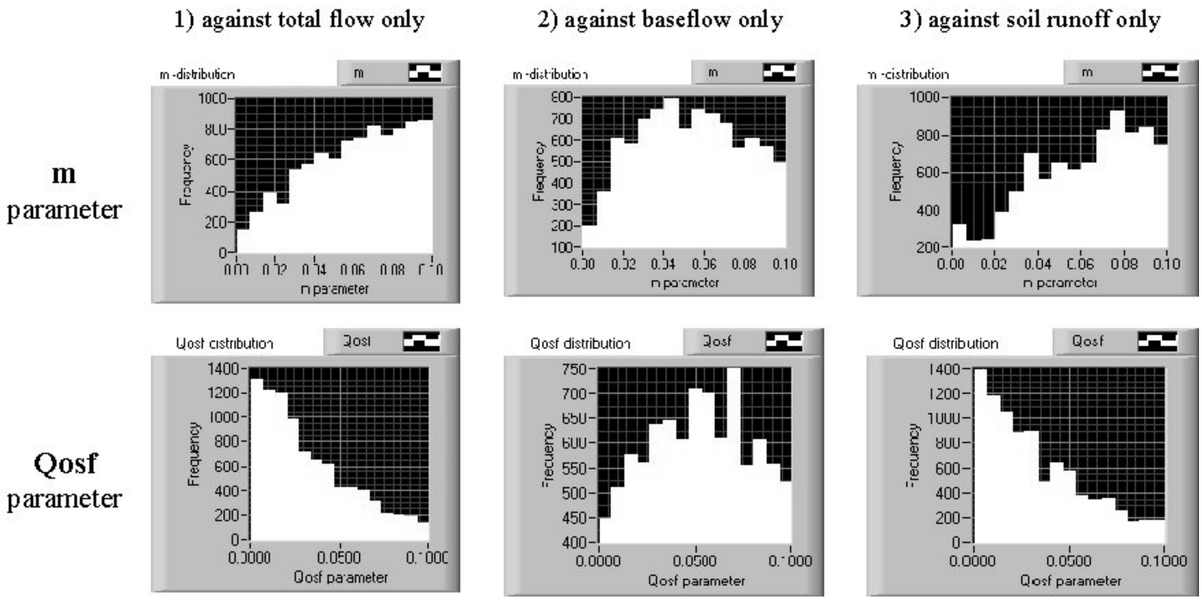

Fig 4: Model parameter distributions (baseflow scale parameter **m** - line 1; stormflow recession parameter **Qosf** - line 2) after calibration against total runoff (column 1) baseflow (column 2) and soil runoff (column 3).

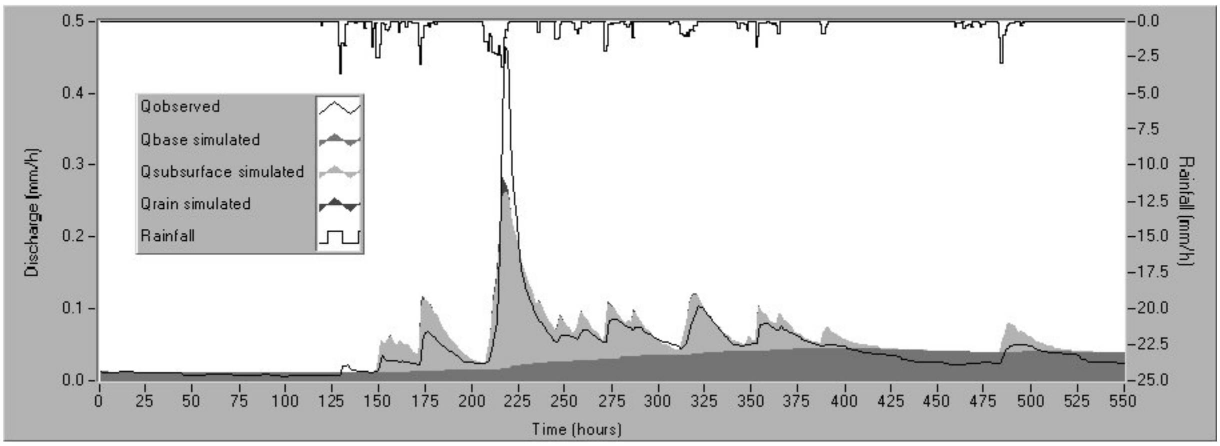

Fig 5: Modified version of TOPMODEL, runoff simulation for Bois-Vuacoz catchment after calibrating the model on both total runoff and baseflow, October 1998.

CONCLUSIONS

This paper presents the first results of considering additional data during the calibration of a semi-distributed model. Several years of intensive environmental tracing on the Haute-Mentue catchment allowed a better understanding of the hydrological behaviour and of the runoff generation processes. The approach presented here is a trade-off between experimental knowledge and "lumped" hydrological modelling. Additional data is introduced by considering different objective functions and by using them within a simulated annealing approach. The first results show the usefulness of multiple criteria in constraining and assessing model performance and process representativity.

REFERENCES

Beven, K. (2001) Calibration, validation and equifinality in hydrological modelling a continuing discussion. *Model Validation: Perspectives in Hydrological Science*. M. G. Anderson and P.D. Bates, John Wiley & Sons, Ltd.

Franks S., Beven K., Chappell N., Gineste P. (1997) The utility of multi-objective conditioning of a distributed hydrological model using uncertain estimates of saturated areas. In A.D. McDonald and M. McAllen: *Proceedings of the International Congress on Modelling and Simulation*, 1, 335-340.

Higy, C. (2000) Modélisations conceptuelle et à base physique des processus hydrologiques: application au bassin versant de la Haute-Mentue. PhD Thesis, Lausanne, EPFL.

Joerin C., Beven K. J., Iorgulescu I., Musy A. (2002) Uncertainty in hydrograph separations based on geochemical mixing models. *Journal of Hydrology*, 255, 90-106.

Lamb R., Beven K., Myrabo S. (1998) Use of spatially distributed water table observations to constrain uncertainty in a rainfall-runoff model. *Advances in Water Resources*, 22, 4, 305-317.

Mroczkovski M., Raper G. Paul., Kuczera G., (1997) The quest for more powerful validation of conceptual catchment models. *Water Resources Research*, 33, 10, 2325-2335.

Scanlon T.J., Raffensperger J.P., Hornberger G. (2000) Shallow subsurface storm flow in a forested headwater catchment: Observations and modelling using a modified TOPMODEL. *Water Resources Research*, 36, 9, 2575-2586.

Seibert, J. J.J. McDonnell (2001) Towards a better process representation of catchment hydrology in conceptual runoff modelling. IAHS Freiburg Conference on Meso-scale modelling, Proc. of the *Int. Workshop on Runoff Generation and Implications for River Basin Modeling*, 9-12.

Suppapitnarm A., Seffen K. A., Parks G.T., Clarkson P.J. (2000) A simulated annealing algorithm for multiobjective optimisation. *Engineering Optimisation*, 33, 59-85.

METHODS OF RUNOFF SEPARATION APPLIED TO SMALL STREAM AND TILE DRAINAGE RUNOFF

František Doležal, Zbyněk Kulhavý, Tomáš Kvítek, Mojmír Soukup, Martin Tippl

Research Institute for Soil and Water Conservation, Žabovřeská 250, 156 27 Praha 5 - Zbraslav, Czech Republic, dolezal@vumop.tel.cz

ABSTRACT

Runoff hydrographs from several small agricultural catchments and tile drainage (subdrainage) systems in these catchments were analysed using several runoff separation techniques. A semi-empirical method, GROUND (Kulhavý et al., 2001), based on a conceptual model of delayed reaction of the slow flow component to the total flow ascent, was used to separate the quick runoff component (direct runoff). A digital filter (Chapman and Maxwell, 1996) was calibrated for two of the catchments studied, using the Kliner and Kněžek (1974) method based on the analysis of groundwater table vs. stream discharge relation, and the Kille (1970) method based on the distribution of minimum monthly flows. The digital filter was then used to separate the slowest flow component (baseflow), while the difference between the GROUND results and the digital filter results was taken as an estimate of interflow, interpreted as shallow groundwater flow. The quick flow / total flow ratios as obtained by GROUND and the digital filter are mutually correlated (r^2 = 0.717). On the average, direct flow, interflow and baseflow represented 30 %, 40 % and 30 % of the total flow, respectively. The results show significant differences between individual catchments and subdrainage systems. Low direct runoff proportions are found when a subdrainage system or a stream drains perennial aquifers. On the other hand, high direct runoff correspond to the cases when a subdrainage system is located upslope and does not cut a perennial aquifer, or when the catchment of a stream has an extremely elongated shape. In general, the runoff patterns of subdrainage systems are not notably different from those of surface streams, which suggests that the runoff formation mechanisms in these two systems are similar.

Keywords hydrograph separation, agricultural catchments, tile drainage, runoff formation

INTRODUCTION

One approach in studying runoff processes is to separate different components of the total runoff hydrograph as it has been observed in the closing profile of a catchment. These components inevitably reflect, directly or indirectly, the different processes taking place within the catchment. The smaller the catchment, the easier the deciphering of its runoff hydrograph. This paper explores the potential of several runoff separation methods, applied to the data from small, prevailingly agricultural catchments in the foothill zones of Central and East Bohemia and from agricultural subdrainage systems located in these catchments.

METHODS AND MATERIALS

Surface runoff and subdrainage runoff were measured in several small agricultural catchments in Central and East Bohemia (see Tables 1 and 2). The separation of runoff components was performed in the same way for both stream flow and subdrainage runoff data (daily flow series in both cases). The subdrainage systems studied consist of underground pipe (tile or plastic) drains about 1 m deep and 11 to 16 m apart (the term "subdrainage" is used in this paper, as proposed by the reviewer, to denote a subsurface tile drainage system). For an overview of the subdrainage systems, see the left part of the last five rows in Table 3. Some data series are relatively short, except for the Žejbro stream. The contribution of subdrainage runoff to the total stream flow in the catchments studied is not known exactly, because not all subdrainage systems were monitored. Its estimates vary between 10 and 30 % of the annual stream runoff.

Table 1: Basic characteristics of the main RISWC experimental catchments.

Catchment name:	Cerhovický potok	Černičí	Dolský potok	Kopanin-ský tok	Kotelský potok
Catchment code	CP/A1*)	CE/P1	DP	KT/T7	KP
Average latitude:	49° 51' E	49° 37' N	49° 47' N	49° 28' N	49° 47' N
Average longitude:	13° 50' E	15° 04' E	15° 59' E	15° 17' E	15° 59' E
Altitude (m): min – max (average)	390 – 572 (481)	448 - 543 (496)	456 - 676 (566)	467 - 578 (523)	438 - 663 (551)
Area (km^2)	7.36	1.42	4.78	6.69	3.21
% crop land:	18 %	73 %	68 %	52 %	76 %
% grassland:	22 %	7 %	7 %	14 %	10 %
% forest:	60 %	17 %	1 %	30 %	3 %
% drained land:	16 %	17 %	22 %	10 %	38 %
An. Precipitation (mm):	617	722	764	665	764
Av. Temperature (°C):	7.5	7.5	6.3	7.0	6.3
Main parent rock:	mica schist	paragneiss	phyllite	paragneiss	phyllite
Measured since:	1973	1991	1982	1985	1982

*) The characteristics relate to the actual experimental catchment (CP/A1). Some results below refer to a larger catchment which was operational before 1994 (CP/UPF, 8.98 km^2, containing more arable land) or to an upper subcatchment of CP/A1 (CP/B1, 3.15 km^2, mainly forested).

Table 2: Basic characteristics of the other experimental catchments.

Catchment name:	Žejbro *)	Křepelka §)	Ovesná Lhota +)
Catchment code:	ZE	KR	OL
Average latitude:	49° 48' N	50° 28’ N	49° 49' N
Average longitude:	15° 59' E	16° 14’	15° 27' E
Altitude (m): min - max (average)	355-676 (516)	360-410 (385)	506-550 (528)
Area (km^2)	48.3	2.0	0.66
% crop land:	63 %	75 %	76 %
% grassland:	15 %	20 %	15 %
% forest:	16 %	5 %	9 %
% drained land:	23 %	about 20 %	59 %
An. precipitation (mm):	764	742	671
Av. temperature (°C):	6.3	7.3	7.0
Main parent rock:	phyllite, deep igneous, Cretaceous sedimentary	loess loam over Cretaceous sandstone	paragneiss
Measured from-to:	1977-97	1965-1982	1977-91

*) A regular gauging site of the Czech Hydrometeorological Institute.
§) A former experimental catchment of the Czech University of Agriculture.
+) A former experimental catchment of RISWC, now abandoned.

Two methods of runoff separation were applied systematically to all data. The first method is the digital filter suggested by Chapman and Maxwell (1996; referred to as Method 1 in Grayson et al., 1996), defined by equations:

$$Q_{total} = Q_{quick} + Q_{slow}\ ; \quad Q_{slow}(i) = \frac{k}{2-k} Q_{slow}(i-1) + \frac{1-k}{2-k} Q_{total}(i)\ ; \quad Q_{slow}(i) \le Q_{total}(i)$$

where $Q(i)$ is the average daily flow on i-th day, either the total flow or the slow component or the quick component (as indicated by the subscript), and k is the flow recession constant. The initial condition was taken as $Q_{slow}(1) = Q_{total}(1)$. The other procedure used, GROUND (Kulhavý et al., 2001), contains a parameter C determining the rate at which the slow flow component rises when the total flow rises. Neither GROUND nor the digital filter can distinguish more than two flow components. In this paper, these components are referred to as Q_{slow} and Q_{quick}. However, experience shows that at least three components must be distinguished, i.e., the genuinely quick direct runoff on one hand, the genuinely slow and quasi-constant baseflow on the other hand, and the rest, usually being referred to as interflow, which can be visualised as perched, shallow groundwater flow. The GROUND method is more suitable for direct runoff separation because it assumes that the slow component (i.e. interflow plus baseflow) immediately reacts to each total flow ascent. Its suitability was verified by comparing it with a semi-distributed model, EPIC (Jain, 1997). We therefore used GROUND to separate the direct flow component, leaving C = 0.075 as proposed by Kulhavý et al. (2001).

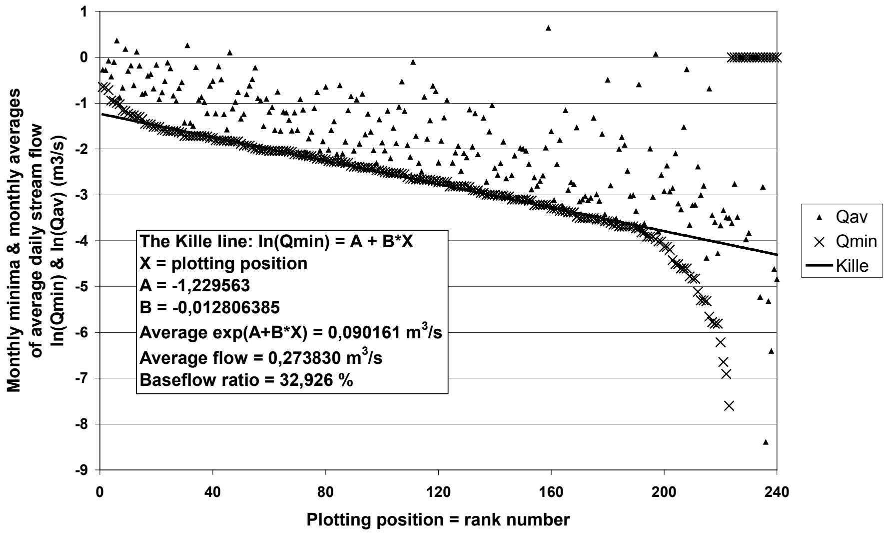

Fig 1: Baseflow separation using the Kille method for Žejbro, November 1977 to October 1997.

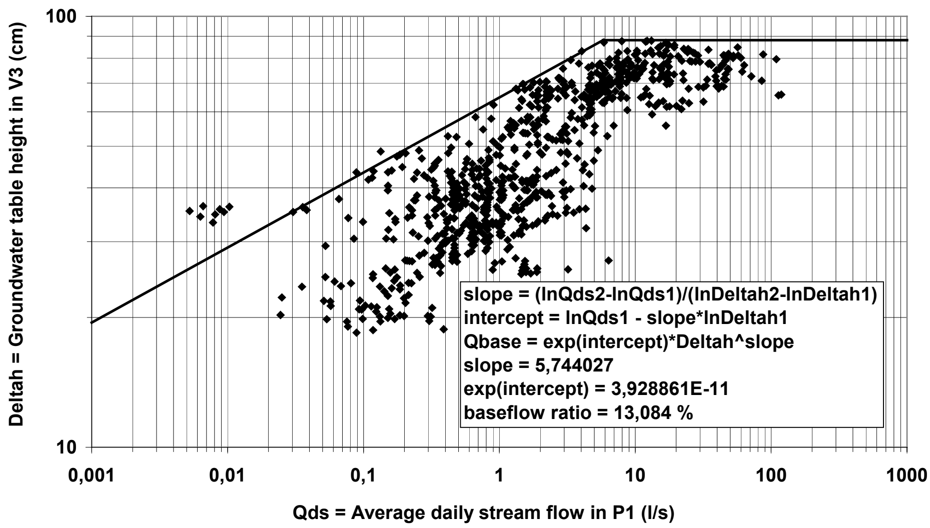

Fig 2: Baseflow separation using the Kliner-Kněžek method for Černičí, stream (P1), 6/1/98-31/5/2000.

The digital filter described above is more suitable for the separation of baseflow, and we applied it with $k = 0.99483$ (see below). For calibration of the digital filter, we used the method of baseflow separation by Kille (1970) based on the frequency analysis of minimum monthly flows, applied to the Žejbro stream data only (Fig 1), and the method by Kliner and Kněžek (1974) based on the relation between the stream flow and the groundwater table elevation, used with the Černičí stream data (Fig 2). The effect of the two methods (the digital filter and GROUND) is demonstrated in Fig 3.

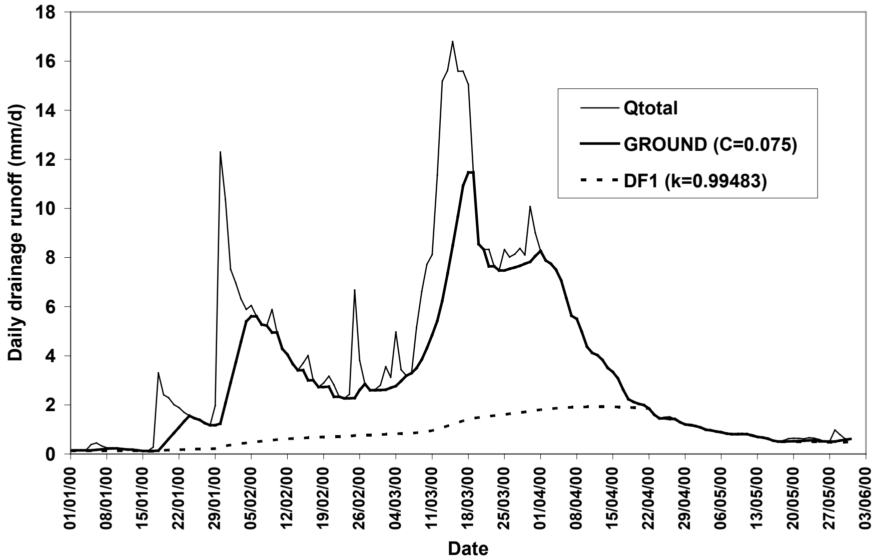

Fig 3: Comparison of runoff separation results using the GROUND method with $C = 0.075$ and the digital filter (DF1) with $k = 0.99483$ at Černičí, the subdrainage system S2, January-May 2000.

RESULTS AND DISCUSSION

The Kille method gave $Q_{quick}/Q_{total} = 67.1$ % for the Žejbro stream. The digital filter gave the same result with $k = 0.991525$. The Kliner-Kněžek method indicated that $Q_{quick}/Q_{total} = 86.9$ % for the Černičí stream. The digital filter gave the same result with $k = 0.998135$. In the absence of other information, we decided to take an arithmetic average of the two k-values, namely 0.99483, for use with all data. The results of the GROUND method and the digital filter method are given in Table 3, together with average runoff coefficients over the period of separation. High runoff coefficients of subdrainage systems suggest that they collect water from larger areas. With some reservation, the GROUND ratios can be interpreted as direct flow / total flow ratios, while the digital filter ratios can be understood as (direct flow + interflow) / total flow ratios. The quick flow / total flow ratios as obtained by the two methods are mutually correlated ($r^2 = 0.717$, $y = 0.894\ x + 43.434$, y being the digital filter results and x the GROUND results). On the average, direct flow, interflow and baseflow represented 30 %, 40 % and 30 % of the total flow, respectively. This is in agreement with environmental isotope studies, which indicate that under conditions roughly similar to ours the direct flow portion lies between 10 and 40 % (cf. Chapter 6 in FRIEND, 1997).

The relatively low baseflow contribution obtained by the digital filter, as well as by the Kille and the Kliner-Kněžek methods, indicate that there is indeed a considerable part of the total runoff which is neither direct runoff nor baseflow. Hence the use of the interflow concept is fully warranted. Otherwise the results show significant variation from case to case. The results are presented graphically in Fig 4. While the low direct runoff proportion found in Ovesná Lhota may be partly explained by the absence of winter months in the data (this is also indicated in Table 3 by a relatively low runoff coefficient), similar results were also obtained for the subdrainage system S2 in Černičí, which drains a perennial spring, and for the Kopaninský tok stream. The Kliner-Kněžek method was independently applied to the Kopaninský tok stream (Kvítek et al., 2001, unpublished). The discharge of a local spring was used instead of the groundwater table data. The resulting slow flow percentage was 31 % (close to the 38 % obtained with the digital filter). High direct runoff contributions were found for the subdrainage system in Křepelka, which is explainable by its upslope location in absence of a perennial aquifer, and for the Kotelský potok stream which has a very narrow and elongated catchment, facilitating direct runoff. The twin catchment (Dolský potok) is similar in shape and geology but its runoff pattern is modified by a few fishponds. In the Cerhovický potok catchment, a gradual downstream decrease of both direct flow and baseflow can be observed. In general, the runoff patterns of subdrainage systems are not notably different from those of surface streams (except for runoff coefficients), suggesting that the runoff formation mechanisms in subdrainage systems are similar to those in small streams.

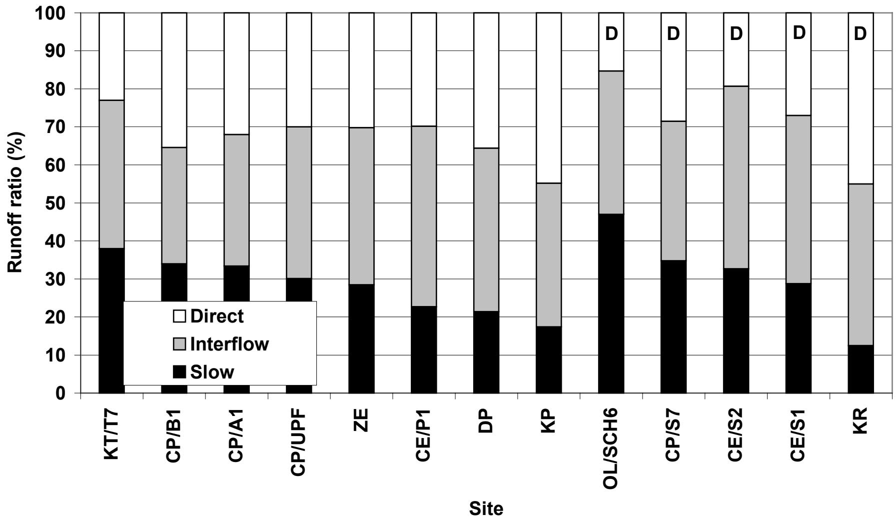

Fig 4: Comparison of hydrograph separation results. Both the catchments and the subdrainage systems (the latter denoted by D) are arranged in descending order in terms of the slow flow component (i.e. baseflow). See Table 3 for the meaning of symbols.

Table 3: Results of runoff separation.

Catchment (S = stream D = sub-drainage)	Code	Area (ha)	Observation period	Runoff coeff.	Q_{quick}/Q_{total} (%)	
					GROUND	Digital filter
Cerhov. p. (S)	CP/B1	315	23.10.96-31.8.99 *)	0.18	35.4	66.0
Cerhov. p. (S)	CP/A1	736	23.10.96-29.11.00 §)	0.19	32.0	66.6
Cerhov. p. (S)	CP/UPF	898	7.9.92-7.8.94	0.31	30.0	69.9
Černičí (S)	CE/P1	142	6.1.98-22.7.01	0.24	29.8	77.3
Dolský p. (S)	DP	478	1.4.82-31.3.00 *)	0.19	35.6	78.6
Kopan. tok (S)	KT/T7	669	26.6.91-31.10.00	0.18	23.0	62.0
Kotel. p. (S)	KP	321	1.4.82-31.3.00 *)	0.34	44.8	82.6
Žejbro (S)	ZE	4830	1.11.77-31.10.97	0.26	30.2	71.5
Cerhov. p. (D)	CP/S7	40.5	1.9.94-3.6.99	0.76	28.5	65.2
Černičí (D)	CE/S1	0.605	1.3.97-31.5.00	0.67	27.0	71.2
Černičí (D)	CE/S2	1.815	1.3.97-31.5.00	1.02	19.3	67.3
Křepelka (D)	KR	0.80	1.7.78-30.6.82 §)	0.42	45.0	87.5
Ov. Lhota (D)	OL/SCH6	17.8	1979-81, 83-91 +)	0.42	15.3	53.0

*) The gaps in data were omitted.
§) The gaps in data were filled by linear interpolation.
+) The data are only available for the growing season (1.4.-30.9.) of each year.

CONCLUSIONS

Three runoff components were distinguished in stream and subdrainage hydrographs from small catchments on crystalline rocks in the foothill zones of Central and East Bohemia. It is demonstrated that the differences between individual catchments and the subdrainage system in terms of proportions of runoff components can be explained with reference to local hydrogeology and geomorphology. In future work, the values of the parameters k and C should be individualised for each hydrological unit in question, based on independent calibration. The subdrainage runoff separation appears to be a suitable tool for recognising whether or not the subdrainage system drains a perennial aquifer.

ACKNOWLEDGEMENT

This study was made possible by the RISWC programme MZE-M07-99-01, the National Agency for Agricultural Research projects RE 5501, EP 096006150, EP 9155 and QC 0242, the Grant Agency of the Czech Republic projects 502/95/0826 and 103/99/1470, the EU Copernicus project CIPA-CT-93-0241 and other donors. Substantial contribution of all who measured and processed the data is gratefully acknowledged. We thank Prof. Jiří Fídler and his colleagues (Czech University of Agriculture) for the Křepelka data.

REFERENCES

Chapman, T. G., Maxwell, A. I. (1996) Baseflow separation - comparison of numerical methods with tracer experiments. I. E. Aust. Natl.Conf. Publ. 96/05, 539-545. Cited after Grayson et al. (1996).

FRIEND - Flow Regimes from International Experimental and Network Data. Projects H-5-5 and 1.1, Third report: 1994-1997. UNESCO, Paris, June 1997.

Grayson, R. B., Argent, R. M., Nathan, R. J., McMahon, T. A., Mein, R. G. (1996) Hydrological recipes: estimation techniques in Australian hydrology. Cooperative Research Centre for Catchment Hydrology, Clayton, Victoria, Australia, 125 pp.

Jain, S. K. (1977) Evaluation of catchment management strategies by modelling soil erosion / water quality in EPIC supported by GIS. M.Sc. thesis, Galway, National University of Ireland, Department of Engineering Hydrology.

Kille, K., (1970) Das Verfahren MoMNQ, ein Beitrag zur Berechnung der mittleren langjährigen Grundwasserneubildung mit Hilfe der monatlichen Niedrigwasserabflüsse. *Z. Deutsch. Geol. Gesell*.

Kliner, K., Kněžek, M. (1974) The underground runoff separation method making use of the observation of groundwater table. (In Czech). *J. Hydrol. Hydromech.*, 23, 5, 457-466.

Kulhavý, Z., Doležal, F., Soukup M. (2001) Separation of drainage runoff components and its use for classification of existing drainage systems (In Czech). *Vědecké práce VÚMOP Praha*, 2001, 12: 29-52.

PROCESS-ORIENTED SUBDIVISION OF BASINS TO IMPROVE THE PREPROCESSING OF DISTRIBUTED PRECIPITATION-RUNOFF MODELS

F. Hellie, G. Peschke †, C. Seidler, D. Niedel

International Graduate School Zittau, Markt 23, D-02763 Zittau, Germany

ABSTRACT

Hydrological processes are characterised by a high degree of spatial variability. Therefore a spatial subdivision of the basins has to be carried out in the preprocessing of distributed precipitation-runoff models. To include more process knowledge into the simulation of runoff production and to overcome the problem of overparameterisation a functional discretisation is necessary. Thus, an expert system (XPS) was developed that allows a process-oriented subdivision of the basins. It offers the possibility to identify spatial units with functional hydrological similarity focussing on the homogeneity of runoff generation processes. In this publication the methodology and the structure of the XPS are presented and a result of its application in a mesoscale basin is shown.

Keywords runoff generation, spatial distribution, regionalisation, expert system

INTRODUCTION

One of the fundamental qualities of the landscape is the regulation of runoff. The runoff generation processes in a catchment are influenced by many different factors and thus, they are characterised by great spatial and temporal variability. Knowledge about the spatial distribution of runoff components and their temporal behaviour is an important basis for regional planning, water conservation, water projects and flood forecasting. It is useful to solve different hydrological problems.

The classical discretisation is based on the tope-principle. Hydrological similarity is often defined only by formal structural similarity based on relief, soils, land use and other geoparameters, and derived from the overlay functions of the GIS. A large number of elementary discretisation units can arise. In the process of up-scaling it is necessary to aggregate these units to reduce their number per se as well as the number of parameters that have to be determined for the precipitation-runoff model. Here we investigate a method for the subdivision of catchments functionally - based on the runoff generation processes.

METHODOLOGY

The required subdivision should be handled by methods of Artificial Intelligence because our knowledge about runoff processes is gained to a considerable extent by empirical knowledge containing significant uncertainties. Therefore an expert system was developed named XPS-FLAB (Peschke et al., 1999; Zimmermann, 1999) as an instrument of regionalisation in order to identify process-related spatial units with a dominant runoff generation process. We attached great importance to the quick runoff components (Table 1). Basics of the knowledge-based system XPS-FLAB are generally available information, such as maps of soil types, geological formations, land use, stream networks and a digital elevation model. These data on geofactors and basin features represent fuzzy knowledge. To reach the desired goal of a functional spatial discretisation, two steps are necessary:

1. GIS supported overlay of information to generate the smallest units with identical feature combinations.
2. Classification of these units and aggregation to areas with functional hydrological similarity (up-scaling).

The GIS solves the problem of data acquisition and management and generates the smallest spatial units (topes) from the overlay of different geo-information. The knowledge-based XPS-FLAB represents process understanding (semantic) and determines how a precipitation-runoff model should be parameterised for simulating basin runoff. Rules and facts evaluate the topes resulting from the GIS application considering the runoff generation process (Fig 1). To derive this rule system we used our own long-time experiences in hydrological experimental work (e.g., Etzenberg, 1998; Peschke et al., 1998; Müller and Peschke, 2000) as well as the investigation results from other teams (e.g., Gutknecht and Kirnbauer, 1996; Kirnbauer and Haas, 1998; Merz and Plate, 1997; Uhlenbrook, 1999; Tilch et al., 2002). Different feature combinations may produce equal runoff components and the units with the same processes are aggregated and represented in a map. Thus, the XPS is a module of qualitative evaluation and classification of landscape elements. Furthermore it can be coupled with a distributed precipitation-runoff model for a quantitative description of the basin. In a first step, the system indicates dominant processes under given conditions. If the input data (e.g. precipitation features) or the state of the system (e.g. antecedent soil moisture or plant cover) were changed, other processes would become dominant (Fig 3). Threshold values are used to consider this variability, e.g. when the soil moisture surpasses a given value, the interflow process gains dominance or when the precipitation reaches a specific intensity, infiltration gives way to quick overland flow.

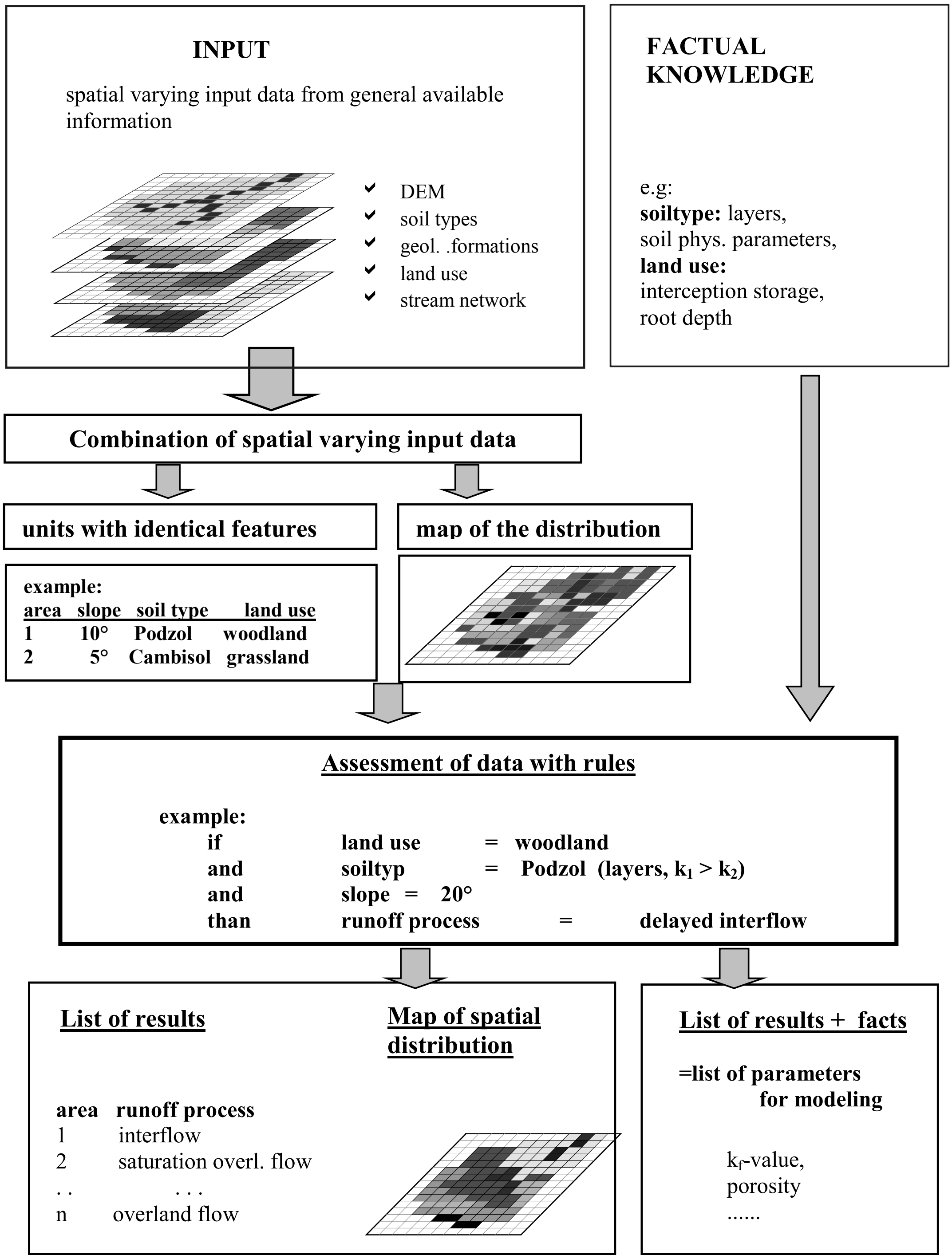

Fig 1: Structure of the XPS-FLAB.

Table 1: Quick runoff components considered in the XPS-FLAB

Runoff components		Specification of components	
1	**OVERLAND FLOW**	1	Sealed urban areas
		2	Partly sealed urban areas
		3	Rock areas
		4	Areas with small infiltration
		5	Hydrophobe responding areas
2	**SATURATION OVERLAND FLOW**	1	Overland flow from permanent saturated areas resp. delayed saturating soils
3	**INTERFLOW**	1	Quick interflow
		2	Delayed interflow
		3	Strongly delayed interflow
4	**DEEP PERCOLATION**	1	Areas with mainly vertical water movement
5	**NOT ASSESSED**		The data cannot be assessed

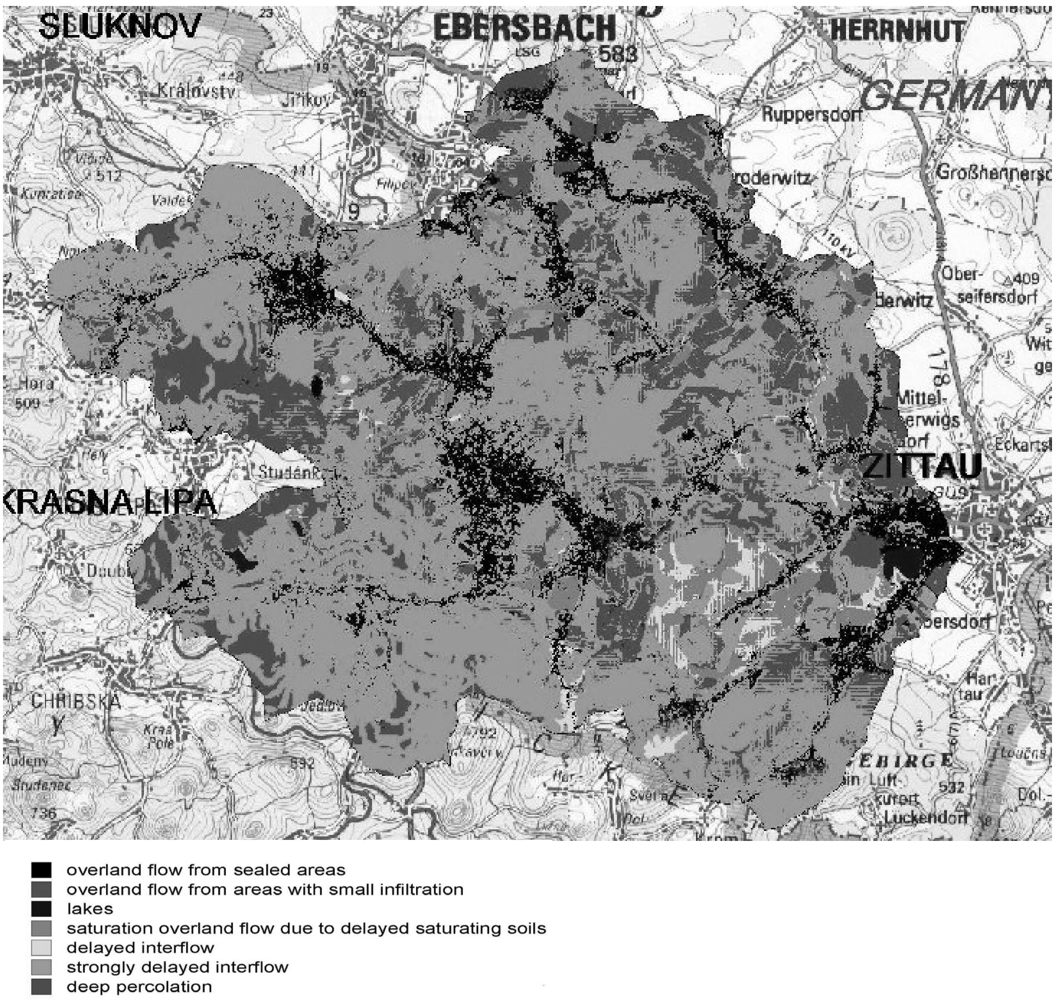

Fig 2: Distribution of dominant runoff components in the Mandau basin.

RESULTS AND CONCLUSIONS

Application of the XPS-FLAB in a mesoscale basin

The knowledge-based system XPS – still under development – seems to be an appropriate instrument to identify spatial units on which a certain process of runoff generation dominates. It has already been used for several basins with different basic information. As an example, its application in a mesoscale basin is shown here. The Mandau basin (294 km^2) is located in the eastern part of Germany at the border with Poland and the Czech Republic (1/3 of the catchment area is in the Czech Republic). The altitude ranges between 230 and 800 m a.s.l. and the slopes reach up to 50%. Agricultural acreage (61%) dominates the land use, only 27% of the area is forested and 11% are settlements. Large parts of the basin are characterised by loess formations, silty soils with small infiltration intensities. Annual precipitation (650 mm) and annual evapotranspiration (550 mm) are similar in magnitude.

Fig 2 shows the spatial subdivision of the Mandau basin created by the expert system. A DEM, maps of land use, soil types and river network were available for the procedure. Together with integrated expert knowledge, the XPS-FLAB was able to assess these input data regarding the runoff generation processes. However this map shows only one possible situation dependent on the geomorphological conditions in the basin. The dominant runoff generation process can alter with changing conditions. Every raster cell has special, temporally less variable features, such as slope, soil type, land use etc., and these characteristics influence the runoff processes strongly. But the actual dominant process finally depends on the degree of ground cover, the soil moisture and the nature of the precipitation event. Therefore the dominance of a process is variable and time dependent. Within the XPS-FLAB these changes are reflected by threshold values that describe the transfer from one process to another. For instance, Fig 3 shows a rough example of the differentiation of runoff components for a sloped field of luvic stagnosol and bare soil, two soil layers with a higher hydraulic conductivity of the upper one. Hydraulic conductivity is used as a substitute for infiltration intensity. Different potential reactions in the units are possible depending on antecedent soil moisture and rainfall event characteristics. The results can be presented in maps of varying system states. Besides the list and the map of the identified runoff components, the system generates parameter files for the modeller.

Conclusions

The XPS-FLAB is a combination of strongly abstracted process modelling and the use of comprehensive experimental experience (expert knowledge). The combination of both offers the possibility of analyses based on spatial hydrological responses and on a discretisation of the investigated basin into units of equal runoff generation processes. It enables spatial discretisation, parameter reduction and a process-oriented justification of the parameters of a precipitation-runoff model. Therefore, scale transitions do not affect the transformation of parameters. A change in land use, for example, requires a new evaluation of corresponding spatial types by the XPS-FLAB, but not a new calibration. The area-related identification of runoff components also characterises spatial origins of water and transport paths, thus, it is an important basis for the consideration of the processes of transport of matter.

The developed Knowledge Based System can be enlarged with additional runoff processes if the generation conditions are well known. It seems to be necessary to consider anthropogenic changes like drainages, because they influence the runoff production strongly. In addition to that in the future other input information like remote sensing data should be used in the rule system.

ACKNOWLEDGEMENTS

The basic research has been supported by the “Deutsche Forschungsgemeinschaft” in the focal program “Regionalisation in hydrology” and further on in the bundle-project “Runoff generation and catchment modelling”.

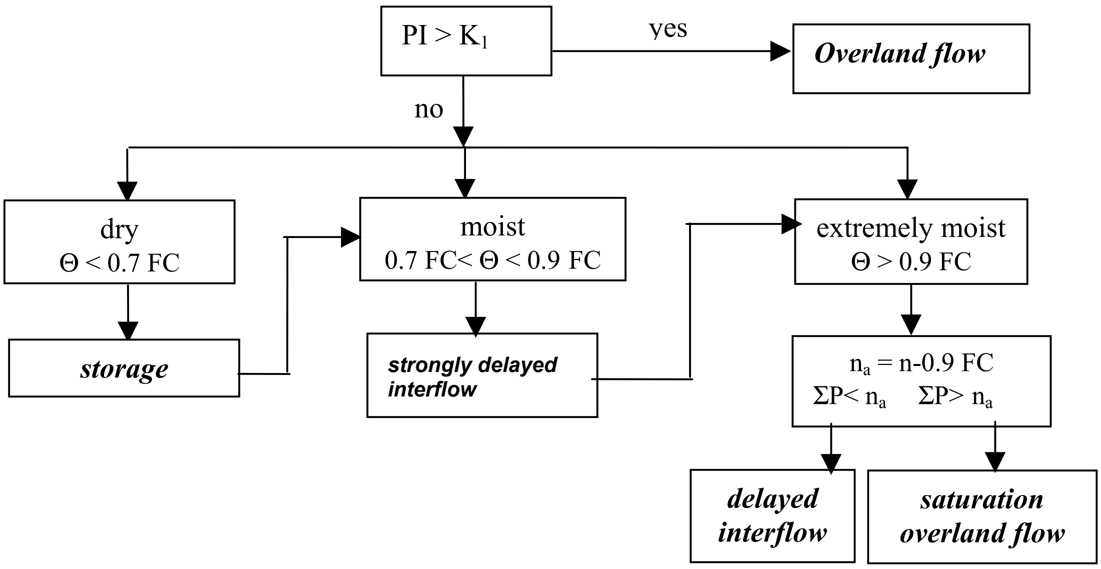

Fig 3: Differentiation of runoff generation processes by threshold values (rough example) P-precipitation, FC-field capacity, n-porosity, n_a-replenishing porosity, Θ-soil moisture

REFERENCES

Etzenberg, C. (1998) Zur Regionalisierung der Abflussbildung - Bestimmung flächenspezifischer Abflussbeiträge aus Gebietseigenschaften. (On regionalization of the runoff generation – determination of areal specific runoff contributions from basin features). Thesis Internationales Hochschulinstut Zittau.

Gutknecht, D., Kirnbauer, R. (1996) Abflußentstehung - Einflußfaktoren und Konzeption. (Runoff formation – influencing factors and conception). *IHI-Schriftenreihe*, H.2, Zittau, 182-191.

Kirnbauer, R., Haas, P. (1998) Observations on runoff generation mechanisms in small Alpine catchments. In: *Hydrology, Water Resources and Ecology in Headwaters* (ed by K. Kovar, U. Tappeiner, N.E. Peters and R.G. Craig; Proc. of the HeadWater '98 Conference, Meran, Italy, Apr. 1998). IAHS Publ. No. 248, 239-247.

Merz, B., Plate, E.J. (1997) An analysis of the effects of spatial variability of soil and soil moisture on runoff. *Water Resour. Res.* 33, 2909-2922.

Müller, G., Peschke, G. (2000) Hydrologische Prozessuntersuchungen auf der Basis adäquater Meßnetze. *Österr. Wasser- und Abfallwirtschaft*, H. 5/6, 94-104.

Peschke, G., Etzenberg, C., Müller, G. (1998) Experimental analysis of different runoff generation mechanismus. In: Bucek, J. et at. (eds): *Catchment Hydrological and Biochemical Processes in a Changing Environment*. Proceed. of the ERB-Conference, Liblice, 109-112.

Peschke, G., Etzenberg, C., Müller, G., Töpfer, J., Zimmermann, S. (1999) Runoff generation regionalization - analysis and a possible approach to a solution. IAHS Publ. 254, 147-156.

Tilch, N., Uhlenbrook, S., Leibundgut, Ch. (2002) Ausweisung hydrogeologischer und hydrologischer Homogenbereiche mesoskaliger Einzugsgebiete mit breitenverfügbaren Daten. (Identification of hydrogeological and hydrological homogenous areas of mesoscale basins with general available data. [manuscript submitted in „*Grundwasser*“].

Uhlenbrook, S. (1999) Untersuchung und Modellierung der Abflußbildung in einem mesoskaligen Einzugsgebiet. (Investigation and modeling of runoff generation in a mesoscale basin). Thesis, Universität Freiburg.

Zimmermann, S. (1999) Wissensbasierte Regionalisierung. (Knowledge based regionalization) Thesis, Internationales Hochschulinstitut Zittau.

RAINFALL-RUNOFF MODELS WITH PARZEN REGRESSION

R. Wójcik, P. Torfs, P. Warmerdam

Wageningen University, Department of Environmental Science, Sub-Department Water Resources, Nieuwe Kanaal II, 6709 PA, Wageningen, The Netherlands

ABSTRACT

In this paper a black box technique for rainfall-runoff modelling on a daily scale will be discussed. The following aspects: incorporation of memory, periodicity and non-linearity will be highlighted. An application to the catchment of the Beerze in the Netherlands will be shown. It will be demonstrated that it is feasible to model the runoff of a catchment with black box models, using rainfall data only.

Keywords non-linear black box models, rainfall-runoff process, Parzen densities, non-stationary time series

INTRODUCTION

The rainfall-runoff process of a catchment involves "hydrological" memory, as rainfall ($P(n)$) is not immediately transferred into discharge ($Q(n)$). A classical black box approach towards incorporating this memory into a rainfall-runoff model (see e.g. Minns and Hall, 1996 and references therein) is to apply the concept of delay reconstruction and then build the model using the following equation:

$$Q(n) = f(Q(n-\tau_Q), Q(n-2\,\tau_Q), \ldots, Q(n-K\,\tau_Q), P(n), P(n-\tau_P), P(n-2\,\tau_P), \ldots\ldots, P(n-L\,\tau_p)) \qquad (1)$$

where τ_Q, τ_P, K and L are delay reconstruction parameters and $f(\cdot)$ stands for a black box model. This methodology, recently cast into the broader framework of non-linear systems theory (see Takens, 1981 and Casdagli, 1992 for theoretical background and Porporato and Ridolfi, 1997; 2001 or Silvakumar et al., 2002 for hydrological applications), suffers from several technical flaws. Firstly, there is no straightforward algorithmic way to find the optimal delay reconstruction given noisy non-linear time series, so usually several subjective decisions concerning the choice of τ_Q , τ_P ,K and L must be taken. Secondly, if the number of inputs on the right-hand side of (1) is large and the sample size is limited (as frequently happens in practice) there might not be enough data points to populate the reconstructed input-output space and then statistical models $f(\cdot)$ (both linear and non-linear) will show large uncertainty in the estimated parameters and tend to overfit. In statistical literature this phenomenon is referred to as the curse of dimensionality (Hastie et al. 2002). Finally, it is important to note that the discharge estimate $Q(n)$ is always conditioned on antecedent discharges. This restriction stems from the fact that in (1) the use of rainfall inputs alone would be insufficient to calculate $Q(n)$ with reasonable accuracy as pointed out by Minns and Hall (1996). So (1) is actually a discharge prediction model which in the literature is sometimes mistakenly referred to as rainfall-runoff model. A considerable part of its predictive power (especially for daily and sub-daily time resolution) is due to strong correlation of $Q(n)$ with $Q(n-\tau_Q)$.

In this paper a new methodology that solves the above-mentioned problems is presented. It will be shown that combining simple conceptual models with a black box model is an effective way of computing rainfall-runoff transformation based on rainfall information only.

INCORPORATING MEMORY INTO BLACK BOX MODELS – A CONCEPTUAL APPROACH

The problem of accounting for a memory in statistical rainfall-runoff models can be tackled by using two linear (parallel) reservoir models S_1 and S_2 of the form:

$$S_i(n+1) = \alpha_i\, S_i(n) + P(n) \qquad (2)$$

where $S_i(n)$ is the storage of ith reservoir and α_i are identified by investigating the recession curves of the discharge. The first reservoir accounts for slow processes involved in runoff formation such as fluctuations in groundwater flow, changes in soil moisture etc., while the second reservoir accounts for fast processes such as surface runoff. Combining measured rainfall input $P(n)$ with storage functions of the reservoirs $S_1(n)$ and $S_2(n)$ leads to a black box model of the following type:

$$Q(n) = f(P(n), S_1(n), S_2(n)) \qquad (3)$$

Catchments in temperate climate systems also show a clear yearly periodic pattern. This is mainly due to the annual cycle in temperature, land use and evapotranspiration. If that extra information is not directly used in the model (as we assume in this study), the basic approach would therefore be to fit a model (3) for every day:

$$Q(n) = f_{d(n)}(P(n), S_1(n), S_2(n)) \qquad (4)$$

where $d(n)$ stands for the day number of time n. This multiplies the number of parameters by a factor 365, which makes it as such inapplicable. Therefore, the use of an artificial input is proposed:

$$t(n) = \sin(\omega(n+n_f)) \qquad (5)$$

where $\omega = 2\pi/365$ and n_f is an appropriately chosen phase constant. Inclusion of this input into (3) yields:

$$Q(n) = f(P(n), S_1(n), S_2(n), t(n)) \qquad (6)$$

By letting $f(\cdot)$ to be a universal function approximator, the form of $t(n)$ is not so important, i.e. other forms that account for certain periodic components present in data can be used as well.

In this paper, a rainfall-runoff model of the type described by (6) will be shown to be an attractive alternative to the type described by (1). As $f(\cdot)$ we will use the Parzen regression technique. Fig 1 illustrates this new way of rainfall-runoff modelling schematically.

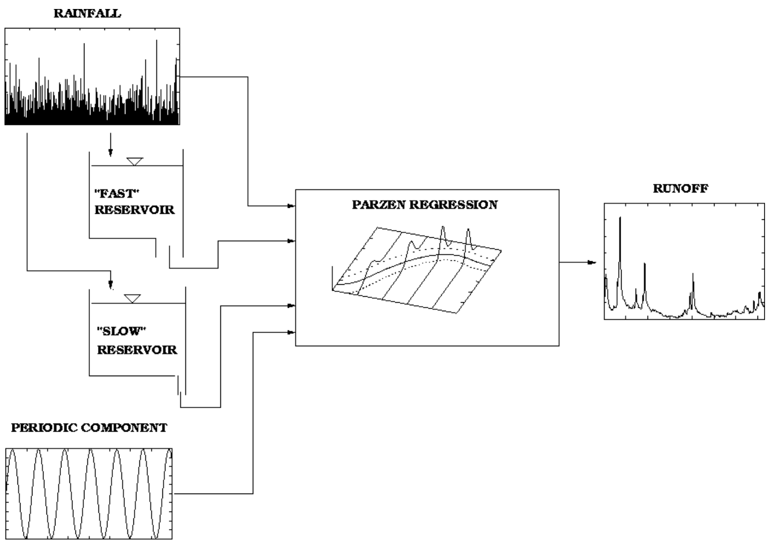

Fig 1: A new methodology for incorporating “hydrological” memory into statistical rainfall - runoff models.

PARZEN REGRESSION

Parzen (Parzen, 1962; see also Silverman, 1986 and Wand and Jones, 1995) used the sum of Gaussian densities to approximate arbitrary densities, as shown in Fig 2. To fit a Parzen density to the joint input-output sample, a maximum likelihood principle was used, but with a new twist being an inclusion of an extra penalty term that prevents degeneration of the Parzen density in question and controls locality of the fit. The maximised fitting criterion Λ can then be written as:

$$\Lambda = \mathrm{L} - \gamma\, d_{KL}(P;G) \qquad (7)$$

where L denotes the likelihood function, γ is the locality constant and $d_{KL}(P;G)$ is the average *Kullback-Leibler* distance (see Kullback, 1959) between components of the Parzen density P and reference Gaussian density G. Once the optimal value of γ is found by a validation procedure and the density is fitted to the inputs and outputs, conditional means and standard deviation bands can be calculated, as depicted in Fig 3.

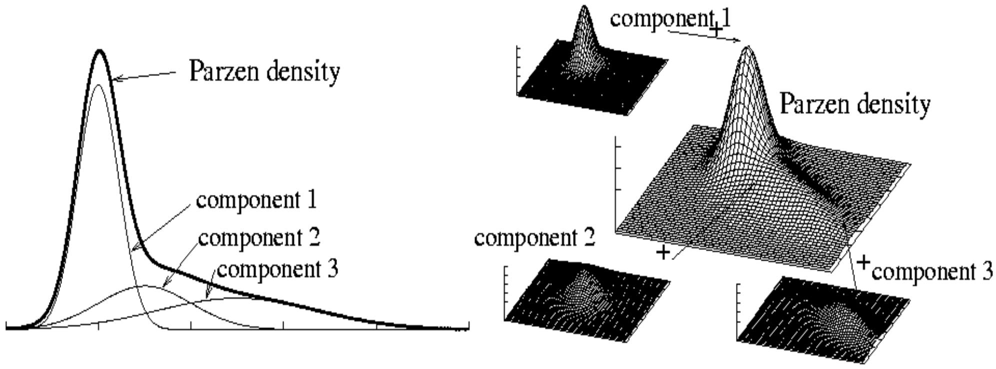

Fig 2: A one and two dimensional example of Parzen densities (in both cases as the sum of three Gaussian components).

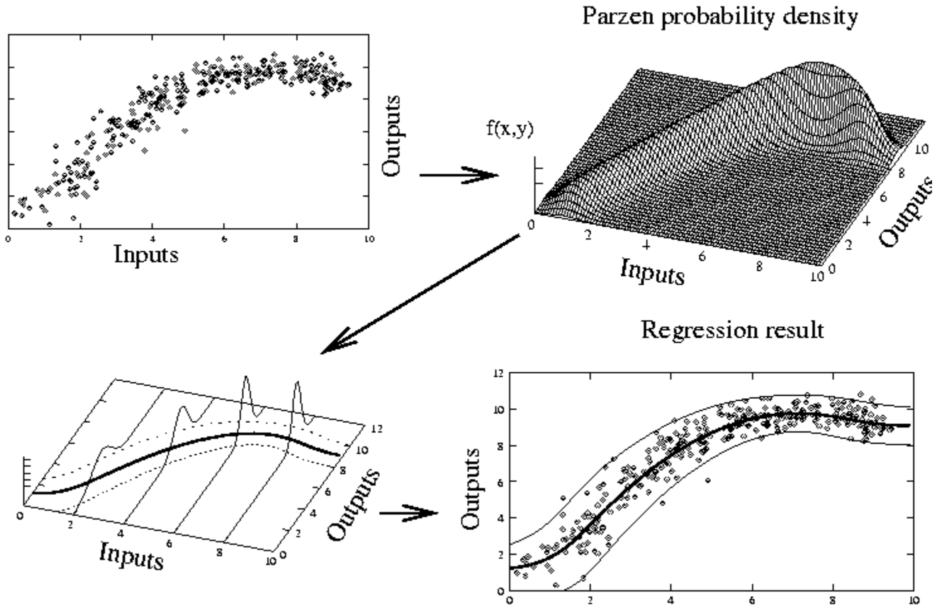

Fig 3: The steps involved in Parzen regression: first a Parzen density is fitted to the data, then conditional densities are estimated, from which mean and e.g. confidence intervals may be extracted.

DATA AND RESULTS

The rainfall and runoff data used for regression experiments in this study are a sequence of daily values registered at the Beerze catchment in the Netherlands over a period of 8 years (January 1980-December 1987). The catchment area covers 240 km^2 and the mean annual rainfall is about 800 mm. The data set was divided into three parts: a calibration set, a validation set and a testing set. The parts consisted of 3 years, 2 years and 3 years of daily records respectively. The calibration set was used to fit regression models, the validation set was used for selection of model parameters, and the testing set was used for assessment of the final chosen models. Two types of models $f(\cdot)$ in (6) were considered: a linear regression model and a non-linear Parzen regression model.

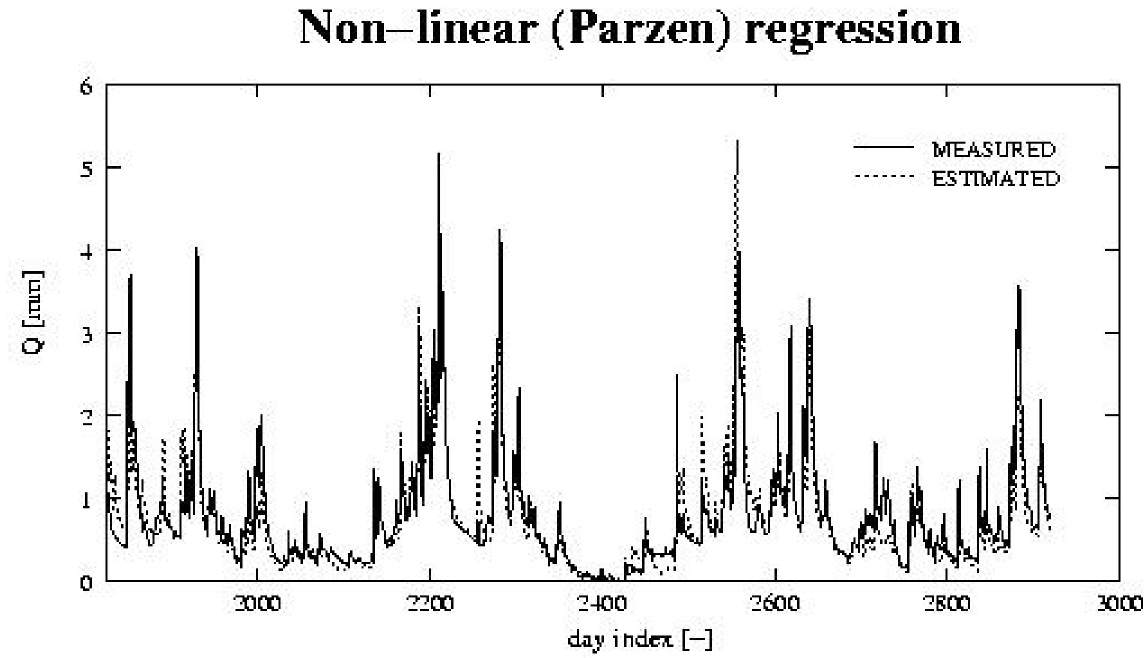

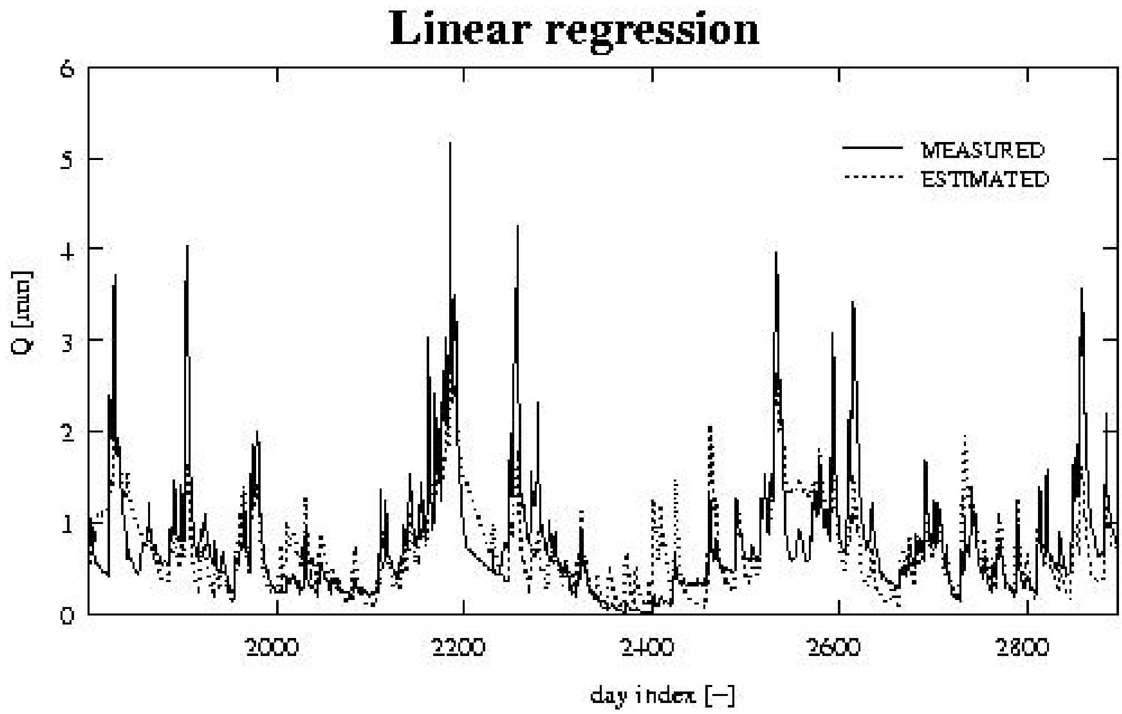

Fig 4: Performance of non-linear and linear regression technique on the testing set.

Fig 4 shows the testing results for both types of models. It can clearly be seen that the non-linear model performed better. Apart from the visual judgement, we also calculated normalised mean squared error for the testing set. This error was always lower for Parzen regression. The strong point of the non-linear model is that apart from discharge estimates, extra information in the form of conditional Parzen densities is available. Fig 5 shows a segment of the testing set for which several such conditional densities are plotted together with the conditional mean (estimated discharge), standard deviation bands, and measured discharge. It is interesting to see that there are three cases (designated as A, B and C) for which the conditional density is bimodal. The reason for that kind of behaviour might be that the mapping of rainfall into runoff is not exactly functional, i.e. the same values of rainfall are sometimes associated with different values of runoff. Therefore, the mean and the standard deviation have to be interpreted through these two modes.

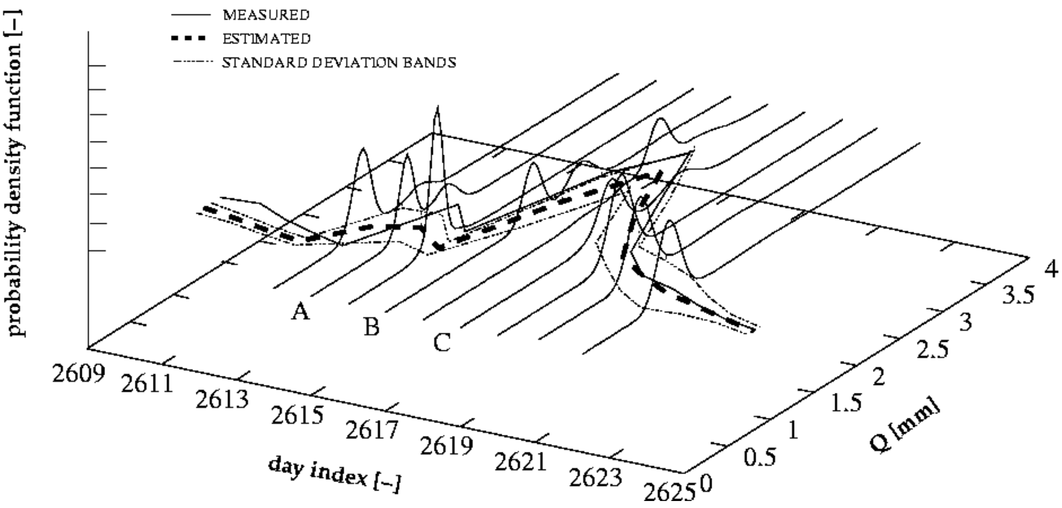

Fig 5: X-Y plane: Parzen regression on a segment of the testing set with error bands given by standard deviations; Z-plane: conditional densities.

CONCLUSIONS

1. The use of conceptual reservoir models solves efficiently a memory incorporation problem for statistical rainfall - runoff models.
2. The Parzen regression model performed better as a rainfall-runoff transformation tool than the linear regression model.
3. In addition to runoff estimates, Parzen regression offers other results that can be useful for the modeller: standard deviation error bands, full conditional density. All these concepts have their standard probabilistic interpretation.

REFERENCES

Casdagli, M. (1992) A dynamical systems approach to modelling input-output systems. In: Casdagli, M., Eubank, S. (eds.), *Nonlinear Modelling and Forecasting*. Santa Fe Institute Studies in the Science of Complexity. Addison-Wesley, Redwood City.

Hastie, T., Tibshirani, R., Friedman, J.H. (2002) The Elements of Statistical Learning: Data Mining, Inference, and Prediction. Springer-Verlag, London.

Kullback, S. (1959) Information Theory and Statistics. Dover Publications, New York.

Minns, A.W., Hall, M.J. (1996) Artificial neural networks as rainfall - runoff models. *Hydrological Sciences Journal*, 41, 399-417.

Parzen, E. (1962) On estimation of a probability density function and mode. *Annals of Mathematical Statistics*, 33, 1065-1076.

Porporato, A., Ridolfi, L. (1997) Non-linear analysis of river flow time sequences. *Water Resources Research*, 33, 1352-1367.

Porporato, A., Ridolfi, L. (2001) Multivariate nonlinear prediction of river flow. *Journal of Hydrology*, 248, 109-122.

Silvakumar, B., Jaywardena, A.W, Fernando, T.M.K.G. (2002) River flow forecasting: use of phase-space reconstruction and artificial neural networks approaches. *Journal of Hydrology*, 265, 225-245.

Silverman, B.W. (1986) Density Estimation for Statistics and Data Analysis. Chapman and Hall, New York.

Takens, F. (1981) Detecting strange attractors in turbulence. In: Rand, D.A., Young, L.S. (eds.), *Dynamical Systems and Turbulence*. Lecture Notes in Mathematics, vol. 898. Springer-Verlag, New York.

Wand, M.P., Jones, M.C. (1995) Kernel Smoothing, Chapman & Hall, London.

IMPLEMENTATION OF A MATHEMATICAL MODEL OF WATER AND SOLUTE VERTICAL TRANSPORT IN THE PLANT-SOIL COLUMN IN THE POŻARY BASIN

Maciej Lenartowicz

Department of Hydrology, Faculty of Geography and Regional Studies, University of Warsaw
Krakowskie Przedmieście 30, 00-927 Warszawa, e-mail: mlenarto@uw.edu.pl, tel. +48225520635

ABSTRACT

The vertical component predominates in the water balance of lowland swampy catchments. The one-dimensional mathematical model developed here couples a description of the following processes taking part in the vertical migration of water: land evaporation, interception on plant canopy, infiltration and soil moisture changes in the unsaturated zone. These processes are handled as a background for the migration of solutes to the groundwater table. Every part of the model describing individual processes is physically based and related to another part by input-output parameters. The identification of model parameters was performed in the Pożary basin in three selected representative plant-soil columns: in wetlands, dunes and in the transitional zone between wetlands and dunes. The model was tested using chloride ion as an example. This paper presents the results of modelling over a short summer period. It was found that the greatest role in summer recharge is played by long lasting intense precipitation episodes. Precipitation is also the main source of chloride ions in the basin. Since the results were considered to be quite good, it is possible to use the model for the simulation of water and solute vertical transport in swampy basins.

Keywords mathematical model, water and solute vertical transport, interception, infiltration, soil moisture changes, unsaturated zone

RESEARCH GOALS AND STUDY BASIN

The goal of this research is to implement and test a mathematical one-dimensional model for the vertical migration of water and chemical substances in the Pożary lowland swampy basin located in central Poland within the Kampinos National Park. Because vertical water migration dominates in these types of catchments, its detailed description can answer many questions related to the water balance and circulation of chemical substances in the Pożary basin. This paper presents the first results of modelling. In this phase of the project, the migration of an exemplary ion (chloride) in three selected representative plant-soil columns was modelled.

The Pożary basin is part of the Łasica River catchment, a right tributary of the Bzura River. Most of the basin is protected within the Kampinos National Park. The total area of the Pożary basin to the streamflow gauge at Józefów is 20,17 km^2 of which 7,01 km^2 is blind drainage area, that is area without surface runoff (Fig 1). Nearly 90% of the basin area consists of land with 0% inclination or slightly larger. The whole area of the Pożary basin consists of Quaternary sediments. Loose sands and weakly loamy sands dominate (49.4% of the whole basin area). Peat covers 27.2% of the area in depressions filled with organic sediments. Pine forest is dominant among vegetation communities found on sandy formations (20.3%). In hydrogenic landscapes the most characteristic community is alder wood with currant (16.1%) and lowland bog (12.0%). There are meadows and deciduous forests in the transitional zones between the dunes and lowland bog areas. During the period of 1994-2000, average annual temperature was +7.7°C and average annual measured precipitation was 569.2 mm (Zintegrowany Monitoring 1999). In the central part of the Pożary basin the groundwater table is very close to the surface throughout most of the year. In periods of intensive precipitation the groundwater table rises above the terrain level, flooding wide areas. A detailed lithological survey enables us to state that there is one main aquifer in the area of the Pożary basin and its thickness reaches more than a dozen meters (Kazimierski et al.,1995).

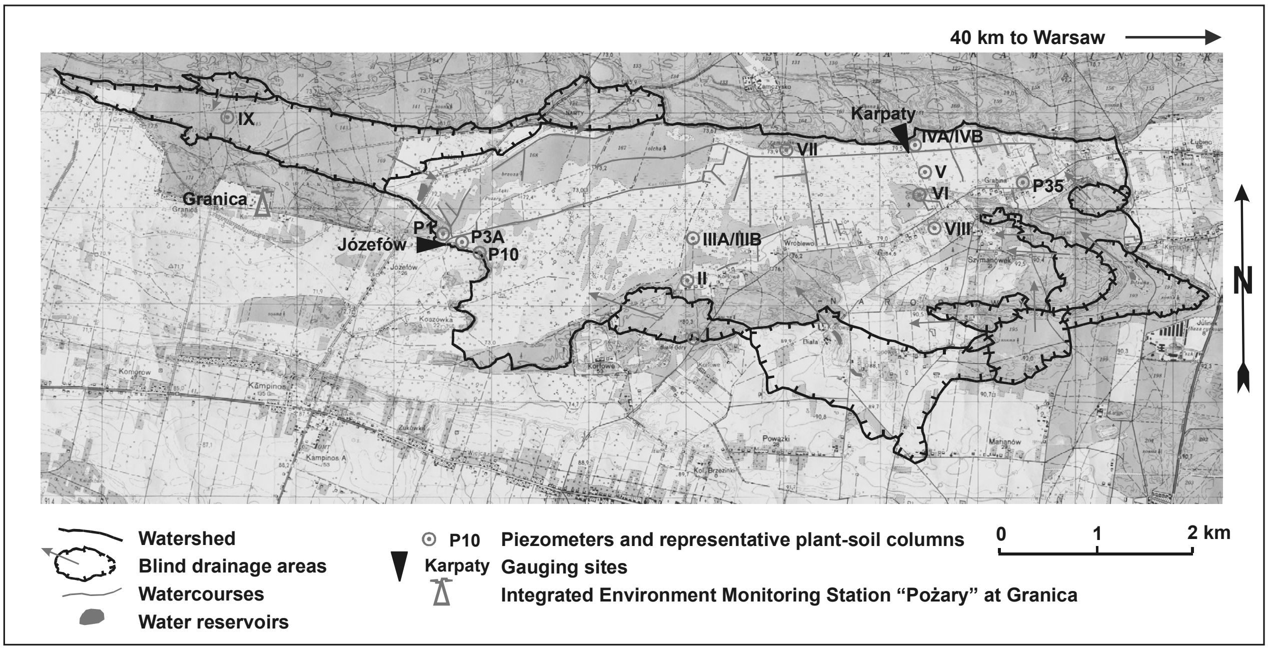

Fig 1: The Pożary basin: topography, piezometers and gauging sites.

MATHEMATICAL MODEL STRUCTURE

The one-dimensional model of the vertical migration of water and chemical substances in the plant-soil column describes processes at the interface between the atmosphere, biosphere and pedosphere (Fig 2). The proposed mathematical model uses physically based parameters. This means that all its parameters have an unequivocal physical sense and may be estimated by direct field measurements (Soczyńska, 1997). All processes are examined in a 24-hour time step. The model input data is the daily sum of liquid precipitation and its chemical composition in the form of ion concentration in water measured in mg dm^{-3}.

Precipitation is an input to the mathematical model and reliable data about the daily totals are fundamental for the proper functioning of all the modules. The rain gauge measuring method applied at meteorological stations and posts creates serious difficulties with the evaluation of the real sums of water reaching the ground. A method developed by Kowalczyk et al. (1978) was used to calculate the corrected precipitation in the Pożary basin. The daily corrected precipitation totals are input data for the model of plant cover interception, and are calculated according to the following formula:

$$P_r = 1.135\,(P_1 + 1)^{0.165} + P_1 + k_1 - 1 \text{ [mm d}^{-1}\text{]} \quad (1)$$

where: P_1 - daily precipitation total measured at a height of 1 m (mm), k_1 - calculated precipitation loss caused by rain gauge collector surface moistening (mm), P_r - corrected precipitation total (mm).

Due to the lack of sufficient data for the calculation of daily totals of land evaporation, a method that does not require data such as radiation balance had to be selected. The best results were obtained by the Konstantinov method. This method is based on a nomograph relating the measurements of land evaporation to air temperature and water vapour pressure (Konstantinov, 1968). Measurements of only those two meteorological parameters are necessary in order to use this method. An adaptation of the Konstantinov nomograph to Polish conditions was made based on numerous research studies done in the 60’s (Cetnarowicz, 1961; Mikulik, 1961; Dębski, 1963).

A mathematical model developed by Fleming (1975) was applied to describe the flora interception process. Flora characteristics used in this model are stand density (D_c) representing the relation between the vertical projection area of tree crowns and total forest area, and the maximum interception storage capacity (S_{max}). These are functions of the composition and development stage (age) of flora species. The interception increment (ΔS) over a time step may be described by a simple equation:

$$\Delta S = P_r \cdot D_c - E_t \quad (2)$$

where: E_t - evaporation (mm).

Throughfall (Z) is calculated as follows:

$$Z = P_r \cdot (1 - D_c) \tag{3}$$

The interception retention surplus (T) is estimated according to the conditional equation (Soczyńska, 1997):

$$T = \begin{cases} S(t_{i-1}) + \Delta S(t_i) - S_{max} \\ 0 \end{cases} \text{when} \begin{matrix} \left(S(t_{i-1}) + \Delta S(t_i)\right) \geq S_{max} \\ \left(S(t_{i-1}) + \Delta S(t_i)\right) < S_{max} \end{matrix} \tag{4}$$

where: T - interception surplus (mm), $S(t_{i-1})$ - interception storage at time t_{i-1} (mm), $\Delta S(t_i)$ - interception storage increment over the time interval between the (i-1)-th and i-th time instants (mm), S_{max} - maximum interception storage capacity (mm).

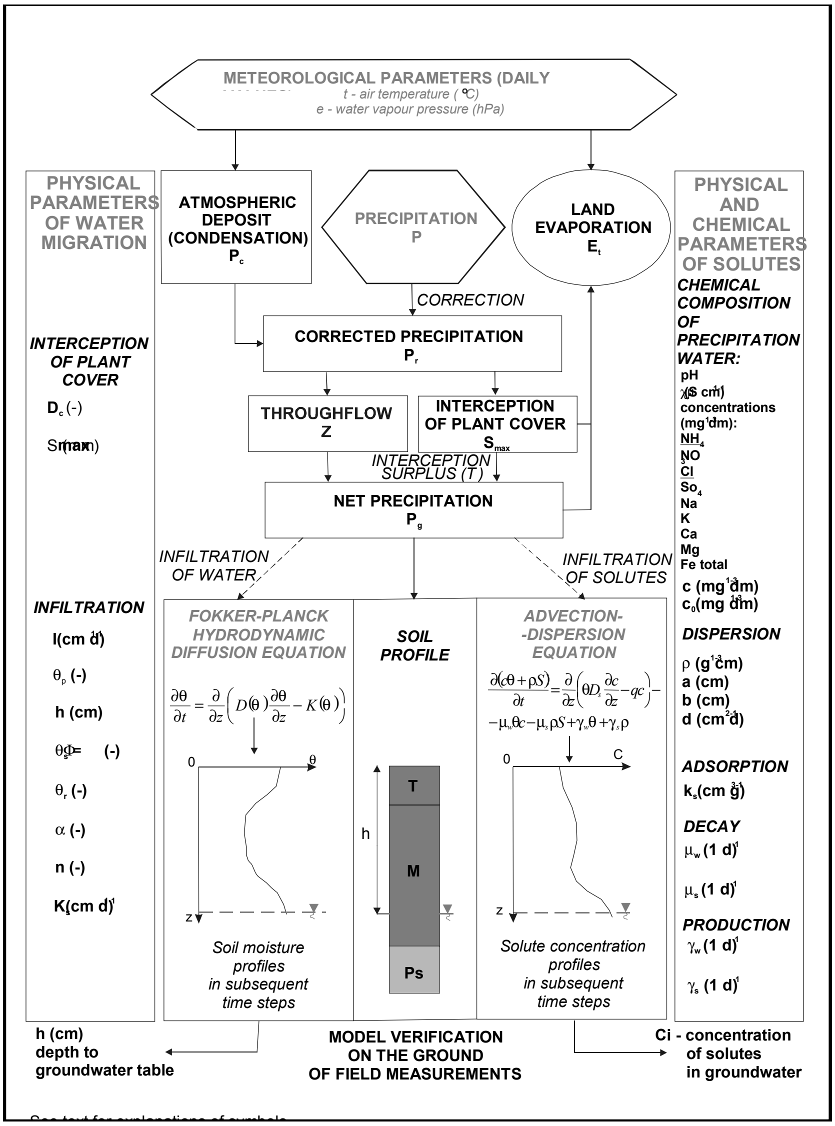

Fig 2: Structure of the one-dimension mathematical model of the vertical migration of water and chemical substances in the plant-soil column.

The sum of the interception surplus and throughfall reduced by the evaporation sum is equal to net precipitation (P_g). It is the output from the vegetation cover interception module and the input to the soil infiltration module and to the transport of the chemical substance in the unsaturated zone, calculated on a daily time step.

The mathematical model developed by the Academy of Agriculture in Wrocław (Szulczewski, 1990) was used to describe the water and solute migration in the unsaturated zone. Soil moisture changes are evaluated using the Fokker-Planck differential equation (5). The dependence of the soil water diffusivity (D), unsaturated hydraulic conductivity (K), and soil water matrix potential (or pressure head) (h) on soil water content (θ) has been modelled after Van Genuchten (1980). This dependence is described by the parameters θ_r, θ_s, α, n and K_s. The Fokker-Planck equation reads:

$$\frac{\partial \theta}{\partial t} = \frac{\partial}{\partial z}\left(D(\theta)\frac{\partial \theta}{\partial z} - K(\theta) \right) \tag{5}$$

where: z, t - independent variables: space (L) and time (T), θ - actual volumetric water content ($L^3\ L^{-3}$), $D(\theta)$ - soil water diffusivity ($L^2\ T^{-1}$), $K(\theta)$ - unsaturated hydraulic conductivity ($L\ T^{-1}$).

The description of soil moisture changes by the Fokker-Planck equation requires some simplifications:

- the soil profile is a non-deformed and isotropic medium,
- the flowing flux of liquid is of constant density,
- during modelling there are no water phase changes,
- the flow takes place at a virtually constant temperature,
- water uptake by plants is omitted.

For $z = 0$ (top of the soil profile), Szulczewski's model allows the use of the boundary condition of Dirichlet as well as that of Neumann, but for $z = L$ (bottom of the soil profile) the no-flow Neumann condition is used ($q(t) = 0$). The solution of the Fokker-Planck equation is used to determine the pore water velocity (v) and the soil water content (θ) which are necessary for the parallel modelling of solute transport in the soil. The application of the model is limited to situations when the wetland is not fully saturated (summer dry period).

To model the solute transport, the advection-dispersion equation (Maciejewski, 1998) was used (6). It is a differential equation included in a system of equations together with the Fokker-Planck equation:

$$\frac{\partial (c\theta + \rho S)}{\partial t} = \frac{\partial}{\partial z}\left(\theta D_s \frac{\partial c}{\partial z} - qc \right) - \mu_w \theta c - \mu_s \rho S + \gamma_w \theta + \gamma_s \rho \tag{6}$$

where: c - concentration of substance per unit volume of solution ($M\ L^{-3}$), S - adsorption coefficient ($M\ M^{-1}$), which was taken in the form $S = k_s \cdot c$, k_s = const., D_s - dispersion coefficient ($L^2\ T^{-1}$), q - volumetric flux of water $q = v \cdot \theta$ ($L\ T^{-1}$), ρ – soil bulk density ($M\ L^{-3}$), μ_w, μ_s - constants characterising substance decay (first-order reactions) in fluid and solid phase respectively (T^{-1}), γ_w, γ_s - constants characterising substance production (zero-order reactions) in fluid and solid phase respectively (T^{-1}).

According to Maciejewski (1998), the dispersion coefficient D_s is dependent on soil water content and pore water velocity in the soil:

$$D_s = (-a\theta + b)v + d \tag{7}$$

where: a, b, d - constants describing variability of the dispersion process (cm) equal to the longitudinal and transverse dispersivity and molecular diffusion respectively.

The Dirichlet or Neumann boundary conditions can be taken for (6) at the top of the soil profile (z=0). At the bottom of the profile the zero concentration gradient was taken, which in the case of no water flow means no flow of solute. The concentration distribution of the modelled substance in the soil profile, in individual time steps, is found by solving the hydrodynamic dispersion equation.

IDENTIFICATION OF MODEL PARAMETERS AND INPUTS

For the model to properly reflect the physiogeographical conditions in the Pożary basin, it was necessary to choose representative plant-soil columns. After a detailed analysis, 13 representative plant-soil columns were selected, based on soil type, real vegetation type and the thickness of the vadose zone (Fig 1). For the needs of the present paper, the migration of the chloride ion in three research profiles (Fig 1): IV (swamp), II (transition between swamp and dune areas) and P1 (dune) have been selected as an example. The modelling period was chosen between 3 June and 18 June1999.

In 1998, Kruk developed relations between the type, age and species composition of forest assemblages on the one hand and the parameters of the interception process in the Łasica catchment on the other hand.

Table 1: Physical parameters of the interception process in selected representative plant-soil columns in the Pożary basin (according to Kruk 1998).

Profile	Type of assemblage	Dominating species	Age (years)	Stand density *Dc* (-)	Maximum interception storage capacity *Simax* (mm)
P1	Unclassified assemblage of pine forest and mixed oak-pine forest (association *Dicrano-Pinion*)	Pine (*Pinus silvestris*)	40	1	3.2
II	Meadow (*Arrhenatheretum elatioris*)	-	-	1	1.1
IV	Alder wood (*Ribo nigri-Alnetum*) juvenile form	Alder (*Alnus glutinosa*) 70%	20	0.89	3.07

This enables a quick estimation of these parameters based on the analysis of forest stand maps (Tab. 1). In the case of non-forest communities, the data from literature was used (Soczyńska, 1997).

In order to describe the soil water flow process, it is necessary to estimate the physical parameters of the soil. The set of parameters included in this model required field research. Bulk density and saturated water content were determined by laboratory analyses of soil samples (Tab. 2). The grain size distribution curves were used to calculate saturated hydraulic conductivity according to the so-called American formula (Pazdro and Kozerski, 1990):

$K_s = 0.36\, d_{20}^{2.3}$ (cm^1 s^{-1}) (8)

where: d_{20} - the effective diameter (in mm) of particles, such that 20 % of the soil mass is composed of particles smaller than d_{20}.

Table 2: Physical parameters of the infiltration process in selected plant-soil columns in the Pożary basin, estimated from field surveys.

Profile	Type of material	Saturated hydraulic conductivity K_s (cm d^{-1})	Bulk density ρ (g^1 cm^{-3})	Saturated volumetric water content (porosity) $\theta_s=\Phi$ (-)	Van Genuchten's soil parameters (-)		Volumetric water content at permanent wilting point (pF4.2) θ_r (-)
					α	n	
P1	sand	404.67	1.528	0.369	0,0112	1,364	0.011
II	sand	335.54	1.409	0.372	0,0117	1,363	0.011
IV	peat	69.98	0.215	0.836	0,0133	1,261	0.255

The volumetric water content at pF 4.2 (residual water content, taken as equal to the wilting point) was estimated according to the formula proposed by Ślusarczyk (1979):

$WTW = 0{,}709 + 0{,}386\, X$ (9)

Where: WTW - residual water content (at pF 4.2), X - content of soil fraction below 0,002 mm (clay) in %. In the case of peat soil, the residual water content was determined in the laboratory.

The Van Genuchten parameters α (α>0 (-)) and n (n>1 (-)) were estimated using relations given by Rawls and Brakensiek (1982), based on soil porosity and the content of sand and clay. The dispersion coefficient according to (7) is described by 3 parameters *a, b* and *d*. The values of *a* and *b* were taken after Maciejewski (1998) as: $a = 0.2$ cm, $b = 0.1$ cm. The value of $d = 0.17$ (cm^2 g^{-1}) was taken according to research by De Smedt et al. (1981). The parameter k_s (cm^3 g^{-1}) represents substance adsorption in the soil and is otherwise called the equilibrium constant. In the case of an ideal migrant, thus a non-adsorbed substance or ion, $k_s = 0$. The k_s coefficient for the chloride ion was estimated as 0.05 cm^3 g^{-1}. The remaining model parameters (μ_w, μ_s, γ_w, γ_s) describing substance (ion) degradation and production in the soil were assumed equal to 0, because the chloride ion does not decay in the soil and is not produced either. The initial soil water content (θ_p (-)) and the thickness of the unsaturated zone (h (cm)) were obtained by field surveys. It was assumed that the initial concentration of chloride c_0 (mg^1 dm^{-3}) was constant and equal to 0 in the unsaturated zone and a concentration greater than 0 was only present within the aquifer. Initial soil water content and chloride concentrations are shown in Figs 3, 4, and 5 as the curves with time equal to zero.

The input variables to the infiltration and solute transport model were the net precipitation (P_g) intensity on the ground surface I (cm d^{-1}), the chloride ion concentration in precipitation water c (mg^1 dm^{-3}) and the daily totals of land evaporation E_t (cm d^{-1}). Precipitation data were obtained from the Granica meteorological station (Fig 1). Measurement results were corrected in order to obtain P_r according to formula (1) (Tab. 3). A chemical analysis of precipitation water at the station in Granica was made once a month in a collective sample test (from the whole month). Therefore, it was assumed that the concentration of individual ions is constant within one month. In the modelling period, the chloride ion concentration in precipitation water was 0.2 mg Cl^- dm^{-3} in June 1999 (Tab. 4). The daily totals of land evaporation as mentioned above were calculated using the Konstantinov method, based on meteorological data from the Granica station: daily mean air temperature and water vapour pressure (Tab. 3).

Table 3: Daily corrected precipitation (P_r) and land evaporation (E_t) totals at the Granica station and net precipitation in profiles IV, II and P1 in the period from 1 June to 18 June 1999.

Date	P_r (mm/d)	E_t (mm/d)	P_g (mm/d)			Date	P_r (mm/d)	E_t (mm/d)	P_g (mm/d)		
			IV	II	P1				IV	II	P1
1.06	0.0	3.5	0.00	0.00	0.00	10.06	0.0	3.6	0.00	0.00	0.00
2.06	0.0	3.4	0.00	0.00	0.00	11.06	30.4	3.3	27.07	27.07	27.70
3.06	7.5	3.1	4.38	4.38	4.28	12.06	8.4	1.2	5.34	7.18	5.21
4.06	14.1	2.3	10.98	11.73	10.95	13.06	10.8	2.8	7.96	7.96	7.96
5.06	0.0	3.3	0.00	0.00	0.00	14.06	5.1	1.5	2.02	3.56	1.89
6.06	0.0	3.4	0.00	0.00	0.00	15.06	1.7	1.5	0.19	0.21	0.16
7.06	0.3	3.9	0.00	0.00	0.00	16.06	0.3	2.6	0.00	0.00	0.00
8.06	11.5	2.7	8.42	8.78	8.29	17.06	26.6	1.0	23.58	25.55	23.45
9.06	0.0	3.6	0.00	0.00	0.00	18.06	3.3	2.1	1.16	1.16	1.16

Table 4: Chloride ion concentration in precipitation water at the Granica station in 1999.

Month	I	II	III	IV	V	VI	VII	VIII	IX	X	XI	XII
Concentration (mg Cl^- dm^{-3})	2.3	1.8	1.5	0.8	0.5	0.2	0.6	0.8	0.8	1.0	2.0	2.2

RESULTS

The calculated soil moisture distribution in the swamp profile (Fig 3a) shows a strong sensitivity to rainfall totals. There was a large rainfall event (10.98 mm) on the second day after the beginning of the simulation. The soil immediately reached full saturation (θ = 0.836) and water started to collect on the ground surface. This can be seen in the calculation results. A decrease of soil moisture over the first day was caused by the absence of precipitation. In the case of the chloride ion concentration, a decrease in the lower part of the profile is related to a small content of chloride in the precipitation water. The measured concentration in the groundwater, which initially was equal to 10 mg Cl^- dm^{-3}, decreased to 7 mg Cl^- dm^{-3}. The modelling result was 8 mg Cl^- dm^{-3} (Fig 3b), which agrees quite well with the measurement, taking into consideration a very small input of chloride with precipitation. The increase of the chloride concentration in the upper soil layers must be a numerical modelling artefact because the boundary conditions adopted did not make any upward flow possible.

In the transitional soil profile II (Fig 4), the measured groundwater level during the period of 14 days raised from 72 to 59 cm b.t.l. (below terrain level). The daily precipitation total once even exceeded 20 mm. The initial soil moisture content above the capillary fringe zone was about θ = 0.275. The measured chloride ion concentration in the groundwater was quite high at the beginning (27 mg Cl^- dm^{-3}) but it drastically fell during the 14 days (to 8 mg Cl^- dm^{-3}). This was due to little chloride supply with the precipitation water and due to the effect of the previous period, when the chloride ion concentration both in the soil and in the precipitation water was higher (Tab. 4). The calculation results show quite a strong reaction to precipitation of overdried soil in terms of the soil moisture content (Fig 4a). High daily precipitation totals have an immediate effect on the top soil layer to a depth of about 70 cm. The calculated groundwater level at the end of the modelling period is 3 cm higher than the measured one. The chloride ion concentration in the soil shows variability only in the saturation zone (Fig 4b). Above the groundwater table, concentrations are very small as a result of the low chloride content in precipitation water and quick ion migration in the soil. The calculated chloride ion concentration at the end of the simulation period in the unsaturated zone is 0.5 mg $Cl^{-}dm^{-3}$ higher than the measured value.

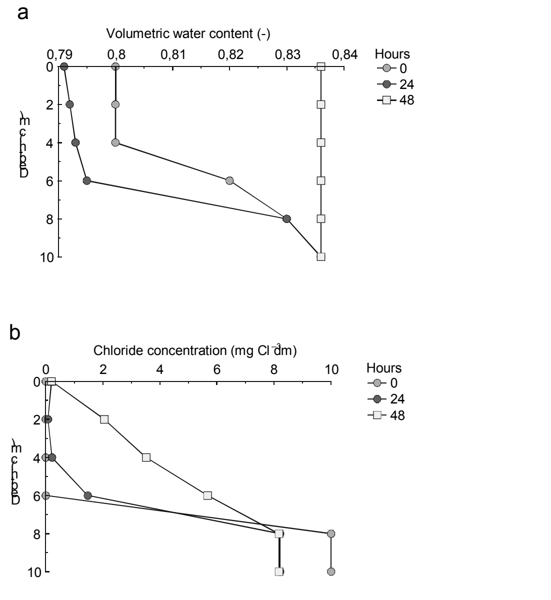

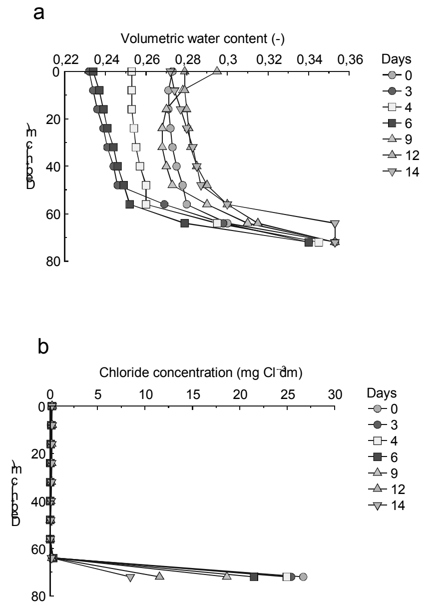

Fig 3: Results of soil moisture distribution (a) and chloride ion concentration (b) modelling in profile IV during the period 3-4 June 1999 (time in hours).

Fig 4: Results of soil moisture distribution (a) and chloride ion concentration (b) modelling in profile II during the period 3-18 June 1999 (time in days).

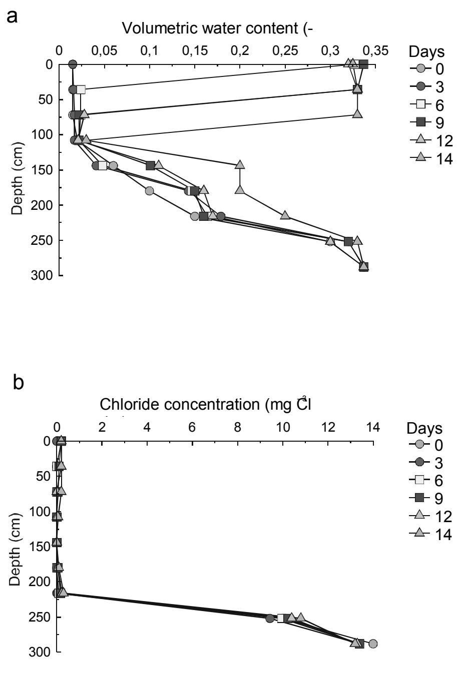

Fig 5: Results of soil moisture distribution (a) and chloride ion concentration (b) modelling in profile P1 during the period 3-18 June 1999 (time in days).

The dune profile (P1), 280 cm thick, was the deepest of the analysed soil profiles. Initially the whole profile was strongly overdried and water content was close to the permanent wilting point (θ_r = 0.011), whereas the groundwater table was measured at 258 cm b.t.l. Quite a large precipitation event in the period from 3 June to 18 June 1999, exceeding 27 mm/d, caused the water table to rise to 250 cm b.t.l. The measured chloride ion concentration in the groundwater did not vary in time, staying constant at 14 mg Cl^- dm^{-3}. In the top soil layer, due to abundant precipitation, a strong variability in water content was observed (Fig 5a). The results show that water migration in this profile, composed of loose sands, is very fast and after intense precipitation a state close to saturation can be observed in the top layers. Below 100 cm, the percolating water is only partially able to replenish the soil moisture deficiency. The calculated groundwater level at the end of simulation is about 7 cm higher than the measured level. Changes in the calculated chloride ion concentration are only visible in the top soil layer, which is clearly a result of the ion's small concentration in precipitation water (Fig 5b). The calculation results show that the chloride ion concentration in the middle part of the profile nearly always approach zero. The highest calculated chloride concentration occurred in the lower part of the profile and slightly changed over the modelling period (it decreased from 14 mg Cl^- dm^{-3} to about 13 mg Cl^- dm^{-3}). The difference between the calculated and measured concentration in groundwater at the end of simulation is about 1 mg Cl^- dm^{-3}.

CONCLUSIONS

The modelling results confirm the presumptions concerning the basic rules governing water circulation in the Pożary basin:

- Because of favourable infiltration conditions in the dune area, and less favourable conditions on the wetlands, the dune zones are the main place of groundwater recharge in the basin.
- The greatest role in the summer recharge of groundwater is played by long lasting intense precipitation, which causes an immediate reaction of the swamp area groundwater. Precipitation events with intensities less than 4 mm/d cause no reaction of the groundwater, because during the summer period evaporation is very high.
- The main source of chloride ions in the basin is precipitation water. The chloride concentration in groundwater decreases as soon as a reduced chloride load in precipitation water is observed.
- The influence of chloride concentration variability in precipitation water on chloride content in groundwater decreases with depth. The most visible reaction takes place in relatively shallow sandy profiles (II).

The presented mathematical model of water and solute transport in the vertical plant-soil column may be applied in various other catchments where groundwater is shallow and the vertical components of water flow and solute transport in the saturated zone are negligible. An attempt to apply this model in a wetland area shows that it is also possible to use it there, even if the unsaturated zone is not very thick. The only limitation for the application of the presented mathematical model seems to be the availability of data and the proper identification of model physical parameters.

REFERENCES

Cetnarowicz, M. (1961) Wyniki zastosowania w zlewniach o charakterze górskim i podgórskim niektórych empirycznych metod obliczenia parowania terenowego [Results of selected empirical methods applying for calculation of land evaporation in mountain and piedmont basins]. *Biuletyn PIHM* 2.

De Smedt, F., Wierenga, P.J., Van der Beken, A. (1981) Theoretical and experimental study of solute movement through porous media with mobile and immobile water. Vrije Universiteit Brussel, Laboratory of Hydrology and the Centre for Statistics and Operational Research, Brussel.

Dębski, K. (1963) Przystosowanie nomogramu Konstantinowa do obliczeń parowania terenowego w Polsce [Adaptation of Konstantinov nomograph for land evaporation calculations in Polish conditions]. *Prace i Studia Komitetu Inżynierii i Gospodarki Wodnej PAN,* vol.VI, PWN, Warszawa, 59-96.

Fleming, G. (1975) *Computer simulation techniques in hydrology*. Elsevier, New York-Oxford-Amsterdam.

Kazimierski, B., Pilichowska-Kazimierska, E., Sikorska-Maykowska, M. (1995) Studium warunków wodnych [Study of water conditions]. In: *Plan Ochrony Kampinoskiego Parku Narodowego* [*The protection plan of the Kampinos National Park*]. unpubl. Narodowa Fundacja Ochrony Środowiska, Warszawa.

Konstantinov, A.R. (1968) Isparenije w prirodje [*Evaporation in Nature*]. Gidrometeorologiczeskoje Izdatel'stwo, Leningrad.

Kowalczyk, S., Godziemska, T., Wolska, A. (1978) Pomiary porównawcze opadów atmosferycznych [Comparative measurements of precipitation]. unpubl. IMiGW, Warszawa.

Kruk, A. (1998) Ocena obiegu wody w zlewni Łasicy w strefie bio- i pedosfery [Water circulation assessment in bio- and pedosphere in the Łasica catchment]. unpubl. Thesis. Zakład Hydrologii, Wydział Geografii i Studiów Regionalnych Uniwersytetu Warszawskiego.

Maciejewski, S. (1998) Procesy przepływu rozpuszczonych w wodzie substancji w gruncie nienasyconym [Solute transport processes in unsaturated soil]. *Biblioteka Naukowa Hydrotechnika* no. 26. Instytut Budownictwa Wodnego PAN, Gdańsk.

Mikulik, S. (1961) Zbadanie przydatności niektórych empirycznych metod wyznaczania normalnego parowania terenowego dla Polski Środkowej [Research on usefulness of some empirical methods of normal land evaporation determination in Middle Poland]. *Biuletyn PIHM* no. 2.

Pazdro, Z., Kozerski, B. (1990) Hydrogeologia ogólna [Hydrogeology]. Wyd. Geolog., Warszawa.

Rawls, W.J., Brakensiek, D.L. (1982) Estimating Soil Water Retention from Soil Properties. *J. Irrig. Drain. Eng.,,* vol. 108, no. IR2, 166-171.

Soczyńska U. [Ed.] (1997) Hydrologia dynamiczna [Dynamic Hydrology]. PWN, Warszawa.

Szulczewski, W. (1990) Model matematyczny rozprzestrzeniania substancji chemicznych w strefie aeracji [A modelling of chemical substance transport in aeration zone]. (Engl. summ.), *Zeszyty Naukowe Akademii Rolniczej we Wrocławiu. Melioracja*, vol. XXXVI, no. 192, 99-110.

Ślusarczyk, E. (1979) Określenie retencji użytecznej gleb mineralnych dla prognozowania i projektowania nawodnień [Estimation of useful storage of mineral soils for forecasting and designing purposes in irrigation]. *Melioracje Rolne, Biuletyn Informacyjny* 3, 1-10.

Van Genuchten, M.Th. (1980) A Closed-Form Equation for Predicting the Hydraulic Conductivity of Unsaturated Soil. *Soil Sci. Soc. Am. J.*, vol. 44, 892-898.

Zintegrowany Monitoring Środowiska Przyrodniczego, Stacja bazowa "Pożary" w Kampinoskim Parku Narodowym [Integrated Monitoring of the Natural Environment, Base station "Pożary" in Kampinos National Park]. (1999) Biblioteka Monitoringu Środowiska, Inspekcja Ochrony Środowiska, Warszawa.

MEASURING TECHNIQUES FOR CONTAMINANT HYDROLOGY

Lubomir Lichner[1], Andrea Cipakova[2], Miloslav Sir[3]

[1]*Institute of Hydrology, Slovak Academy of Sciences, Bratislava, Slovakia*
[2]*State Institute of Public Health, Kosice, Slovakia*
[3]*Institute of Hydrodynamics, Czech Academy of Sciences, Prague, Czech Republic*

ABSTRACT

Three original measuring techniques are presented in this paper. Radioactive tracer techniques can be used for in-situ measurements of the solute (contaminant) velocity, the longitudinal dispersion coefficient and bypassing ratio, as well as for laboratory measurements of the solute (contaminant) sorption, distribution coefficient and partitioning among individual fractions of studied soil. The retardation factor of a contaminant can be estimated from the breakthrough curves measured in a laboratory on the undisturbed soil column with the System of European Water Monitoring (SEWING) developed in the 5th EC Framework Programme Project IST-2000-28084.

Keywords radioactive tracer techniques, FET sensors, contaminant hydrology

INTRODUCTION

The water issue is set to become one of the major questions of the 21st century. The world's water problems arise not so much from a shortage of freshwater as from its uneven distribution, from ever-increasing demand, and from practices detrimental to water quality (Falkenmark et al., 1999). Preferential flow of water and chemicals contributes substantially to contaminant transport under field conditions (Jury and Fluhler, 1992; Cislerova et al., 2002). The aim of this paper is to present three original measuring techniques that can serve to measure the quantities connected with preferential movement of water and contaminants in structured soils.

MATERIAL AND METHODS

The Danubian Lowland is a large (1260 km^2) agriculturally utilised area, with a shallow (0.5–3 m) underlying aquifer. Three different soils from this region were studied. A light soil was sampled in Kalinkovo (loamy-sand soil, Calcaric Fluvisol (WRB, 1998)), a medium heavy soil in Macov (loamy soil, Calcari-Haplic Chernozem (WRB, 1998)), and a heavy soil in Jurova (clay soil, Calcari-Mollic Fluvisol (WRB, 1998)). Basic characteristics of the soils used in this study are presented in Table 1 (Fulajtar et al., 1998). The quality of humus is assessed by the ratio of humic acids to fulvic acids content (HA/FA).

A radioactive tracer technique was used to measure freshwater contaminant relative concentration vs. depth distributions in a soil, with radioactive iodine isotope $^{131}I^-$ as the tracer of non-reactive fertilizer transport, and radioactive cadmium isotope $^{115}Cd^{2+}$ as the tracer of cadmium transport in the studied soils. The probe (Fig 1) consists of a duralumin tube (3) in which a Geiger-Mueller (G-M) detector and analog interface unit (1), connected to the nuclear analyser (2) with coaxial cable, can be placed in any desired position. The tubes (10-mm O.D., 8-mm I.D., and 1500-mm length) are inserted vertically from the soil surface into holes made by a 10-mm-diametre steel rod into the soil below the 1-m^2 square infiltrometer (4). Conical soil sealing (5) made for each vertical probe prevents water from penetrating next to the probe, as was proved by a dye test with Methylene Blue. Owing to its small size (21-mm length and 6.3-mm O.D.) the G-M detector can be considered as a point detector. The bypassing ratio (partition of water and solutes between the macropore domain and the matrix domain) and an impact of land-use change on nutrient fluxes in a structured soil were also measured in this region using radioactive tracer techniques (Alaoui et al., 1997; Lichner, 1997; Lichner et al., 1999).

The conventional (Selim et al., 1992; Cipakova and Mitro, 1997) and modified batch technique (Lichner and Cipakova, 2002) serve to measure the sorption of contaminants on soil particles and to estimate the distribution coefficient K_d. In this paper, the results of Cd sorption and its relation to the duration of Cd-soil interaction are presented. The radioactive cadmium isotope ^{109}Cd was used as a tracer of cadmium behaviour in soil because of its easy and fast detectability. Each sorption experiment involved 10 g of soil (< 2 mm particles), 40 ml of distilled water, and cadmium ^{109}Cd (in the form of $CdCl_2$) with a concentration of 50.9 mg.l^{-1} and specific activity a_0.

Table 1: Particle size distribution, mineral composition of the clay fraction and selected chemical properties of the soils used in this study (Fulajtar et al., 1998).

Soil studied	Kalinkovo	Macov	Jurova
≥ 0.25 mm (%)	6.0	0.9	1.5
0.25–0.05 mm (%)	55.8	36.1	11.4
0.05–0.01 mm (%)	22.5	28.8	27.8
0.01–0.001 mm (%)	10.2	19.9	37.3
≤ 0.001 mm (%)	5.5	14.2	21.9
≤ 0.01 mm (%)	15.7	34.2	59.3
Illite (%)	60–80	60–80	50–70
Chlorite (%)	10–20	10–20	10–20
Smectites (%)	5–10	10–20	10–20
Calcite (%)	2–5	2–5	2–5
Dolomite (%)	1–3	1–3	1–2
Quartz (%)	2–5	1–3	1–3
pH (H_2O)	7.8	8.0	8.6
pH (KCl)	7.4	7.7	7.4
$CaCO_3$ (%)	27	26	16
C_{ox} (%)	0.8	1.4	2.2
Humus (%)	1.4	2.4	3.8
HA/FA	0.6	1.6	1.8

In the conventional batch technique, the soil, water and cadmium were placed into a 100-ml polyethylene bottle and shaken for 5 s. Then a 5-ml sample of eluate was taken 1 min after shaking, centrifuged, and the specific activity a of the ^{109}Cd in aqueous phase was measured with a multichannel gamma spectrometer with Ge/Li detector. The measurements took 10–60 minutes depending on the measured specific activity. The Cd sorption S on all the soil particles, and the distribution coefficient K_d were calculated from the equations:

$$S = (a_0 - a)/\, a_0 \qquad (1)$$

$$K_d = (V/m)\,(a_0 - a)/\, a \qquad (2)$$

The same procedure was chosen for the 2-, 3-, 5-, 10-, 30-, and 60-min durations of Cd-soil interaction.

The modified batch technique is identical to the conventional batch technique, except for centrifuging. Therefore, the ^{109}Cd in aqueous phase and that adsorbed on the soil particles < 10 µm occur in the 5-ml sample of solution taken 1 min after shaking. The specific activity a' was measured for 90 seconds with a multichannel gamma spectrometer with Ge/Li detector. Cadmium sorption S' on the clay particles < 10 µm, which did not settle on the bottom of a polyethylene bottle in one minute after shaking, and the modified distribution coefficient K_d' were calculated as follows:

$$S' = (a' - a)/\, a_0 \qquad (3)$$

$$K_d' = (V/m)\,(a_0 - a')/\,a' \qquad (4)$$

A similar procedure was chosen for the 2-, 3-, 5-, 10-, 30-, and 60-min durations of Cd-soil interaction with one essential difference: 1 min before taking the sample of eluate, the mixture was shaken for 5 s. Time t = 1 min, in which all the particles > 10 µm settle on the bottom of a bottle, was calculated according to Stokes law:

$$v = l/t = 2\,g\,r^2\,(\rho_s - \rho_w)/9\,\eta \qquad (5)$$

where: v – velocity of the soil particle in water, l – path, t – time, g – gravitational acceleration, r – radius of the soil particle, ρ_s – density of the soil-water mixture, ρ_w – density of water, η – dynamic viscosity of water.

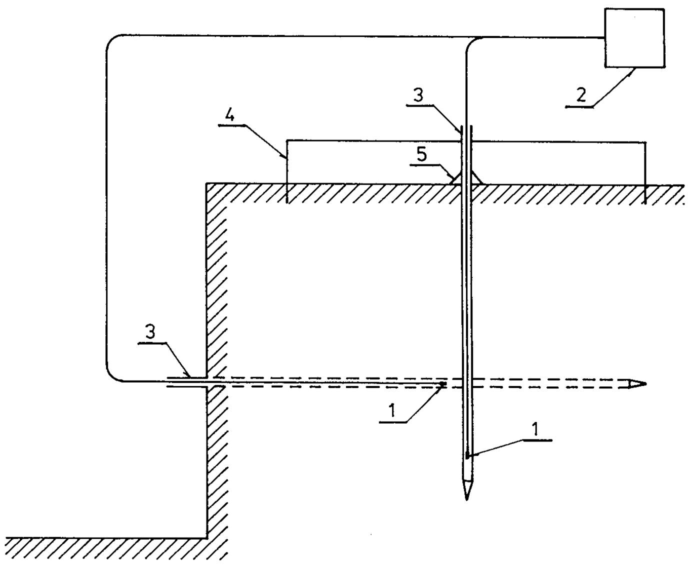

Fig 1: Schematic arrangement for radioactive tracer technique.

The retardation factor R is equal to the ratio between the time that a reactive and a non-reactive solute needs to travel a given distance in the soil. It is related to the distribution coefficient K_d by

$$R = 1 + \rho\,K_d\,/\,\theta \qquad (6)$$

where ρ is soil dry bulk density and θ is volumetric water content.

The retardation factor R can be estimated from the breakthrough curves of the studied reactive and non-reactive solute. The breakthrough curves could be measured in a laboratory on the undisturbed soil column with the System of European Water Monitoring (SEWING) (Filipkowski, 2001). Sensors of this system, based on the ion sensitive field effect transistor (ISFET) or chemically-modified field effect transistor (CHEMFET), are able to simultaneously measure concentrations of 5 selected inorganic ions in the column outflow water.

RESULTS AND DISCUSSION

Using the radioactive tracer technique (Fig 1), a deep Cd penetration up to 60 cm was measured in a loam soil under meadow in the study region. Using the equilibrium distribution coefficient K_d^{eq} and a convective-dispersion equation, it was predicted that all the Cd should remain in the 10-cm thick top layer. In spite of that prediction it was found that more than 40 % of Cd penetrated deeper than expected.

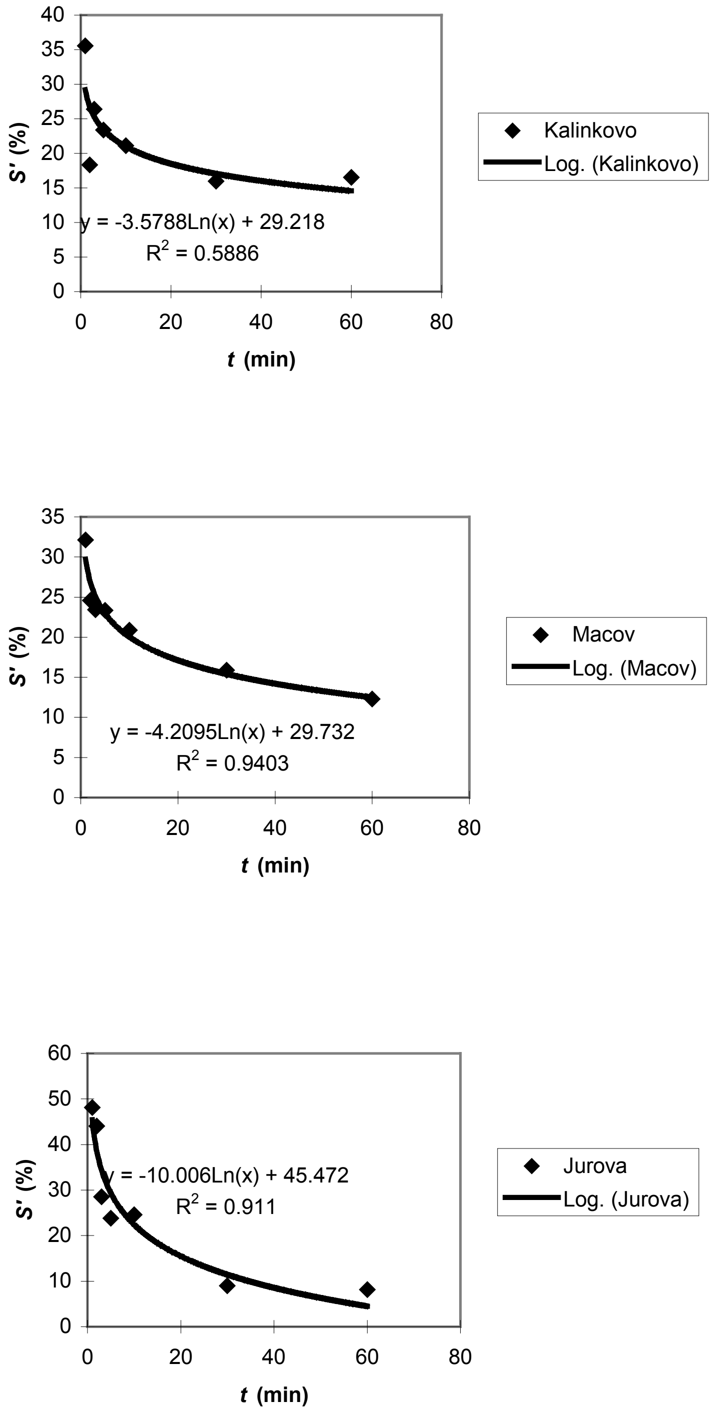

Fig 2: Sorption *S'* of cadmium on the soil particles < 10 μm, which did not settle on the bottom of a bottle in one minute after shaking, vs. duration *t* of the Cd-soil contact (♦ measured value, ▬ fitted curve).

This discrepancy could be explained by the particle-facilitated Cd transport (transport of Cd sorbed on clay particles) via soil macropores (Jacobsen et al., 1997; Laegsmand et al., 1999) which was studied on three various soils. The results of conventional and modified batch techniques show that for the Cd-soil contact lasting 1 min, more than 35 %, 32% and 48% of Cd was adsorbed on the particles < 10 μm of the soil from Kalinkovo, Macov, and Jurova, respectively. It was found that, when the contact time was extended, the percentage of Cd adsorbed on the particles < 10 μm decreased (Fig 2). At Jurova, after the 30-min and 60-min lasting Cd-soil interaction, only 9.0 and 8.2 % respectively of cadmium was adsorbed on the particles < 10 μm. This sediment fraction forms > 59 % of all the particles in the Jurova soil. A similar decrease in reversibly sorbed ^{109}Cd was observed by Almas et al. (2000) for Cd-soil contact lasting from 30 min up to 1 year.

Next, the distribution coefficient K_d for 60-min lasting Cd-soil contact was set equal to the matrix distribution coefficient K_{dm}, and the distribution coefficient K_d' for 1-min lasting Cd-soil contact was set equal to the macropore distribution coefficient K_{dM}. It was found that using the coefficient K_{dm} instead of K_{dM} would underestimate a penetration of the part of Cd transported in the macropores by about 255-times in the loamy-sand soil in Kalinkovo, 20-times in the loam soil in Macov, and 122-times in the clay soil in Jurova. Fasko (Lichner et al., 1999) gave evidence from 10-year-lasting observations that macropore flow can appear 24 times on the average during the vegetation season in south-western Slovakia. This flow can be the cause of rapid Cd transport from the soil surface to a depth well below the root zone.

CONCLUSION

The ease and speed of measurement are the most significant advantages of the radioactive tracer techniques presented. When used on a field soil, the radioactive tracer technique is non-destructive, able to locate heterogeneities in a field soil, and does not influence solute transport. The duration of the measurement of each point in a breakthrough curve or in tracer concentration distribution was only one minute. Installation or removal required about 10 minutes per probe. The time reduction is profitable in studies of spatial variability of transport properties in field soils, where an extensive set of values is required for statistical processing. The dose of radioactive tracer necessary for one measurement is very small and in the case of $^{131}I^-$ it is one sixth of the dose used in thyroid gland therapy (Lichner, 1995). Nevertheless, permission from the national public-health officer and fulfilling strict safety precautions by staff is necessary for the radioactive tracer measurements mentioned.

The SEWING system is intended for the concentration measurement of 5 various ions (in the first variant NO_3, NH_4, Ca, Na, and H) in industrial and municipal waste water, irrigation water, fresh water, groundwater, and surface water (e.g., in the studies on fertilizer washout from hillside fields into rivers or brooks), for solute breakthrough curve measurements in a soil-physical laboratory, for early warnings in rivers near a factory or other contaminant producer, etc.

ACKNOWLEDGEMENT

The financial support from the Slovak Scientific Grant Agency Project 2/7065/20, Slovak-Czech Scientific Co-operation Project KONTAKT no. 185, and 5th EC Framework Programme Project IST-2000-28084 is gratefully acknowledged.

REFERENCES

Alaoui, A. M., Germann, P., Lichner, L., Novak, V. (1997) Preferential transport of water and 131 Iodide in a clay loam assessed with TDR-technique and boundary layer flow theory. *Hydrol. Earth System Sci.*, 1 (4), 813–822.

Almas, A.R., Salbu, B., Singh, B.R. (2000) Changes in partitioning of cadmium-109 and zinc-65 in soil as affected by organic matter addition and temperature. *Soil Sci. Soc. Am. J.*, 64(6), 1951–1958.

Cipakova, A., Mitro, A. (1997) Influence of agrochemical characteristics on ^{85}Sr and ^{137}Cs sorption in soil samples from the localities around nuclear power plants in Slovak Republic. *J. Radioecology*, 5(2), 3–8.

Cislerova, M., Vogel, T., Votrubova, J., Robovska, A. (2002) Searching Below Thresholds: Tracing the Origins of Preferential Flow within Undisturbed Soil Samples. In: Smiles, D. et al. (eds.): *Environmental Mechanics: Water, Mass and Energy Transfer in the Biosphere*. AGU Geophysical Monograph 129, 265–274.

Falkenmark, M., Andersson, L., Castensson, R., Sundblad, K. (1999) Water – a reflection of land use. Swedish Natural Science Research Council, Stockholm, pp. 128.

Filipkowski, A. (2001) System for European Water Monitoring (SEWING). IST-2000-28084. Project Presentation. Brussels, pp. 4.

Fulajtar, E., Barancikova, G., Curlik, J., Sedlakova, B., Surina, B. (1998) An impact of the water work Gabcikovo on agricultural soils. (in Slovak), VUPU, Bratislava, pp. 204.

Jacobsen, O. H., Moldrup, P., Larsen, C., Konnerup, L., Petersen, L. W. (1997) Particle transport in macropores of undisturbed soil columns. *J. Hydrol*., 196, 185–203.

Jury, W. A., Fluhler, H. (1992) Transport of chemicals through soil: mechanisms, models, and field applications. *Adv. Agronomy*, 47, 141–201.

Laegsmand, M., Villholth, K. G., Ullum, M., Jensen, K. H. (1999) Processes of colloid mobilization and transport in macroporous soil monoliths. Geoderma, 93, 33–59.

Lichner, L. (1995) A nuclear tracer technique for investigation of solute transport in the unsaturated zone of soil. In: Leibundgut, Ch. (ed): Proc. Int. Symp. *Tracer technologies for hydrological systems*, Boulder 1995. IAHS Publication No. 229, Wallingford, 109–116.

Lichner, L. (1997) In-situ measurement of bypassing ratio in macroporous soil. *J. Hydrol. Hydromech.*, 45(5), 365–376.

Lichner, L., Cipakova, A. (2002) Cadmium distribution coefficients and Cd transport in structured soils. *Rostlinna Vyroba* (*Plant Production*), 48, 3, 96–100.

Lichner, L., Meszaros, I., Germann, P., Alaoui, A. M., Sir, M., Fasko, P. (1999) Impact of land-use change on nutrient fluxes in structured soils. In: Heathwaite, L. (ed): Proc. Int. Symp. *Impact of land-use change on nutrient loads from diffuse sources*, Birmingham 1999. IAHS Publication No. 257, Wallingford, 171–177.

Selim, H. M., Buchter, B., Hinz, C., Ma, L. (1992) Modeling the transport and retention of cadmium in soils: Multireaction and multicomponent approaches. *Soil Sci. Soc. Am. J*., 56, 4, 1004–1015.

WRB (1998) World reference base for soil resources. *World Soil Resources Reports*, No. 84. FAO, Rome, 88 pp.

DATA ACQUISITION AND PROCESSING IN A SMALL DEBRIS FLOW PRONE CATCHMENT

M. Arattano[1], L. Marchi[2], A.M. Deganutti[2]

[1]*CNR-IRPI, Strada delle Cacce 73, 10135 Torino, Italy ,m.arattano@irpi.to.cnr.it*
[2]*CNR IRPI, Corso Stati Uniti 4, 35127 Padova, Italy, lorenzo.marchi@irpi.pd.cnr.it*

ABSTRACT

The Moscardo Torrent, a small stream of the Eastern Italian Alps, was instrumented for debris flow monitoring starting in 1989. Two raingauges were installed, respectively close to the basin divide and at the centre of the basin. Ultrasonic sensors and a fixed video camera were placed in the mid-fan area. A network of ground vibration detectors was set up about 1 km upstream from the ultrasonic gauging stations; two more ground vibration detectors were placed close to an ultrasonic gauge on the fan. The data collected by this equipment allowed measurement of triggering rainfall, flow stage and ground vibrations caused by debris flows. Other important debris flow variables, i.e. mean front velocity, propagation velocity of the debris flow wave along the channel, peak discharge and flowing volume were estimated from instrumental records. Video pictures have proved to be very useful for the visual interpretation of the behaviour of debris flow waves and have made possible the estimation of debris flow surface velocity.

Keywords debris flow, triggering rainfall, hydrograph

INTRODUCTION

The aim of this paper is to describe the field research carried out in the Moscardo Torrent, a debris flow prone basin in the Eastern Italian Alps. Important and well-known monitoring activities on debris flows have been carried out in several geographical regions of the world (Okuda et al., 1980; Watanabe and Ikeya, 1981; Pierson, 1986; Zhang, 1993; Suwa et al., 1993; Marcial et al., 1996). In alpine basins, the relatively low frequency of debris flows makes monitoring activities, carried out by instruments permanently installed in the field, very difficult and expensive. These activities become worthwhile only if enough data can be recorded in a sufficiently short period of time. The Moscardo Torrent appeared to be suitable for the installation of a debris flow monitoring system because it displayed, in particular, a very high frequency of debris flow occurrences in addition to several other favourable characteristics. The Moscardo Torrent was first instrumented for debris flow monitoring in 1989. At that time the Moscardo Torrent represented a pioneering site for debris flow monitoring by permanent equipment in Europe. Recently, more alpine basins have been instrumented for debris flow measurement (Genevois et al., 2000; Rickenmann et al., 2001).

GEOLOGICAL AND MORPHOLOGICAL CHARACTERISTICS OF THE CATCHMENT

The Moscardo Torrent is a small creek, with an area of about 4 km^2, located in the Eastern Italian Alps (Fig 1). The bedrock of the Moscardo basin is made of Carboniferous flysch, consisting of shale, slates, siltstone, sandstone and breccia that continuously outcrop in the upper portion of the basin and locally along the torrent. The poor mechanical properties of the rocks, the instability caused by the presence of a deep seated gravitational slope deformation and the steepness of the upper basin slopes facilitate frequent widespread falls and toppling of rocks. The very large quantity of debris that reaches the drainage network by gravitational and erosion processes and by snow avalanches explains the strong tendency of the Moscardo Torrent to generate debris flows and hyperconcentrated flows. The debris flows of the Moscardo Torrent led to the construction of a huge fan that progressively invaded the receiving valley bottom, forcing the stream to flow on the opposite side of the valley. The main morphological parameters of the basin closed at the fan apex are listed in Table 1; the length of the channel reach on the fan is about 1000 m (Arattano et al., 1997).

The Moscardo debris flows are composed by material with a wide range of dimensions. Lateral levees and debris flow lobes are mostly formed by small and medium boulders; larger boulders of over two meters are also common. Grain size analyses have been carried out on several matrix samples (Arattano et al., 1997; Moscariello and Deganutti, 2000) from old and fresh deposits. The high percentage of fine particles in the matrix (from 13% to 35% less than 40 μm) underlines the muddy character of the Moscardo debris flows.

Table 1: Main morphometric parameters of the Moscardo basin.

Basin area [km^2]	Maximum elevation [m]	Minimum elevation [m]	Average Basin slope [%]	Channel length [km]	Average channel slope [%]
4.1	2043	890	63	2.76	37

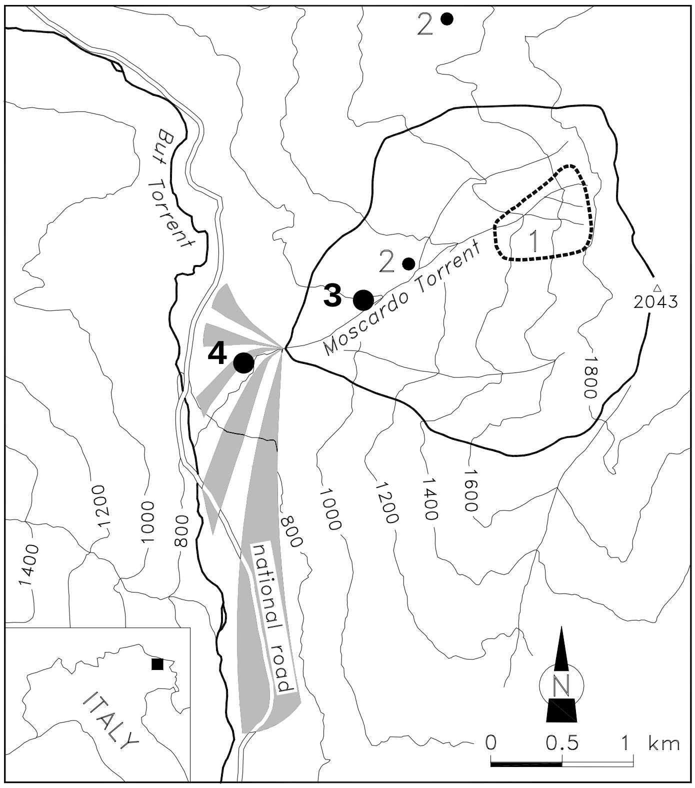

Fig 1: The Moscardo Torrent basin and its alluvial fan. 1: debris flow initiation site; 2: raingauges; 3 and 4: instrumented channel stretches.

The Moscardo debris flow material has been studied also from the rheological point of view, using a large amount of material sampled from a fresh deposit left by a debris flow which occurred on 5 July 1995. Several suspensions, obtained by mixing the material with water, were analysed for a range of different solid concentrations using two parallel plate rheometers and a tilting plane. The material showed a shear thinning viscous behaviour which can be well represented by a Herschel-Bulkley model (Coussot et al., 1998).

MONITORING SYSTEM AND RECORDED DATA

The first installations in 1989 consisted of two ultrasonic sensors, placed on the fan at a distance of about 300 m. A raingauge was installed in the upper portion of the basin. In 1995 the ultrasonic sensors were replaced by new detectors and a third ultrasonic sensor was added 150 m upstream. A fixed video camera was positioned close to the intermediate of the three ultrasonic sensors and a network of four ground vibration detectors was set up about 1 km upstream from the ultrasonic gauging stations. In 1997 a second raingauge was installed in the centre of the basin and two ground vibration detectors were set up close to the intermediate ultrasonic gauge on the fan. From 1990 to 1998, 15 debris flows occurred, 14 of which were recorded by the installed gauges. Several types of measurements have been carried out on the recorded debris flows during the years, including mean front velocity, surface velocity, volume, flow stage, hydrograph deformation, triggering rainfalls, etc.

The instrumentation installed in the Moscardo Torrent basin (raingauges and sensors which detect debris flow passage) gives the possibility of analysing the relations between rainfall characteristics and debris flow occurrence more precisely than usually possible in alpine basins. Rainfalls recorded in the Moscardo Torrent from 1990 to 1998 were analysed and storm characteristics of two classes, i.e. debris flow triggering storms (15 cases) and storms which did not trigger debris flows (58 cases) were compared (Deganutti et al., 2000). Several storm variables were taken into account, including total storm rainfall, average intensity, maximum 60-minute intensity, and antecedent precipitation. A statistical analysis showed that only total storm rainfall and maximum 60-minute intensity were significantly different between debris flow triggering storms and storms that did not trigger debris flows. The analysis of rainfall has shown that rainstorm characteristics and antecedent precipitation play an important role but are not sufficient to define debris flow initiation conditions (Deganutti et al., 2000). A critical combination of sediment availability and hydrologic conditions is necessary to cause debris flow formation. This is particularly true when sediment moisture is influenced by a complex groundwater flow regime and sediment availability depends on bank and slope failures, as well as on the previous occurrence of debris flows, as it occurs in the Moscardo basin.

The ultrasonic sensors measure the torrent stage, making it possible to record the debris flow hydrographs. A logging interval of 60 seconds was initially set between two consecutive recordings of the sensors. The logging interval was then reduced to 10 seconds in 1990, to grant a better accuracy of the data and further reduced to 1 second in 1995, thanks to the updating and improvement of the recording system. A time lag of 1 second between two consecutive recordings of the sensors allows a careful detection of the passage of the debris flow wave below the sensors (Fig 2).

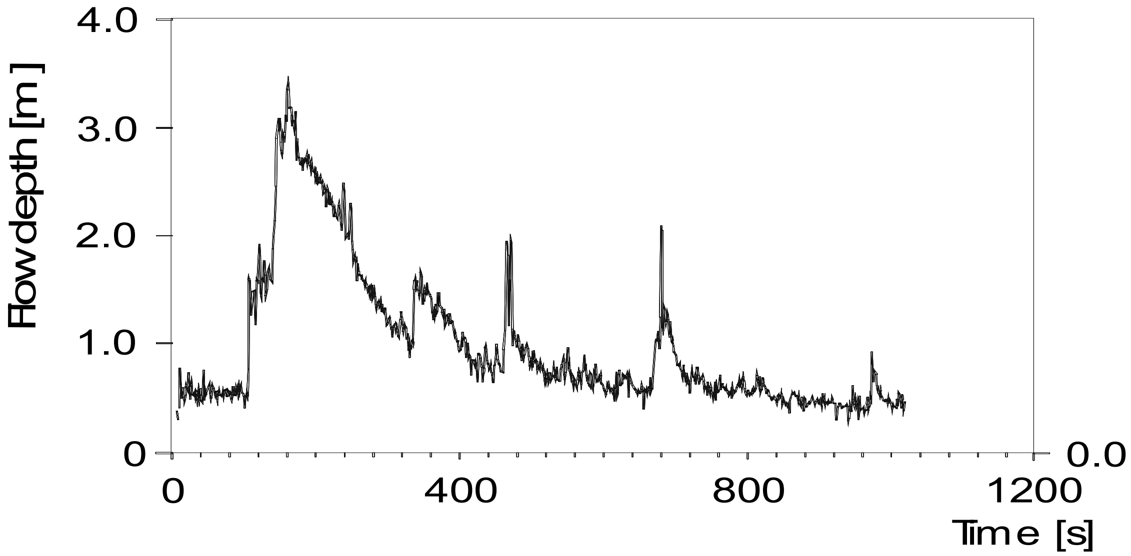

Fig 2: Hydrographs of a debris flow recorded by ultrasonic gauges (event recorded on 22 June 1996).

The mean propagation velocity of the front can be calculated in the monitored reach as the ratio of the distance between the sensors to the time interval between the appearance of the peak of the debris flow surge in the two recorded hydrographs. The calculated velocity data are shown in Table 2.

The analysis of the hydrographs recorded by the ultrasonic sensors may show the aggradation or degradation of the channel bed at the recording sites. Flow stage measurements and topographic surveys of the monitored sections make it possible to estimate peak discharges and total volume of debris flows (Arattano et al., 1997, Marchi et al., 2002). Debris flow volumes *Vol* have been estimated as:

$$Vol = \int_{t_0}^{t_f} vA(t)\,dt = v\int_{t_0}^{t_f} A(t)\,dt \qquad (1)$$

where v is the mean velocity of the flow, which was assumed constant for the entire debris flow wave and equal to the mean front velocity, $A(t)$ is the cross section area occupied by the flow at the time t, known from topographic surveys and the ultrasonic data, t_0 is the time of arrival of the surge at the gauging site and t_f is the time at the end of the debris flow wave. Mean velocity of the main front was used for volume computation because it is the only velocity datum available for all recorded events: additional information on velocity variations during the debris flow wave has been obtained only for two events. This approach to the computation of the discharged volume assumes that the material flows through the considered section at a constant velocity during the surge. Thus computed debris flow volumes should be regarded as approximate estimates (Table 2).

Table 2: Velocity, discharge and volume calculated from ultrasonic sensor measurements.

Event date	Mean front velocity (m s^{-1})	Peak discharge (m^3s^{-1})	Discharged volume (m^3)	Event date	Mean front velocity (m s^{-1})	Peak discharge (m^3s^{-1})	Discharged volume (m^3)
17.08.1990	1.0	-	-	20.07.1993	4.3	16	6500
13.08.1991	5.0	88	19000	14.09.1993	2.5	10	3800
30.09.1991	1.9	24	3250	18.07.1994	4.0	-	-
01.09.1992 a	2.5	46	5800	22.06.1996	3.5	140	16130
01.09.1992 b	10.0	-	-	08.07.1996	4.0	195	57800
11.07.1993	3.0	14	5600	27.06.1997	2.9	25	3000
19.07.1993	0.9	3	730				

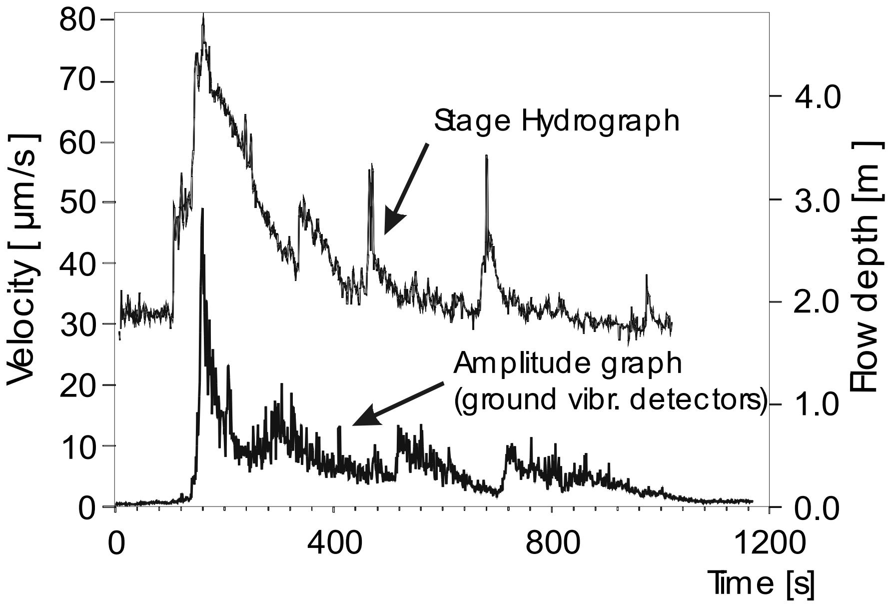

Fig 3: Amplitude graph for the 22 June 1996 debris flow as derived from the ground vibration recordings. The stage hydrograph recorded at the ultrasonic gages is shown for comparison.

The ground vibration detectors (seismometers and geophones) record ground vibrations induced by the passage of a debris flow. The purpose of the seismic sensors installation, in the initial phase of the research, was essentially to verify which information could be obtained through this type of device during a debris flow event. However, the first results that have been obtained showed the possibility of using these detectors also as tools for velocity measurements (Arattano and Moia, 1999). The debris flow passage generates ground vibrations whose amplitude graph corresponds to the stage hydrograph (Fig 3). The ground vibrations peak is detectable by a seismic sensor placed at a safe distance of some tens of meters from the channel bed. The mean front velocity can then be measured by placing a pair of these detectors at a known distance along the torrent adopting the same procedure previously described for velocity measurement with ultrasonic sensors.

A fixed video camera like that installed in 1995 on the alluvial fan of the Moscardo Torrent allows a visual interpretation of the debris flow features. The video camera records slantwise a straight channel reach about 80 meters long and is triggered by the upstream ultrasonic sensor by means of a triggering software that identifies abrupt increases of the stage in the torrent and starts the video recordings. The possibility was also investigated of using the video recordings for estimating debris flow surface velocity. A simple method to process the recorded images was developed that maps 2D image points on the screen and points in the 3D space (Arattano and Marchi, 2000). The average velocity of the features floating on the surface was then computed as the ratio of their travelled distance to the time elapsed between the shooting of the video frames that contained them (Fig 4). Average debris flow velocities estimated through image processing were consistent with measurements based on the recordings of the ultrasonic gauges; velocity variations in debris flow waves are discussed in Arattano and Marchi (2000).

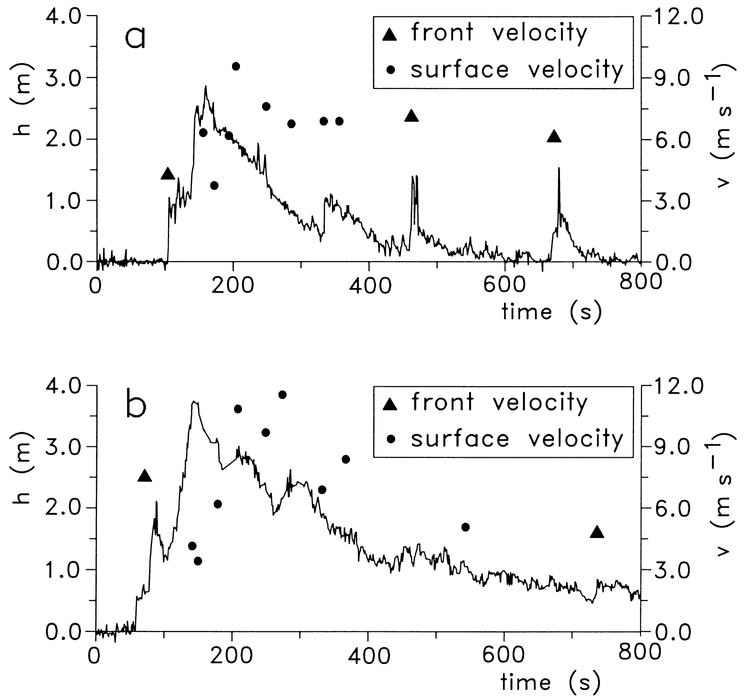

Fig 4: Plot of the surface velocity values v (dots) and mean front velocity of precursory and secondary surges (triangles) that have been measured with the corresponding flow depth h measured by the ultrasonic sensor no. 1 (Fig 1). a) 22 June 1996; b) 8 July 1996.

CONCLUDING REMARKS

Field monitoring of debris flows gives an important contribution to an improved knowledge of these hazardous flow processes. Debris flow research in the Moscardo Torrent pioneered studies on debris flow monitoring in Europe. Data regarding flow depth, velocity, peak discharge and volumes, recorded in the Moscardo Torrent since 1990, have contributed to broaden the database on debris flow characteristics collected worldwide. Even though debris flow monitoring in the Moscardo Torrent was intended for research purposes, the results can provide suitable indications also for the design of debris flow warning systems.

ACKNOWLEDGMENTS

The research activities in the Moscardo Torrent were carried out in the context of the Research Projects «Debris flow risk» (Contract No. ENV4 CT96 0253) and «THARMIT» (Contract No. EVG1-CT-1999-00012) funded by the European Union; partial funding derived from the National Research Council of Italy - Special Project GNDCI, U.O. 1.29. The authors wish to thank the Forest Department of Friuli - Venezia Giulia Region (Dr. S. Sanna and Dr. P. Stefanelli) for the collaboration in installing and managing field instrumentation.

REFERENCES

Arattano, M., Deganutti, A.M., Marchi, L. (1997) Debris flow monitoring activities in an instrumented watershed of the Italian Alps. In: *Chen, C. (Ed.), Proceedings, First International Conference on Debris-flow Hazard Mitigation: Mechanics, Prediction, and Assessment*. Water Resources Engineering Division / ASCE, New York, 506-515.

Arattano, M., Moia, F. (1999) Monitoring the propagation of a debris flow along a torrent. *Hydrological Sciences Journal*, 44, 5, 811-823.

Arattano, M., Marchi, L. (2000) Video-derived velocity distribution along a debris flow surge. *Physics and Chemistry of the Earth Part B*, 25, 8, 781-784.

Coussot, Ph., Laigle, D., Arattano, M., Deganutti, A.M., Marchi, L. (1998) Direct determination of rheological characteristics of debris flow. *Journal of Hydraulic Engineering ASCE*, 124, 8, 865-868.

Deganutti, A.M., Marchi, L., Arattano, M., (2000) Rainfall and debris flow occurrence in the Moscardo basin (Italian Alps). In: Wieczorek, G., Naeser, N. (Eds.), Proc. *Second International Conference on Debris-flow Hazard Mitigation: Mechanics, Prediction, and Assessment*. A.A. Balkema, Rotterdam, 67-72.

Genevois, R., Tecca, P.R., Berti, M., Simoni, A. (2000) Debris flow in the Dolomites: experimental data from a monitoring system. In: Wieczorek, G., Naeser, N. (Eds.), Proc. *Second International Conference on Debris-flow Hazard Mitigation: Mechanics, Prediction, and Assessment*. A.A. Balkema, Rotterdam, 283-291.

Marchi, L., Arattano, M., Deganutti, A.M. (2002) Ten years of debris-flow monitoring in the Moscardo Torrents (Italian Alps). *Geomorphology*, 46, 1/2, 1-17.

Marcial, S., Melosantos, A.A., Hadley, K.C., LaHusen, R.G. (1996) Instrumental lahar monitoring at Mount Pinatubo, 1996. In: Newhall, C.G., Punongbayan, R.S., (Eds.), *Fire and mud: eruptions and lahars of Mount Pinatubo, Philippines*. Philippine Institute of Volcanology and Seismology, Quezon City, Philippines, 1015-1022.

Moscariello, A., Deganutti, A.M. (2000) Sedimentary and hydrologic processes of a debris-flow dominated alluvial fan - Moscardo Fan, Italy. In: Wieczorek, G., Naeser, N. (Eds.), Proc. *Second International Conference on Debris-flow Hazard Mitigation: Mechanics, Prediction, and Assessment*. A.A. Balkema, Rotterdam, 301-310.

Okuda, S., Suwa, H., Okunishi, K., Yokoyama, K., Nakano, M. (1980) Observations on the motion of a debris flow and its geomorphological effects. *Z. Geomorph. N.F.*, Suppl. Bd. 35, 142-163.

Pierson, T.C. (1986) Flow behavior of channelized debris flows, Mount St. Helens, Washington. In: Abrahms, A.D., (Ed.), *Hillslope Processes*. Allen and Unwin, Boston, 269-296.

Rickenmann, D., Hurlimann, M., Graf, C., Näf, D., Weber, D. (2001) Murgang-Beobachtungsstationen in der Schweiz. *Wasser, Energie, Luft - Eau, Energie, Air*, 93, 1/2, 1 – 8.

Suwa, H., Okunishi, K., Sakai, M. (1993) Motion, debris size and scale of debris flows in a valley on Mount Yakedake, Japan. In: Hadley, R.F., Mizuyama, T. (Eds.), *Sediment Problems: Strategies for Monitoring, Prediction and Control*. IAHS Publ. no. 217, 239-248.

Watanabe, M., Ikeya, H. (1981) Investigation and analysis of volcanic mud flows on Mt. Sakurajima, Japan. In: *Erosion and Sediment Transport Measurement*. IAHS Publ. no. 133, 245-256.

Zhang, S. (1993) A comprehensive approach to the observation and prevention of debris flows in China. Natural Hazards 7, 1, 1-23.

AN INTEGRATED APPROACH TO WATER EROSION, SEDIMENT TRANSPORT AND RESERVOIR SEDIMENTATION

W. Saenyi, H. Holzmann

Institute of Water Management, Hydrology and Hydraulic Engineering, University of Agricultural Sciences (BOKU), Muthgasse 18, Vienna, Austria.

ABSTRACT

The Water Erosion Prediction Project (WEPP) model has been applied to the Masinga catchment in Kenya for the estimation of soil loss due to surface runoff resulting from intense tropical rainfall. The WEPP model is a distributed parameter continuous simulation model for predicting daily soil loss and deposition due to rainfall, snowmelt and irrigation. Most computer models for the simulation and prediction of sediment transport in rivers and reservoirs are one-dimensional. Although truly two- or three-dimensional models are available, they require extensive field data for calibration and may be difficult to apply. A semi-two-dimensional model for water and sediment routing, GSTARS 2.1, may be an alternative for solving river engineering problems. This paper provides a brief description of the systematic and integrated approach based on well established sediment transport equations and the Bureau of Reclamation's Generalized Stream Tube model for Alluvial River Simulation (GSTARS 2.1) and its applications. Examples of computed results are presented to illustrate the applicability of different components of this approach.

Keywords water erosion, sediment transport, modelling

INTRODUCTION

As a result of runoff from rainfall, soil particles on the surface of a watershed can be eroded and transported through the processes of sheet, rill and gully erosion. Once eroded, sediment particles are transported through a river system and are eventually deposited in a reservoir, lake or at sea. Therefore, an erosion model capable of predicting surface erosion and routing sediment through a channel system is desirable. Engineering techniques used for the determination of reservoir sedimentation processes rely mainly on field surveys. Field surveys can be used for the determination of what has happened but not for predictive purposes.

During the 1997 Congress of the International Commission on Large Dams (ICOLD), the Sedimentation Committee passed a resolution encouraging all member countries to (a) develop and apply methods for the prediction of the rate of surface erosion based on rainfall and soil properties, and (b) develop and apply computer models for the simulation and prediction of reservoir sedimentation processes. This paper provides a brief description of an ongoing study in compliance with the above two ICOLD resolutions. Preliminary results will be presented to demonstrate the feasibility of a systematic and rational approach for the determination of surface erosion rates and sediment transport in rivers. In addition, the application of a reservoir sedimentation model is presented.

WATER EROSION AND SEDIMENT ROUTING THROUGH CHANNELS

Soil erosion and sediment yield modelling

The Water Erosion Prediction Project (WEPP) model current version (v2001.3) was released in April 2001 (Flanagan et al., 2001). The model represents erosion prediction technology based on fundamentals of infiltration theory, hydrology, soil physics, plant science, hydraulics, and erosion mechanics. The model provides several major advantages over existing erosion prediction technology: (a) its capabilities for estimating spatial and temporal distributions of soil loss - the net soil loss for an entire hillslope or for each point on a slope profile can be estimated on daily, monthly, or average annual basis; and (b) since the model is process-based, it can be applied on a broad range of conditions that may not be practical or economical when field tests are used.

The model can be used in both hillslope and watershed applications. Runoff characteristics, soil loss and deposition are first calculated on each hillslope with the hillslope component of WEPP for the entire simulation period. Main results are saved in a pass file that is used during the watershed routing. Then the model combines simulation results from each hillslope and performs runoff and sediment routing through the channels and impoundments each time runoff is produced on one of the hillslopes or channels, or if there is an outflow from one of the impoundments. In this study, no impoundments are considered.

The first step in the application of WEPP on the Masinga catchment (7,335 km^2) for sediment yield prediction was to sub-divide it into subcatchments using the available topographic map. Each subcatchment was further subdivided into representative hillslopes. A total of 31 representative hillslopes were identified (Fig 1). Eight of the 31 hillslopes drain into the Thika arm of the Masinga reservoir while the remaining 23 drain into the Tana arm (Fig 4a).

WEPP can give an output of over 100 variables. In this paper only a few were selected for presentation (Saenyi, 2002). These included daily values of sediment yield, runoff, evapotranspiration and total soil water. Sediment yield from the WEPP watershed simulation was correlated to discharge by the least squares method to obtain the sediment discharge rating curves used in GSTARS 2.1 as:

Thika arm: $Q_s = 0.89Q^{1.707}$, r = 0.85 n = 107 (1)

Tana arm: $Q_s = 0.52Q^{0.887}$, r = 0.79 n = 153 (2)

where Q_s = sediment discharge (metric tonne/day), Q = water discharge (m^3/s) r = correlation coefficient, n = number of data points.

Sediment transport in river channels

Since there is a high concentration of wash load in the flow entering the Masinga reservoir (Bobotti, 1998), its effect on sediment fall velocity, flow viscosity, and relative specific weight of sediment is significant. Hence, a modified sediment transport function for sediment-laden flow with high concentration of wash load (Yang et al., 1996) was used for sediment transport computations in the river channels.

RESERVOIR SEDIMENTATION SIMULATION USING GSTARS 2.1 MODEL

The generalized Stream Tube model for Alluvial River Simulation (GSTARS) was first released by the US Bureau of Reclamation in 1986 (Molinas and Yang, 1986) for CYBER mainframe computer application. A revised and enhanced model GSTARS version 2.0 (GSTARS 2.0) was released by Yang et al. (1998). The most recent version, GSTARS 2.1, was released by Yang and Simoes (2000).

With proper selection of a sediment transport function, GSTARS 2.1 can be applied to a wide range of sediment conditions with particle sizes ranging from clay, silt, sand, to gravel. GSTARS 2.1 also has the ability to consider the effects of wash load on the sediment transport rate by using the modified unit stream power formula proposed by Yang et al. (1996). An earlier version, GSTARS 2.0, was applied to the Willow Creek emergency spillway to demonstrate its capabilities in predicting the sediment transport and channel forming processes downstream (Yang et al., 1998). In this study, Yang's (1973) and (1979) formulae were used. It was shown that both channel width and depth can change during the channel forming process (Yang et al., 1998).

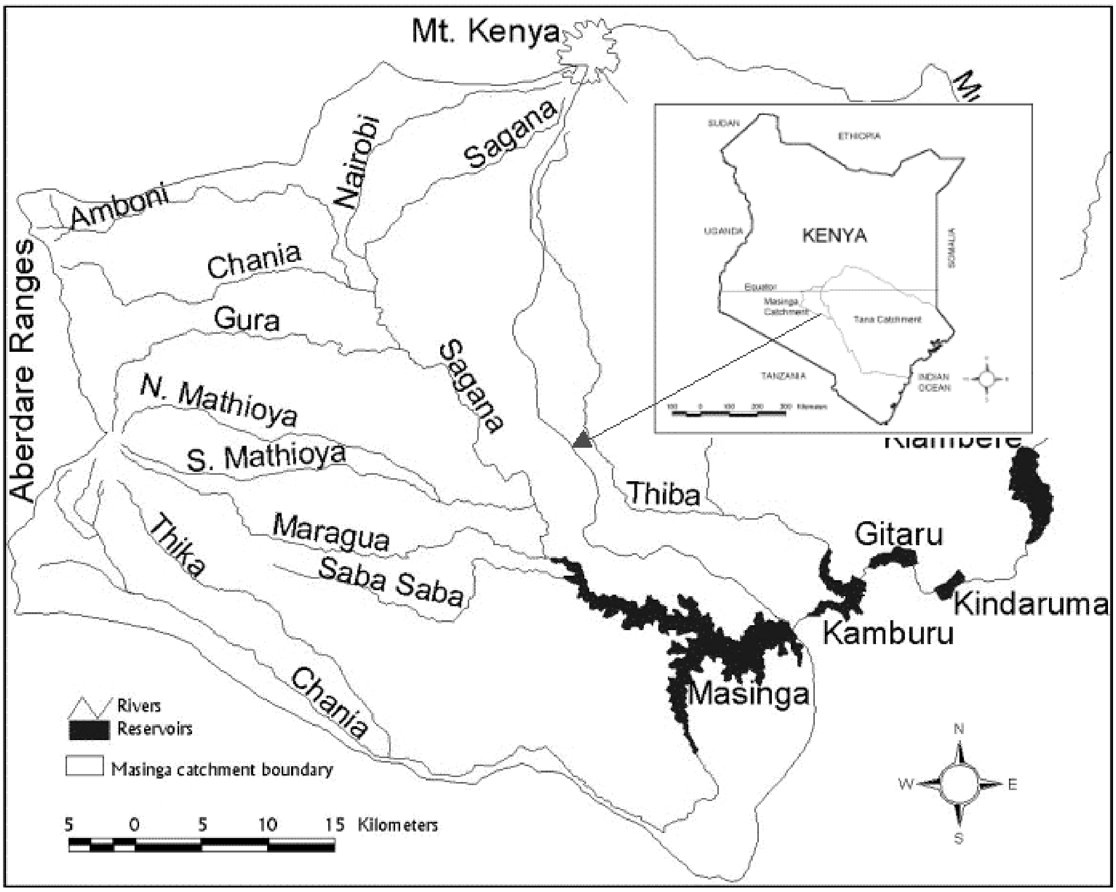

Fig 1: Location of the Masinga catchment and reservoir.

CALIBRATION PROCESS AND DIFFICULTIES ENCOUNTERED

The first step in the application of GSTARS 2.1 to the Masinga reservoir was to calibrate the model. The following parameters were adjusted to fit the simulated cross-sections to the measured cross-sectional data:

- shear threshold for deposition of clay and silt (STDEP), used to determine the initial condition for deposition,
- shear threshold for particle erosion of clay and silt (STMERO),
- slope of the erosion rate curve for mass erosion (ERMASS),
- size gradation distribution of the incoming sediment.

To calibrate GSTARS 2.1, first the size gradation distribution of incoming sediment was varied and predicted reservoir cross-sections were obtained. The predicted cross-sections and thalweg were then compared with measured ones to establish whether the two sets matched. The reason for varying the size gradation distribution of incoming sediment was to distribute sediment deposits longitudinally in such a way that predicted and measured cross-sections and thalweg approximately matched. Normally, the bed load and the coarser fraction of the suspended load are deposited at the mouth of the reservoir, while fine sediments with lower settling velocities are transported and deposited deeper into the reservoir or near the dam wall.

Some problems were encountered while calibrating the model. It was difficult to adjust the model parameters so that the simulated and observed cross-sections matched for all the stations. For instance, there was a bigger deviation between the measured and observed cross-sections for the sections around the confluence. This could be attributed to the formation of eddy and/or secondary currents at the confluence of the two arms (Thika and Tana). Since GSTARS 2.1 is based on a stream tube concept, the presence of secondary and eddy currents may cause the model to fail. It was also found that there was a big deviation between simulated and observed data for cross-sections near the dam wall. This could be attributed to backwater flow and the formation of eddy currents. Otherwise, for other cross-sections, the observed and simulated bed elevation changes were in good agreement.

GSTARS 2.1 SIMULATED RESULTS

Figs 2a, 2b, and 3 demonstrate GSTARS 2.1 capabilities in computing the transverse and longitudinal bed profile of a reservoir due to sedimentation. Yang's (1996) modified formula was employed in the Masinga reservoir sedimentation study because of the presence of a high concentration of wash load in the flow. Since most of the sediments entering the Masinga reservoir are fine grained silt and clay, the cohesive sediment part of GSTARS 2.1 was used in conjunction with the non-equilibrium sediment transport option. The processing and visualization of GSTARS 2.1 results were performed using a two-dimensional BOSS SMS model (1996) to yield the sediment distribution in the reservoir (Figs 4b,c). Changes from Fig 4b to Fig 4c show that the model is capable of simulating the sedimentation process in the reservoir. From the figures, it can be seen that the reservoir bathymetry has been altered drastically due to siltation.

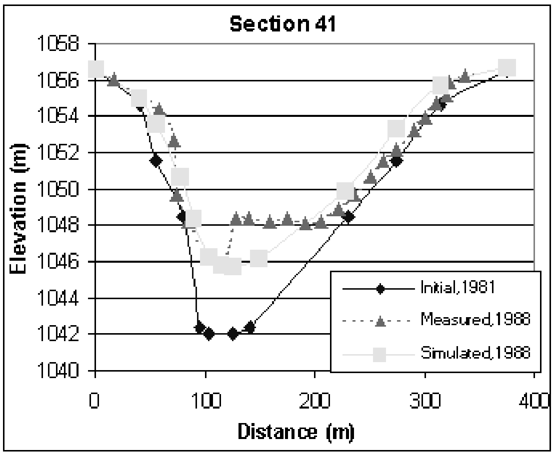

Fig 2a: Predicted channel development compared with a measured cross-section in 1988, for a station 10 km upstream of Masinga dam.

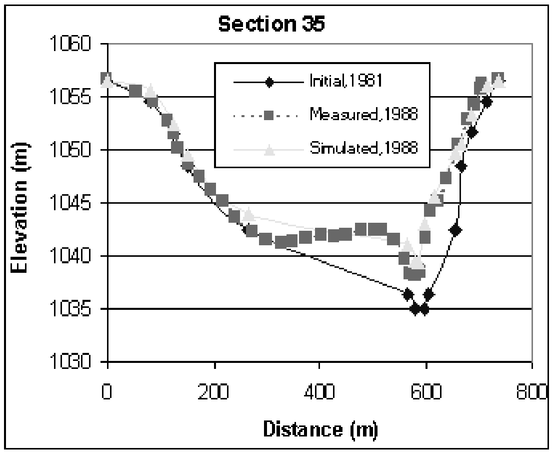

Fig 2b: Predicted channel development compared with a measured cross-section in 1988, for a station 5 km upstream of Masinga dam.

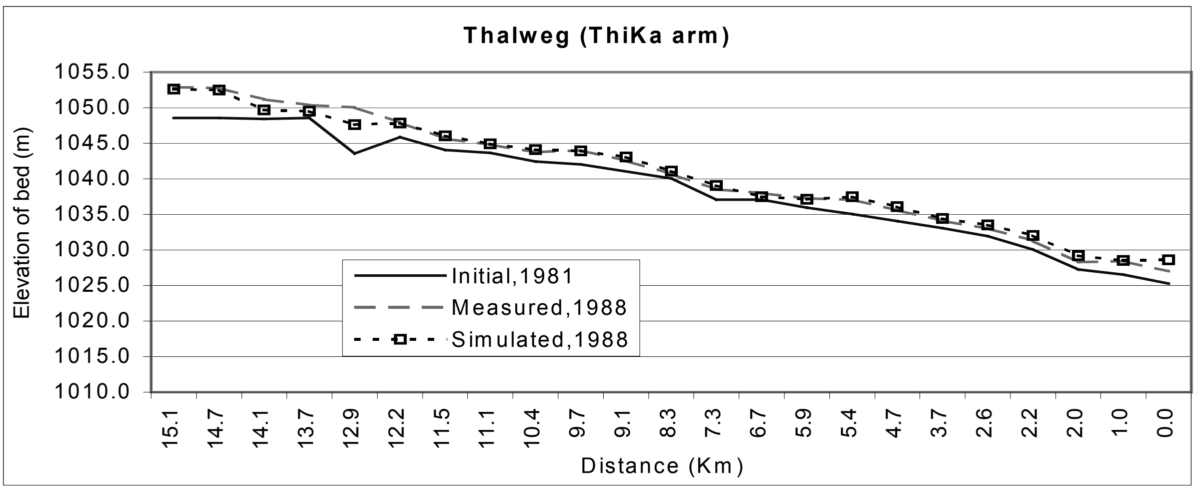

Fig 3: Thalweg from the mouth of the reservoir to station 29.9 km upstream of Masinga dam.

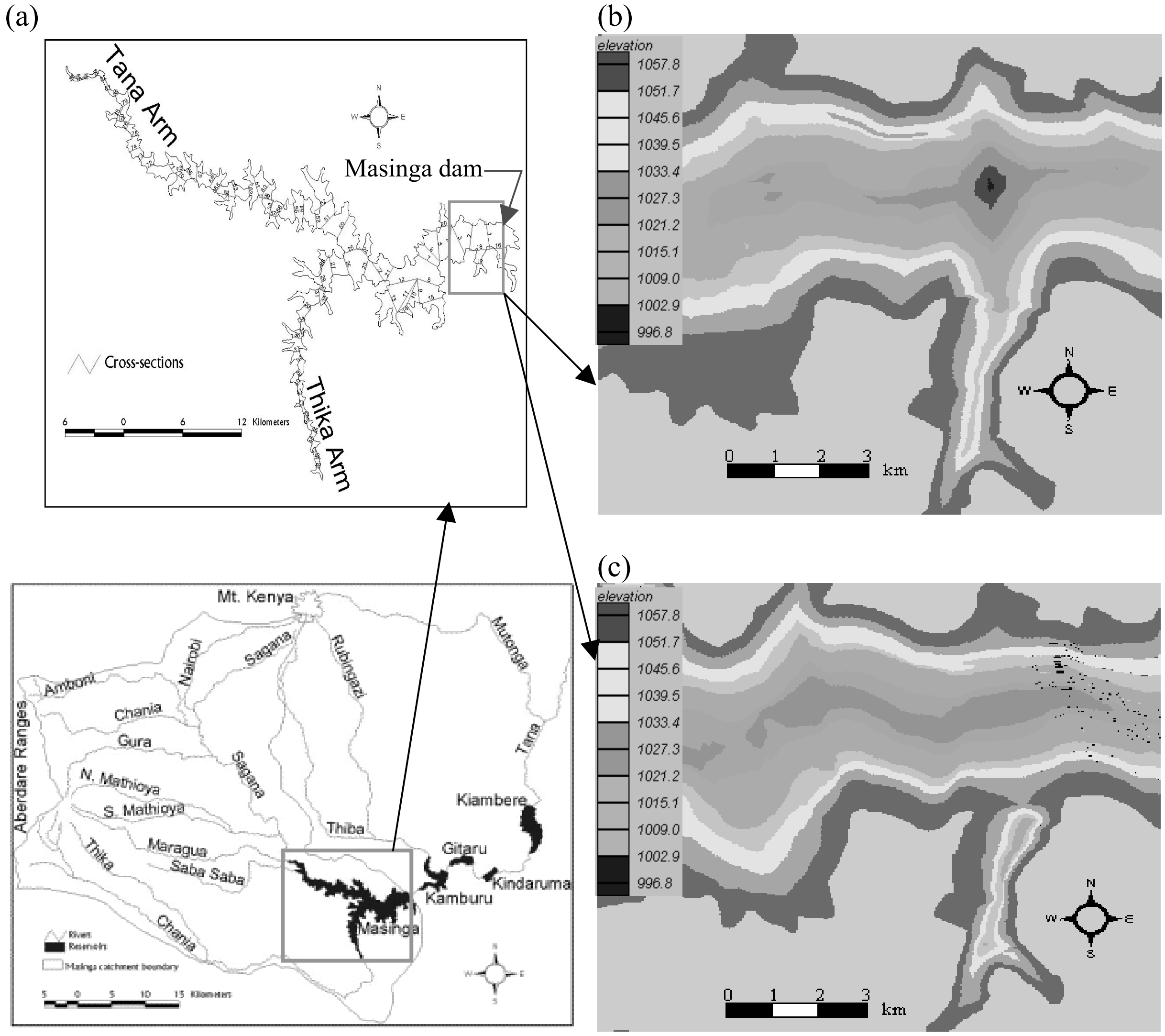

Fig 4: (a) Masinga reservoir showing the location of cross-sections. (b) Initial bathymetry of the reservoir in 1981. (c) Bathymetry of the reservoir in 1988.

SUMMARY AND CONCLUSION

The results from WEPP watershed simulations were used to derive sediment rating curves for both Tana and Thika subcatchments. These curves were then used as input into the sedimentation model for describing suspended load inflow as a function of water discharge. The focus of the sedimentation modelling was to see how the reservoir bed elevations change after 20 years of reservoir operation. From the plotted cross sections, it was found that most deposition occurred along the thalweg with deposition depths typically in the range of 1.5 m to 3 m. Most of the sediment delivered to the reservoir was deposited along the main channel and a smaller fraction on the reservoir terraces. The model predicted highest sedimentation at the mouth of the reservoir, at the confluence of the two arms (Tana and Thika), and near the dam wall.

ACKNOWLEDGEMENTS

This ongoing study is partly supported by Austrian Academic Exchange Service (ÖAD), and the Institute of Water management, Hydrology and Hydraulic Engineering of the University of Agricultural Sciences, BOKU, Vienna.

REFERENCES

Bobotti, O.K. (1998) Masinga Reservoir Capacity and Sedimentation, Kenya. A World Bank Project; Tana and Athi Rivers Development Authority, TARDA Report, Vol. 2: Data Annexes.

BOSS SMS model (1996) BOSS SMS Computer program user's manual version 4.3. Engineering Computer Laboratory, Brigham Young University.

Flanagan, D.C., Laflen, J.M., Lane, L.G., Nearing, M.A. (2001) Water Erosion Prediction Project (WEPP) Computer Program (version 2001.3) for Windows. USDA-Water erosion prediction project: *Hillslope profile and watershed model documentation*. NSERL Report No. 10, National Soil Erosion Research Laboratory, USDA-ARS-MWA, West Lafayette, Indiana.

Molinas, A., Yang, C.T. (1986) Computer program users manual for GSTARS. Technical report, U.S. Department of Interior Bureau of Reclamation Engineering and Research Centre, Denver, Colo.

Saenyi, W.W. (2002) Sediment Management in Masinga Reservoir, Kenya. A Ph.D thesis submitted to the University of Agricultural Sciences, BOKU; Institute of Water Management, Hydrology and Hydraulic Engineering Vienna, Austria.

Yang, C.T. (1973) Incipient motion and sediment transport. *J. of the Hydr. Div. ASCE*, 99(HY10).

Yang, C.T. (1979) Unit stream power equations for total load. *J. of Hydrology*, 40.

Yang, C.T. (1984) Unit stream power equation for gravel. *J. of the Hydr. Div. ASCE,* 110(HY12).

Yang, C.T. (1996) Sediment transport: theory and practice. McGraw-Hill Companies, Inc., New York, NY.

Yang, C.T., Molinas, A., and Wu, B. (1996) Sediment transport in the Yellow River. *J. of Hydr. Engineering, ASCE*, 122, 5.

Yang, C.T, Randle, T.J., Hsu, S.K. (1998) Surface erosion, sediment transport, and reservoir sedimentation. In Summer, W., Klaghofer, E., and Zhang, W., editors, IAHS Publication no. 249. 3-12.

Yang, C.T., Trevino, M.A., Simoes, F.J.M. (1998) User's manual for GSTARS 2.0 (Generalized Stream Tube model for Alluvial River Simulation version 2.0). U.S. Bureau of Reclamation, Technical Service Center, Denver, Cororado.

Yang, C.T., Simoes, F.J.M. (2000) User's manual for GSTARS 2.1 (Generalized Stream Tube model for Alluvial River Simulation version 2.1). U.S. Bureau of Reclamation, Technical Service Center, Denver, Cororado.

LONG-TERM WATER BALANCE OF THE EXPERIMENTAL AGRICULTURAL MICROBASIN RYBÁRIK

Pavol Miklánek, Alojz Koníček, Pavla Pekárová

Institute of Hydrology, Slovak Academy of Sciences, Bratislava, Slovakia

ABSTRACT

The paper presents the analysis of the annual and monthly long-term water balance elements in the experimental agricultural microbasin Rybárik of the IH SAS. The analysis is based on the data series of water years 1964/1965-2000/2001. The mathematical relations between precipitation and runoff were developed for the vegetation and non-vegetation seasons. Monitoring of the basic water elements in the experimental agricultural basin Rybárik has shown a decreasing trend of both annual and seasonal precipitation and runoff over the last 37 years (precipitation by 2.7 mm/year, runoff by 3.3 mm/year on average). The decrease of both precipitation and runoff in the non-vegetation season is higher than in the vegetation season.

Keywords experimental basin, long-term water balance, trends, Rybárik

MEAN ANNUAL WATER BALANCE CHARACTERISTICS

The Institute of Hydrology SAS operates several experimental basins (Herrmann et al., 1997; Kostka and Holko, 1996; Holko and Kostka, 1999). The experimental microbasin Rybárik (Fig 1) is an agricultural basin extending over 0.12 km^2 (15 % grassland, 85 % arable land). More details about the basin were given by Koníček et al. (1997), Bača (2001, 2002).

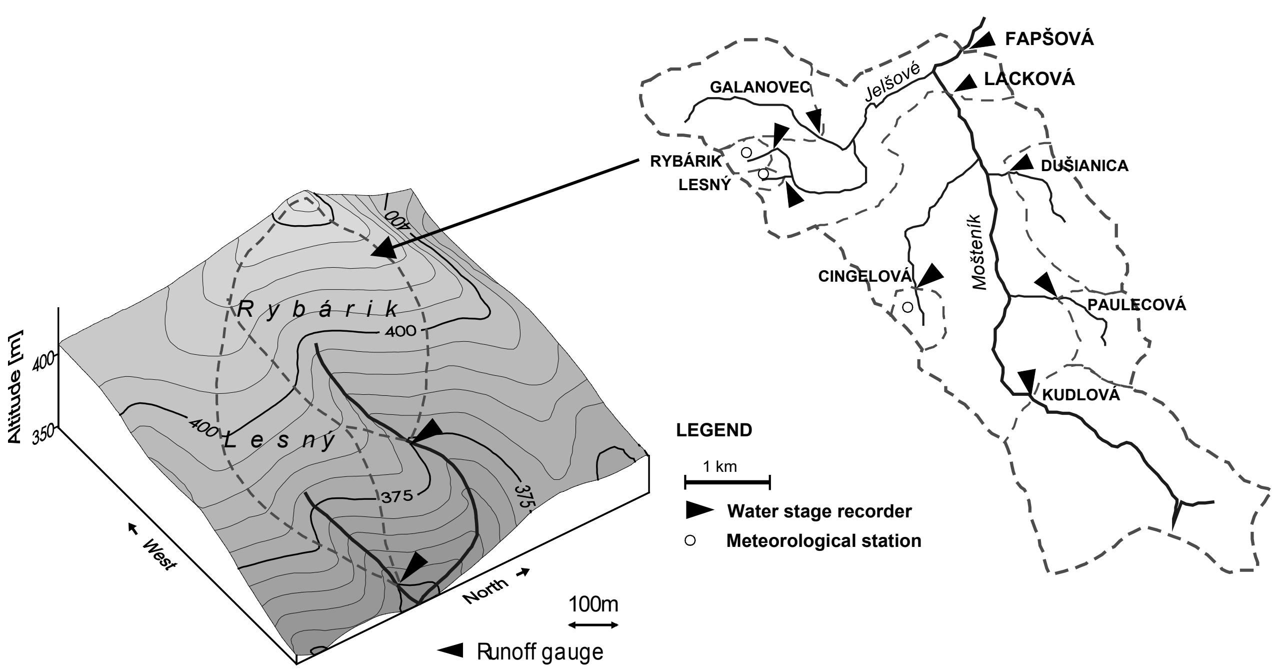

Fig 1: Location of the experimental basins in the Strážov highlands.

The mean annual precipitation over the study period was 741 mm. Maximum annual precipitation was 996 mm in the water year 1965/1966 (in Slovakia the water year starts in November of the previous year). The minimum annual precipitation was observed in 1972/1973 and only reached 539.6 mm.

The long-term mean annual discharge of Jelšové creek at the Rybárik station is 0.877 $l.s^{-1}$, with a mean annual specific yield of 7.31 $l.s^{-1}km^{-2}$ (1964/1965–2000/2001). The minimum mean annual discharge was observed in 1991, Qmin = 0.42 $l.s^{-1}$, and the maximum was observed in 1966, Qmax = 1.67 $l.s^{-1}$. The yearly water balance components of the experimental microbasin Jelšové (Rybárik) are shown in Table 1 for the period of water years 1964/1965–2000/2001. Evapotranspiration was calculated from measured precipitation and runoff depth. The whole period 1964/1965–2000/2001 was characterised by a rapid decrease of available water. The deviations from the long-term mean annual discharge 1964/65–2000/2001 are evident in Fig 2.

Table 1: Annual water balance of the Rybárik basin during the years 1964/1965 - 2000/2001

P - annual precipitation, R - annual runoff depth, ET - annual evapotranspiration as difference P-R, Qa - average annual discharge, q - specific yield, c_s - coefficient of symmetry (decades), c_v - coefficient of variation (decades).

Year	P Mm	R mm	ET mm	Qa $l.s^{-1}$	q $l.s^{-1}.km^{-2}$	k	c_s	c_v	T °C
1965	872.4	297.3	575.1	1.13	9.43	0.34			6.8
1966	996.0	437.9	558.1	1.67	13.89	0.44			8.6
1967	720.9	316.3	404.6	1.20	10.03	0.44			8.3
1968	821.1	277.0	544.1	1.05	8.78	0.34			7.8
1969	578.7	169.5	409.2	0.64	5.37	0.29	0.81	0.28	7.6
1970	854.9	246.1	608.8	0.94	7.80	0.29	0.93	0.28	7.5
1971	610.3	232.2	378.1	0.88	7.36	0.38	-0.08	0.20	7.9
1972	872.7	261.6	611.1	1.00	8.30	0.30	0.62	0.24	8.3
1973	539.6	190.4	349.2	0.72	6.04	0.35	0.92	0.25	8.3
1974	882.4	325.1	557.3	1.24	10.31	0.37	1.15	0.22	8.4
1975	721.3	275.0	446.3	1.05	8.72	0.38	1.12	0.22	8.4
1976	704.7	212.2	492.5	0.81	6.73	0.30	0.98	0.22	8.4
1977	912.5	378.5	534.0	1.44	12.00	0.41	1.12	0.23	7.8
1978	736.9	208.0	528.9	0.79	6.60	0.28	1.28	0.20	6.6
1979	738.2	246.8	491.4	0.94	7.83	0.33	0.37	0.27	7.6
1980	791.2	251.9	539.3	0.96	7.99	0.32	0.54	0.27	6.3
1981	841.7	261.2	580.5	0.99	8.28	0.31	0.57	0.27	7.7
1982	671.2	215.1	456.1	0.82	6.82	0.32	-1.90	0.19	7.4
1983	710.7	249.9	460.8	0.95	7.92	0.35	-2.20	0.18	8.8
1984	702.6	120.8	581.8	0.46	3.83	0.17	-1.41	0.21	7.5
1985	750.6	246.5	504.1	0.94	7.82	0.33	-0.79	0.24	6.8
1986	796.5	199.0	597.5	0.76	6.31	0.25	-0.46	0.29	7.6
1987	745.3	241.0	504.3	0.92	7.64	0.32	-0.50	0.29	7.1
1988	768.5	247.7	520.8	0.94	7.85	0.32	-0.04	0.31	8.4
1989	699.5	167.5	532.0	0.64	5.31	0.24	-0.17	0.31	8.8
1990	641.2	139.7	501.5	0.53	4.43	0.22	-0.03	0.31	8.7
1991	552.4	109.1	443.3	0.42	3.46	0.20	0.23	0.34	8.1
1992	618.5	226.6	391.9	0.86	7.19	0.37	0.51	0.33	9.3
1993	569.3	122.7	446.6	0.47	3.89	0.22	0.65	0.32	8.5
1994	925.9	293.0	632.9	1.11	9.29	0.32	0.63	0.32	9.8
1995	666.1	210.3	455.8	0.80	6.67	0.32	0.37	0.30	9.3
1996	742.7	127.1	615.6	0.48	4.03	0.17	0.12	0.27	8.3
1997	711.2	186.0	525.2	0.71	5.90	0.26			7.6
1998	743.1	212.1	531.0	0.81	6.73	0.29			8.2
1999	652.4	172.6	479.8	0.66	5.47	0.26			9.1
2000	684.8	194.5	490.3	0.74	6.17	0.28			9.5
2001	858.2	260.7	597.5	0.99	8.27	0.30			8.3
mean	***740.7***	***230.5***	***510.2***	***0.88***	***7.31***	***0.31***	***0.64***	***0.30***	*8.1*
min	539.6	109.1	349.2	0.42	3.46	0.17	-2.20	0.18	6.30
max	996.0	437.9	632.9	1.67	13.89	0.44	1.28	0.34	9.80

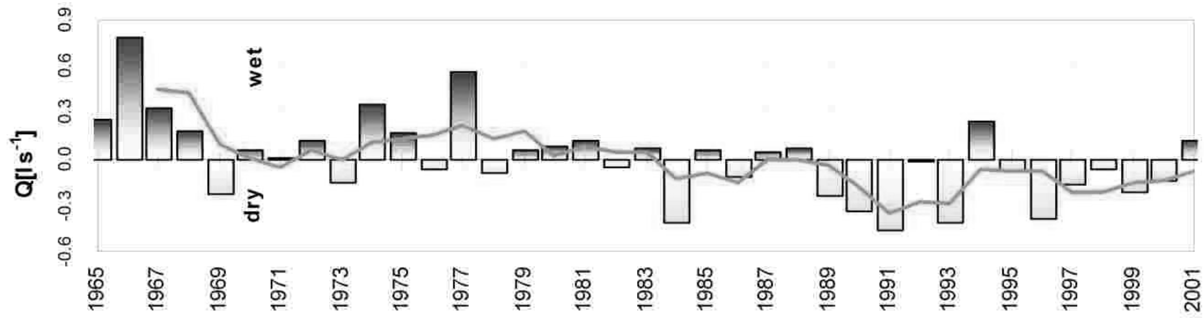

Fig 2: Deviations of the mean annual discharge in individual years from the long-term mean annual discharge 1965–2001, Rybárik.

Trends of precipitation and runoff in vegetation and non-vegetation seasons

The basic water balance elements show the following trends in 1964/65-2000/01:

P (mm) = 791.4 – 2.67 x	(precipitation)	(1)
R (mm) = 293.9 – 3.34 x	(runoff)	(2)
ET (mm) = 497.5 + 0.67 x	(evapotranspiration)	(3)

where: x - order of the year, 1.....37, starting with 1965.

The relations indicate a significant decreasing trend of annual precipitation and runoff in the basin during the last 37 years. The following relations were found for vegetation (Pv, Rv) and non-vegetation (Pnv, Rnv) seasons:

Pnv (mm) = 338.3 – 2.39 x	(4)
Pv (mm) = 453.1 – 0.28 x	(5)
Rnv (mm) = 200.3 - 2.39 x	(6)
Rv (mm) = 93.6 - 0.94 x	(7)

The results are presented in Figs 3 and 4. Precipitation significantly decreases in the non-vegetation period, while the decrease in the vegetation period is much lower. Runoff in the non-vegetation season decreases by 2.4 mm annually on average from 1965 to 2001, while in the vegetation period it only decreases by 0.9 mm. Evapotranspiration, computed as the difference between precipitation and runoff, remains constant in the non-vegetation season and increases in the vegetation season.

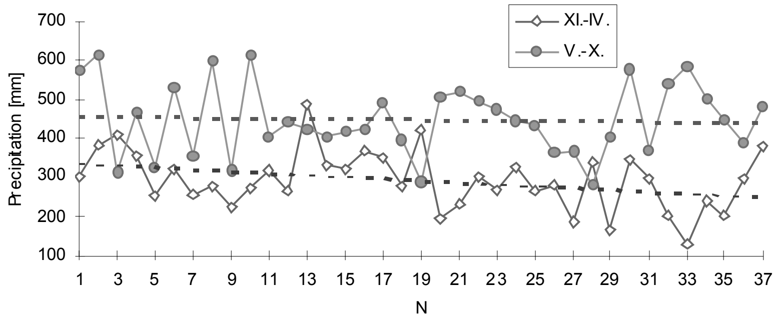

Fig 3: Trend of precipitation during the vegetation and non-vegetation seasons.

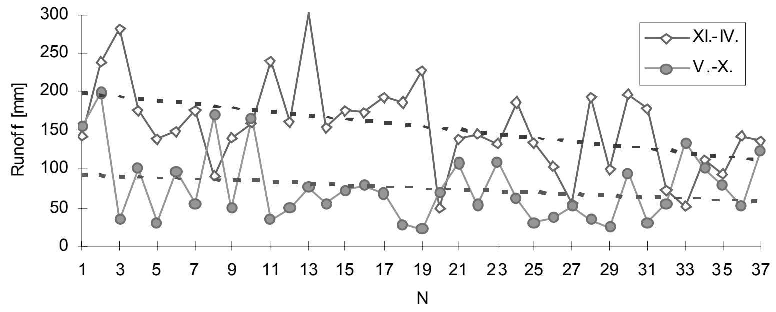

Fig 4: Trend of runoff during the vegetation and non-vegetation seasons.

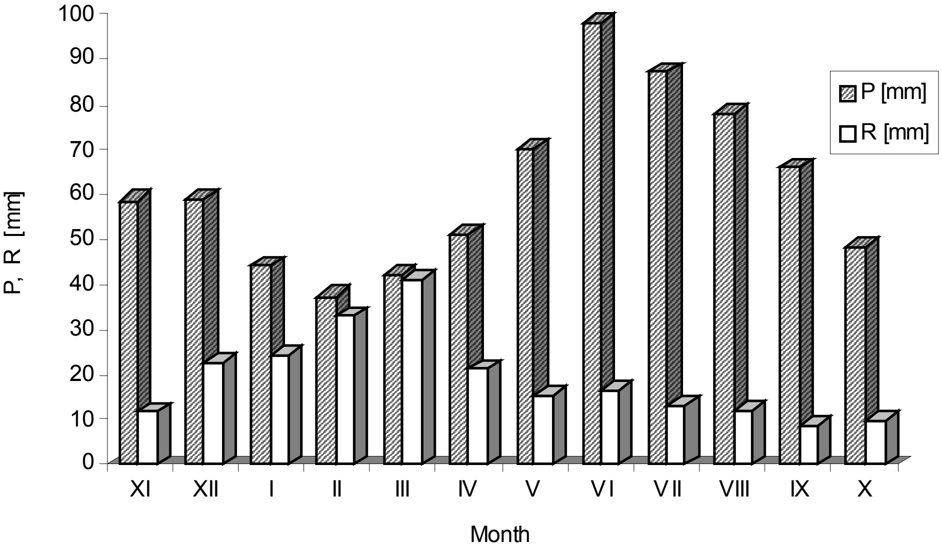

Fig 5: Mean monthly precipitation and runoff (in mm) in the period of water years 1964/65 - 2000/2001.

Mean monthly water balance characteristics

From the point of view of monthly values, the highest precipitation occurs in June (97.9 mm) and the lowest in February (37.5 mm). Maximum runoff occurs in March (41.4 mm), and minimum runoff is observed in November (8.8 mm).

Table 2: Mean monthly runoff coefficients k_m [%], mean monthly precipitation P_m [mm], mean monthly runoff depth R_m [mm], mean monthly contribution to the mean annual runoff depth R_m/R_a[%], and other statistical characteristics related to R_m, period 1964/1965-2000/2001.

	XI	XII	I	II	III	IV	V	VI	VII	VIII	IX	X
k_m	20.3	38.6	55.0	88.1	97.9	41.5	21.9	16.7	15.3	15.4	13.4	20.4
P_m	58.7	58.9	44.3	37.5	42.3	51.2	70.2	98	87.2	78.1	66	48.2
R_m	11.9	22.8	24.4	33.1	41.4	21.3	15.4	16.3	13.3	12.0	8.8	9.8
R_m/R_a %	5.1	9.9	10.6	14.6	18.0	9.2	6.7	7.2	5.5	5.3	3.4	4.3
Min	1.9	3.4	2.0	4.5	8.4	5.0	3.6	3.5	2.5	1.3	1.1	1.2
Max	37	118	88	113	96	61	46	56	75	120	35	102
Cs	1.12	2.83	1.54	1.38	0.75	1.47	1.81	1.44	3.46	4.38	2.67	4.89
Cv	0.804	0.924	0.852	0.785	0.590	0.592	0.679	0.778	1.021	1.719	0.855	1.728

Cs is coefficient of skewness, Cv is coefficient of variation

The mean annual runoff depth was 230.5 mm and the mean runoff coefficient was 31.1% in the 1964/65–2000/01 period. Maximum runoff is related to the snowmelt period (33.1 mm in February, and 41.4 mm in March). About 1/3 of the annual runoff occurs during these two months (32.6 %). The runoff coefficients are also highest during February and March: 0.88 and 0.98, respectively. The minimum runoff coefficients occur in the summer: 0.153 and 0.154 in July and August, respectively. The mean monthly values of precipitation and runoff are shown in Fig 5. The mean monthly runoff coefficients (k_m) and the mean monthly contribution to mean annual runoff are provided in Table 2.

Long-term monthly water balance

In Table 3 the values of long-term monthly water balance elements are shown. Precipitation and runoff are measured values. Monthly evapotranspiration was calculated from the annual water balance (ET= P-R) proportionally distributed between months according to the monthly evaporation observed in the neighbouring areas. The storage of water (S) in the agricultural microbasin increases from August to January, while from February to August the accumulated water storage decreases. Runoff (R) and evapotranspiration (ET) is augmented by soil moisture and groundwater until July-August. The course of the long-term water balance elements is presented in Fig 6.

Table 3: Mean monthly water balance elements of Rybárik (Jelšové) basin, period 1965–2001.

	XI	XII	I	II	III	IV	V	VI	VII	VIII	IX	X	Year
P [mm]	58.7	58.9	44.3	37.5	42.3	51.2	70.2	98.0	87.2	78.1	66.0	48.2	740.7
R [mm]	11.9	22.8	24.4	33.1	41.4	21.3	15.4	16.3	13.3	12.0	8.8	9.8	230.5
ET [mm]	7.1	2.6	2.6	9.7	24.0	40.3	76.0	99.5	103.6	75.5	40.8	28.6	510.2
Diff=P-R-ET	39.7	33.6	17.4	-5.2	-23.1	-10.4	-21.1	-17.9	-29.7	-9.4	16.3	9.8	0.0
S	***19.7***	***53.3***	***70.7***	***65.4***	***42.3***	***32.0***	***10.8***	***-7.0***	***-36.7***	***-46.1***	***-29.8***	***-20.0***	
ET [%]	1.4	0.5	0.5	1.9	4.7	7.9	14.9	19.5	20.3	14.8	8.0	5.6	100.0
ET+R	19.0	25.3	26.9	42.8	65.4	61.6	91.4	115.8	116.9	87.5	49.7	38.4	740.7

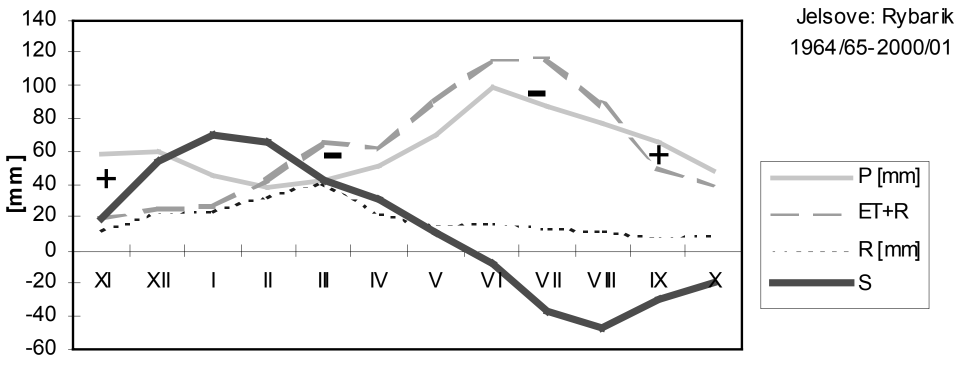

Fig 6: Course of the water balance elements computed from the long-term monthly averages in the Rybárik basin, period 1964/1965–2000/2001.

Relation between runoff and precipitation

The relation between seasonal runoff and precipitation is linear in the non-vegetation season (R_{nv}, P_{nv}), and quadratic in the vegetation season (R_v, P_v) in the Rybárik basin (see also Figs 7a, b):

$$R_{nv}\,(\mathrm{mm}) = 0.6594\, P_{nv} - 38.4 \qquad (8)$$
$$R_v\,(\mathrm{mm}) = 0.0013\, P_v^2 - 0.795\, P_v + 154.53 \qquad (9)$$

where: R_{nv}, P_{nv} - seasonal runoff and precipitation in November-April, and
R_v, P_v - seasonal runoff and precipitation in May-October.

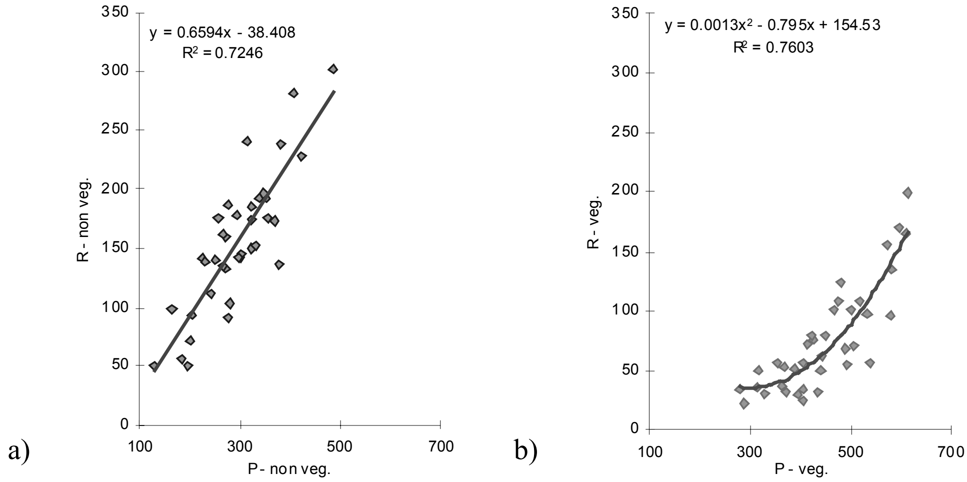

Fig 7: Seasonal precipitation - runoff relation in (a) the non-vegetation and (b) the vegetation season (years 1965-2001).

CONCLUSION

Monitoring of the basic water elements in the experimental agricultural basin Rybárik has shown a decreasing trend of both annual and seasonal precipitation and runoff in the past 37 years (precipitation by 2.7 mm/year, runoff by 3.3 mm/year on average). The decrease of both precipitation and runoff in the non-vegetation season is higher than in the vegetation season.

Annual and seasonal linear trend equations were found (Eq. (1) - (7)). The long-term monthly water balance was also estimated in Table 3 and Fig 6. Seasonal relations between precipitation and runoff were developed as well (Eq. (8) - (9)).

ACKNOWLEDGEMENT

Financial support from the Slovak Scientific Grant Agency Project 2016 is gratefully acknowledged.

REFERENCES

Bača, P. (2001) Analysis and modeling of the surface runoff and erosion process in small basin. (in Slovak.) *Acta Hydrologica Slovaca*, 2, 1, 93-97.

Bača, P. (2002) Temporal variability of suspended sediment availability during rainfall-runoff events in a small agricultural basin. Proc. 9th ERB and NEFRIEND5 Int. Conf. *Interdisciplinary Approaches in Small Catchment Hydrology: Monitoring and Research*, Slovak NC IHP UNESCO / UH SAV, 198-201.

Herrmann, A., Eliáš, V., Buchtele, J., Tesař, M., Vuglinsky, V., Zhuravin, S., Holko, L., Kostka, Z., Molnár, Ľ. (1997) Process Studies. Advances in Regional Hydrology through East European Cooperation (ISBN 0948540834), Institute of Hydrology, Wallingford., 25–27.

Holko, L., Kostka, Z. (1999) Study of runoff formation in the Western Tatra mountains. Proc. Int. Workshop *Experimental Hydrology with Reference to Hydrological Processes in Small Research Basins* (Ed. A. Herrmann). State Hydrological Institute, St. Petersburg, 88–92.

Koníček, A., Miklánek, P., Pekárová, P. (1997) The estimation of pollutant loads from experimental microbasins during extreme hydrological events. In: *Technical Documents in Hydrology*, No. 14, UNESCO, Paris, 65–70.

Kostka, Z., Holko, L. (1996): Estimation of Hydrological Balance Components at Variable Conditions of the Mountainous Catchment. Proc. *Ecohydr. High Mount. Areas*, ICIMOD, Kathmandu, 181–186.

LONG TERM HYDROLOGICAL MONITORING OF TWO MICRO-CATCHMENTS IN SEMI-ARID SE SPAIN

Albert Solé-Benet, Yolanda Cantón, Francisco Domingo, Gabriel DelBarrio, Roberto Lázaro, Miguel Angel Domene, Sebastián Vidal, Juan Puigdefábregas

Estación Experimental de Zonas Aridas, Consejo Superior de Investigaciones Científicas
C. General Segura, 1 04001-Almería, Spain

ABSTRACT

Arid and semi-arid lands are characterised by a combination of high temporal variability in rainfall and spatial heterogeneity of soil surface properties. As a consequence, little information is available about their hydrology. In addition, during the past half century, changes have occurred in most semi-arid lands in the Northern Mediterranean: agricultural abandonment and consequently a change in land use. In order to investigate the hydrological consequences of such abandonment, two representative field sites on contrasting lithologies in SE Spain were instrumented in 1989 and 1991. Additional field observations, experiments and model simulations were performed with a variety of soil, plant, water runoff, and atmospheric parameters. A summary of the first long term results of analyses of runoff, erosion and other hydrological variables at plot and micro-catchment scales is presented here, including the main monitoring problems encountered.

Keywords runoff, erosion, long-term monitoring, soil water content, semi-arid environment

INTRODUCTION

The Rambla Honda (37.1297°N, 2.3713°W) and the El Cautivo (37.0109N, 2.4391°W) field sites, both in Almeria province, SE Spain, are permanently equipped research sites, aimed at gathering information on climate, vegetation, and hydrological and geomorphic processes and their interactions at two lithologically contrasting locations in a dry Mediterranean climate (see references). Both sites are under very low grazing pressure after the abandonment of agriculture.

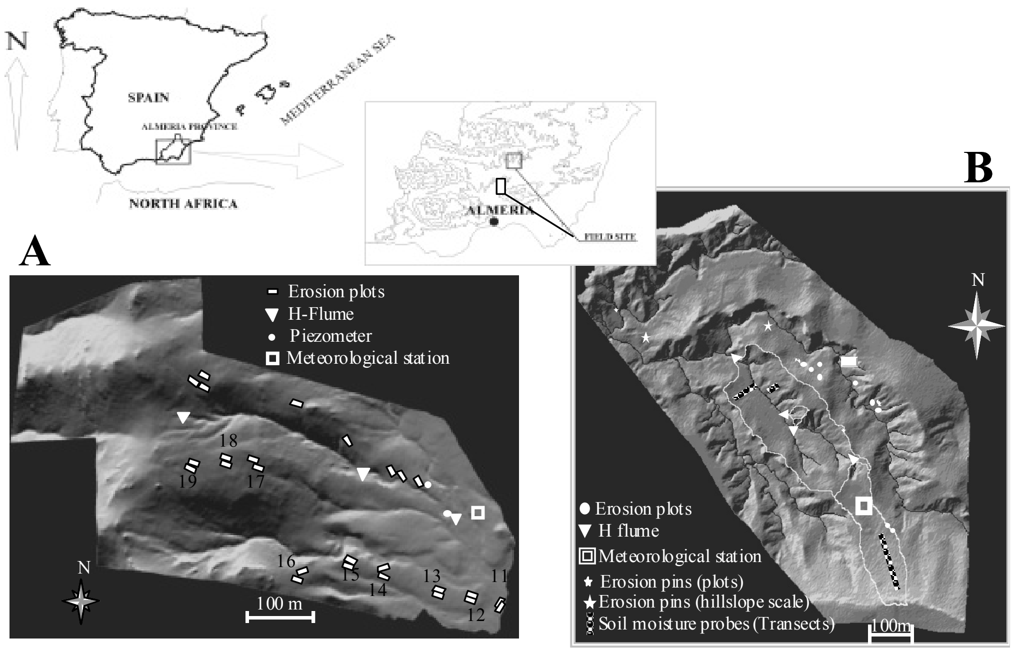

Fig 1: Location and maps compiled from DEM, showing runoff and erosion plots (Nº 11 to Nº 19, from the lower to the upper part of the catena). H-flumes are gauging devices in micro-catchments 1 to 3 in Rambla Honda (Fig 1A) and micro-catchments 1 to 4 in El Cautivo (Fig 1B) (numbered from the lower to the upper part of the catchment).

Rambla Honda (Fig 1A) is a semi-arid Mediterranean rangeland on top of mica schist bedrock including: a) tussock grasslands of *Stipa tenacissima* on shallow sandy-loam soils at the rocky upper part; b) open shrubland of *Anthyllis cytisoides* on thick loamy-sand soils developed on the alluvial fans at the foot slope; and c) open shrubland of *Retama sphaerocarpa* on very thick loamy-sand soils over the river bank terrace at the bottom of the catena (Nicolau et al., 1996; Puigdefábregas et al., 1996).

El Cautivo (Fig 1B) is located in one of the most extensive badland areas in Spain over calcitic gypsiferous mudstone. Main geomorphic features include valley asymmetry and a variety of different soil-surface types over silt-loams, including many types of both mineral and biological crusts, with contrasted erosion and hydrological behaviour (Calvo and Harvey, 1996; Solé-Benet et al, 1997; Cantón et al., 2001b).

Meteorological, hydrological and ecological variables are being monitored at several time scales at both field sites. Runoff and sediment yield is monitored in plots ranging from 0.25 m^2 to 20 m^2, some equipped with divisors and tipping buckets, and in micro-catchments from 57 to 45,000 m^2, equipped with H-flumes and automatic samplers. The sites also have dielectric sensors (TDR). Other variables have been monitored during specific campaigns: soil hydrology (Nicolau et al., 1996; Puigdefábregas et al., 1996), actual evapotranspiration for three main plant communities (Domingo et al., 1999), rainfall interception and rainfall partitioning (Domingo et al., 1998), as well as plant biomass budgets and fluxes, such as net primary productivity, death biomass and litter fall (Puigdefábregas et al., 1996).

RESULTS

In both sites a strong seasonal and inter-annual variability in rainfall is observed. On average, up to 75 % of the annual rainfall is recorded during autumn and winter (Fig 2). Temperatures show mild annual averages with warm summers and mild winters, due to a high insulation and mild winds. There is a strong spatial variability in runoff along hillslopes in both field sites due to soil surface types (crusted), soil depth (< 30 cm in rocky slopes and > 1 m in the alluvial fans or pediments), plant cover (Fig 4) and spatial vegetation pattern. The widespread occurrence of structural surface crusts (coarse-pavement sieving crusts, Fig 3, in Rambla Honda and slaking crusts in El Cautivo) explains rainfall thresholds for runoff occurrence of around 18 mm in the alluvial fan and 3 mm in the upper slopes of Rambla Honda, and about 5 mm in bare areas of El Cautivo.

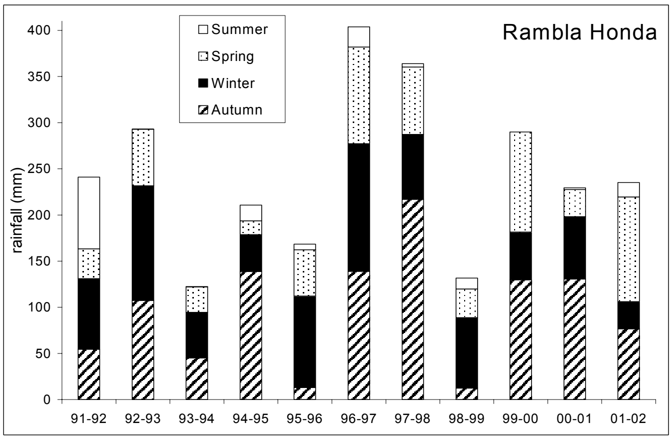

Fig 2: Seasonal rainfall from 1991 to 2002.

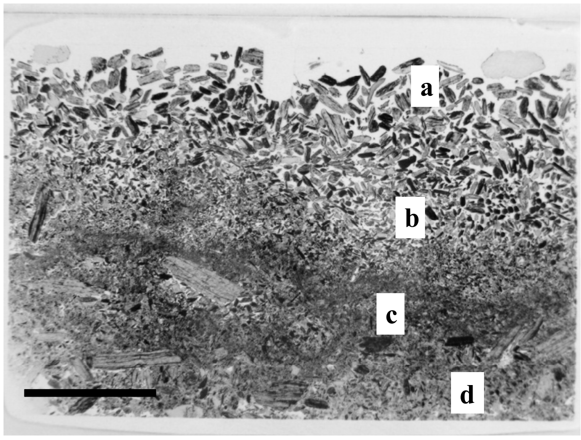

Fig 3: Coarse pavement sieving crust from Rambla Honda. a = gravel and coarse sand layer, b = sand layer, c = very fine sand layer, d = heterogeneous layer. Length of black bar = 15 mm.

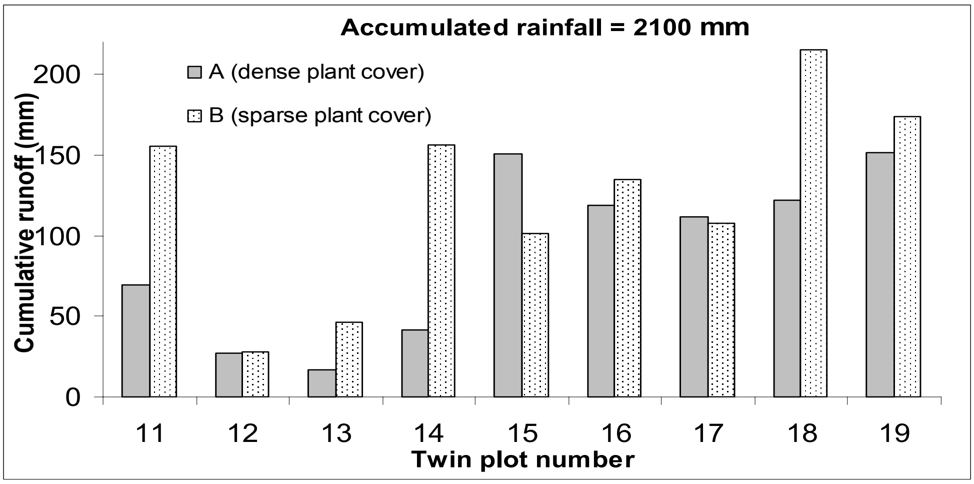

Fig 4: Accumulated runoff (from Sept 91 to Aug 2000) along the catena, from lower (nº 11) to upper hillslope (nº 19). A and B are twin runoff-erosion plots as shown in Fig 1.

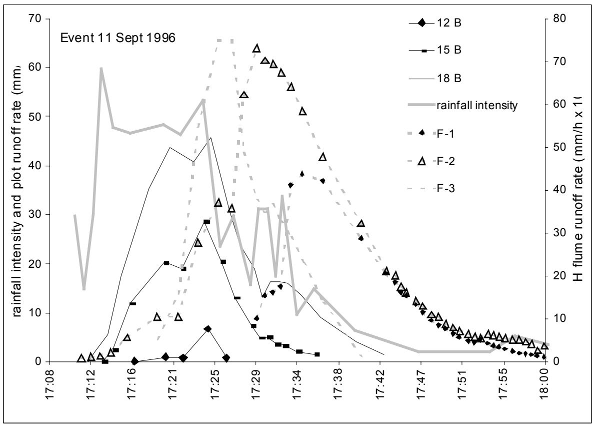

Fig 5: Cumulative saturation of subsurface layers in Rambla Honda

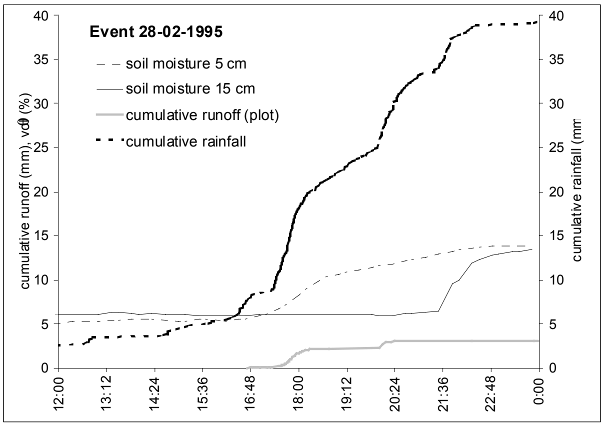

Fig 6: Runoff by infiltration excess (Horton).

Two mechanisms of overland flow generation have been identified (Puigdefábregas et al, 1998). The first mechanism is saturation from subsurface layers (low frequency, high magnitude events in Rambla Honda). An example is shown in Fig 5. The second mechanism is infiltration excess. These are frequent but short lived, high intensity events in Rambla Honda and always in El Cautivo (Fig 6). Hillslope connectivity is rare, as in most arid and semi-arid regions, and only occurs with the first runoff mechanism. The relation between the area of the catchment and runoff coefficients is relatively similar at both sites (Figs 7A, 7B).

The influence of scale and soil surface types on runoff is evident when the cumulative runoff in different micro-catchments is compared. As an example, the event of 31 October 1993 in El Cautivo is shown in Fig 8: micro-catchments 2 (260 m^2) and 3 (60 m^2), mainly covered by bare soil surfaces with low infiltration capacity, show the highest runoff (Solé-Benet et al., 1997; Cantón et al., 2001), while micro-catchment 4, mostly covered by vegetation with medium to high infiltration rates, shows the lowest runoff. Micro-catchment 1 (2 ha) shows also a quite reduced overall runoff due to its heterogeneous mosaic of soil surfaces, where runoff from bare areas can reinfiltrate in plant-covered areas downslope (Cantón et al., 2001, 2002).

Soil erosion is very limited in Rambla Honda (up to 9 g m^{-1} $year^{-1}$ in erosion plots and < 0.01 g m^{-2} $year^{-1}$ in a 5 ha catchment) and more significant in El Cautivo (up to 628 g m^{-1} $year^{-1}$ in small plots and up to 0.037 g m^{-2} $year^{-1}$ in micro-catchment 1 (2 ha), with a runoff threshold of 5 mm to produce over 300 g m^{-2} of sediment).

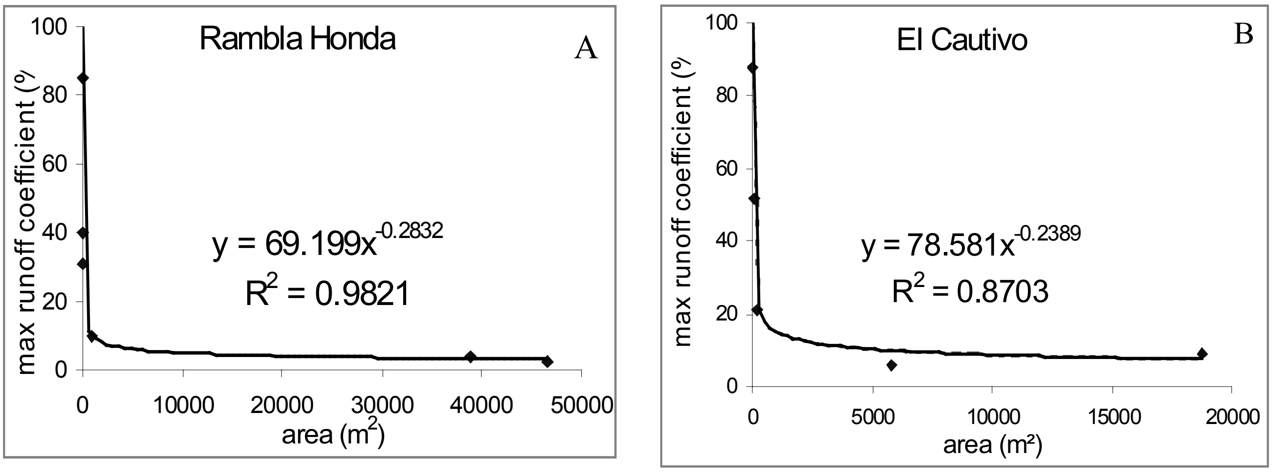

Fig 7: Relationships between catchment size and runoff coefficients.

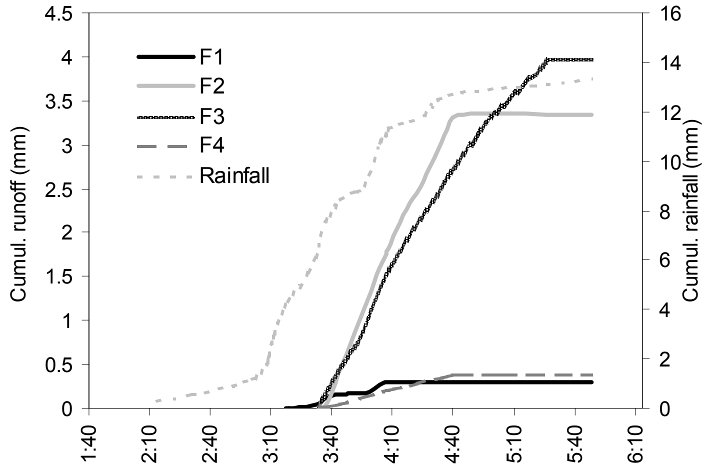

Fig 8: Accumulated runoff and accumulated rainfall for micro-catchments 1 (F1), 2 (F2), 3 (F3) and 4 (F4) during the event of 31 October 1993 (Cantón et al., 2001).

Soil erosion in El Cautivo also shows a strong correlation with the dominant soil surface type. Where plant cover is scarce, as in micro-catchments 2 and 3, soil erosion can be very high. During some events, highly charged (up to 0.4 kg L^{-1}) to hyper-concentrated flows (up to 0.8 kg L^{-1}) are recorded. In areas mostly covered by annual and perennial plants, as in micro-catchment 4, the erosion rates are low (during one event a maximum of 60 g m^{-2} was measured).

Flow peaks coincide with the highest sediment discharge peaks. Fig 9 shows the evolution of both runoff and sediment yield (particles < 1 mm) during a rainfall event in micro-catchment 1.

The research on erosion at a patch scale has particularly focused on the role of vegetation as a source of spatial heterogeneity that affects the short-range distribution of water and sediments. Results from Rambla Honda, based on field observations, experiments and simulation models (Sánchez and Puigdefábregas, 1994), show that a range of positive feedback mechanisms, like the trapping of water and sediments by vegetated patches and the concentration of flow between herbs and bushes, leads to nucleation or to the increase in spatial heterogeneity by concentrating resources of the soil beneath plant clumps at the expense of neighbouring bare ground (Puigdefábregas et al, 1999). Concerning sediment at the micro-catchment scale, channels are the main redistribution structures as well as the main sources when they cut into alluvial fans (Puigdefábregas et al., 1999).

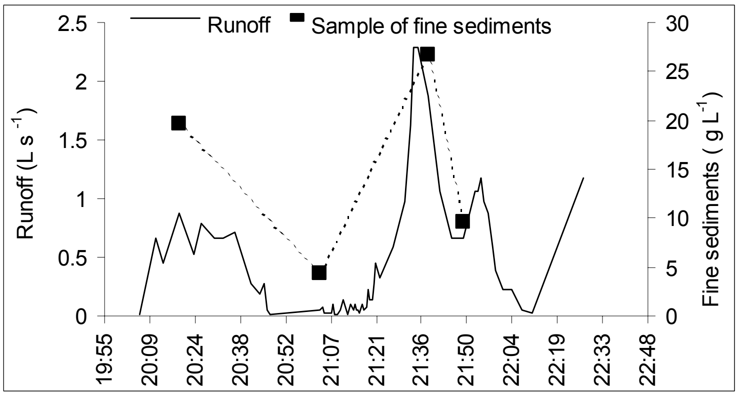

Fig 9: Hydrograph and sedimentograph (particles < 1 mm) for the event of 1 February 1993 in micro-catchment 1.

A validated evapotranspiration model applied to an area of about 2 ha in the lower section of the catena in Rambla Honda shows that actual evapotranspiration (ET_{act}) largely exceeds (by about 100 mm per year) precipitation (P) at annual scales. The estimated deficit may be compensated by: a) infiltration of local rainfall during extreme events; b) runon from the surrounding hillslopes; or c) infiltration of channel flow during flash floods originating from the upper part of the catchment. Data from long term monitoring show that possibilities a) and b) cannot explain the water deficit but do show that deep storage of water during floods in the main channel can be as much as 60 mm to 150 mm per event, and may have been 160 mm year^{-1} to 400 mm year^{-1} during a period of four years (1994-1997) (Domingo et al, 2001).

DRAWBACKS AND SUSTAINABILITY OF LONG TERM MONITORING

Several problems occurred during the experiments on the runoff plots: A) Bounded runoff plots stop sediment flux from upslope and therefore might suffer from sediment exhaustion after several years of no runon. B) Soil moisture surplus near a collector trough enhances the growth of annual plants, thus triggering a feedback mechanism of progressive sediment trapping and enhanced plant growth. C) An important part of runoff collected from runoff plots comes from a few decimetres upslope of the collector trough. D) The changes in spatial structure of vegetation within runoff plots during the monitoring period may influence the magnitude of the measured variables. E) Several types of external changes (galleries and/or latrines of rabbits or other vertebrates, feeding grounds or rooting areas of wild boars, ant nests, etc.) may cause an important non-homogeneity in the monitored variables, a fact especially acute in bounded runoff plots. F) Periodical calibration of tipping buckets and levelling flow divisors is highly recommended to avoid a progressive drift in the measured variables. All these problems, because of the small scale of the experiments, make it difficult to upscale the results.

Detected problems in small instrumented catchments: A) It is not easy to select the right gauging device for ephemeral channels, nor its right dimension. A combination of large devices (large range, reduced precision) with small ones (short range, higher precision) seems to be the most adequate approach. B) Hyper-concentrated flows, where they occur, usually cause clogging of gauging devices and sensors. C) No simple devices are adequate for sediment measurements from hyper-concentrated flows. Weight sensors coupled to water levels in gauged channel sections are a promising technique which should be improved. D) In semi-arid areas, where runoff events normally occur with low frequency (1 year^{-1}), it may take a long time to collect a good data series in order to test homogeneity assumptions.

Data obtained in micro-catchments from arid and semi-arid regions should be used with caution when trying to extrapolate to either larger or different areas: because of the occurrence of spatial heterogeneity (in soil depth, vegetation type and cover and rooting depth) along with high temporal variability in rainfall and other meteorological data. This may have very important hydrological consequences, and thus extrapolations might only apply for very similar environmental conditions.

In dry environments, looking at fine time scales is essential to obtain information on processes, especially those leading to extreme events (such as rainfall), which are the main drivers of landscape change. Moreover, permanent research facilities afford the paradox that funding is mainly through specific research projects the time scale of which is usually not compatible with the longer term evolution of the geomorphic processes. The approach should be to develop and monitor low cost indicators, including remotely sensed data.

REFERENCES

Boer, M.M. (1999) Assessment of dryland degradation: linking theory and practice through site water balance modelling. *Netherlands Geographical Studies,* 251, KNAG – Utrecht, The Netherlands, pp. 294.

Calvo, A., Harvey, A.M. (1996) Morphology and development of selected badlands in SE Spain: implications of climatic change. *Earth Surface Processes and Landforms*, 21, 725-735.

Cantón, Y., Solé-Benet, A., Queralt, I., Pini, R. (2001) Weathering of a gypsum-calcareous mudstone under semi-arid environment at Tabernas, SE Spain: laboratory and field-based experimental approaches. *Catena*, 44, 111–132.

Cantón, Y., Domingo, F., Solé-Benet, A., Puigdefábregas, J. (2001) Hydrological and erosion response of a badlands system in semiarid SE Spain. *Journal of Hydrology*, 252, 65–84.

Cantón, Y., Domingo, F., Solé-Benet, A., Puigdefábregas, J. (2002) Influence of soil surface types on the overall runoff of the Tabernas badlands (SE Spain). Field data and model approaches. *Hydrological Processes*, 16, 2621-2643.

Domingo, F., Sánchez, G. Moro, M.J., Brenner, A.J., Puigdefábregas, J. (1998) Measurement and modelling of rainfall interception by three semi-arid canopies. *Agricultural and Forest Meteorology*, 91, 275–292.

Domingo, F., Villagarcía, L., Brenner, A. J., Puigdefábregas, J. (1999) Evapotranspiration model for semi-arid shrub-lands tested against data from SE Spain. *Agricultural and Forest Meteorology,* 95, 67–84.

Domingo, F., Villagarcía, L., Boer, M. M., Alados-Arboledas, L., Puigdefábregas, J. (2001) Evaluating the long-term water balance of arid zone stream bed vegetation using evapotranspiration modelling and hillslope runoff measurements. *Journal of Hydrology*, 243, 17–30.

Lázaro, R., Rodrigo, F.S., Gutiérrez, L., Domingo, F.& Puigdefábregas, J. (2001) Analysis of a 30-year rainfall record (1967-1997) in semi-arid SE Spain for implications on vegetation. *Journal of Arid Environments*, 48, 373–395.

Nicolau, J. M., Solé-Benet, A., Puigdefábregas, J., Gutiérrez, L. (1996) Effects of soil and vegetation on runoff along a catena in semi-arid Spain. *Geomorphology*, 14, 297–309.

Puigdefábregas, J., Alonso, J. M., Delgado, Domingo, F., Cueto, M., Gutiérrez, L., Lázaro, R., Nicolau, J. M. Sánchez, G., Solé, A., Vidal, S., Aguilera, C., Brenner, A., Clark, S., Incoll, L. (1996) The Rambla Honda field site: interactions of soil and vegetation along a catena in semi-arid southeast Spain. J. Brandt & J. Thornes eds. In *Mediterranean Desertification and Land Use*, John Wiley & Sons, Ltd., 137–168.

Puigdefábregas, J., del Barrio, G., Boer, M.M., Gutiérrez, L. & Solé-Benet, A. (1998) Differential responses of hillslope and channel elements to rainfallevents in a semi-arid area. *Geomorphology*, 23, 337–351.

Puigdefabregas, J., Sole-Benet, A., Gutierrez, L., del Barrio, G., Boer.M.M. (1999) Scales and processes of water redistribution in drylands: results from the Rambla Honda field site in southeast Spain. *Earth Science Reviews*, 48, 39-70.

Sánchez, G., Puigdefábregas, J. (1994) Interactions of plant growth and sediment movement on slopes in a semi-arid environment. *Geomorphology*, 9, 243–260.

Solé-Benet, A., Calvo, A., Cerdà, A., Lázaro, R., Pini, R., Barbero, J. (1997) Influences of micro-relief patterns and plant cover on runoff related processes in badlands from Tabernas (SE Spain). *Catena*, 31, 23-38.

Solé-Benet, A., Pini, R., Raffaelli, M. (2002) Hydrological consequences of soil surface type and condition in colluvial mica schist soils after the agricultural abandonment. In J.L.Rubio, R.P.C.Morgan, S.Ansins & V.Andreu (eds) *Proceedings of the 3rd International Congress Man and Soil at the Third Millenium*, Geoforma Ediciones, Logroño, Spain, 523-533.

LONG-TERM HYDROMETEOROLOGICAL MEASUREMENTS AND MODEL-BASED ANALYSES IN THE HYDROLOGICAL RESEARCH CATCHMENT RIETHOLZBACH

J. Gurtz[1], M. Verbunt[1], M. Zappa[1], M. Moesch[1], F. Pos[2], U. Moser[1]

[1]*Institute for Atmospheric and Climate Science, Swiss Federal Institute of Technology (ETH) Zürich, Winterthurerstr. 190, CH-8057 Zürich, Switzerland, E-mail: gurtz@geo.umnw.ethz.ch*
[2]*Department of Environmental Sciences, Sub-department Water Resources, Wageningen University (NL), De Nieuwlanden, Nieuwe Kanaal 11, 6709 PA Wageningen, The Netherlands*

ABSTRACT

In this study 25-year (1976-2000) observations of precipitation, temperature and runoff in a pre-alpine research catchment have been analysed. Lysimeter measurements are investigated and discussed with respect to precipitation, evapotranspiration and percolation rates. A comparison of precipitation volumes derived from lysimeter measurements and from rain gauges shows a strong underestimation of (especially) winter precipitation. Therefore, monthly precipitation correction factors have been calculated. Results of the runoff simulation for the period 1981-1998 are presented and compared with observed discharges.

Keywords hydrological research catchments, water balance, precipitation correction, hydrological modelling

INTRODUCTION

The pre-alpine hydrological research catchment Rietholzbach was established in 1975 and provides since then observations of several hydro-meteorological variables. These long-term measurement series are important to obtain a better insight into the understanding of the hydrometeorological processes (Menzel, 1997). Besides the better process understanding, the measurements also are of great importance for the calibration, validation and development of hydrological models (Kirnbauer et al., 2000).

CHARACTERISTICS OF RIETHOLZBACH RESEARCH CATCHMENT

The hilly pre-alpine research catchment *Rietholzbach* is located in the central part of the Thur river basin (tributary of Rhine) in north-eastern Switzerland with an area of 3.2 km^2 and the main water flow running west to east. The elevation ranges from 682 to 950 m a.s.l. It is primarily used as pasture land (76%). The geology of the catchment is characterized by the tertiary deposits of the Upper Freshwater Molasse. Pleistocene sandy and silty gravel pockets of glacial moraines occur in the flat riparian zones along the creek. A variety of soil types is observed; from less permeable gley soils to more permeable brown soils and regosols with relatively large soil water storage capacities. The soil depth exceeds 50 cm. The catchment is equipped with a complete meteorological station, a weighting lysimeter, continuous TDR soil moisture measurements at different depths all situated at the station Büel in the centre of the catchment, 3 access tubes for groundwater level observations and 3 runoff gauging stations (Rietholzbach/Mosnang, Huwilerbach and Upper Rietholzbach). The first measurements of some hydrometeorological variables and of discharge at the catchment outlet began in 1975. For some variables observations for a period of more than 25 years are now available. The internet homepage of Rietholzbach can be accessed at http://www.iac.ethz.ch/en/research/riet/.

ANALYSIS OF 25 YEARS OF OBSERVATIONS

The 25-year observation period 1976-2000 with air temperature, precipitation, discharge and lysimeter measurements is analysed. Fig 1 presents the mean annual air temperature at the station Büel. The mean air temperatures are in a range from about 5 up to 9°C and show a clear increasing trend. Corresponding to this trend the number of frost days shows a clear decreasing trend.

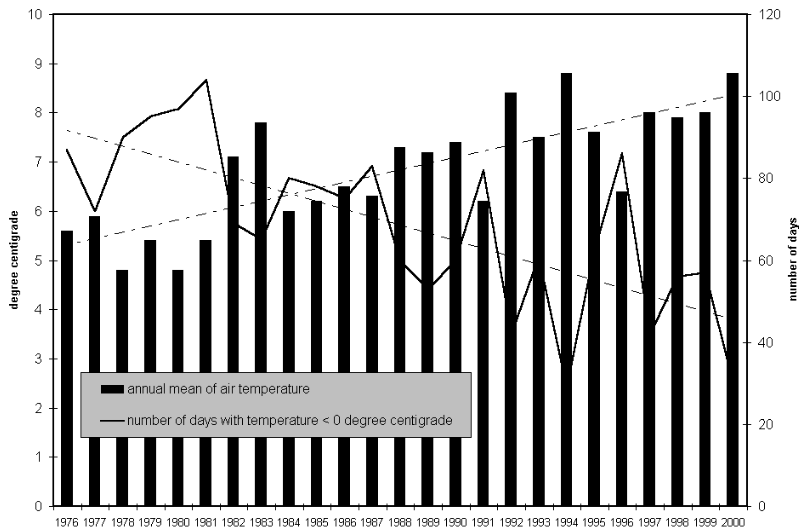

Fig 1: Mean annual air temperature and number of days with air temperature <0°C and linear trends at the meteorological station Büel for the period 1976-2000.

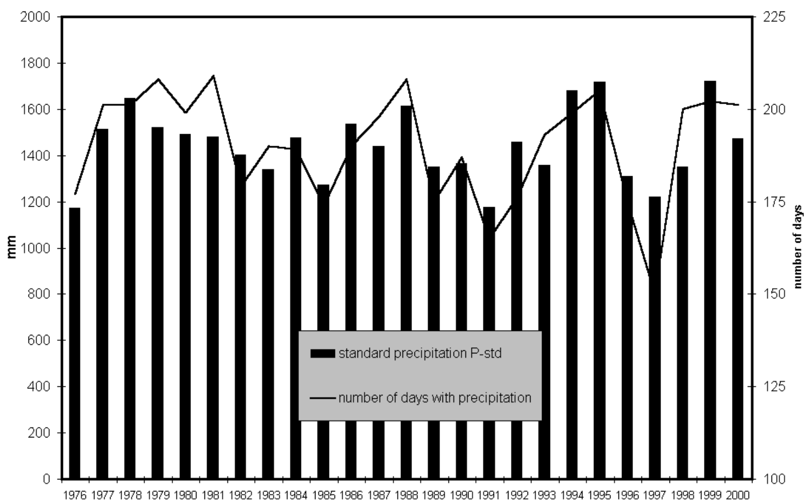

Fig 2: Annual measured precipitation totals (P-std) and the number of days with precipitation at the meteorological station Büel for the period 1976-2000.

The annual precipitation totals P_{std} measured at the standard height of 1.5 m (Fig 2) range between 1200 $mm \cdot y^{-1}$ and 1700 $mm \cdot y^{-1}$, and show a tendency toward higher variability in the last 8 years. Such tendency is found in the number of days with precipitation, as well.

The same tendency toward higher variability in the last 8 years is also observed in the case of the catchment runoff (Fig 3) which ranges between 650 and 1500 $mm \cdot y^{-1}$. Precipitation and runoff do not show any temporal trend.

The lysimeter outflow R_{lys} and the change in lysimeter weight D_{lys} are measured with a time resolution of five minutes. From these values the annual totals of lysimeter evapotranspiration E_{lys} and lysimeter precipitation P_{lys} (Fig 4) are obtained (see next section). P_{lys} ranges from 1200 $mm \cdot y^{-1}$ up to about 2000 $mm \cdot y^{-1}$. P_{lys} is often more than 200 mm higher than P_{std}. P_{lys} is assumed to be the correct precipitation, because it is not affected by wind error. The lysimeter outflow is of the same order as the catchment outflow at the gauge. The lysimeter evapotranspiration E_{lys} ranges from 450 mm·y^{-1} to up to more than 600 mm·y^{-1}. E_{lys} shows no clear temporal trend. The average seasonal maximum of E_{lys} is reached in July with 100 mm (Fig 5). The winter evaporation is on the order of 10 mm·month^{-1}. The average seasonal maximum of P_{lys} is in June with about 170 mm.

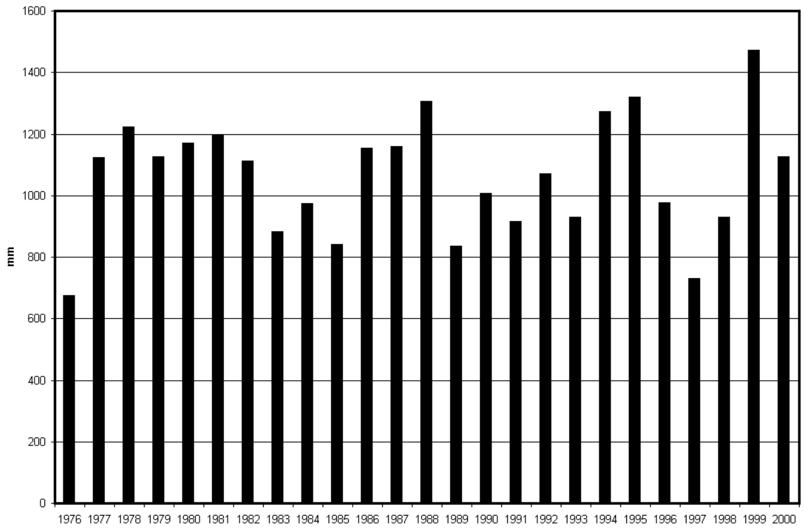

Fig 3: Annual runoff of the Rietholzbach catchment at the outlet gauge Mosnang for the period 1976-2000.

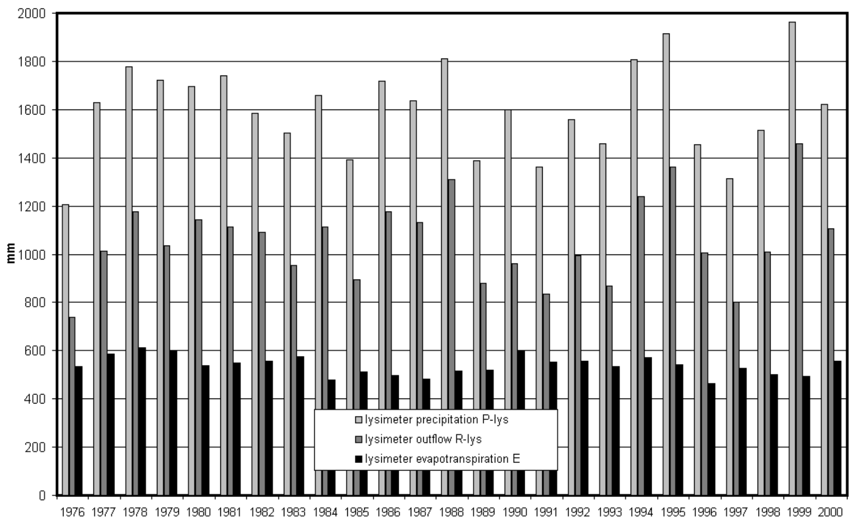

Fig 4: Annual totals of lysimeter precipitation, lysimeter outflow and lysimeter evapotranspiration for the period 1976-2000.

As a result, the highest lysimeter outflows are in winter (100-130 mm·month^{-1}). The main period of soil moisture extraction in the lysimeter (negative D_{lys}) coincides with the periods with lowest outflow and lasts from March to July.

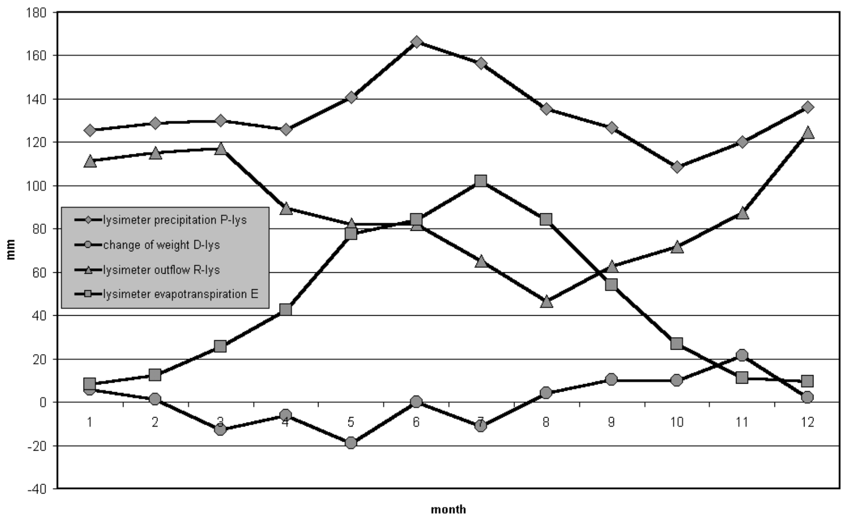

Fig 5: Mean monthly lysimeter precipitation, outflow, evapotranspiration and change of lysimeter weight for the period 1976-2000.

PRECIPITATION MEASUREMENT ERROR

Precipitation at the meteorological station Büel is measured by a standard rain gauge (P_{std}) (heated tipping bucket). The gauge is installed 1.5 m above the ground. A similar rain gauge is installed at ground-level (P_{ground}). The ground-level rain gauge is only representative in summer because of the influence of wind induced snow drift in winter. A precipitation amount can also be calculated from the lysimeter measurements using the water balance equation (Moesch, 2001):

$$P_{lys} = E_{lys} + R_{lys} + D_{lys} \quad (1)$$

where E_{lys} is the actual lysimeter evapotranspiration [mm·dt^{-1}], P_{lys} the precipitation derived from the lysimeter [mm·dt^{-1}], R_{lys} the lysimeter outflow [mm·dt^{-1}], D_{lys} the weight change of the lysimeter [mm·dt^{-1}] and dt the used time interval. In equation (1) there are two unknowns: P_{lys} and E_{lys}. During precipitation (P_{std}> 0.1 mm·dt^{-1}), E_{lys} is set to zero and P_{lys}can be computed. Otherwise P_{lys} is zero and E_{lys} can be computed with equation 1.

The comparison between P_{lys} and P_{std} (Fig 6) indicates that the standard rain gauge measures significantly less precipitation in winter. In summer months, with the exception of August, P_{lys} is only slightly higher than P_{std}. A comparison of P_{ground} with P_{std} for summer months shows the same result as when comparing P_{lys} with P_{std} for summer months. Since the average wind speed is significantly larger in winter months than in summer (Moesch, 2001), the precipitation measurement with the standard gauge is more influenced by wind in winter than in summer. Wind strongly influences the losses in the precipitation measurements, especially in case of snowfall. The reason is that the wind field above the gauge is deformed. The precipitation particles are also lighter in case of snowfall in winter than the rain in summer, the wind has therefore more influence on the particles in winter than in summer. Sevruk (1983) showed that the total losses of snow measurements during winter months for the heated tipping bucket at Weissfluhjoch near Davos was about 55%. Alongside with wind, evapotranspiration can also cause important water losses for heated precipitation gauges.

Monthly precipitation corrections for the Rietholzbach catchment can be estimated by comparing the mean measured monthly values of P_{std} and P_{lys} in the period 1976-2000. These monthly corrections are applied on the standard rain gauge, and can be estimated in the first instance from the deviation between P_{lys} and P_{std} (total correction in Table 1). The correction factors are divided into a snow and a rain correction factor (Table 1). This is done by analysing the amount of snow and rain in the Rietholzbach catchment for the period 1981-2000 (Pos, 2001) on the basis of hydrological simulation experiments.

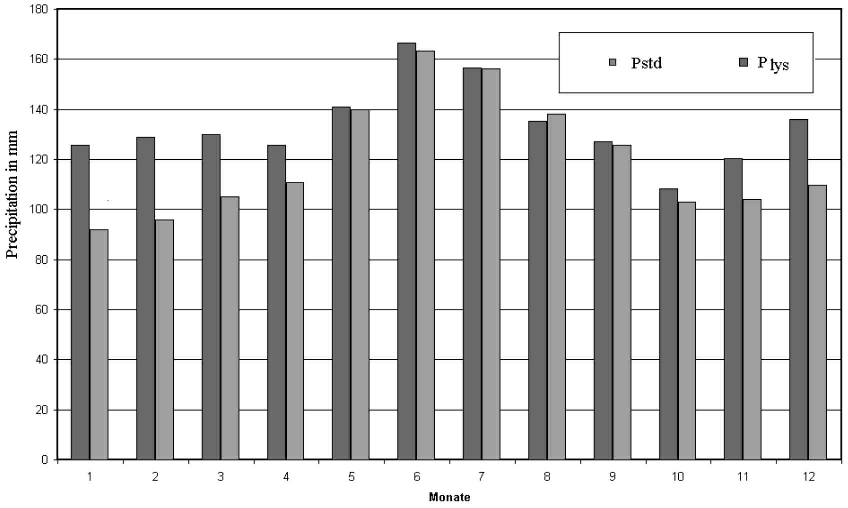

Fig 6: Comparison of the mean monthly P_{lys} with P_{std} at the meteorological station Büel for the period 1976-2000.

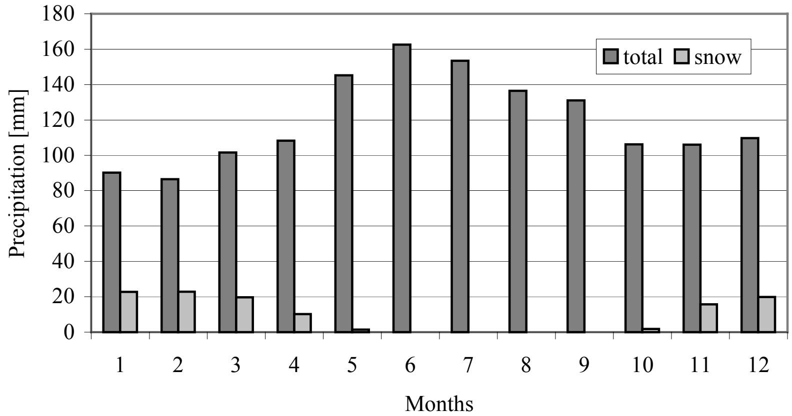

Fig 7: The measured mean monthly total precipitation amount and the mean monthly snow amount in the Rietholzbach catchment for the period 1981-2000.

Table 1: Monthly correction factors for snow and rain and total precipitation correction, as used for hydrological simulations in the Rietholzbach catchment.

Month	Jan	Feb	Mar	Apr	May	Jun	Jul	Aug	Sep	Oct	Nov	Dec
Snow correction [%]	61.0	62.0	62.2	58.0	35.0	-	-	-	-	8.0	58.0	60.0
Rain correction [%]	23.3	23.0	25.5	14.0	4.0	3.0	0.0	0.0	0.0	5.0	5.0	15.0
Total correction [%]	36.4	34.5	23.8	13.6	4.0	2.2	0.7	-0.9	1.7	7.2	15.5	24.1

The portion of snow expressed as water equivalent when compared to the total precipitation amount is given in Fig 7. Snow is only falling from October till May. The portion of snow is below 25% in all of these months. The need of precipitation corrections (up to +60%) is confirmed by both a water balance and runoff components analysis (König et al., 1994) and by the improvements these corrections provide when applied in a rainfall-runoff modelling experiment with a spatially distributed hydrological model for the period 1981-2000 (Pos, 2001).

MODEL RESULTS

Two differently structured rainfall-runoff models were applied to the Rietholzbach research catchment for the simulation of hydrological processes and runoff hydrographs for the period 1981-1998. The adopted models are the more physically based WaSiM-ETH model with grid-oriented computation of the water balance elements and the stronger conceptual hydrological response unit based PREVAH model. Gurtz et al. (2000, 2003) discuss the simulation results in comparison with the observed catchment discharges, with measurements of evapotranspiration, soil moisture, outflow of the lysimeter and with groundwater levels in 3 access tubes. The model intercomparison outlined that these two approaches for determining runoff generation with different degrees of complexity, performed with similar statistical Nash and Sutcliffe efficiency r^2 (Table 2). The contribution of the runoff components strongly depends on the applied modelling approach. About 50% of the computed runoff is generated by interflow. Similar results were derived from a discharge component analysis of the observed discharge hydrograph (König et al., 1994) and from the estimation of water residence times using natural tracers (Vitvar et al., 1999). Also, the fast response of the ground water table observed in the wells situated at slopes in contrast to the observations in the well situated in the moraine valley clearly confirms the existence of interflow. In comparison to PREVAH, the WaSiM-ETH model generates a clearly higher surface runoff contribution and a lower baseflow contribution. This seems to outline that surface runoff is underestimated by PREVAH and slightly overestimated by WaSiM-ETH, whereas baseflow is simulated more realistically by PREVAH as compared to WaSiM-ETH. The reasons for such differences are connected to the models' different runoff generation approaches (Gurtz et al., 2003).

Table 2: Rietholzbach (1981-1998) - measured and modelled mean annual water balance [$mm \cdot y^{-1}$] (P = precipitation, ET = evapotranspiration, R_{sim} = simulated runoff, R_{obs} = observed runoff) and runoff components [$mm \cdot y^{-1}$] (RS = surface runoff, RI= interflow, RG= baseflow), storage change (DS) and obtained averaged efficiency score [-] (linear = r^2_{lin} and logarithmic = r^2_{log}) for the simulation of hourly discharges.

Method	Location	P	ET	R_{sim}	R_{obs}	RS	RI	RG	DS	r^2_{lin}	r^2_{log}
Measured	Lysimeter	1576	529	-	1049	--	--	--	--	--	--
PREVAH	Lysimeter	1570	549	1020	1049	--	--	--	--	0.61	--
PREVAH	Rietholzbach	1593	583	1010	1013	73	561	376	0	0.713	0.890
WaSiM	Rietholzbach	1596	587	1011	1013	385	494	132	-2	0.796	0.825

CONCLUSIONS

- Long-term observations, in situ measurements and special investigations in selected sites and research catchments are very important for the investigation of long-term behaviour of the water balance elements and for a successful calibration and validation of hydrological models and their components.
- The precipitation measurement errors in the Rietholzbach catchment are considerable, especially in the winter months due to the wind effect, and can be evaluated by the above-mentioned methods.
- Detailed modelling of the runoff hydrograph and of the water balance elements in mountainous catchments needs to consider the spatial variability in topography, landuse, soil characteristics and meteorological inputs.
- Interflow is the dominating runoff component in this catchment. Depending on the concepts of the applied models, the contributions of the various runoff components to the total runoff can be different.

REFERENCES

Gurtz, J., Zappa, M., Jasper, K., Verbunt, M., Badoux, A., Vitvar, T., Lang, H. (2000) Modelling of runoff and its components and model validation in Swiss Pre-Alpine and Alpine catchments. In: Leibundgut, Ch., Uhlenbrook, S., and McDonnell, J. (Eds.) 2000. Runoff Generation and

Implications for River Basin Modelling. Proceedings of the International Workshop 9-13 October 2000, *Freiburger Schriften zur Hydrologie 13*, Institute of Hydrology, University of Freiburg i.Br., Germany, 206-220.

Gurtz, J., Zappa, M., Jasper, K., Lang, H., Verbunt, M., Badoux, A., Vitvar, T . (2003) A Comparative Study in Modelling Runoff and its Components in Two Mountainous Catchments. *Hydrological Processes*, 17, in print.

Kirnbauer, R., Lang, H., Forster, F. (2000) Hydrological research basins - Sources of information for science and practice. (in German), *Österreichische Wasser- und Abfallwirtschaft,* 52, 87-94.

König, P., Lang, H., Schwarze, R. (1994) On the runoff formation in the small pre-alpine research basin Rietholzbach. Proceedings of the Braunschweig Conference in October 1993 *"FRIEND: Flow Regimes from International Experimental and Network Data"*, IAHS Publ. no. 221, 391-398.

Menzel, L. (1997) Modellierung der Evapotranspiration im System Boden-Pflanze-Atmosphäre. *Zürcher Geographische Schriften*, Heft 67, Geographisches Institut der ETH Zürich, 1-128.

Moesch, M. (2001) Untersuchungen zur hydrologischen und klimatologischen Charakterisierung des Forschungsgebietes Rietholzbach. Diploma thesis, Institute of Climate Research, ETH Zurich.

Pos, F. (2001) Spatially distributed modelling of snow accumulation and melt in pre-alpine and alpine catchments. Diploma thesis, Institute of Climate Research, ETH Zurich and Wageningen University.

Sevruk, B. (1983) Correction of measured precipitation using the water equivalent of new snow. *Nordic Hydrology*, 14, 2, 49-58.

Vitvar, T., Gurtz, J., H. Lang, H. (1999) Application of GIS-based distributed hydrological modelling for estimation of water residence times in the small Swiss pre-alpine catchment Rietholzbach. *Integrated Methods in Catchment Hydrology-Tracer, Remote Sensing and New Hydrometric Techniques*. Proceedings of IUGG 99 Symposium HS4, Birmingham, July 1999, IAHS Publ. No. 258, 241-248.

MONITORING AND MODELLING OF LONG-TERM CHANGES IN THE STREAMWATER CHEMISTRY OF TWO SMALL CATCHMENTS WITH CONTRASTING VULNERABILITY TO ACIDIFICATION

Pavel Krám[1], Jakub Hruška[1], Kevin Bishop[2]

[1]*Czech Geological Survey, Dept. of Geochemistry, Klárov 3, 118 21 Prague 1, Czech Republic; kram@cgu.cz*
[2]*Swedish University of Agricultural Sciences, Dept. of Environ. Assessment, POB 7050, Uppsala, SE-750 07 Sweden*

ABSTRACT

Long-term streamwater patterns in two catchments underlain by different bedrock (leucogranite at Lysina vs. serpentinite at Pluhův Bor) were studied by intensive field monitoring in 1989-2002 and computer modeling which simulated the period 1851-2030. A marked decrease in the concentration of acidifying compounds including sulfate was evident in the monitored precipitation inputs. Streamwater sulfate declined at mean rates of 28 μeq L^{-1} yr^{-1} (Lysina) and 50 μeq L^{-1} yr^{-1} (Pluhův Bor) during the monitoring period. At the chronically acidic Lysina catchment, pH increased at a mean rate of 0.02 pH units yr^{-1}, however pH did not change appreciably at Pluhův Bor. Rates of the decrease in sulfate concentration in the streamwater at Lysina and Pluhův Bor were faster than the declines in any other reported European catchment. Pre-industrial streamwater pH of 5.5 was simulated by the MAGIC model at Lysina. According to the model, the pH dropped below 3.9 in the 1980s and should increase to 4.3 by 2030. Soil base saturation declined dramatically from about 25% to only 6% at Lysina. This severely acidified site will not return to good environmental conditions in the upcoming decades. According to MAGIC, pH was at a similar level (between 6.9 and 7.2) during the whole simulation period as well as the soil base saturation (between 84 and 95%) at the acid resistant Pluhův Bor catchment. Therefore it is obvious that the Pluhův Bor was able to mitigate long-term acidification. The two catchments served as valuable end-members of central European spruce regions of middle altitude.

Keywords acidification recovery, Czech Republic, leucogranite, long-term monitoring, MAGIC model, serpentinite, small catchments, water chemistry

INTRODUCTION

Severe impacts of air pollution on forested and aquatic environments were documented in the Czech Republic (Moldan and Schnoor, 1992). There is an interest in long-term monitoring of small forested catchments to document changes in biogeochemical patterns (Likens et al., 1996). There is also considerable interest in computer simulations of these patterns (Tiktak and van Grinsven, 1995), especially the predicted recovery from acidification (Evans et al., 2001).

The main objective of this study was to investigate long-term streamwater patterns in two catchments with different geology. These catchment serve as end-members of sensitivity to acidic atmospheric deposition. Another objective was to simulate expected recovery after a decade of massive reduction of sulfur emissions in the "Black Triangle" of central Europe. The MAGIC model was also tested in this application in very acidic as well as alkaline environments.

SITE DESCRIPTION AND METHODS

The catchments are situated in the Slavkov Forest (Slavkovský les), in western Bohemia, Czech Republic (Fig 1). The 27.3 ha Lysina catchment is underlain by base cation-poor leucogranite and the 22.0 ha Pluhův Bor catchment is underlain by base cation-rich (predominantly Mg) serpentinite. They are both forested mainly by Norway spruce *(Picea abies)* plantations, and they are located only 7 km apart. The spruce stands have an average age of 50 years at Lysina. At Pluhův Bor, the dominant spruce stands are about 100 years old. The elevation at Pluhův Bor is slightly lower than at Lysina (Fig 1). Mean annual air temperature is 5°C at Lysina and 6°C at Pluhův Bor.

Surface water flow from the catchments was monitored continuously since 1989 at Lysina and 1991 at Pluhův Bor using V-notch weirs and water level recorders. Runoff samples were collected usually weekly. Bulk precipitation from the open areas was collected since 1990, and throughfall (precipitation below tree canopy) since 1991. Soils were sampled mainly in 1993, tree tissue samples were collected in 1994. Procedures for chemical analyses are described in detail in Krám et al. (1997).

MAGIC (Model of Acidification of Groundwater in Catchments) was designed to reconstruct the historical development of acidification and to predict future drainage water and soil chemistry (Cosby et al., 1985). It uses a lumped representation of geochemical processes in the catchment. Water fluxes, atmospheric deposition, net vegetation uptake, weathering rates, and properties of organic acids are required as external inputs to the model. MAGIC simultaneously solves equilibrium reactions between the soil exchanger and soil solution, usually in annual time steps. The simulation outputs are fluxes and volume-weighted concentrations in soil water and surface water as well as basic soil chemistry. Version 5.01 of MAGIC (Cosby, 1991) was used in this application.

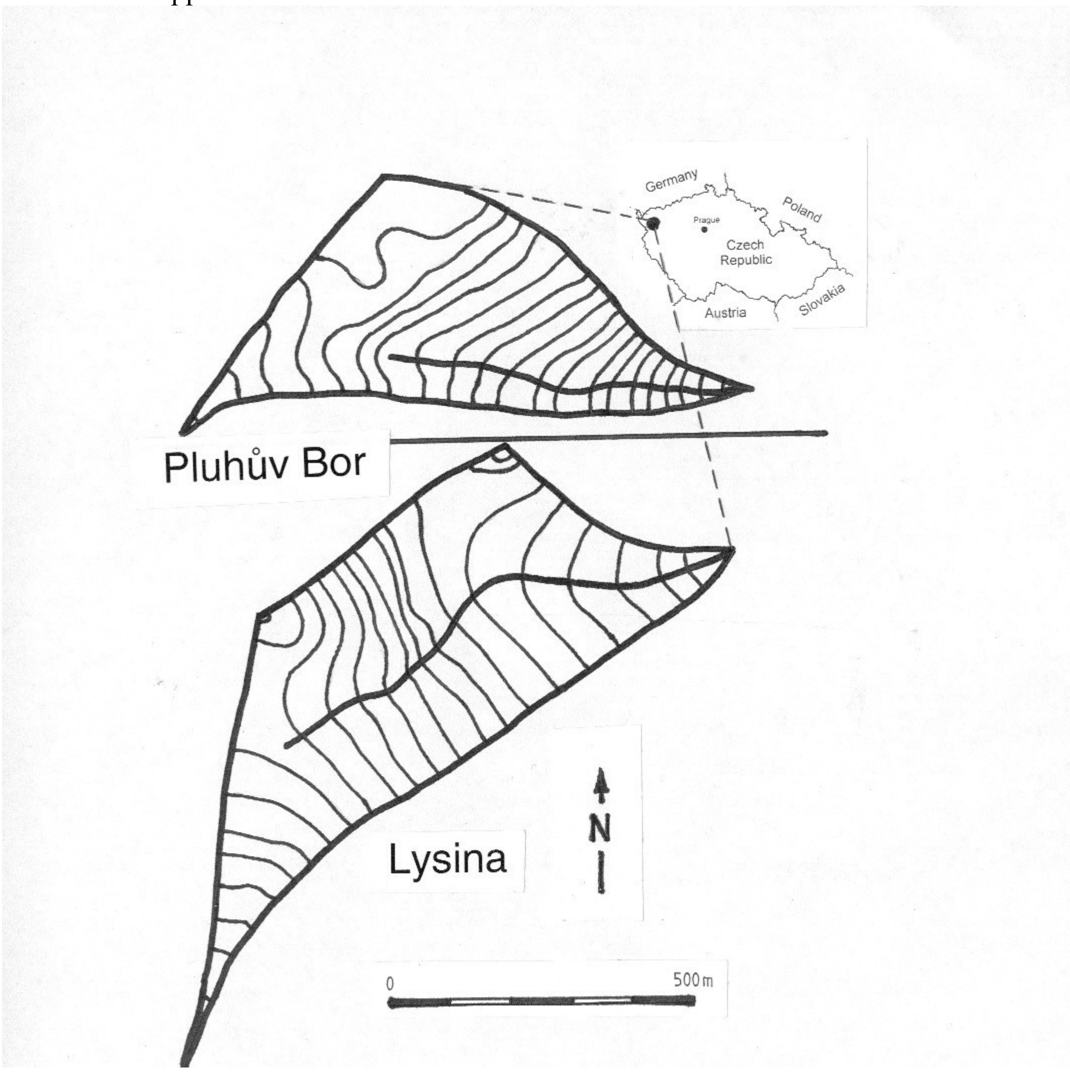

Fig 1: Maps of the Lysina and Pluhův Bor catchments in the western Czech Republic. Topographic contours are shown every 5 meters. Elevation range of Lysina is 829-949 m a.s.l., the elevation of Pluhův Bor is 690-804 m a.s.l. Only the major stream channels are shown.

RESULTS AND DISCUSSION

Pluhův Bor is drier than the Lysina catchment. Mean annual precipitation in open areas was about 950 mm at Lysina compared to approximately 850 mm at Pluhův Bor. Less precipitation at Pluhův Bor reflects its lower altitude compared to Lysina and partially also a rainfall shadow east of the major peaks of the Slavkov Forest. Mean annual throughfall was approximately 820 mm at Lysina, and 670 mm at Pluhův Bor. The lower throughfall flux was influenced by slightly higher temperatures at Pluhův Bor. Annual runoff averages are 430 mm at Lysina and 270 mm at Pluhův Bor. Calculated evapotranspiration was 390 mm at Lysina and 400 mm at Pluhův Bor, given the reported throughfall and runoff values and the assumption of zero storage.

Lysina exhibited incomplete neutralization of mineral acids and it showed low streamwater pH (Fig 2) and higher concentrations of Al. Pluhův Bor exhibited efficient neutralization of acids by weathering of Mg-rich silicates. It showed near neutral streamwater pH (Krám et al., 1997, 2000). Measured Gran alkalinity (by titration) was always negative at Lysina, even during baseflow conditions (Fig 3). However the alkalinity was very high at Pluhův Bor, except during snowmelt periods or large storms.

Marked decreases in the concentration of major acidifying compounds (SO_4, F, H), dust representing solutes (Al, Si) and trace metals (As, Pb, Be) was evident in the bulk precipitation and throughfall during the 1990s. The strong decline in atmospheric deposition of sulfur in the study area in the 1990s (Hruška et al., 2002) resulted in changes of streamwater chemistry in the study catchments. Time series of streamwater concentrations showed a significant decrease of SO_4 at Lysina and Pluhův Bor over the periods 1989-2001 and 1991-2001, respectively. SO_4 declined at mean rates of 28 μeq L^{-1} yr^{-1} (Lysina) and 50 μeq L^{-1} yr^{-1} (Pluhův Bor). Annual volume-weighted mean SO_4 declined from 568 μeq L^{-1} in 1990 to 232 μeq L^{-1} in 2000 at Lysina (Fig 4), while pH increased at a mean rate of 0.02 pH units yr^{-1}. Pluhův Bor experienced an extremely large decline of SO_4 from 1035 μeq L^{-1} in 1992 to 332 μeq L^{-1} in 2000. Despite the large decrease in SO_4 concentrations, pH did not change appreciably at Pluhův Bor. A decrease in concentrations of Mg (13 μeq L^{-1} yr^{-1}) and Ca (2 μeq L^{-1} yr^{-1}) were observed in this catchment. At Lysina the decline of SO_4 was accompanied by a decrease of base cations at a mean rate of 16 μeq L^{-1} yr^{-1} (11 μeq L^{-1} yr^{-1} by Ca, 3 μeq L^{-1} yr^{-1} by Mg). Charge balance acid neutralization capacity (ANC) increased by 15 μeq L^{-1} yr^{-1} at Lysina and by 35 μeq L^{-1} yr^{-1} at Pluhův Bor. Rates of the decrease in the concentration of sulfate and the increase of ANC in the streamwater at Lysina and Pluhův Bor were faster than the changes in any other monitored European catchments (Evans et al., 2001; Fölster and Wilander, 2002).

The MAGIC model (Cosby, 1991) was applied to estimate streamwater and soil chemistry between 1851-2030 at Lysina (Hruška et al., 2002) and at Pluhův Bor. Estimated atmospheric deposition was used for 1851-1989, and the measured deposition was used in 1990-2000. The average of the measured deposition from the last two years (1999-2000) was applied for the future deposition in 2001-2030. According to the MAGIC simulation, sulfate concentrations in streamwater peaked in the middle 1980s (Fig 4), several years after the peak of sulfur deposition in 1979 (due to soil adsorption of part of the incoming sulfur). Similarly the decrease of concentrations of sulfate will be slowed down partially by desorption of previously stored sulfur in the soil. Both catchments should be close to a new equilibrium with respect to sulfur in 2030. Streamwater pH at Lysina will increase to 4.3 (Fig 5), and soil base saturation will increase to 6.2% by 2030 (from a minimum of 5.7% estimated for 2002). Pre-industrial pH was estimated to be 5.5 and soil base saturation 24.7%. The loss of base cations was caused predominantly by atmospheric acidity, but intensive forestry was responsible for approximately one third of the net base cation loss via accumulation in harvested biomass at Lysina (Hruška et al., 2002). Severely damaged sites, under continued pressure from forestry, will not suddenly (if ever) return to a good environmental condition when the acid deposition input is only partially reduced. According to MAGIC, the Pluhův Bor streamwater pH will stabilise by 2030 (pH 7.1) at a level similar to the simulated pre-industrial value (pH 7.2) (Fig 5). Similarly, soil base saturation, simulated as 95% in 1851, declined to 84% in 1993 and was predicted to remain at 84% in 2030.

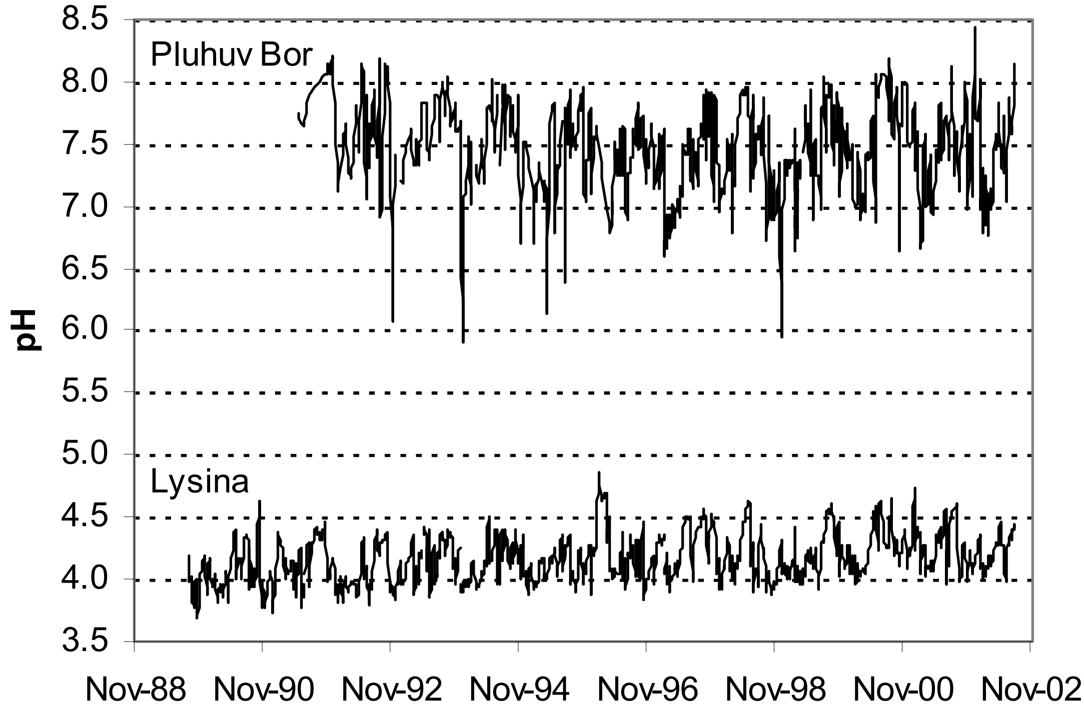

Fig 2: Measured streamwater pH at Lysina and Pluhův Bor catchments for 1989-2002.

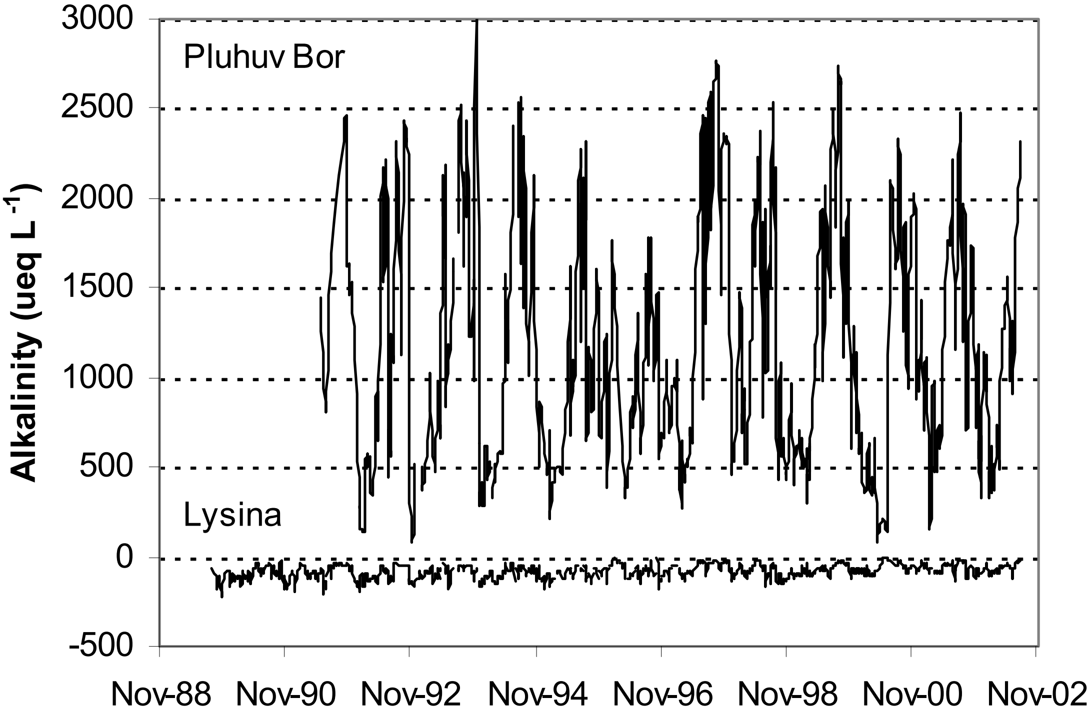

Fig 3: Measured streamwater Gran alkalinity at Lysina and Pluhův Bor catchments for 1989-2002

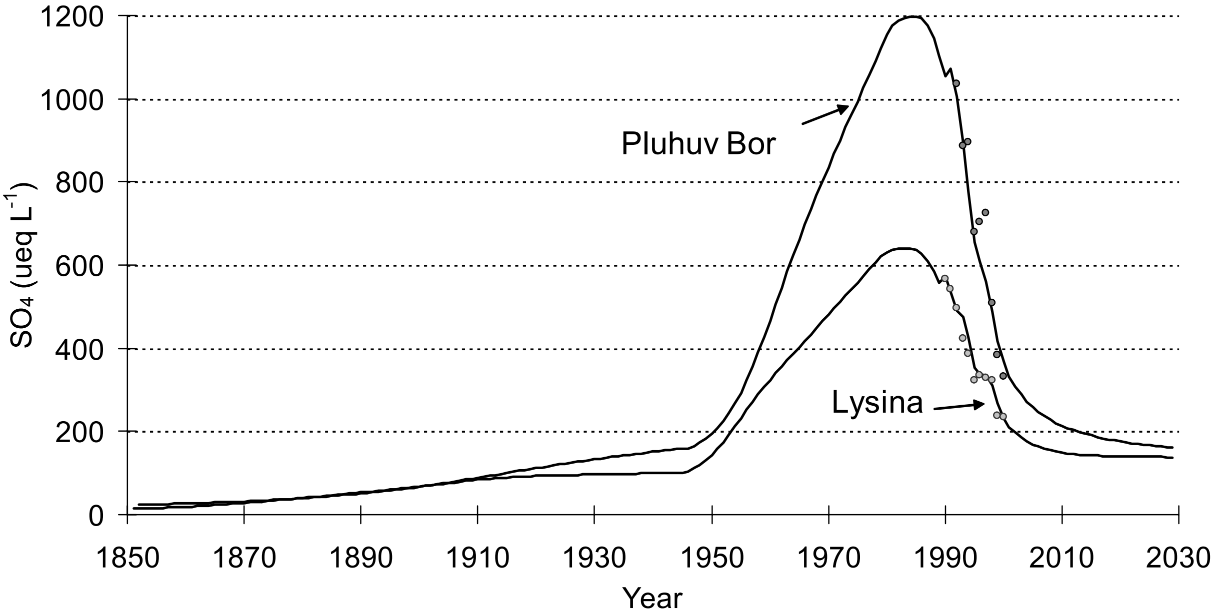

Fig 4: Observed (dots) and simulated (lines) changes in annual volume-weighted streamwater concentrations of sulfate at Lysina and Pluhův Bor catchments. Estimated deposition was used for 1851-1989, measured deposition was used for 1990-2000, and the average deposition of 1999-2000 was used for the forecast period 2001-2030.

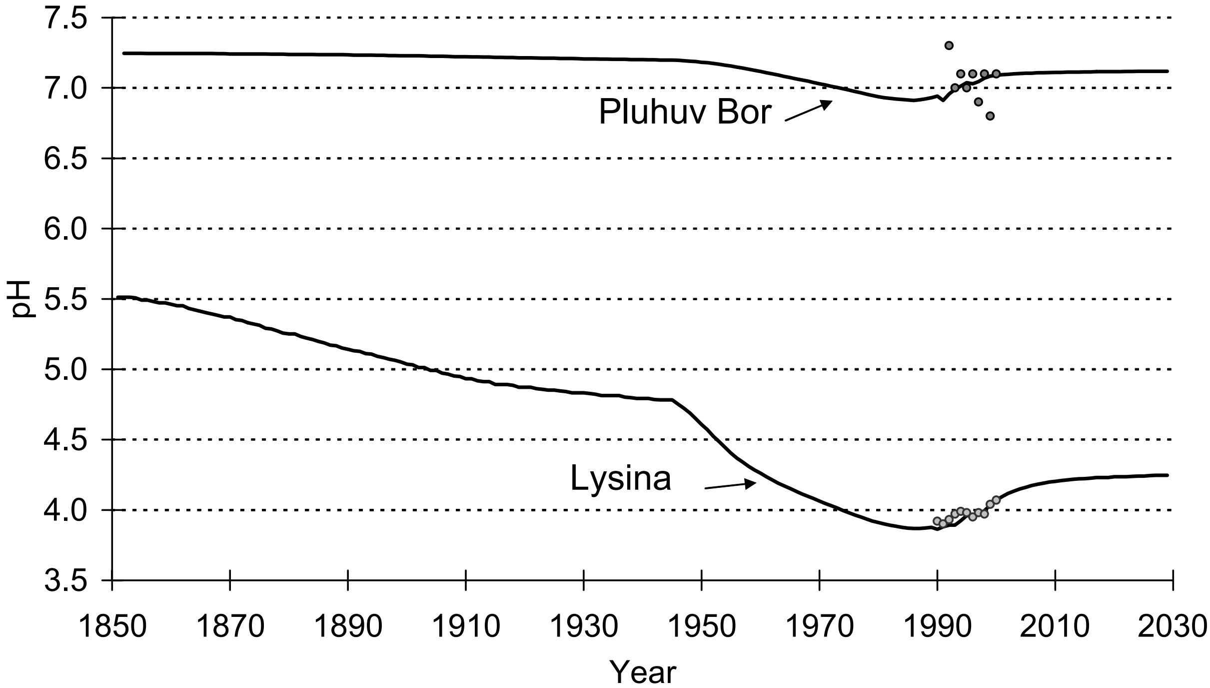

Fig 5: Observed (dots) and simulated (lines) changes in annual volume-weighted streamwater pH at Lysina and Pluhův Bor catchments. Estimated deposition was used for 1851-1989, measured deposition was used for 1990-2000, and the average deposition of 1999-2000 was used for the forecast period 2001-2030.

The most pronounced difference between the catchments, which caused marked differences in long-term responses to acidic inputs, is the weathering rate. Weathering of base cation (Ca+Mg+K+Na) was estimated to be only 62 meq m^{-2} yr^{-1} in the granitic Lysina catchment, but for the serpentinite at Pluhův Bor, a weathering rate of 241 meq m^{-2} yr^{-1} (96% of Mg) was estimated. Predicted recovery of biologically important parameters is small in streamwater and soil compared to the pre-industrial estimate at the chronically acidified Lysina catchment. The acid resistant Pluhův Bor catchment, however, was able to mitigate significant long-term surface water acidification. The MAGIC model simulated successfully both the acidic and alkaline catchments.

CONCLUSIONS

The Lysina and Pluhův Bor catchments served as valuable end-members of ecosystem behaviour in the period of marked acidification and recovery. The Lysina catchment was significantly acidified in the past and predicted recovery is very small in comparison to the estimated pre-industrial pH. Pluhův Bor was able to mitigate long-term acidification. It was partially acidified only during short-term hydrological episodes.

ACKNOWLEDGEMENTS

This study was supported by the Grant Agency of the CR (grant 526/01/1135). Significant part of the field water sampling was performed by Václav Kmínek and Jiří Václavek. We appreciate the help of Bedřich Moldan, Charles T. Driscoll, Chris E. Johnson and Filip Moldan during different stages of our research. Helpful comments were provided by anonymous reviewers.

REFERENCES

Cosby, B.J. (1991) MAGIC (Model of Acidification of Groundwater In Catchments), version 5.01. Executable file. Norwegian Institute for Water Research (NIVA), Oslo.

Cosby, B.J., Hornberger, G.M., Galloway, J.N., Wright, R.F. (1985) Time scales of catchment acidification. *Environmental Science and Technology*, vol. 19, 1144-1149.

Evans, C.D., Cullen, J.M., Alewell, C., Kopáček, J., Marchetto, A., Moldan, F., Prechtel, A., Rogora, M., Veselý, J., Wright, R. (2001) Recovery from acidification in European surface water. *Hydrology and Earth System Sciences*, vol. 5, 283-297.

Fölster, J., Wilander, A. (2002) Recovery from acidification in Swedish forest streams. *Environmental Pollution*, vol. 117, 379-389.

Hruška, J., Moldan, F., Krám, P. (2002) Recovery from acidification in central Europe – observed and predicted changes of soil and streamwater chemistry in the Lysina catchment, Czech Republic. *Environmental Pollution*, vol. 120, 261-274.

Krám, P., Hruška, J., Wenner, B.S., Driscoll, C.T., Johnson, C.E. (1997) The biogeochemistry of basic cations in two acid-impacted forest catchments with contrasting lithology. *Biogeochemistry*, vol. 37, 173-202.

Krám, P., Hruška, J., Driscoll, C.T. (2000) Biogeochemistry of forest catchments with contrasting lithology. In: V. Elias and I.G. Littlewood (eds.) *Catchment hydrological and biochemical processes in the changing environment*, International Hydrological Program-V, Technical Documents in Hydrology, No. 37, UNESCO, Paris, 65-72.

Likens, G.E., Driscoll, C.T., Buso, D.C. (1996) Long-term effects of acid rain: response and recovery of a forest ecosystem. *Science*, vol. 272, 244-246.

Moldan, B., Schnoor, J. (1992) Czechoslovakia: examining a critically ill environment. *Environmental Science and Technology*, vol. 26, 14-21.

Tiktak, A., van Grinsven, H.J.M. (1995) Review of sixteen forest-soil-atmosphere models. *Ecological Modelling*, vol. 83, 35-54.

RECONSTRUCTING GROUNDWATER LEVEL FLUCTUATIONS IN THE 20TH CENTURY IN THE FORESTED CATCHMENT OF DRWINKA (NIEPOŁOMICE FOREST, S. POLAND)

Wojciech Chełmicki[1], Stanisław Ciszewski[2], Mirosław Żelazny[1]

[1]*Jagiellonian University, Institute of Geography and Spatial Management, Kraków, Poland.*
[2]*Stanisław Staszic University of Mining and Metallurgy, Dept. of Computer Science, Kraków, Poland.*

ABSTRACT

The paper presents a method of groundwater level reconstruction in the Niepołomice Forest during a period with no available instrumental measurement records. A neural network model was developed using measured average monthly air temperature, total precipitation and average groundwater level data. The data were then extrapolated spatially using linear regression between one-year-long groundwater level data from different forest sites. The groundwater levels were adjusted with trial correction for changes in water consumption due to the tree-stand ageing.

Keywords groundwater levels, neural networks, forested catchments

INTRODUCTION

The Drwinka catchment drains part of the Niepołomice Forest located near one of Poland's largest industrial enterprises, an early 1950s steel plant in Nowa Huta, Kraków. Over the last 50 years, extensive industrial emissions were influencing the local forest environment. The magnitude of this influence and the resulting destruction have been investigated by many forest-ecology teams (Kleczkowski, 1981; Grodziński et al., 1984; Weiner et al., 1998). The groundwater table, along with industrial emissions, has the potential to influence the state of the forest. Information on groundwater levels before and after the opening of a steel complex should make an assessment possible as to what extent the groundwater table fluctuations have been influencing the state of the forest environment, and to what extent its destruction has resulted from industrial emissions.

The paper aims at reconstructing the groundwater fluctuations in the Drwinka forested catchment for the period 1901-1960, using the available groundwater table data for 1961-2000 and meteorological data for the whole 20th century.

The Niepołomice Forest and the Drwinka catchment are situated in the Vistula River valley, between the Vistula itself and its tributary Raba River, at 190-214 m a.s.l. The dominant bedrock is Pleistocene sand, clay and gravel of glacifluvial and fluvial origin covering deeper layers of the Miocene silt and clay. The sand has been partly wind-transformed and forms chains of dunes. The groundwater table depth is usually between 1-4 m, except at glacifluvial hills and dunes, where it locally exceeds 8-10 m below the surface. The dominant plant communities include coniferous fresh and wet mixed forests (50%), deciduous forests (24%) and fresh and wet mixed forests (20%) (Kleczkowski, 1981).

RECONSTRUCTION OF GROUNDWATER LEVEL FLUCTUATIONS

The only groundwater monitoring well in the Niepołomice Forest in Poszyna (Fig 1) provided weekly records from as early as 1953, but reliable data without major gaps are available since 1961. Other sites distributed around the Niepołomice Forest were operating irregularly and only for short periods. In contrast to this patchy picture, very long and reliable meteorological data series (air temperature and precipitation since the mid 18th century) are available for the nearby city of Kraków (20 km west). Assuming a relationship between the meteorological and groundwater variables and provided meteorological data for 1901-2000 (Kraków) and the groundwater table data for 1961-2000 (Poszyna), the authors embarked on building a neural-network model (Masters 1996) with the aim to use it in reconstructing groundwater level fluctuations at Poszyna prior to 1961.

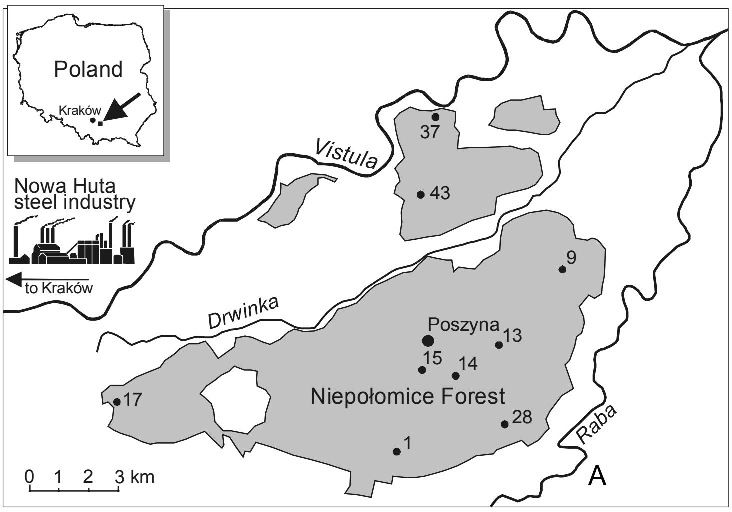

Fig 1: Location of the Drwinka catchment and groundwater measuring sites in the Niepołomice Forest.

Neural network modelling procedure

The predictor concept was applied to solve the issue of groundwater level modelling based on artificial neural networks. A predictor is a conversion of past data series into a simulated present value. The artificial neural network learning method is a classical algorithm of back-propagation with momentum, mixed with pruning by optimal brain surgery (Stork and Hassibi, 1993).

The neural model was applied to fill the gaps in the data series and to reconstruct the groundwater level fluctuation history. The following values were used in the model development: average monthly groundwater table data (Poszyna), average monthly air temperatures (Kraków) and monthly precipitation totals (Kraków), during 1961-2000.

To build the neural model the following questions had to be answered: (1) Are the Krakow meteorological data and the Poszyna hydrological data sufficient to model groundwater table fluctuations at Poszyna? (2) Is the Krakow meteorological series sufficient as input to model groundwater table fluctuations at Poszyna?

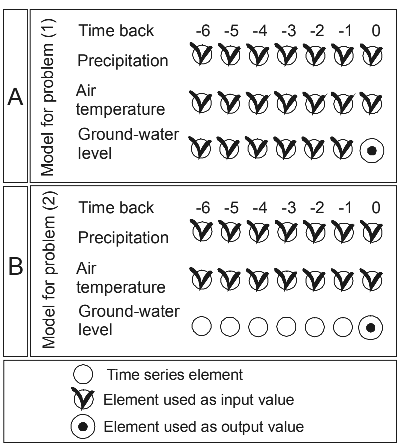

Fig 2: Time series elements used in experiments

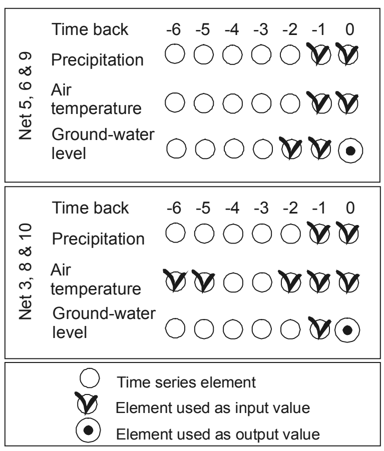

Fig 3: Time series elements used by nets.

To answer the first question in an experimental way a model was built that derived future groundwater table values at Poszyna using both the Krakow weather data and the past groundwater table data from Poszyna (Fig 2A). The transformation sought (model structure) had to turn these data strings into single water table values.

The learning process involved seeking *nets*, which minimised the following formula:

$$\Sigma\| \text{net}(P_{t-6}..., P_t, T_{t-6},..,T_t,H_{t-6,...,}H_{t-1}) - H_t\|^2 \rightarrow \min \tag{1}$$

where $\|.\|$ was an Euclidean standard and P_t, T_t and H_t denoted, respectively, monthly total precipitation, average air temperature and average water table values at a given time t. The data was subject to linear transformation into the range [0.02, 0.98]. Then, for each of the issues, separate sets were built consisting of all (452) 7-components of the time series corresponding to the input and output of the models. The learning sets were created by random selection of 300 components. The remaining components constituted an independent testing set. Identical learning processes were applied based on the standard back-propagation with momentum method. A perceptron with one hidden layer and sigmoid activations is the architecture. To optimise the architecture, a series of experiments was performed where the network was trained for a defined period of time and various learning factors. The best of such networks were then selected and subjected to pruning with the Optimal Brain Surgery method (Stork and Hassibi, 1993). The final step involved yet another selection of the best solutions which were trained again on small learning factors.

The pruned networks contain lower numbers of input units and a much lower number of links. Fig 3 summarises the input parameters, while Table 1 shows the experiment results.

Table 1: Error measures for the best nets in the first numerical experiment.

Learning set										
Measure\Net	1	2	3	4	5	6	7	8	9	10
Median [cm]	6.6	5.7	6.5	6.3	6.1	6.1	6.2	6.3	6.3	5.5
Mean [cm]	8.1	7.1	7.9	7.5	7.7	7.7	7.3	7.8	7.8	7.4
Std. dev. [cm]	6.7	5.5	6.5	5.7	6.3	6.3	5.6	6.4	6.5	6.5
Correlation coef.	0.95	0.96	0.95	0.96	0.95	0.95	0.96	0.95	0.95	0.95
Testing set										
Measure\Net	1	2	3	4	5	6	7	8	9	10
Median [cm]	8.0	7.1	6.4	6.7	6.2	6.2	6.5	6.5	6.4	6.4
Mean [cm]	9.3	8.3	8.2	8.2	8.3	8.3	8.2	8.3	8.3	8.4
Std. dev. [cm]	7.1	6.3	6.6	6.6	7.0	7.0	6.6	6.5	7.2	6.5
Correlation coef.	0.94	0.96	0.96	0.95	0.95	0.95	0.96	0.95	0.95	0.95

Shadowed columns show the measures before pruning, non-shadowed after pruning

Table 2: Error measures for the best nets in the second numerical experiment.

Learning set										
Measure\Net	1	2	3	4	5	6	7	8	9	10
Median [cm]	11.0	16.3	12.8	11.2	11.7	12.1	11.9	11.3	11.3	11.4
Mean [cm]	15.2	20.5	15.6	15.2	15.5	15.8	15.4	15.1	15.3	15.5
Std. dev. [cm]	13.0	16.5	12.8	12.9	12.8	12.9	13.2	12.9	12.9	13.0
Correlation coef.	0.81	0.73	0.81	0.81	0.81	0.80	0.81	0.82	0.81	0.81
Testing set										
Measure\Net	1	2	3	4	5	6	7	8	9	10
Median [cm]	13.8	16.3	14.1	13.8	13.0	15.2	13.5	13.9	14.4	14.8
Mean [cm]	17.7	20.1	18.0	17.7	17.6	18.1	17.7	17.7	17.7	17.7
Std. dev. [cm]	14.5	16.2	15.3	14.5	15.3	14.3	14.4	14.6	14.2	14.4
Correlation coef.	0.72	0.70	0.71	0.72	0.71	0.72	0.73	0.72	0.72	0.72

Shadowed columns show the measures before pruning, non-shadowed after pruning

Two architecture types clearly emerged after pruning. The first is represented by network No. 5, 6 and 9 involving two elements of each time series (hydrological/meteorological parameters). The other type of networks (3,8 and 10) only used a single value of the water table and relied heavily on multiple historical air temperature values.

To answer the second question a model was required that would only rely on the Kraków meteorological data to yield groundwater table values at Poszyna (Fig 2B). A model based on this relationship can be used to fill the gaps and reconstruct groundwater table levels, because there are no groundwater table values at the input. Here, the minimised formula has the following form:

$$\Sigma\| \text{net}(P_{t-6}..., P_t, T_{t-6},..,T_t) - H_t\|^2 \rightarrow \min \quad (2)$$

For the independent test set the error measures are shown in Table 2. Although the results were not as good as in the previous case they were still useful in obtaining values close to the real ones. This model was used to perform a full conversion of the Kraków meteorological data into the Poszyna groundwater level series. Comparison of measured and simulated groundwater levels is shown in Fig 4.

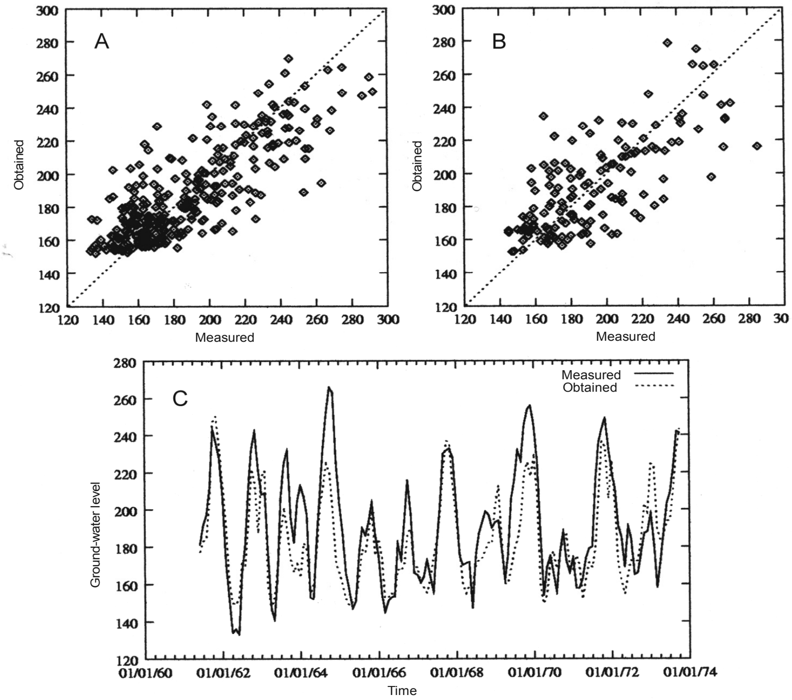

Fig 4: Comparison of the measured and simulated groundwater levels for learning (A) and test (B) sets and comparison of the course of measured and simulated groundwater levels (C) obtained in the second numerical experiment for the example net.

Assigning groundwater fluctuations in different parts of the catchment area

Both the reconstructed and observed groundwater levels at Poszyna mirrored periods of dry, medium and wet years. Having the groundwater levels for Poszyna available for the whole 20th century, the next step of the procedure was to reconstruct groundwater table fluctuations in other parts of the catchment area. In order to find the relationship between groundwater fluctuations at Poszyna and other parts of the catchment, nine piezometric wells were set up in different parts of the forest, and then used for a one-year-long (May 1999-April 2000) monitoring, which was simultaneous with the one at Poszyna (Fig 5). The wells were located in tree stands aged at least 100-years, to make future studies possible on the relationship between groundwater levels and annual tree-ring increments.

The one-year-long series of measurements displayed a clear linear relationship between water levels in the piezometric wells and Poszyna. This relationship was used to calculate the groundwater levels at the monitoring sites for the whole 20th century. As the linear relationship between the Poszyna and piezometric wells was based on a one-year-long series of observations, the question rose whether this relationship is valid for the whole 20th century. One of the factors to consider is the changing age of the tree stands and resulting changes in transpiration efficiency influencing groundwater levels over the period studied. An attempt to solve the issue was made using Suliński's formula (1990) illustrating a relationship between the mean groundwater table depth *H* [m], tree stand age *A* [years] and the filtration coefficient in water-bearing deposits *K* [10^{-5} m s^{-1}]:

$$H_A = 40{,}05\ K^{0{,}198}\ A^{0{,}278}\ e^{-0{,}020A} \quad (3)$$

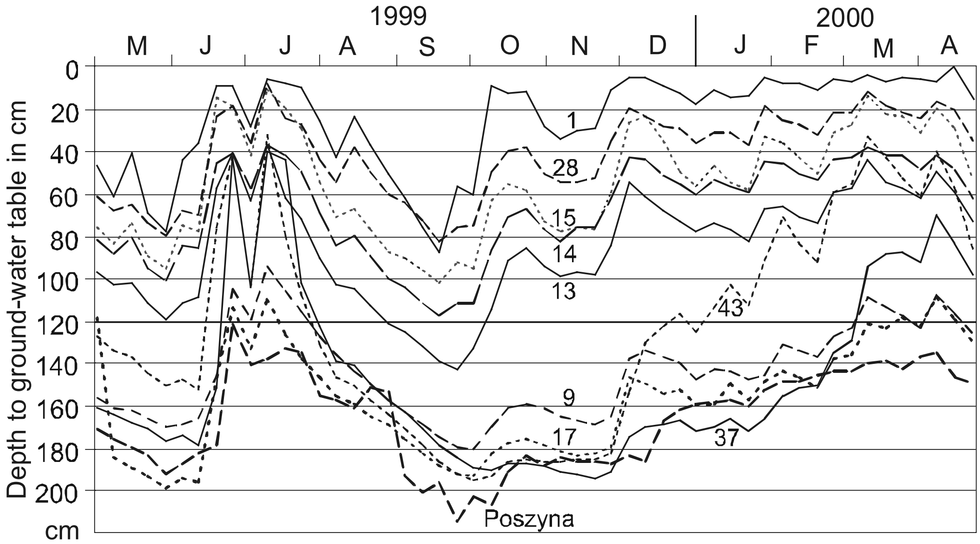

Fig 5: Groundwater levels in Niepołomice Forest from 3 May 1999 to 23 April 2000.

Fig 6 shows the groundwater levels for the 140-year-old pine stand (*Molinio-Pinetum*) at site 15 (A) without any adjustment for tree age, and (B) with adjustment based on the formula (3). The doubts connected with the use of the formula rose due to the unknown effect of tree ageing at the Poszyna well, which is situated in a woodland glade, surrounded by forest with an unknown effect on the groundwater level at the monitoring site. The whole reconstruction procedure is shown in Fig 7.

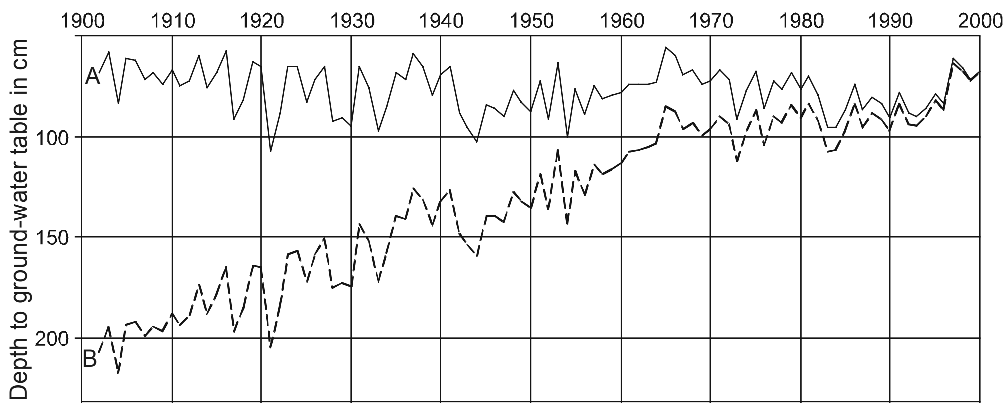

Fig 6: Long-term course of groundwater level at site 15 unadjusted (A) and adjusted (B) for tree-stand age.

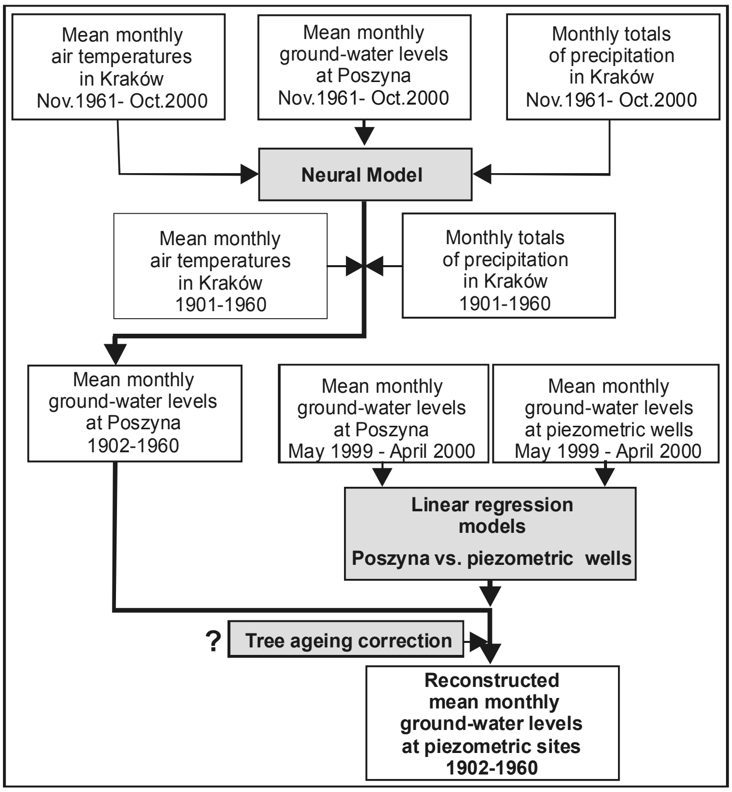

Fig 7: Reconstruction procedure of the groundwater level fluctuations in the Niepołomice Forest.

CONCLUSIONS

Neural networks provide a useful tool for groundwater level modelling based on meteorological variables. They were used to perform a successful conversion of the Kraków meteorological data into the Poszyna groundwater level series. Linear regression between groundwater levels at Poszyna and different forest sites can be used for the spatial extrapolation of data. Further studies are needed to assess the impact of tree ageing on the long-term groundwater level trends.

ACKNOWLEDGEMENTS

The project was sponsored by State Committee for Scientific Research (Project 6P04 F02315/P01).

REFERENCES

Grodziński, W., Weiner, J., Maycock, P. F. (1984) Forest Ecosystems in Industrial Regions. Springer Vlg., Heidelberg.

Kleczkowski, A. S., (ed.) (1981) Resources of the natural environment of the Niepołomice Forest and problems of its protection. (in Polish), *Studia Ośr. Dok. Fizjogr*., 9.

Masters, T. (1996) Neural networks in practice. Programming in language C++. (in Polish), Wyd. Nauk.-Techn., Warszawa.

Stork, D., Hassibi, B. (1993) Second order derivatives for network prunning: Optimal Brain Surgery. In: Sejnowski T.J., Hinton G.E. (ed.), *Advances in Neural Information Processing Systems (NIS)*, 5, Morgan Kaufmann Publ. Inc., San Mateo.

Suliński, J. (1990) Influence of the age of pine tree stands onto average groundwater levels. (in Polish), *Gosp. Wodna*, 5.

Weiner, J., Fredro-Boniecki, S., Reed, D., Maclean, A., Strong, M. (1998) Niepołomice Forest – A GIS analysis of ecosystem response to industrial pollution, *Env. Pollution*, 98, 3.

LONGTERM EVALUATION OF THE IMPACT OF AFFORESTATION OF ARABLE LAND ON LANDSCAPE WATER BALANCE

Martin Wegehenkel

Institute of Landscape Systems Analysis, Centre of Agricultural Landscape and Land Use Research Eberswalder Str.84, D-15374 Müncheberg, mwegehenkel@zalf.de

ABSTRACT

In this paper, longterm effects of an afforestation scenario on the landscape water balance are analysed using the GIS-coupled conceptual hydrological model THESEUS for the spatially distributed calculation of water balance and discharge. In a regional case study, longterm model runs were performed using a spatial data set from a mesoscale catchment including time series for the period 1953-1997. This catchment is located in the moraine landscape of North-East Germany. For the afforestation scenario, the model calculates a decrease in discharge on the order of 4-50 % with an average of 24 % and an increase in evapotranspiration on the order of 3-31 % with an average of 14 % in comparison with the actual landuse. As a result of the afforestation scenario, extreme peak discharges decrease on the order of 4-5 %.

Keywords afforestation, landscape water balance

INTRODUCTION

Due to a changing agricultural funding policy of the European Communities, a discussion came up, that agricultural areas with a low agricultural production potential should be set aside in the state of Brandenburg, Northeast-Germany (MLUR, 2002). This concerns about 15-20 % of the actual area of arable land (Bork et al., 1995). A suggested future land use of these set-aside areas is afforestation with mixed deciduous forest. Mean annual precipitation rates in Brandenburg range between 480-530 mm y^{-1}, with dry periods in the early summer months (Krumbiegel and Schwinge, 1991). People opposing larger scale afforestation often argue that forests would increase interception as well as evapotranspiration losses and strongly reduce ground water recharge (Bork et al., 1995). To predict the effect of afforestation at the catchment scale, hydrological simulation models were used in several studies (e.g. Bultot et al., 1990; Lukey et al., 2002). In a previous paper, a conceptual hydrological model was tested and calibrated using data from the Stobber catchment located in Brandenburg (Wegehenkel, 2002). Within a simple afforestation scenario, the forested area increases from 34 % to 80 % of the catchment area. The impact of this change in the forest cover was analysed using the calibrated hydrological model (Wegehenkel, 2002). In this paper, results of longterm water balance calculations based on the actual landuse and the afforestation scenario over a time period of 47 years with a focus on extreme precipitation and discharge events will be presented.

MATERIAL AND METHODS

Stobber catchment

The Stobber catchment with an area of 220 km^2 is located about 35 km east of Berlin in the moraine landscape of Brandenburg, North-East Germany. The elevation range is between 5 and 139 m above sea level. The database in the Geographical Information System (GIS) consists of a land use map, soil map, digital elevation model with a grid resolution of 50 m x 50 m, and a map of the river network in the catchment (Fig 1). The actual land use of the Stobber catchment is 51 % arable land and 34 % forests. The remaining 15 % include meadows, settlement areas and water bodies. Most soils in the catchment are of sandy texture indicating relatively high infiltration and percolation rates. The mean channel slope of the river network is $\leq$ 0.1%. The main flow direction is north-east draining into the Odra River (Fig 1). Daily values of precipitation, air temperature, saturation deficit of air, wind speed and solar radiation were available for the period 1953-1997. These data were obtained from a meteorological station in Müncheberg located within the catchment (Fig 1). Annual precipitation for this time period ranged between

412-944 mm y^{-1}, the mean annual rate was 650 mm y^{-1}. Furthermore, daily discharge rates used for the calibration of the model were measured for 1994-1997 at a gauging station located within the catchment (Fig 1). Annual precipitation for the period 1994-97 ranged between 583-855 mm y^{-1}, the mean annual rate was at 673 mm y^{-1}. In comparison with the mean value and the range of annual precipitation obtained from the period 1953-1997, the data from 1994-1997 are representative for the hydrometeorological conditions of the total time period, with some restrictions. A detailed overview of the database and data preprocessing procedures can be found in Wegehenkel and Steidl (2000) and will not be repeated here.

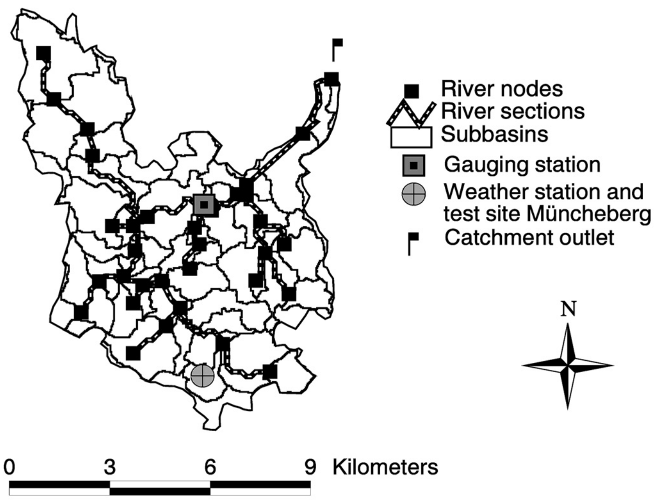

Fig 1: Simplified river network and subbasins of the Stobber catchment (adapted from Wegehenkel and Steidl, 2000).

Table 1: General characteristics of the hydrological model THESEUS.

Spatial discretisation	Hydrotopes, subbasins, catchment
Time discretisation	1 day
Characterisation	Conceptual
Evapotranspiration	PENMAN, HAUDE, TURC, WENDLING, PENMAN-MONTEITH
Vegetation cover	Semi-empirical plant modelling approach
Interception	Single linear storage
Snowmelt	Degree-day approach
Infiltration	Modified Holtan approach
Unsaturated Zone	Multiple layer capacity model
Overland- Channel Flow	Linear storage routing over subbasins and catchments
Saturated Zone	Single linear storage – routed over watersheds and catchment

Simulation model THESEUS

An overview of the hydrological catchment model THESEUS is shown in Table 1.

THESEUS is coupled with a GIS and needs three coverages:

- Hydrotopes - this coverage results from the overlay of the landuse map with the soil map. For each hydrotope, information about the soil type, the soil quality index, the land use class or crop type, the corresponding subbasin, the ground water level and the mean elevation are stored in the database.
- Subbasins (Fig 1) - this coverage results from the GIS-based delineation of the digital elevation model (DEM) and consists of information about the mean elevation and the subsoil of each subbasin.

- Rivernet (Fig 1) - this coverage results from an overlay of the subbasins map, the DEM and river network and includes information about the cross-section profiles and the elevation of the river nodes of each river section as well as a reference to the corresponding downstream river section.

Surface runoff and ground water recharge computed separately for each hydrotope are accumulated for the corresponding subbasin per modelling time step. For each subbasin, accumulated surface runoff is routed by a fast linear storage and accumulated ground water recharge is routed by a slow linear storage. The discharge comprised of the outflows of these two storages is assigned to the corresponding river section of the subbasin. Streamflow through the river network is simulated by a linear storage cascade of all river sections down to the outlet of the catchment. A detailed description of the model can be obtained from Wegehenkel (2002).

Modelling procedures

The model calculations were performed using the actual landuse distribution and an afforestation scenario. In this scenario, all arable land will be afforested with mixed forest (beech-oak) and the forest cover proportion increases from 34 % to 80 % of the total catchment area. The initial soil water contents of all hydrotopes were set equal to the corresponding field capacity. Daily rates of measured precipitation were empirically corrected within the model by multiplying the precipitation rates with a factor of 1.1. Former investigations indicate that the precipitation rates obtained from the weather station Müncheberg can be assumed to be representative for the total Stobber catchment (Wegehenkel and Steidl, 2000). According to Koitzsch and Günther (1990), the maximum interception capacity of crops Sc_{max} was set at 2.5 mm d^{-1}. The maximum interception capacity of forests was set to 6 mm d^{-1} for coniferous, and to 4 mm d^{-1} for mixed and deciduous forests. Results of water balance calculations from different experimental forest test sites in Brandenburg show that these values of Sc_{max} result in the best fit of measured versus simulated canopy interception (Wegehenkel et al., 2001). In this study, measured canopy interception rates were determined by the difference between measured precipitation rates and measured throughfall rates (Wegehenkel et al., 2001). The rooting depth was set to 200 cm for all forest types (Raissi et al., 2002).

RESULTS

Longterm simulations for the Stobber catchment

The model was calibrated using measured daily discharge rates from the period 1994-1997. A detailed description of the calibration procedure and the performance of the model can be obtained from Wegehenkel (2002). The results of the longterm calculations of daily discharge rates for the actual landuse and for the afforestation scenario are presented in Figs 2-4 for selected time periods.

The daily discharge rates obtained for the afforestation scenario are in general lower than those obtained for the actual landuse. This is due to higher evapotranspiration and interception rates of forested areas in comparison with arable land. The most extreme precipitation events occur on 9.6.1953 with a daily rate of 106 mm d^{-1}, on 12.6.1966 with 115 mm d^{-1}, and on 8.8.1978 with the highest recorded daily precipitation rate of 202 mm d^{-1}. For the first event (9.6.1953), the peak discharge for the actual landuse was 9.2 m^3 s^{-1} and for the afforestation scenario 8.7 m^3 s^{-1} (Fig 2). For the second event (12.6.1966), the peak discharge for the actual landuse was 8.3 m^3 s^{-1} and for the afforestation scenario 7.9 m^3 s^{-1} (Fig 3).

For the third event (8.8.1978), the peak discharge for the actual landuse was 16.7 m^3 s^{-1} and for the afforestation scenario 16.0 m^3 s^{-1} (Fig 4). Annual rates of precipitation, actual evapotranspiration and discharge for the Stobber catchment for the time period 1953-97 are shown in Fig 5. For the actual landuse, the mean annual rate of actual evapotranspiration for 1953-97 was 450 mm y^{-1} and the annual rates ranged between 323-531 mm y^{-1}. For the afforestation scenario, the mean annual rate of actual evapotranspiration was 511 mm y^{-1} and the annual rates ranged between 409-582 mm y^{-1}. Annual discharge rates varied between 48-434 mm y^{-1} with an average of 201 mm y^{-1} for the actual landuse, and ranged between 33-366 mm y^{-1} with an average of 155 mm y^{-1} for the afforestation scenario (Fig 5). Annual rates of evapotranspiration calculated according to the afforestation scenario increased on the order of 3-31 % (with an average of 14 %) compared to the evapotranspiration due to the actual landuse.

Annual discharge rates calculated according to the afforestation scenario decreased on the order of 5-40 % (with an average of 24 %) compared to the discharge due to the actual landuse (Fig 5).

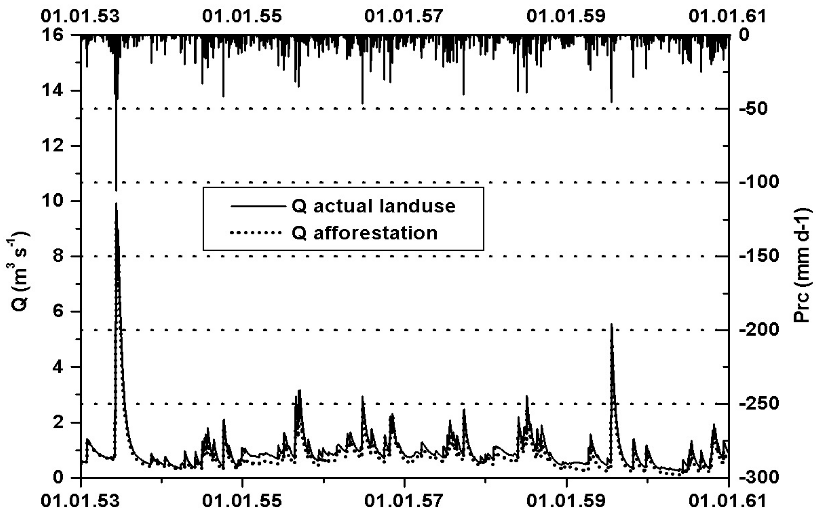

Fig 2: Daily rates of precipitation (Prc) and discharge (Q) simulated according to the actual landuse and according to the afforestation scenario, 1953-1960.

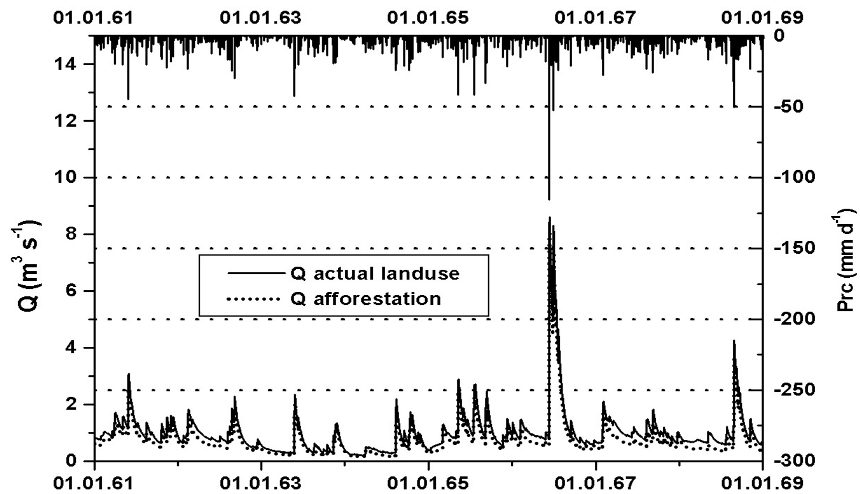

Fig 3: Daily rates of precipitation (Prc) and discharge (Q) simulated according to the actual landuse and according to the afforestation scenario, 1961-1968.

DISCUSSION

The relationship between the change in forest canopy and the catchment water yield depends on the age and the type of forest canopy such as mixed, coniferous and deciduous forests and has been analysed in many papers (e.g. Bosch and Hewlett, 1982; Bultot et al., 1990; Hornbeck et al., 1993; Lukey et al., 2000; Sahin and Hall, 1996; Stednick; 1996). In general, afforestation increases evapotranspiration and interception, and decreases ground water recharge as well as surface runoff. In a study by Bultot et al. (1990), a reduction of the discharge on the order of 18 % was predicted for an afforestation scenario of set-aside areas in a 114 km^2 catchment in Belgium using a calibrated hydrological catchment model. In another study, the SHETRAN model predicted a reduction of annual discharge rates in the case of afforestation on the order of 20-54 % of the discharge simulated on the basis of the actual landuse, for a six-year period with annual rates of precipitation ranging between 878-1012 mm y^{-1} (Lukey et al., 2000). Sahin and Hall (1996) analysed the relationship between forest canopy reduction and change in catchment water yield, analysing data from 145 experiments. According to their results, a 10 % reduction in forest canopy leads to a mean increase in water yield of 20-25 mm y^{-1} for coniferous forests and to a mean increase of 17-19 mm y^{-1} for deciduous forests. Another study by Bosch and Hewlett (1982) using data from 94 experiments reports an average increase in water yield of approximately 40 mm y^{-1} for a 10 % removal of cover in pine forests, and an average increase of 25 mm y^{-1} for a 10 % cover reduction in deciduous forests. Similar results were obtained by Stednick (1996) and Hornbeck et al. (1993). The results for the Stobber catchment are similar to those obtained in the literature. However, the simulated decrease in three extreme peak discharges due to the afforestation scenario was only on the order of 4-5 %.

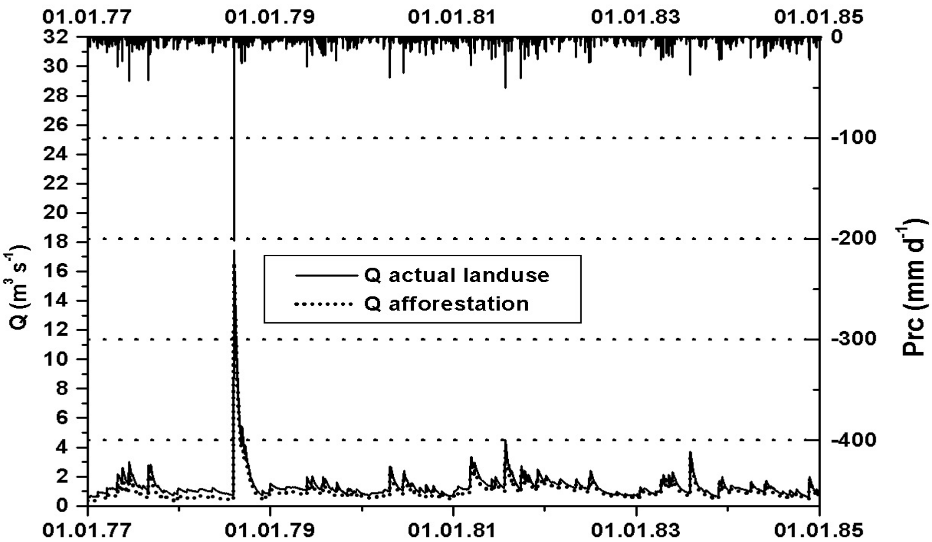

Fig 4: Daily rates of precipitation (Prc) and discharge (Q) simulated according to the actual landuse and according to the afforestation scenario, 1977-1984.

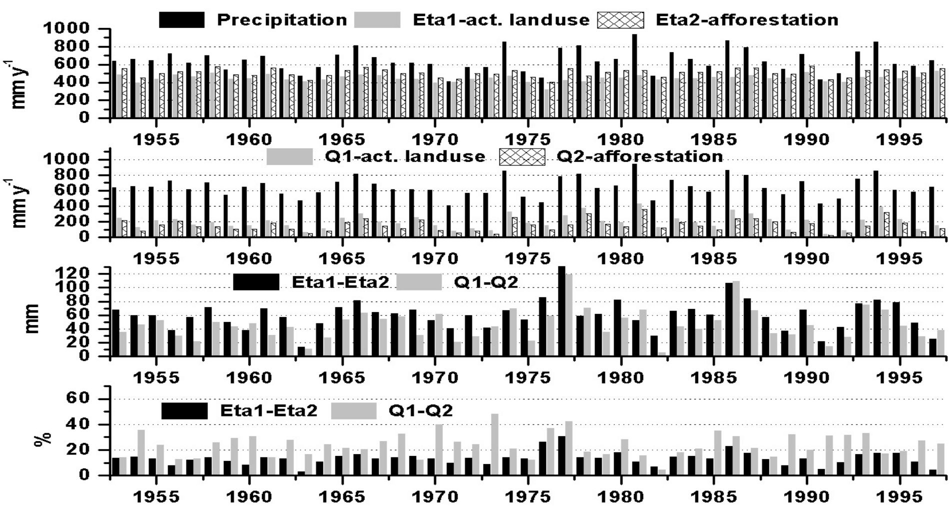

Fig 5: Simulated annual rates of precipitation, evapotranspiration and discharge based on the actual landuse (Eta1, Q1) and the afforestation scenario (Eta2, Q2), differences Eta1-Eta2 as well as Q1-Q2 in mm and in % of Eta1 or Q1 respectively.

CONCLUSIONS

In comparison to short-term studies, long-term simulations give a more detailed overview of the range of climatological conditions, especially precipitation rates, and the range of increasing evapotranspiration and decreasing discharges in the case of afforestation. The results of such simulations can be used for future decisions about the afforestation of distinct areas taking into account criteria such as the amount of ground water recharge which is necessary for the replenishment of the ground water resources. The definition of such thresholds can improve landscape planning issues for the related catchment. The results also indicate that the THESEUS model is sensitive to large changes in forest cover in the catchment. Therefore, the model seems to be an appropriate tool for predicting the impact of such large land use changes. However, further research including model improvement is needed to test the model performance in water balance simulations for additional landuse types.

ACKNOWLEDGEMENTS

The work was funded by the Germany Federal Ministry of Consumer Protection, Food and Agriculture (BMVEL) and the Ministry of Agriculture, Environmental Protection and Landscape Planning (MLUR), Brandenburg.

REFERENCES

Bork, H.R., Dalchow, C., Kächele, H., Piorr, H.P., Wenkel, K.O. (1995) Agrarlandschaftswandel in Nordostdeutschland unter veränderten Rahmenbedingungen – ökologische und ökonomische Konsequenzen. Ernst, Berlin, pp. 419.

Bosch, J.M., Hewlett, J.D. (1982) A review of catchment experiments to determine the effects of vegetation changes on water yield and evapotranspiration. *J. Hydrol*., 55, 3-23.

Bultot, F., Dupriez, G.L., Gellens, G. (1990) Simulation of land use changes and impacts on the water balance – a case study for Belgium. *J. Hydrol*., 114, 327-348.

Hornbeck J.W., Adams B.M., Corbett E.S., Verry E.S., Lynnch P.J. (1993) Long-term impacts of forest treatment on water yield: a summary for northern USA., *J. Hydrol*., 150, 323-344.

Koitzsch R., Günther R. (1990) Modell zur ganzjährigen Simulation der Verdunstung und der Bodenfeuchte landwirtschaftlicher Nutzflächen. *Arch. Acker Pflanzenbau Bodenkd*., 24, 717-725.

Krummbiegel D., Schwinge W. (1991) Witterung-Klima Mecklenburg-Vorpommern, Brandenburg, Berlin. – DWD, Wetteramt Potsdam, pp. 80.

Lukey, B.T., Sheffield, J., Bathurst, J.C., Hiley, R.A., Mathys, N. (2000) Test of the SHETRAN-technology for modelling the impact of reforestation on badlands runoff and sediment yield at Draix, France. *J. Hydrol*., 253, 44-62.

MLUR (2002) Forstliche Rahmenplanung im Land Brandenburg.- http://www.bildung.brandenburg.de/land/mlur/f/rahmen:2,htm.

Raissi, F., Müller, U., Meesenburg, H. (2001) Ermittlung der effektiven Durchwurzelungstiefe von Forst standorten. *Geofakten*, Mr.9, NFLB Hannover.

Sahin, V., Hall, M.J. (1996) The effects of afforestation and deforestation on water yield. *J. Hydrol*., 178, 293-309.

Stednick, J.D. (1996) Monitoring the effects of timber harvest on annual water yield. *J. Hydrol*., 176. 79-95.

Wegehenkel, M., Steidl, J. (2000) Simulation des Wasserhaushaltes in einem Einzugsgebiet der glazial geprägten nordostdeutschen Moränenlandschaft. *Zeitschr. f. Kulturtechnik u. Landentw*., 41, 2, 57-61.

Wegehenkel, M., Jochheim, H., Einert, P., Kallweit, R., Konopatzki, A., Riek, W., Strohbach, B. (2001) Wasserhaushaltssimulation der Level-II-Kiefernbestände Brandenburgs- Vergleich von Speichermodell und deterministischem Modellansatz. *Beitr. f. Forstwirschaft und Landschaftsökologie*, 1, 5-8.

Wegehenkel, M. (2002) Estimating the impact of landuse changes using the conceptual hydrological model Theseus. *Physics and Chemistry of the Earth*, 27, 631-640.

TREND AND CLIMATE CHANGE IMPACT ANALYSES ON THE MESOSCALE

W. Lahmer

Potsdam Institute for Climate Impact Research (PIK), Telegrafenberg, P.O.Box 60 12 03 D-14412 Potsdam, GERMANY, lahmer@pik-potsdam.de

ABSTRACT

Climate change impacts on the regional water cycle belong to the most urgent issues of today's hydrological research. Stronger research efforts are needed especially at the regional and local scale, where political and technical adaptation measures can be taken to avoid critical developments for the environment and society. Studies in the past indicate considerable regional vulnerabilities to changes of both temperature and precipitation patterns. The present study describes a methodology that allows an assessment of the influence of climate change on the mesoscale. Results of a high temporal and spatial resolution modelling approach are presented for the State of Brandenburg in Eastern Germany, which suffers from water deficit. The study indicates strong impacts on various water balance components under changed climatic conditions in the period 1996-2050 and possible water availability problems in the future. Basis for the impact study are trend analyses in Brandenburg, which indicate a significant decrease in percolation for areas with a shallow groundwater table already in the observation period 1961-1998.

Keywords climate change impacts, trend analyses of percolation, State of Brandenburg

INTRODUCTION

Studies of climate change impacts on the hydrological cycle play a growing role in today's hydrological research. Stronger research efforts are needed especially on the regional and local scale, where political and technical measures can be taken to reduce negative effects on the environment and society. Thus, the regional scale is crucial for an improved understanding of climate change and related processes. Both the understanding of global climate systems and human concern about future climatic changes have considerably increased in recent years. Since hydrological processes directly depend on climatic conditions, important consequences are expected in regional hydrological cycles, with subsequent effects on regional water resources. However, influences of climatic changes on these processes will differ from region to region. Which effects will be most relevant depends on the magnitude and spatial distribution of the climatic changes in combination with the hydrologic characteristics of the region. Studies in the last years have shown important regional vulnerabilities to changes of temperature and precipitation patterns (Becker and Lahmer, 1996; Becker et al., 1999; Müller-Wohlfeil et al., 2000; Lahmer and Becker, 2000; Lahmer et al., 2000a, 2001ab; Lahmer, 2002). They suggest that climatic changes will alter basic components of the hydrological cycle such as soil moisture, groundwater availability and the magnitude and timing of runoff. As a consequence, this would induce dramatic environmental alterations and have widespread implications for water resources planning and management in the future. Based on the results of spatially distributed regional trend analyses for percolation (Lahmer and Pfützner, 2001), the main objectives of the present study were to investigate the direction and magnitude of possible climate change impacts on the regional hydrological cycle and to identify specifically vulnerable landcover types. High resolution water balance calculations were performed for the State of Brandenburg in Germany both for a reference state (period 1951-1990) and two climate change scenarios, assuming a temperature increase of 1.5 K and 3 K in the period 1996-2050. These calculations reveal a high sensitivity of the regional water cycle to relatively small changes in meteorological variables, and the need for suitable adaptation strategies.

STUDY REGION

The results of trend analyses for percolation and of climate change impacts on the regional water balance are discussed for the State of Brandenburg, Germany (30,000 km^2). The major part of Brandenburg is situated in the German part of the Elbe basin (see Fig 1), which is characterized by water scarcity, resulting from a mean annual precipitation of about 610 mm or less. Water deficiencies (droughts) occur more frequently here, in strong contradiction to the situation in the rest of Germany, where the meteorological conditions in general do not induce water availability problems.

Fig 1: Overview of the German part of the Elbe river basin and the State of Brandenburg.

METHODOLOGY

In order to forecast possible effects of climate change, appropriate modelling approaches as well as high resolution spatial and hydro-meteorological data are necessary. Only with a sufficient density of such data can all necessary input parameters be taken into account in the simulation calculations. However, regional scale applications of fully distributed physically based hydrological models are often constrained by the availability of required input data (Gleick, 1986; Beven, 1993). Therefore, a GIS-based modelling approach is applied in the present study, which allows an effective simulation of the regional hydrological cycle. It is based on variable spatial disaggregation and aggregation techniques to take the spatial heterogeneity of the study region properly into account (see e.g. Becker et al., 2002; Lahmer, 1998; Lahmer and Becker, 1998; Lahmer et al., 1999), and consequently uses the GIS-based derivation of model parameters from generally available spatial data. The basic element of this approach is the modelling system ArcEGMO (Pfützner et al., 1997; Becker et al., 2002; Pfützner, 2002), which was successfully applied in various investigations (i.e. Lahmer, 1998; Becker and Lahmer, 1999; Lahmer et al., 1999a, 2001c; Lahmer and Pfützner, 2001).

In general, the assessment of the actual hydrological situation represents the basis for the evaluation of changes due to scenarios of climate change. Therefore, crucial components of the meso- to macro-scale modelling approach are a proper description of all hydrological processes relevant at that scale and the knowledge of modelling sensitivities. With respect to the processes, only algorithms can be used which are fed by available input parameters. For example, for actual evapotranspiration only approaches like that of Turc (1961) can be used, since then the necessary meteorological input parameters can be provided with a sufficient spatial density. With respect to modelling sensitivities, problems generally arise from the quality of the available spatial and temporal data and the procedures of spatial aggregation and disaggregation (e.g. an adequate hydrotope classification). Several sensitivity studies were performed in the past to assess both the influences of data uncertainties, as well as interpolation and aggregation techniques (Lahmer et al., 1999b; Lahmer et al., 2000b; Lahmer and Pfützner, 2000). Taking a common data situation into account, the uncertainties of the modelling approach can be assumed to be on the order of 5 to 10 %.

More information on the general characteristics of ArcEGMO and details of model application is available at www.arcegmo.de.

TREND ANALYSES OF PERCOLATION

Trend analyses of percolation performed for the State of Brandenburg were the reason to study climate change impacts in that region. The results of these analyses are part of two studies performed for the Brandenburg Environmental Agency (Lahmer et al., 2001c; Lahmer and Pfützner, 2001) using the GIS-based modelling approach introduced above. They indicate some considerable changes in water balance components already under the current climate, and agree with observations of numerous groundwater logging stations in Brandenburg which indicate a considerable decrease of groundwater table depth. Variations of percolation due to a decrease in precipitation and/or an increase in temperature are thought to be the reason for this decrease.

Water balance calculations were performed on 57,836 spatial units, which result from the GIS-based combination of landuse, soil, groundwater table depth and subbasin maps. These units were aggregated into 1,599 hydrotopes and 15 hydrotope classes. The aggregation method and the reason for its application are outlined in several publications (e.g. Lahmer and Becker, 1998; Lahmer et al., 1999a; Becker et al., 2002). Since the spatial distribution of meteorological input variables plays a key role in meso- to macroscale hydrological modelling (see e.g. Lahmer, 1998; Lahmer et al., 2000b), reliable results for evapotranspiration, groundwater recharge, surface runoff and basin discharge can be achieved only if the spatial and temporal resolution of climatic information is high enough to represent the meteorological heterogeneities of the study region. Therefore, meteorological time series from 23 climate and 54 precipitation stations were included in the simulations runs. In addition, an appropriate interpolation method was used to distribute the meteorological information over all spatial units (see e.g. Lahmer and Becker, 1998; Lahmer et al., 1999b, 2000b).

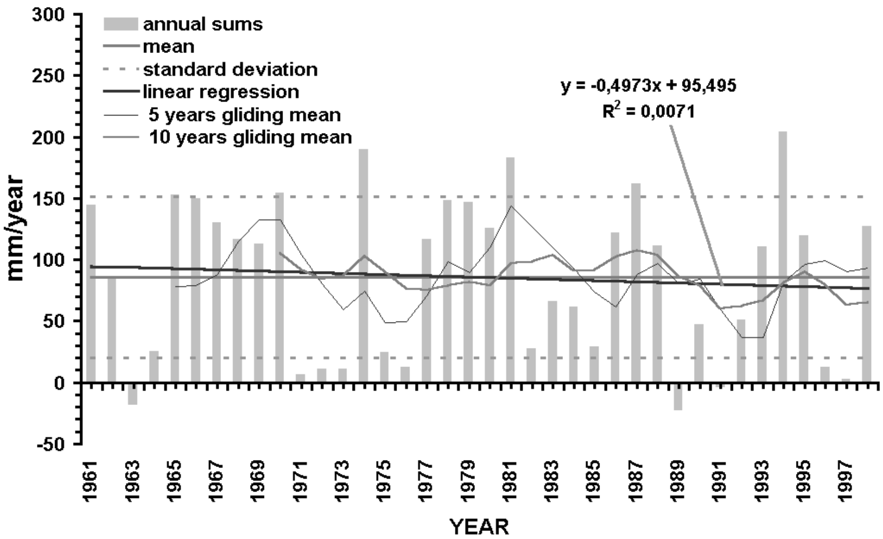

Fig 2: Annual sums of percolation calculated for the State of Brandenburg in the period 1961-1998. Besides the mean and the standard deviation, a linear regression curve as well as moving averages for 5 and 10 years are shown. The decrease indicated by the regression curve turns out to be not significant.

Based on the aggregated digital maps and the spatially distributed meteorological information, various water balance components were calculated on a daily basis for the period 1961-1998. Trend analyses show whether and to what extent percolation changes occur in Brandenburg, and how the extreme summers in the last decade of the 20th century contribute to this change. One result of the simulation calculations is the high variability of the annual sums of percolation given in Fig 2. The annual mean for the period 1961-1998 amounts to +86 mm (+107 mm in the winter and -21 mm in the summer period), resulting in a mean annual total runoff of 106 mm (60 % of which occurs in the winter period).

Since climatic variations are assumed to be the reason for the observed decreasing groundwater table in Brandenburg, analyses of corresponding time series can reveal tendencies, which influence the regional water cycle in general, and percolation in particular. In such analyses, based on annual values for the period 1961-1998 only, the increase of the mean daily temperature by about 1 °C turns out to be statistically significant. All other meteorological variables show more or less pronounced, but not significant changes. This is also true for precipitation, which decreases by almost 13 mm between 1961 and 1998. Performing such analyses on a half-year basis results in statistically significant changes (trends) only for mean daily temperature and potential evapotranspiration in the winter. With changes of +1,6 °C and +24,2 mm, respectively, the trends are rather evident.

Since percolation and its changes vary both in time and space, this water balance component was statistically analysed for different periods and temporal aggregations (annual, winter, summer, quarterly and monthly values). The linear regression of annual sums given in Fig 2 indicates a decrease of percolation in Brandenburg from 95 mm in 1961 to about 77 mm in 1998. However, this decrease by almost 20 % turns out to be statistically not significant. The same is true for winter, summer and quarterly values. Only for May is a significant negative trend in percolation derived. In order to identify areas characterized by a significant change in percolation in the state of Brandenburg, trend analyses were performed for all 1,599 hydrotopes. According to Fig 3, the absolute changes in the period 1961-1998 range from -140 mm to +50 mm. About 75 % of the total area shows a decrease in percolation. However, following the Mann-Kendall significance test, only 4.4 % (or 1,331 km²) of the total area is characterized by a significant (negative) change in percolation, ranging from -12 mm to -98 mm.

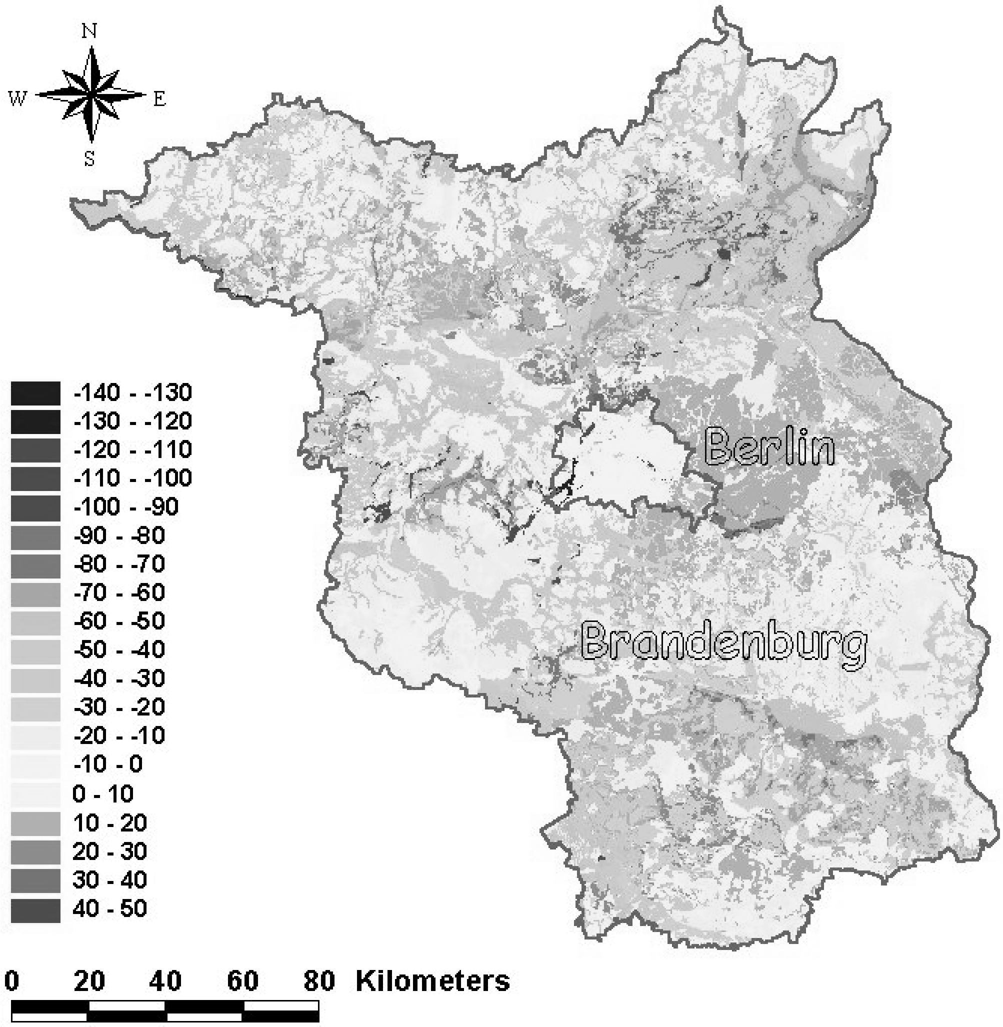

Fig 3: Absolute changes of percolation calculated for the State of Brandenburg in the period 1961-1998 (in mm).

To answer the question which areas show the largest changes in percolation, the map shown in Fig 3 was differentiated based on the 15 hydrotope classes used for the simulation runs. The analysis shows that only the classes ‘wetland‘, ‘farmland‘, ‘forest‘ and ‘meadow‘, which are characterized by a shallow groundwater table depth, show a significant decrease in percolation. With about 31 % and 23 % of their total area, the last two classes contribute particularly to this trend. However, due to their comparatively small fractional area of only 4.4 %, the total area of Brandenburg does not show a significant decrease in percolation (see Fig 2). In summary, in the period 1961-1998 the already negative values of percolation decrease further, especially for areas with a shallow groundwater table. The basic reasons are a decrease in precipitation (statistically not significant) and an increase in mean daily temperature (significant). The last decade (1991-1998), which was characterized by many hot summers, contributes considerably to this result. It should also be mentioned that the simulation calculations do not take into account water withdrawal from the groundwater reservoir in the period 1961-1998. However, as compared to the climatic impacts, the anthropogenic influence on the regional water balance is supposed to be rather small.

CLIMATE CHANGE IMPACT STUDY

Already some early studies (e.g. Nemec and Schaake, 1982; Gleick, 1986) provided first tentative evidence that relatively small changes in regional precipitation and evapotranspiration patterns might result in large changes in regional water availability. In principle, influences of climate change on the regional water balance may result from both spatial and temporal precipitation shifts, temperature-driven changes of actual evapotranspiration, and an increase in extreme meteorological events (prolongation of dry periods, droughts, high intensity precipitation events etc.). In order to assess the impacts of climatic changes on regional hydrological processes, quantitative estimates are needed for the major long-term climatic variables such as temperature or precipitation. However, General Circulation Models (GCMs) are still not able to provide valuable detailed information on regional impacts on water supply. Therefore, alternative approaches must be used to promote the understanding of climatic vulnerabilities.

CLIMATE CHANGE SCENARIOS

Among the various types of regional climate change scenarios currently used in the scientific community, the present study is based on physically consistent regional scenarios, which include general trends of GCM model calculations. This method assumes that GCM results on the average are more exact for large scales than for a defined region. Then, long-term observed time series can be prepared by statistical methods to reflect the changes calculated by GCMs (Lahmer et al., 2001a; Werner and Gerstengarbe, 1997). In case of a further unlimited increase of the CO_2 concentration in the atmosphere, the current GCMs calculate a global warming between 1.5 and 4.5 K by 2100. For Central Europe a temperature increase of about 2 to 4 K can be assumed within the next 100 years. Two scenarios were applied in the present study. These assume a temperature increase of 1.5 K (‘business as usual‘) and 3 K (extreme scenario) in the period 1996-2050, which were imposed on the observed values at 40 meteorological stations in Brandenburg in the period 1951-1990 (actual meteorological conditions, reference scenario).

RESULTS OF THE IMPACT ANALYSES

Based on the spatial data used for the trend analyses, water balance calculations were performed for the State of Brandenburg, both for the reference state (period 1951-1990) and the two climate change scenarios (period 1996-2050). From the variety of results obtained for evapotranspiration, percolation, surface runoff and basin discharge only some will be discussed hereafter. Fig 4 shows the development of the annual sums of percolation for the reference scenario and the two climate change scenarios. Percolation is dramatically reduced under the assumed climate change conditions. Based on linear regression curves, percolation decreases from 161 mm in 1951 to 129 mm in 1990 (-20 %) for the reference state. For the climate change scenarios, the reductions in the period 1996-2050 amount to 68 % and 83 %, respectively.

Table 1 gives an overview of all meteorological input variables and derived water balance components calculated for the three climate conditions, both on an annual and a half-annual basis. In Fig 5 the values given in Table 1 are shown in the form of differences between the scenarios and the reference state. On the average, annual precipitation P in the climate scenarios is only slightly reduced by 5.8 % (1.5 K scenario) and 6.1 % (3 K scenario) as compared to the reference state. The reductions in winter are, however, much more pronounced. Also the increase in mean daily temperature T is considerably higher in winter. Due to the changes in P and T, potential evapotranspiration EP increases under climate change conditions by 5.5 % (1.5 K) and 9.2 % (3 K) in summer, and by 18.8 % and 25.8 % in winter. Due to the general water deficit, actual evapotranspiration EAT almost does not change in summer. During winter EAT increases considerably: by 18.6 % for the 1.5 K scenario and by 25.4 % for the 3 K scenario.

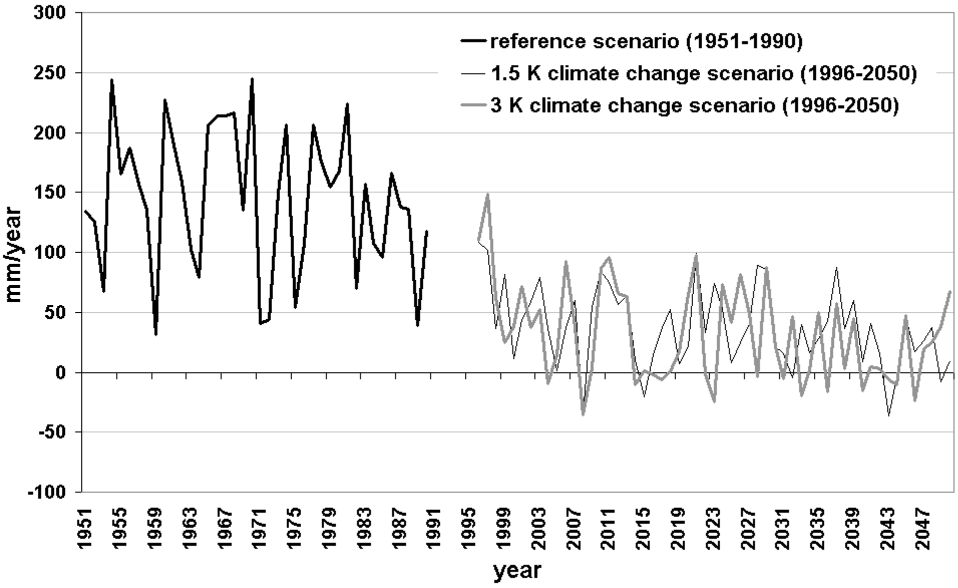

Fig 4: Annual sums of percolation calculated for the State of Brandenburg for the reference state (period 1951-1990) and the two climate change scenarios (period 1996-2050) assuming a temperature increase of 1.5 K and 3 K, respectively.

Table 1: Impacts of climate change on various water balance components in the State of Brandenburg, calculated on an annual basis and for the summer and winter seasons. Besides the means for the meteorological input variables precipitation (P) and mean daily temperature (T), the values for potential evapotranspiration (EP), climatic water balance (WB), actual evapotranspiration (EAT), percolation (PER), surface runoff formation (SRO) and total runoff (R) are given, both for the reference state (1951-1990) and the 1.5 K- and 3 K-climate change scenarios (1996-2050) (all values in mm/y, T in °C/day).

	P	T	EP	WB	EAT	PER	SRO	R
Reference state								
Mean annual sums	614.8	8.71	629.6	-14.9	515.6	88.3	11.7	107.5
Mean summer sums	348.1	14.87	522.7	-174.5	410.6	-19.8	5.5	42.8
Mean winter sums	266.6	2.56	107.0	159.7	105.0	108.1	6.2	64.7
1.5K scenario								
Mean annual sums	579.1	9.85	678.3	-99.2	533.1	37.9	9.5	60.4
Mean summer sums	342.9	16.03	551.2	-208.3	408.5	-27.8	5.1	26.3
Mean winter sums	236.2	3.67	127.1	109.1	124.5	65.7	4.4	34.1
3K scenario								
Mean annual sums	577.5	10.60	705.2	-127.7	537.8	31.9	9.0	54.1
Mean summer sums	343.1	16.79	570.7	-227.5	406.1	-29.5	4.8	23.7
Mean winter sums	234.4	4.42	134.5	99.9	131.7	61.4	4.2	30.4

Percolation PER is drastically influenced by climate change. The reductions are considerably high in winter, where PER drops by about 40 % both for the 1.5 K and the 3 K scenarios. The mean annual total runoff R drops from about 108 mm for the reference scenario to 60 mm and 54 mm in the case of the two climate change scenarios. Again, the reductions are lower in summer (39 % and 19 %, respectively) than in winter (47 % and 53 %). Since the water balance components PER and R are dramatically reduced by the assumed climate changes particularly in the winter season, the already existing water deficit in summer would intensify in Brandenburg under changed climate conditions. The main reasons are the considerable increases in mean daily temperature and evapotranspiration in the winter period.

In addition to time series analyses, the spatial distributions of water balance components were calculated as well. Maps of mean annual sums of percolation for the climate change scenarios show a considerable decrease under climate change conditions as compared to the reference state. The reductions are especially high for open water bodies and areas with a shallow groundwater table (up to about 100 mm). For the total area, the decrease amounts to -57 % (1.5 K scenario) and -64 % (3 K scenario). Almost the whole area is affected by this negative change, which results both from the reduction of precipitation and the increase in mean daily temperature.

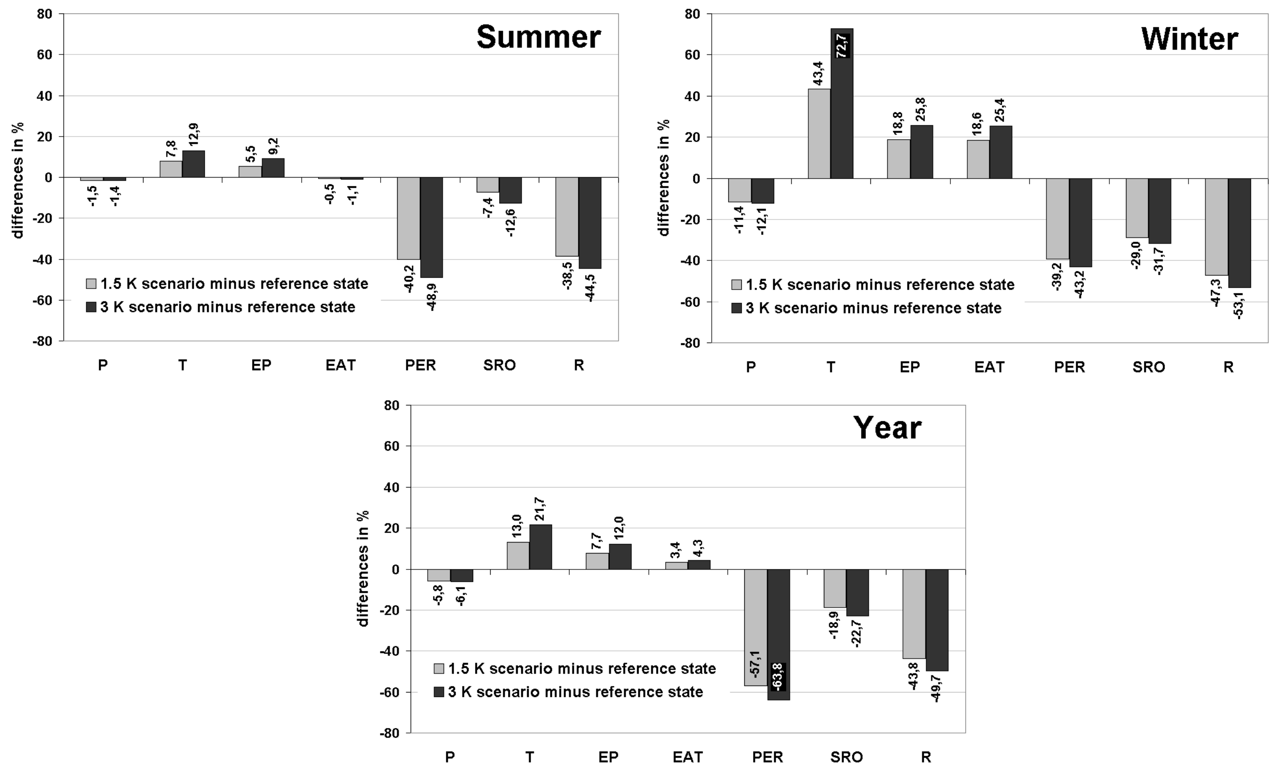

Fig 5: Differences in various water balance components (mean annual as well as summer and winter sums) between the 1.5 K and 3 K climate change scenario (1996-2050) and the reference state (1951-1990) calculated in the State of Brandenburg. Variable names and remarks as in Table 1.

SUMMARY AND CONCLUSIONS

The high resolution GIS-based modelling approach based on the modelling system ArcEGMO has turned out to be an effective way to study trends in various water balance components as well as impacts of climate change on the regional hydrological cycle. The trend analyses in the State of Brandenburg indicate considerable changes in water balance components already under the current climate. Areas with a shallow groundwater table show a significant decrease in percolation in the period 1961-1998. The main reason for this decrease is the increasing mean daily temperature in that period. Based on observed meteorological conditions (period 1951-1990), the regional hydrological consequences of climatic changes (period 1996-2050) were demonstrated. The climate change impact study shows that some of the water balance components in Brandenburg will undergo considerable changes. Due to their high evaporation potential, open water bodies and areas characterized by a shallow groundwater table (lowlands, wetlands, riparian areas) are the most sensitive areas. The percentage of such areas is rather high in Brandenburg, which suffers from water deficit already under current climate conditions. Since the 1.5 K climate change scenario used in the present study can be characterized as relatively 'conservative', the calculated impacts on the regional water balance might be even more severe. The dramatic changes in various water balance components under climate change conditions indicate possible water availability problems in the future. Therefore, the study clearly emphasizes a strong need to understand and appropriately simulate the hydrological regime of water deficient regions.

REFERENCES

Becker, A., Lahmer, W. (1996) Klimawandel und seine Auswirkungen auf den Wasserhaushalt. *gwf-Wasser Special,* 14/96.

Becker, A., Lahmer, W. (1999) GIS-basierte großskalige hydrologische Modellierung. In: Kleeberg, H.-B., Mauser, W., Peschke, G. und Streit, U. (Hrsg.). *Hydrologie und Regionalisierung – Ergebnisse eines Schwerpunktprogramms (1992 bis 1998)*, Forschungsbericht, Deutsche Forschungsgemeinschaft (DFG). Wiley-VCH, Weinheim, 1999, ISBN 3-527-27145-7, 115-129.

Becker, A., Wenzel, V., Krysanova, V., Lahmer, W. (1999) Regional analysis of global change impacts: Concepts, tools and first results. *Env. Modelling and Assessment*, 4, 243-257.

Becker, A., Klöcking, B., Lahmer, W., Pfützner, B. (2002) The Hydrological Modelling System ARC/EGMO. In: *Mathematical Models of Large Watershed Hydrology* (Eds.: Singh, V.P. and Frevert, D.K.). Water Resources Publications, Littleton/Colorado. 891pp. ISBN 1-887201-34-3, 321-384.

Beven, K. J. (1993) Prophesy, reality and uncertainty in distributed hydrological modelling. *Adv. Wat. Resour.*, 16, 41-51.

Gleick, P.H., (1986). Methods for evaluating the regional hydrologic impacts of global climatic changes. *J. Hydrol.*, 88, 99-116.

Lahmer, W. (1998) Macro- and Mesoscale Hydrological Modelling in the Elbe River Basin. In: Proceedings of the International Conference '*Catchment Hydrological and Biochemical Processes in Changing Environment*' in Liblice, Czech Republic, September 22-24, 1998, 57-61.

Lahmer, W., Becker, A. (1998) Grundprinzipien für eine GIS-gestützte großskalige hydrologische Modellierung. Beitrag zum Workshop „*Modellierung des Wasser- und Stofftransportes in großen Einzugsgebieten*" vom 15. bis 16. Dezember 1997 in Potsdam. PIK-Report No. 43, PIK 1998, 55-66.

Lahmer, W., Becker, A., Müller-Wohlfeil, D.-I. and Pfützner, B. (1999a). A GIS-based Approach for Regional Hydrological Modelling. In: B. Diekkrüger, M.J. Kirkby, U. Schröder (Eds.): *Regionalization in Hydrology*. IAHS publication no. 254, ISSN 0144-7815, 33-43.

Lahmer, W., Klöcking, B. and Pfützner, B. (1999b). Meteorological Input Variables in Meso and Macroscale Hydrological Modelling. In: *Extended abstracts of the International Conference on Quality, Management and Availability of Data for Hydrology and Water Resources Management*, Koblenz, 22-26 March, 1999, 165-168.

Lahmer, W., Becker, A. (2000) Mögliche Auswirkungen von Klimaveränderungen am Beispiel einer Untersuchung für das Land Brandenburg. In: *Auswirkungen von Klimaänderungen auf die Wasserwirtschaft*. KA – Wasserwirtschaft, Abwasser, Abfall 2000 (47), Nr. 2, 170-175.

Lahmer, W., Pfützner, B. (2000) Scaling problems in large-scale hydrological modelling. In: Verhoest, N.E.C., Van Herpe, Y.J.P. and De Troch, F.P. (Eds.). *Monitoring and Modelling Catchment Water Quantity and Quality*. Conference proceedings. Laboratory of Hydrology and Water Management, Ghent University, Ghent, Belgium, 95-99.

Lahmer, W., Pfützner, B., Becker, A. (2000a) Influences of Environmental Changes on Regional Flood Events. In: Bronstert, A., Bismuth, C. and Menzel, L. (Eds.). *European Conference on Advances in Flood Research*. PIK-Report No. 65, 238-254. Potsdam Institute for Climate Impact Research, November 2000.

Lahmer, W., Pfützner, B., Becker, A. (2000b) Data-related Uncertainties in Meso- and Macroscale Hydrological Modelling. In: Heuvelink, G.B.M. and Lemmens, M.J.P.M (Eds.). *Accuracy 2000*. Proceedings of the 4th international symposium on spatial accuracy assessment in natural resources and environmental sciences. Amsterdam, July 2000, 389-396.

Lahmer, W., Pfützner, B., Becker, A. (2001a) Assessment of Land Use and Climate Change Impacts on the Mesoscale. *Phys. Chem. Earth (B)*. vol. 26, no. 7-8, 2001 Elsevier Science Ltd., 565-575,

Lahmer, W., Pfützner, B., Ströbl, B. (2001b) Possible Impacts of Climate and Land Use Changes on the Water Balance of Semi-arid German River Basins. 19th European Regional ICID Conference *Sustainable Use of Land and Water*, Brno and Prague, Czech Republic, 4-8 June 2001 (CD-ROM).

Lahmer, W., Steidl, J., Dannowski, R., Pfützner, B., Schenk, R. (2001c) Spatially distributed modelling of water balance components in the country of Brandenburg. (in German), Nature Protection Agency Brandenburg (Ed.), 27, *ISSN 0948-0838,* Potsdam.

Lahmer, W., Pfützner, B. (2001) High resolution trend analyses of percolation in the country of Brandenburg. (unpublished, in German), Potsdam Institute for Climate Impact Research.

Lahmer, W. (2002) Hydrologische Auswirkungen von Klimaänderungen. In: *Klimaszenarien und Derivate - Vorsorge für Regionen und Unternehmen*. Beitrag des Potsdam-Instituts für Klima-folgenforschung zur Umweltwoche des Bundespräsidenten „Treffpunkt Zukunft – Innovation für den Umweltschutz“ vom 3. - 7. Juni 2002.

Müller-Wohlfeil, D.-I., Bürger, G., Lahmer, W. (2000) Response of a River Catchment to Climatic Change in Northern Germany. *Climatic Change*, vol. 47, 61-89.

Nemec, J., Schaake, J. (1982) Sensitivity of Water Resource Systems to Climate Variation. *Hydrological Sciences*, 27, 327-343.

Pfützner, B., Lahmer, W., Becker, A. (1997) ARC/EGMO – a program system for GIS-based hydrological modelling. Short documentation to version 2.0. (in German, unpubl.), Potsdam Institute for Climate Impact Research.

Pfützner, B. (2002) ARC/EGMO. In: Barben, M., Hodel, H.-P., Kleeberg, H.-B., Spreafico, M. und Weingartner, R. (Hrsg.). *Übersicht über Verfahren zur Abschätzung von Hochwasserabflüssen – Erfahrungen aus den Rheinanliegerstaaten*. Bericht Nr. I-19 der Internationalen Kommission für die Hydrologie des Rheingebietes-KHR, ISBN 90-36954-11-8, 151-154.

Turc, L. (1961) Évaluation des besoin en eau d’irrigation évapotranspiration potentielle. *Ann. Agron.*, 12, 113-149.

Werner, P.C., Gerstengarbe, F.-W. (1997) A Proposal for the Development of Climate Scenarios. *Climate Research*, 8, 171-182.

THE NORTH ATLANTIC OSCILLATION IMPACT ON THE HYDROLOGICAL REGIME OF POLISH CARPATHIAN RIVERS

Joanna Pociask-Karteczka[1], Zenon Nieckarz[2], Danuta Limanówka[3]

[1]*Institute of Geography and Spatial Management, Jagiellonian University, jpociask@arsenal.geo.uj.edu.pl, 31 044 Kraków, ul. Grodzka 64, Poland,*
[2]*Institute of Physics, Jagiellonian University, 30 059 Kraków, ul. Reymonta 4, Poland,*
[3]*Institute of Meteorology and Water Management,30 215 Kraków, ul. Borowego 14, Poland*

ABSTRACT

The impact of the North Atlantic Oscillation on the discharge of some Polish Carpathian rivers was investigated over the period 1951-2000. Pearson's linear correlation analysis was used. Some synchronic and asynchronic relations between the NAO index and river discharges were observed. During a positive NAO phase, the annual river discharge is low. NAO conditions during winter influence spring and summer river flow. The analysis was based on particular circulation phases, distinguished on the basis of Hurrell's NAO irregularity index. The annual NAO index explains about 41% of the summer river discharge variability and 30% of the variability of annual river discharge during the period 1951-1970. The annual NAO index also explains several percent of the variability of annual discharges of the Vistula and Dunajec rivers during the period 1971-1995. Accordingly, there is a possibility to use the NAO index as a predictor in hydrological modelling.

Keywords North Atlantic Oscillation, river discharge, Carpathian Mts.

INTRODUCTION

A river flow regime reflects the meteorological and physiographic conditions over a basin. Regional climate is generated by the simultaneous action of atmospheric circulation at local, regional and global scales. The North Atlantic Oscillation (NAO) is one of the most important regional systems affecting the climate in North America, Europe and some other regions (Bonsal et al., 2001; Hurrell and Van Loon, 1997; Shabbar et al., 1997). The meteorological conditions in Poland are influenced by NAO too, in particular during the winter season (Marsz and Styszyńska, 2001; Wibig, 2000). This creates a possibility of an indirect influence of NAO on river runoff. However, the connections between NAO and river runoff in Poland have not been given enough attention. Some interactions were introduced by Stahl and Demuth (2001) and Styszyńska (2002).

The impact of the North Atlantic Oscillation was analysed for the following rivers in this paper (Fig 1):
- Skawa River - 835 km^2,
- Dunajec River - 4 341 km^2,
- Wisła River - 31 846 km^2.

Data on river discharges were available for the period 1951-2000. Data sets of long-term monthly mean, seasonal, minimum and maximum values of river discharge were taken into consideration, as well as Hurrell's NAO index and Rogers's NAO index for the winter period (www.cgd.ucar.edu/ ~jhurrell/nao.html). A linear correlation analysis was used.

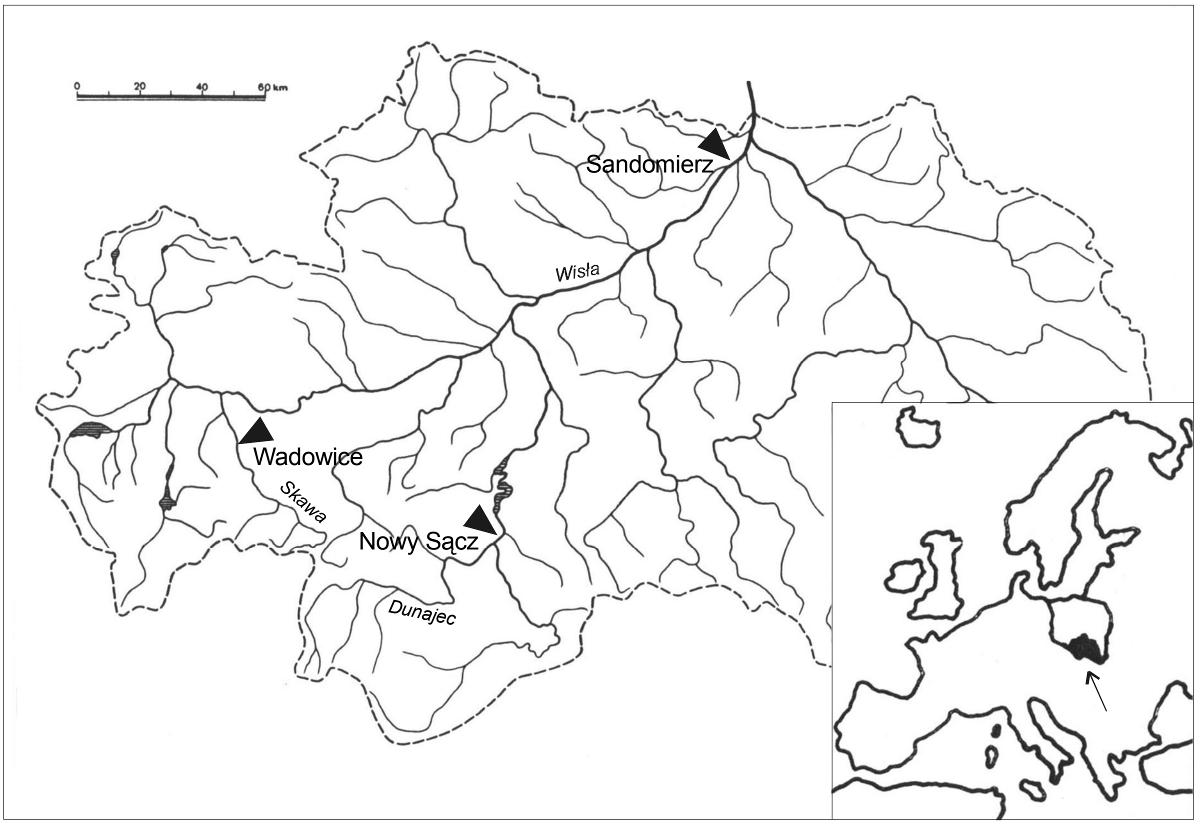

Fig 1: Location of the investigated area.

Table 1: Correlation coefficients between the maximum and minimum discharges and the annual NAO index (R_r) and the winter NAO index (R_z) (bold – $p < 0,01$).

Basin	Discharge	R_r	R_z
Skawa – Wadowice	Maximum	**-0,39**	-0,11
	Minimum	0,05	0,05
Dunajec – Nowy Sącz	Maximum	**-0,43**	**-0,43**
	Minimum	-0,16	-0,16
Wisła – Sandomierz	Maximum	-0,34	-0,22
	Minimum	0,16	0,29

RESULTS AND DISCUSSION

On the basis of the analysis of the Roger and Hurrell NAO indexes and the Carpathian river discharge, some relationships were identified. Generally, correlation coefficients were very low and were not statistically significant in many cases. However, significant correlations were obtained for maximum discharge values: there is a relationship between the winter and annual NAO indices and maximum discharge of Dunajec, and between the annual NAO index and the maximum discharge of Skawa (Table 1).

The correlation between the winter NAO index and mean monthly winter discharge is significant only in the case of Dunajec in January ($R = 0,38$, $p < 0,01$). Lower correlations are observed between the winter NAO index and the discharge of all rivers in August, and Wisła in September (Table 2). There is quite a strong correlation between the annual NAO index and the mean monthly discharge of Wisła in August (–0.39; p < 0,05) (Table 3).

A correlation analysis between the mean monthly NAO index and the mean monthly discharge has also been conducted. There are some remarkable correlations between:

- the December NAO index and the discharge of Skawa in May and September respectively (R = - 0,37, R = -0,36; p < 0,05),
- the December NAO index and the discharge of Dunajec in May and September (respectively R = -0,32, R = -0,34; p < 0,05),
- the January NAO index and the discharge of Dunajec in January (R = 0,43; p < 0,01),
- the December NAO index and the discharge of Wisła in September (R = -0,36; p < 0,05),
- the January NAO index and the discharges of Wisła in August (R = 0,31; p < 0,05),
- the March NAO index and the discharges of Wisła in April (R = -0,36; p < 0,05).

Table 2: Correlation coefficients between mean monthly discharges and the winter NAO index (bold – p < 0,01).

Basin	XI	XII	I	II	III	IV	V	VI	VII	VIII	IX	X
Skawa – Wadowice	-0.03	0.18	0.22	0.02	0.01	-0.16	-0.21	-0.09	-0.11	-0.26	-0.19	-0.05
Dunajec – Nowy Sącz	0.05	0.19	**0.38**	0.13	0.21	-0.15	0.13	-0.01	-0.06	-0.25	-0.10	0.05
Wisła – Sandomierz	0.04	0.17	0.21	0.04	-0.12	-0.20	-0.13	-0.14	-0.12	-0.25	-0.24	-0.05

According to the analysis above, the relationships between mean monthly values have not been strong, contrary to expectations. Therefore, three-month mean values were analysed. The correlation between the XI-XII-I NAO index and discharges of all rivers in the spring (III-IV-V), and discharge of Skawa and Wisła in summer and autumn, and discharge of Dunajec in winter months, are significant. This delay may be caused by the snow-cover ablation processes during spring. There are also synchronic relationships in autumn and winter months in Skawa and Dunajec (Fig 2). However, a good correlation does not guarantee a physical cause and effect.

Table 3: Correlation coefficients between mean monthly discharges and the annual NAO index (bold – p < 0,01).

Basin	XI	XII	I	II	III	IV	V	VI	VII	VIII	IX	X
Skawa – Wadowice	0.17	0.25	0.13	-0.22	-0.03	-0.28	-0.30	-0.18	-0.20	-0.34	-0.20	-0.09
Dunajec – Nowy Sącz	0.13	0.25	0.31	-0.06	0.11	-0.26	-0.05	-0.14	-0.23	-0.34	-0.19	-0.05
Wisła – Sandomierz	0.17	0.28	0.23	-0.12	-0.09	-0.30	-0.17	-0.17	-0.25	**-0.39**	-0.31	-0.14

The NAO conditions over the period 1951-2000 were very variable, and therefore a few air-circulation phases were distinguished (Marsz and Styszyńska, 2001). One of them, the phase E-II, began in 1930 and lasted until 1970, while phase E-III began in 1971 and finished in 1995. Remarkable correlations over particular periods were found: there is a significant correlation between the annual mean NAO index and the annual and summer-half-year discharge of Skawa in phase E-II (respectively: R = - 0,55, p < 0,05; R = -0,64, p < 0,01) (Table 4). There are also some significant correlations in phase E-III , i.e. correlations between the annual NAO index and the annual discharge of Wisła and Dunajec (respectively: R = -0,40, R = -0,49; p < 0,05) (Table 4).

CONCLUSIONS

The present analysis of Hurrell's and Roger's North Atlantic Oscillation indices and Carpathian river discharges demonstrates very interesting large-scale connections: the positive NAO phases in winter are associated with low discharges in summer and at the beginning of autumn. The mean monthly NAO indices in winter are influencing river discharges during winter, spring and autumn: December and January NAO affect river discharge in January, August and September. It is interesting that Styszyńska (2002) stated similar relationships between NAO and the Warta River (western Poland) discharge. She also found a link between the winter NAO index and precipitation during late summer: the winter NAO index explains about 30% of precipitation variability in August of the following year (Styszyńska, 2001).

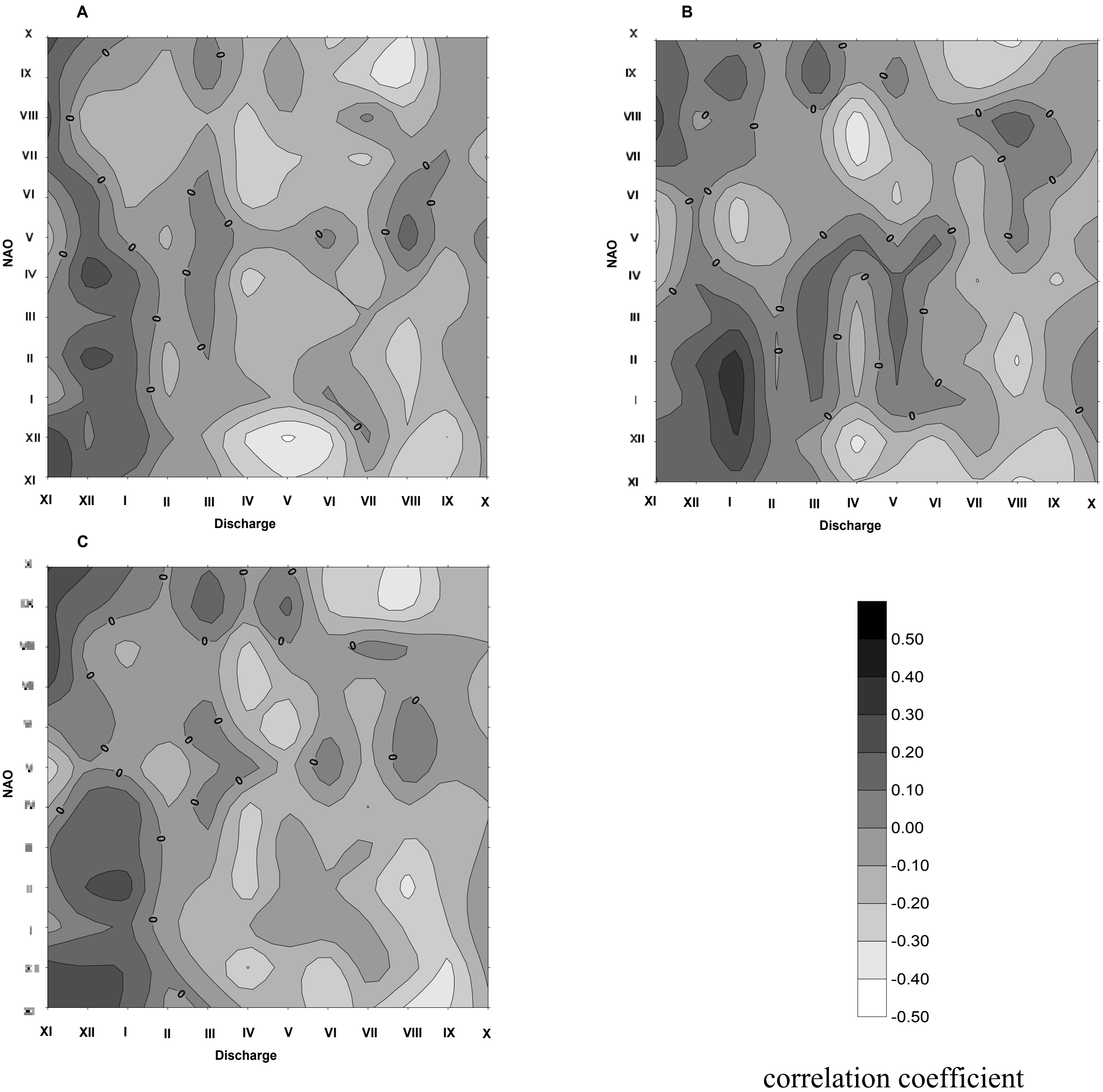

Fig 2: Correlation between three-month mean values of NAO and discharges of Skawa (A), Dunajec (B) and Wisła (C) (month in the figure corresponds to the centre of the three-month period).

Table 4: Correlation coefficients between the annual NAO index (R_r) and the winter NAO index (R_z) and discharges of Skawa, Dunajec and Wisła (bold – p < 0,01) in two phases.

Mean discharge	River	Phase E-II (1951-1970)		Phase E-III (1971-1995)	
		R_r	R_z	R_r	R_z
Annual	Skawa	-0,55	-0,32	-0,38	-0,33
	Dunajec	-0,32	-0,18	**-0,40**	-0,06
	Wisła	-0,39	-0,24	**-0,49**	-0,38
Summer months	Skawa	**-0,64**	-0,33	-0,26	-0,23
	Dunajec	-0,40	-0,25	-0,26	0,06
	Wisła	-0,50	-0,33	-0,34	-0,20
Winter months	Skawa	-0,26	-0,20	-0,29	-0,25
	Dunajec	0,03	0,05	-0,28	-0,02
	Wisła	0,05	0,08	-0,30	-0,35

This delay in runoff/precipitation is related to the activity of two systems: ocean and atmosphere. The ocean system is controlled by the atmospheric system, and inversely. Variations of the sea surface temperature cause changes in the redistribution of heat and substantially control the weather conditions. There is a correlation between the winter NAO index and the sea surface temperature in March-May and August-September of the following year. According to Marsz (2002), the behaviour of NAO is responsible for the activity of ocean currents. A strong positive NAO phase in winter influences the activity of the Gulf Stream: discharges of this ocean current increase and the water temperature is higher than usual from January to July. It causes the advectional transport of heat from low to moderate latitudes. After a positive phase of NAO, the sea surface temperatures of the North Atlantic Current, the Labrador Current and the Norway Current change. So, air circulation in summer in Europe is linked to the anomaly of the sea surface temperature over the North Atlantic during the previous two winters. The anomaly of the sea surface temperature in grids 34°N-40°W and 54°N-30°W explains about 50% of the variability of the incoming winter NAO index. It has also been stated, that the higher Sargasso Sea surface temperature in recent decades is responsible for the increase in the frequency and intensity of a positive winter NAO index after 1971.

The most remarkable relationships were obtained in the analysis performed for the atmospheric circulation phases: the mean annual NAO index explains 41% of the variability of the mean river discharge in summer and 30% of the variability of the mean annual river discharge in period II. NAO played a smaller role during period III. The connection between atmospheric circulation over the North Atlantic and river discharges in particular periods may vary according to meteorological conditions.

It may be stated that NAO plays an important role as an indirect factor influencing river discharge, as well as it might offer the possibility of improving runoff forecasts of some Polish rivers. The study of large-scale connections between atmospheric circulation and hydrology is also important for a better understanding and explanation of river discharge variability. More research focused on the precipitation phenomena during positive and negative phases of NAO that influence river runoff response is however required.

REFERENCES

Bonsal, B.R., Shabbar, A., Higuchi, K. (2001) Impact of low frequency variability modes on Canadian winter temperature, *Intern. J. of Climatology*, 21, 95-108.

Hurrel, J.W., Van Loon, H. (1997) Decadal variations in climate associated with the North Atlantic Oscillation, *Clim. Change*, 36, 301-306.

Marsz, A.A. (2002) NAO a cyrkulacja wód Północnego Atlantyku, związki NAO z polem temperatury powierzchni oceanu (NAO and water circulation in the North Atlantic, links NAO with the sea surface temperature) [in] *Oscylacja Północnego Atlantyku i jej rola w kształtowaniu zmienności wzrunków klimatycznych i hydrologicznych Polski* (The North Atlantic Oscillation and its links with climatic and hydrological conditions in Poland), ed. A.A. Marsz, A. Styszyńska, Akademia Morska, Gdynia, 47-74.

Marsz, A., Styszyńska, A. (2001) Oscylacja Północnego Atlantyku a temperatura powietrza nad Polską (The North Atlantic Oscillation and the air temperature in Poland), Wyższa Szk. Morska, Gdynia, pp. 101.

Shabbar, A., Higuchi, K., Skinner, W., Knox J.L. (1997) The association between the BWA index and winter surface temperature variability over eastern Canada and west Greenland, *Intern. J. of Climatology*, 17, 1195-1210.

Stahl, K., Demuth S. (2001) Atmospheric Circulation and Drought [in] *Assessment of the Regional Impact of Droughts in Europe*, ed. Demuth S., Stahl K, ARIDE Final Report, Institute of Hydrology, Freiburg, 95-110.

Styszyńska, A. (2001) Oscylacja Północnego Atlantyku a opady na obszarze Polski (The North Atlantic Oscillation and precipitation in Poland), *Prace i Studia Geogr*., 29, 232-241.

Styszyńska, A. (2002) Związki między przepływem Warty w Poznaniu a wskaźnikami NAO (1865-2000) (Relation between the Warta River discharge in Poznan and the NAO indexes (1865-2000), http://ocean.wsm.gdynia.pl/konf_NAO/stysa-stre.html.

Wibig, J. (2000) Oscylacja Północnoatlantycka i jej wpływ na kształtowanie pogody i klimatu (The North Atlantic Oscillation influencing weather and climat), *Prz. Geofiz*., 45, 2, 121-137.

www.cgd.ucar.edu/~jhurrell/nao.html (web-site of J. Hurrell, National Center for Atmospheric Research)

EVALUATION OF A DISTRIBUTED HYDROLOGY MODEL TO SUPPORT RESTORATION EFFORTS IN SMALL WATERSHEDS WITH LIMITED DATA: FROM RESEARCH SCALE TO MANAGEMENT SCALE

E.S. Brooks, J. Boll

Department of Biological and Agricultural Engineering, University of Idaho, Moscow, ID 83844-0904, USA

ABSTRACT

This project focuses on testing and developing a distributed hydrologic model for the Pacific Northwest region of the United States, which can be used to simulate the hydrology of small watersheds with minimal calibration and publicly available data. A modified version of the Soil Moisture Routing model is applied to and tested on a small research watershed (~2 ha) with site-specific data. The model also is applied to a management scale watershed (~100 km^2) using publicly available data. The model simulates perched water fluctuations with reasonable accuracy at the research watershed and the hydrograph is well represented at three different management scales for the non-drought year. Over-prediction of stream hydrographs during the drought year indicates a more detailed forest evapotranspiration algorithm may be necessary. The release of snowmelt water from an existing snow pack contributed to errors in the timing of the hydrograph from the research scale watershed.

Keywords GIS, distributed modelling, hillslope hydrology, fragipan

INTRODUCTION

Throughout the Pacific Northwest region of the United States awareness has increased of the impact of point and non-point source pollution on stream and lake water quality. In Idaho, over 900 streams have been listed on the 303(d) list for exceeding the total maximum daily loads (TMDL) as defined by the Clean Water Act (USEPA, 1992) for a number of pollutants, including suspended sediment, phosphorous and water temperature. To decrease pollutant loading to acceptable levels in a limited amount of time, watershed managers must rely on general observations or computer modelling to assist in decision making. This project focuses on developing and testing a distributed hydrologic model to simulate the hydrology of small watersheds with minimal calibration and publicly available data. This model can then be used to identify regions within a watershed having a high risk of runoff or pollutant transport to assist the watershed manager in directing watershed restoration efforts. The primary objectives are:

1.) Evaluate a GIS-based distributed hydrologic model on a small (~2 ha) research scale watershed using publicly available data and detailed spatial measurements of soil hydraulic properties without calibration;
2.) Apply the same model to a management scale (~100 km^2) watershed without calibration using publicly available input data and the grid scale hydraulic properties from the research scale watershed.

SOIL MOISTURE ROUTING MODEL

The variable source area hydrology model used in this project is a modified version of the Soil Moisture Routing (SMR) model (Frankenberger et al., 1999; Boll et al., 1998) developed originally at Cornell University. The SMR model allows for distributed prediction of surface runoff and soil moisture, integrated prediction of streamflow, needing minimal calibration, and also a limited amount of publicly available input data. The model is written as a set of batch programs that can be implemented into most grid based GIS programs. The model tracks the flow into and out of grid cells using a basic mass balance (Eq. (1)) assuming step by step quasi-steady state conditions.

$$D_i \frac{d\theta_i}{dt} = P(t)_i - ET(t)_i + \sum Q_{in.i} - \sum Q_{out.i} - L_i - R_i \quad (1)$$

where **i** is the cell address, θ_i is the volumetric moisture content of the cell, D_i is the depth to a hydraulically restricting layer (m), P is the effective precipitation (rain + snowmelt, m), ET_i is the actual evapotranspiration (m), $\Sigma Q_{in.i}$ is the lateral inflow from surrounding upslope cells (m), $\Sigma Q_{out.i}$ is the lateral outflow to surrounding downslope cells (m), L_i is the leakage out of the surface soil layer to bedrock (m), R_I is the surface runoff (m), and t is time (hr).

Snow accumulation and snowmelt is determined using a threshold air temperature and a snowmelt degree-day equation (U.S. Army Corps of Engineers, 1960), respectively. For watersheds having significant elevation differences, air temperature and precipitation are distributed linearly by elevation using any available weather data. It is assumed that all rain and snowmelt infiltrates during the modelling time step unless the soil is or becomes saturated. Actual evapotranspiration is determined using the relationship developed by Thornthwaite and Mather (1955). Evapotranspiration occurs at the potential rate when the matrix potential is below -1/3 bar. No evapotranspiration takes place when moisture content is below wilting point, and a linear relationship is assumed between wilting point and 1/3 bar moisture contents.

The primary modifications to the SMR model from that presented by Frankenberger et al. (1999) include an exponential decrease in the saturated hydraulic conductivity (K_s) and the ability to predict the exact location of the water table by including a capillary fringe above the water table. The location of a perched water table is determined based on an assumed or measured drainable porosity relationship. The total saturated amount of water within a soil column is related to a linear relationship between the saturated volumetric moisture content and depth above a restricting layer. The total amount of water held in the soil column when a perched layer is present (S) is described by the following equation:

$$S = \frac{a}{2} D^2 + bD - \frac{f}{2}(D-h)^2 \quad (2)$$

where a is the change in saturated moisture content with depth (m^{-1}), b is the saturated volumetric moisture content at the restricting layer, f is the change in moisture content with depth above the water table (m^{-1}) and h is the water table depth (m). The depth of the water table is determined by solving Eq. (2) for h. Knowing the perched layer depth, the total lateral flow is determined by Darcy's law assuming the hydraulic gradient is equal to the land slope. The transmissivity is determined by integrating the K_s relationship with depth from the fragipan to the perched water depth. The total subsurface lateral flow is routed from a given cell to one or more neighbouring, downslope cells based on a slope weighted average (Quinn et al., 1991). Vertical percolation through the restricting layer occurs only when a perched layer is present and is calculated assuming a unit gradient and the K_s of the restricting layer. Surface runoff occurs when input to the cell exceeds the saturated storage amount of the cell.

SITE DESCRIPTION

Troy, ID Catchment

The SMR model was first applied and tested in a small, intensively instrumented 1.7 ha catchment planted in perennial grasses having a single soil type with a shallow restrictive soil layer. The soil is classified in the Santa series, which consists of moderately well-drained soils with a moderately deep profile extending to a fragipan at an average depth of 73 cm. Soil hydraulic measurements indicate the fragipan layer is nearly impermeable. Within the catchment 99 shallows wells, installed on a 10 m x 15 m grid, are read every 12 hrs (Fig 1). At each well location, soil horizons have been characterized. A weather station at the site records solar radiation, wind speed, relative humidity, precipitation, and air temperature every hour. A flume at the outlet of the catchment records changes in flow every 15 min. Analysis of lateral flow draining from an isolated hillslope plot indicates that the K_s decreases exponentially from approximately 20 m/day at the soil surface to 0.2 m/day at the fragipan. The saturated moisture content of the soil decreases from approximately 0.50 cm^3/cm^3 at the soil surface to 0.35 cm^3/cm^3 at the fragipan. Analysis of the soil moisture data show that the volumetric moisture content at a point decreases linearly at the rate of 0.14% per cm above the water table. This linear water retention function was assumed to be applicable to the shallow soils at the site and was necessary to account for the capillary effects on moisture content near a water table. These site-specific soil hydraulic properties were incorporated into the model to predict perched water table thickness and surface runoff through the flume.

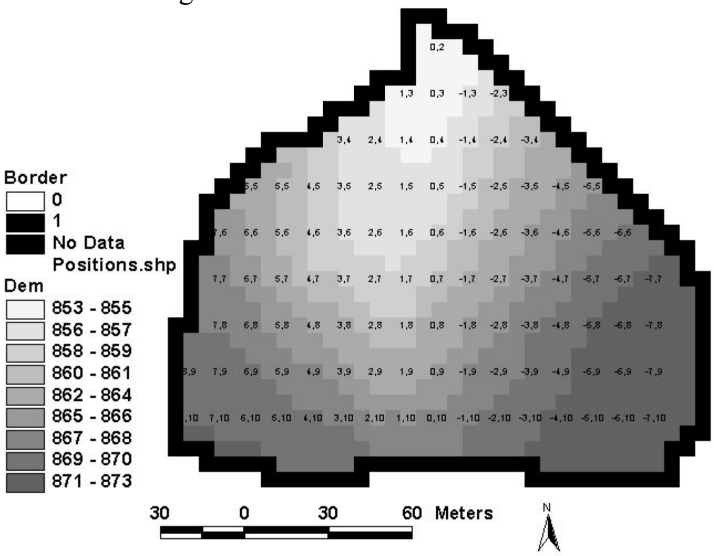

Fig 1: The DEM (metres) for the Troy ID with locations and location numbers of shallow wells.

Paradise Creek Watershed

The Paradise creek watershed, which includes the city of Moscow, Idaho, represents a typical management scale watershed in northern Idaho. Annual total precipitation increases with elevation from approximately 600 mm at the lowest elevation to 1000 mm at the highest elevation. The watershed is split into three distinct land types (16% forested, 18% urban, 66% agricultural land) (Fig 2). Stream monitoring stations define three nested watersheds referred to as the Forest, Ag, and Urban watersheds. Both a low elevation and high elevation weather station were available to distribute precipitation and temperature. The SSURGO soil database, available digitally for most agriculturally dominated regions of the U.S.A., was used for the soil hydraulic properties. Data from the Troy ID catchment showed that the K_s of the A-horizon is ~10 times larger than the maximum K_s of the A-horizon listed on the database. The exponential decrease of the K_s was found directly using the K_s of the A-horizon and the minimum K_s of the bottom horizon. The vertical K_s was taken to be 10 times smaller than the minimum K_s in the SSURGO database.

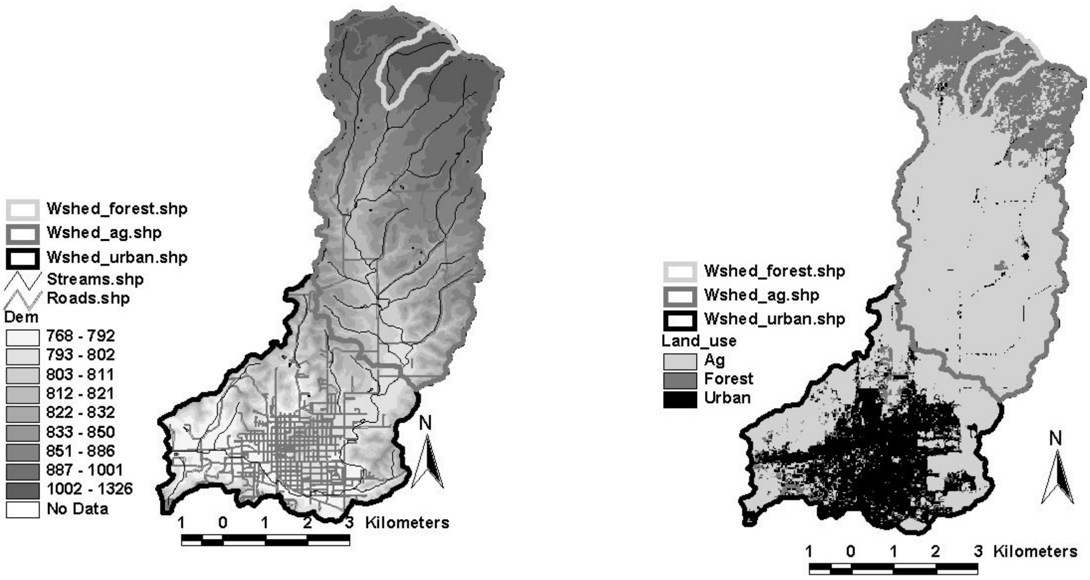

Fig 2: The DEM (metres) and landuse maps for the Paradise creek watershed.

RESULTS

The Nash-Sutcliffe (NS) efficiency (Nash and Sutcliffe, 1970) was used to assess the performance of the SMR model. A NS value of 1 indicates a perfect fit; a NS value of 0 or less indicates the model is no better than using the average observed value for the entire period of record. Separate NS efficiencies were calculated within the entire period of record focusing only on periods of time having flow. The NS values for the entire simulation are larger since there are significant periods of time having no flow. Simulation results are shown in Figs 3, 4, and 5, and discussed below.

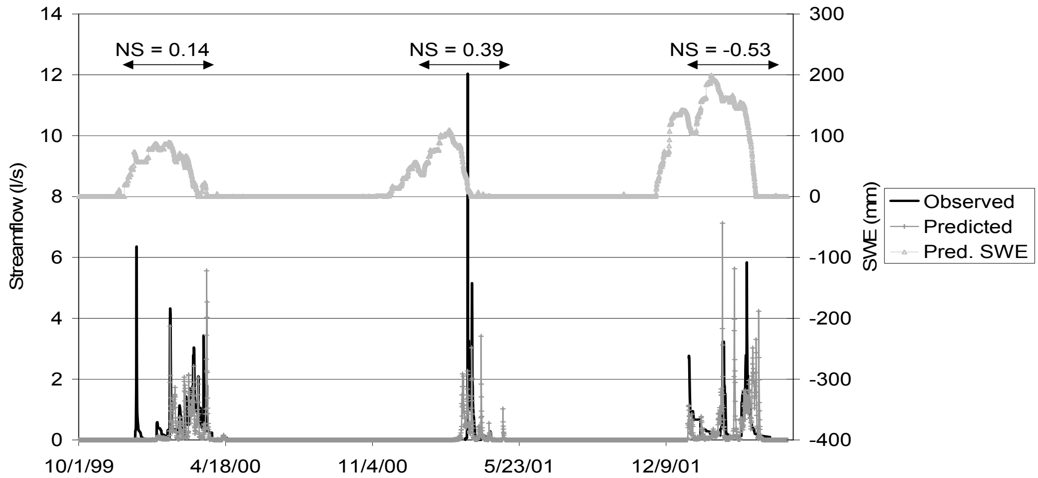

Fig 3: Observed and predicted surface runoff at the outlet of the Troy watershed.

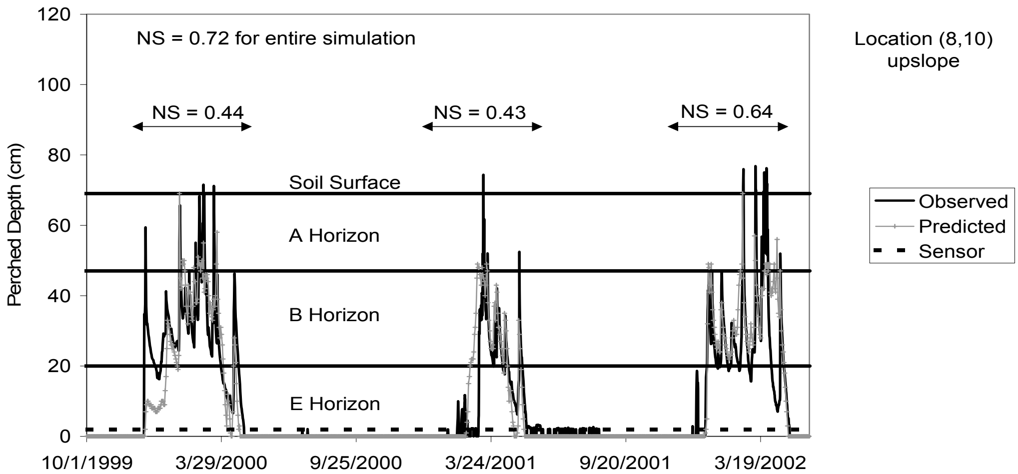

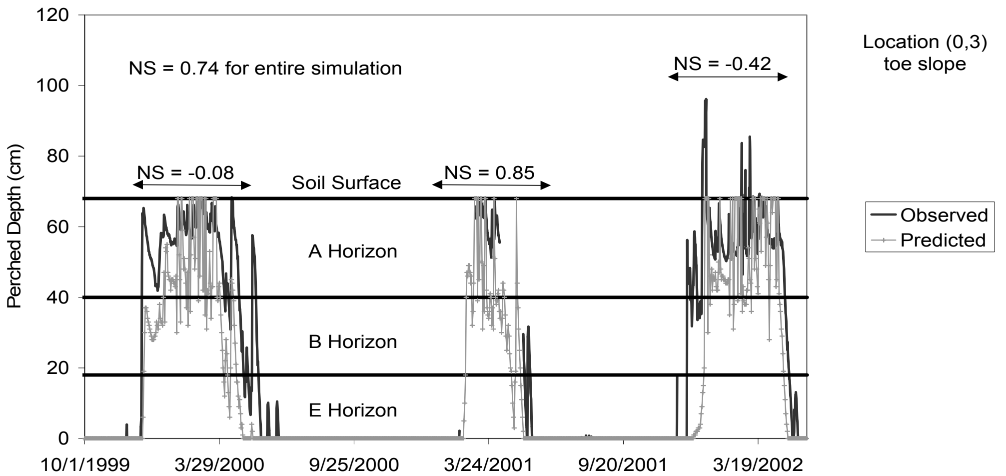

Fig 4: Predicted and observed perched water levels for shallow well locations (8,10) and (0,3) located at upslope and toe slope positions, respectively.

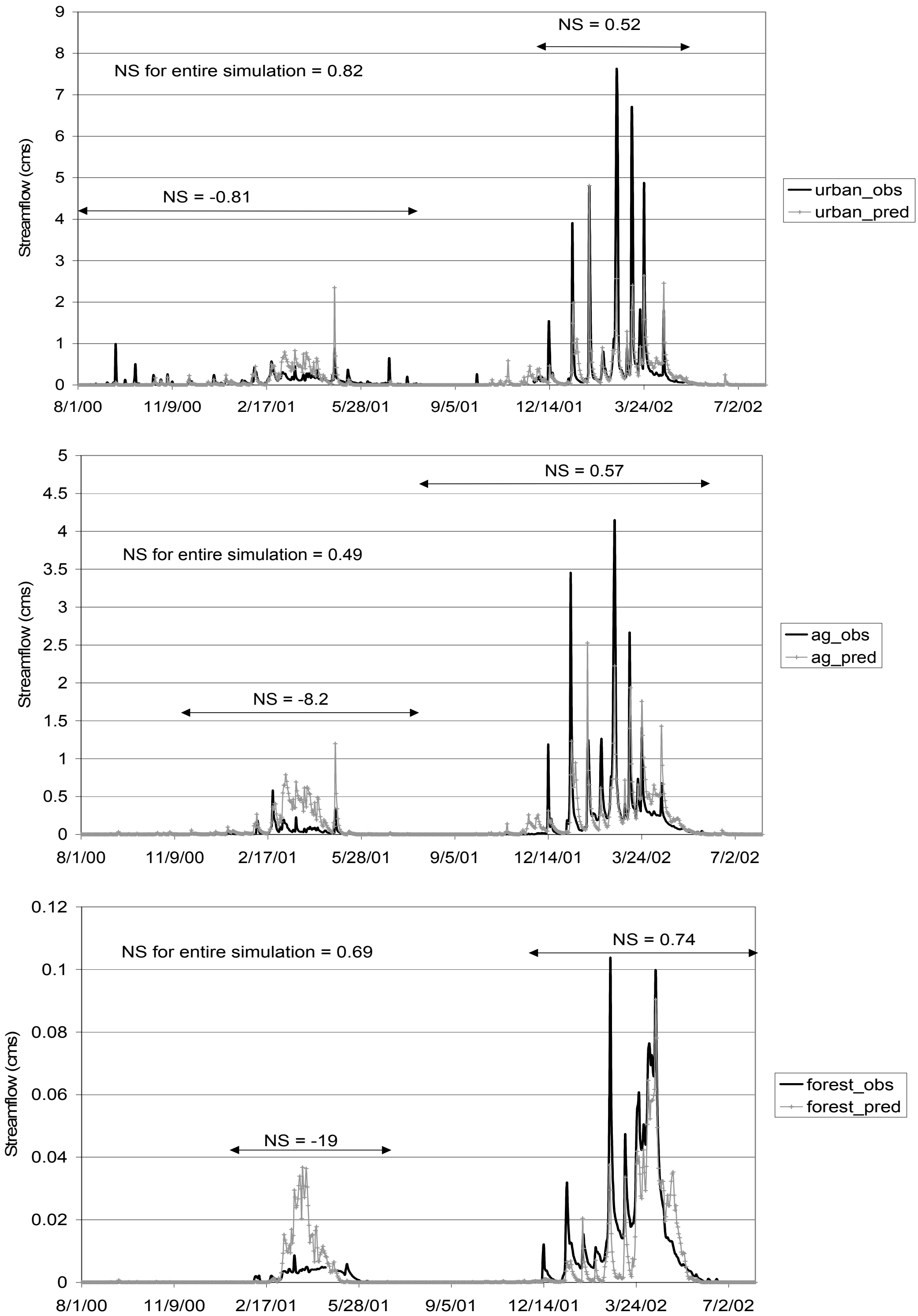

Fig 5: Measured and predicted streamflow leaving the Forest, Ag, and Urban watersheds.

Troy ID catchment

The SMR model was applied to Troy research catchment for the hydrological years 2000, 2001, and 2002. As seen from Figs 3 and 4, the model was able to reflect the perching and subsequent surface runoff trends at the watershed outlet. Timing of runoff peaks was in error due to standing water in the snow pack in the flat lowland areas just above the flume, a process not simulated in the SMR model. The water perching within the snowpack can be observed in the shallow well measurements at the toe slope location (0,3) where the water table readings indicate a water level above the soil surface (see Fig 4). The discrepancy of timing of runoff peaks leads to a negative NS value for the 2002 spring thaw.

For management purposes, the response at individual cell locations (i.e., the distributed response) is more valuable since this response can be used to assess critical source areas in the watershed (Frankenberger et al., 1999). Observed and predicted water table levels were compared at two shallow well locations 8,10 and 0,3 (see Fig 4). Horizontal lines in Fig 4 represent the interfaces between soil horizons. For the entire three-year period, the model agreed well with measurements made at these shallow wells (NS = 0.72 and 0.74, respectively). For the periods when perched water was present, the prediction of perched water tables at a shallow well (8,10) located near the top of the catchment was reasonable with NS values between 0.43 and 0.64. Simulated water fluctuations at the toe slope position (0,3) had lower NS efficiencies during the perched water periods in 2000 and 2002, but still the overall position of the water table within a given soil horizon was well represented by the model.

Paradise creek watershed

The SMR model was applied to the Paradise creek watershed for the hydrological years 2001 and 2002 (Fig 5). The average annual flow recorded for hydrological year 2001 (Oct 1, 2000 – Sept 30, 2001) was one of the lowest recorded over the last 22 years. Streamflow was over-predicted by the SMR model for the hydrological year 2001 with the greatest error occurring within the forested watershed. This possibly indicates that the simple evapotranspiration algorithm in SMR cannot fully account for water uptake by trees especially during a drought year, or that interception losses which were not accounted for in the model, were more significant during the drier year. Flows during the hydrological year 2002 represent a more typical average annual flow pattern. Model performance during the 2002 water year for all watersheds was very good with NS values of 0.52, 0.57 and 0.74 for the Forest, Ag, and Urban watersheds, respectively. In each case, the timing of event peak flows was very good. The magnitude of these peak flows, however, was over- and under-predicted at different times during the year.

CONCLUSION AND DISCUSSION

The SMR model agrees reasonably well with both distributed seasonal perched water levels within a catchment and the integrated streamflow response leaving a watershed. Improvements to the model can be made by simulating the ponding and release of runoff from an existing snowpack, and forest canopy effects during drought years. The mapping capabilities of the GIS model allow for site-specific prediction of runoff which could prove to be a valuable management tool for watershed restoration within the Pacific Northwest.

REFERENCES

Boll, J., Brooks, E.S., Campbell, C.R., Stockle, C.O., Young, S.K., Hammel, J.E., McDaniel, P.A.. (1998) Progress toward development of a GIS based water quality management tool for small rural watersheds: modification and application of a distributed model. *ASAE Annual International Meeting* in Orlando, Florida, July 12-16, Paper 982230, ASAE, 2950 Niles Road, St. Joseph, MI 49085-9659, USA (Poster).

Frankenberger, J.R., Brooks, E.S., Walter, M.T., Walter, M.F., Steenhuis, T.S. (1999) A GIS-based variable source area hydrology model. *Hydrological Processes*, 13, 805-822.

Nash, J.E., Sutcliffe, J.V. (1970) River flow forecasting through conceptual models, Part 1 - A discussion of principles. *J. Hydrol.*, 10, 238-250.

Quinn, P., Beven, K.J., Chevallier, P., Planchon, O. (1991) The prediction of hillslope flow paths for distributed hydrological modelling using digital terrain models. *Hydrological Processes,* 5, 59-79.

Thornthwaite, C.W., Mather, J.R. (1955) The Water Balance. Laboratory of Climatology, Publ. No. 8, Centerton NJ.

U.S. Army Corps of Engineers (1960) Engineering and Design: Runoff from Snowmelt. EM 1110-2-1406.

United States Environmental Protection Agency. 1992. National Water Quality Inventory, 1992 Report to Congress. EPA 841-R-94-001, Office of Water, Washington DC, pp. 328.

TYPES OF STREAM ALIMENTATION IN LOWLAND AREAS OF NW POLAND. A GEOSTATISTICAL ANALYSIS.

Alfred Stach[1], Andrzej Kostrzewski[1], Małgorzata Mazurek[1], Grażyna M. Michalska[2], Zbigniew Zwoliński[1]

[1]Institute of Quaternary Research and Geoecology, Adam Mickiewicz University, Fredry 10, 61-701 Poznań, Poland
[2] Adam Mickiewicz University Geoecological Station, Storkowo 32, 78-450 Grzmiąca, Poland

ABSTRACT

Areas of the Last Glaciation in northern Poland differ widely as to the conditions controlling the formation of river runoff and solute loads. The aim of the research was to identify chief mechanisms of stream alimentation in this area depending on the scale of a catchment. The analysis was based on data from hydrochemical profiling. Three types of systems were found to occur: in spring-head catchments with areas of the order of 10^{-2} km^2, in small catchments (10^0 km^2), and in medium-sized ones (10^1-10^2 km^2). The first is connected with the mixing of soil- and groundwater; the second with the mixing of waters from relatively homogeneous subcatchments; and the third with the mixing of groundwater from various water-bearing horizons. In headwater catchments, river waters reach a new physico-chemical equilibrium at a distance of 20-40 m; in small catchments, two nested autocorrelation structures (150 and 400 m) reflect the sequence of land cover changes and distances between main tributaries; in medium-sized catchments, river waters demonstrate similarity at a distance of between 300 and 450 m which is controlled by the sequence of successive valley reaches of different origins (melt-out basins & ravines).The reported analysis justifies the hypothesis that in the areas of northern Poland covered by the Last Glaciation it is possible to identify zones and forms of channel alimentation on the basis of hydrochemical interpretation of runoff recorded in gauging profiles only in the case of small catchments no larger than $n \times 10^0$ km^2. In larger catchments, it is only possible to differentiate between 'new water' (direct precipitation on the channel and overland flow) and 'old water', composed of a mixture of soil water and the alimentation from various water-bearing horizons.

Keywords stream alimentation, catchment scale, hydrochemical profiling, semivariograms, NW Poland

INTRODUCTION AND STUDY AREA DESCRIPTION

Since 1985, interdisciplinary research has been carried out in the upper Parsęta catchment (NW Poland, Fig 1) concerning the processes of energy and matter fluxes in areas with postglacial relief and varying land-use patterns (Kostrzewski et al., 1994). An element of the research has been the monitoring of hydrological and geomorphological processes in catchments of various sizes, starting with first-order ones, covering 10^{-2} km^2 (Michalska, 2001; Stach, 1993), and ending with a fifth-order one, covering 10^2 km^2 (Kostrzewski et al., 1994; Mazurek, 1999, 2000). The operation of even the smallest catchment in this area is very complex, owing to a poor organisation of the drainage system, a complicated geological structure of the Quaternary, diversified lithology, and a mosaic of land uses, including numerous water bodies and peat bogs (Table 1). The characteristic features of the hydrology of this northern part of the Polish Lowland are a high proportion of areas with no surface outlet, a large retaining capacity of catchments and hence big hydrological inertia of streams, and the dominance of seasonal over short-term variability connected with rainfall or snowmelt episodes. The spatial and temporal variations in the conditions controlling the channel flow are reflected in a high variation, primarily spatial, of the unit flow modulus, and in the physico-chemical properties of waters (Table 1). In small, even adjacent catchments, water mineralisation levels and solute loads can differ by more than one order of magnitude. That is why a hydrological interpretation of the channel flow in water-gauging profiles on those streams (in terms of the identification of sources and ways of feeding) is impossible without spatial studies and analyses. Apart from traditional hydrological mapping, a wealth of valuable data have been derived from hydrochemical profiling of the streams.

The aim of the present work is to elucidate the mechanisms of the channel flow formation in catchments of various sizes in areas with postglacial relief on the Polish Plain. For this purpose use was made, among other things, of a geostatistical analysis (Goovaerts, 1997; Gringarten and Deutsch, 2001) of data from the hydrochemical profiling.

METHODOLOGY

The studies were conducted in four subcatchments as well as in the entire catchment of the upper Parsęta (Table 1). The catchment areas varied from 0.05 km^2 to 74.0 km^2, the length of streams from 0.16 km to 13.26 km, and sampling intervals from 2 m to 100 m. The basic range of *in situ* measurements included the temperature, reaction, and specific electrical conductivity of water. Additionally, samples were taken in order to determine the basic ionic macrocomposition. Mapping was carried out in periods of steady runoff lasting a maximum of one day. The periods chosen corresponded to high water resources in the catchments, with all other forms of channel feeding besides non-saturation (Hortonian) overland flow present.

The classical analysis of semivariance is intended for the study of series of stationary data, i.e., ones in which the deviation from the mean is random in nature (Goovaerts, 1997; Gringarten and Deutsch, 2001). The analysed measurement series are non-stationary and there is often a strong tendency for water coming from upstream to "mask" changes occurring at a given point. In most cases, the actual spatial structure of the analysed data can be discerned after the elimination of the tendency or the local average (Table 2). The nugget variance of semivariance models (Table 2) is in most cases close to the measurement error. This means that the variability of the parameters measured at a distance shorter than the sampling interval was negligibly small.

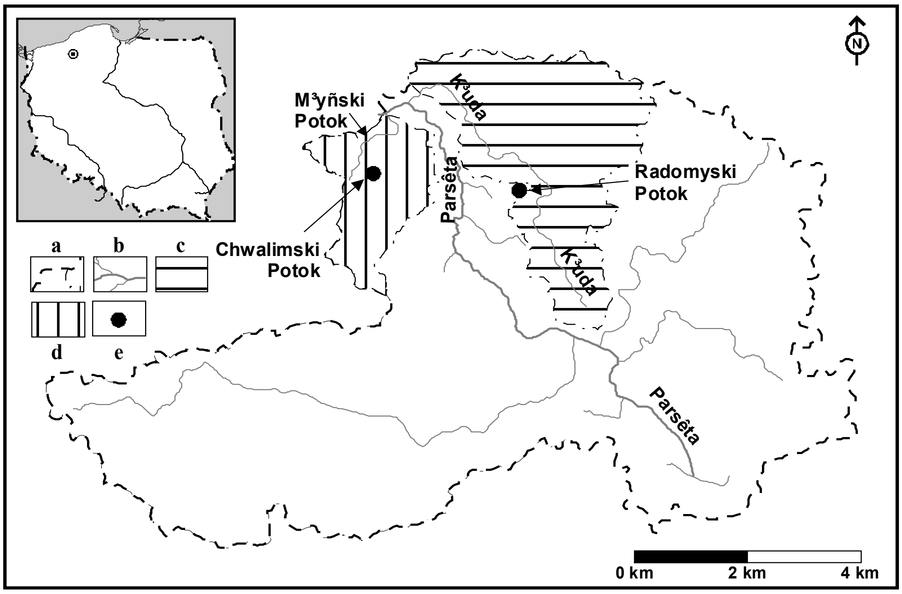

Fig 1: The location and hydrological system of the upper Parsęta catchment. a - watershed of the upper Parsęta catchment and its subcatchments, b - hydrographic network, c - Kłuda catchment, d - Młyński Potok catchment, e - first-order catchments (of Chwalimski Potok and Radomyski Potok).

RESULTS

Each investigated stream turned out to have its own, unique features. However, there were noticeable differences at three spatial catchment scales.

In spring-head catchments covering 0.05-0.10 km^2 and stream lengths of 0.16-0.23 km, variations in the measured physico-chemical properties of waters were relatively big, but nonetheless gradual (Fig 2C).

The range of autocorrelation roughly equalled 20 m (Fig 3C, Table 2). The basic processes responsible for this pattern were:

- the gradual attaining of a physico-chemical equilibrium by water reaching the ground surface under current conditions of temperature and atmospheric pressure; mainly the establishment of a new carbonate equilibrium and a new pH of water.
- the mixing of soil- and groundwater differing significantly in total mineralisation levels and ionic composition.

Table 1: Characteristics of analysed rivers and their catchments (morphometric indices after Zăvoianu 1985).

Parameter / river / reference	**the upper Parsęta** (Kostrzewski et al. 1994)	**Kłuda** (Mazurek 1999, 2000)	**Młyński Potok**	**Radomyski Potok** (Stach 1993)	**Chwalimski Potok** (Michalska 2001)
Catchment area [km^2]	74.00	10.69	3.94	0.109	0.051
River length [km]	13.26	6.99	2.46	0.157	0.231
River slope [-]	0.0041	0.0063	0.0139	0.0422	0.0156
Basin height H_{max}-H_{min} [m]	119.5	96.2	79.1	26.0	10.36
Index of catchment relief H_{source} – H_{outlet} [m]	137.5 - 83.4	132.0 - 88.7	117.5-83.4	116.6-110.0	114.3-110.7
Basin slope [-]	0.008	0.017	0.025	0.060	0.035
Drainage density [$km\,km^{-2}$]	2.24	2.97	2.35	2.12	5.71
Mean annual discharge [$dm^3\,s^{-1}$]	610.0 [1)]	94.9 [2)]	20.7 [3)]	1.33 [4)]	1.47 [5)]
Mean annual unit runoff [$dm^3 s^{-1}\,km^{-2}$]	8.2 [1)]	8.9 [2)]	5.3 [3)]	12.20 [4)]	28.82 [5) 6)]
Surface lithology [7)]	85%S, 13%P, 2% O	88%S, 7%P, 5%O	91.9%S, 5,4%P, 2,8%O	93%S, 3%P, 6%O	93%S, 5%P, 2%O
Landuse [8)]	[9)] 43%A, 34%F, 15%M/P, 8%O	[9)] 37%A, 41%F, 18%M/P, 4% O	[9)] 40%A, 35%F, 23%M/P, 2%O	94%A, 3%F, 3%M/P, 0% O	14%A, 0%F, 26%M/P, 60%O
Water chemistry at the outlet (anions and cations concentrations are in meq dm^{-3}) Anions: $HCO_3 > SO_4 > Cl$ Cations: Ca > Mg > Na > K	388.1 µS, 7.85 pH, 10.53 mg dm^{-3} SiO_2, A: 2.86 > 0.83 > 0.38 C: 3.54 > 0.44 > 0.25 > 0.06	409.5 µS, 7.90 pH, 12.30 mg dm^{-3} SiO_2, A: 3.14 > 0.74 > 0.33 C: 3.41 > 0.43 > 0.34 > 0.05	353,3 µS, 7,10 pH, 9,61 mg dm^{-3} SiO_2, A: 2.75 > 0.78 > 0.35 C: 3.23 > 0.34 > 0.28 > 0.05	362,4 µS, 7.46 pH, 12,60 mg dm^{-3} SiO_2, A: 2.74 > 0.40 > 0.29 C: 2.90 > 0.42 > 0.29 > 0.04	382,0 µS, 7,94 pH, 8.89 mg dm^{-3} SiO_2, A: 2.51 > 0.96 > 0.29 C: 3.36 > 0.34 > 0.28 > 0.09

1) – gauge of the Institute of Meteorology and Water Management at Storkowo, hydrological years 1985-2000
2) – hydrological years 1990-1993
3) – hydrological years 1994-2001
4) – mean of 105 irregular measurements taken in the hydrological years 1987-1991
5) – weekly measurements in the hydrological years 1992-1995
6) – extraordinary high value because of big difference between surface and subsurface catchment,
7) – S - sands (loamy and loose sands), P - sediments of organic origin, mostly peat, O - other
8) – A - arable land, F - woodland, M/P - meadows/pastures, O - other.
9) – Data from early 1990s; there have been rapid changes in land-use pattern: drop in proportion of arable land and increase in area of wasteland and woodland.

Also visible were more subtle elements of the spatial structure, like the cyclicity of semivariance after it had reached the level of structural semivariance (Fig 3C) and a similar cyclicity of cross-correlograms. The length of the cycle is roughly twice as large as the autocorrelation range, which is indicative of the presence (corroborated by the results of other studies, cf. Stach, 1993) of at least two zones of groundwater feeding into the analysed stream section, and hence, of two zones of establishment of a physico-chemical equilibrium and the mixing of waters.

In a third-order catchment of 3.94 km^2 and a stream length of 2.46 km (Klimczak, 1993), sampling was carried out every 20 m. Sudden changes were recorded in the parameters downstream of the tributaries, while they were negligibly small between them (Fig 2B). Hence, in this case the crucial factor is the spatial variability of the feeding sources. The tributary catchments are relatively homogeneous in terms of lithology/soils and land-use patterns, and at this spatial scale they differ significantly. Because the discharge in the tributaries is comparable with the amount of water flowing in the principal stream, changes in the physico-chemical parameters of water are stepwise. To some extent, the storm/melting runoff-related and seasonal changes in solute concentrations recorded in a gauging profile can be interpreted in terms of changes in the relative contributions of water flowing from the individual subcatchments. The analysis of semivariance, after the mean 'tributary effect' has been eliminated, indicates the presence of two ranges of data autocorrelation: 0.15 km and 0.40 km (Fig 3B, Table 2), which reflects the sequence of land cover changes and distances between the main tributaries.

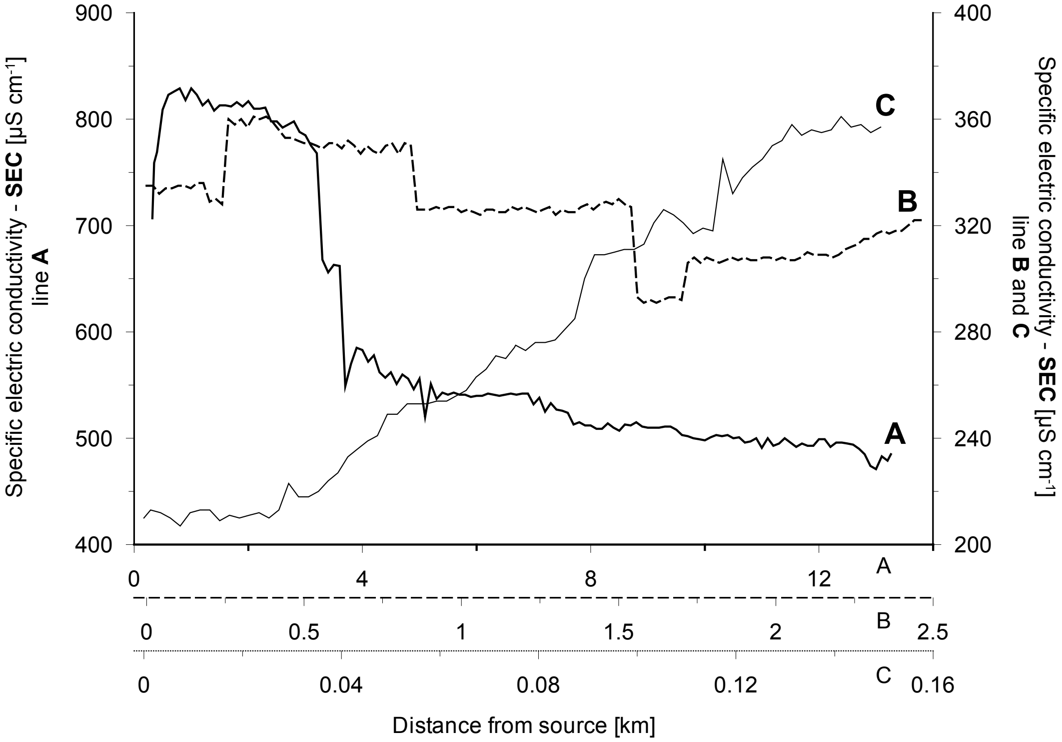

Fig 2: Profiles of variations in the electrical conductivity of water in the channels of the upper Parsęta (line A), Młyński Potok (line B), and Radomyski Potok (line C).

In two larger catchments with respective areas of 10.7 km^2 and 74.0 km^2, and principal stream lengths of 7.0 km and 13.3 km, sampling was carried out every 100 m (Kostrzewski et al., 1994; Mazurek, 2000). Two types of structures can be observed here. Relatively small changes in the channel of the principal stream downstream of the biggest tributaries overlap with trends embracing longer channel sections characterised by different gradients, and sometimes also directions of change (Fig 2A). Of basic importance in this case is a belt pattern of the main geomorphological-lithological zones forming distinct hypsometric levels within the catchments of the two streams. On cutting through them, the streams are fed from several levels of groundwater with different circulation times, and hence also mineralisation and ionic composition. However, owing to the abundance of readily soluble carbonates in various types of glacial and fluvioglacial deposits, the proportions of chief solution components are similar. The best hydrochemical indicator differentiating groundwater with respect to the circulation time has been found to be ionised silica. In these catchments, therefore, the crucial factor controlling the runoff is the 'vertical' variability of feeding sources, i.e. groundwater levels at a variety of depths and with a variety of alimentation areas. Also in those streams, after the trend has been eliminated, one can observe an autocorrelation of measurement results at a distance of 300-450 m (Fig 3A, Table 2). It is controlled by the sequence of successive valley reaches of different origins (melt-out basins & ravines).

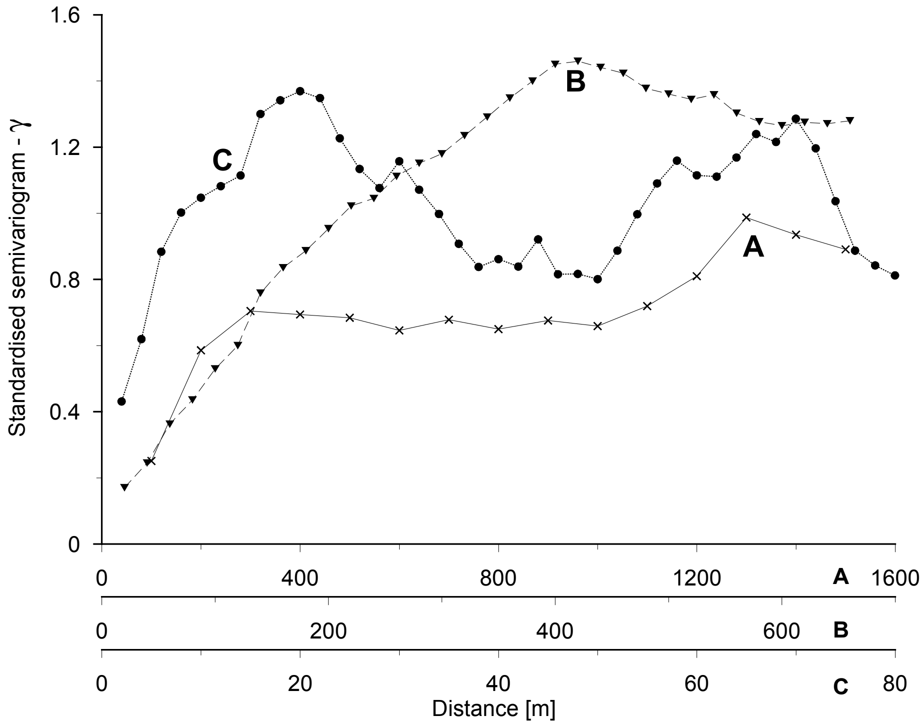

Fig 3: Standardised semivariograms of the electrical conductance of water in long profiles from the catchments of the Kłuda (line A), Młyński Potok (line B), and Radomyski Potok (line C).

A significant role in controlling the flow of dissolved salts between the catchment area and the stream channel is played by the valley zone, which is filled with mineral-organic sediments (with a large proportion of silt, calcareous gyttja, lacustrine chalk and peat). A comparison of the chemical composition of river water and groundwater examined on the morainic plateau shows that the alimentation of the stream channel occurs through the shallow groundwater of the valley zone. The properties of this shallow groundwater result from the mixing of waters flowing from the catchment to the valley floors. The chemical composition of the inflowing water also undergoes a transformation under the influence of calcium carbonate contained in the mineral-organic sediments characteristic especially of melt-out basin sections of the valleys.

CONCLUSIONS

The reported analysis confirms the hypothesis that in the areas of northern Poland covered by the Last Glaciation it is possible to identify zones and forms of channel alimentation on the basis of hydrochemical interpretation of runoff recorded in gauging profiles only in the case of small catchments no larger than $n \times 10^0$ km^2. In larger catchments, it is only possible to differentiate between "new water" (direct precipitation on the channel and overland flow) and "old water", composed of a mixture of soil water and the alimentation from various water-bearing horizons. The hypothesis is being verified by studying a bigger catchment sample in diversified hydrological conditions. An examination of the stable isotope content of the water might shed new light on this issue.

REFERENCES

Goovaerts, P. (1997) Geostatistcs for natural resources evaluation. Oxford University Press, 1-483.

Gringarten, E., Deutsch, C.V. (2001) Teacher's aide. Variogram interpretation and modeling. *Mathematical Geology*, vol. 33, no. 4, 507-534.

Klimczak, R. (1993) The processes of slope wash in areas with diversified land use patterns – their role in contemporary morphogenetic environment (The Młyński Brook catchment, West Pomerania). (in Polish with English summary), In: Komitet Naukowy przy Prezydium PAN "Człowiek i Środowisko", *Zeszyty Naukowe*, 6, 61-77.

Kostrzewski, A., Mazurek, M., Zwoliński, Z. (1994) Dynamics of fluvial transport of the upper Parsęta River as a response of the catchment system). (in Polish with English summary), The Association of Polish Geomorphologist, Poznań, pp. 165.

Mazurek, M. (1999) Solute transport as an indicator of morphodynamic zonation in a postglacial environment, West Pomerania. *Earth Surface Processes and Landforms*, 24, 1-14.

Mazurek, M. (2000) Variations in solute transport in the Kłuda catchment as a reflection of the present-day processes of chemical denudation (West Pomerania). (in Polish with English summary), *Adam Mickiewicz University Press, Ser. Geographia*, no. 62, Poznań, pp. 125.

Michalska, G. (2001) Nutrient wet deposition, cycle and runoff from the agricultural catchment (Chwalimski Potok, the upper Parsęta). (in Polish with English summary), In: M. Jóźwiak, A. Kowalkowski (red.) *Zintegrowany Monitoring Środowiska Przyrodniczego w Polsce. Funkcjonowanie i Monitoring Geoekosystemów z uwzględnieniem zanieczyszczenia powietrza*, Bibl. Monitoringu Środowiska, 373-386.

Stach, A. (1993) Uwarunkowania i funkcjonowanie procesów denudacji chemicznej i ich wpływ na morfodynamikę stoków mikrozlewni na obszarze młodoglacjalym (zlewna górnej Parsęty, Pomorze Zachodnie). Unpublished PhD thesis (in Polish), Adam Mickiewicz University, Poznań, pp. 188.

Zăvoianu, I. (1985) Morphometry of drainage basins. *Developments in Water Science*, 20, Elsevier, 1-238.

Table 2: Profiling results of the studied streams.

Name of river	Length of section sampled / Sampling interval	Sampling date	Parameters measured [1)]	Range of parameters in sampled river section	Mean for sampled river section	Data preparation before semivariogram calculation [2)]	Nugget variance $\sqrt{C_0}$	Sill (nugget variance + structural variance) $\sqrt{C+C_0}$	Range A_0
Units	[m]			SEC - µS cm^{-1} in 25°C, Tw - °C					[m]
Chwalimski Potok	215 / 5	2001-03-13	SEC / pH / Tw	SEC: 160 – 455 pH: 7.90 – 8.39 Tw: 6.0 – 7.9	SEC: 419.2 pH: 8.23 Tw: 7.0	SEC: none pH: none Tw: CLTR	SEC: 1.0 pH: 0.02 Tw: 0.1	SEC: 37.9 pH: 0.05 Tw: 0.18	SEC: 25.2 pH: 42 Tw: 36.4
Radomyski Potok	149,5 / 2	1992-03-05	SEC / pH / Tw	SEC: 207 – 361 pH: 5.45 – 7.73 Tw: 3.8 – 6.1	SEC: 277.8 pH: 6.33 Tw: 5.0	SEC: CLTR pH: CLTR Tw: LTR	SEC: 2.63 pH: 0.14 Tw: 0.05	SEC: 6.0 pH: 0.27 Tw: 0.15	SEC: 17.9 pH: 23.1 Tw: 17.1
Młyński Potok	2460 / 20	2002-03-09	SEC / Tw	SEC: 291 – 361 Tw: 4.1 – 6.3	SEC: 326.5 Tw: 5.44	local means removal	SEC: 0.9 Tw: 0.08	SEC: 3.8 Tw: 0.23	SEC: 150/400 Tw: 430
Kłuda	6990 / 100	1992-08-20	SEC / pH	SEC: 352 – 419 pH: 7.29 – 8.15	SEC: 401.8 pH: 7.82	None	SEC: 0 pH: 0	SEC: 7.5 pH: 0.12	SEC: 310 pH: 315
the upper Parsęta	12940 / 100	1993-07-04	SEC / pH	SEC: 471 – 829 pH: 7.59 – 8.50	SEC: 590.0 pH: 7.92	SEC: CLTR pH: none	SEC: 7.21 pH: 0.06	SEC: 14.5 pH: 0.31	SEC: 436 pH: 1200/2600

[1)] SEC – Specific Electric Conductivity of water, pH – reaction, Tw – water temperature,
[2)] CLTR – curvilinear trend removal, LTR – linear trend removal

Annex: List of posters presented at the conference

Struma river basin data acquisition and processing system
Koshnichanov G., Dimitrov D.

The Attert river basin: a transnational experimental river basin in Luxembourg
Iffly J.F., Drogue G., El Idrissi A., Pfister L., Salvia M., Hoffmann L.

Effect of climate change on the hydrology of the Hupselse Beek catchment area
Warmerdam P., Torfs P., Kole J., Crespi E.

Impact of climate and vegetation changes on hydrological processes in the Jalovecký creek catchment
Kostka Z., Holko L.

Assessment of the runoff regime changes under various climate conditions in the Uh River basin
Halmová D., Mitková V., Pekárová P.

Investigation of runoff changes after deforestation-comparison of runoff in three experimental basins
Buchtele J., Buchtelová M., Martin C., Didon-Lescot J.-F.

Changes in runoff conditions depending on the way of farming in the small catchment
Podhrázská J., Toman F.

Soil and water conservation through the land consolidation
Uhlířová J.

Seasonal dynamics of runoff variable contributing areas in a Mediterranean mountain catchment (Vallcebre, Catalan Pyrenees)
Latron J., Gallart F.

Water retention in the river Opava catchment during the floods in July 1997
Spitz P., Podhrázská J., Prudký J.

Assessment of extreme events in the Čierny Hron representative river basin
Šipikalová H., Kyselová D., Hrušková K.

Reconstruction of extreme floods in small ungaged catchment
Hlavčová K., Szolgay J., Kohnová S., Zvolenský M.

Regional calibration of water balance model for estimating mean monthly flow in small ungaged catchment
Szolgay J., Hlavčová K., Kohnová S., Kubeš R.

Nutrients fluxes dynamics in two rural watersheds in the Haute-Sûre river basin
Iffly J.F., Pihan J., Hoffmann L.